SINTEF

TR A7603- Unrestricted

Report

EERA DeepWind'2016 Conference
20 – 22 January 2016

Radisson Blu Royal Garden Hotel, Trondheim

Author(s)
John Olav Tande (editor)

SINTEF Energy Research
Power Conversion and Transmission
2016-11-01

SINTEF Energi AS
SINTEF Energy Research
Address:
Postboks 4761 Sluppen
NO-7465 Trondheim
NORWAY
Switchboard: +47 73597200
Telefax: +47 73598354
energy.research@sintef.no
www.sintef.no/energi
Enterprise /VAT No:
NO 939 350 675 MVA

KEYWORDS:

Report

EERA DeepWind'2016 Conference
20 – 22 January 2016

Radisson Blu Royal Garden Hotel, Trondheim

VERSION
1.0

DATE
2016-12-12

AUTHOR(S)
John Olav Tande

CLIENT(S)

CLIENT'S REF.
Client's reference

PROJECT NO.
502000965-2

NUMBER OF PAGES/APPENDICES:
314

ABSTRACT

This report includes the presentations from the 13th Deep Sea Offshore Wind R&D Conference, EERA DeepWind'2016, 20 – 22 January 2016 in Trondheim, Norway.

Presentations include plenary sessions with broad appeal and parallel sessions on specific technical themes:

a) New turbine and generator technology
b) Grid connection and power system integration
c) Met-ocean conditions
d) Operations & maintenance
e) Installation & sub-structures
f) Wind farm optimization
g) Experimental Testing and Validation
x1) Online technology transfer network for wind energy research
x2) Numerical reference wind farms

Plenary presentations include frontiers of science and technologies and strategic outlook. The presentations and further conference details are also available at the conference web page: https://www.sintef.no/projectweb/deepwind_2016/

PREPARED BY
John Olav Tande

SIGNATURE

CHECKED BY
Hans Christian Bolstad

SIGNATURE

APPROVED BY
Knut Samdal

SIGNATURE

REPORT NO.	ISBN	CLASSIFICATION	CLASSIFICATION THIS PAGE
TR A7603	978-82-594-3676-4	Unrestricted	Unrestricted

SINTEF

Document history

VERSION	DATE	VERSION DESCRIPTION
1.0	2016-11-01	

SINTEF

Table of contents

1. Development of a FAST model for a floating 10MW wind turbine, M. Borg, DTU Wind Energy
2. Investigation on Fault-ride Through Method for VSC-HVDC Connected Offshore Wind Farms, W. Sun, NTNU
3. Design and Modelling of a LFAC transmission system for offshore wind, J. Ruddy, Univ College Dublin
4. A Review on Wind Power Plant Control and Modelling Requirements, O. Anaya-Lara, Univ of Strathclyde
5. Synthetic inertia from wind power plant: Investigation of practical issues based on laboratory-based studies, O. Anaya-Lara, Univ of Strathclyde
6. Provision of Ancillary Services from Large Offshore Wind Farms, W. Ross, Univ of Strathclyde
7. Analysis of cyclone Xaver (2013) for offshore wind energy, K. Christakos, Uni Research Polytec AS
8. OBLO instrumentation at FINO1, M. Flügge, CMR
9. Energy systems on autonomous offshore measurement stations, T.K. Løken, NTNU
10. A Site Assessment of the Hywind Floating Wind Turbine location, L. Sætran, NTNU
11. Gust factors in gale and storm conditions at Frøya, L.M. Bardal, NTNU
12. Proof of concept for wind turbine wake investigations with the RPAS SUMO, J. Reuder, UiB
13. Development of a TLP substructure for a 6MW wind turbine – use of steel concrete composite material, F. Adam, Wind Power Construction GMBH
14. First results from an offshore 40m high TLP met. mast at 65m deep waters in the Aegean Sea, D. Foussekis, Centre for Renewable Energy Sources (CRES)
15. Project schedule assessment with a focus on different input weather data sources, G. Wolken-Möhlmann, Fraunhofer IWES
16. Nonlinear wave propagation and breaking in the coastal area, M.B. Paskyabi, UiB
17. Lagrangian Study of Turbulence Structure Near the Sea Surface, M.B. Paskyabi, UiB
18. Evaluation of ensemble prediction forecasts for estimating weather windows, B.R. Furevik, MET
19. A surrogate model for simulations – finding optimal operation & maintenance strategies for offshore wind farms, M.R. Gallala, NTNU
20. Risk and reliability based maintenance planning for offshore wind farms using Bayesian statistics, M. Florian, Aalborg Univ.
21. The operation and maintenance planning based on reliability analysis of fatigue fracture of a wind turbine drivetrain components. A. Beržonskis, Aalborg Univ.
22. Operation and maintenance and logistics strategy optimisation for offshore wind farms, I.B. Sperstad, SINTEF Energi
23. Vessel fleet optimization for maintenance operations at offshore wind farms under uncertainty, M. Stålhane, NTNU
24. Maintenance polar and marine traffic validation on existing wind farm, Colone, L., DTU
25. Assessment of the dynamic responses and operational sea states of a novel OWT tower and rotor nacelle assembly installation concept based on the inverted pendulum principle, W. G. Acero, NTNU
26. Multi-level hydrodynamic modelling of a 10MW TLP wind turbine, A.P. Jurado, DTU
27. A model for jacket optimization in Matlab, K. Sandal, DTU
28. Strategy and costs of installing floating offshore wind farms, L.B. Savenije, ECN
29. Analysis of second order effects on a floating concrete structure for FOWT's, Prof. Climent Molins, Universitat Politecnica de Catalunya
30. Vibration-based identification of hydrodynamic loads and system parameters for offshore wind turbine support structures, D. Fallais, Delft University of Technology
31. Improved Simulation of Wave Loads on Offshore Structures in Integral Design Load Case Simulations, M.J. de Ruiter, Knowledge Centre WMC
32. Adaptation of Control Concepts for the Support Structure Load Mitigation of Offshore Wind Turbines, B. Shrestha, ForWind
33. Comparison of experiments and CFD simulations of a braceless concrete semi-submersible platform, L. Oggiano, IFE
34. Parametric Wave Excitation Model for Floating Wind Turbines, F.Lemmer, né Sandner, University of Stuttgart
35. On Fatigue Damage Assessment for Offshore Support Structures with tubular Joints B. Hammerstad, NTNU
36. Influence of Soil Parameters on Fatigue Lifetime for Offshore Wind Turbines with Monopile Support Structure, S. Schafhirt, NTNU
37. Mooring Line Dynamics Experiments and Computations. Effects on Floating Wind Turbine Fatigue Life and Extreme Loads, J. Azcona, CENER
38. Semisubmersible floater design for a 10MW wind turbine, J. Azcona, CENER
39. Sizing optimization of a jacket under many dynamic loads, A. Verbart, DTU Wind Energy
40. Rational upscaling of a semi-submersible floating platform, M. Leimeister, NTNU
41. Numerical and experimental investigation of breaking wave impact forces on a vertical cylinder in shallow waters, M.A. Chella, NTNU
42. Irregular Wave Forces on Circular Cylinders placed in Tandem, A. Aggarawal, NTNU
43. New design concepts of an upwind turbine rotor and their impact on wake characteristics, F. Mühle, NMBU
44. Wake modelling: the actuator disc concept in PHOENICS, N. Simisiroglou, WindSim AS
45. Wind farm control applications for Windscanner infrastructure, T.I. Reigstad, SINTEF Energi AS

46. Real-Time Hybrid Model Testing of a Floating Wind Turbine: Numerical validation of the setup, V. Chabaud, NTNU
47. Experimental Wind Turbine Wake Investigation towards Offshore Wind Farm Performance Validation, Y. Kim, LSTM, FAU
48. Validation of a Semi-Submersible Offshore Wind Platform through tank test, G. Aguirre, Tecnalia R&I
49. Field site experimental analysis of a 1:30 scaled model of a spar floating offshore wind turbine, M. Collu, Mediterranea University
50. A Review and Comparison of Floating Offshore Wind Turbine Model Experiments, G. Stewart, NTNU
51. Wind Model for Simulation of Thrust Variations on a Wind Turbine, E. Smilden, NTNU
52. Numerical simulations of the NREL S826 aerofoil performance characteristics – A CFD validation and simulation of 3D effects in wind tunnel testing, K. Sagmo, NTNU
53. A Single-Axis Hybrid Modelling System for Floating Wind Turbine Basin Testing, M. Hall, University of Maine
54. A design support multibody tool for assessing the dynamic capabilities of a wind tunnel 6DoF/HIL setup, M. Belloli, Politecnico di Milano
55. Assessment and evaluation of a wind turbine condition using a time-frequency signal processing method, P. McKeever, Offshore Renewable Energy Catapult
56. Development, Verification and Validation of 3DFloat; Aero-Servo-Hydro-Elastic Computations of Offshore Structures, T.A. Nygaard, IFE
57. Effect of upstream turbine tip speed variations on downstream turbine performance: a wind farm case optimization, J. Bartl, NTNU
58. Droplet Erosion Protection Coatings for Offshore Wind Turbine Blades, A. Brink, SINTEF M&C
59. Design of an airfoil insensitive to leading edge roughness, T. Bracchi, HIST
60. Socio-economic evaluation of floating substructures within LIFES 50+ project, M. de Prada, IREC
61. Coordinated control of DFIG-based offshore wind power plant connected to a single VSC-HVDC operated at variable frequency, M. de Prada , IREC
62. Implications of different regulatory approaches for offshore wind in Europe, L. Kitzing, DTU Management Engineering
63. Fiskarstrand Verft AS tooling up for renewable energy, Einar Kjerstad, Fiskerstrand Verft AS
64. LIFES50+: Innovative floating offshore wind energy .P.A.Berthelsen, Marintek
65. Aerodynamic modeling of offshore floating vertical axis wind turbines, Z. Cheng, NTNU
66. Scalability of floating Vertical Axis Wind Turbines, E. Andersen, UiS
67. Advanced Wind Energy Systems Operation and Maintenance Expertise, J. Melero, CIRCE

FINAL 15 JANUARY 2016

Wednesday 20 January		
09.00	Registration & coffee	
	Opening session – Frontiers of Science and Technology Chairs: John Olav Tande, SINTEF/NOWITECH and Trond Kvamsdal, NTNU/NOWITECH	
09.30	Opening and welcome by chair	
09.40	Initiative for Global Leadership in Offshore Wind, Matthijs Soede, Research Programme Officer, European Commission	
10.10	Innovations in offshore wind energy, John Olav Tande, director NOWITECH	
10.35	Cooperation as a key to cost reductions for offshore wind, Kristin Guldbrandsen Frøysa, director NORCOWE	
11.00	Hywind Scotland, Knut Erik Steen, Technical Manager, Statoil	
11.30	EERA research programme on wind energy and the offshore challenges, Thomas Buhl, DTU	
11.55	Closing by chair	
12.00	Lunch	
	Parallel sessions	
	A1) New turbine and generator technology Chairs: Karl Merz, SINTEF	**C1) Met-ocean conditions** Chairs: Valerie-Marie Kumer, Uni of Bergen, Joachim Reuder, Uni of Bergen, Birgitte Rugaard Furevik, met.no
13.00	Introduction by Chair	Introduction by Chair
13.05	Development of a TLP substructure for a 6MW wind turbine – use of steel concrete composite material, F. Adam, Wind Power Construction GMBH	Turbulence Intensity Model for offshore wind energy applications, K. Christakos, Uni Research Polytec AS
13.30	A parametric CFD study of morphing trailing edge flaps applied on a 10 MW offshore wind turbine, Eva Jost, Univ of Stuttgart	Boundary-Layer Study of FIN0vale1, M. Flügge, CMR
13.50	Latest results from the EU project AVATAR: How to model large wind turbines aerodynamically? J.G. Schepers, ECN	High-resolution simulations of surface wind climate, ocean currents and waves, H. Agustsson, Kjeller Vindteknikk AS
14.10	Design Load Cases investigation and comparison between Vertical and Horizontal Axis Wind Turbines, C. Galinos, DTU	Analysis of offshore turbulence intensity – comparison with prediction models, K. Lamkowska, Lodz Univ of Technology
14.30	Closing by Chair	Closing by Chair
14.35	Refreshments	
	A2) New turbine and generator technology (cont.)	**C2) Met-ocean conditions (cont.)**
15.05	Introduction by Chair	Introduction by Chair
15.10	Development of an analysis and simulation tool for a multi-rotor wind turbine floater, P.E. Thomassen, Simis	Coherence of turbulent wind under neutral wind conditions at FINO, L. Eliassen, NTNU / Statkraft
15.30	Influence of Aerodynamic Model Fidelity on Rotor Loads during Floating Offshore Wind Turbine Motions, D. Matha, Ramboll Wind	Assessment of offshore wind coherence by pulsed Doppler lidars, J.B. Jakobsen, UiS
15.50	A coupled floating offshore wind turbine analysis with high-fidelity methods, V. Leble, Univ of Glasgow	Turbulent Structure over Air-Sea Wavy Interface: Large-Eddy Simulation, M.B. Paskyabi, UiB
16.10	Closing by Chair	Closing by Chair
18.00	**Conference reception** Guided tour at Erkebispegården followed by entertainment (Trondheim Bassorkester*) and ligh*t food	

Side event

16.10 – 18.00: Planning meeting for EERA SP Offshore Wind Energy

FINAL 15 JANUARY 2016

Thursday 21 January		
	Parallel sessions	
	X1) Online technology transfer network for wind energy research Chair: Martijn van Roermund, ECN	**E1) Installation and sub-structures** Chairs: Prof Hans Gerd Busmann, Fraunhofer IWES Jørgen Krokstad, Statkraft; Michael Muskulus, NTNU
09.00	Introduction by Chair	Introduction by Chair
09.05	▪ Background on the initiative to set up an online tech transfer network on wind energy research. How does industry interact with the research community? ▪ Presentation of the online IP repository as developed for EERA. How to present your IP/technology? ▪ Discussion on further development of the online tech transfer network.	Accurate frequency domain method for monopiles K. Merz, SINTEF Energi
09.30		Crack growth fatigue modeling for monopiles, L. Ziegler, Rambøll/NTNU
09.50		The effect of slamming on a one degree of freedom model of an offshore wind turbine: experimental results, L. Suja-Thauvin, Statkraft/NTNU
10.10		Towards a risk-based decision support for offshore wind turbine installation and operation & maintenance, T. Gintautas, Aalborg Univ.
10.30	Refreshments	
	X2) Numerical reference wind farms Chair: Kristin Guldbrandsen Frøysa, director NORCOWE and Karl Merz, SINTEF Energy	**E2) Installation and sub-structures (cont.)**
11.00	▪ NORCOWE Reference Wind Farm, Kristin Guldbrandsen Frøysa, director NORCOWE ▪ NOWITECH Dogger Bank Reference Wind Farm, Karl Merz, SINTEF Energy Research	SATH platform concept study, Carrascosa, Saitec
11.20		Methodology for risk assessment of floating wind substructures, R.Proskovics, ORE Catapult
11.40		Scaling up floating wind – investigating the potential for platform cost reductions, M.I. Kvittem, DNVGL
12.00	Closing by Chair	Closing by Chair
12.05	Lunch	
	B1) Grid connection and power system integration Chairs: Prof Olimpo Anaya-Lara, Strathclyde University	**G1) Experimental Testing and Validation** Chairs: Tor Anders Nygaard, IFE Ole David Økland, MARINTEK, Amy Robertson, NREL
13.05	Introduction by Chair	Introduction by Chair
13.10	High Density MMC for platform-less HVDC offshore wind power collection systems (KEYNOTE), Chong NG, Offshore Renewable Catapult	Validation of a FAST Model of the Statoil-Hywind Demo Floating Wind Turbine, J. Jonkman, NREL
13.35	Cluster Control of Offshore Wind Power Plants Connected to a Common HVDC Station, J.N. Sakamuri, DTU Wind Energy	Real-time hybrid testing of a braceless semi-submersible wind turbine, E. Bachynski, MARINTEK
13.55	Coordinated Tuning of Converter Controls in Hybrid AC/DC Power Systems for System Frequency Support, A. Endegnanew, SINTEF Energi	OC5 Project Phase I: Validation of Hydrodynamic Loading on a Fixed Cylinder, A.N. Robertson, NREL
14.15	Fulfilment of Grid Code Obligations by Large Offshore Wind Farms Clusters Connected via HVDC Corridors, A.B. Attya, Univ of Strathclyde	Hydro-Elastic Contributions to Fatigue Damage on a Large Monopile, J-T. Horn, NTNU
14.35	Refreshments	
	B2) Grid connection and power system integration (cont.)	**G2) Experimental Testing and Validation (cont.)**
15.05	Optimal transmission voltage for very long HVAC cables, T.K.Vrana, SINTEF Energi AS	Validation of uncertainty in IEC damage calculations based on measurements from alpha ventus, K. Müller, Univ of Stuttgart
15.25	Investigation on Fault-ride Through Method for VSC-HVDC Connected Offshore Wind Farms, Raymundo Torres, NTNU	Experimental Validation of the W2Power Hybrid Floating Platform, P. Mayorga, W2Power
15.45	Minimizing Losses in Long AC Export Cables, O. Mo, SINTEF Energi	Unsteady aerodynamics of floating offshore wind turbines: toward experimental validation of equivalent lumped-element models, A. Zasso, Politecnico di Milano
16.05	Scaled Hardware Implementation of a Full Conversion Wind Turbine for Low Frequency AC Transmission, R. Meere, UCD	Aerodynamic damping of a HAWT on a Semisubmersible, S. Gueydon, Maritime Institute of The Netherlands
16.25	Closing by Chair	Closing by Chair
16.30	Refreshments	
17.00	**Poster session**	
19.00	Conference dinner	

FINAL 15 JANUARY 2016

Thursday 21 January: 17.00 Poster Session with refreshments

1. *Development of a FAST model for a floating 10MW wind turbine, M. Borg, DTU Wind Energy*
2. *Investigation on Fault-ride Through Method for VSC-HVDC Connected Offshore Wind Farms, W. Sun, NTNU*
3. *Design and Modelling of a LFAC transmission system for offshore wind, J. Ruddy, Univ College Dublin*
4. *A Review on Wind Power Plant Control and Modelling Requirements, O. Anaya-Lara, Univ of Strathclyde*
5. *Synthetic inertia from wind power plant: Investigation of practical issues based on laboratory-based studies, O. Anaya-Lara, Univ of Strathclyde*
6. *Provision of Ancillary Services from Large Offshore Wind Farms, W. Ross, Univ of Strathclyde*
7. *Analysis of cyclone Xaver (2013) for offshore wind energy, K. Christakos, Uni Research Polytec AS*
8. *OBLO instrumentation at FINO1, M. Flügge, CMR*
9. *Energy systems on autonomous offshore measurement stations, T.K. Løken, NTNU*
10. *A Site Assessment of the Hywind Floating Wind Turbine location, L. Sætran, NTNU*
11. *Gust factors in gale and storm conditions at Frøya, L.M. Bardal, NTNU*
12. *Proof of concept for wind turbine wake investigations with the RPAS SUMO, J. Reuder, UiB*
13. Development of a TLP substructure for a 6MW wind turbine – use of steel concrete composite material, F. Adam, Wind Power Construction GMBH
14. *First results from an offshore 40m high TLP met. mast at 65m deep waters in the Aegean Sea, D. Foussekis, Centre for Renewable Energy Sources (CRES)*
15. *Project schedule assessment with a focus on different input weather data sources, G. Wolken-Möhlmann, Fraunhofer IWES*
16. *Nonlinear wave propagation and breaking in the coastal area, M.B. Paskyabi, UiB*
17. *Lagrangian Study of Turbulence Structure Near the Sea Surface, M.B. Paskyabi, UiB*
18. *Evaluation of ensemble prediction forecasts for estimating weather windows, B.R. Furevik, MET*
19. *A surrogate model for simulations – finding optimal operation & maintenance strategies for offshore wind farms, M.R. Gallala, NTNU*
20. *Risk and reliability based maintenance planning for offshore wind farms using Bayesian statistics, M. Florian, Aalborg Univ.*
21. *The operation and maintenance planning based on reliability analysis of fatigue fracture of a wind turbine drivetrain components. A. Beržonskis, Aalborg Univ.*
22. *Operation and maintenance and logistics strategy optimisation for offshore wind farms, I.B. Sperstad, SINTEF Energi*
23. *Vessel fleet optimization for maintenance operations at offshore wind farms under uncertainty, M. Stålhane, NTNU*
24. *Maintenance polar and marine traffic validation on existing wind farm, Colone, L., DTU*
25. *Assessment of the dynamic responses and operational sea states of a novel OWT tower and rotor nacelle assembly installation concept based on the inverted pendulum principle, W. G. Acero, NTNU*
26. *Multi-level hydrodynamic modelling of a 10MW TLP wind turbine, A.P. Jurado, DTU*
27. *A model for jacket optimization in Matlab, K. Sandal, DTU*
28. *Strategy and costs of installing floating offshore wind farms, L.B. Savenije, ECN*
29. *Analysis of second order effects on a floating concrete structure for FOWT's, Prof. Climent Molins, Universitat Politecnica de Catalunya*
30. *Vibration-based identification of hydrodynamic loads and system parameters for offshore wind turbine support structures, D. Fallais, Delft University of Technology*
31. *Improved Simulation of Wave Loads on Offshore Structures in Integral Design Load Case Simulations, M.J. de Ruiter, Knowledge Centre WMC*
32. *Adaptation of Control Concepts for the Support Structure Load Mitigation of Offshore Wind Turbines, B. Shrestha, ForWind*
33. *Comparison of experiments and CFD simulations of a braceless concrete semi-submersible platform, L. Oggiano, IFE*
34. *Parametric Wave Excitation Model for Floating Wind Turbines, F.Lemmer, né Sandner, University of Stuttgart*
35. *On Fatigue Damage Assessment for Offshore Support Structures with tubular Joints B. Hammerstad, NTNU*
36. *Influence of Soil Parameters on Fatigue Lifetime for Offshore Wind Turbines with Monopile Support Structure, S. Schafhirt, NTNU*
37. *Mooring Line Dynamics Experiments and Computations. Effects on Floating Wind Turbine Fatigue Life and Extreme Loads, J. Azcona, CENER*
38. *Semisubmersible floater design for a 10MW wind turbine, J. Azcona, CENER*
39. *Sizing optimization of a jacket under many dynamic loads, A. Verbart, DTU Wind Energy*
40. *Rational upscaling of a semi-submersible floating platform, M. Leimeister, NTNU*
41. *Numerical and experimental investigation of breaking wave impact forces on a vertical cylinder in shallow waters, M.A. Chella, NTNU*
42. *Irregular Wave Forces on Circular Cylinders placed in Tandem, A. Aggarawal, NTNU*
43. *New design concepts of an upwind turbine rotor and their impact on wake characteristics, F. Mühle, NMBU*
44. *Wake modelling: the actuator disc concept in PHOENICS, N. Simisiroglou, WindSim AS*
45. *Wind farm control applications for Windscanner infrastructure, T.I. Reigstad, SINTEF Energi AS*
46. *Real-Time Hybrid Model Testing of a Floating Wind Turbine: Numerical validation of the setup, V. Chabaud, NTNU*
47. *Experimental Wind Turbine Wake Investigation towards Offshore Wind Farm Performance Validation, Y. Kim, LSTM, FAU*
48. *Validation of a Semi-Submersible Offshore Wind Platform through tank test, G. Aguirre, Tecnalia R&I*
49. *Field site experimental analysis of a 1:30 scaled model of a spar floating offshore wind turbine, M. Collu, Mediterranea University*

FINAL 15 JANUARY 2016

Thursday 21 January: 17.00 Poster Session with refreshments (cont.)

50. *A Review and Comparison of Floating Offshore Wind Turbine Model Experiments, G. Stewart, NTNU*
51. *Wind Model for Simulation of Thrust Variations on a Wind Turbine, E. Smilden, NTNU*
52. *Numerical simulations of the NREL S826 aerofoil performance characteristics – A CFD validation and simulation of 3D effects in wind tunnel testing, K. Sagmo, NTNU*
53. *A Single-Axis Hybrid Modelling System for Floating Wind Turbine Basin Testing, M. Hall, University of Maine*
54. *A design support multibody tool for assessing the dynamic capabilities of a wind tunnel 6DoF/HIL setup, M. Belloli, Politecnico di Milano*
55. *Assessment and evaluation of a wind turbine condition using a time-frequency signal processing method, P. McKeever, Offshore Renewable Energy Catapult*
56. *Development, Verification and Validation of 3DFloat; Aero-Servo-Hydro-Elastic Computations of Offshore Structures, T.A. Nygaard, IFE*
57. *Effect of upstream turbine tip speed variations on downstream turbine performance: a wind farm case optimization, J. Bartl, NTNU*
58. *Droplet Erosion Protection Coatings for Offshore Wind Turbine Blades, A. Brink, SINTEF M&C*
59. *Design of an airfoil insensitive to leading edge roughness, T. Bracchi, HIST*
60. *Socio-economic evaluation of floating substructures within LIFES 50+ project, M. de Prada, IREC*
61. *Coordinated control of DFIG-based offshore wind power plant connected to a single VSC-HVDC operated at variable frequency, M. de Prada , IREC*
62. *Implications of different regulatory approaches for offshore wind in Europe, L. Kitzing, DTU Management Engineering*
63. *Fiskarstrand Verft AS tooling up for renewable energy, Einar Kjerstad, Fiskerstrand Verft AS*
64. *LIFES50+: Innovative floating offshore wind energy .P.A.Berthelsen, Marintek*
65. *Aerodynamic modeling of offshore floating vertical axis wind turbines, Z. Cheng, NTNU*
66. *Scalability of floating Vertical Axis Wind Turbines, E. Andersen, UiS*
67. *Advanced Wind Energy Systems Operation and Maintenance Expertise, J. Melero, CIRCE*

Friday 22 January

	Parallel sessions	
	D) Operations & maintenance Chairs: Thomas Welte, SINTEF Energi AS Michael Durstewitz, Fraunhofer IWES	**F) Wind farm optimization** Chairs: Annette F. Stephansen, CMR Henrik Bredmose, DTU Wind Energy
09.00	Introduction by Chair	Introduction by Chair
09.05	A Risk Based Inspection Methodology for Offshore Wind Jacket Structures, M. Shafiee, Cranfield Univ	A parametric investigation into the effect of low induction rotor (LIR) wind turbines on the LCoE of a 1GW offshore wind farm in a North Sea wind climate, G. Scheepers, ECN Wind Energy
09.25	Effect of Tower-top Axial Acceleration on Monopile Offshore Wind Turbine Drivetrains, A.R. Nejad, NTNU	ProdBase: Theoretical power production in the time domain using Wind Farm Simulator, M.S. Grønsleth, Kjeller Vindteknikk
09.45	Safety Indicators for the Marine Operations in the Installation and Operating Phase of an Offshore Wind Farm, H. Seyr, NTNU	A continuously differentiable turbine layout optimization model for offshore wind farms, A. Klein, UiB
10.05	Probabilistic assessment of floating wind turbine access by catamaran vessel, M. Martini, Inst of Cantabria	Experimental testing of axial induction based control strategies for wind farm power optimization, J. Bartl, NTNU
10.25	Closing by Chair	Closing by Chair
10.30	Refreshments	
	Closing session – Strategic Outlook Chairs: John Olav Tande, SINTEF/NOWITECH and Trond Kvamsdal, NTNU/NOWITECH	
11.00	Introduction by Chair	
11.05	DeRisk project on extreme wave loads, H. Bredmose, DTU	
11.35	Type Validation for the SeaWatch Wind Lidar Buoy, V. Neshaug, Fugro OCEANOR	
12.05	Increasing wind farm profit through integrated condition monitoring and control, Berit Floor Lund, Kongsberg Renewables	
12.35	Poster award and closing	
13.00	Lunch	

Side event
08.30 – 17.00: IEA OC5 meeting

List of participants – EERA DeepWind'2016 Conference

Surname	First name	Institution
Adam	Frank	University Rostock
Aggarwal	Ankit	NTNU FAKULTET FOR INGENIØRVITENSKAP OG TEKNIKK
Aguirre	Goren	TECNALIA
Ágússson	Hálfdán	Kjeller Vindteknikk
Alagan Chella	Mayilvahanan	Norwegian university of Science and Technology
Anaya-Lara	Olimpo	Strathclyde University
Andersen	Elin	University of Stavanger
Andersen	Håkon	Dr. techn. Olav Olsen
Andersen	Søren	Technical University of Denmark
Argyriadis	Kimon	DNV GL
Attya	Ayman Bakry Taha	University of Strathclyde
Azcona	Jose	CENER
Bachynski	Erin E.	MARINTEK
Bakhoday Paskyabi	Mostafa	University of Bergen
Bardal	Lars Morten	NTNU
Barrera Sanchez	Carlos	FUNDACION INSTITUTO DE HIDRAULICA AMBIENTAL
Bartl	Jan	NTNU
Berthelsen	Petter Andreas	MARINTEK
Beržonskis	Arvydas	Aalborg University
Bolstad	Hans Christian	SINTEF Energi
Borg	Michael	DTU Wind Energy
Bozonnet	Pauline	IFPEN
Bracchi	Tania	NTNU
Bredmose	Henrik	DTU Wind Energy
Brink	Angelika	SINTEF
Brown	Stuart	FloWave Ocean energy Research Facility
Buhl	Thomas	DTU Wind Energy
Buils Urbano	Ricard	DNV GL – Energy Advisory
Busmann	Hans-Gerd	Fraunhofer IWES
Busturia	Jesús M.	NAUTILUS Floating Solutions, S.L.
Capaldo	Matteo	EDF R&D
Carrascosa	David	SAITEC, S.A.
Cecotti	Clio	NTNU
Chabaud	Valentin	NTNU
Cheng	Zhengshun	NTNU
Cheynet	Etienne	Universitetet i Stavanger
Chivaee	Hamid	DTU Wind Energy
Christakos	Konstantinos	Uni Research Polytec AS
Collu	Maurizio	Cranfield University
Colone	Lorenzo	Technical University of Denmark
Couñago	Bernardino	ESTEYCO SAP

De Prada Gil	Mikel	IREC-FUND.INST.RECERCA ENERGIA CATALUNYA
De Ruiter	Marten Jan	Knowledge Centre WMC
De Vaal	Jacobus	IFE
Domagalski	Piotr	Lodz University of Technology
Durstewitz	Michael	Fraunhofer IWES
Eecen	Peter	ECN
Eide	Anja	NTNU
Eikill	Rannveig Oftedal	University of Bergen
Eliassen	Lene	Ntnu/Statkraft
Endegnanew	Atsede	NTNU
Endrerud	Ole-Erik	Shoreline
Fallais	Dominik	TU Delft
Favre	Mathieu	IDEOL
Ferriday	Thomas	NTNU
Florian	Mihai	Aalborg University
Flügge	Martin	Christian Michelsen Research
Foussekis	Dimitrios	CRES
Fretheim	Harald	ABB AS
Frühmann	Richard	DEWI, UL International
Frøysa	Kristin Guldbrandsen	Christian Michelsen Research
Furevik	Birgitte	Norwegian Meteorological Institute
Galinos	Christos	DTU-Technical University of Denmark
Gao	Zhen	NTNU
Gintautas	Tomas	Aalborg University
Gonzalez-Pinto	Luis	SAITEC, S.A.
Gravdahl	Arne R.	WindSim AS
Grimwade	Jamie	FloWave Ocean Energy Research Facility
Grønsleth	Martin	Kjeller Vindteknikk
Guachamin Acero	Wilson	NTNU
Guanche Garcia	Raul	FUNDACION INSTITUTO DE HIDRAULICA AMBIENTAL DE CANTABRIA
Gueydon	Sebastien	MARIN
Hall	Matthew	University of Maine
Hammerstad	Benedicte Hexeberg	Norwegian University of Science and Technology (NTNU)
Hanssen	Jan Erik	W2Power
Hanssen-Bauer	Øyvind W.	NTNU
Horn	Jan-Tore H.	AMOS/NTNU
Hussain	Azeem	Universitetet i Tromsø
Jakobsen	Jasna	University of Stavanger
Jonkman	Jason	National Wind Technology Center
Jost	Eva	Institute of Aerodynamics and Gas Dynamics, University of Stuttgart
Kim	You-Jin	LSTM, Friedrich-Alexander-Universität Erlangen-Nürnberg
Kjerstad	Einar	Fiskerstrand Verft AS
Klein	Arne	Institutt for informatikk, Universitetet i Bergen

Knutsen	Anna N.	NTNU
Koizumi	Kazuhiro	Globalfoundries
Kringelum	Jon	DONG Energy Wind Power
Krokstad	Jørgen	Statkraft
Kumer	Valerie-Marie	University of Bergen
Kvamsdal	Trond	NTNU
Kvittem	Marit Irene	DNV GL
Lacas	Pierre Paul	STX France Solutions
Lamkowska	Karolina	Lodz University of Technology
Landbø	Trond	Dr.techn:olav Olsen AS
Leble	Vladimir	University of Glasgow
Leimeister	Mareike	NTNU
Lemmer	Frank	University of Stuttgart (SWE)
Lund	Berit Floor	Kongsberg Maritime AS
Løken	Trygve	NTNU
Malmo	Oddbjørn	Kongsberg Maritime AS
Martini	Michele	IH Cantabria
Matha	Denis	Ramboll
Mayorga	Pedro	EnerOcean SL
McKeever	Paul	ORE Catapult
Meere	Ronan	University College Dublin
Merz	Karl	SINTEF Energi
Mo	Olve	SINTEF Energi
Mochet	Clement	LE BEON MANUFACTURING
Molins	Climent	Universitat Politècnica de Catalunya (UPC)
Mork	Bruce	MTU
Muskulus	Michael	NTNU
Mühle	Franz V.	NTNU
Müller	Kolja	University of Stuttgart
Myhr	Anders	Dr.tech. Olav Olsen
Mælan	Jostein	StormGeo
Mørch	Hans Jørgen	CFD marine AS
Nejad	Amir	NTNU
Ng	Chong	ORE Catapult
Nygaard	Tor Anders	Institute for Energy Technology
Oggiano	Luca	IFE
Oh	Sho	ClassNK
Ormberg	Harald	MARINTEK
Page	Ana	NTNU
Paillard	Benoit	ACE
Pegalajar Jurado	Antonio M.	DTU Wind Energy
Peppas	Antonios	FLOATMAST LTD
Perez	German	TECNALIA
Piel	Jan-Hendrik	Leibniz Universität Hannover

Pierella	Fabio	IFE
Preede Revheim	Pål	Nasjonalt Vindenergisenter Smøla AS
Qvist	Jacob	4Subsea
Reigstad	Tor Inge	SINTEF Energi As
Reuder	Joachim	University of Bergen
Rikheim	Harald	Norges Forskningsråd
Rise Gallala	Marius	NTNU
Robertson	Amy	National Renewable Energy Laboratory
Ross	William	University of Strathclyde
Ruddy	Jonathan	University College Dublin
Sagmo	Kristian	NTNU
Sakamuri	Jayachandra Naidu	Department of Wind Energy, Technical University of Denmark
Sandal	Kasper	DTU Wind Energy
Schafhirt	Sebastian	Norwegian University of Science and Technology (NTNU)
Schepers	Gerard	ECN Wind Energy
Seyr	Helene	NTNU
Shafiee	Mahmood	Cranfield University
Shin	Hyunkyoung	University of Ulsan
Shrestha	Binita	ForWind Oldenburg
Simisiroglou	Nikolaos	WindSim/Uppsala University
Smilden	Emil	NTNU
Soede	Matthijs	European Commission
Sperstad	Iver Bakken	SINTEF Energi AS
Spiga	Andrea	NTNU
Steen	Knut Erik	Statoil
Stephansen	Annette	Christian Michelsen Research
Stewart	Gordon	NTNU
Stenbro	Roy	IFE
Stokke	Marit	NTNU
Stålhane	Magnus	NTNU
Suja-Thauvin	Loup	Statkraft
Svean	Magnus	NTNU
Sætran	Lars Roar	NTNU
Sørlie	John Are	NTNU
Tande	John Olav	SINTEF Energi AS
Thomassen	Paul	Simis AS
Torres-Olguin	Raymundo	NTNU
Totsuka	Yoshitaka	Wind Energy Institute of Tokyo Inc.
Van Der Mijle Meijer	Harald	TNO
Van Roermund	Martijn	ECN
Van Wingerde	Arno	University of Glasgow
Vatne	Sigrid	MARINTEK
Verbart	Alexander	Technical University of Denmark (DTU)
Vrana	Til Kristian	SINTEF Energi

Ward	Dawn	Cranfield University
Welte	Thomas	SINTEF Energy Research
Wolken-Möhlmann	Gerrit	Fraunhofer IWES
Zasso	Alberto	Politecnico di Milano
Ziegler	Lisa	Ramboll
Zwick	Daniel	Fedem Technology AS
Økland	Ole David	MARINTEK

SINTEF

3 Scientific Committee and Conference Chairs

An international Scientific Committee is established with participants from leading institutes and universities. These include:

Anaya-Lara, Olimpo, Strathclyde
Durstewitz, Michael, Fraunhofer IWES
Eecen, Peter, ECN
Furevik, Birgitte, R., MET
Jørgensen, Hans Ejsing, DTU
Kumer, Valerie, University of Bergen
Krogstad, Jørgen, Statkraft
Kvamsdal, Trond, NTNU
Leithead, William, Strathclyde
Lekou, Denja, CRES
Madsen, Peter Hauge, DTU
Merz, Karl, SINTEF Energi AS
Moan, Torgeir, NTNU
Muskulus, Michael, NTNU
Nielsen, Finn Gunnar, Statoil/UiB
Nygaard, Tor Anders, IFE
Reuder, Joachim, UiB
Robertson, Amy, NREL
Rohrig, Kurt, Fraunhofer IWES
Sempreviva, Anna Maria, CNR
Stephansen, Annette, CMR
Tande, John Olav, SINTEF Energi AS / NOWITECH
Uhlen Kjetil, NTNU
Van Bussel, Gerard, TU Delft
Welte, Thomas, SINTEF Energi AS
Økland, Ole David, MARINTEK

The Scientific Committee will review submissions and prepare the programme. Selection criteria are relevance, quality and originality.

The conference chairs were:

- John Olav Giæver Tande, Director NOWITECH, Chief scientist, SINTEF Energi AS
- Trond Kvamsdal, Chair NOWITECH Scientific Committee, Professor NTNU
- Michael Muskulus, vice-chair NOWITECH Scientific Committee, Professor NTNU

Opening session – Frontiers of Science and Technology

Initiative for Global Leadership in Offshore Wind, Matthijs Soede, Research Programme Officer, European Commission

Innovations in offshore wind energy, John Olav Tande, director NOWITECH

Cooperation as a key to cost reductions for offshore wind, Kristin Guldbrandsen Frøysa, director NORCOWE

Hywind Scotland, Knut Erik Steen, Technical Manager, Statoil

EERA research programme on wind energy and the offshore challenges, Thomas Buhl, DTU


European Commission
HORIZON 2020
Initiative for Global Leadership in Offshore Wind
Disclaimer © European Union, 2016
The content of this presentation may not reflect the official legal opinion of the European Union. The European Commission does not accept responsibility for any use made of the information contained therein.
Matthijs SOEDE
Research Programme Officer
Unit G3 Renewable Energy Sources
DG Research and Innovation
Research and Innovation

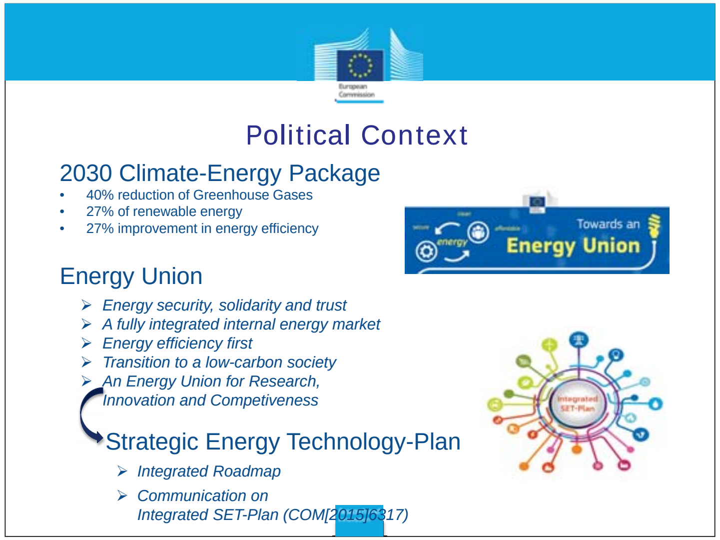
Political Context
2030 Climate-Energy Package
40% reduction of Greenhouse Gases
27% of renewable energy
27% improvement in energy efficiency
Towards an Energy Union
Energy Union
Energy security, solidarity and trust
A fully integrated internal energy market
Energy efficiency first
Transition to a low-carbon society
An Energy Union for Research, Innovation and Competiveness
Strategic Energy Technology-Plan
Integrated Roadmap
Communication on Integrated SET-Plan (COM[2015]6317)
Integrated SET-Plan

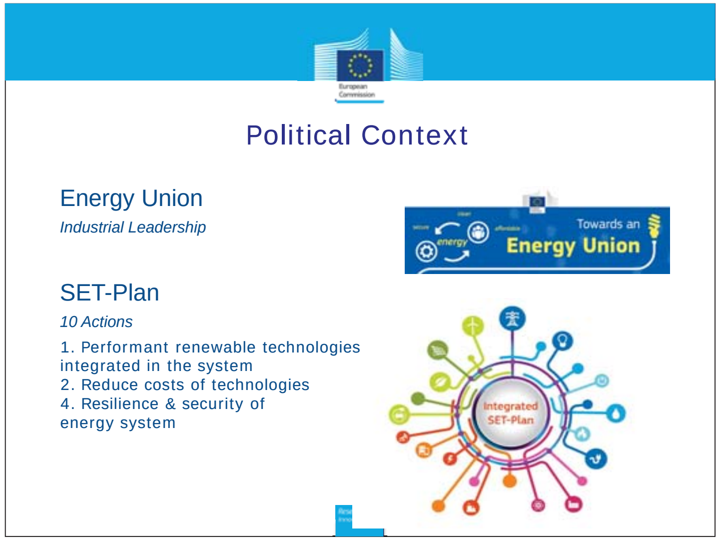
Political Context
Energy Union
Industrial Leadership
Towards an Energy Union
SET-Plan
10 Actions
1. Performant renewable technologies integrated in the system
2. Reduce costs of technologies
4. Resilience & security of energy system
Integrated SET-Plan

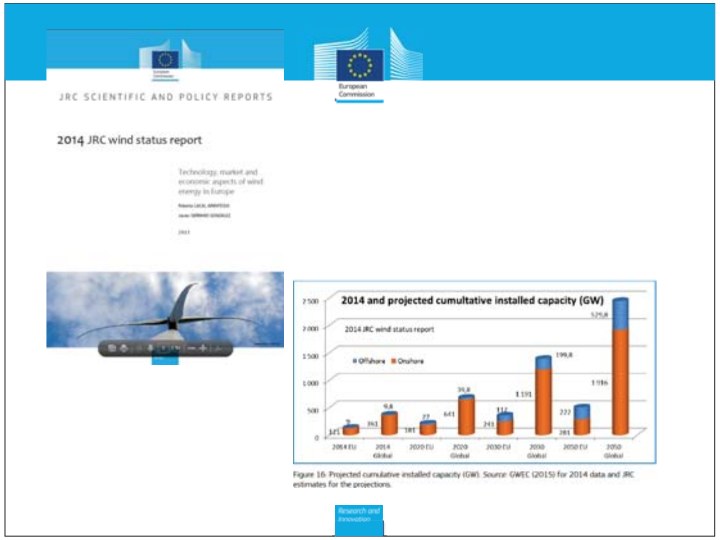
JRC SCIENTIFIC AND POLICY REPORTS
2014 JRC wind status report
2014 and projected cumultative installed capacity (GW)
Offshore
Onshore
Figure 16: Projected cumulative installed capacity (GW). Source: GWEC (2015) for 2014 data and JRC estimates for the projections.
Research and Innovation


JRC SCIENTIFIC AND POLICY REPORTS
2014 JRC wind status report
"The main driver for developing wind technology further is to minimise the cost of energy (CoE) production, for which efforts focus on minimising capital and operation and maintenance costs and maximising reliability and energy production."
https://setis.ec.europa.eu/sites/default/files/reports/2014JRCwindstatusreport.pdf
Research and Innovation


Integrated SET-plan actions
Strategic Targets in the context of an Initiative for Global Leadership in Offshore Wind
Two key issues need to be tackled:
1) Offshore wind costs must be reduced through, but not only, increased performance and reliability in order to meet its full potential contribution to the European energy mix.
2 - There is a need to develop (floating) substructures or integrated floating wind energy systems for deeper waters and wind energy systems for use in other marine climatic conditions, to increase the deployment possibilities and to improve the European position in the global market.
Research and Innovation

Agreed strategic targets for offshore wind energy

1) Reduce the levelised cost of energy (LCoE) *at final investment decision (FID) for fixed offshore wind* by improvement of the performances of the entire value chain to*

- **less than 10 ct€/kWh by 2020 and to**
- **less than 7ct€/kWh by 2030;**

** the costs for delivering the electricity to onshore substations are taken into account within the LCoE*

Agreed strategic targets for offshore wind energy

2) *Develop cost competitive* ***integrated wind energy systems*** *including substructures which can be used in* ***deeper waters (>50m) at a maximum distance of 50 km from shore with a LCoE* of***

- **less than 12 ct€/kWh by 2025 and to**
- **less than 9 ct€/kWh by 2030**

** the costs for delivering the electricity to onshore substations are taken into account within the LCoE*

How?

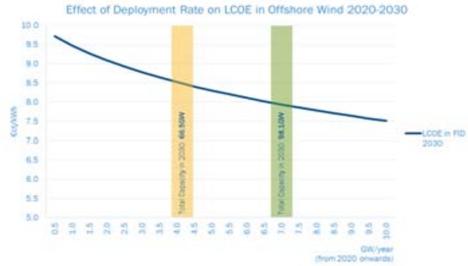

How?

- ***Production value chain performance/cost competitiveness:***

Larger and lighter turbines (>10 MW while maintaining top-head mass below 50t/MW); more reliable turbines (materials and components of better quality; condition monitoring and control strategies); lower-cost, fast deployment installations, including foundations, and improved cable laying and protection methods; development of lower cost interconnection systems. Substructures or integrated wind energy systems for water depths beyond 50m and possibly in other climates conditions for instance for offshore wind farms in the Baltic Sea and Mediterranean.

- ***Production value chain***

Standardisation; better infrastructure for large scale deployment including appropriate and sufficient test and validation centers, effective methods for repowering and recycling, lighter, stronger and cheaper materials; new control and power electronics.

Better system integration

- *Grid development (enhancing system security, grid integration) and reliability of the grid at very high levels of wind power penetration, up to 70% of the electricity demand, and accuracy of wind power forecasting. .*

How?

- ***Wind conditions***

Efficiency and accuracy of wind design conditions, siting, resource assessment and forecasting. An uncertainty of less than 3% in the forecasting is expected by 2030.

- ***Non technological aspects***

A coordinated, continuous pipeline of offshore wind projects until 2030 enabling a continuous learning curve and cost reduction. New market designs and optimal business models for a power system with high shares of non-dispatchable renewables generation, improved financing conditions for wind energy projects especially reducing the cost of capital for offshore wind. Knowledge exchange (sharing best practice, seeking common solutions and standards, seeking common ground for economically viable investments)

- ***Environmental and societal issues***

Knowledge on potential impacts of wind energy on the environment and cost-effective solutions to minimise it, increase social acceptance and support for wind energy.

European Technology and Innovation Platform on Wind (ETIP Wind)

Industry and Research organisations working together

- Research, Innovation & Technology Industry Leaders group
- Working group Research and Innovation
- EERA JP Wind

- Developing Action plan to deliver on the targets
- Contributing to the implementation of this plan: private investments, research strategy, joint projects, ...

HORIZON 2020

How H2020 can contribute to value creation and cost reductions of offshore wind energy

More information:
www.ec.europa/research/horizon2020

Horizon 2020 – Overall Objectives

HORIZON 2020

- Responding to the economic crisis by investing in future jobs and growth
- Strengthening the EU's global position in research, innovation and technology
- Addressing people's concerns about their livelihoods, safety and environment
- Contributing to sustainable development (at least 35% of the overall budget)
- Supporting EU policies (e.g. Europe 2020 / Energy Union)

Systemic approach of the Energy Challenge 'Secure, clean and efficient Energy'

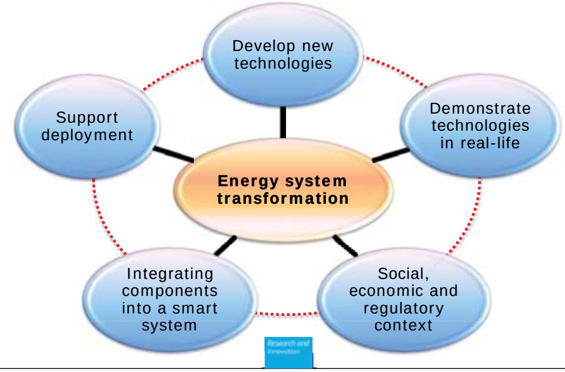

The 2016-2017 calls of the Energy Challenge

Energy Efficiency (EE)
- Heating and Cooling
- Engaging consumers
- Buildings
- Industry, services and Products
- Innovative financing

Competitive low-carbon energy Technologies (LCE)
- Energy system (grids, storage)
- Renewable energies
- Decarbonising fossil fuels
- Socio-economic research
- European Research Area in energy

Smart Cities and Communities (SCC)
- Light-house demonstration projects

SME instrument (SIE)

Call budgets (in Mio €)

Call	2016	2017
EE	93	101
LCE	352,66	367,62
SCC	60	71,50
SME	46	50

Strategy for research and demonstration projects in the area of wind energy

- Main focus on offshore wind energy where major cost reductions are needed
- Focus on increased performance of wind energy technologies and to increase deployment possibilities

Expected impacts

- Increased performance, reliability and lifetime of wind energy systems making it fully competitive, through a better design of wind turbines and having an impact on the turbine efficiency and therefore on the cost of energy produced

SC3 LCE – selection of topics

Towards an integrated EU energy system

LCE-1-2016-2017: Next generation innovative technologies enabling smart grids, storage and energy system integration with increasing share of renewables: distribution network

LCE-2-2016: Demonstration of smart grid, storage and system integration technologies with increasing share of renewables: distribution system

LCE-3-2016: Support to R&I strategy for smart grid and storage

LCE-4-2017: Demonstration of smart transmission grid, storage and system integration technologies with increasing share of renewables

LCE-5-2017: Tools and technologies for coordination and integration of the European energy system

SC3 LCE – selection of topics

Developing the next generation of renewable energy technologies

LCE-6-2017: New knowledge and technologies

LCE-7-2016-2017: Developing the next generation technologies of renewable electricity and heating/cooling

Demonstrating innovative renewable energy technologies

LCE-13-2016: Solutions for reduced maintenance, increased reliability and extended life-time of wind turbines/farms

LCE-14-2017: Demonstration of large >10MW wind turbine

LCE06 – New knowledge and technologies

- 2017 – Wind energy: *Improved understanding of the physics of wind as a primary resource and wind energy technology*

-Will improve the simulation capability for multi-scale wind flows, loads and materials failure
-Significant high-performance computing (HPC) resources needed
-Results can contribute to IEA tasks and international cooperation with leading groups outside Europe is encouraged.
-Further research after the project is expected and, therefore data should be with open access

LCE07 – Next generation of technologies

- 2016 – Wind energy: *Advanced control of large scale wind turbines and farms*
  - Current progress in wind energy like larger wind turbines and farms, floating offshore wind, but also specific geographical challenges, require the development of advanced control strategies. Overall challenge is to design an integrated approach to advanced operation of a wind turbine and/or farm.
- 2017 – Wind energy: *Reduction of environmental impact of wind energy*
  - Develop potential mitigating strategies or alternative solutions and to increase public acceptance of wind energy
  - Increased scientific understanding of the social and environmental impact of wind turbines and (clusters of) wind farms both on and off-shore (including floating)
  - Cooperation with NGOs and civil society groups is essential for further investigation of the roots of resistive behaviour as engaging and involving concerned communities can facilitate addressing this specific challenge.

2016 – LCE13 – Solutions for reduced maintenance, increased reliability and extended life-time of offshore wind turbines/farms

Specific Challenge: The challenge is to achieve a very substantial reduction in Operation and Maintenance (O&M) costs through new O&M and control concepts, including logistics planning, decision making and operation

Scope: The focus is to reduce the need for maintenance of wind turbines/farms and to develop measures for life-time extension, demonstrating innovative solutions and tools, and thereby the levelised cost of wind energy.
The actions should consider not only the wind turbines but also the substructure and the soil conditions.
Participation of wind turbine manufacturers and large wind farm operators is expected.
Demonstration project: TRL 7 should be achieved,
Expected EC contribution 7-10 M€

2017 – LCE14 – Demonstration of large >10MW wind turbine

Specific Challenge: To demonstrate and construct a full scale >10MW turbine and provide proof of a significant cost reduction potential.

Scope: The development of large scale (>10MW) turbines will have intrinsically logistical requirements regarding handling, installation, operation and maintenance. Improved handling (storage, loading, transport, etc.) on land, in the harbours and/or at sea, as well as improved logistics around operations and maintenance have to be taken into account in this innovation action.

Demonstration project: TRL 7 should be achieved,
Expected EC contribution 20-25 M€

LCE-21-2017: Market uptake of renewable energy technologies

- ***Wind energy**: One of the following specific sub-challenges need to be addressed:*
  - i) Develop spatial planning methodologies and tools for new onshore wind and repowering of old wind farms taking into account environmental and social impacts but also the adoption of the latest developments in wind energy technology;
  - ii) Identify the bottlenecks for further deployment in Europe and the regulations which limit the adoption of technological innovation and their deployment possibilities;
  - iii) Increase the social acceptance and support for wind energy in 'wind energy scarce regions' using, with solid involvement of social sciences and humanities and local communities and civil society to understand best practices and to increase knowledge about social and environmental impact of wind energy.

Fast-track to Innovation Pilot

- Innovation from the demonstration stage through to market uptake (starting as of TRL 6)
- Completely bottom-up – covers all areas addressed by H2020
- Small consortia with strong participation from industry
- Business plans mandatory
- 3 submission deadlines in 2016 (15/3, 1/6, 25/10/2016)
- Budget 100 M€ (no earmarking for areas)

The SME Instrument

- Seamless business innovation support
- Completely bottom-up – all areas of the Energy Challenge covered
- Only open to SMEs – also single-beneficiaries possible

3 phases of support (no need to start with phase 1)

1. **Business innovation grants** (feasibility studies, lump sum of EUR 50,000 per project);
2. **Business innovation grants for innovation development & demonstration purposes** (between EUR 0.5 – 2.5 million / project)
3. **Free-of-charge business coaching,** access to a wide range of innovation support services and facilitated access to risk finance to facilitate the commercial exploitation of the innovation.

- ✓ 4 submission deadlines per year for phase 1 and 2
- ✓ Budget for the Energy SME topic (SMEInst-09-2016-2017):
  - ✓ **46 M€ in 2016**
  - ✓ **50 M€ in 2017**

Energy outside the Energy Challenge

Cross-thematic priorities
- Materials, Key Enabling Technologies
- ICT
- Energy-efficiency in buildings/industry
- Biomass production
- Energy in transport
- Socio-economics
- Access to risk finance
- Research Infrastructures

Bottom-up activities
- European Research Council (ERC)
- Marie Skłodowska-Curie actions
- Future and Emerging Technologies (FET)
- Fast-track to Innovation

Implementation
- European Commission/ Executive Agencies
- Public-Private Partnerships
- Joint Technology Initiatives (JTI)
- EIT – KIC InnoEnergy
- European Investment Bank

Risk finance for demonstration projects

InnovFin Energy Demo Projects Pilot Facility (EDP)
(Other Action#28)

- First-of-a kind commercial-scale industrial demonstration projects (TRL 7-8) for unproven pre-commercial technologies in the field of innovative **renewable energy**, **fuel cells and hydrogen** in support of the SET-Plan
- Loan amount: min EUR 7.5 M€, max EUR 75 M€
- Loan maturity: max 15 years

InnovFin Energy Demo Projects

Application & inquiries: directly with the EIB - New Products & Special Transactions, EIB, Luxembourg
Tel: +352 4379 85002, E-mail: innovfinFDP@eib.org
http://www.eib.org/products/blending/innovfin/products/index.htm

Results first 2 years

FP7 projects

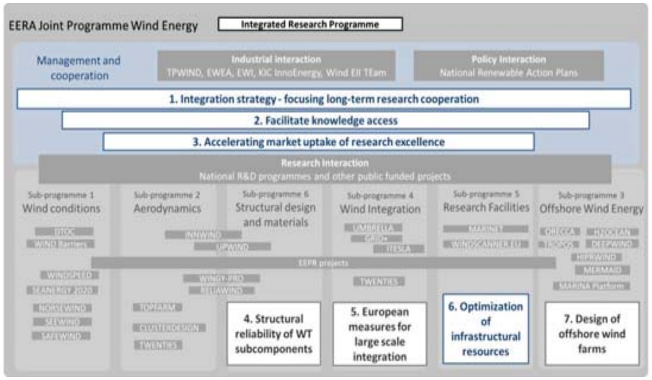

Figure 7- Rationale behind IRPWIND: Identification of gaps within the framework of EERA JP Wind

H2020 – projects

- *Wind turbine*
  - Ecoswing – Energy Cost Optimization using Superconducting Wind Generators - World's First Demonstration of a 3.6 MW Low-Cost Lightweight DD Superconducting Generator on a Wind Turbine (<TRL7, IA, 10.591.734 €, 1/3/2015 – 28/2/2019, Envision Energy (DK))

H2020 – projects

- *Substructures*
  - TELWIND – Integrated telescopic tower and evolved spar floating substructure for low-cost deep offshore wind and next generation of 10MW+ turbines (<TRL5, RIA, 3.498.530 €, 30 months, 1/12/2015 – 31/5/2018, ESTEYCO SAP)
  - LIFES50+ - Qualification of innovative floating substructures for 10 MW wind turbines and water depths greater than 50 m (<TRL5, RIA, 7.274.838 €, 40 months, 1/6/2015 – 30/9/2018, Marintek (NO))
  - ELISA/ELICAN – Self-bouyant precast concrete foundation for the craneless installation of complete offshore wind turbines: full scale offshore protype (SME -2, IA , 13.679.850 €, 24 months, 1/6/2015 – 31/5/2017, ESTEYCO SAP)
  - DEMOGRAVI3, innovative gravity based foundation for offshore wind turbines (TRL7, IA, 19.243.042 €, 48 months, 1/1/2016 – 31/12/2019, EDP (PT))

H2020 – projects

- *Cost reduction in offshore wind*
  - DEMOWIND (Eranet Cofund, IA, 10.000.000 €, 60 months, 1/1/2015 – 31/12/2019, DECC (UK)) combined with national funding of UK, DK, NL, ES, PT and BE total: 31.000.000 €
  - DEMOWIND 2 (Eranet Cofund, IA, 8.300.000 €, 60 months, 1/1/2016 – 31/12/2020, DECC (UK)) combined with national funding of UK, DK, NL, ES, BE and NO total: 25.000.000 €

H2020 – projects

- *Small wind*
  - Briareo – Implementation of a vertical axis micro-wind turbine capable of working at high efficiency even at a low wind speed (SME-1, 50.000 € funding, 6 months, 2015, Arken SPA)
  - IRWES Integrated Roof Wind Energy System (SME-2, 1.696.381 € funding, 24 months, 2015 – 2017, IBIS Power BV)
  - Omniflow – Next-generation hybrid wind and solar power technology (SME-1, 50.000 €, 6 months, 2015, Omniflow SA (PT))

H2020 – projects

- *Airborne Wind*
  - AMPYXAP3 – Commercial introduction of the first Airborne Wind Energy system: renewable eneryg at costs below fully depreciated coal fired power plants (SME-2, 2.500.000€ funding, 23 months, 2015, Ampyx Power BV)
  - REACH – Resource Efficient Automatic Conversion of High Altitude Wind (FTIPilot -1, 2.675.132€ funding, 36 months, 2015, ENEVATE BV) Kite Power

H2020 – projects

- *Education and training*
  - ICONN – European Industrial DoCtorate on Offshore WiNd and Wave ENergy (MSCA-ITN-EID, 845.838 €, 48 months, 2015 – 2019, Trinity College Dublin)
  - AWESOME – Advanced Wind Energy Systems Operation and Maintenance Expertise (MSCA-ITN-ETN, 2.862.074 €, 48 months, 2015 – 2019, CIRCE (ES))
  - AWESCO – Airborne Wind Energy System Modelling, Control and optimisation (MSCA-ITN-ETN, 2.999.015 €, 48 months, 01/01/2015 – 31/12/2018, TU Delft (NL))
  - SPARCARB – Lightning protection of wind turbine blades with carbon fibre composite materials (MSCA-ITN-ETN, 1.093.151 €, 48 months, 01/01/2015 – 31/12/2018, GLPS (DK) and Univ Southampton (UK))
  - AEOLUS4FUTURE – Efficient harvesting of the wind energy (MSCA-ITN-ETN, 3.811.805 €, 48 months, 01/01/2015 – 31/12/2018, LULEA Tekniske Univ (S))

H2020 – projects

- *Varia*
  - HPC4E – HPC for Energy (LEIT, RIA, 1.998.176 €, 24 months, 1/1/2016 – 31/12/2017, Barcelona supercomputing centre)
  - Opti-LPS – Optimal Lightning Protection System (SME-1, 50.000 €, 6 months, 2015, GLPS AS (Dk))
  - MEWi-B – More efficient Wind Blades (SME-1, 50.000 €, 6 months, 2015, ETA Srl (IT))
  - FLOATMAST – An Innovative Wind Resource Assessment Tension Leg Platform for combined Anemometer and Lidar reliable and bankable wind measurements for offshore wind parks (SME-1, 50.000 €, 6 months, 2015, ETME Streamlined (EL))
  - SEAMETEC – Smart Efficient Affordable Marine Energy Technology Exploitation using Composites (SME-1, 50.000 €, 6 months, 2015, Eirecompoisites Teoranta (IE))

H2020 – projects

- *Varia*
  - I-WSN – Intelligent Wireless Sensor Networks for Asset Integrity Monitoring (SME-1, 50.000 €, 6 months, 2015, Inertia Technology BV (NL))
  - EeC WITUR – Efficient energy cleaning robotic platform for wind turbines (SME-1, 50.000 €, 6 months, 2014, Tratamiento Superficial Robotizado SL (ES))
  - CLOUD DIAGNOSIS – Providing Predictive Maintenance for Wind Turbines Over Cloud (SME-1, 50.000 €, 6 months, 2014, ITESTIT (ES))
  - AIRCRANE – New Building methodology for improved full-concrete wind towers for wind turbines (SME-1, 50.000 €, 6 months, 2014, Structural Research S.L. (ES))
  - Aeropaft – Delay of flow separation and stall on Aerofoils using a passive flow control technology which will improve aerodynamic performance and stabilty of wind turbines increasing their range of operation (SME-1, 50.000 €, 6 months, 2014, Jarilo Limited (UK))

TOP INNOVATIONS *Northern Europe remains the hotbed for wind power's pioneering technology*

Make/Model	Description	Noteworthy	Status
Fraunhofer IWES Dynalab (Germany)	Industry's most advanced drivetrain and nacelle test rig	Incorporates the world's biggest and most advanced grid simulator; focused on full system tests rather than highly accelerated life testing (HALT)	Operational since autumn 2014
Vestas LDST (large diameter steel tower) (Denmark)	Patented lighweight wide-based tubular steel tower for high hub heights	Bottom sections are manufactured in tapering circles, then sliced into 120-degree segments. The sections can be transported by flatbed trucks and the parts, which fit together precisely, re-assembled on site	More than 80 turbines mounted on LDST are now in operation
Max Bögl wind turbine tower and energy storage solution (Germany)	High tower with incorporated power storage	Pumped storage device comprises a water basin with a hollow 40-metre structure with varying water column level; provides the basis for tower mounting; hub height of 178 metres	Prototype under construction
Seatower Cranefree Gravity Foundation (Norway)	Offshore gravity base foundation	Self-installing hollow-concrete foundation base; floating structure that is towed to its location; installation implemented by filling concrete part with water and, in final step, replacing with sand	One unit now installed at French Fécamp offshore development
Lagerwey L136 turbine (Netherlands)	3.6/4.0MW turbine for IEC Class IIA	Compact direct-drive turbine design with 225-tonne head mass; features innovative simplified inner-rotor generator with traditional stator housing and 100% passive air cooling	Design under construction; first commercial deliveries expected in second half of 2017

Thank you for your attention!

More information:
www.ec.europa/research/horizon2020

NOWITECH
Innovations in offshore wind energy

January 2016

www.nowitech.no

John Olav Giæver Tande
Director NOWITECH
Senior Scientist / Research Manager
SINTEF Energy Research
John.tande@sintef.no

NOWITECH in brief

- **A joint pre-competitive research effort**
- **Focus on deep offshore wind technology (+30 m)**
- **Budget (2009-2017) EUR 40 millions**
- **Co-financed by the Research Council of Norway, industry and research partners**
- **25 PhD/post doc grants**
- **Key target: innovations reducing cost of energy from offshore wind**
- **Vision:**
  - **large scale deployment**
  - **internationally leading**

Research partners:
- SINTEF Energy (host)
- IFE
- NTNU
- MARINTEK
- SINTEF ICT
- SINTEF MC

Industry partners:
- CD-adapco
- DNV GL
- DONG Energy
- Fedem Technology
- Fugro OCEANOR
- Kongsberg Maritime
- Norsk Automatisering
- Statkraft
- Statoil

Associated research partners:
- DTU Wind Energy
- Michigan Tech Uni.
- MIT
- NREL
- Fraunhofer IWES
- Uni. Strathclyde
- TU Delft
- Nanyang TU

Associated industry partners:
- Devold AMT AS
- Energy Norway
- Enova
- Innovation Norway
- NCEI
- NORWEA
- NVE
- Wind Cluster Norway

NOWITECH is in very good progress

- Strong consortium with leading industry and research partners
- Progress according to plan delivering successful innovations, excellent research and a strong educational programme

Successful innovations

Excellence in research

Strong educational program

European Wind Energy Technology Platform

Offshore wind main challenge: Reduce Cost of Energy

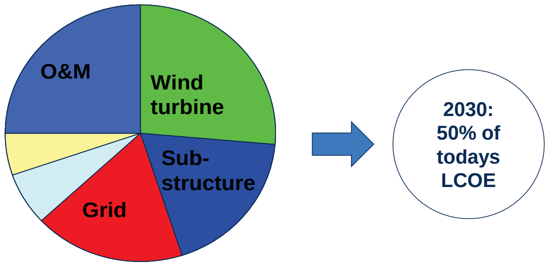

EU TP wind KPI in new SRA:
Reduce LCOE by 50% from present levels for similar sites by 2030

SET-plan initiative: Global Leadership in Offshore Wind

- ✓ **Offshore wind costs must be reduced** and performance and reliability increased to meet its full contribution to the European energy mix.
- ✓ There is a need to **develop (floating) substructures or integrated floating wind energy systems for deeper waters** and for use in other climate conditions, to increase the deployment possibilities and to improve the European position in the global market.

Working document of the EC for consultation (SET Plan Secretariat – 09 October 2015):

Proposed targets in offshore wind energy

1. **Reduce the levelised cost of energy (LCoE)** for fixed offshore wind* by improvement of the performances of the entire value chain to
   - **less than 10 ct€/kWh by 2020** and to
   - **less than 7ct€/kWh by 2030;**
2. **Increase the reliability of offshore wind turbines to 99% and the capacity factor to 55% by 2020;**
3. Develop cost competitive **integrated wind energy systems** including substructures which can be used in **deeper waters (>50m)** at any distance from shore and for use in different climate conditions with LCoE of:
   - **less than 14 ct€/KWh by 2020** and to
   - **less than 9 ct€/KWh by 2030**

DRAFT

*within the LCoE, the costs for delivering the electricity to onshore substations are taken into account

From R&I to cost reductions

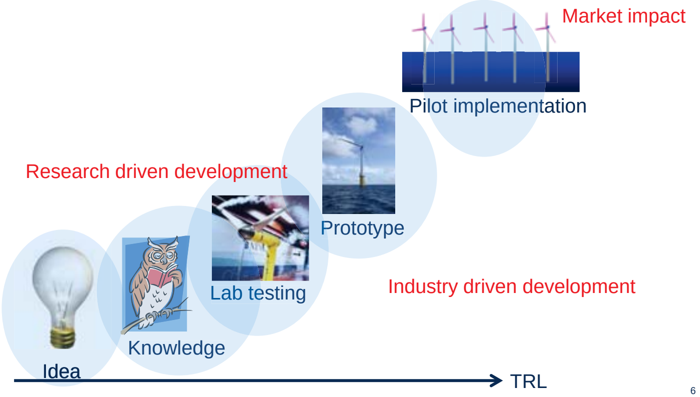

Hywind – Statoil is taking the next step

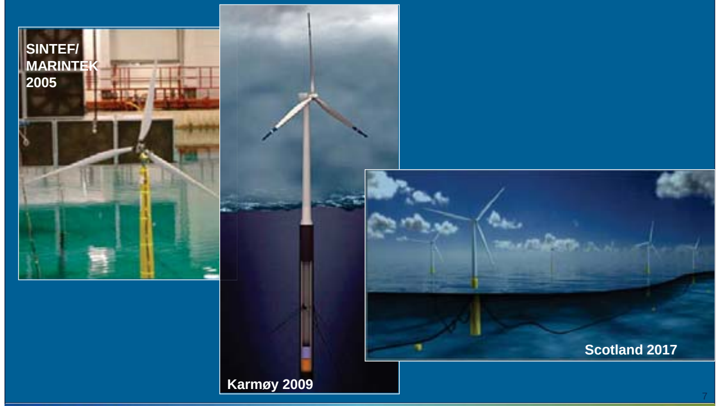

NOWITECH results provide cost reductions

- ✓ A total of 40 results are assigned a Technology Readiness Level (TRL)
- ✓ The results include new methods, software tools and hardware products
- ✓ The results are migrating to commercial use, licence agreements, and business developments providing value creation and cost reductions.

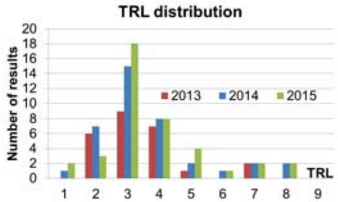

An attractive partner on the international scene

- ▶ Active in EERA, TPwind, EAWE, IEA, IEC
- ▶ Heading offshore works within EERA JPwind and TPwind
- ▶ Partner in EU projects, e.g.: Twenties (2009-), DeepWind (2010-), HiPRWind (2010-), EERA-DTOC (2012-), InnWind (2012-), WindScanner (2012-), LeanWind (2014-), EERA IRP wind (2014-), BestPaths (2014-) , Lifes50+ (2015-), AWESOME (2015-)

LIFES50+ | Best Paths | EERA European Energy Research Alliance WIND ENERGY

Thermally sprayed silicon carbide coating

- ✓ Patented process result of NOWITECH PhD work.
- ✓ Being developed as a commercial product through the new spinout company Seram Coatings AS.
- ✓ The process provides for an extremely hard, wear-resistant, low friction ceramic coating that can be applied to rotating machinery like main bearings in large direct drive wind turbines; ultimately increasing lifetime and reducing cost for maintenance.

Remote presence

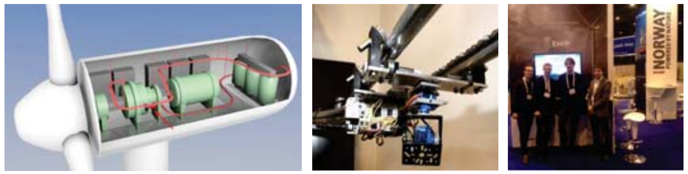

- ✓ Technology developed in part through NOWITECH PhD work
- ✓ Remote presence through a small robot on a track in the nacelle equipped with camera / heat sensitive, various probes, microphone etc. reducing offshore work by service personnel, downtime and costs
- ✓ Technology is commercialized by Norsk Automatisering AS through the new company EMIP

Savings costs with knowledge, models and labs

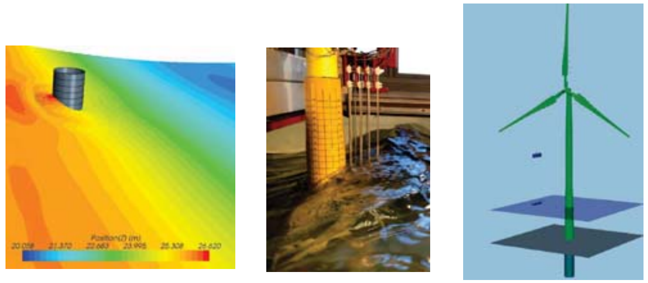

De-risking monopole for Dudgeon 402 MW Offshore Wind Farm
MARINTEK using CFD, lab experiments and FE SIMA analysis

SEAWATCH Wind Lidar Buoy

- Cost efficient and flexible compared to offshore met mast
- Measure wind profiles (300 m), wave height and direction, ocean current profiles, met-ocean parameters
- Result of NOWITECH "spin-off" joint industry project by Fugro OCEANOR with Norwegian universities, research institutes and Statoil.

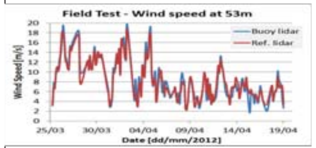

NOWIcob – O&M analysis tool

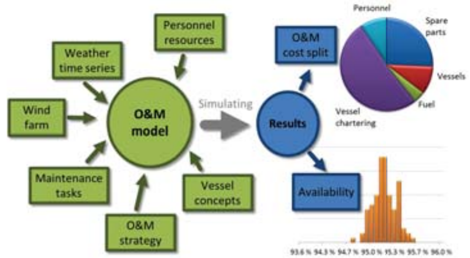

- ✓ Strategic discrete-event simulation tool for analysis of different offshore wind farm maintenance and logistics strategies
- ✓ Developed by SINTEF Energy in NOWITECH
- ✓ In use by Statkraft and others for wind farm O&M planning

Extending HVAC transmission beyond 100 km

- Low frequency AC (16 2/3 Hz)
- Reactive power compensation
- Optimizing cable voltage
- Development by SINTEF Energy Research

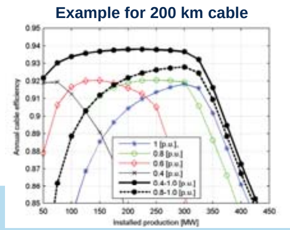

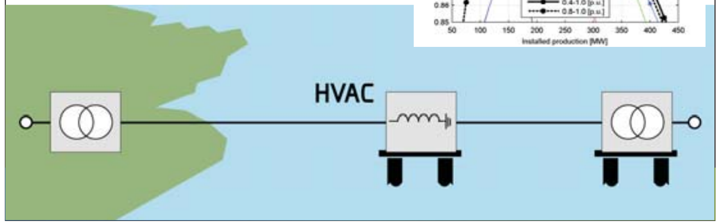

New software tools are developed and applied by industry

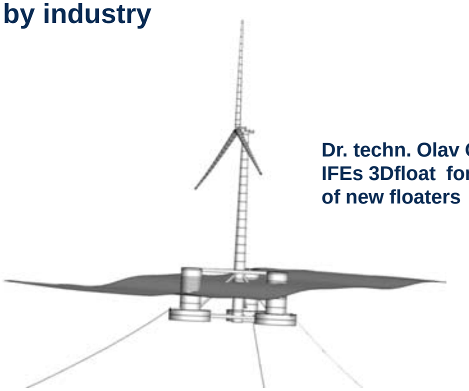

Dr. techn. Olav Olsen use IFEs 3Dfloat for development of new floaters

Norwegian industry is ready for a green transition

To make Norway a leading exporter of offshore technology and services requires:

- ✓ Enhanced R&D efforts
- ✓ Support for a offshore demonstration wind farm

COWIND: Centre for Offshore Wind Energy Research

Application for a new FME on offshore wind energy research is submitted to the RCN

- **Key ambitions:**
  - Reduce offshore wind LCOE with 30 %
  - Increase value creation
  - Accelerate innovation and commercialization.
- **Work programme:**

- **Start-up in 2016/2017, pending on funding. Duration 8 years. Decision by RCN 26 May 2016.**
- **Annual budget 60 MNOK:** financed by RCN (50 %), user partners (25 %) and research partners (25 %)
- **Host: SINTEF Energy Research**
- **Research partners: CMR, IFE MARINTEK, met.no, NGI, NTNU, SINTEF Foundation, UiA, UiB, UiS + international**
- **User partners:** ABB, Amon, Axys Technologies, CFD Marine, DNV GL, Olav Olsen, ESNA, Fedem, Ferrx, Fred Olsen Ocean, Fugro Oceanor, Impello, Kjeller Vindteknikk, Kongsberg, Maritime Robotics, Meventus, Mitsubishi Electric, Norsk Automatisering, Ship Modelling & Simulation Centre, SIMIS, Statkraft, Statoil, Vattenfall, Windmaster Technologies
- **Still open for more user partners**
- **Contact: John Olav Giæver Tande** john.tande@sintef.no; +47 91368188

Norwegian Parliament decision on floating offshore wind farms (1/12-2015)

Vedtak 50

Stortinget ber regjeringen i forbindelse med energimeldingen legge frem en strategi som bidrar til realisering av demonstrasjonsprosjekter for flytende havvind og andre former for havbasert fornybar teknologi, og ser på mulighetene for norsk leverandørindustris utvikling innenfor fornybar energiproduksjon.

Vedtak 51

Dokument 8:118 S (2014–2015) – representantforslag fra stortingsrepresentant Rasmus Hansson om en storsatsing på flytende vindkraft i Norge – vedlegges protokollen.

Cooperation as a key to cost reductions for offshore wind

Kristin Guldbrandsen Frøysa
Director NORCOWE/CMR
kristin@cmr.no

Outline

- Norwegian oil and gas industry
  - Cooperation
  - Govermental regulations
  - Support schemes for Norwegian research
- Examples from NORCOWE
  - OBLEX-F1
  - Improved understanding of turbulence
  - NORCOWE Reference Wind Farm
- 1+1=5!

Ownership of oil and gas licences
Statfjord as an example

Statoil	44,34 %
ExxonMobil	21,37 %
ConocoPhillips	15,17 %
Centrica Resources	9,69 %
Shell	8,55 %
Enterprise Oil Norge	0,89 %

Norwegian oil and gas industry

- Business sensitive information
  - Geological information
  - Interpretation of geological information
- Common interests in developing the oil&gas vendor industry
  - Close cooperation on development of the techical solutions, transperency between the vendor and the customer
  - Detailed technical information available to the oil&gas companies from the vendors
  - Use of JIP to mature the vendor industry
  - A development project is considered succesful when implemented in the vendor industry

Strong governmental involvement

- Oljedirektoratet founded in 1972 (first oil detected in August 1969)
- Petroleumstilsynet founded in 2004 (demerged from Oljedirektoratet)

NORWEGIAN PETROLEUM DIRECTORATE

PETROLEUM SAFETY AUTHORITY NORWAY

Investment in Norwegian research

- Strong incentives to invest in Norwegian research by governmental regulations
- Norwegian authorities told the oil companies to install instruments on their offshore installations
- Norwegian Petroleum Directorate (OD) collected the data, and set up R&D programs to analyze the data. The analyses were paid by the oil companies
- OD still collects data from the Norwegian continental shelf
- Investment in R&D in Norway was important to get licences on the Norwegian continental shelf

Cooperation in the Norwegian oil and gas industry

- The Norwegian Oil and Gas association (Norsk olje og gass) consists of 54 oil/gas companies and 55 supplier companies. The companies represent about 35 000 employees.
- Founded in 1965 as Norsk Industriforening for Oljeselskapene
- Have organized joint projects to meet regulatory requirements
- An example of commercial cooperation: Turbinpool, a joint maintenance contract for 97 gas turbines from Norsk Hydro, Statoil and Exxcon Norge towards GE.

Why is scientific cooperation needed?

Mesoscale	Park scale	Rotor scale	Blade scale
10000 -10 km	10 -1 km	200 – 50 m	5 - .5 m
Days -Hours	20 min – 20 s	10 – 2 s	0.5 – 0.01 s

Factor of 10^6 in relevant length and time scales

By courtesy of Finn-Gunnar Nielsen

Examples from NORCOWE

- OBLEX-F1 – measurement campaign at FINO1
- LIMECS – Lidar measurement campaign at Sola (Stavanger)
- Improved understanding of turbulence and loads on offshore wind turbines
- NORCOWE Reference Wind Farm
- Validation of models with data from Sheringham Shoal
- Lysefjord bridge (UiS, NPRA, UiB, CMR, DTU)

FINO 1

- Research platform
- Commissioned 2003
- Owner: Federal Ministry (BMWi)
- Administration: Projektträger Jülich
- Operator 2012-2017: FuE-Zentrum FH Kiel
- Public available data

Measurement concept

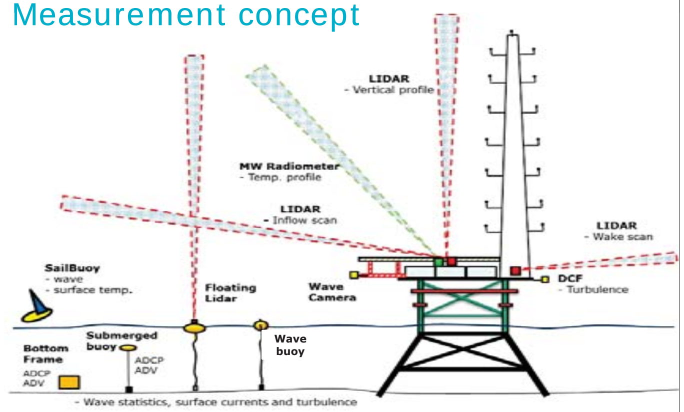

CONFIDENTIAL

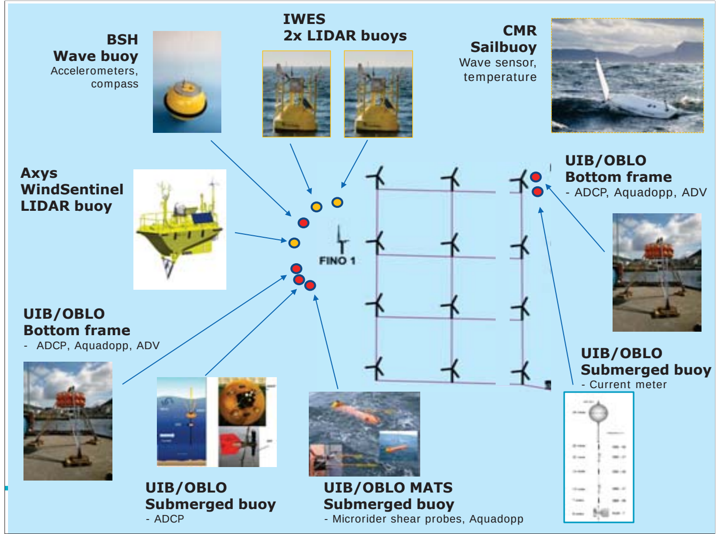

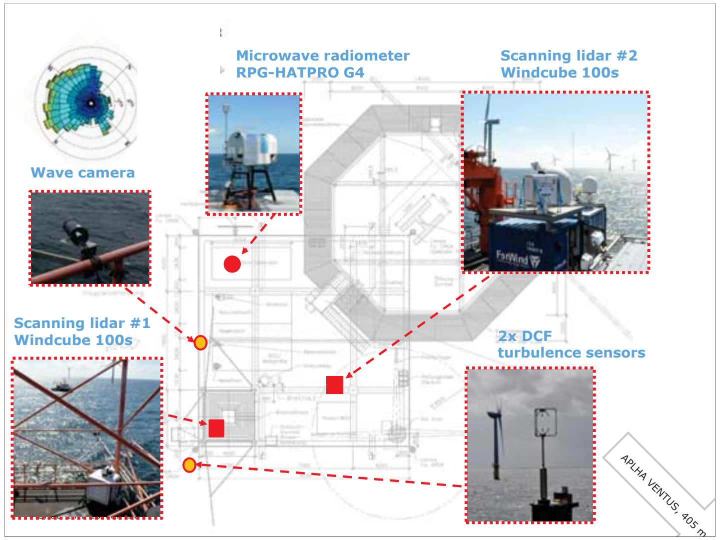

Scanning lidars

- Online instrument control and webcam monitoring
- Real-time access to wind profiles for inflow and wake

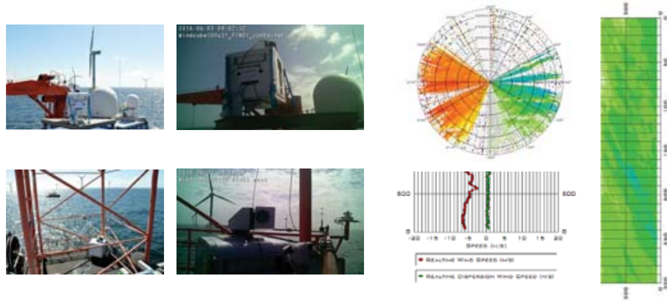

Validation of turbulence models

- Industrial motivation: accurate estimation of loads
- Validation of tubulence models, with a particular focus on applications to loads is a main focus area in NORCOWE in 2016-2017
- Coherence investigations of atmospheric turbulence as collaboration between UiB, UiS, UiA, CMR and Statoil
- Utilizing the OBLEX-F1 data to see if waves, atmospheric stability, wind and wave field influence the turbulence characteristics

Norcowe reference wind farm

Thomas Bak, Angus Graham, Alla Sapronova, Zhen Chen, Torben Knudsen, John D Sørensen, Mihai Florian, Peng Hou, Masoud Asgarpour

Key parameters

- Reference zone: FINO3
- Installed capacity: 800 MW
- Number of turbines: 80
- Turbine: DTU 10 MW turbine, rotor* 178m, hub height 119m
- Water depth / foundations is not in the initial focus – 22 meter, monopile

*Bak C, Zahle F, Bitsche R, Kim T, Yde A, Henriksen LC, Natarajan A, Hansen MH. Description of the DTU 10 MW Reference Wind Turbine. DTU Wind Energy Report-I-0092, 2013.

Baseline turbine layouts of the NORCOWE reference wind farm

Developmental work on Norcowe's reference wind farm (RWF) has taken place at Aalborg University and Uni Research.
The RWF comprises a fictitious 800 MW wind farm at the location of the FINO3 met mast, 80 km west of the island of Sylt at the Danish-German border.

- The farm involves a set of 80 reference wind turbines and two substations.
- DTU's 10 MW reference wind turbine is the chosen turbine type, a variable-speed rotor of diameter 178 m and hub height 119 m.
- Foundations are monopiles: mean water depth at FINO3 is 22.5 m, soil type comprises medium dense to very dense sand deposits with gravel and silt constituents.
- There is a real wind farm at FINO3, DanTysk, owned by Vattenfall.

NORCOWE RWF

AALBORG UNIVERSITY

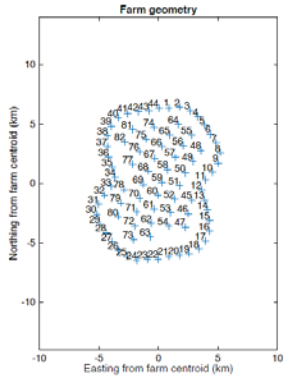

Alternative layout:

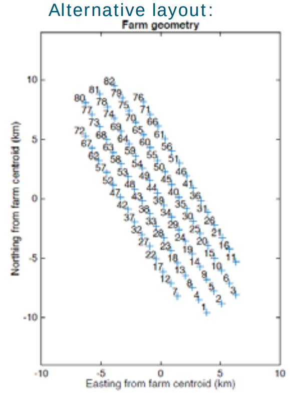

How can 1+1=5?

- Common goals, joint effort
- Skilled people
- Clusters (industry, academia, education and public sector)
- Good management systems in the industry
- Govermental regulations
- Industrialization and standardization

It's all about people!

Thank you for your attention!

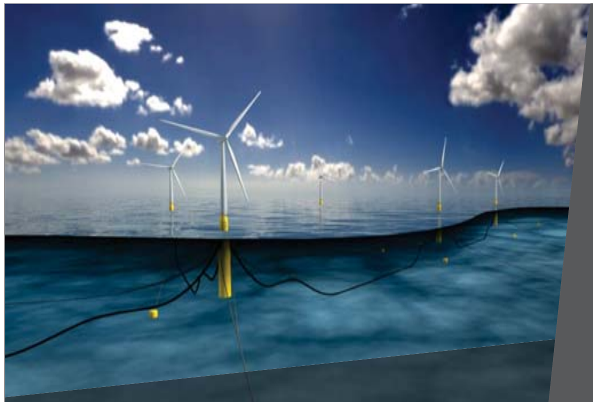

Statoil

Hywind Scotland – status and plans

EERA DeepWind' 2016, Trondheim

Knut Erik Steen, Statoil

Offshore wind

Playing at our strengths

- Financial control and project management excellence
- Multi contracting interfaces
- Marine operations
- Managing technology and subsurface
- Operations excellence
- Managing technology risks and use
- Safety culture and community engagement

Statoil

Statoil positioning in offshore wind

Current Portfolio

2.3MW	317MW 1.11 Twh / yr	402MW 1.7 Twh / yr	30MW 0.14 Twh / yr
Hywind Demo	**Sheringham Shoal**	**Dudgeon**	***Hywind pilot park***
In operation	In operation	FID Construction and installation phase	FID Construction and installation phase

Increase Portfolio & Acreage

North West Europe · *Japan* · *US*

Dogger Bank · *Hywind Commercial Park*

1200MW each project

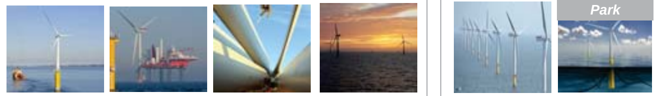

2009- · 2012- · 2017 · 2017- · 2020-

Statoil

Floating wind - *Potential markets*

North sea – Norway and UK

US, Atlantic and Pacific coast – and Great Lakes

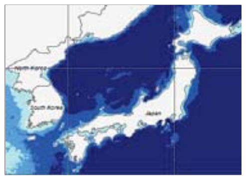

Japan and Korea

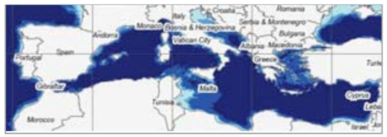

Iberian Peninsula and Mediterranean Sea

Statoil

HYWIND

Statoil

What is Hywind?

- Floating wind turbine (FWT)
- A standard offshore wind turbine placed on a ballasted vertical steel cylinder, anchored to the seabed
- Active motion controller
- Statoil-owned technology

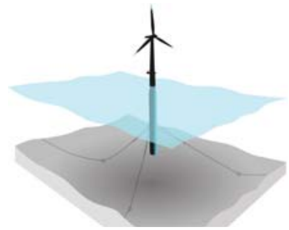

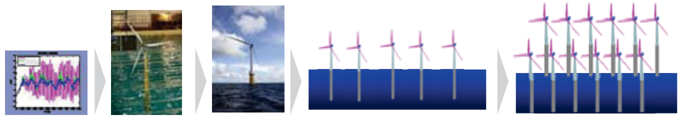

Concept *2001* · Model test *2005* · Full-scale prototype *2009* · Pilot Park, 3-6 turbines *<5 years* · Large Parks, 500-1000MW *<10 years*

Statoil

HYWIND DEMO

Hywind Demo – the World's first full scale prototype

10 km offshore Norway at 200 meter depth:

Conventional technology used in a new way

- **slender floating cylinder (simple sub-structure)**
- **conventional 3-line mooring system**
- **use of standard offshore wind turbine**

In operation from September 2009

- **produced ~40 GWh since start-up**
- **capacity factor 50% in 2011 (overall 40%)**
- **experienced wind speed of 40 m/s and maximum wave height of 19 m**

Blade pitch control to dampen out motions

Floater motions have no negative impact on turbine performance

Concept verified

Hywind Demo - assembly and installation - 2009

HYWIND SCOTLAND

Commercialisation of Hywind

Status:	Next step:	End goal:
• The technical concept is considered proven	• Pilot park to demonstrate improvements and cost reductions	• Commercial scale parks of 500-1000 MW • Cost competitive with bottom fixed

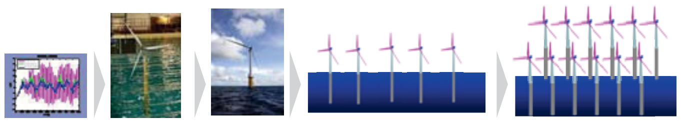

Concept *2001* — Model test *2005* — Full-scale prototype *2009* — Pilot Park, 3-6 turbines *<5 years*

Hywind Scotland - project objectives

Demonstrate cost-efficient and low risk solutions for commercial scale parks

- Test multiple units in park-configuration
- Verify up-scaled design
- Verify reliability and availability of optimized multi-turbine concept
- Mobilize supply chain

Hywind Scotland Pilot Park

Hywind Scotland	
Area (sea level)	~4 km²
Water depth	95-120 m
Average wind speed (@100 m)	10.1 m/s
Mean waves, Hs	1.8 m
Installed capacity (5 WTGs)	30 MW
Offshore export cable length	30 km
Onshore cable length	2-3 km
Transmission voltage	33 kV
Tentative milestones: • Final Investment Decision • Offshore installation & commissioning	Q3 2015 2017

Hywind Scotland test park at a glance

- Electrical swichgear plant
- Export cable
- 5 x 6MW WTG units
- Mooring system

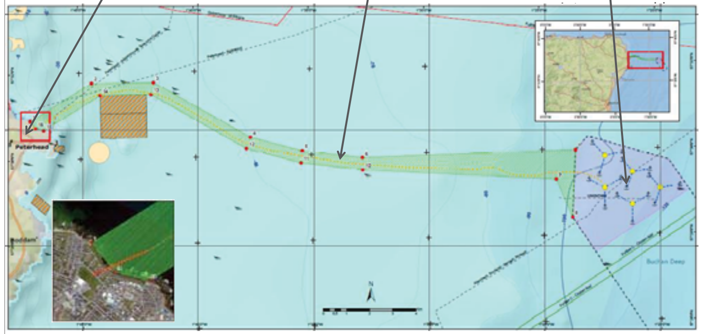

Upscaling from Demo 2009 to Hywind Scotland 2014

Dimension	Hywind Demo	Hywind Scotland
Mass	5300 tons	~11500 tons
Hub height	~65 m	~100 m
Draught	100 m	~75 - 80 m
Diameter of sub-structure	8.3 m	~14 - 15 m
Water depth	220 m	~95 - 120 m
Rotor diameter	~85 m	154 m
Capacity	2.3 MW	6.0 MW

Substructure & Tower

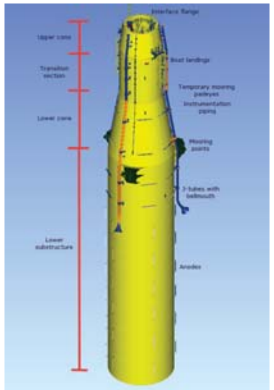

Height : 91m
Diameter : 14,4m →7,5m

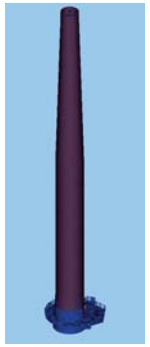

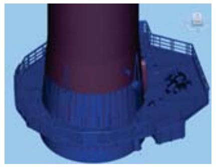

Height : 83m
Diameter : 7,5m →6,5m

Mooring System

- Normal safety class (confirm
  - Suction anchor: 5m dia x

	T3_A
Bridle dimension	132 mm
Bridle length	50 m
Moring line dimension	147 mm
Pretension at triplate	900 kN
Mooring line length (in DeepLines model)	609.4 m
Anchor radius (in DeepLines model)	640 m

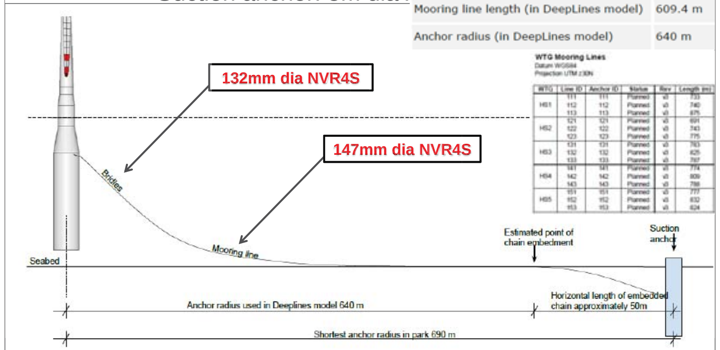

Mooring Details

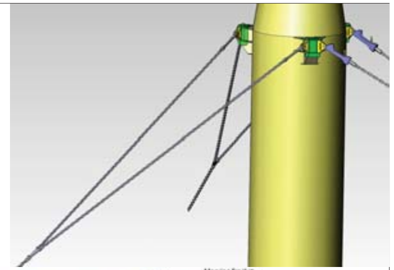

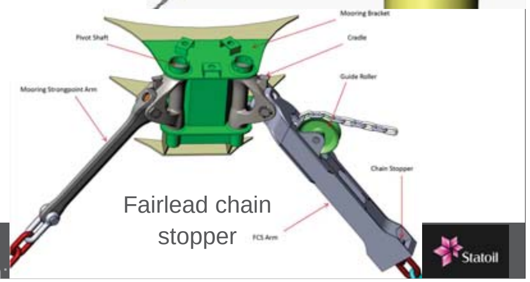

Dynamic cable layout (Lazy-Wave)

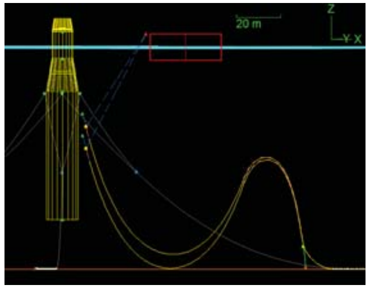

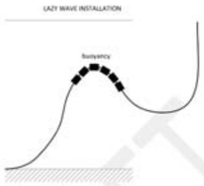

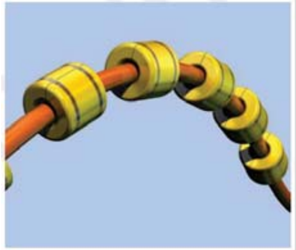

SWT-6.0-154 turbine

Rotor Diameter: 154m

Rotor Area : 18.600m²

Upscaling effects

- Fabrication
  - Increased diameter of the substructure is an important challenge for the fabrication
- Marine operations, assembly site
  - Lifting heigth increased significantly
  - Available vessels to install under floating conditions very limited
  - The operation related to lifting from a floating installation to another floating installation is very challenging with regards to load transfer

Hywind – WTG and tower assembly on shore

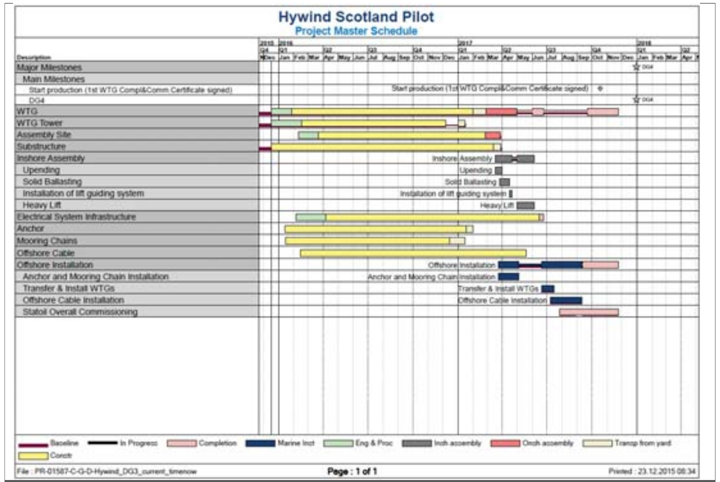

Project execution strategy

Contract overview

CONTRACTS	Offshore Wind Turbine (EPC)	Substructure (FC)	WTG Towers (FC)	Mooring chain (FC)	Suction anchors (FC)	Marine operations (EPCI)	Export and inter array cable (EPC+I)	Electrical System Infrastructure (EPCI)	Assembly site
Project Mgmt/planning Facility Scope									
Studies		Parallel studies with several contractors. Mooring design part of substructure	D.I.S (tower study)	Olav Olsen		Marine operation studies	Cable study	Landfall study	
FEED, Engineering& Mgmt Assistance	Siemens	Aibel						ESI Class D study	
Detail Engineering									
Procurement	Siemens	Navantia	Competition through prequalified tenderers	Single Source or competition through prequalified tenderers	Competition through prequalified tenderers	Competition through pre-qualified tenderers	Competition through prequalified tenderers	Competition through pre-qualified tenderers.	Competition through pre-qualified tenderers
Fabrication									
Installation/transport Offshore/onshore	Marine Operation						Separate cable installation contract. Competition		
Trenching and backfilling							Option in cable installation contract		
Seabed intervention						Competition or Call off Frame agreements			
Filling of ballasting material						Competition or Call off Frame agreements			
Fairlead chain stopper		Company provided item to substructure contract. Single Source							
Commissioning	Siemens								
RFO/Start up		Statoil							
O&M	Statoil and Siemens	Statoil							

- Multi-contracting strategy to minimise CAPEX and maximize market effects
- Building on Hywind Demo, Sheringham and Dudgeon experience
- Reuse existing supplier relations, where possible
- Ensure competition where possible
- Bundling explored
- Synergies with other Statoil projects for inshore heavy lift & marine operations
- Synergies with vessels on long-term hire for Statoil
- Enable Scottish content
- Interfaces

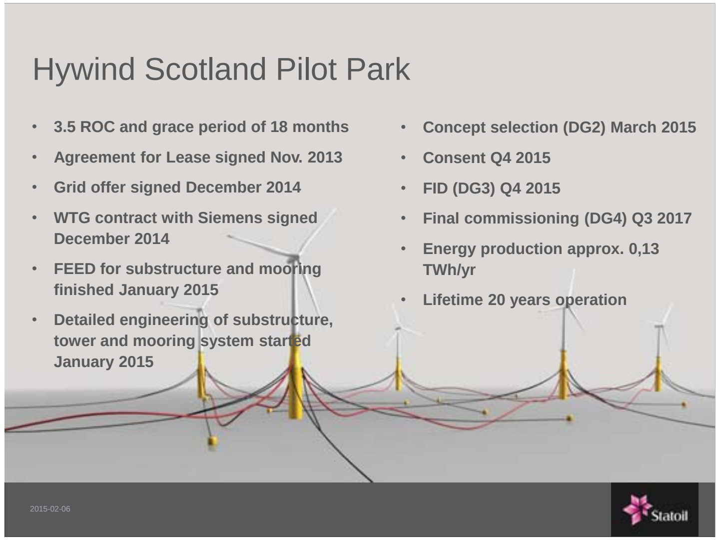
Hywind Scotland Pilot Park
• 3.5 ROC and grace period of 18 months
• Agreement for Lease signed Nov. 2013
• Grid offer signed December 2014
• WTG contract with Siemens signed December 2014
• FEED for substructure and mooring finished January 2015
• Detailed engineering of substructure, tower and mooring system started January 2015
• Concept selection (DG2) March 2015
• Consent Q4 2015
• FID (DG3) Q4 2015
• Final commissioning (DG4) Q3 2017
• Energy production approx. 0,13 TWh/yr
• Lifetime 20 years operation
2015-02-06
Statoil

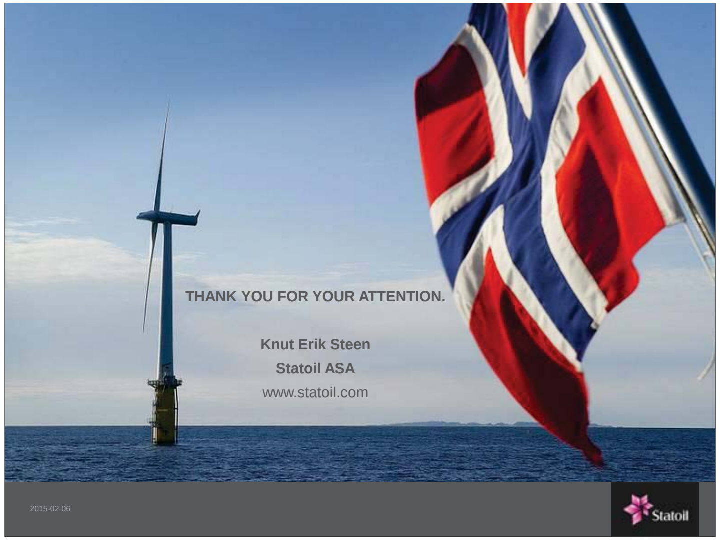
THANK YOU FOR YOUR ATTENTION.
Knut Erik Steen
Statoil ASA
www.statoil.com
2015-02-06
Statoil

EERA

EERA research programme on wind energy and the offshore challenges

Trondheim, EERA DeepWind' 2016

20 January, 2016

Thomas Buhl & Peter Hauge Madsen, DTU Wind Energy

EERA IRPWind

EERA JPWIND and IRPWIND

- The vision of the EERA Joint Programme for Wind Energy is to move from a voluntary network of research organisations towards a "virtual research centre" running an Joint Research Programme and help develop a common European Research Area.
- JPWind started in 2010 on a voluntary basis. Since then activities and the number of members have grown substantially.
- In March 2014 the Integrated Research Programme scheme co-funded by the European Commission called "IRPWIND" was started.
- **IRPWIND is designed to take EERA JP Wind to the next level towards creating a European Integrated Research Programme on wind energy and comprises both CSA and research components**

EERA

EERA JP WIND structure and sub-programmes

Application areas

Enabling research areas

Research area	Coordination
Wind Conditions	Coordinated by DTU, DK
Aerodynamics	Coordinated by ECN, NL
Structures and materials	Coordinated by CRES, GR
Grid integration	Coordinated by IWES, DE
Research infrastructures	Coordinated by CENER, SP
Economic & social aspects	Coordinated by DTU, DK

Offshore Wind Energy Coordinated by SINTEF, NO

New pilot programme on cold climate in the making

EERA

EERA JP WIND Members

Full participants		Associated Participants	
DTU Wind Energy	DK	DHI, University of Aalborg, Dublin(IR)	DK
ECN	NL	TU Delft, WMC	NL
SINTEF	NO	NTNU, IFE, UoB, CMR MARINTEK, Sintef MC	NO
CRES	GR	NKUA	GR
CENER	ES	CIEMAT, IREC, CTC, CIRCE, Tecnalia, IK4 Alliance	ES
Fraunhofer IWES	GER	IEN (PO), DLR, TU München	GER
Forwind - University of Oldenburg	GER	Forwind Hannover, Uni. of Stuttgart, RWTH Aachen	GER
LNEG	POR	University of Porto	POR
VTT	FI		
TUBITAK	TU	METUWIND	
University of Strachclyde	UK	NAREC, Loughborough Uni.	UK
CNR	IT	POLIMI, RSE	IT
Belgian Energy Research Alliance	BE		
EPFL	CH		

14 full participants & 30 associated participants from 14 countries.
Applicants in process: NTUA (GR), TNO (NL), UCC (IR)

IRPWind

IRPWIND objectives

- The aim of EERA and the IRPWIND is to foster **better integration of European research activities in the field of wind energy research** with the aim to accelerate the transition towards a low-carbon economy and maintain and increase European competitiveness.
- The IRPWIND is expected to both benefit existing priority settings as well as to improve the quality and implementation of future priority settings through **the coordinating effect on the research communities**.
- An objective is to **integrate the various capacities and resources in the joint research activities** described in this IRP- with other ongoing European and National projects carried out by IRPWIND partners and/or other EERA JP Wind members.

Supported by

IRPWind

IRPWIND – what it's all about?

Integration, coordination and alignment (as well as R&D)

- Strategic level (ETIP, EERA Wind Strategy, National strategies)
- Operational level
  - Integration of activities (EERA DoW, workshops, IRPWIND mobility scheme)
  - New joint activities (ERA NET+, Berlin model, ad hoc)
- Transparency – who does what, national programmes
- Complete research programme

Towards a European Wind Energy Programme and a virtual research institute based on national and European activities

Supported by

EERA Wind Energy R&D Strategy

Example– Offshore sub-programme Roadmap and priorities

IRPWind

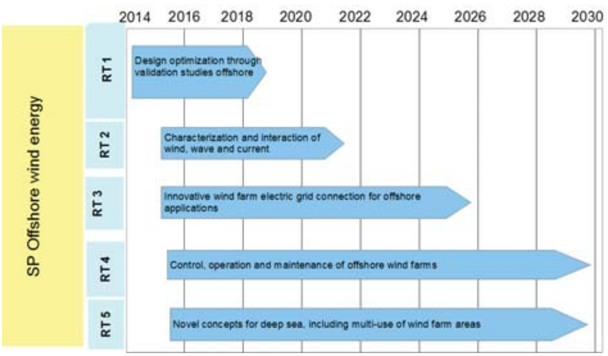

Supported by

IRPWIND mobility

IRPWind

- A very concrete way of facilitating more integration of national activities
  - **Flexible and non-bureaucratic** programme:

  Mobility scheme of 2 to 4 weeks for IRP Wind and EERA Managers.

  Mobility scheme of 4 to 26 weeks for all scientists.
  - 4 yearly cycles of calls
- Basic idea: Travelling researcher bring own project which are "related to" similar project at the hosting institution

The fourth call is now open with a deadline on 31 January 2016.

- Report: each report such provide input to the overall reporting of the IRP and possibly also be presented at the yearly event.
- Application: The mobility programme is **open for all** EERA JPWIND partners.
- **16 researchers** have until made use of the programme and we have room for more mobility applicants.

IRPWIND: Research Infrastructure

IRPWind

Key activities in 2015:

- Network creation:
  - Research Wind Turbines
  - Wind Tunnels
  - Grid integration
- Mapping of existing Research Infrastructure in Europe

Upcoming activities:

- Call for joint experiments
  - Subjects for the call for experiments will be research wind turbines, wind tunnels and grid integration.
  - The call will be open to all EERA JP WIND members and will be issued no later than February 2016.
  - The call is supported by the criteria in the document on "Rules & Conditions for joint experiments" elaborated in the IRPWIND work package on Research Infrastructure.
  - **Total budget**: 850.000€ - to be split between to calls and among 3 types of experiments.
  - **Reference budget per experiment:** 150.000€

Supported by

IRPWIND core research projects

IRPWind

WP 6: Design of offshore wind farms

WP 7: Improved & validated Structural Reliability

WP 8: European-wide measures and structures for a large-scale wind energy integration

Nationally funded collaborative projects

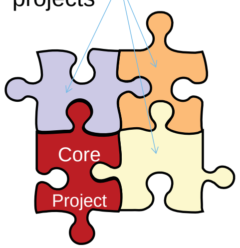

Supported by

IRPWIND WP6: Design of offshore wind farms

WP	Lead	PM	Start	End
WP6.1: Data assimilation	Hannover	46.0	12	36
WP6.2: Benchmark of models	CENER	105.5	1	36
WP6.3: Model development	Strathclyde	97.0	12	48

Participants

- ✓ DTU Wind Energy
- ✓ CRES
- ✓ ECN
- ✓ SINTEF Energy Research (WP lead)
- ✓ CENER
- ✓ NTNU
- ✓ University of Strathclyde
- ✓ Tecnalia
- ✓ ForWind – Oldenburg & Hannover
- ✓ MARINTEK

Objective

to accelerate the design optimization of wind turbines and support structures for offshore wind farms, through validation of integrated design models, and subsequent development of methods and design criteria

11

EERA

The EERA JP Wind project portfolio (with and without IRPWIND)

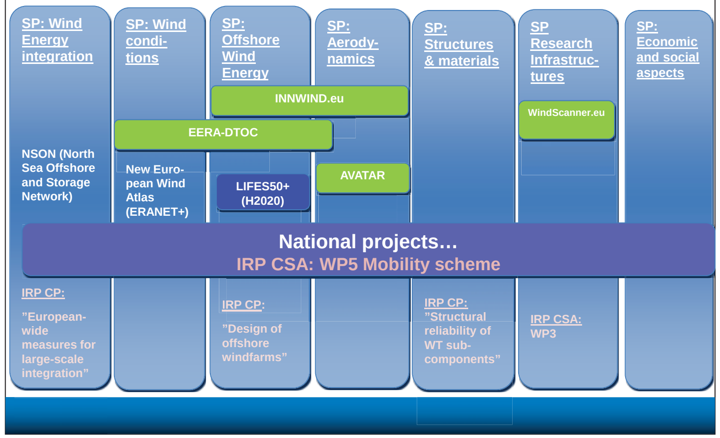

IRPWIND WP6:
Results providing basis for value creation

- **Database of measurements from offshore wind farms, both bottom-fixed and floating, and also from relevant lab-scale experiments. IRPwind will provide open data.**
- **Development of a benchmark validation procedure and an inventory of validation test cases.**
- **Implementation of a web-based European platform for the management of model benchmarking activities.**
- **Integrated design tools and guidelines taking into account loads, control and grid support, on turbine and wind farm level, providing reduced uncertainties and reduced cost of energy.**
- **Investigation of new control systems, at the turbine level and the farm level, providing additional protection to individual turbines and enabling optimized wind farm operation minimizing the cost of energy.**

13

IRPwind WP6:
Design of offshore wind farms

Status (cont.)
- ✓ Activities are coordinated with EERA SP offshore wind energy
- ✓ Sharing knowledge for joint benefits and efficient use of resources through expert workshops and conferences
- ✓ Preparation of strategy aligning with national and EU priorities
- ✓ Joint national and EU projects
  - ABYSS (DK-NO), kick-off 2014
  - NSON (NO-UK-DE), kick-off 2014
  - EERA DTOC, kick-off 2012
  - EERA InnWind, kick-off 2013
  - EERA IRPWind, kick-off 2014
  - LIFE50+, kick-off 2015
  - COWIND, FME application (NO)

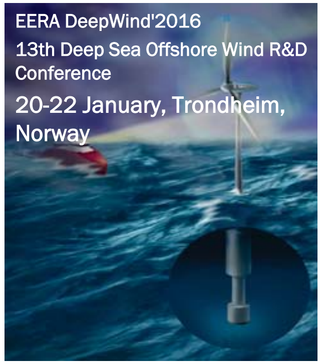

14

Offshore milestones in 2016

IRPWind

Mile-stone	Description
M1	EERA DeepWind R&D Offshore Wind Conference: EERA partners will contribute in total to about 50 oral and 50 posters, and approx. 30 papers from the conference will go through peer-review and be published in Energy Procedia
M2	Benchmarks scheduled and launched; IRPwind milestone MS22
M3	Data in database for benchmark exercise; IRPwind milestone MS20

Supported by

Innovative Support Structures

Innovative Jackets

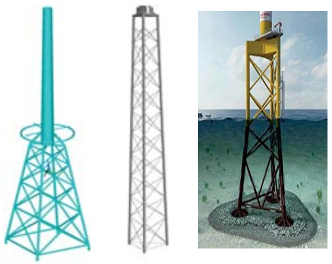

Three legged frame structures, also as a full length structure to the nacelle or for legged structures with vibration absorption devices

Floating Solutions

Guyed Tower with buoyancy and ballast chambers and Semi Submersible designed for a 10 MW wind turbine.

An Innovative Support Concept

2 Bladed rotor on a Semi-floating platform:

- Jointed to the seabed
- Buoyancy chamber
- Mooring lines
- Avoid 2p, 4p excitation

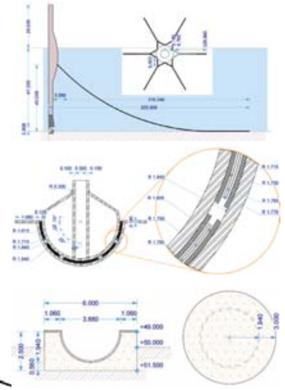

Monopiles at 50m water depth!

MONOPILE for the DTU 10 MW Reference turbine

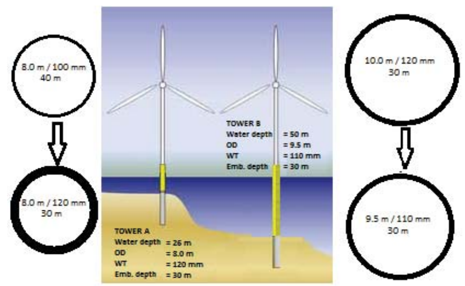

2700 tons

Wind Measurements for Controls

Spinner LIDAR

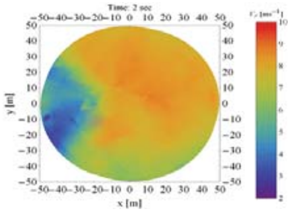

Spinner Anemometer

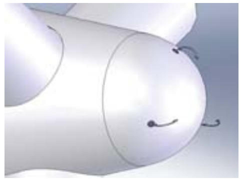

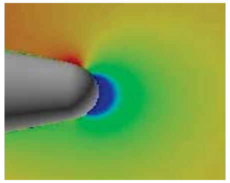

Advanced Blades

- Reynolds no. and compressibility effects separated
- Blade add-ons validated, spoilers, serrations, Gurney flaps
- Design of 2-bladed rotor, Low induction
- Bend-twist coupled RWT blade+ IPC+stretched = load and cost reduction
- New blade structure, truss, grid stiffeners,
- Scaled blade with BT coupling, wind tunnel test

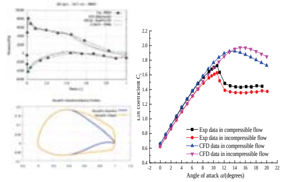

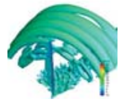

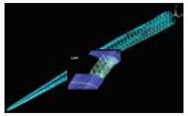

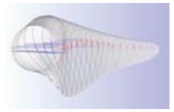

Direct Drive SC and PDD

CONCEPT	BRIEF DESCRIPTION	
DRIVE TRAIN		
Superconducting Generator	Two SC generator options are considered, the MgB_2 option and the RBCO one. The high price for the RBCO tape is indicating that MgB2 is most likely the fastest technology to be implemented bur RBCO is considered to become the cheapest technology in the long run.	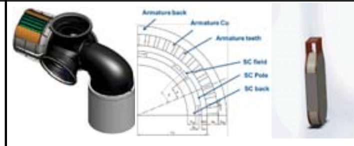
PDD Generator	The magnetic pseudo direct-drive (PDD) generator is realizing the possibility of applying magnetic gears in wind turbines. In a PDD generator, the magnetic gear and the electrical generator are mechanically as well as magnetically integrated.	

Synthesis

ROTOR	Component Mass (Δ%)	Component Cost (Δ%)	Overall CAPEX (Δ%)	Turbine CF (Δ%)	Wind Farm CF (Δ%)	LCOE (Δ%)
Low Induction Rotor	7.9%	15.4%	3.8%	7.5%	9.1%	-6.0%
Two-Bladed Rotor R1.08	-20.9%	-19.4%	-1.6%	4.7%	4.7%	-5.3%
Two-Bladed Rotor R1.12	-4.1%	-4.0%	-0.3%	8.3%	8.1%	-7.6%
Smart Rotor (Flaps)	-10.7%	-6.5%	-0.5%	0.2%	0.2%	-0.5%
Carbon Truss Blade Structure	-25.7%	-13.2%	-0.9%	0.0%	0.0%	-0.6%
Bend-Twist Coupled Rotor	-2.0%	-2.0%	-1.2%	0.0%	0.0%	-0.8%
Integrated BTC with IPC	18.4%	18.5%	1.0%	7.5%	7.2%	-6.1%
DRIVE TRAIN & NACELLE	Component Mass (Δ%)	Component Cost (Δ%)	Overall CAPEX (Δ%)	Turbine CF (Δ%)	Wind Farm CF (Δ%)	LCOE (Δ%)
SC MgB2-CSI Generator	47.2%	2.8%	0.7%	0.8%	0.7%	-0.4%
PDD Generator	2.5%	-13.1%	-3.0%	1.4%	1.2%	-3.2%
OFFSHORE SUPPORT STRUCT	Component Mass (Δ%)	Component Cost (Δ%)	Overall CAPEX (Δ%)	Turbine CF (Δ%)	Wind Farm CF (Δ%)	LCOE (Δ%)
Bottom-Mounted OSS		-14.7%	-4.5%			-3.0%
Semi-Sub Floater Design	95.1%	32.0%	9.8%			6.5%
Semi-Floater Concept		-34.8%	-10.6%			-7.0%
COMBINATIONS			Overall CAPEX (Δ%)	Turbine CF (Δ%)	Wind Farm CF (Δ%)	LCOE (Δ%)
LIR + PDD + Adv. Jacket			-4.4%	8.3%	10.0%	-11.5%
2B R1.12+PDD+Adv.Jacket			-9.5%	9.1%	9.1%	-13.0%
BTC/ITC+ PDD + Adv. Jacket			-6.5%	8.9%	8.4%	-10.8%

IRPWind

irpwind@eerawind.eu

Thank you and enjoy the conference!

Supported by

A1) New turbine, generator and wind farm technology

Development of a TLP substructure for a 6MW wind turbine – use of steel concrete composite material, F. Adam, Wind Power Construction GMBH

A parametric CFD study of morphing trailing edge flaps applied on a 10 MW offshore wind turbine, Eva Jost, Univ of Stuttgart

Latest results from the EU project AVATAR: How to model large wind turbines aerodynamically? J.G. Schepers, ECN

Design Load Cases investigation and comparison between Vertical and Horizontal Axis Wind Turbines, C. Galinos, DTU

WPC WINDPOWER CONSTRUCTION GMBH — GICON Firmengruppe

Development of a TLP substructure for a 6 MW wind turbine – use of steel concrete composite material

A cooperation between industry and research institutions

Frank Adam
EERA DeepWind'2016 – 20.01.2016 - Trondheim

LWET

WPC Floating foundations for offshore - wind turbines — LWET

WPC Preliminary GICON-TLP for wind turbines — LWET

Components of the platform:

- Cylindrical buoyancy bodies (BB)
- Horizontal pipes (HP)
- Vertical pipes (VP)
- Cantilever beam (CB)
- Transition piece (TP)
- Ice-breaking Cone (IC)

Dimensions (L x B x H)	32 m x 32 m x 28 m
TLP Weight incl. sec. Steel	**≈ 742 t**
Total weight incl. WT	**≈ 1062 t**
min. # of Anchor points	4

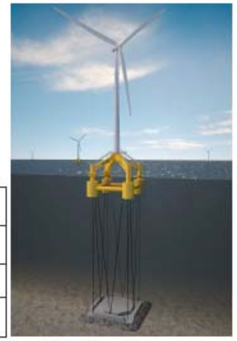

WPC Objectives for floating offshore wind sub-structures — LWET

- Economical solution
  → Mass as low as possible
- LCOE as low as possible
- Steel is not the cheapest material
- Steel-concrete composite material would be an alternitve:
  - Tension?
  - Life time?
  - Surface qualtiy?

WPC WINDPOWER CONSTRUCTION GMBH

TLP for OWT

Steel-concrete components

Economical aspects

Pre-design 6 MW

WPC WINDPOWER CONSTRUCTION GMBH

TLP for OWT

Steel-concrete components

Economical aspects

Pre-design 6 MW

WPC Examples for TLPs or TLBs

LWET

		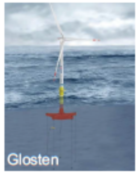	
Tank tests 2012	Tank tests 2013	Tank tests 2013	Tank tests 2012-14
Vertical ropes	Angled ropes	Vertical ropes	Vertical and angled ropes
TRL 4	TRL 3	TRL 4	TRL 4

WPC Path of development

LWET

Mass in t	ca. 2000	2214	1790	742
Width in m	70	68	50	32
High in m	25	24	39	28

→ **These values are for a 2.3 MW wind turbine (~ 320 t/MW)**

WPC Preliminary Design of a 6 MW substructure

LWET

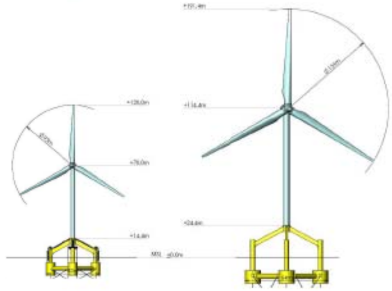

WPC WINDPOWER CONSTRUCTION GMBH

TLP for OWT

Steel-concrete components

Economical aspects

Pre-design 6 MW

WPC Pre-Stressed Steel-Concrete shell elemets – state of the art

LWET

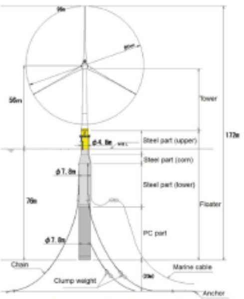

Source: T. Utsunomiya (2015). "Design and Installation of a Hybrid-Spar Floating Wind Turbine Platform". In: *Proc. OMAE2015*

WPC Pre-Stressed Steel-Concrete shell elemets – state of the art

LWET

Advantages:

- Modular system
- External fabrication – independently from the yard
- Transport via truck or ships

Challenges:

- Lifetime
- Tightening

Source: T. Utsunomiya (2015). "Design and Installation of a Hybrid-Spar Floating Wind Turbine Platform". In: *Proc. OMAE2015*

WPC Centrifugally spun concrete pile

LWET

Advantages:

- Modular system
- External fabrication – independently from the yard
- Simple pre-fabrication
- Good surface via centrifugal force

Challenges:

- Lifetime
- Pre-tensioning
- Tightening

Source: DBZ Deutsche Bauzeitschrift

Source: Europoles

WPC WINDPOWER CONSTRUCTION GMBH

TLP for OWT

Steel-concrete components

Economical aspects

Pre-design 6 MW

WPC Offshore CapEx breakdown

LWET

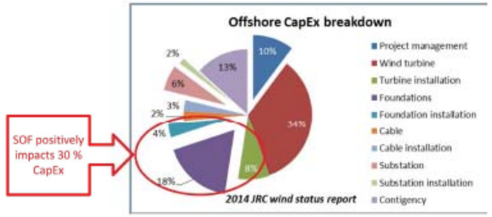

Source: 2014 JRC Wind Status Report 'Technology, market and economic aspects of wind energy in Europe'

WPC Substructure mass – one economical driver

LWET

Platform weight, post-ballast, by typology (steel concepts only)

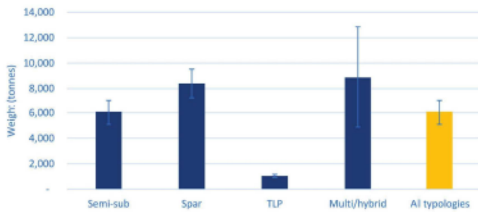

Source: 'Floating Offshore Wind: Market and Technology Review' Prepared for the Scottish Government. Carbon Trust, June 2015

WPC LCOE for the presented design

LWET

- First results show the technical feasibility of the 6 MW system
- The system will be an economically viable solution

SOF - Economic Viability highlighted by estimated LCOE (independent analysis by ECO915 based on Prognos Fichtner Scenarios 2013)

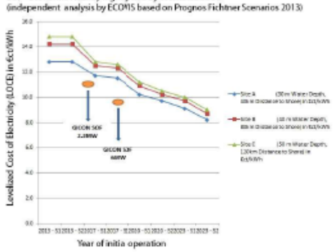

WPC WINDPOWER CONSTRUCTION GMBH

TLP for OWT

Steel-concrete components

Economical aspects

Pre-design 6 MW

WPC Requirements for the 6 MW sub-structure

Mass (incl. sec. steel) ≤ 1200 t

Floating stability for the sub-structure and anchor incl. wind turbine

Fabrication – 1 ½ sub-TLPs/week

Aim: 80 TLPs/year

Economical solution for water depths ≥ 30/35 m – comparable with fixed sub-structures

WPC Calculation

- ANSYS AQWA for the floating stability
- Analysis → FEM
- Using ULS interface forces for the pre-design (no coupled calculation):
  - Normal Force – 7300 kN
  - Shear Force – 2400 kN
  - Overturning Moment – 210000 kNm
  - Torsional Moment – 25000 kNm

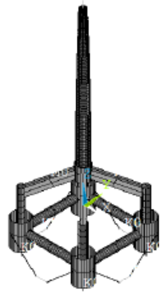

WPC Mass (incl. sec. steel) ≤ 1200 t

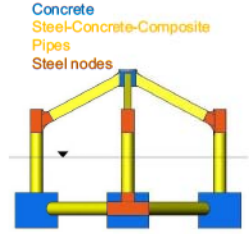

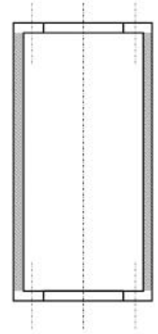

WPC Floating stability incl. Wind Turbine

	Deviation Maximum				
	Acceleration (ms^-2)			Rotation (Degree)	
Angle of Attack	X	Y	Z	RX	RY
180	-0,616	-0,155	-3,014	0,058	0,716
135	0,365	-0,495	-2,799	0,078	0,855
90	-0,017	-0,661	-2,716	0,164	-7,970
45	-0,384	-0,496	-2,801	0,040	0,736
0	0,617	-0,155	-3,017	0,098	4,268

Mass	5000t
Wave Freq	0.1Hz
Wave Height	2m

	Deviation Maximum				
	Acceleration (ms^-2)			Rotation (Degree)	
Angle of Attack	X	Y	Z	RX	RY
180	-0,705	-0,101	-3,281	0,104	11,971
135	-0,411	0,590	-3,205	0,105	12,232
90	0,002	-0,717	-3,246	0,556	-0,487
45	0,408	0,591	-3,209	0,043	12,426
0	0,705	-0,101	-3,282	0,013	11,979

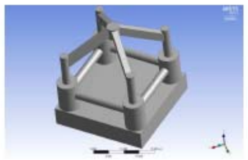

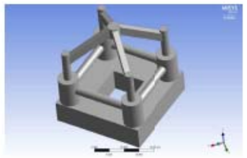

WPC Pre-design Maximum von Mises

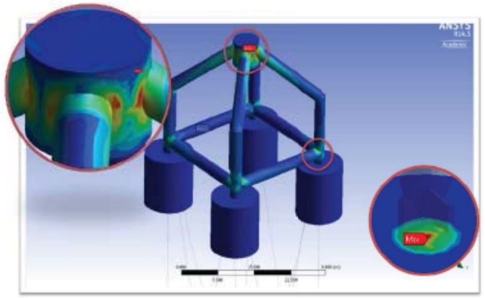

WPC Eigen frequencies – mass participation factors

	Frequency	X	Y	Z	ROTX	ROTY	ROTZ
200m	1.15E-01	0.12607	-0.11983	-34.133	[illegible]	[illegible]	-0.03062
Angled	1.16E-01	0.11878	0.12509	0.87388	[illegible]	[illegible]	-1.6672
and	2.47E-01	0.00236	0.003176	-0.04248	604.21	604.14	-0.00028475
Vertical	2.48E-01	0.01567	0.00492	0.001667	-602.1	601.81	1.9038
	2.55E-01	0.01821	-0.06862	5.2954	1648.7	1971.2	0.0094054
50m	0.01378	0.20017	0.20011	-3E-05	4779.2	-4779.2	[illegible]
Angled	0.02611	12.456	-12.395	-0.00176	-739.34	-742.8	1.6528
and	0.02612	18.073	17.023	-0.0038	1029.4	-1091	-87.716
Vertical	0.20771	-0.00943	0.007796	39.867	[illegible]	[illegible]	0.92508
	0.20867	-0.00772	-0.00937	-3.82	[illegible]	[illegible]	9.5983
	0.45705	0.010201	-0.00256	0.1162	-59.501	-237.26	0.16141
	0.45762	0.063893	-0.03888	0.94007	-905.67	-1488.7	0.5471
200m	0.0117	24.491	-24.131	-0.09312	-5291.2	-5370.5	4.6527
Vertical	0.01171	51.618	52.365	-0.00176	11321	-11160	916.54
	0.01172	57.685	-56.791	-0.23205	-12479	-12676	10.269
	0.08985	0.019853	-0.01897	38.706	[illegible]	[illegible]	0.00072706
	0.09103	0.018239	0.019105	-0.5743	[illegible]	[illegible]	-0.16997
	0.42944	-0.00134	0.001261	-1439.6	-198.33	-480.87	-0.0096311
50m	0.17175	0.005659	-0.00497	36.067	[illegible]	[illegible]	-0.001375
Vertical	0.17267	0.004895	0.005579	-2.2369	[illegible]	[illegible]	-0.029769

WPC Conclusion

LWET

- Coupled simulations
- Basic design of the new steel-concrete components
- Solving logistical issues
- Development of high performance concrete
- Cooperation with the certification body

WPC Quellen

LWET

Acknowledgment:

We like to express our special gratitude to the German Federal State of Mecklenburg-Vorpommern, for the financial support provided to the ESG GmbH, a member of the GICON group (project number: V-630-1-260-2012/103).

Prepared by:
Dr.- Ing. Frank Adam
WPC Wind Power Construction GmbH
Carl-Hopp-Straße 4a
18069 Rostock
Phone +49 (0) 174 3236545

Universität Stuttgart

www.iag.uni-stuttgart.de

A Parametric CFD Study Of Morphing Trailing Edge Flaps Applied On A 10 MW Offshore Wind Turbine

Universität Stuttgart

WINDFORS Wind Energy Research Cluster

AVATAR AdVanced Aerodynamic Tools for lArge Rotors

13th EERA DeepWind conference, 20 January 2016, Trondheim, Norway

Eva Jost

e.jost@iag.uni-stuttgart.de

Thorsten Lutz, Ewald Krämer

Universität Stuttgart

www.iag.uni-stuttgart.de

Overview

Universität Stuttgart

www.iag.uni-stuttgart.de

Overview

Universität Stuttgart

www.iag.uni-stuttgart.de

Why trailing edge flaps?

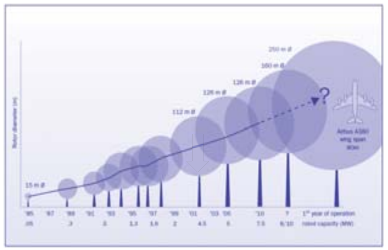

Scaling rules

Parameter	Proportionality
Power	$\sim R^2$
Thrust	$\sim R^2$
Rotor mass	$\sim R^3$

Demand of new technologies to reduce loads, load variations and mass:

Structure, Control, Aerodynamics, …

Active trailing edge flaps

Figure top left: UpWind – Final report, March 2011, www.upwind.eu
Figure bottom right: http://www.renewableenergyfocus.com/view/7457/wind-turbine-controllable-rubber-trailing-edge-flap-tested/

Universität Stuttgart

www.iag.uni-stuttgart.de

Functioning

Reduction of dynamic load variations due to:

- Tower shadow
- Atmospheric boundary layer and turbulence
- Yawed inflow

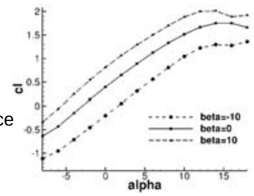

Basic functioning:

Undisturbed inflow

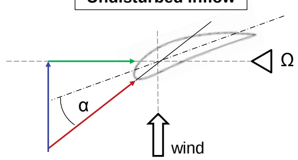

Disturbed inflow

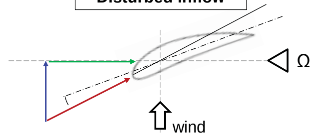

approach velocity c, wind velocity v, rotational velocity u=ωR

Universität Stuttgart

www.iag.uni-stuttgart.de

Previous work

- Prove of concept based on BEM and vortex methods
- Fatigue load reduction of blade root bending moment
  - BEM method ~ 18 %[1] ,Vortex method ~ 30 %[2]
- Difficulty: Modeling of steady and unsteady viscid 3D aerodynamics

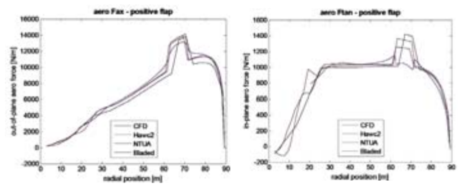

Next step: CFD simulation as high fidelity method

[1] S. Navalkar, J. van Wingerden, E. van Solingen, T. Oomen, E. Pasterkamp and G. van Kuik, "Subspace predictive control to mitigate periodic loads on large scale wind turbines," *Mechatronics* , vol. 24, pp. 916-925, February 2014.

[2] V. Riziotis and S. Voutsinas, "Aero-elastic modelling of the active flap concept for load control," in *Proceedings of the EWEC*, Brussels, Belgium, 2008

Figures: E.Jost, A. Barlas, V. Riziotis, S.T. Navalkar, "Innwind Report D2.3.2", www.innwind.eu

Objectives

Investigate the influence of steady 3D effects:

Simulation of the pure rotor with different flap configurations (varying chord and radial extension)

→ Comparison to 2D airfoil simulations

Selected rotor: DTU 10 MW reference wind turbine

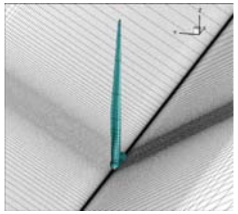

3D aerodynamic effects

Steady deflection, beta positive:

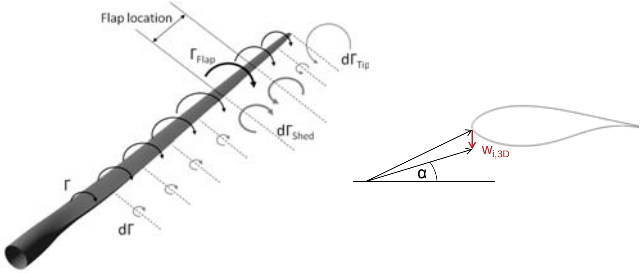

Overview

Simulation process chain

Mesh generation

- Gridgen/Pointwise
- Automesh: Automatic parameterized blade meshing

CFD code

FLOWer:
- developed by DLR[1]
- Compressible block structured finite-volume solver
- Moving/overlapping meshes (CHIMERA)

Extensions with regard to wind turbine application
- Dirichlet boundary condition for turbulent inflow
- **Grid deformation based on radial basis functions**
- Load integration during runtime

Post-processing

- Load integration
- Angle of attack extraction
- FFT analysis

[1]N. Kroll and J. Fassbender, MEGAFLOW – Numerical Flow Simulation for Aircraft Design, Berlin/Heidelberg/New York: Springer Verlag, 2002.

Extension for trailing edge flaps

- Mesh deformation based on radial basis functions[1]

2D simulation with flaps:

Baseline airfoil
Deformed airfoil

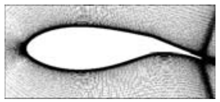

Rigid flap

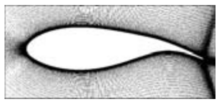

Morphing flap

3D simulation with flaps:

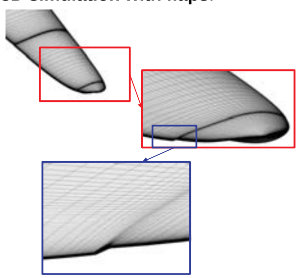

[1]M. Schuff, P. Kranzinger, M. Keßler and E. Krämer, "Advanced CFD-CSD coupling: Generalized, high performant, radial basis function based volume mesh deformation algorithm for structured, unstructured and overlapping meshes," in *40th European Rotorcraft Forum*, Southhampton, 2014.

Simulation setup - Baseline

Baseline without trailing edge flaps:
- Setup used in the code-to-code validation within FP7 project AVATAR (Deliverable 2.3[1])
- 120°-model with periodic boundary conditions
- 4 different grids: blade, spinner, nacelle and background
- Turbulence model: Menter SST
- Fully turbulent boundary layer

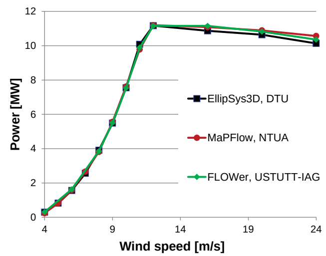

[1] and plot modified from: N. Sørensen, M. Hansen, N. Garcia, L. Florentie, K. Boorsma, S. Gomez-Iradi, J. Prospathopoulus, G. Barakos, Y. Wang, E. Jost and T. Lutz, "AVATAR Deliverable 2.3: Power Curve Predictions," 1 June 2015. [Online]. Available: http://www.eera-avatar.eu/fileadmin/mexnext/user/report-d2p3.pdf.

Simulation setup with trailing edge flaps

Simulated flap configurations:

- 4 different flap configurations: Combination of two different chord extensions (10% , 30%) with two radial extensions (10% and 20%)
- Flap centered at 75% blade radius (~ 66.86m)
- Deflection angle β=+/-10°

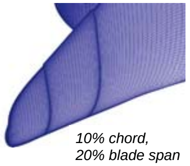
10% chord, 20% blade span

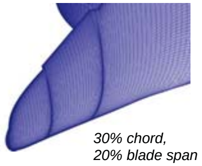
30% chord, 20% blade span

Operational conditions:

- 15 m/s wind speed, 10.96° pitch angle, 9.6 rpm

Overview

Radial thrust +/-10° deflection angle

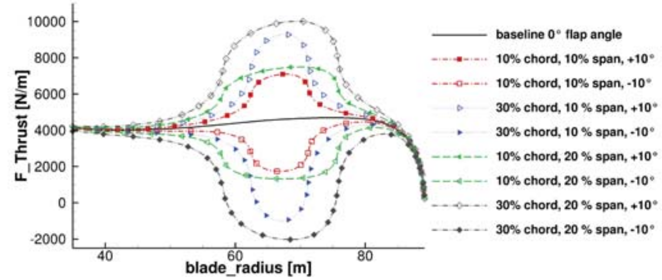

Radial driving force +/-10° deflection angle

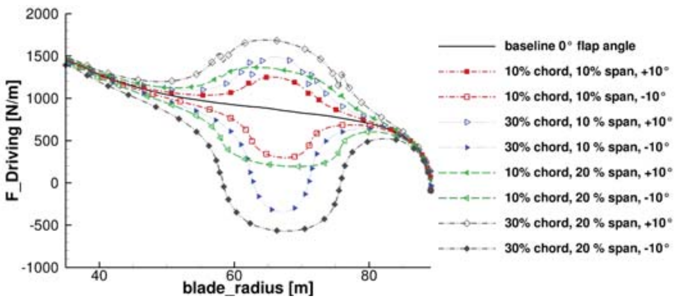

Comparison of lift coefficients 3D at mid flap position

- Extraction of the angle of attack and lift coefficient based on the reduced axial velocity method[1]

	No flap	β=10°, 20% blade span		β=10°, 10% blade span	
		10% chord	30% chord	10% chord	30% chord
c_l	0.488	0.788	1.05	0.751	0.979
$\Delta c_{l,\beta=0}$	-	0.3	0.562	0.263	0.491

- Results for β=-10° are comparable and will be presented in the conference paper.

[1] J. Johansen, N. Sørensen, "Aerofoil characteristics from 3D CFD Rotor Computations", Wind Energy, vol. 7, pp 283-294, 2004

Comparison of aerodynamic coefficients 2D/3D

- Simulation of the airfoil at mid flap position (75 % radius, FFA-w3-241) in 2D
- Conditions extracted from 3D simulation: Re=15.6e6, Ma=0.2, α=1.13
  → **Comparison of c_l and $\Delta c_{l,\beta=0}$**

	No flap	β=10	
		10% chord	30% chord
$c_{l,2D}$	0.483	0.859	1.198
$\Delta c_{l,\beta=0,2D}$	-	0.376	0.715
$\Delta c_{l,3D,10\%span}/\Delta c_{l,2D}$	-	**70 %**	**69 %**
$\Delta c_{l,3D,20\%span}/\Delta c_{l,2D}$	-	**80 %**	**79 %**

- Results for β=-10° are comparable and will be presented in the conference paper.

Universität Stuttgart

Adaption of deflection angle

20 % blade span:

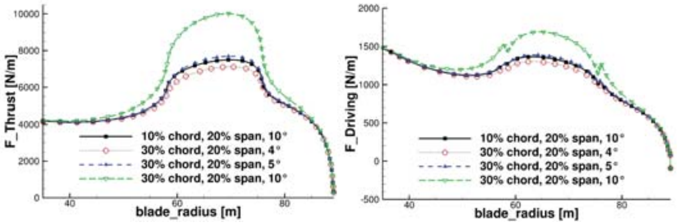

www.iag.uni-stuttgart.de

IAG Institute of Aerodynamics and Gasdynamics

Universität Stuttgart

Different wind speeds

20 % blade span, 10% chord:

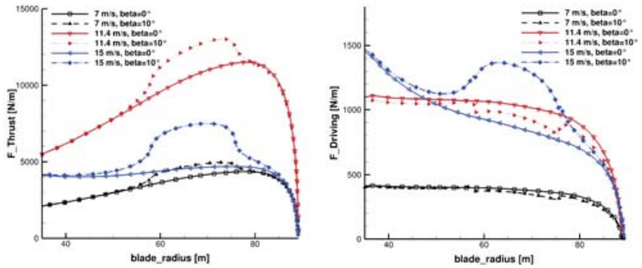

www.iag.uni-stuttgart.de

IAG Institute of Aerodynamics and Gasdynamics

Universität Stuttgart

Overview

www.iag.uni-stuttgart.de

IAG Institute of Aerodynamics and Gasdynamics

Universität Stuttgart

Conclusion

- 3D effects play an important role on trailing edge flaps and reduce their efficiency.
- Up to 35 % reduction of the lift variation compared to the 2D airfoil case have been found.
- A longer extension along the blade span is thus favorable.
- Trailing edge flaps are more efficient at higher wind speeds.

Outlook

- Unsteady effects (Theodorsen theory)
- Simulation of the full turbine

www.iag.uni-stuttgart.de

IAG Institute of Aerodynamics and Gasdynamics

Universität Stuttgart

Thank you for your attention.
Questions?

WINDFORS Wind Energy Research Cluster

University of Stuttgart Germany

AVATAR AdVanced Aerodynamic Tools for lArge Rotors

www.iag.uni-stuttgart.de

IAG Institute of Aerodynamics and Gasdynamics

AdVanced Aerodynamic Tools for lArge Rotors

www.eera-avatar.eu

AVATAR project
Advanced Aerodynamic Tools for lArge Rotors

Gerard Schepers
January 20th, 2016

EERA Deepwind
Trondheim, Norway

This project has received funding from the European Union's Seventh Programme for research, technological development and demonstration under grant agreement No FP7-ENERGY-2013-1/n° 608396 .

List of Contents

- Introduction into the project
- Design of AVATAR Reference Wind Turbine [1])
- Aerodynamics at high Reynolds numbers
  - Results from a blind test on airfoil measurements taken in the pressurized DNW-HDG tunnel [2])
- Aero-elasticity of large turbines
  - BEM versus free wake aerodynamic modelling[3])

1) Acknowledgement G. Sieros, M. Stettner
2) Acknowledgement O. Ceyhan, O. Pires
3) Acknowledgement K. Boorsma, S. Voutsinas
And all other project partners!

EU FP7 Project initiated by EERA

1. Energy Research Centre of the Netherlands, ECN (Coordinator)
2. Delft University of Technology, TUDelft
3. Technical University of Denmark, DTU
4. Fraunhofer IWES
5. University of Oldenburg, Forwind
6. University of Stuttgart, USTUTT
7. National Renewable Energy Centre, CENER
8. University of Liverpool/University of Glasgow, ULIV/UoG
9. Centre for Renewable Energy Sources and Saving, CRES
10. National Technical University of Greece, NTUA
11. Politecnico di Milano, Polimi
12. GE Global Research, Zweigniederlassung der General Electric Deutschland Holding GmbH, GE
13. LM Wind Power, LM

Period

- Project period:
  November 1st 2013- November 1st 2017

Main motivation for AVATAR: Aerodynamics of large wind turbines (10-20MW

- We simply don't know if present aerodynamic models are good enough to design 10MW+ turbines
- 10MW+ rotors violate assumptions in current aerodynamic tools, e.g.:
  - Reynolds number effects,
  - Compressibility effects
  - Thick(er) airfoils
  - Flow transition and separation,
  - (More) flexible blades
  - Flow devices
- **Hence 10MW+ designs fall outside the validated range of current state of the art tools.**

Avatar: Main objective

To bring the aerodynamic and fluid-structure models to a next level and calibrate them for all relevant aspects of large (10MW+) wind turbines

Avatar: Work procedure

- Problem: No 10 MW turbines are on the market yet for validation
- Hence: Validate *submodels* against experiments
  - *Pressurized* HDG tunnel of German Dutch Wind Tunnel facilities (DNW)
    - Airfoil measurements at Reynolds numbers up to *RE = 15 M* and low Mach (< 0.2)
  - LM: Wind tunnel airfoil measurements also at dynamic conditions
  - Forwind: Wind tunnel airfoil measurements at *representative turbulence*
  - TUDelft: Wind tunnel experiments on airfoils with *vortex generators, flaps*
  - NTUA: Wind tunnel experiments on airfoils with/without *vortex generators*
  - DTU : Danaero: Aerodynamic *field* experiments on a *2.3 MW* turbine and supporting 2D wind tunnel measurements
  - Note: Several experiments are supplied *in-kind*

Avatar: Work procedure

Use the different models from partners in the project
- It is a ***cooperation*** project!
- In the project we have many models which range from computational efficient '*engineering*' tools to *high fidelity* but *computationally expensive* tools
- Engineering tools are needed in *industrial* design codes [1])
- *High fidelity* models (*and intermediate* models) feed information towards *engineering* models

[1]) J.G. Schepers '*Engineering models in wind energy aerodynamics*', (2012). TUDelft PhD thesis **ISBN**: 9789461915078

Avatar: Work procedure

- Demonstrate the value of the improved tools on *10 MW reference rotors* with and without flow control devices
  1. INNWIND.EU reference rotor (more or less *conventional* design philosophy)
  2. AVATAR reference rotor which should be more *challenging* from an aerodynamic point of view (e.g. lower induction, longer, more slender blades, thicker airfoils, higher tip speed).
- Compare results from 'old' and improved models at the end of the project

List of Contents

- Introduction into the project
- *Design of AVATAR Reference Wind Turbine [1])*
- Aerodynamics at high Reynolds numbers
  - Results from a blind test on airfoil measurements taken in the pressurized DNW-HDG tunnel [2])
- Aero-elasticity of large turbines
  - BEM versus free wake[3]

1) Acknowledgement G. Sieros, M. Stettner
2) Acknowledgement O. Ceyhan, O. Pires
3) Acknowledgement K. Boorsma, S. Voutsinas
And all other project partners!

ECN

AVATAR RWT

	INNWIND.EU	AVATAR
Power:	10 MW	10 MW
Rotor diameter:	178.3m	205.8m
WTPD:	400 W/m²	300 W/m²
Axial induction:	0.3	0.24
RPM→Tip speed	9.8rpm→ 90m/s	9.8 →103.4 m/s
Hub height:	119m	132.7m

Classical Approach versus Low Induction

- Power Coefficient flat around Betz maximum (a = 1/3)

$$C_p = \frac{P}{\frac{1}{2}\rho A U_\infty^3} = 4a(1-a)^2$$

- Aerodynamic load coefficient strongly dependant on a

$$C_{D.ax} = \frac{D.ax}{\frac{1}{2}\rho A U_\infty^2} = 4a(1-a)$$

- Increase diameter→ maintain aerodynamic loads→ increase power

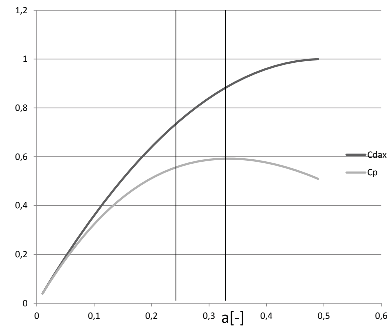

Design of AVATAR RWT

- 5% Increase in energy production due to larger diameter
- Key rotor load levels are maintained
- Non-rotor loads exceeded→ Redesign of AVATAR rotor at end of project
- Note: LCOE of AVATAR turbine assessed in [1]) taking into account additional advantage of lower wake effects

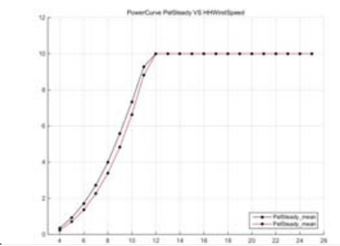

[1]) R. Quinn, B. Bulder, J.G. Schepers
A parametric investigation into the effect of low induction rotor (LIR) wind turbines on the LCoE of a 1GW offshore wind farm in a North Sea wind climate, EERA-Deepwind 2016

Design of AVATAR RWT

- The operational conditions

Section Thickness	Re (rated)	Ma (rated)	Re (Min)	Ma (Min)
60.0%	**7.0×106**	**0.05**	4.4×106	0.03
40.1%	**11.0×106**	**0.07**	7.0×106	0.05
35.0%	**14.0×106**	**0.09**	9.0×106	0.06
30.0%	**17.0×106**	**0.12**	10.0×106	0.07
24.0%	**20.0×106**	**0.16**	12.0×106	0.10
24.0%	**16.0×106**	**0.25**	11.0×106	0.15
24.0%	**13.0×106**	**0.30**	8.0×106	0.18
21.0%	**20.0×106**	**0.16**	12.0×106	0.10
21.0%	**16.0×106**	**0.25**	11.0×106	0.15
21.0%	**13.0×106**	**0.30**	8.0×106	0.18

List of Contents

1) Acknowledgement G. Sieros, M. Stettner
2) Acknowledgement O. Ceyhan, O. Pires
3) Acknowledgement K. Boorsma, S. Voutsinas
And all other project partners!

Measurements in DNW-HDG pressurized tunnel

- Airfoil: DU00-W-212
  - Measurements up to Re = 15M
  - DU00-W-212 is also measured by LM up to RE=6M and by Forwind at controlled turbulent conditions up to 1M
- Results are brought into a 'blind test'
  - including participants outside project

DNW-HDG model, c=15 cm

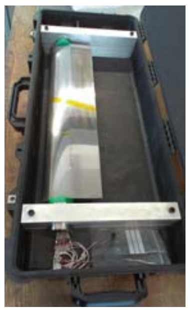

DNW-HDG Wind Tunnel

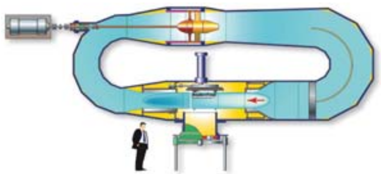

General Tunnel Characteristics

Test section : 60cmx60cm
Fan Rpm : 200 – 820 Fan blade angle fixed
Tunnel Pres. : 1 – 100 × 10^5 Pa
Tunnel Temp. : ambient to 45° C

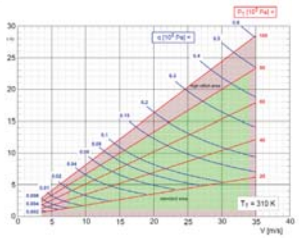

Test Section

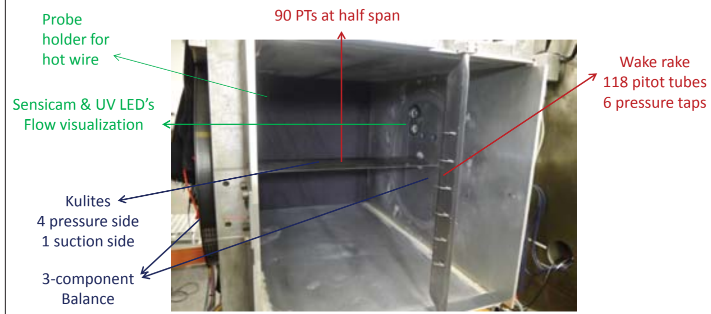

Participants/Codes

			Test 1. Re=3mil	Test 2. Re=6mil-1	Test 3. Re=6mil-2	Test 4. Re=9mil-1	Test 5. Re=9mil-2	Test 6. Re=12mil	Test 7. Re=15mil
		P_t [bars]	12	34	67	34	67	67	60
		V_{tunnel} [m/s]	25.6	19	10	28.6	15	20	28.4
Full CFD	DTU/EllipSys	Fully turbulent							
		Transition	Yes	Yes	Yes	Yes	Yes	Yes	Yes
	KIEL/TAU	Fully turbulent							
		Transition	Yes	Yes	Yes	Yes	Yes	Yes	Yes
	NTUA/Mapflow	Fully turbulent							
		Transition	Yes	Yes	Yes	Yes	Yes	Yes	Yes
	UoG/HMB	Fully turbulent	Yes						Yes
		Transition	Yes		Yes				
	Forwind-IWES/OpenFOAM	Fully turbulent	Yes	Yes	Yes	Yes	Yes	Yes	Yes
		Transition							
Panel Methods	USTUTT/XFOILvUSTUTT	Fully turbulent							
		Transition	Yes	Yes	Yes	Yes	Yes	Yes	Yes
	ORE Catapult/XFOILv6.96	Fully turbulent							
		Transition	Yes	Yes	Yes	Yes	Yes	Yes	Yes

DNW-HDG Full CFD calculations vs measurements
Effect in Blade Design parameter: Cl/Cd

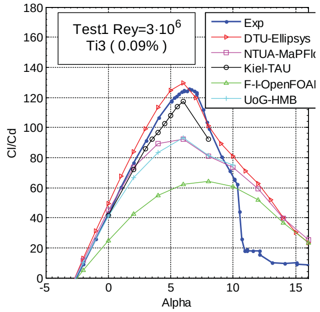

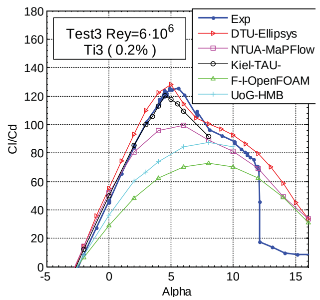

DNW-HDG Full CFD calculations vs measurements
Effect in Blade Design parameter: Cl/Cd

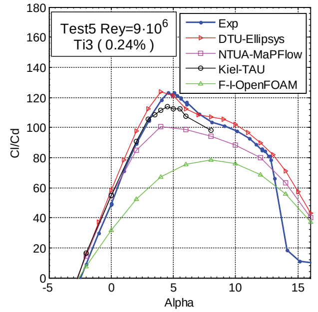

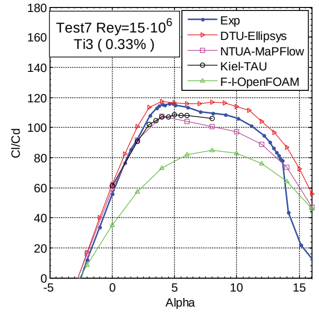

DNW-HDG Panel code calculations vs measurements
Effect in Blade Design parameter: Cl/Cd

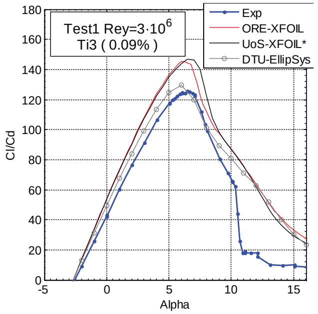

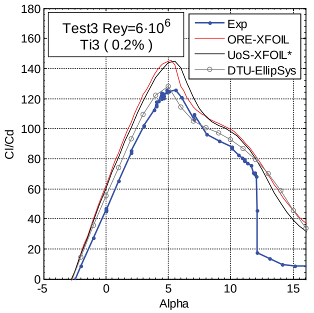

DNW-HDG Panel code calculations vs measurements
Effect in Blade Design parameter: Cl/Cd

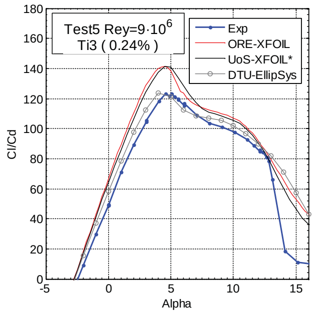

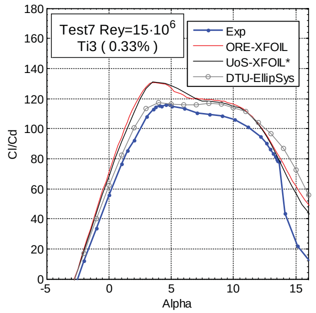

Results
Re effects in Cl/Cd trends

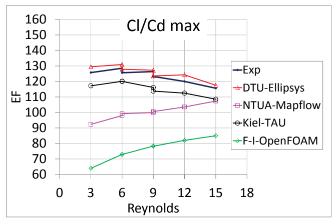

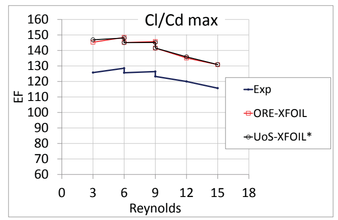

List of Contents

- ❑ Introduction into the project
- ❑ Design of AVATAR Reference Wind Turbine [1])
- ❑ Aerodynamics at high Reynolds numbers
  - Results from a blind test on airfoil measurements taken in the pressurized DNW-HDG tunnel [2])
- ❑ *Aero-elasticity of large turbines*
  - *BEM versus free wake*[3]

1) Acknowledgement G. Sieros, M. Stettner
2) Acknowledgement O. Ceyhan, O. Pires
3) Acknowledgement K. Boorsma, S. Voutsinas
And all other project partners!

ECN Aero-module

- ECN Aero Module: One code with aero-models of different degrees of fidelity (BEM and free/prescribed vortex wake) coupled to same structural solver (PHATAS/FOCUS)
  - Straightforward comparison of different aerodynamic models

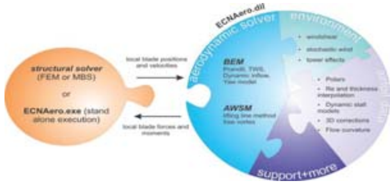

Results: Extreme transient shear

- INNWIND, rated power

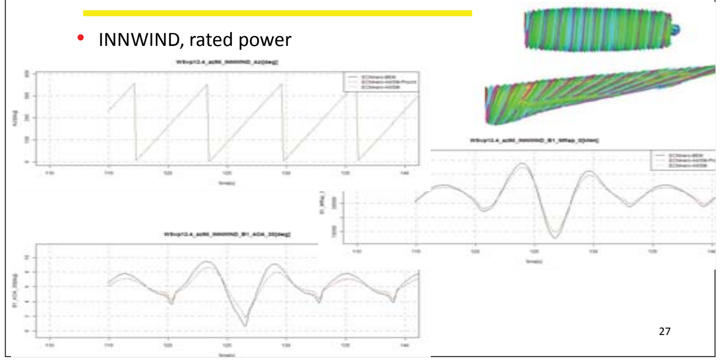

Results: Extreme transient shear

- AVATAR, partial load

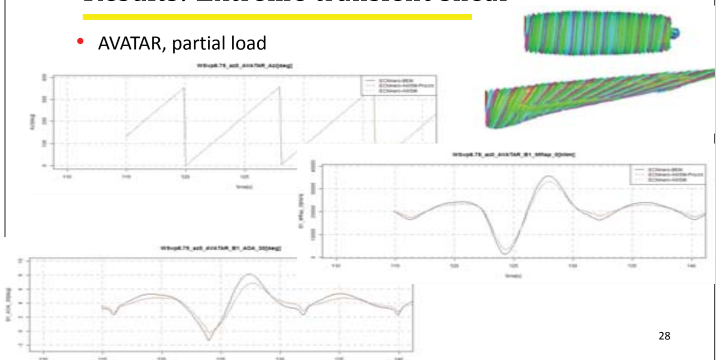

Results: Half wake

- AVATAR, rated conditions

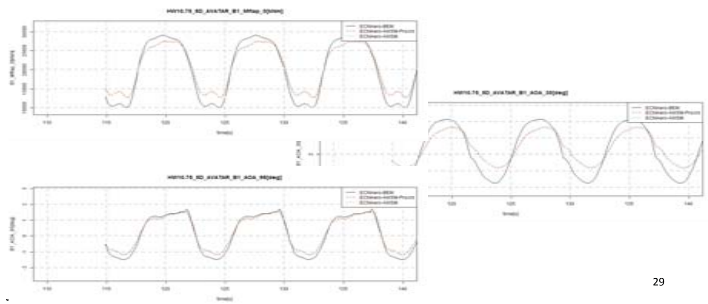

Summary

- AVATAR is an EU FP7 projects which aims to validate, improve and calibrate aerodynamic models for 10MW+ turbines with and without flow devices and with and without aero-elastic effects
- Several (wind tunnel) measurements have been taken which have helped to validate and improve (sub) models relevant for 10MW+ turbines
  - Correlation based transition models shown to be deficient at high Reynolds numbers
- Models of different degrees of fidelity are evaluated on two 10 MW reference wind turbines:
  - AVATAR low induction turbine with special aerodynamic challenges
  - INNWIND.EU conventional induction turbine
  - Engineering prediction of load fluctuations at transients/wake operation overestimated
- The amount of results is far too much to present in 20 minutes
  - All technical deliverables are public:
    http://www.eera-avatar.eu/publications-results-and-links/

Consortium

Coordinator:

ECN

Partners in alphabetical order:

CENER

KAΠE CRES CENTRE FOR RENEWABLE ENERGY SOURCES AND SAVING

DTU

ForWind Center for Wind Energy Research

Fraunhofer IWES

GE

LM WIND POWER

National Technical University of Athens

POLITECNICO DI MILANO

TU Delft

UNIVERSITY OF LIVERPOOL

University of Stuttgart Germany

FP7-ENERGY-2013-1/ n° 608396

Thank you for your attention

This project has received funding from the European Union's Seventh Programme for research, technological development and demonstration under grand agreement No FP7-ENERGY-2013-1/n° 608396 .

Vertical-axis wind turbine design load cases investigation and load comparison with horizontal axis wind turbine

C. Galinos, T.J. Larsen, H.A. Madsen, U.S. Paulsen
cgal@dtu.dk

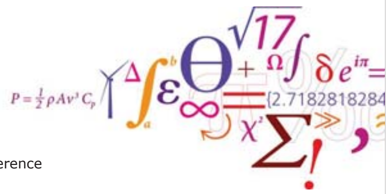

13th Deep Sea Offshore Wind R&D Conference
EERA DeepWind'2016

DTU Wind Energy
Department of Wind Energy

Outline

- Introduction
- Wind turbine minimum design requirements
  - Design load cases
  - Definition considerations
- Wind Turbine models
- Simulation tool
- Results
- Conclusions

Introduction

Large scale VAWT development

Past: Sandia 34m test bed, Eole 4MW, FloWind 19m
Present-Future: 5MW DeepWind concept, Nenuphar Vertiwind

Need to set the minimum design requirements for the structural integrity of VAWTs according to IEC/standardisation.

Wind turbine minimum design requirements

- IEC 61400-1 ed.3 standard sets minimum structural requirements for onshore wind turbines
  - The Design Load Cases (DLCs) are a combination of external conditions and wind turbine states
- DNV·GL similar criteria

Main research question
Are the IEC 61400-1, ed.3 DLCs applicable for vertical-axis wind turbines?

Wind turbine minimum design requirements

Design load cases

- Design situations
  - ➢ Normal power production
  - ➢ Emergency shut down
  - ➢ Parked rotor
- Not considered
  - ➢ Power production plus occurrence of fault
  - ➢ Start up and normal shut down
  - ➢ Transportation, assembly, maintenance and repair

Design situation	DLC	Wind condition		Other conditions
1) Power production	1.1	NTM	$V_{in} < V_{hub} < V_{out}$	For extrapolation of extreme events
	1.2	NTM	$V_{in} < V_{hub} < V_{out}$	
	1.3	ETM	$V_{in} < V_{hub} < V_{out}$	
	1.4	ECD	$V_{hub} = V_r - 2$ m/s, V_r, $V_r + 2$ m/s	
	1.5	EWS	$V_{in} < V_{hub} < V_{out}$	
2) Power production plus occurrence of fault	2.1	NTM	$V_{in} < V_{hub} < V_{out}$	Control system fault or loss of electrical network
	2.2	NTM	$V_{in} < V_{hub} < V_{out}$	Protection system or preceding internal electrical fault
	2.3	EOG	$V_{hub} = V_r \pm 2$ m/s and V_{out}	External or internal electrical fault including loss of electrical network
	2.4	NTM	$V_{in} < V_{hub} < V_{out}$	Control, protection, or electrical system faults including loss of electrical network
3) Start up	3.1	NWP	$V_{in} < V_{hub} < V_{out}$	
	3.2	EOG	$V_{hub} = V_{in}$, $V_r \pm 2$ m/s and V_{out}	
	3.3	EDC	$V_{hub} = V_{in}$, $V_r \pm 2$ m/s and V_{out}	
4) Normal shut down	4.1	NWP	$V_{in} < V_{hub} < V_{out}$	
	4.2	EOG	$V_{hub} = V_r \pm 2$ m/s and V_{out}	
5) Emergency shut down	5.1	NTM	$V_{hub} = V_r \pm 2$ m/s and V_{out}	
6) Parked (standing still or idling)	6.1	EWM	50-year recurrence period	
	6.2	EWM	50-year recurrence period	Loss of electrical network connection
	6.3	EWM	1-year recurrence period	Extreme yaw misalignment
	6.4	NTM	$V_{hub} < 0.7\ V_{ref}$	
7) Parked and fault conditions	7.1	EWM	1-year recurrence period	
8) Transport, assembly, maintenance and repair	8.1	NTM	V_{maint} to be stated by the manufacturer	
	8.2	EWM	1-year recurrence period	

IEC 61400-1,ed.3 DLCs p35

Wind turbine minimum design requirements

Considerations of the IEC 61400-1 ed.3 for VAWTs

1. The **hub-height** where the wind reference values are applied
   - ➢ In this study the rotor swept area (projected area) centre location at nominal rotor speed

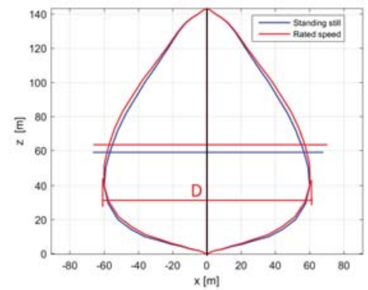

Darrieus-VAWT

Wind turbine minimum design requirements

Considerations of the IEC 61400-1 ed.3 for VAWTs

1. The **hub-height** where the wind reference values are applied
   - ➢ The rotor swept area (projected area) centre location at nominal rotor speed

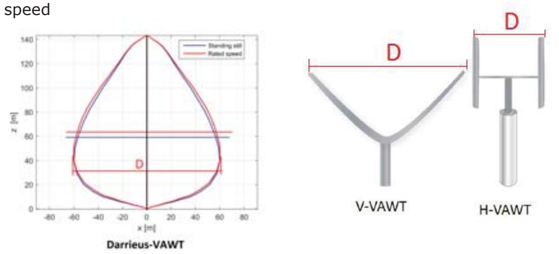

2. The **rotor diameter** is used in equations for the definition of the wind characteristics
   - ➢ The largest rotor diameter of the wind turbine at nominal rotor speed

Wind turbine models and aeroelastic code

	VAWT	HAWT
Model	Modified DeepWind rotor	NREL reference wind turbine
Rated electrical power	5 MW	5 MW
Number of blades	2	3
Power regulation	Stall	Pitch

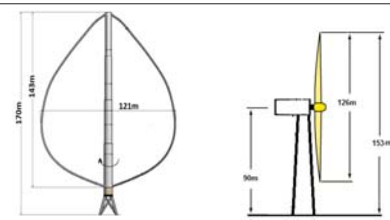

- **Simulation Tool:** HAWC2 aeroelastic code
- **Outputs:** Turbine base bottom BM, blade root BM, blade deflection

Simulation results

Power production under NTM

- Extrapolated 50 year return period extremes VAWT-HAWT

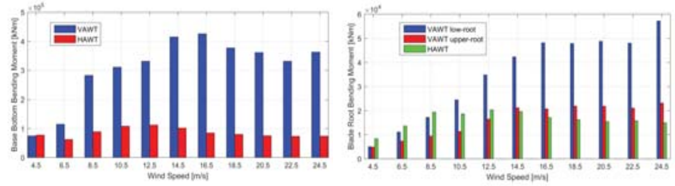

1. Larger turbine base BM for VAWT
2. VAWT blade upper root BM similar with HAWT blade root

Simulation results

Power production under NTM

- Blade equivalent 1Hz fatigue VAWT-HAWT

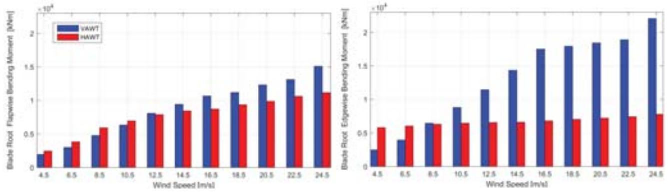

1. Flapwise BM similar magnitude
2. VAWT edgewise BM much larger at high winds

Simulation results

Extreme Operating Gust VAWT

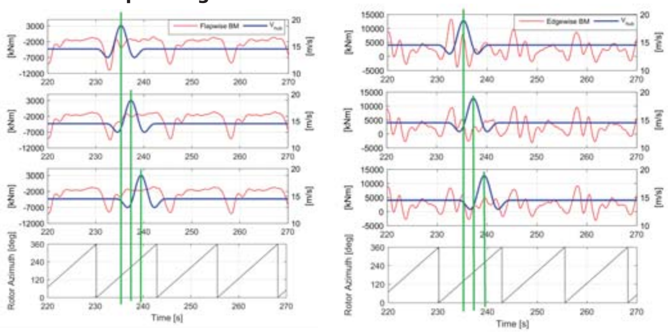

- Loads depend on the rotor orientation during the gust passage (rotor extends in 3-dimensions)

Simulation results

Emergency Shut Down VAWT

- Mechanical brake
- Emergency shut down at 220s
- 0.5s before grid loss (zero generator torque)

} Set-up

1. Turbine deceleration to 10%ω_{rated} within 11s
2. Blade loads & deformation not extreme

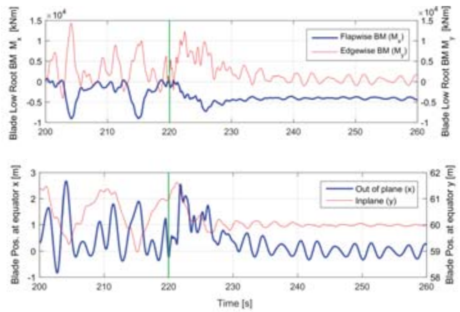

Simulation results

VAWT Parked Rotor under 50-year EWM

1. Idling rotor → non reaching equilibrium rotor speed
2. Forced rotor rotation at low rotor speed → Possible
3. Standing still (locked rotor at different orientations) → Blade instabilities

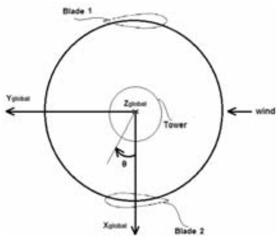

Simulation results

VAWT Parked Rotor under 50-year EWM

1. Idling rotor → non reaching equilibrium rotor speed
2. Forced rotor rotation at low rotor speed → Possible
3. Standing still (locked rotor at different orientations) → Blade instabilities

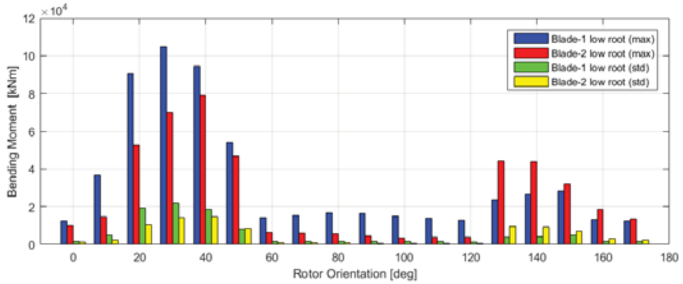

Simulation results

VAWT Parked Rotor under 50-year EWM

1. Idling rotor → non reaching equilibrium rotor speed
2. Forced rotor rotation at low rotor speed → Possible
3. Standing still (locked rotor at different orientations) → Blade instabilities

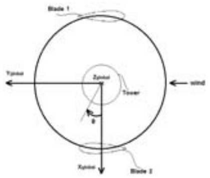

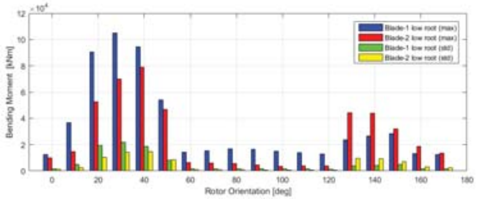

- Sensitivity analysis on blade stiffness and damping for the standing still case → Instabilities present

Simulation results

Comparison of DLCs VAWT-HAWT

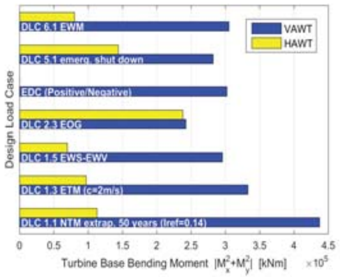

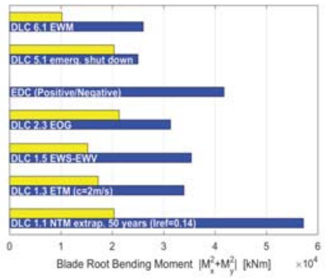

1. VAWT extreme loads emerged from DLC 1.1 higher than the transient wind events
2. HAWT load results from transients more severe (DLC 2.3)

Conclusions

VAWT DLCs

1. The examined DLCs of IEC 61400-1, ed.3 are applicable for VAWTs
2. Definitions of equivalent hub height and rotor diameter were specified
3. The loads emerged from EOG depend on the rotor orientation - gust passage combination (3D rotor in space)
4. Parked standing still rotor under extreme winds (DLC 6.2) led to blade instabilities for specific rotor orientations and seems be design driver for VAWTs

Conclusions

VAWT-HAWT load comparison

1. Under power production with NTM both VAWT ultimate and 1 Hz fatigue base bottom bending moments were higher compared to the HAWT
2. The blade root loads are of similar magnitude at low and moderate winds between the two wind turbines under normal power production
3. DLC 1.1 simulations returned the highest base bottom and blade root loads for the VAWT where the DLC 2.3 and 5.1 for the HAWT

DTU

The present work is a result of the contributions within the INFLOW project, supported by the European Commission, Grant No 296043, and by the INFLOW beneficiaries: NENUPHAR(F), IFP(F), EDF(F), EIFAGE(F), FRAUNHOFER(D), VICINAY(E), VRYHOF(NL), and DTU(DK)

A2) New turbine and generator and wind farm technology

Development of an analysis and simulation tool for a multi-rotor wind turbine floater, P.E. Thomassen, Simis

Influence of Aerodynamic Model Fidelity on Rotor Loads during Floating Offshore Wind Turbine Motions, D. Matha, Ramboll Wind

A coupled floating offshore wind turbine analysis with high-fidelity methods, V. Leble, Univ of Glasgow

INFLUENCE OF AERODYNAMIC MODEL FIDELITY ON ROTOR LOADS DURING FLOATING OFFSHORE WIND TURBINE MOTIONS

DENIS MATHA[1,2*], LEVIN KLEIN[3], DIMITRIOS BEKIROPOULOS[3], PO WEN CHENG[2]

[1]RAMBOLL WIND, GERMANY * (PREVIOUSLY WITH [2])
[2]STUTTGART WIND ENERGY, UNIVERSITY OF STUTTGART, GERMANY
[3]INSTITUTE OF AERODYNAMICS AND GAS DYNAMICS, UNIVERSITÄT STUTTGART, GERMANY

RAMBØLL

INTRODUCTION

RAMBØLL

INTRODUCTION

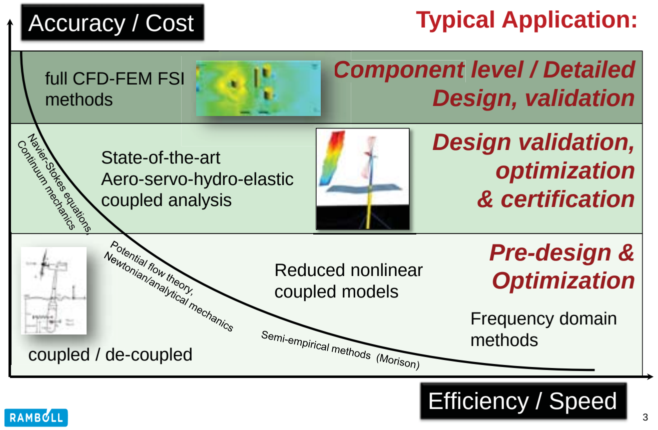

RAMBØLL 3

INTRODUCTION

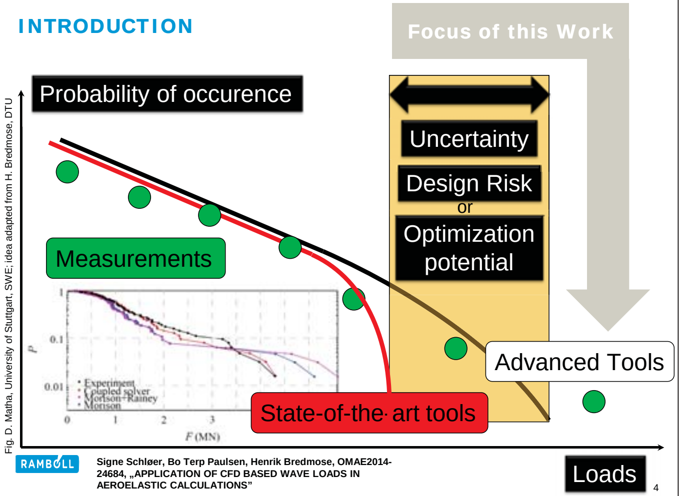

RAMBØLL Signe Schløer, Bo Terp Paulsen, Henrik Bredmose, OMAE2014-24684, „APPLICATION OF CFD BASED WAVE LOADS IN AEROELASTIC CALCULATIONS" 4

INTRODUCTION

FOWT modelling research primarily focuses on hydrodynamics and mooring line dynamics

Leading Question for this Study

- **What is the impact of Aerodynamic Model Fidelity on Rotor Loads during Floating Offshore Wind Turbine Motions?**

Presented work is related to

- OFFWINDTECH Project within EU KIC Framework and associated PhD projects in Stuttgart
- Similar questions related to model fidelity are also investigated in ongoing EU project, e.g. LIFES50+
- (no results from LIFES50+ are presented)

RAMBØLL Presented results were generated primarily at Stuttgart Wind Energy 5

INTRODUCTION

Aerodynamic effects on a floating offshore wind turbine

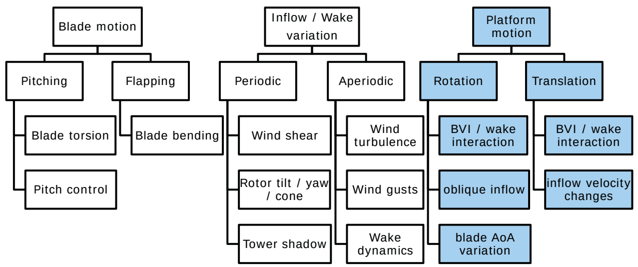

RAMBØLL 6

INTRODUCTION

- Complex 3d viscous & rotational effects
- Complex rotor interaction with
  - tower & nacelle
  - turbulent atmospheric boundary layer
  - (half) wake
  - Structure
- Wave & wind induced platform motion
- unsteady aerodynamic effects

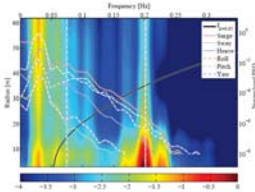

OC3 Hywind @ rated wind speed
Contour: normalized α PSD over radius
Curves: PSD of platform motions

Percentage of **aerodynamically unsteady (k > 0.05)** to total energy from α PSDs:

	Monopile	OC3Spar
Below Rated	0.3 %	18.0 %
Rated	1.7 %	17.9 %
Above Rated	0.1 %	17.9 %

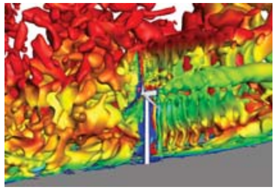

*Thomas Sebastian, "THE AERODYNAMICS AND NEAR WAKE OF AN OFFSHORE FLOATING HORIZONTAL AXIS WIND TURBINE", UMASS Dissertation, 2012

APPROACH

APPROACH
REFERENCE MODEL

Platform & Tower:
OC3 Hywind Spar Buoy
Turbine: **modified** 5MW **NREL WT**

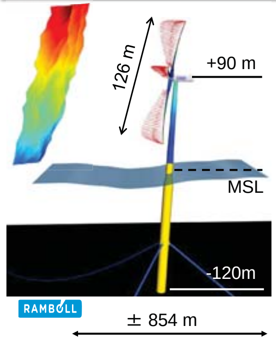

Modification of Blades & Controller:

- Recalculated airfoil tables
  - XFOIL (panel & BL code) generated to ensure comparability with new airfoils
  - Applied Viterna extrapolation, Snel 3D corrections & DS parameters for use in BEM
- Changed aerodynamic & structural twist angle
  - Goal: At rated wind speed, a lift coefficient close to todays high performance blade designs
    $c_L > 1.1$ (from $c_L > 0.95$)
- Changed generator torque controller constant
  - Adjusted for blade modifications

APPROACH
AERODYNAMIC MODELS

BEM: Blade Element Momentum Theory

- State-of-the-art in aero-servo-hydro-elastic FOWT load simulation
- Basic idea: Balance of forces in axial (and tangential) directions from global momentum balance with Forces at the local blade element
- Encompasses various assumptions & semi-empirical correction models

LLFVWM: Lifting Line Free Wake Vortex Method (Potential Flow)

- vorticity in the volume is lumped into vortex lines
  - Blade: Lifting Line (airfoil tables req.)
  - Wake: Free surface of shed vortices
- dynamic wake effects and local blade aerodynamics are inherently represented

CFD: (U)RANS (Unsteady Reynolds-Averaged Navier-Stokes)

- State of the art for complex turbulent flow simulations (not yet in wind)
- Turbulence models are applied to solve the NSE

BEM	AeroDyn 13 (NREL) AeroModule BEM (ECN)
FVM	WInDS (UMASS) AeroModule AWSM (ECN)
CFD	FLOWER (DLR/IAG) ANSYS CFX (for validation)

APPROACH
CFD MODEL

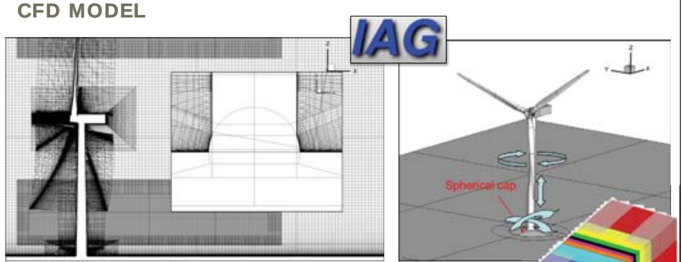

- Extended Block-structured Code FLOWER (DLR)
- 14 components
- CHIMERA overlapping mesh technique

- Background mesh
  - 400m x 400 m x 520 m
  - Δxyz ≈ 2 m
- Approx. 30 million cells
- 0.014s time-step size (≡1°)
- k-ω turbulence model

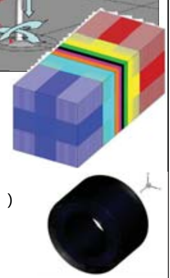

APPROACH
AERODYNAMIC ANALYSIS

1. Model Setup in 5 different aerodynamic codes, covering 3 methodologies using SIMPACK as structural WT model
2. Verification of baseline onshore loads
3. Selection of Floating Cases
   a) Extreme motions for CFD analyses for limited conditions
   b) IEC operating DLCs for inflow condition analysis
4. Performing load cases a) & b)
5. Analyzing extreme loads & inflow conditions

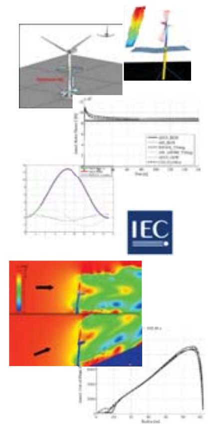

RESULTS

RAMBØLL

RESULTS
VERIFICATION OF ONSHORE LOADS

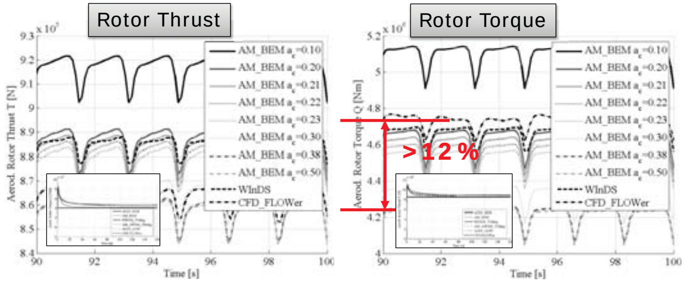

- Parametric correction model study performed to identify causes for large >12% torque deviations
- Significant influence from turbulent wake state (Glauert) correction observed due to high rotor induction level

RAMBØLL

$a_c = 0.2$

RESULTS
TURBULENT WAKE STATE CORRECTION

- Turbulent wake state correction is an empirical modification for high induction factors, where the momentum equation breaks down and predicts multiple flow directions in the wake

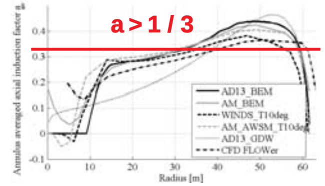

$$a = \frac{4a_c^2 F - CT}{(8a_c - 4)F}$$

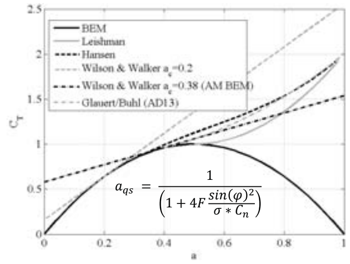

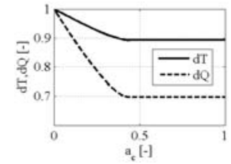

RESULTS
EXTREME MOTION ANALYSIS - THRUST

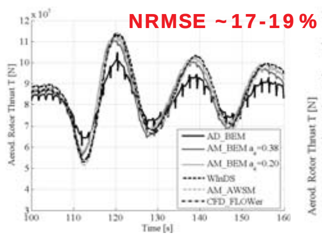

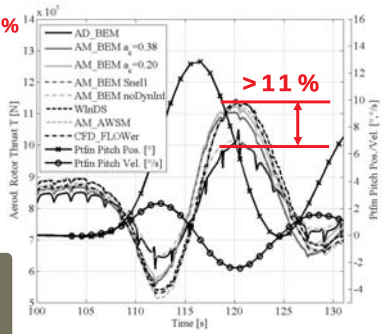

Dynamic Inflow identified as largest influence on thrust and torque differences of BEM and FVM/CFD loads
*additional pos. timeshifts

RAMBØLL

RESULTS
EXTREME MOTION ANALYSIS - TORQUE

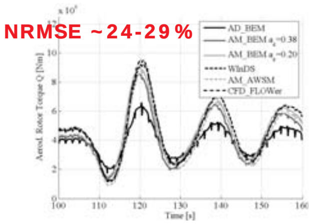

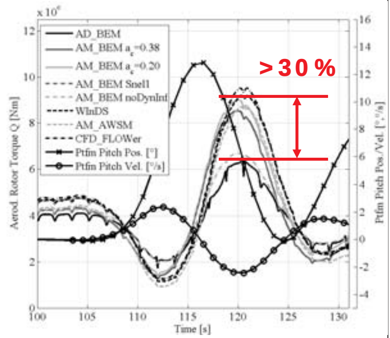

	$NRMSE(T)$	$NRMSE(Q)$
BEM no DynIn	17-19%	24-29 %
AM BEM w. DynIn $a_c = 0.20 - 0.38$	~7%	6-10 %
FVM	1-3%	2-6 %

RESULTS
EXTREME MOTION ANALYSIS – DYNAMIC INFLOW

- Simple model confirms influence of Dynamic Inflow during motions
- Sensitivity to model and time constants
- Particular relevance at specific wave periods

$$L \cdot C_T = \tau \cdot \dot{a} + a$$

$$T_{DynInf} = \frac{D}{V_\infty} = \frac{126m}{11.3m/s} = 11.15s$$

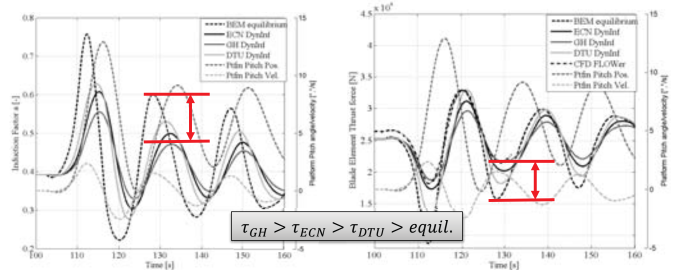

RESULTS
FLOW FIELD ANALYSIS

$$k_i = \frac{\omega c}{2|\vec{V}|} = \frac{\omega_{ptfm} c_i}{2\sqrt{U_\infty^2 + (r_i\Omega)^2}}.$$

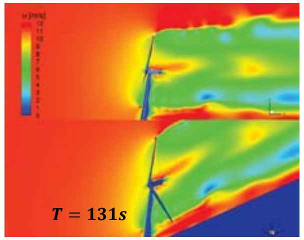

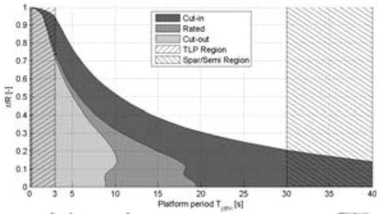

FVM: Sensitive to vortex core models
CFD: Sensitive to y⁺ and turbulence models

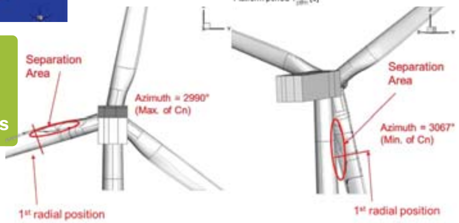

RAMBØLL

RESULTS
FLOW FIELD ANALYSIS

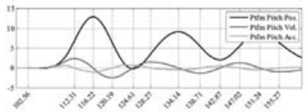

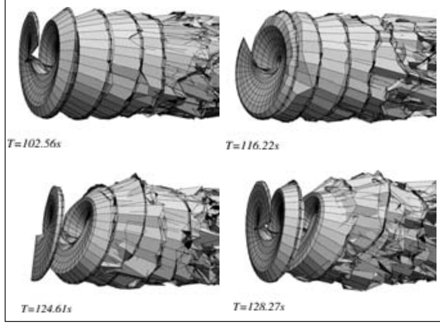

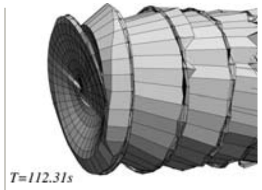

Unsteady effects
Local blade load distrib. differences:

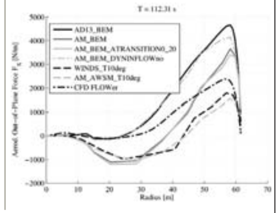

RESULTS
INFLOW CONDITIONS

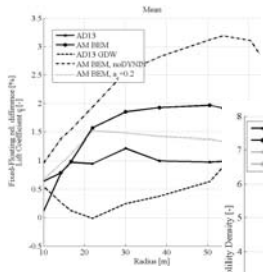

IEC DLC 1.1 @ rated wind

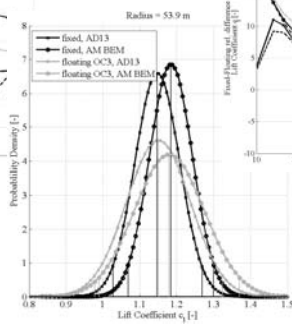

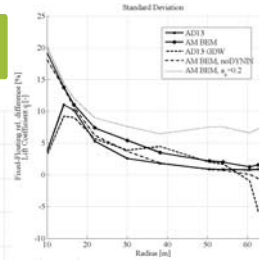

Minor impact on design point: $c_{l,ref}, Ma_{ref}, Re_{ref}$

Larger airfoil design range: $\Delta c_l, \Delta Ma, \Delta Re$

RAMBØLL

CONCLUSION

RAMBØLL

CONCLUSION

- **Study on aerodynamic model fidelity influence on FOWTs**
- **Models setup for BEM, FVM and CFD methods**

Dynamic Inflow
with important influence on thrust and torque loads and timeshifts for FOWTs

TWS correction
is important for rotors operating at high induction levels, as likely for FOWTs

Other unsteady effects
Local blade loads influenced by flow separation & BVI

Inflow conditions
Design point not-influenced
Design range increased

- **Use Dynamic Inflow models with appropriate time const.**
- **Critical assessment of local blade loads**

CONCLUSION

Upcoming IEC 61400-3-2

"IEC 61400-3-1 clause 7.3.3 is generally applicable. The aerodynamic interaction between the airflow and the FOWT is of special importance due to their additional compliance and increased dynamic response. The interaction of potentially large translational and rotational motions of the floating sub-structure with the aerodynamic loading of the RNA and tower shall be considered, including aeroelastic effects and the ***associated global and local dynamic and unsteady aerodynamic effects (e.g. dynamic inflow, oblique inflow, skewed wake, unsteady airfoil aerodynamics including dynamic stall, blade-vortex interaction).*** *Wind loads on the floating sub-structure shall also be considered, where relevant."*

RAMBØLL

THANK YOU

MARE-WINT new MAterials and REliability in offshore WINd Turbines technology

University of Glasgow

A coupled floating offshore wind turbine analysis with high-fidelity methods

DeepWind 2016
Location: Trondheim, Norway
Date: 20.01.2016
Speaker's name: Vladimir Leble

MARE-WINT
• **Adress:** Fiszera 14 St., 80-231 Gdańsk, Poland
• **Phone :** (+48) 58 699 52 85 | Fax: (+48) 58 341 61 44
• **e-mail :** marewint@marewint.eu
www.marewint.eu

MARE-WINT PROJECT

- MARE-WINT project objectives:
  - Bring together specific partners capabilities:
    - Mechanical engineering
    - Material science
    - Fluid mechanics
    - Condition monitoring
    - Reliability analysis
  - Increase reliability of floating off-shore wind turbine (FOWT) designs
  - Contribute to operation and maintenance (O&M) cost reduction
  - Balanced industry-academia network consortium includes 6 Universities, 7 Research Institutes, 4 Small and Medium-sized Enterprises and 7 Large Industry Partners
- Current research objectives
  - Develop high-fidelity tools for FOWT analysis
  - Coupled aero-hydro-elastic analysis of FOWT

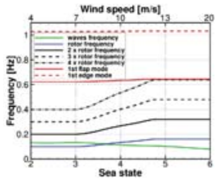

SPH •Hydrodynamics

MBDM •Multi-body solver •Mooring lines

HMB3 • Aerodynamics

→ **Coupled model of FOWT**

FOWT PROTOTYPES

- Several prototypes built including:
  - Blue H prototype
    - 2008, Italy
    - 80kW
    - Tension leg platform
  - Hywind
    - 2009, Norway
    - 2.3MW
    - Spar buoy platform
  - WindFloat
    - 2011, Portugal
    - 2MW
    - Semi-submersible platform
  - Fukushima FORWARD
    - 2013, Japan
    - 2MW
    - Semi-submersible platform


Blue H prototype


Hywind


WindFloat


Fukushima FORWARD

LITERATURE REVIEW

- Most common approach is to combine simplified tools into a hybrid model of FOWT
  - Aerodynamics
    - Simple analytical expression[1,2]
    - Blade element momentum method[3,4,5]
  - Hydrodynamics
    - Morison's equation[6]
    - Airy wave theory (inviscid, incompressible and irrotational flow)[1,3,4]
  - FOWT dynamics
    - Components
      - Rigid
      - Flexible[4,5,6]
    - Mooring lines
      - springs and dampers[6]
      - multi-body chains[7]
      - catenary equation[5]
- Current development of coupled CFD models
- No experimental data available in open literature

[1] Roddier, D., Cermelli, C., Weinstein, A., 2009. WindFloat: A Floating Foundation for Offshore Wind Turbines–Part I: Design Basis and Qualification Process. In: ASME 2009 28th International Conference on Ocean, Offshore and Arctic Engineering. ASME, pp. 845–853
[2] Karimirad, M., Moan, T., 2012. A simplified method for coupled analysis of floating offshore wind turbines. Marine Structures 27 (1), 45 – 63.
[3] Jonkman, J., November 2007. Dynamics modeling and loads analysis of an offshore floating wind turbine. Technical Report NREL/TP-500-41958, NREL
[4] Karimirad, M., Moan, T., 2013. Modeling aspects of a floating wind turbine for coupled wavewind-induced dynamic analyses. Renewable Energy 53, pp. 299–305.
[5] Skaare, B., Hanson, T., Nielsen, F., Yttervik, R., Hansen, A., 2007. Integrated dynamic analysis of floating offshore wind turbines. In: Proceedings of 2007 European Wind Energy Conference and Exhibition.
[6] Savenije, L. B., Ashuri, T., Bussel, G. J. W., Staerdahl, J. W., 2010. Dynamic modeling of a spar-type floating offshore wind turbine. In: Scientific Proceedings European Wind Energy Conference & Exhibition.
[7] Matha, D., Schlipf, M., Cordle, A., Pereira, R., Jonkman, J., June 2011. Challenges in simulation of aerodynamics, hydrodynamics, and mooring-line dynamics of floating offshore wind turbines. In: 21st Offshore and Polar Engineering Conference.

HELICOPTER MULTI-BLOCK (HMB3) SOLVER

- Control volume method
- Parallel - Shared and Distributed memory
- Multi-block (complex geometry) structured grids
- Unstructured mesh method
- Smoothed Particle Hydrodynamics method
- Unsteady RANS - Variety of turbulence models including LES/DES/SAS
- Implicit time marching and harmonic balance methods
- Osher's and Roe's schemes for convective fluxes
- All-Mach schemes based on AUSM/+UP and Roe
- MUSCL scheme for formally 3rd order accuracy
- Central differences for viscous fluxes
- Krylov subspace linear solver with pre-conditioning
- Moving grids, sliding planes, overset method
- Hover formulation, rotor trimming, blade actuation
- Documentation
- Validation database
- Range of utilities for processing data, structural models etc.
- Used by academics and engineers

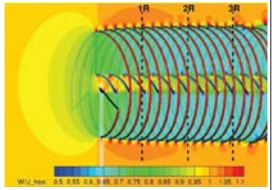

HELICOPTER MULTI-BLOCK (HMB3) SOLVER CONT.

- HMB2 was validated for several wind turbine cases including:
  - NREL Annex XX[1][2] experiment
    - 2 bladed wind turbine
    - 18M cells for the rotor, nacelle and tower
    - k-ω SST turbulence model
    - Wind speed 7m/s
    - Rigid and elastic blades
    - Rotational speed 72RPM
    - Tip speed ratio 5.4

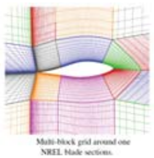

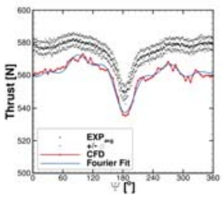

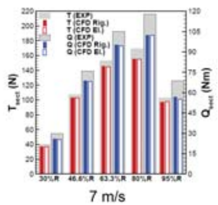

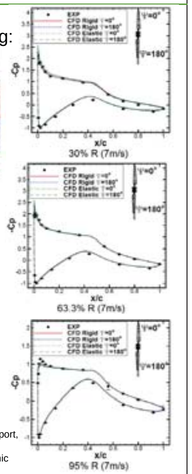

[1] M.M. Hand, D.A. Simms, L.J. Fingersh, D.W. Jager, J.R. Cotrell, S. Schreck, and S.M. Larwood. Unsteady Aerodynamics Experiment Phase VI: Wind Tunnel Test Configurations Available Data Campaigns. NREL Technical Report, December 2001.
[2] Gomez-Iradi, S., Steijl, R., and Barakos, G. N., "Development and Validation of a CFD Technique for the Aerodynamic Analysis of HAWT," Journal of Solar Energy Engineering, Vol. 131, (3), 2009, pp. 031009. doi: 10.1115/1.3139144

HELICOPTER MULTI-BLOCK (HMB3) SOLVER CONT.

- HMB2 was validated for several wind turbine cases including
  - MEXICO[1][2][3] project experiments
    - 3 bladed wind turbine
    - 2000M cells for the full rotor and wake capture
    - Wind speed 15m/s
    - Rotational speed 424.5RPM
    - Tip speed ratio 6.67

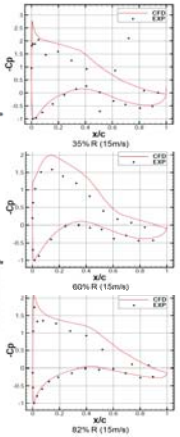
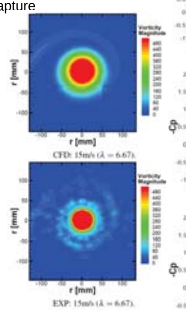
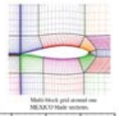
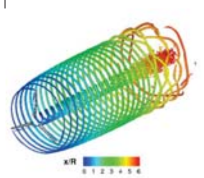
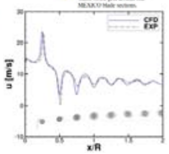

[1] J.G. Schepers and H. Snel. Final Report of IEA Task 29, MexNext (Phase I): Analysis of MEXICO Wind Tunnel Measurements. Technical report, ECN, February 2012.
[2] Carrion, M., Steijl, R., Woodgate, M., Barakos, G., Munduate, X., and Gomez-Iradi, S., "Computational fluid dynamics analysis of the wake behind the MEXICO rotor in axial flow conditions," Wind Energy, 2014. doi: 10.1002/we.1745
[3] Carrion, M., Woodgate, M., Steijl, R., Barakos, G. N., Gomez-Iradi, S., and Munduate, X., "Understanding Wind-Turbine Wake Breakdown Using Computational Fluid Dynamics,"AIAA Journal, Vol. 53, (3), 2015, pp. 588 – 602. doi: 10.2514/1.J053196

SMOOTHED PARTICLES HYDRODYNAMICS (SPH)

- Particle method, where each particle represents the volume of the fluid
- Solves N/S equations in Lagrangian form
- Assumes weak compressibility of the fluid
- Moving boundaries and free surface resolved naturally
- Does not require floating structure-fluid coupling
- Employs weighted average approach limited by kernel function
- Derivatives of field functions are replaced by the derivative of kernel function
- Various kernel functions are implemented
  - Cubic spline
  - Quadratic spline
  - Gaussian
- Various explicit time integration schemes are implemented
  - Symplectic
  - Verlet

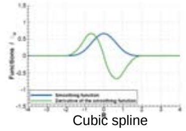
Cubic spline

SMOOTHED PARTICLES HYDRODYNAMICS (SPH) CONT.

- Lagrangian form of governing equations in SPH
  - Continuity equation

$$\frac{D\rho}{Dt} = -\rho\nabla\cdot\mathbf{U} \longrightarrow \frac{D\rho_i}{Dt} = \sum_{i=1}^{N} m_j \mathbf{U}_{ij}\nabla_i W_{ij} \qquad \mathbf{U}_{ij} = \mathbf{U}_i - \mathbf{U}_j$$

  - Momentum equation

$$\frac{D\mathbf{U}}{Dt} = -\frac{1}{\rho}\nabla p + \mathbf{g} + \Gamma \longrightarrow \frac{D\mathbf{U}_i}{Dt} = -\sum_{j=1}^{N} m_j\left[\frac{p_j}{\rho_j^2} + \frac{p_i}{\rho_i^2} + \Pi_{ij}\right]\nabla_i W_{ij} + \mathbf{g}$$

  - Equation of state

$$p = B\left[\left(\frac{\rho}{\rho_0}\right)^{\gamma} - 1\right]$$

More details:
[1] Liu G.R. and Liu M.B. *Smoothed particle hydrodynamics - a meshfree method. World Scientific,* Singapore, 2003.
[2] Monaghan J.J. Smoothed particle hydrodynamics. *Annual review of astronomy and astrophysics,* 30:543–574, 1992.
[3] Monaghan J.J. Simulating free surface flows with sph. *Journal of Computational Physics, 110(2):399* – 406, 1994.

SMOOTHED PARTICLES HYDRODYNAMICS (SPH) CONT.

- SPH method key steps: **a)** represent the problem domain by a set of particles **b)** use particle approximation and iteratively choose particle **c)** find all the particles close to the current particle **d)** flag the interaction particles **e)** solve the NS equations using all the particles within the support domain **f)** update the particle to its new position.

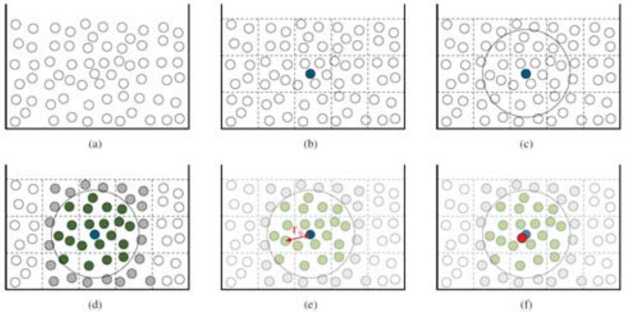

SMOOTHED PARTICLES HYDRODYNAMICS (SPH) CONT.

- High speed entry of a half-buoyant cylinder into calm water.

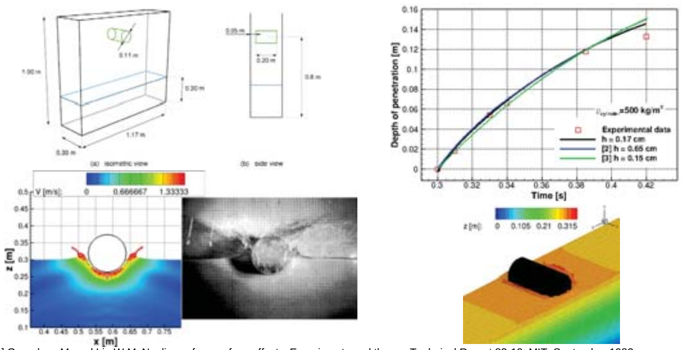

[1] Greenhow M. and Lin W.M. Nonlinear-free surface effects: Experiments and theory. Technical Report 83-19, MIT, September 1983.
[2] Vandamme J., Zou Q., and Reeve D.E. Modeling floating object entry and exit using smoothed particle hydrodynamics. *Journal of Waterway, Port, Coastal and Ocean Engineering, 137(5):213–224, 2011.*
[3] Skillen A., Lind S., Stansby P.K., and Rogers B.D. Incompressible Smoothed Particle Hydrodynamics (SPH) with reduced temporal noise and generalised Fickian smoothing applied to body-water slam and efficient wave-body interaction. *Computer Methods in Applied Mechanics and Engineering, (0):–,* 2013.

MULTI-BODY DYNAMIC MODULE (MBDM)

- Assumptions of the model:
  - Rigid bodies
  - Frictionless joints
- Unit quaternions are employed to orient bodies in space
- The non-linear constraint equations
  - Solved using Newton-Raphson method with exact analytical Jacobian
- System of mixed differential-algebraic equations
  - Solved with the coordinate partitioning method[1]
- Explicit integration schemes
  - Forward Euler
  - Symplectic
  - Runge-Kutta 4th order
- Additionally
  - Arbitrary number of springs and dampers
    - Between bodies
    - Between bodies and prescribed points

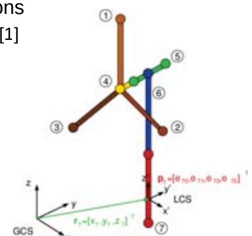
Example of the FOWT modelled with MBDM

[1] Nikravesh, P. E., Computer-aided Analysis of Mechanical Systems, Prentice-Hall, Inc., Upper Saddle River, NJ, USA, 1988.

MBDM VALIDATION

- Slider-crank dynamic model results
  - Constant torque applied to the crank: $41.450 \cdot 10^3$ Nm
  - Gravity force acting in positive *x* direction
  - Slider acts as a compressor with reaction force F_c
  - Runge-Kutta 4th order scheme with Δt=0.001s

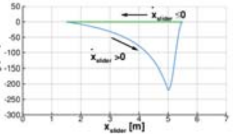

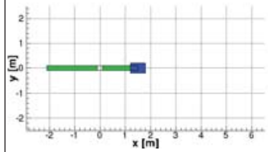

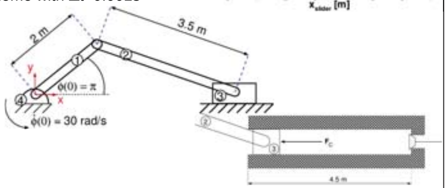

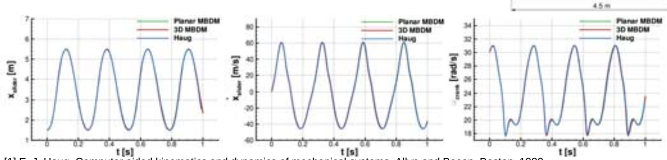

[1] E. J. Haug, Computer aided kinematics and dynamics of mechanical systems. Allyn and Bacon, Boston, 1989.

MBDM VALIDATION CONT.

- Gyroscopic wheel results
  - Constant rotational speed of the wheel:
    $\omega_w = 60 rad/s$
  - Gravitational force applied to all bodies
  - Analytical precession obtained from the gyroscopic approximation:
    $\omega_p = \tau/L = m_w g l / I_{xx} \omega_w$

Name	Mass [kg]	Inertia tensor [$kg \cdot m^2$]
Wheel	28.3	$\begin{bmatrix} 1.45 & 0 & 0 \\ 0 & 0.73 & 0 \\ 0 & 0 & 0.73 \end{bmatrix}$
Rod	0.1	$\begin{bmatrix} 10^{-6} & 0 & 0 \\ 0 & 8.3 \cdot 10^{-5} & 0 \\ 0 & 0 & 8.3 \cdot 10^{-5} \end{bmatrix}$

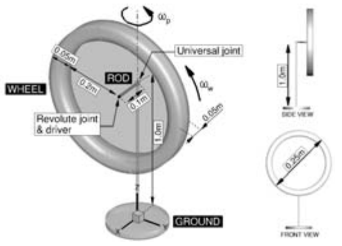

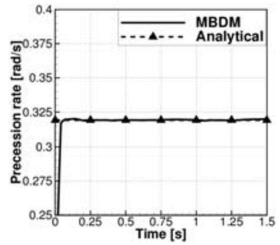

COUPLING

- Coupling problems have been extensively studied
  - Fluid-Structure Interaction
  - Thermal-Structure Interaction
  - Structure-Soil Interaction
- Coupling methods
  - Weak (loose)
    - explicit schemes
    - each solver evaluated only once per time step
    - simple to implement and computationally inexpensive
  - Strong (tight)
    - implicit schemes
    - require multiple evaluation of solution with each step
    - slow convergence with simple relaxation methods
      - Adaptive Aitken relaxation, fixed under-relaxation, steepest descent relaxation
    - fast convergence if Jacobians are employed, most likely requires approximation of Jacobian-vector product
      - Interface Quasi-Newton algorithm with an approximation for the inverse of the Jacobian from a Least-Squares model
      - Interface Block Quasi-Newton with an approximation for the Jacobian from a Least-Squares model
      - Interface Generalised Minimal Residual method
    - difficult to implement and computationally expensive

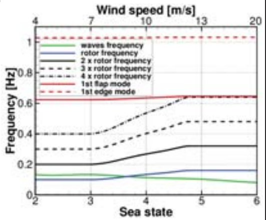

WEAK COUPLING

- Communication through the Message Passing Interface (MPI)
- MBDM substitutes the body motion routines of the SPH solver:
  - reduces the number of coupled solvers to two - SPH and HMB3
- SPH time step of $\Delta t_{SPH} = 2 \cdot 10^{-4}$ s – required by explicit scheme
- HMB3 time step of $\Delta t_{HMB3} = 2 \cdot 10^{-2}$s =100 Δt_{SPH} – dual-time implicit method
- Synchronisation of the solvers at the end of each HMB3 step
- Parallel conventional staggered method
  - At each synchronisation time step
    - position and velocities of the rotor are transferred to the HMB3
    - forces and moments on the rotor are passed to the SPH
  - Advance both solvers in parallel to a new time level
    - SPH performs 100 symplectic steps keeping forces constant
    - HMB2 performs 250 implicit pseudo-time steps keeping position and velocities constant
  - Once the synchronisation point is reached, repeat

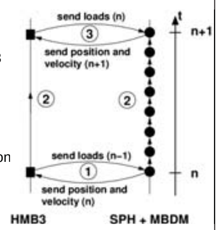

MPI IMPLEMENTATION

- MBDM is in charge of starting both solvers
- MBDM replaces SPH's body motion routines
- MBDM gathers all the information about forces and moment and returns positions and velocities

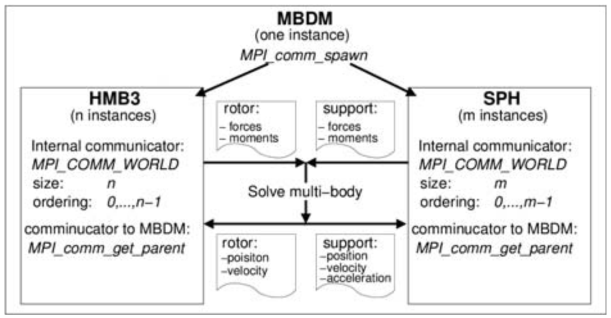

TEST CASE DESCRIPTION

- DTU 10MW reference wind turbine[1]
  - Designed for offshore application
  - Only tower is designed, no floating support
  - Number of blades 3
  - Rotor diameter 178.3m
  - Hub height 119 m
  - Rated power 10-MW
  - Rated wind speed 11.4 m/s
  - Rotor pre-cone angle -2.5°
  - Blade pre-bend 3.3m
  - Nacelle tilt 5°
  - Upwind configuration

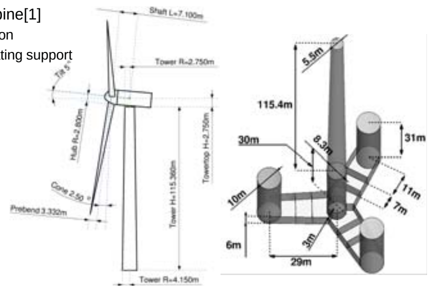

- Floating support design
  - mass properties

Component	Mass [kg]
Support	$2,351,188 \cdot 10^3$
Tower	$628,442 \cdot 10^3$
Nacelle	$446,036 \cdot 10^3$
Rotor	$227,962 \cdot 10^3$
Total	$3,653,628 \cdot 10^3$
Total with balast	$4,451,900 \cdot 10^3$

– estimated mechanical properties

Draft	7.25 m
CoG below SWL	0.0 m
Roll inertia about centre of mass (Ixx)	$2.030 \cdot 10^{10}$ kg·m²
Pitch inertia about centre of mass (Iyy)	$2.030 \cdot 10^{10}$ kg·m²
Yaw inertia about centre of mass (Izz)	$2.809 \cdot 10^{9}$ kg·m²

[1] Bak C., Zhale F., Bitsche R., Kim T., Yde A., Henriksen L.C., Andersen P.B., Natarajan A., and Hansen M.H. Description of the DTU 10 MW Reference Wind Turbine. DTU Wind Energy Report-I-0092, Technical University of Denmark, June 2013.

TEST CASE DESCRIPTION CONT.

- HMB2 aerodynamic domain
  - 8M cells mesh for the full rotor and nacelle
  - k-ω SST turbulence model
- SPH hydrodynamic domain
  - 5M particles
  - Artificial viscosity model
  - Cubic spline kernel
- MBDM configuration
  - 2 rigid bodies
  - 3 mooring lines as springs and dampe
  - 1 revolute driver of constant speed
- Waves imposed by sinusoidal paddle motion and dissipated by a beach-like slope
- Initial conditions obtained separately before coupling

Rotor	
m [kg]	227,962
I [kg·m²]	[1.56·10⁸ 0 0; 0 7.84·10⁷ 0; 0 0 7.84·10⁷]
Nacelle, support and tower	
m [kg]	4,223,938
I [kg·m²]	[2.03·10¹⁰ 0 0; 0 2.03·10¹⁰ 0; 0 0 2.81·10⁹]
Mooring lines	
120.0	Angle between adjacent lines [°]
20.6	Depth of anchors below SWL [m]
7.0	Depth of fairleads below SWL [m]
116.73	Length of the relaxed line [m]
400·10⁶	Mooring line extensional stiffness [N/m]
40,000	Mooring line damping coefficient [Ns/m]

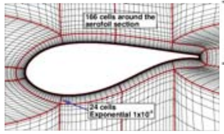

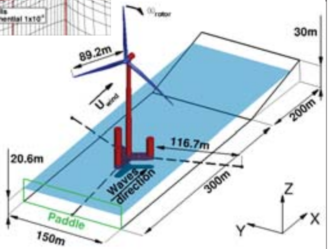

DECOUPLED COMPUTATIONS

- Aerodynamic forcing is prescribed: constant or time varying thrust applied at the location of nacelle
- Variation of thrust estimated form CFD computation
- Calm water
- Inertia properties of the rotor not considered – no gyroscopic effect
- Centre of mass offset due to rotor overhung not included

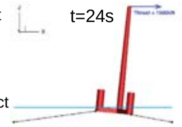

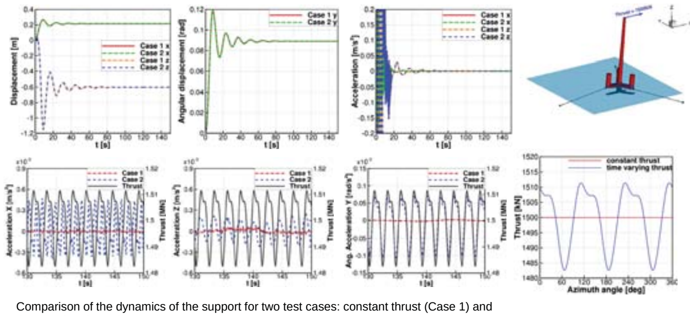

Comparison of the dynamics of the support for two test cases: constant thrust (Case 1) and time varying thrust (Case 2)

RESULTS OF WEAKLY COUPLED COMPUTATION

- Parallel conventional staggered method

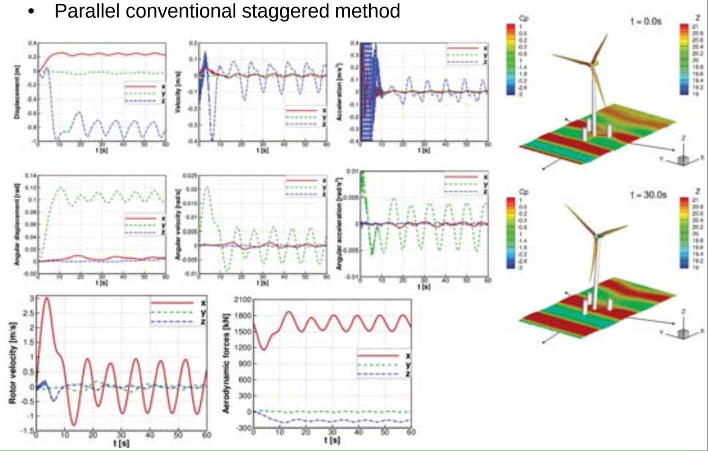

RESULTS OF WEAKLY COUPLED COMPUTATION CONT.

- Displacement in the direction of wind and waves by ~0.25m
- Sinking by ~0.9m
- Maximum dynamic pitch ~0.12rad (~6.9deg)
- Initial settling dominates over the first wave passage
- The effect of consecutive wave passages clearly visible
- Initial high frequency response due to the sudden release of the floating body

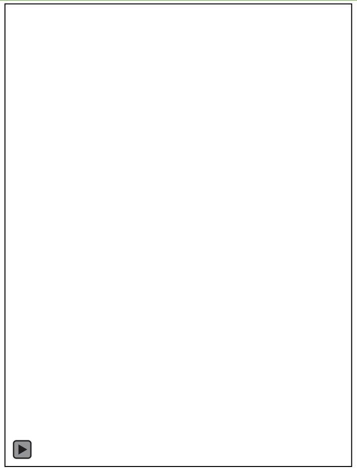

SUMMARY AND FUTURE WORK

- The work has so far developed the weakly coupled method necessary for realistic simulation of dynamic FOWTs
- Strongly coupled model is being developed
- There is a clear need for validation data from scaled or full-size FOWTS
- There is also a clear need for time-resolved aerodynamic data alongside the usual forces, accelerations and moments measured in water-basins
- Future work includes
  - Implementation of other coupling algorithms – weak and strong
  - Implementation of mooring lines as set of rigid bodies linked by springs and dampers, or alternatively with the catenary line equation
  - FOWT model with tower, elastic blades and actuated flaps
  - Attempt to couple a load control algorithm with the flap actuation
  - Analysis of the WT undergoing prescribed yawing and pitching motion

MARE-WINT new MAterials and REliability in offshore WINd Turbines technology
University of Glasgow

THANK YOU FOR YOUR ATTENTION

www.marewint.eu

B1) Grid connection and power system integration (Windgrid)

High Density MMC for platform-less HVDC offshore wind power collection systems (KEYNOTE), Chong NG, Offshore Renewable Catapult

Cluster Control of Offshore Wind Power Plants Connected to a Common HVDC Station, J.N. Sakamuri, DTU Wind Energy

Coordinated Tuning of Converter Controls in Hybrid AC/DC Power Systems for System Frequency Support, A. Endegnanew, SINTEF Energi

Fulfilment of Grid Code Obligations by Large Offshore Wind Farms Clusters Connected via HVDC Corridors, A.B. Attya, Univ of Strathclyde

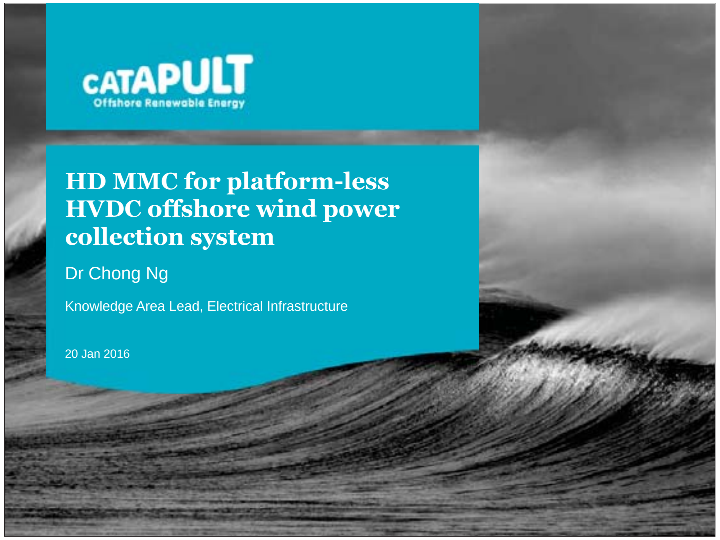

CATAPULT Offshore Renewable Energy

HD MMC for platform-less HVDC offshore wind power collection system

Dr Chong Ng

Knowledge Area Lead, Electrical Infrastructure

20 Jan 2016

Content

- ORE Catapult introduction
- Platform-less Offshore HVDC System
  - Research History
  - Current Status
- HD MMC
  - State of the art
  - HD Proposed Solution

Catapults: A long-term vision for innovation & growth

Cell Therapy Catapult | Connected Digital Economy Catapult | Future Cities Catapult | High Value Manufacturing Catapult | Offshore Renewable Energy Catapult | Satellite Applications Catapult | Transport Systems Catapult

- Established and overseen by the Technology Strategy Board
- Bridging the gap between business, academia, research and government to create new products and services
- Open up global opportunities and generate sustained economic growth for the future
- Delivering the 'know-how' economy

7 Catapults

£1.4bn private and public sector investment

Offshore Renewable Energy (ORE) Catapult

3

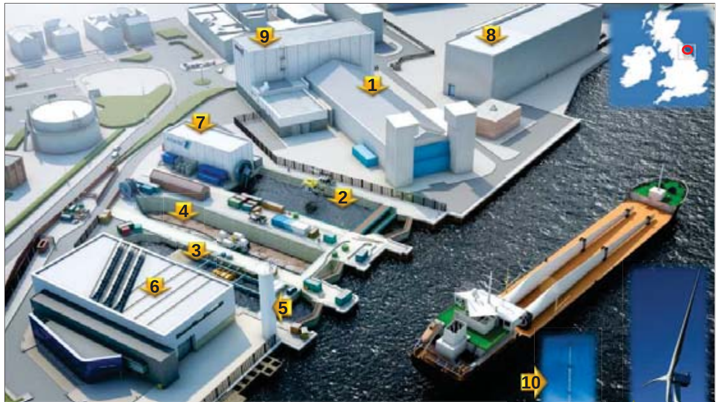

A Controlled and Independent Development Platform

Existing
1. 50m blade test
2. Still water tank
3. Wave flume
4. Simulated seabed
5. Wind turbine training tower
6. Electrical and materials laboratories

New
7. 3MW tidal turbine drive train
8. 100m Blade Test Facility
9. Wind Turbine Nacelle Test Facility-2013
10. Offshore anemometry hub
11. 7MW Wind Turbine

Electrical (HV & LV) Test Lab – Brief

- HV development laboratories – 600kVac, 1MVdc, 8kA, Rain drop simulator, Material lab
- Live environmental chamber – HV and current into chamber
- Flexible three phase LV network – generators & converters array (up to 100kW)
- Grid conformance testing – G59 test equipment in the facility
- 11kV 50Hz network available
- Vibration test rig – loads up to 500kg for endurance and accelerated ageing programmes

Project Example

HD MMC for Platform-less Offshore HVDC System

EPSRC narec

Project Example

Research History in here

Platform-less Offshore HVDC System

Objective: Develop a dedicated high fault tolerances, flexible and cost effective power collection technology for offshore wind industry

Features:

- HVDC power transmission from the very beginning
  - Reduce losses and components
- Decentralised multi-terminal HVDC system
  - Increase availability – Offers flexibility and redundancy
  - Reduce cost – Removal/minimise offshore substation
- Increase MMC voltage level without additional hardware

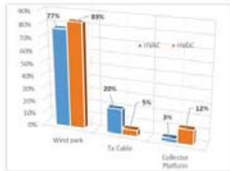

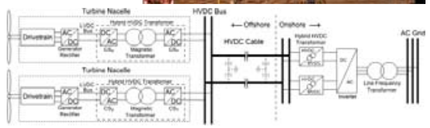

Converter topology analysis

Analysed across frequency range; 100Hz to 2kHz, single phase

Findings:
Transformer core loss ≤ converter loss
Transformer core loss ≤ copper loss

HB-HB configuration:
+ Lower component count
+ Lower converter loss
- Less stable (power control) due to higher voltage gradient
- Higher transformer loss (i.e. 1% higher than MMC)

MMC-MMC configuration:
+ Better control stability (<500Hz)
+ Lower transformer core loss
- Higher component count
- Higher converter loss

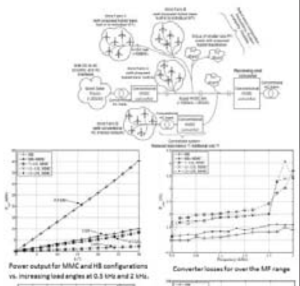

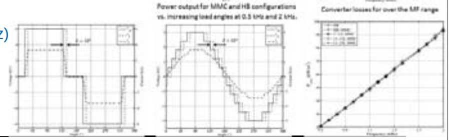

Results

- Different converter configurations modelled in Simulink
  - HB-HB
  - HB-MMC
  - MMC-MMC
- Based on input waveforms, the transformer specifications are optimised and losses calculated
- Repeated for frequencies between 500 – 2,000 Hz
- Optimum configuration found to be HB-MMC at 1.4 kHz
- Majority of losses attributed to converter conduction losses
- This can be decreased by moving to 3-phase

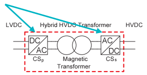

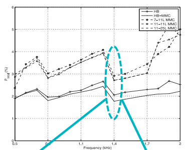

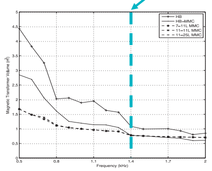

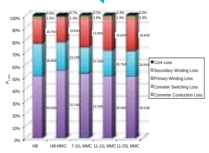

The Modular Multilevel Converter

- Its modular design make it ideal for scaling up.
  - Now used in a variety of applications, including HVDC
- Very attractive for offshore wind
  - Low THD on AC terminal therefore no bulky filters
  - High Efficiency
  - High degree of controllability

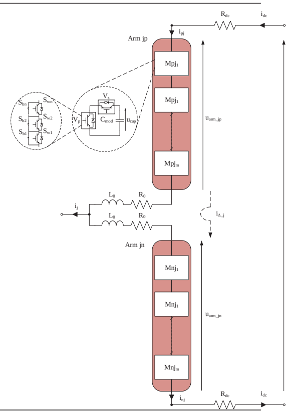

The Modular Multilevel Converter (MMC) Limitations

- Each module can only create 1 AC voltage level L_{conv}:

$$L_{conv} = n_{mod} + 1$$

- Therefore many modules required to reduce THD < 3 % (≈ 30)
- Each module requires 2 valves and a large capacitor
  - Capacitor contributes to roughly 50 % of the module volume
- Therefore low THD increases converter losses but crucially converter size and weight
- A LARGE offshore platform required to support it.
- Platform accounts for ≈ 70 % of substation cost therefore significant savings possible by reducing size

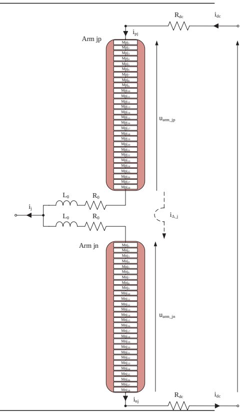

The High Definition Modular Multilevel Converter

- By using the novel HD-MMC control algorithm 1 module corresponds to **multiple AC voltage levels**
- Using the HD-MMC algorithm only **12 modules** are required to create **29 L**
- This is achieved by grouping modules into sets, controlling each to provide additional voltage levels such that L_{HD} is given by:
- Therefore **fewer** capacitors and **fewer** valves
- This results in a more compact converter reducing platform size and cost

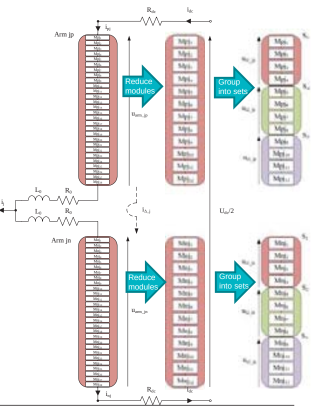

Proposed HD-MMC Control

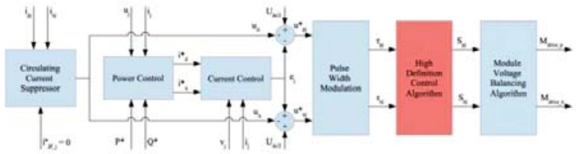

- Non intrusive, the HD-MMC control algorithm (red) can be inserted as an add on to the standard control methods (blue) of the MMC.
- This simplifies implementation

HD-MMC Simulation Results

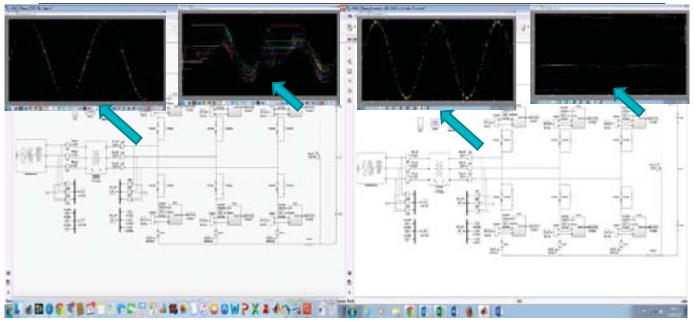

- On the left is a standard 28 level MMC and on the right is the HD-MMC concept.
- Capacitor voltages are maintained at set value throughout simulation

Contact us

ORE Catapult
Inovo
121 George Street
Glasgow
G1 1RD

T +44 (0)333 004 1400
F +44 (0)333 004 1399
info@ore.catapult.org.uk

ORE Catapult
National Renewable Energy Centre
Offshore House, Albert Street
Blyth, Northumberland
NE24 1LZ

T +44 (0)1670 359 555
F +44 (0)1670 359 666
info@ore.catapult.org.uk

ore.catapult.org.uk

Cluster Control of Offshore Wind Power Plants Connected to a Common HVDC Station

Ömer Göksu[1], Jayachandra N. Sakamuri[1], C. Andrea Rapp[2], Poul Sørensen[1], Kamran Sharifabadi[3]
[1]DTU Wind Energy, [2]Halvorsen Power System AS, [3]Statoil ASA

EERA DeepWind'2016
13th Deep Sea Offshore Wind R&D Conference
20-22 January 2016, Trondheim, Norway

DTU Wind Energy
Department of Wind Energy

Outline

- Offshore Wind Power Plant (WPP) Clusters
- Generic benchmark layout with 3 WPPs
- ENTSO-E Generator and HVDC requirements
- IEC 61400-27 Wind Turbine and WPP control models

- Offshore AC Grid Voltage Control
  - Problem: Uncontrolled reactive power flow between WPPs and HVDC
  - Proposal: Droop control at each WPP

- Power Oscillation Damping (POD) with the Offshore WPP Cluster
  - Problem: Unsynchronized active power from the WPPs
  - Proposal: Coordinated closed loop cluster regulator at the HVDC

- Conclusion

Cluster connected WPPs to common HVDC examples from the North Sea

[http://www.siemens.com/press/pool/de/pressebilder/2013/photonews/300dpi/PN201312/PN201312-10e_300dpi.jpg]

Clusters due to distance between the WPPs,
combination of different WT models, WT / HVDC manufacturers

Cluster connected WPPs to common HVDC a generic benchmark layout with individual WPP controllers

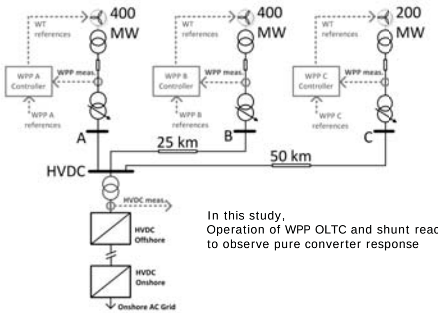

In this study,
Operation of WPP OLTC and shunt reactors are omitted
to observe pure converter response

Cluster with individual WPP controllers (plus offshore cluster controller);
promising for future installations at the North Sea and UK

ENTSO-E Grid Code Requirements

Network Code on Requirements for Grid Connection Applicable to all Generators (NC-RfG)

Final Draft: June 2015

Network code on requirements for grid connection of HVDC systems and DC-connected power park modules (NC-HVDC)

Final Draft: October 2015

Offshore AC Grid Voltage Control by HVDC station
(WPPs are considered to contribute to voltage control)

POD by HVDC stations
(DC-connected WPPs may potentially contribute to POD)

IEC 61400-27-1 Wind Turbine Models

- RMS models for dynamic response of
  - Type 1, Type 2, Type 3, and Type 4A/B (with full/partial chopper)
- Being validated by wind turbine manufacturers (IEC working group)

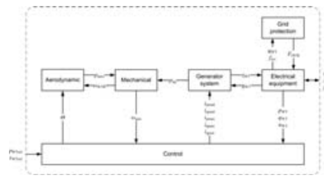

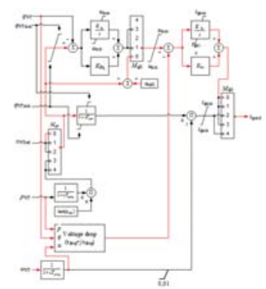

- Local fast voltage control at WT terminals
- Active power control (deloaded operation)
- Fault ride-through functions

Type 4B is utilized in this study

IEC Wind Power Plant Voltage Control

Reactive Power Options: Power factor / **voltage** / reactive power / U(Q) Static control
WPP closed loop active power control (deloaded operation)

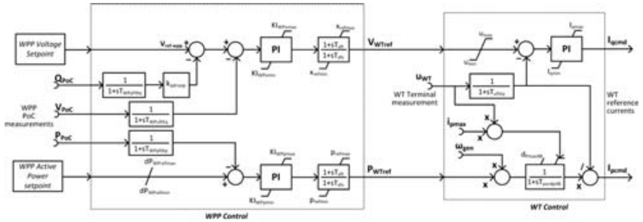

Voltage control with droop compensation (K_{qdroop})

$$V_{WPPref-compensated} = V_{WPPref} - Q_{WPPactual} \cdot K_{qdroop}$$

WPP voltage reference is modified with the actual Q of the WPP

Offshore AC Grid Voltage Control: via Local Voltage Control by the WPPs

Problem: Uncontrolled reactive power flow between WPPs and HVDC
HVDC injects & WPPs absorb Q → Increase of losses

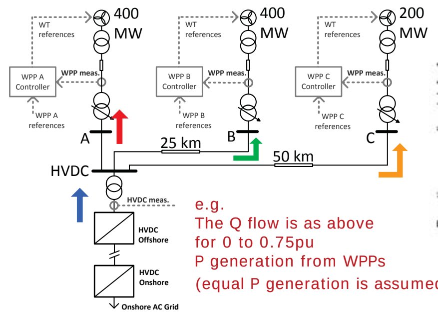

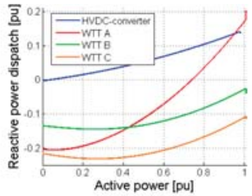

e.g.
The Q flow is as above
for 0 to 0.75pu
P generation from WPPs
(equal P generation is assumed for WPPs)

Equal Sharing of Reactive Power between Converters – via droop

Proposal: Droop control at the WPPs (tuning is based on load flow analysis)

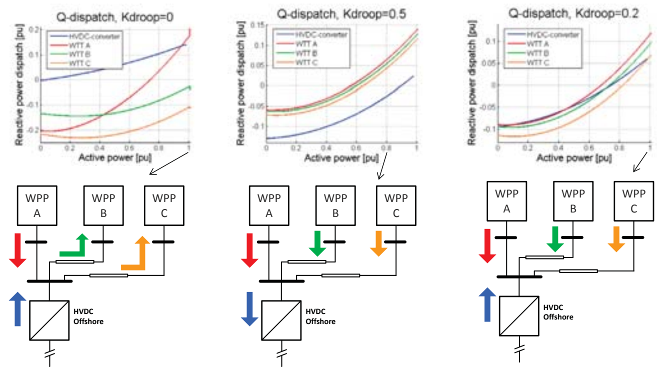

From HVDC&A to B&C From A&B&C to HVDC **Harmonized behaviour !**

POD at the onshore by active power: Active power modulation by the OWPPs

Oscillation is sensed by the onshore HVDC
Required P modulation signal is sent to offshore HVDC
Question: How to realize P modulation by the WPP cluster? Open loop or closed loop?

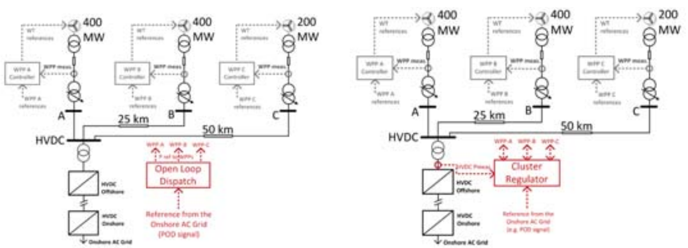

POD at the onshore by active power: Active power modulation by the OWPPs

Open loop dispatch:
Comm. Delay and WPP dynamics are compensated

But compensation is imperfect with mismatch!!

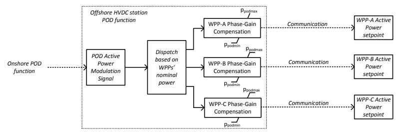

Closed loop cluster control:
Regulation based on total P feedback at the HVDC

Dispatch based on WPPs P generation feedback

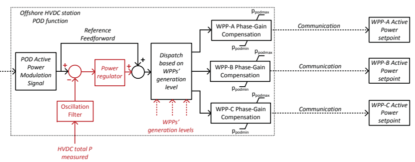

POD at the onshore grid by active power: Closed loop cluster regulator at the Off-HVDC

Problem: Uncoordinated open loop P references to the WPPs
→ unsynchronized response from the WPPs → Ineffective POD !!

Proposal: Closed loop regulation and weighted dispatch to the WPPs
→ synchronized response from the WPPs → Effective POD !!

P reference to the Off-HVDC
Off-HVDC measured P with open loop dispatch
Off-HVDC measured P with closed loop cluster control

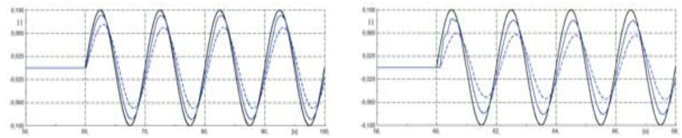

0.1 Hz P modulation 0.5 Hz P modulation

The closed loop cluster controller can realize the reference to a great extent!

Conclusion

- IEC 61400-27-1 models can be utilized in DC-connected offshore WPP studies
- Offshore AC Grid Voltage Control
  - Droop sharing between WPPs helps to improve reactive power flow
  - Better utilized converter capacities
- POD can be potentially provided by closed loop cluster control
  - Coordination helps to mitigate communication sourced insufficiencies
- DC-connected offshore WPPs can contribute to ancillary services
  - Cluster controller is needed for effective support
- Future work;
  - Voltage control settings optimization based on active power losses
  - Adaptive control design for POD cluster controller
  - Frequency support with cluster controller

References

[1] V. C. Tai and K. Uhlen, "Design and Optimisation of Offshore Grids in Baltic Sea for Scenario Year 2030," EERA DeepWind'2014, Energy Procedia, vol. 53, pp. 124–134, 2014

[2] Siemens SylWin1 Press Release, 25 April 2015 [online] Available:
http://www.siemens.com/press/en/pressrelease/?press=/en/pressrelease/2015/energymanagement/pr2015040192emen.htm&content[]=EM

[3] L. Harnefors, N. Johansson, Z. Lidong, and B. Berggren, "Interarea Oscillation Damping Using Active-Power Modulation of Multiterminal HVDC Transmissions," IEEE Transactions on Power Systems, vol.29, no.5, pp. 2529-2538, Sept. 2014

[4] ENTSO-E Draft Network Code on High Voltage Direct Current Connections and DC-connected Power Park Modules, 30 April 2014 [online] Available:
https://www.entsoe.eu/Documents/Network%20codes%20documents/NC%20HVDC/140430-NC%20HVDC.pdf

[5] T. Hennig, L. Löwer, L. M. Faiella, S. Stock, M. Jansen, L. Hofmann, and K. Rohrig "Ancillary Services Analysis of an Offshore Wind Farm Cluster – Technical Integration Steps of a Simulation Tool," EERA DeepWind'2014, Energy Procedia vol. 53, pp. 114–123, 2014

[6] J. Glasdam, L. Zeni, M. Gryning, J. Hjerrild, L. Kocewiak, B. Hesselbæk, K. Andersen, T. Sørensen, M. Blanke, P. E. Sørensen, A. D. Hansen, C. L. Bak, P. C. Kjær, "HVDC Connected Offshore Wind Power Plants: Review and Outlook of Current Research," Workshop on Large-scale Integration of Wind Power Into Power Systems, 2013

[7] Wind Turbines—Part 27-1: Electrical Simulation Models - Wind Turbines, IEC Standard 61400-27-1 ed. 1, Feb. 2015.

[8] Cathrine Andrea Rapp, "Control of HVDC connected cluster of wind power plants," Master thesis, Technical University of Denmark, 2015.

[9] Lorenzo Zeni, "Power system integration of VSC-HVDC connected offshore wind power plants," Technical University of Denmark, PhD thesis, 2015.

[10] Zeni, L.; Eriksson, R.; Goumalatsos, S.; Altin, M.; Sorensen, P.; Hansen, A.; Kjaer, P.; Hesselbaek, B., "Power Oscillation Damping from VSC-HVDC connected Offshore Wind Power Plants," in Power Delivery, IEEE Transactions on , available as early access.

THANKS !

Jayachandra N. Sakamuri, DTU Wind Energy, **RISØ**, jays@dtu.dk

This work was supported in part by People Programme (Marie Curie Actions) of the European Union's Seventh Framework Programme FP7/2007-2013/ under REA grant agreement no. 317221, project title MEDOW.

Any opinions, findings, and conclusions or recommendations expressed in this material are those of the authors and do not necessarily reflect those of Statoil ASA or Halvorsen Power System AS.

Coordinated Tuning of Converter Controls in Hybrid AC/DC Grids for System Frequency Support

Atsede G. Endegnanew and Kjetil Uhlen

EERA DeepWind'2016 Deep Sea Offshore Wind R&D Conference
20 - 22 January 2016
Trondheim, Norway

NTNU

Outline

- Motivation for the study
- Frequency support from offshore wind farm
  - High Voltage DC (HVDC)
  - Multi Terminal DC (MTDC)
- Simulation model
- Study cases and proposed coordination of converter controllers
- Results
- Conclusion

2 NTNU

Motivation for the study

- Increased number of HVDC connected offshore wind farms in the North Sea
- Growing interest in multi-terminal dc grids (MTDC) will lead to hybrid AC/DC power systems
- Several research has been conducted on primary frequency support from Offshore wind farm both through HVDC and MTDC
- Focus has been on frequency of the grid under study and does not consider the disturbances introduced in the other grids in the hybrid system

3 NTNU

Frequency support from Offshore Wind through HVDC

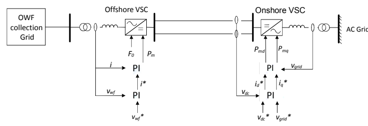

[1]

- Onshore frequency signaling to OWF methods

Method #1

Onshore VSC

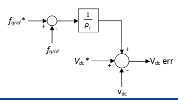

Offshore VSC

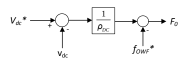

Method #2

Offshore VSC

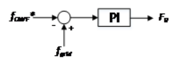

Requires communication

4 NTNU

Frequency support from Offshore Wind via MTDC (1)

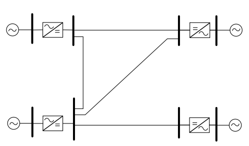

- DC voltage droop control at all terminals
- Power imbalance is shared by all terminals

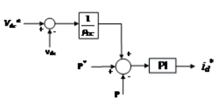

5 NTNU

Frequency support from Offshore Wind via MTDC (2)

- Frequency support can be provided by adding frequency droop
- Frequency support from offshore wind farm
  - AC frequency change signaling through Vdc
  - auxiliary controllers both at onshore VSC and OWF VSC
- All terminals with DC droop controller participate in the frequency support

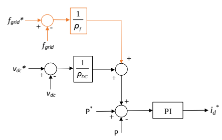

6 NTNU

Study System

- Two multi-machine AC grids
  - Synchronous generators
  - Automatic voltage regulators, governors and Power System Stabilizers(PSS)
- Offshore Wind farm
  - No internal wind farm model
  - Stiff bus behind offshore converter
- DC grid
  - Symmetrical monopolar ±400kV three-terminals VSC-based MTDC
  - π model cables with lumped parameters
- DIgSILENT *PowerFactory*

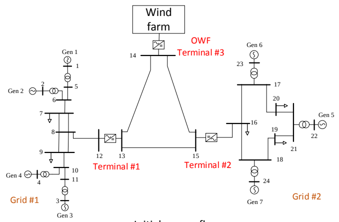

Initial power flows

Terminal #1	400 MW	Import
Terminal #2	200 MW	Import
Terminal #3	600 MW	Export

Study cases

- Loss of load in either of the grids is used to simulate frequency disturbance

	Terminal #1	Terminal #2	Terminal #3
Case 1	Frequency + Vdc droop	Vdc droop	Vdc as freq. change signal
Case 2	Frequency + Vdc droop	Vdc droop	Frequency signal via communication
Case 3	Frequency + Vdc droop	*Frequency + Vdc droop*	Vdc as freq. change signal
Case 4	Frequency + Vdc droop	*Frequency + Vdc droop*	Frequency signal via communication

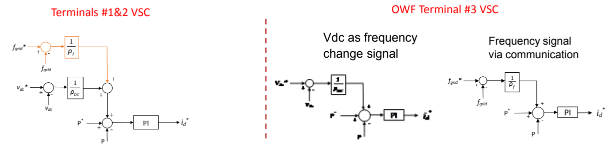

Results (1)

- Loss of load in Grid 1

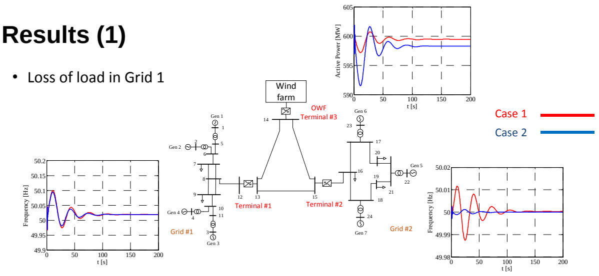

	Terminal #1	Terminal #2	Terminal #3
Case 1	Frequency + Vdc droop	Vdc droop	Vdc as freq. change signal
Case 2	Frequency + Vdc droop	Vdc droop	Frequency signal via communication

Results (2)

- Loss of load in Grid 2

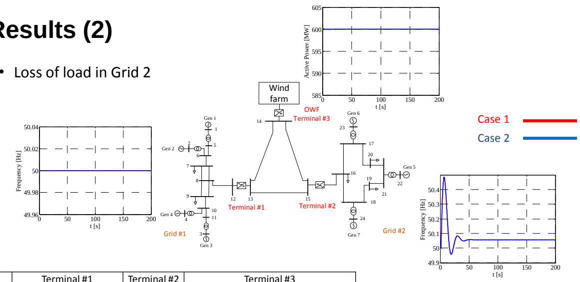

	Terminal #1	Terminal #2	Terminal #3
Case 1	Frequency + Vdc droop	Vdc droop	Vdc as freq. change signal
Case 2	Frequency + Vdc droop	Vdc droop	Frequency signal via communication

Results (3)

- Loss of load in Grid 1

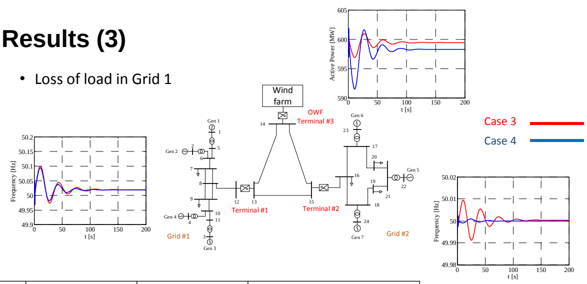

	Terminal #1	Terminal #2	Terminal #3
Case 3	Frequency + Vdc droop	Frequency + Vdc droop	Vdc as freq. change signal
Case 4	Frequency + Vdc droop	Frequency + Vdc droop	Frequency signal via communication

Results (4)

- Loss of load in Grid 2

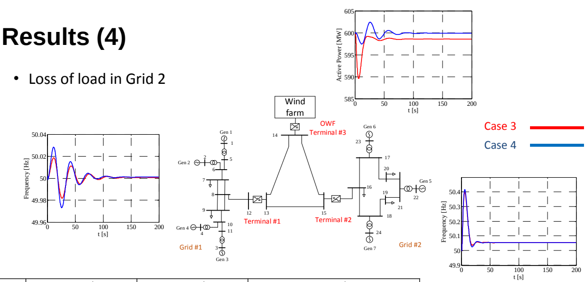

	Terminal #1	Terminal #2	Terminal #3
Case 3	Frequency + Vdc droop	Frequency + Vdc droop	Vdc as freq. change signal
Case 4	Frequency + Vdc droop	Frequency + Vdc droop	Frequency signal via communication

Conclusion

- By coordinating converter controllers at offshore wind farm and one ac grid, it is possible to avoid disturbance in other AC grids connected to the MTDC
- However, the proposed method works when only one terminal is getting frequency support and the remaining AC grid connected MTDC terminals are operating in dc droop or constant power control mode
- If more than one AC grids are going to receive frequency support through MTDC, then distributed dc voltage and frequency droop control is a better control method

References

[1] L. Hongzhi and C. Zhe, "Contribution of Vsc-Hvdc to Frequency Regulation of Power Systems with Offshore Wind Generation," *Energy Conversion, IEEE Transactions on,* vol. 30, pp. 918-926, 2015.

Fulfilment of grid code obligations by large offshore wind farms clusters connected via HVDC corridors

EERA DeepWind'2016 — University of Strathclyde Engineering

A. B. Attya*
O. Anaya-Lara
P. Ledesma
H. G. Svendsen
*presenter Wind Energy Research Group
University of Strathclyde


Source: http://www.evwind.es

Presented research is conducted in the frame of EERA-DTOC project

Outlines

- Motivation
- Grid code and ancillary services
- Implementation challenges
- Benchmark system and case studies
- Results
- Conclusions

Motivation

- High penetration levels of wind power imposes its contribution to voltage stability
- Solving challenges of the utilization of Net-OP tool results to prepare a highly detailed dynamic model using PSS®E
- Investigate the influence of HVDC links connecting the wind farms clusters

Outlines

- ✓ Motivation
- Grid code and ancillary services
- Implementation challenges
- Benchmark system and case studies
- Results
- Conclusions

Grid code and ancillary services

Grid Code specifies the technical requirements and obligations on the connection to, and utilization of, certain transmission system(s). This system could be national or international (e.g. unified European grid)

Ancillary services provided by power plants and **Grid Code requirements** are two sides of one coin

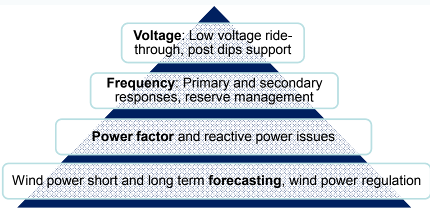

Grid code and ancillary services

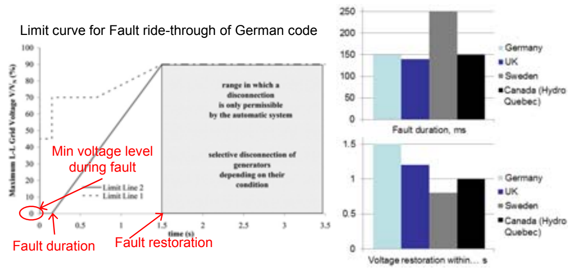

M. Tsili and S. Papathanassiou, "A review of grid code technical requirements for wind farms," *Renewable Power Generation*, vol. 3, 2009

Outlines

- ✓ Motivation
- ✓ Grid code and ancillary services
- ➡ Implementation challenges
- Benchmark system and case studies
- Results
- Conclusions

Implementation challenges

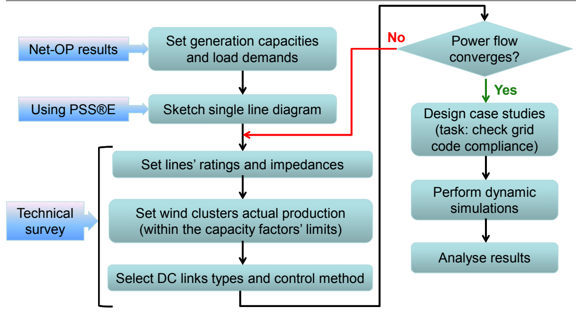

Flowchart: from Net-OP tool *.RAW file to PSS®E dynamic model

Implementation challenges

- In PSS®E, swing bus could not be connected to a DC link → a dummy bus is added to connect the main bus to the DC link(s)
- Setting the rated voltage and power capacities of DC links
- Net-OP does not provide a *.DYR file, thus dynamic models are assigned to all system components from scratch
- Integrating controllers' types of HVDC links (assumed as CDCT4)

Outlines

- ✓ Motivation
- ✓ Grid code and ancillary services
- ✓ Implementation challenges
- ➡ Benchmark system and case studies
- Results
- Conclusions

Benchmark system and case studies

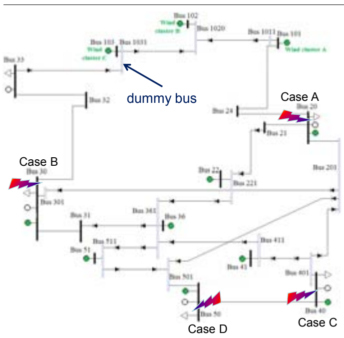

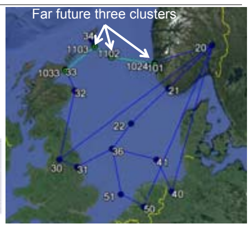

All faults are **3-phase** symmetrical and cleared after **120 ms**

Outlines

- ✓ Motivation
- ✓ Grid code and ancillary services
- ✓ Implementation challenges
- ✓ Benchmark system and case studies
- ➡ Results
- Conclusions

Results– voltage response compared to grid code

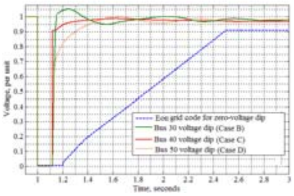

Cases B, C and D

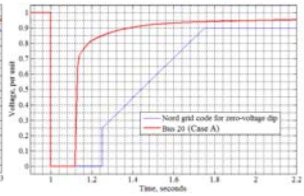

Case A

Results– response of generators' speeds

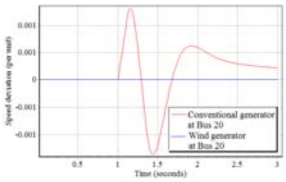

Case A

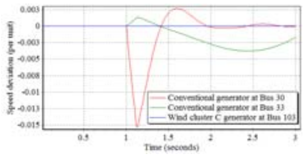

Case B

Results– samples for power flow variations

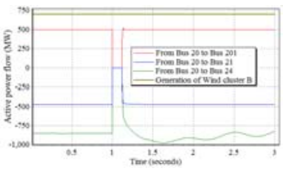

Case A

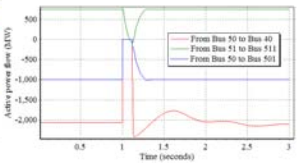

Case D

Outlines

- ✓ Motivation
- ✓ Grid code and ancillary services
- ✓ Implementation challenges
- ✓ Benchmark system and case studies
- ✓ Results
- ➡ Conclusions

Conclusions

- The integration of far future wind clusters does not violate the grid codes during voltage dips
- HVDC failed in some cases to provide the required reactive current to the nearby faulted bus because the converters' models in PSS®E are not equipped with the suitable control methods
- Efforts are required to obtain the real (i.e. generic) values for all the parameters applied in the PSS®E model
- Industrial parties are encouraged to publish samples from real data of related components (e.g. HVDC links converters)
- Comprehensive efforts are required to design new grid codes which specify clearly the role of HVDC links in providing ancillary services

Thanks for your attention

Appendix— numerical values of the parameters of HVDC controllers

EERA DeepWind'2016

University of Strathclyde Engineering

VSCDCT			
J Tpo_1, Time constant of active power order controller, sec (VSC # 1).	0.05	J+14 AC_VC_Limits_2, Reactive power limit for ac voltage control, pu on converter MVA rating	0
J+1 AC_VC_Limits_1, Reactive power limit for ac voltage control, pu on converter MVA rating	0	J+15 AC_Vctrl_kp_2, AC Voltage control proportional gain, converter MVA rating/BASEKV (VSC#2).	2.4
J+2 AC_Vctrl_kp_1, AC Voltage control proportional gain, converter MVA rating/BASEKV (VSC # 1).	2.4	J+16 Tac_2 > 0.0, Time constant for AC voltage PI integral, sec (VSC#2). When 0, VSC#2 is ignored.	0.01
J+3 Tac_1 > 0, Time constant for AC voltage PI integral, sec (VSC#1).	0.01	J+17 Tacm_2, Time constant of the ac voltage transducer, sec (VSC#2), must be longer than simulation step	0.05
J+4 Tacm_1, Time constant of the ac voltage transducer, sec (VSC # 1), must be longer than simulation step	0.05	J+18 Iacmax_2, Current Limit, pu on converter MVA rating (VSC#2).	1
J+5 Iacmax_1, Current Limit, pu on converter MVA rating (VSC#1).	1	J+19 Droop_2, AC Voltage control droop, converter MVA rating/BASEKV (VSC#2).	0
J+6 Droop_1, AC Voltage control droop, converter MVA rating/BASEKV (VSC#1).	0	J+20 VCMX_2, Max. VSC Bridge Internal Voltage (VSC#2).	1.07
J+7 VCMX_1, Max. VSC Bridge Internal Voltage (VSC#1).	1.07	J+21 XREACT_2 > 0.0, Pu reactance of the ac series reactor on converter MVA rating (VSC# 2)	0.17
J+8 XREACT_1 > 0.0, Pu reactance of the ac series reactor on converter MVA rating (VSC#1).	0.17	J+22 QMAX_2, Max. system reactive limit in MVAR (VSC#2).	240
J+9 QMAX_1, Max. system reactive limits in MVAR (VSC#1)	240	J+23 QMIN_2, Min. system reactive limits in MVAR (VSC#2).	-740
J+10 QMIN_1, Min. system reactive limits in MVAR (VSC#1).	-740	J+24 AC_VC_KT_2, feedback from reactive power limiter to ac voltage controller (VSC#2)	1.2
J+11 AC_VC_KT_1, feedback from reactive power limiter to ac voltage controller (VSC#1).	1.2	J+25 AC_VC_KTP_2, feedback from current order limiter to ac voltage controller (VSC#2).	1
J+12 AC_VC_KTP_1, feedback from current order limiter to ac voltage controller (VSC#1).	1	J+26 Tpo_DCL, Time constant of the power order controller, sec (DC Line).	0.05
J+13 Tpo_2, Time constant of active power order controller, sec (VSC#2).	0.05	J+27 Tpo_lim, Time constant of the power order limit controller, sec (DC Line).	0.05

October 19, 2016 | Electronic and Electrical Engineering | Ayman B. Attya | 19

B2) Grid connection and power system integration

Optimal transmission voltage for very long HVAC cables, T.K.Vrana, SINTEF Energi AS

Investigation on Fault-ride Through Method for VSC-HVDC Connected Offshore Wind Farms, Raymundo Torres, NTNU

Minimizing Losses in Long AC Export Cables, O. Mo, SINTEF Energi AS

Scaled Hardware Implementation of a Full Conversion Wind Turbine for Low Frequency AC Transmission, R. Meere, UCD

Optimal Transmission Voltage for Very Long HVAC Cables

Til Kristian Vrana
Olve Mo

Outline

- **Introduction**
- Approach
- Results
- Conclusion

Introduction
Definition

- What is *optimal*?

  Transmission voltage is optimal,…
  …when it enables for maximal power transfer capability

- What is *very long*?

  A HVAC cable can be considered very long,…
  …when the optimal transmission voltage is LOWER than rated voltage

  (This is usually for lengths beyond 100-200 km)
  (depending on cable type)

Introduction
Motivation

- Why considering very long HVAC cables?
  - Used to be seen as economically inferior to HVDC solutions
    - Economic Break-Even-Length (usually referred as 50-100 km)

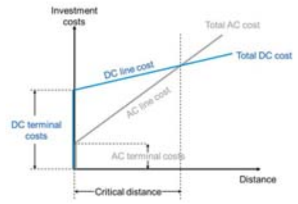

<- ABB

Introduction
Motivation

- Why considering very long HVAC cables?
  - Used to be seen as economically inferior to HVDC solutions
    - Economic Break-Even-Length (usually referred as 50-100 km)
- Offshore HVDC has proven to be more expensive than expected (German Bight)
- L>100 km becoming interesting

Introduction
State of the Art

Introduction
Background

- HVAC cables are operated at rated voltage
- Longest HVAC cables are around 100km (Malta, Ibiza,…)
- European standard voltage (400 kV) not applied for long cables.
- Applied: 220 kV, 155 kV, 132 kV, 110 kV
- Cable capacitance setting the limits.

Soon to come: Martin Linge Cable (162km, 55MW)

SINTEF Technology for a better society 7

Introduction
Today's Approach

- See what cables are available
- Check which cable fits best for the purpose
- Aways operate at rated voltage

Operation voltage (for a given cable)
is taken as given and not as parameter

SINTEF Technology for a better society 8

Introduction
New Systematic Approach

Rated voltage is NOT the operating voltage

Rated voltage is the upper boundary for operating voltage

SINTEF Technology for a better society 9

Introduction
Justification 1

- Why not use a cable with lower voltage rating?
  (instead of lowering the operating voltage)

SINTEF Technology for a better society 10

Introduction
Justification 1

- Why not use a cable with lower voltage rating?
  (instead of lowering the operating voltage)

1. Optimal voltage might lay between available voltage levels

SINTEF Technology for a better society 11

Introduction
Justification 1

- Why not use a cable with lower voltage rating?
  (instead of lowering the operating voltage)

1. Optimal voltage might lay between available voltage levels
2. Power transfer capability is not the same!
   - Lower rated cables have thinner insulation.
   - Thinner insulation gives more capacitance.
   - Power transmission length limited by capacitance.
     -> degrades long distance transmission capability

SINTEF Technology for a better society 12

Introduction
Justification 2

- Comparison of 4 cables
  - l = 200 km
  - U = 132 kV

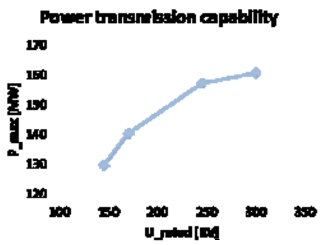

Insulation thickness influences power transfer capability

Introduction
New Systematic Approach

Rated voltage is NOT the operating voltage

Rated voltage is the upper boundary for operating voltage

Introduction
New Systematic Approach

Rated voltage is NOT the operating voltage

Rated voltage is the upper boundary for operating voltage

Great, but...
...how to we make the choice?

Outline

- Introduction
- **Approach**
- Results
- Conclusion

Approach
Calculation

- Purely analytical approach was chosen
- Focus: Deriving the basic equations
  - Cable length
  - Cable parameters
  - Power transmission capability
  - Operation voltage
  - Losses
  - Efficiency

Approach
Degree of Detail

- Lumped model
  - Resistive losses
  - Capacitance

heavily simplified approach!

- Only a starting point / first step
- Focus: Solvable equations

Approach
Simplification issues

- Voltage profile - Higher midpoint voltage
  - Using lower U_max
- Current profile - Lower current in the middle / higher in the ends
  - Ok for losses
  - Problematic for current limit
- Resistive voltage drop
  - Lower charging current @ receiving end
- Losses of reactive compensation equipment
  - Efficiency for cable only
  - Optimum efficiency voltage too high

Approach
Cable Type Example

- Three-core cable
- Copper conductor
- $A = 1000\ mm^2$
- XLPE insulation
- With armour
- 50 % reactive compensation on each end

  (symmetric compensation is also a simplification)

Approach
Cable Data Example

- Data taken from manufacturer brochures:

  (ABB, NKT, (Prysmian))
- Data used for calculations here:
  - $C' = 0{,}18\ \mu F/km$
  - $R' = 0{,}0275\ \Omega/km$
  - $I_{max} = 825\ kV$
  - $U_{max} = 275\ kV$

Outline

- Introduction
- Approach
- **Results**
- Conclusion

Results
Equations 1

- Power Transmission Capability

$$P_{max,trans}(U,l)=\sqrt{3}\,U\sqrt{I_{max}^2-\left(\frac{\omega C' l}{2}\right)^2\left(\frac{U}{\sqrt{3}}\right)^2}-3R' l\, I_{max}^2$$

- Maximum Length at Rated Voltage

$$l_{max,Umax}=\frac{I_{max}}{\sqrt{\frac{3R'^2 I_{max}^4}{U_{max}^2}+\frac{U_{max}^2\omega^2 C'^2}{12}}}=184\,km \quad \text{(for the cable used in the example)}$$

Results
Graphic Visualisation 1

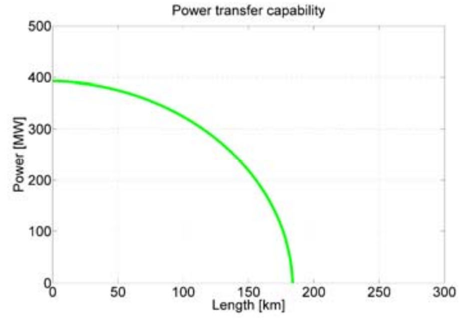

Results
Equations 2 – Optimal Voltage

- Optimal operating voltage

$$U_{opt}(l)=\frac{\sqrt{6}\,I_{max}}{\omega C' l}$$

- Technical Break-Even-Length

$$l_{BE}=\frac{\sqrt{6}\,I_{max}}{\omega C' U_{max}}=130\,km \quad \text{(for the cable used in the example)}$$

- Optimal operating voltage

$$U_{opt}(l)=U_{max}\frac{l_{BE}}{l}$$

Results
Graphic Visualisation 2 – Optimal Voltage

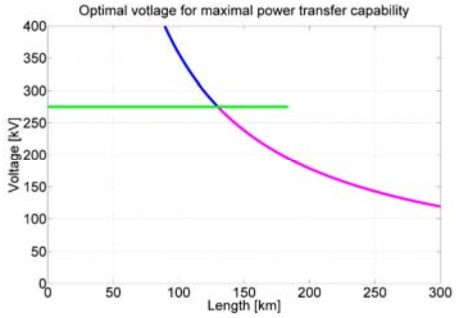

Results
Equations 3 – Maximal Power Transfer

- Maximal power transfer

$$P_{max,trans,Uopt}(l)=3I_{max}^2\left(\frac{1}{\omega C' l}-R' l\right)$$

- Maximal length and resistance

$$l_{max,Uopt}=\frac{1}{\sqrt{\omega R' C'}} \qquad R_{max}=R' l_{max,Uopt}$$

- Maximal power transfer

$$P_{max,trans,Uopt}(l)=3R_{max}I_{max}^2\left(\frac{l_{max,Uopt}}{l}-\frac{l}{l_{max,Uopt}}\right)$$

Results
Graphic Visualisation 3 – Maximal Power Transfer

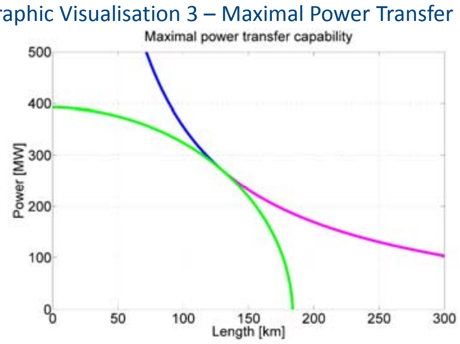

Results
Graphic Visualisation 1+2+3 in 3D

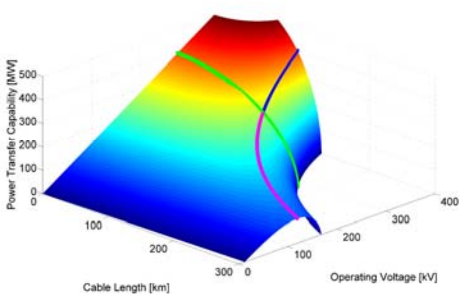

Results
Equations 4 - Efficiency

- Fixed voltage

$$\eta_{Pmax,Umax}(l)=1-\frac{\sqrt{3}R' l I_{max}^2}{U_{max}\sqrt{I_{max}^2-\left(\frac{\omega C' l}{2}\right)^2\left(\frac{U_{max}}{\sqrt{3}}\right)^2}}$$

- Optimal voltage

$$\eta_{Pmax,Uopt}(l)=1-\left(\frac{l}{l_{max,Uopt}}\right)^2$$

Results
Graphic Visualisation 4 - Efficiency

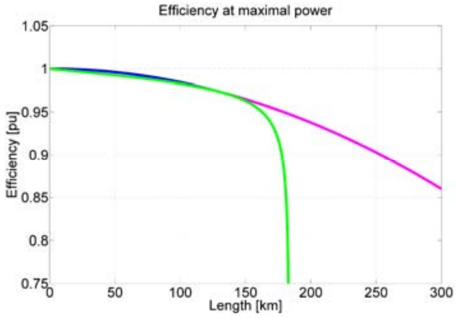

Results
Implications 1

Maximal power transer capability (for all HVAC cables)

$$\cos(\phi) = \frac{1}{\sqrt{(2)}}$$

Results
Implications 1

Maximal power transer capability (for all HVAC cables)

$$\cos(\phi) = \frac{1}{\sqrt{(2)}}$$

(Would require unfeasibly high voltage for non-very-long cables)

Results
Implications 2

- l < 130 km
  - Business as usual
- 130 km < l < 184 km
  - Voltage reduction increases power transfer capability
- 184 km < l
  - Voltage reduction inevitable ($P(U_{rated}) = 0$)

Outline

- Introduction
- Approach
- Results
- **Conclusion**

Conclusion
Summary 1

- Very long HVAC cables have received very little attention
  - Operating at rated voltage always made sense (until now…)
  - Trend goes towards longer and longer HVAC cables
  - Break-Even-Length is in reach
- Operating voltage becomes a constrained parameter

Conclusion
Summary 2

- Analytical equations help to understand phenomena
- Matlab tool gives quick look on long-distance properties
  - Get cable data
  - Calculate:
    - Break-even length
    - Maximal length at rated voltage
    - Maximal length (at optimal voltage)
    - Maximal resistance and maximal length
  - Get a first impression

Conclusion
Outlook 1

- Use of generic cable model

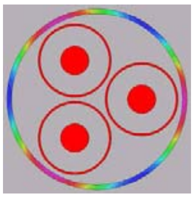

Conclusion
Outlook 2

- More advanced analytical calculations
  - Inductance
  - Distributed parameters

$$Z_{total} = \frac{(2R+2RA^2-2RDA)+j(RB+RBA^2+2RDA^2)+(2R+2RA^2+4R_L A^2)+j(4R_L A)}{(4+4A^2-4DA)+j(2B+2BA^2+4DA^2)}$$

Conclusion
Outlook 3

- Numerical calculations for verification
  - First step indicated valididy of approach
  - Detailed study neccessary

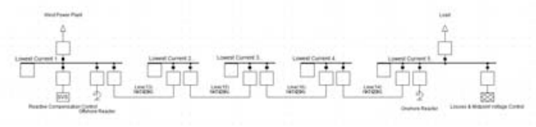

Conclusion
Outlook 4

- Loss-optimal operation with variable power transfer
  (variable voltage / constant cos(ϕ))

Olve Mo presenting soon

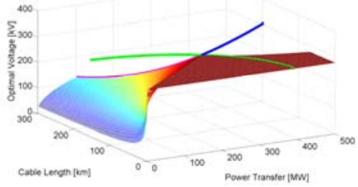

The End

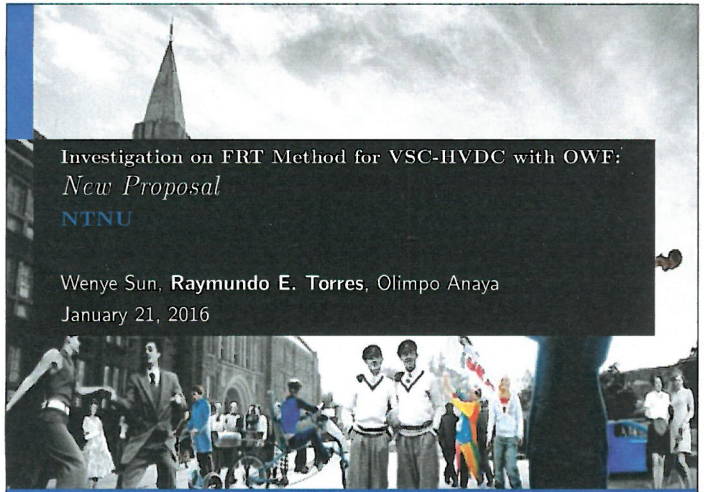

Investigation on FRT Method for VSC-HVDC with OWF: *New Proposal*

NTNU

Wenye Sun, **Raymundo E. Torres**, Olimpo Anaya

January 21, 2016

Outline

Background

Keywords

- Fast development of wind energy in last 20 years
- At end of 2014, total wind power installed around the world was 370 GW.
- The trend is going to offshore, because of good wind condition and less visual impact.
- VSC-HVDC transmission is the latest technology for connecting distant offshore wind farms.

FRT problem

- When a fault occurs at the ac grid, the onshore converter is unable to transmit all the active power to the ac grid, however OWF still inject active power to offshore converter
- This results in power imbalance that will charge the capacitance in the dc-link.
- Without any actions, this will result in a fast increase of the dc voltage, which may damage the HVDC equipment.

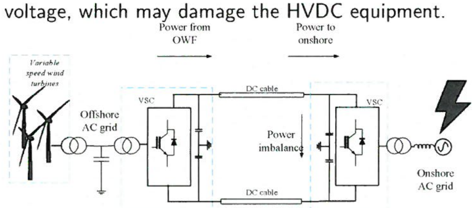

Figure : Fault effect on power transfer

Reference system

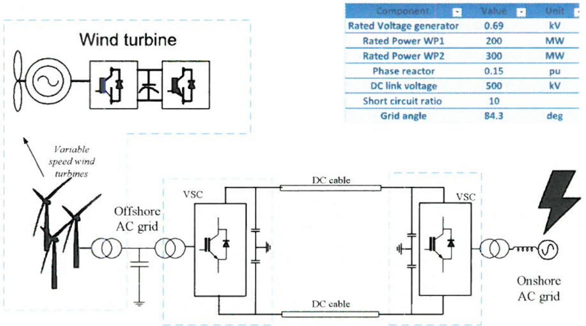

Component	Value	Unit
Rated Voltage generator	0.69	kV
Rated Power WP1	200	MW
Rated Power WP2	300	MW
Phase reactor	0.15	pu
DC link voltage	500	kV
Short circuit ratio	10	
Grid angle	84.3	deg

Offshore converter controller

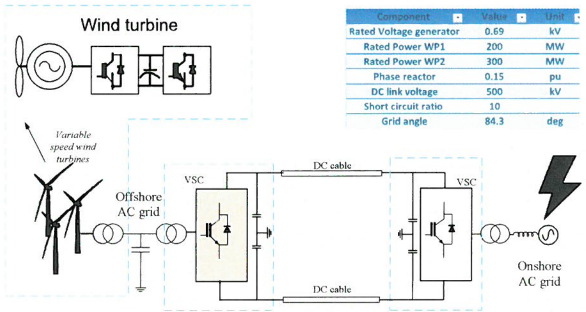

Component	Value	Unit
Rated Voltage generator	0.69	kV
Rated Power WP1	200	MW
Rated Power WP2	300	MW
Phase reactor	0.15	pu
DC link voltage	500	kV
Short circuit ratio	10	
Grid angle	84.3	deg

VSC-HVDC - Offshore converter controller

Control Objective

Generate a three-phase voltage with constant amplitude and frequency for offshore wind farm grid.

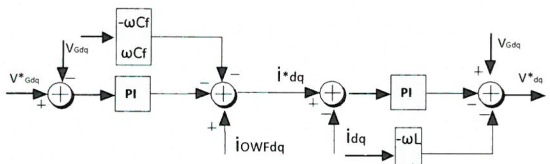

Figure : Offshore converter controller

Onshore converter controller

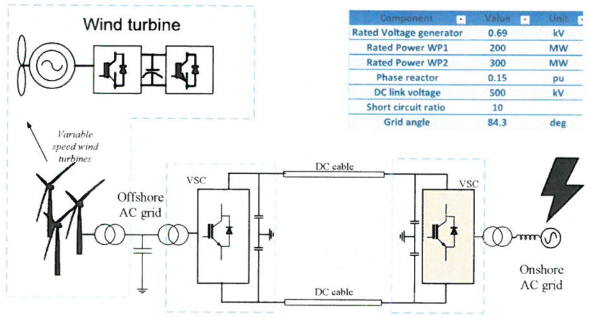

Component	Value	Unit
Rated Voltage generator	0.69	kV
Rated Power WP1	200	MW
Rated Power WP2	300	MW
Phase reactor	0.15	pu
DC link voltage	500	kV
Short circuit ratio	10	
Grid angle	84.3	deg

VSC-HVDC - Onshore converter control design

Control Objective

- Regulate dc-link voltage and reactive power.
- Provide reactive power compensation during onshore grid fault.

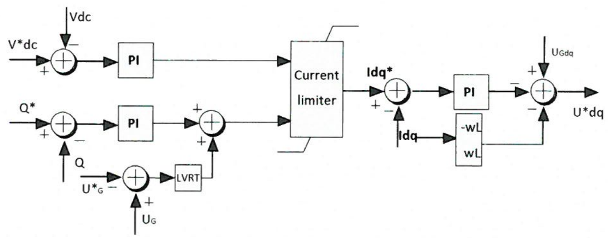

Figure : Onshore converter control design

Wind Turbine - GSC control design

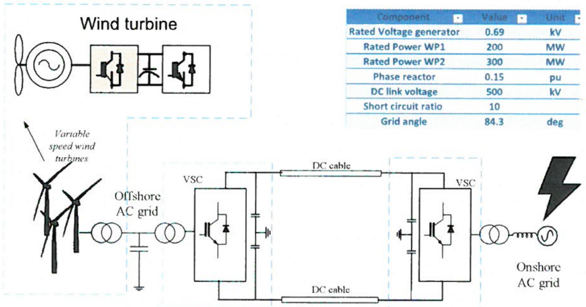

Component	Value	Unit
Rated Voltage generator	0.69	kV
Rated Power WP1	200	MW
Rated Power WP2	300	MW
Phase reactor	0.15	pu
DC link voltage	500	kV
Short circuit ratio	10	
Grid angle	84.3	deg

Wind Turbine - GSC control design

Control Objective

Extract the maximum power from wind turbine.

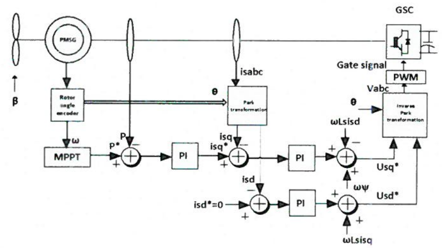

Figure : Generator side converter control design

Wind Turbine - ACGSC control design

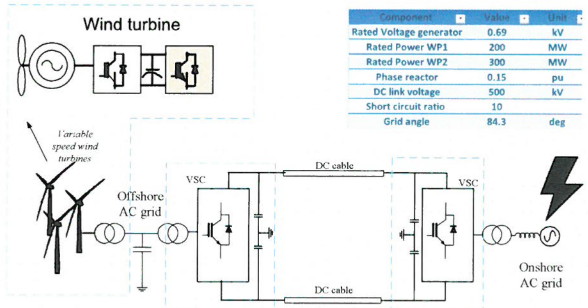

Component	Value	Unit
Rated Voltage generator	0.69	kV
Rated Power WP1	200	MW
Rated Power WP2	300	MW
Phase reactor	0.15	pu
DC link voltage	500	kV
Short circuit ratio	10	
Grid angle	84.3	deg

Wind Turbine - ACGSC control design

Control Objective

Regulate the back-to-back converter dc voltage and reactive power.

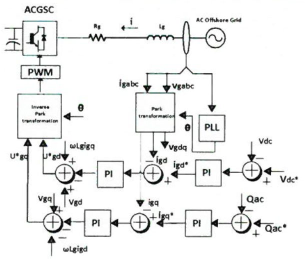

Figure : AC grid side converter control design

Wind Turbine - Pitch control

Control Objective

Limit the power output at rated value.

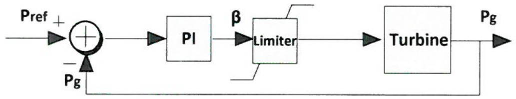

Figure : Pitch control design

FRT Methods

A brief review of the FRT methods.

1. Chopper Resistor
2. Power Setpoint Adjustment
3. Active Current Reduction
4. Offshore Voltage Reduction

FRT Method I- Chopper Resistor

Work principle of chopper resistor

A dc chopper consists of a dc resistor directly controlled through a power electronics switch, e.g. GTO, IGBT. The main function of dc chopper is to limit the dc voltage by dissipating the excess power as heat.

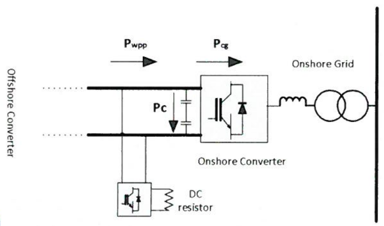

$$R_{chop} = \frac{(1.1V_{dc_{rated}})^2}{P_{rated}}$$

FRT Method II - Power Setpoint Adjustment

Work principle of Power setpoint adjustment method

The principle of this method is to reduce the power setpoint of each wind turbine when onshore fault occurs.

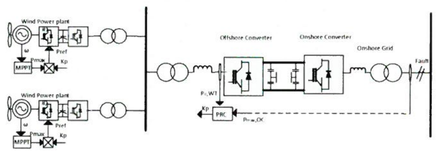

$$K_p = \frac{P_{max}, OC}{P_o, WT}$$

FRT Method III - Active Current Reduction

Work principle of active current reduction method

The WT output power is blocked via wind turbine ACGSC controller using a reduction factor. The reduction factor decreases linearly as the voltage increases up to an specific upper limit.

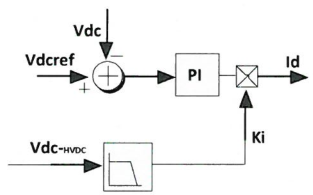

FRT Method IV - Offshore Voltage Reduction

Work principle of offshore voltage reduction

This method calculates the required droop by measuring the dc voltage at the offshore converter, so it is a communication-less scheme with a fast response.

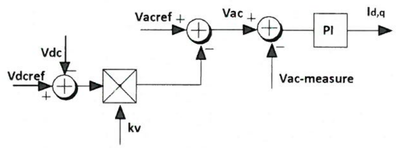

$$V_{ac} = V_{ac_{ref}} - k_v(V_{dc_{ref}} - V_{dc})$$

NTNU

Proposed method FRT

Work principle of the proposed method

When a fault occurs, the dc voltage at the offshore converter will increase. This signal activates the offshore converter controller to control offshore ac voltage magnitude, implemented by block VRC.

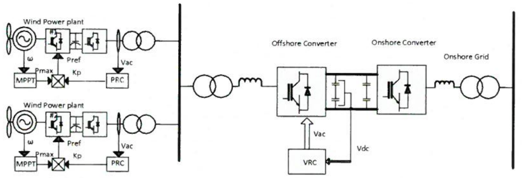

$$V_{ac} = V_{ac_{ref}} - k_v(V_{dc_{ref}} - V_{dc}) \qquad K_p = \frac{V_{reduce}}{V_{rated}}$$

NTNU

Proposed method FRT

Work principle of the proposed method

At the same time, wind turbines detect the offshore ac voltage magnitude reduction. Accordingly, a power droop factor is generated and sent to GSC to de-load active power.

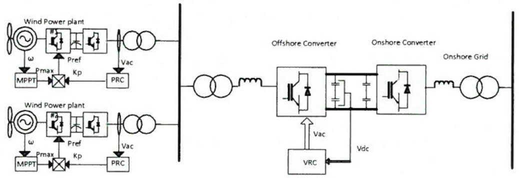

$$V_{ac} = V_{ac_{ref}} - k_v(V_{dc_{ref}} - V_{dc}) \qquad K_p = \frac{V_{reduce}}{V_{rated}}$$

NTNU

Proposed FRT Method

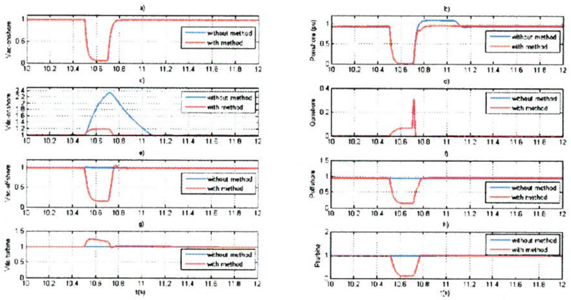

Figure : a)onshore ac voltage b)onshore active power c) onshore dc voltage d)onshore reactive power e) offshore ac voltage f)offshore active power g) dc-link WF h)active power turbine

NTNU

FRT Methods - Summary

	Fault ride through is achieve by	Advantages	Disadvantage
Chopper resistor	External resistor	Straight forward	Extra investment
Power setpoint adjustment	Signal to GSC and reducing wind turbines power	WF controller modification	Communication delay and rely on reliability of communication
Active current control	Signal to ACGSC and reducing wind turbines power	WF controller modification	Communication delay and electrical stress
Offshore voltage reduction	Decreasing offshore grid voltage and blocking output power from OWF	No communication delay, very fast reduction of OWFs power	Electrical stress on wind turbine drive train
Proposed method	Decreasing offshore grid voltage and reducing the output power form each wind turbine	No communication delay, very fast reduction of OWFs output power, no electrical stress	The performance of this method is affected by the measurement of OWF voltage.

NTNU

Conclusion

This paper proposed a FRT method for VSC-HVDC connected OWF system. There are some advantages compared with the described methods:

- The power reduction factor is generated by wind turbine itselft, so the communication delay is eliminated.
- This proposed method combines offshore voltage reduction method and wind turbine power set-point reduction method, so the dc voltage increase in back-to-back converter is reduced. Additionally, the electric stress on wind turbine is reduced.

NTNU

- This work was developed by Wenye Sun in his master thesis
- The European Wind Energy Master consortium is composed of four world leading universities in wind energy and offshore wind energy research and education: Delft university, DTU, NTNU and Carl von Ossietzky Universitt Oldenburg.
- Currently, Wenye Sun works for ABB, China.

Thank You

Questions?

Minimizing Losses in Long AC Export Cables

Olve Mo SINTEF (Presenter)
Bjørn Gustavsen SINTEF

Background

- HVAC compared to HVDC cables have
  - less transfer capacity
  - significantly larger losses
- HVAC are however technically simple and well-proven and seems to still be considered as an attractive alternative
- A natural question to ask is then:

Is it possible to improve efficiency of the export cable?

The simple motivation

- x % transmission loss

↓

+ x % revenue

This presentation will show that

Long AC export cable annual efficiency can be increased by:

Operating the export cable with variable, optimized voltage

alternatively by:

Operating at a fixed, optimal voltage for a given cable based on the actual wind farm production profile

Example study of cable designed for 220kV

Nominal voltage	~~132 kV~~	**220 kV**	~~400 kV~~
Cable section [mm^2]	~~1000~~	**1000**	~~1200~~
R [Ω/km]	~~0.048~~	**0.048**	~~0.0455~~
L [mH/km]	~~0.34~~	**0.37**	~~0.39~~
C [μF/km]	~~0.23~~	**0.18**	~~0.18~~
Nominal current [A]	~~1055~~	**1055**	~~1200~~

Used for all calculations in this presentation

From: "Loss evaluation of HVAC and HVDC transmission solutions for large offshore wind farms", N. Barberis Negra, J. Todorovic, T. Ackermann

The loss calculation

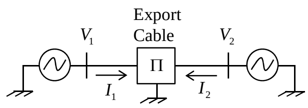

- Cable represented by exact PI-equivalent
  - 50Hz losses can be accurately determined if parameters are known
  - Parameter and temperature uncertainty is the challenge
- Takes into account:
  - Distributed parameter effects
  - Current and voltage variation along the cable
- Losses in other components is ignored in the work presented here

Cable efficiency as function of wind park active power production (200km).

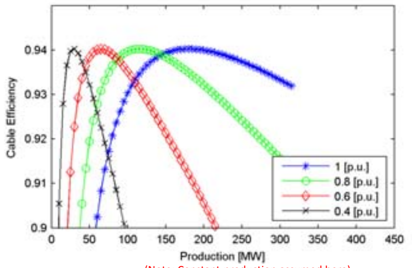

(Note: Constant production assumed here)

The important observation:

Efficiency does not necessarily improve with increasing voltage at long distances

The optimum depends on the production !

200km 220 kV cable, 1000mm2

Wind farm production variability (example)

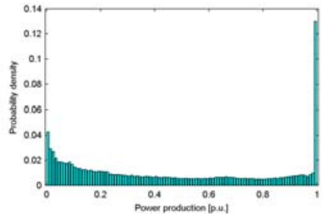

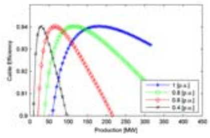

Representative for NOWITECH reference wind farm at Doggerbank.
Average wind speed 9.4 m/s
Utilization factor is 46.

Annual cable efficiency

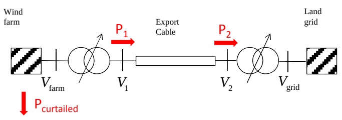

$$\eta_{annual} = \frac{\int P_2\,dt}{\int (P_1 + P_{curtailed})dt}$$

Efficiency for **constant** production

Constant production year around

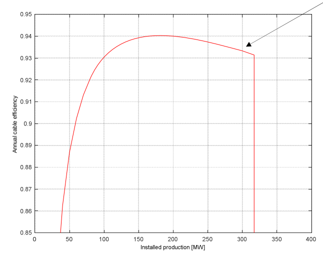

200km 220 kV cable, 1000mm2

Annual efficieny for realistic production variability

Constant production year around

Variable production

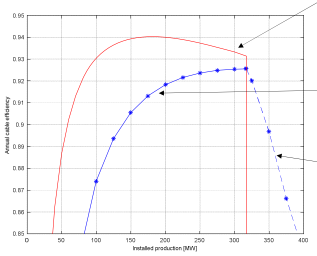

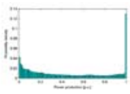

Effect of over-planting (w/curtailment)

Annual efficiency as function of **installed** production

Will now show how to get to this level

Variable production

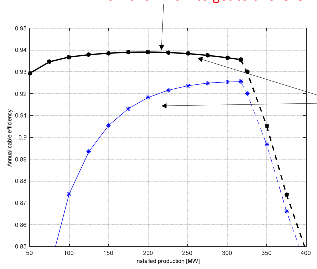

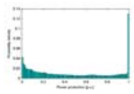

200km 220 kV cable, 1000mm2

Hypothesis:

- Total losses over one year of operation can be reduced by operating the cable at an optimal, **variable voltage**.

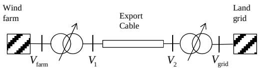

or, if you do not like the idea of tap-changer:

- Total losses over one year of operation can be reduced by operating the cable at a **fixed voltage** optimized for the given wind farm and the given power duration curve.

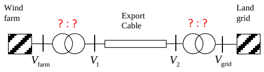

Annual efficiency as function of installed production

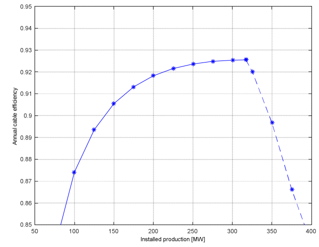

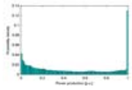

200km 220 kV cable, 1000mm2

Annual efficiency as function of installed production for different constant operating voltages

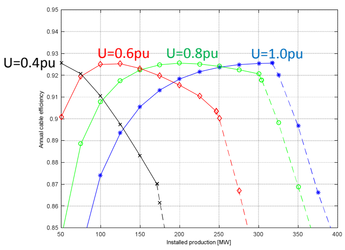

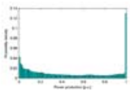

200km 220 kV cable, 1000mm2

Optimal voltage for maximum efficiency

- First step: Find optimal voltage as function of power transfer

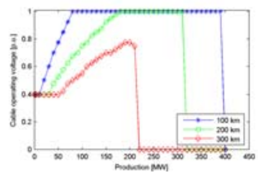

- Next step: Find the annual efficiency when operating at a voltage continuously adapted to the variable wind power production (shown on next slide)

100km, 200km and 300km 220 kV cable, 1000mm2

Annual efficiency as function of installed production

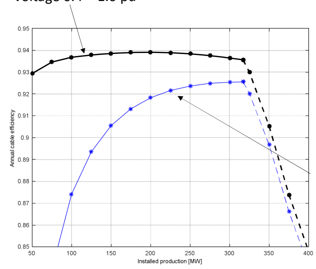

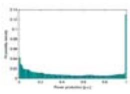

200km 220 kV cable, 1000mm2

Annual efficiency as function of installed production

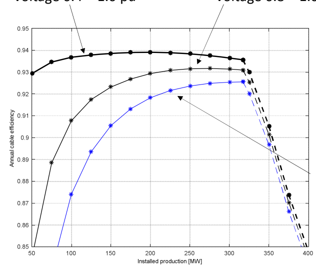

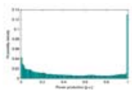

200km 220 kV cable, 1000mm2

Dependency of power production distribution

Power production distribution

Efficiency

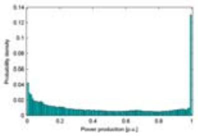

46% Utilization factor

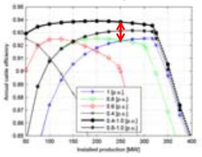

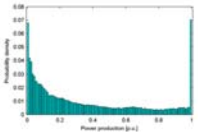

35 % Utilization factor

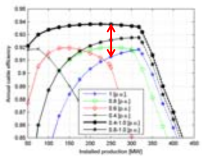

SINTEF Technology for a better society 19

Remains to look into:

- Map the potential loss saving for different cables, distances and wind production profiles
- Look into the practical issues of utilizing the observations:
  - Technology assessment
  - Control methods
  - Stability and transient issues
- Impact of losses in other components (transformers, VAr compensation)
  - Increases or decreases ?
- **Cost-benefit ?**
- Grid codes / regulations challenges

SINTEF Technology for a better society 20

Conclusion

- The Annual efficiency of a long export cable can be improved by operating at variable voltage or in some cases also by operating at a fixed voltage below rated.
- Work remains before it can be concluded whether it will be economically feasible to utilize the results or if it becomes too expensive and technically complicated
- The results do show that it is important to take into consideration the **annual** efficiency when choosing operating voltage and designing the export cable. It might be that the operation below rated voltage improves annual efficiency (project dependent)
- The largest improvement can be expected for:
  - Longest distances (150km ++)
  - Low utilization factor projects (for the whole, or for part of the system life time)

SINTEF Technology for a better society 21

Scaled Hardware Implementation of a Full Conversion Wind Turbine for Low Frequency AC Transmission

Dr. Ronan Meere

EERA DeepWind 2016 Trondheim Norway

Ismail Ibrahim, Jonathan Ruddy, Cathal O'Loughlin and Terence O'Donnell

Ronan Meere (Senior Researcher Power Systems)
Electrical Engineering Department (Electricity Research Centre) (Energy Institute)
University College Dublin
Ireland
ronan.meere@ucd.ie

Presentation Overview

- Background to LFAC transmission for offshore wind
- Design of an LFAC grid compatible wind turbine
- Onshore VSC design

Why Low Frequency AC?

Transmission capability stability limit:

$P_{max} = \frac{V^2}{X}$; $X = 2\pi f L$; $\downarrow f, \downarrow X, \uparrow P_{max}$

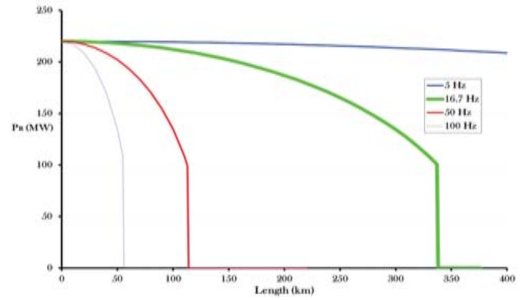

Onshore Frequency Changer

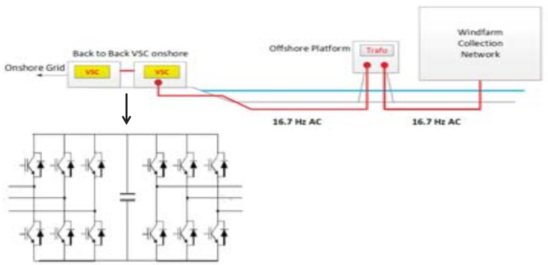

Back to Back VSC converter – Decoupled AC – DC – AC conversion

Ruddy *et al.* 2016 "Low Frequency AC transmission for offshore wind power: A review"
Fischer *et al.* 2012 "Low frequency high voltage offshore grid for transmission of renewable power"
Jafar *et al.* 2014 "Low Frequency AC Transmission for Grid Integration of Offshore Wind Power"
Olsen *et al.* 2014 "Low Frequency AC Transmission on large scale Offshore Wind Power Plants, Achieving the best from two worlds?"

Wind Turbine Collection Network

- Real Time Simulation (RTS) UCD
- Step 1 : Can you design a full conversion WT at 16.7 Hz ?

Step 1 Design Wind Turbine

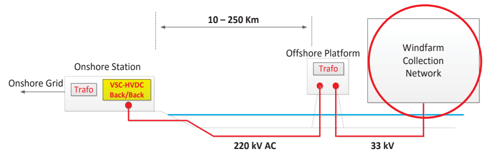

WT Connecting to an LFAC Grid

- Fixed speed and DFIG wind turbine configurations – larger generators to overcome start-up transients
- Full conversion WT – ability to reconfigure the converter to synchronise to the 16.7 Hz grid
- Design of the WT Trafo needs to be relocated on the platform or tower

Overall LFAC Transmission System

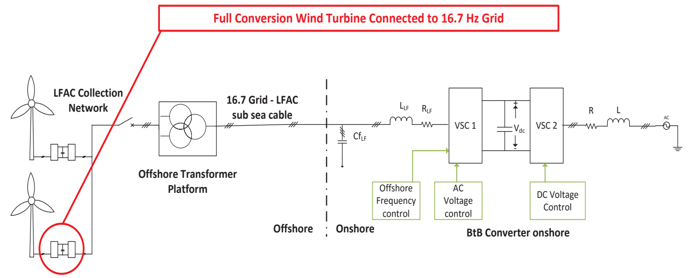

Lab Setup

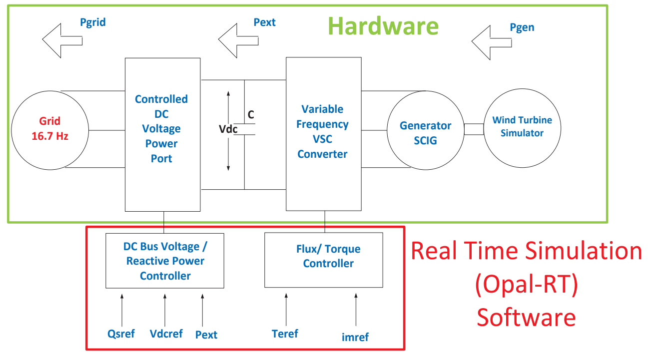

Generator Side VSC Control

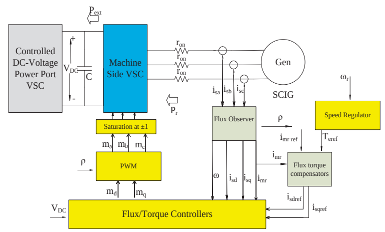

- VSC control maintains a ($T_e \,\alpha\, \omega^2_r$) relationship for the generator so that MPPT (Maximum Power Point Tracking) is guaranteed
- The VSC can set both stator frequency of the generator to control speed and also stator current i_s to control the electrical torque T_e

$$T_e = \frac{3}{2}\frac{L_m}{1+\sigma_r}\hat{i}_{mr} i_{sq}$$

Generator Side Flux Observer

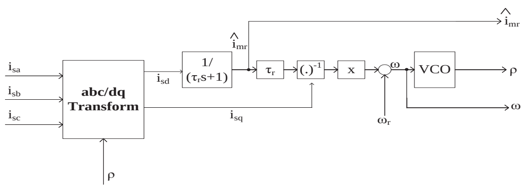

- Torque control maintains i_{mr} (magnetising current) **constant** to a fixed value while using i_{sq} to set T_e
- A flux observer is used to estimate the magnetising current i_{mr}

Flux/Torque Compensator

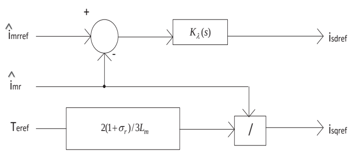

- The flux/torque compensator block receives a reference value for the magnetizing current reference i_{mrref} and an electrical torque reference T_{eref} as inputs and then outputs reference values for the stator d and q currents, i_{sdref} and i_{sqref} which in turn serve as inputs to the inner *dq* current controller

$$\hat{i}_{mrref} = \sqrt{\frac{2}{3}}\frac{V_{sn}}{(1+\sigma_s)L_m\omega_0}$$

Grid Side VSC Control

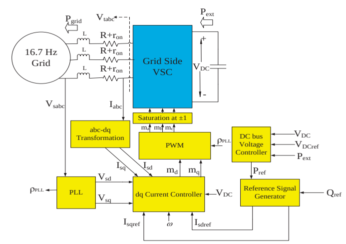

- PLL is utilized to synchronize the converter with the offshore 16.7 Hz grid
- The DC bus voltage controller maintains a constant DC-link voltage

Pictures of the Actual Setup

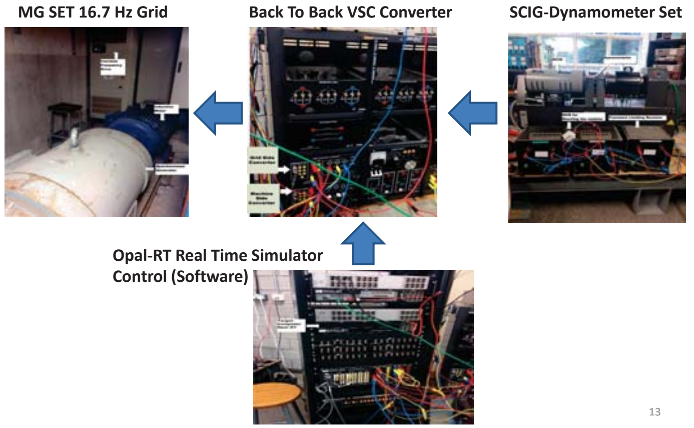

13

Test Procedure

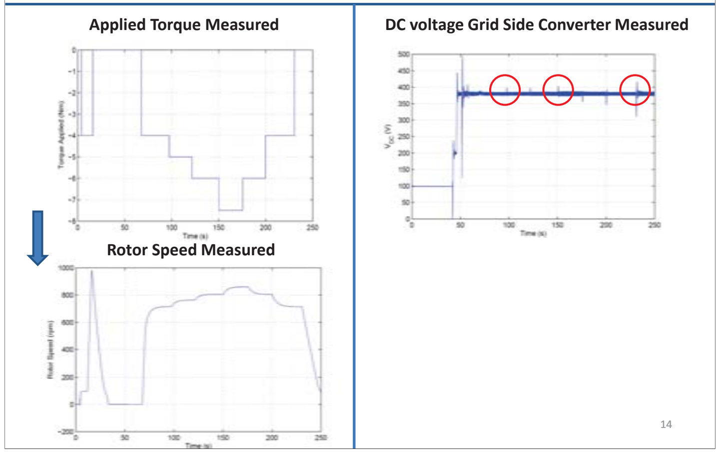

14

Measured Power Export Test

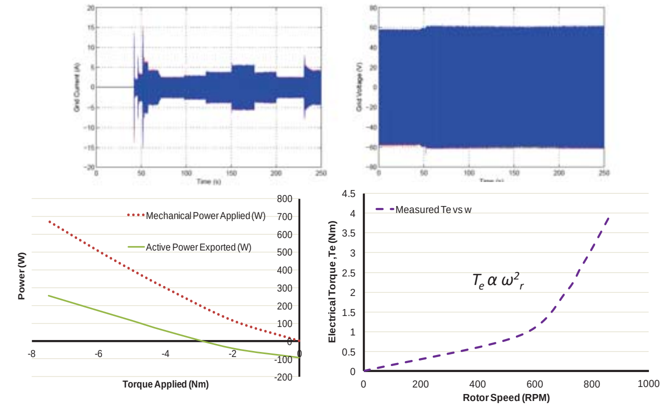

Grid -Side Phase Lock Loop at 16.7 Hz

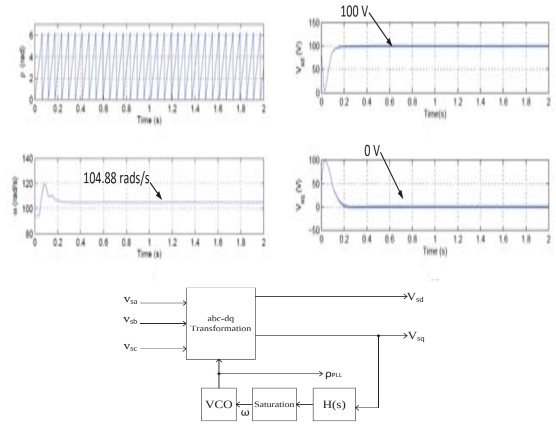

Next Steps

- Step 2 : Onshore VSC Back/Back step 16.7 Hz to 50 Hz

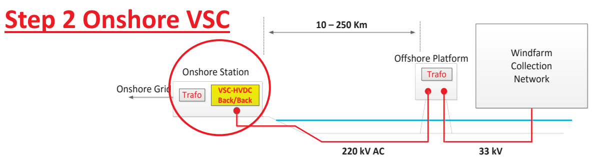

- Poster covers this is detail :

Design and Modelling of a LFAC transmission system for offshore wind

Jonathan Ruddy (jonathan.ruddy@ucdconnect.ie), Dr. Ronan Meere (ronan.meere@ucd.ie), Dr. Terence O'Donnell (terence.odonnell@ucd.ie)

17

Other Work in Progress for LFAC

- Transformer Optimisation 16.7 Hz

  2 – 2.5 times the gross weight of a 50 Hz transformer for the same power

- Hypothetic Nord Sea Grid – *Istvan Erlich "16.7 Hz – The Missing Link"* **Meshed North Sea Grid**

Review

- LFAC is a real alternative to VSC-HVDC
- Demonstrated an operational LFAC connected WT
- Build the onshore BtB converter in hardware
- Evaluate the system under grid connection conditions

Acknowledgements

Ronan Meere is funded under the Third Level Institutions (PRTLI), Cycle 5 and co-funded under the European Regional Development Fund (ERDF).

Terence O'Donnell, Cathal O'Loughlin and Jonathan Ruddy are both funded under the SFI funded SEES Cluster.

Investing in Your Future

Thank You

Questions?

C1) Met-ocean conditions

Turbulence Intensity Model for offshore wind energy applications, K. Christakos, Uni Research Polytec AS

Boundary-Layer Study of FIN0vale1, M. Flügge, CMR

High-resolution simulations of surface wind climate, ocean currents and waves, H. Agustsson, Kjeller Vindteknikk AS

Analysis of offshore turbulence intensity – comparison with prediction models, K. Lamkowska, Lodz Univ of Technology

Turbulence Intensity Model for Offshore Wind Energy Applications

Konstantinos Christakos, Martin Mathiesen, Ole Henrik S. Holvik, Anja K. Meyer
Metocean Group
Uni Research Polytec

Outline

- Motivation
- Wind Parameters
- Offshore Standards: ISO 19901-1:2005
- Turbulence Intensity Model (TIM)
- Estimation of Gust Factor based on TIM
- Further Studies
- Summary

Motivation

Offshore standards:
- Use: Design of offshore structures
- Focus: High wind speed

Need of a model
Valid for:
- All wind conditions

Can be used for:
- Design
- Operation and Fatigue Analysis

Wind Parameters

Mean Wind Speed:

$$U$$

Turbulence Intensity:

$$I = \frac{\sigma_U}{U}$$

Gust Factor:

$$G = \frac{U_{gust}}{U}$$

Offshore Standard: ISO 19901-1:2005

Wind Profile:

$$U(z) = U_0 \cdot \left[1 + C \cdot \ln\left(\frac{z}{z_r}\right)\right]$$

$$C = 5.73 \cdot 10^{-2} \cdot \left[1 + 1.5 \cdot \frac{U_0}{U_{ref}}\right]^{\frac{1}{2}}$$

Turbulence Intensity: $I = 0.06 \cdot \left[1 + 0.43 \cdot \frac{U_0}{U_{ref}}\right] \cdot \left(\frac{z}{z_r}\right)^{-0.22}$

Wind Gust: $U_{gust}(z,t) = U(z) \cdot \left[1 - 0.41 \cdot I(z) \cdot \ln\left(\frac{t}{t_0}\right)\right]$

z_r : Reference elevation above mean sea level, z_r = 10 m
U_o : 1 hour mean wind speed at the reference elevation z_r
U_{ref} : Reference wind speed, U_{ref} = 10 m/s
t_0 : 1 hour

Turbulence Intensity Model (TIM; #1)

Based on offshore wind statistics at FINO platforms, the standard deviation of wind speed is modelled as a function of wind speed using a 2nd order polynomial:

$$\sigma_U = a_1 \cdot U^2 + a_2 \cdot U + a_3$$

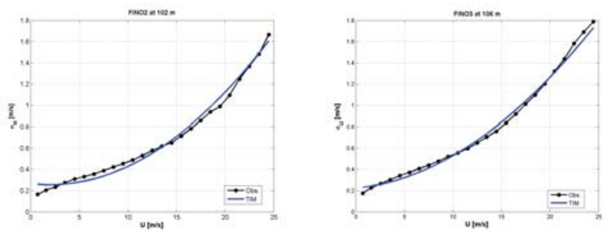

Turbulence Intensity Model (TIM; #1)

$$\sigma_U = a_1 \cdot U^2 + a_2 \cdot U + a_3$$

$$I = \frac{\sigma_U}{U}$$

$$I = a_1 \cdot U + a_2 + \frac{a_3}{U}$$

uni Research
Polytec

Turbulence Intensity Model (TIM; #1)

$$I = a_1 \cdot U + a_2 + \frac{a_3}{U}$$

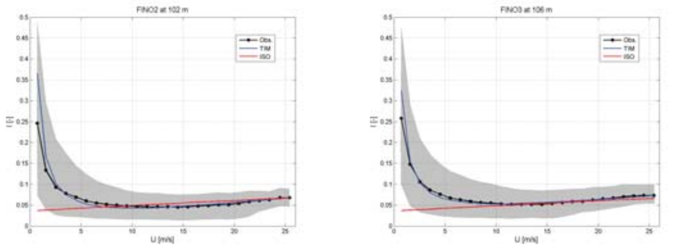

Grey Area: P05 – P95 curves

uni Research
Polytec

Turbulence Intensity Model (TIM; #2)

For wind speed higher than 2 m/s, the standard deviation of turbulence intensity (σ_I) is modelled by:

$$\sigma_I = c_1 + c_2 e^{-c_3 U}$$

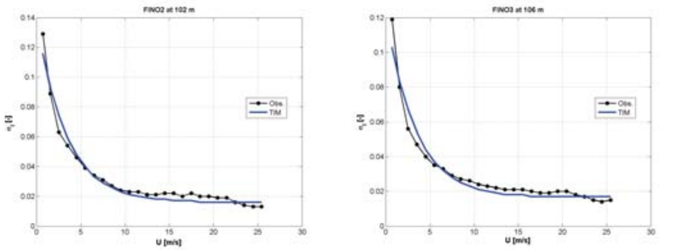

uni Research
Polytec

Estimation of Gust Factor based on TIM

ISO Wind Gust: $U_{gust}(z,t) = U(z) \cdot \left[1 - 0.41 \cdot I(z) \cdot \ln\left(\frac{t}{t_0}\right)\right]$

$$I = a_1 \cdot U + a_2 + \frac{a_3}{U}$$

$$G = \frac{U_{gust}}{U}$$

uni Research
Polytec

Estimation of Gust Factor based on TIM

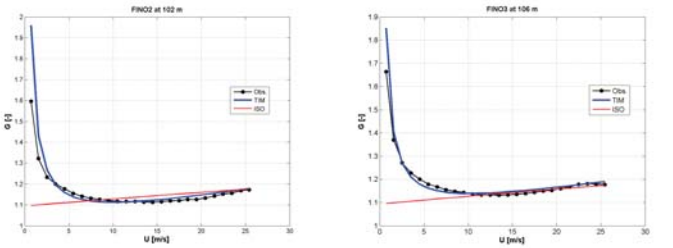

uni Research
Polytec

Further Studies

Apply the TIM to
- other offshore locations
- different heights (higher)

Investigate the possible relation between the TIM and
- atmospheric stability
- wind shear
- sea surface roughness (e.g. effect of waves)

uni Research
Polytec

Summary

- Propose a model for:
- I (valid for all wind conditions)
- σ_I (valid for wind speed > 2m/s)
- Modelled turbulence intensity corresponds to ISO standards for high wind speed
- Model has been tested with good results using data from several locations including FINO 1,2 and 3

uni Research Polytec

Acknowledgement

Wind data provided by BMWi (Bundesministerium fuer Wirtschaft und Energie, Federal Ministry for Economic Affairs and Energy) and the PTJ (Projekttraeger Juelich, project executing organisation)

uni Research Polytec

Thank you

Turbulence Intensity Model (TIM; #1)

$$I = a_1 \cdot U + a_2 + \frac{a_3}{U}$$

Location	Height	Coefficients		
	[m]	a_1 [(m/s)$^{-1}$]	a_2	a_3[m/s]
Fino 1	100	0.0021	0.0104	0.2545
	33	0.0020	0.0351	0.1976
Fino 2	102	0.0027	-0.0102	0.2660
	30	0.0025	0.0252	0.1599
Fino 3	106	0.0021	0.0092	0.2233
	30	0.0025	0.0300	0.1794

uni Research Polytec

Turbulence Intensity Model (TIM; #2)

$$\sigma_I = c_1 + c_2 e^{-c_3 U}$$

Location	Height	Coefficients		
	[m]	c_1	c_2	c_3 [(m/s)$^{-1}$]
Fino 1	100	0.019	0.101	0.237
	33	0.016	0.094	0.166
Fino 2	102	0.016	0.123	0.301
	30	0.012	0.126	0.270
Fino 3	106	0.017	0.107	0.299
	30	0.015	0.123	0.285

uni Research Polytec

Martin Flügge (CMR), Benny Svardal (CMR), Mostafa Bakhoday Paskyabi (UoB), Ilker Fer (UoB), Stian Stavland (CMR), Joachim Reuder (UoB), Stephan Kral (UoB) and Valerie-Marie Kumer (UoB)

Boundary-Layer Study at FINO1

FINO1 and Alpha Ventus

Neighboring wind farms

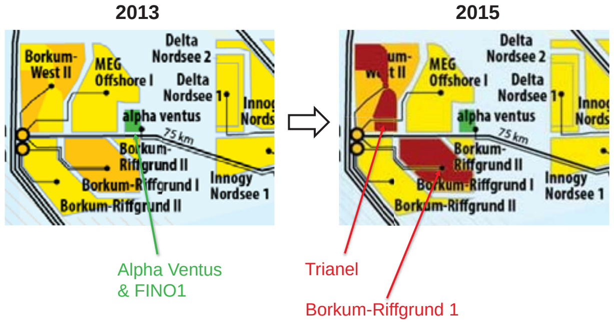

OBLEX-F1 motivation

The key purpose of the campaign is to improve our knowledge of the marine atmospheric boundary-layer (MABL) stability, turbulence generation processes in the water column and MABL, and offshore wind turbine wake propagation effects.

- The collected observational data will be used to validate and improve numerical models and tools for e.g. weather forecasting, marine operations and wind farm layout optimization.
- In order to provide unique datasets for the study of boundary-layer stability in offshore conditions, simultaneous measurements of wind, temperature and humidity profiles in the MABL is performed.

OBLEX-F1

- NORCOWE met-instrumentation: May 2015 – June 2016
- Oceanographic deployment: June – October 2015

Partners:

- *DEWI*, *BSH* and *FuE Kiel* – FINO1 reference measurements data
- *AXYS* – LiDAR buoy deployment
- *ForWind Oldenburg* – cooperation on LiDAR measurements

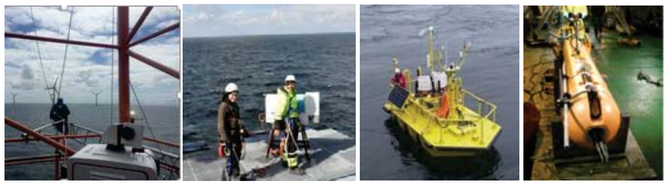

Scanning LiDAR – Leosphere 100s

System 1 (WLS100s-37):
- Installed on top of a container platform
- Scanning across Alpha Ventus wind farm + vertical wind profiles

System 2 (WLS100s-34):
- Installed inside the FINO1 100 m mast
- Scanning across the SE – S wind sector

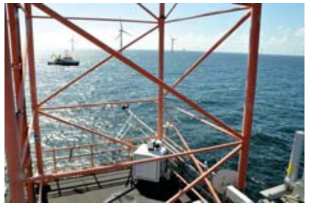

Lidar coverage

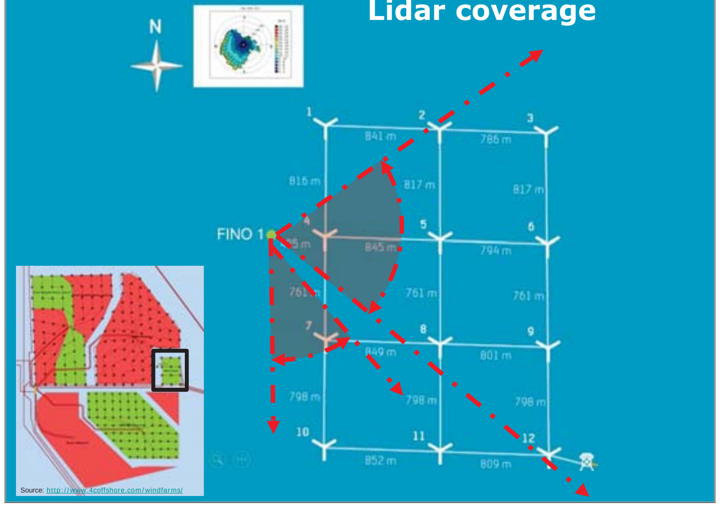

Source: http://www.4coffshore.com/windfarms/

Example of LiDAR scans – PPI and RHI mode

Plan Position Indicator (PPI) mode – constant elevation angle

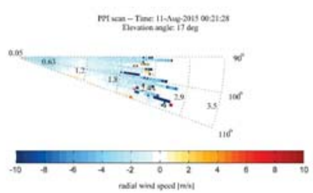

Range Height Indicator (RHI) mode – constant azimuth angle

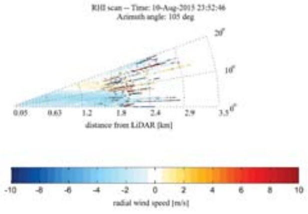

Figures showing an example of a PPI and RHI measurement, pointing towards wind turbine AV5.

- Azimuth angle: 0 – 360 deg, Elevation angle: -10 – 190 deg, Angular resolution: 0.1 deg
- Maximum rotation speed: 0.5 – 8 deg/s while acquiring data
- Measurement resolution: from 50 m up to 3500 m, 25 m intervals

Example of LiDAR scans – 3D wind vector reconstruction in DBS mode

- Radial wind speed accuracy: <0.5 m/s
- Radial wind speed range: -30 to 30 m/s

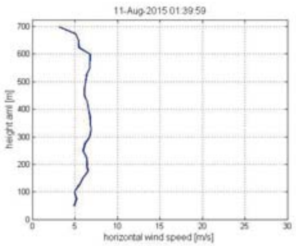

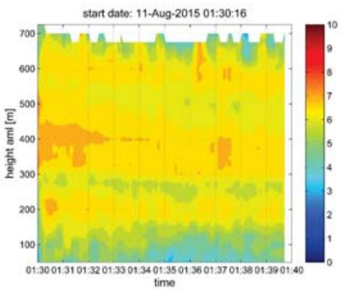

Figures showing an example of a DBS measurement.

HATPRO-R4 passive microwave radiometer

- Installed on top of container platform
- Provides vertical profiles of temperature and humidity up to an altitude of at least 1000 m
- These measurements are combined with the LiDAR wind measurements to obtain information on dynamic stability conditions at FINO1
- First time such measurements are performed continuously nearby an offshore wind farm

Height Range	Vertical Resolution	Accuracy
0-1200 m	30-50 m (BLM)	0.25 K RMS
0-1000 m	100 m (ZM), 30-50	0.25 K RMS
1000-2000 m	200 m	0.35 K RMS
2000-5000 m	200 m	0.50 K RMS
5000-10000 m	400 m	0.50 K RMS

***Table 6**: Typical characteristics of RPG-HATPRO-G4 temperature profiles.*

Height Range	Vertical Resolution	Accuracy (Abs Hum.)	Accuracy (Rel. Hum.)
0-1000 m	100 m	0.4 g/m³ K RMS	5% RMS
1000-2000 m	100 m	0.4 g/m³ K RMS	5% RMS
2000-5000 m	250 m	0.4 g/m³ K RMS	5% RMS
5000-10000 m	400 m	0.4 g/m³ K RMS	5% RMS

***Table 7**: Typical characteristics of RPG-HATPRO-G4 humidity profiles.*

Source: Radiometer Physics GmbH

HATPRO-R4 passive microwave radiometer

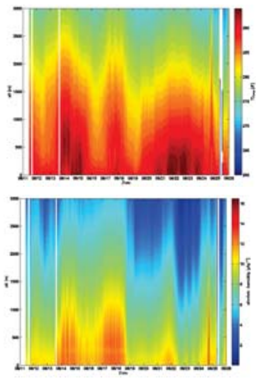

Figures showing an example of temperature (upper panel) and humidity (lower panel) Hovmøller diagrams.

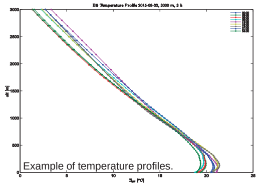

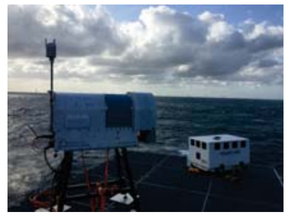

Ultra sonic anemometer (USA) measurements

- Two additional Gill R3-100 anemometers installed on outward facing booms at 15 and 20 masl
- FINO1 USA installed at 40, 60 and 80 masl – NW site of 100 m mast
- High frequency (25 Hz) measurement of the 3D wind vector (U,V,W)
- Provides information about turbulent fluxes at the measurement height

The array of USA provides independent information about the vertical wind profile and the turbulence intensity between 15 – 80 masl.

It also provides information about heat and momentum fluxes which is highly needed for the characterization of the MABL.

Together with the ocean equipment, the lowest measurement level (15 m) provides flux measurements for air-sea interaction.

Availability of met-data

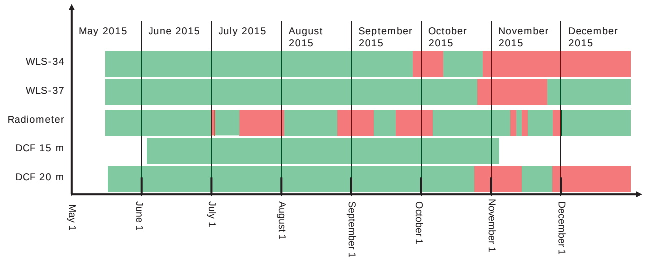

Oceanographic measurements

The overall aim is to gain a better understanding of the interactions between the atmosphere, the ocean and offshore wind farms, such as single turbine and wind farm wake characteristics in the presence of combined wind and wake effects.

⇩

How does the wind field around offshore wind farms influence the ocean and vice versa?

Sullivan et al, 2008

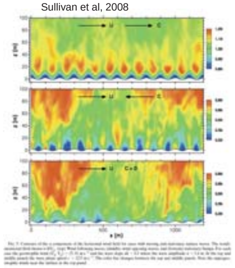

Sullivan et al, 2014

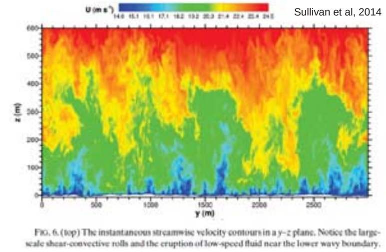

Oceanographic measurements

- Several moorings deployed in close vicinity to FINO1 and the North-East-corner of Alpha Ventus
- Moorings equipped with ADCP and ADV which provide current profiles and directional wave properties
- Mooring M1 equipped with airfoil shear probes and fast response thermistors in order to assess the Reynolds stress

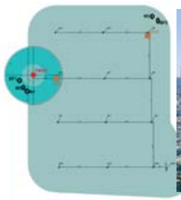

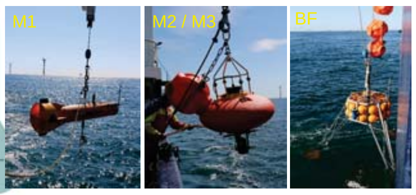

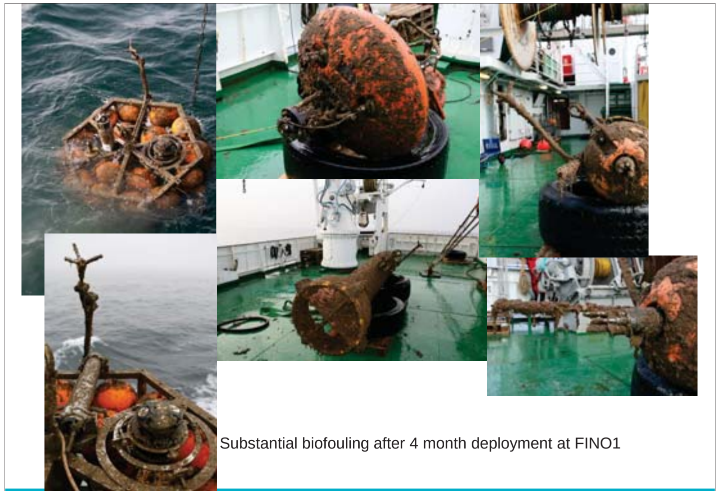

Substantial biofouling after 4 month deployment at FINO1

Availability of ocean data

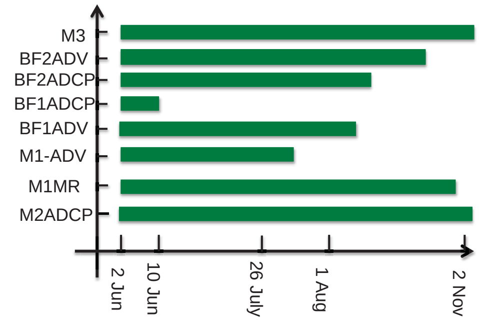

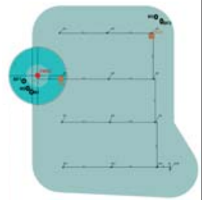

The availability of datasets depends on the quality control criteria which are used.

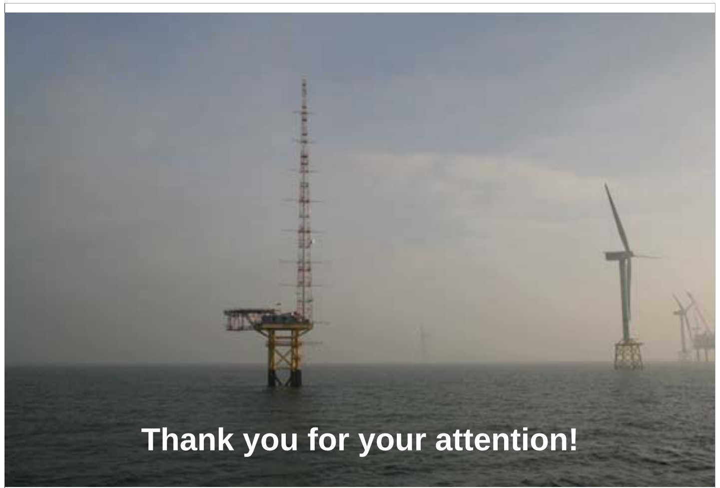

References

- Sullivan, P. P., et al. (2008). "Large-eddy simulations and observations of atmospheric marine boundary layers above nonequilibrium surface waves." Journal of the Atmospheric Sciences **65**(4): 1225-1245.
- Sullivan, P. P., et al. (2014). "Large-Eddy Simulation of Marine Atmospheric Boundary Layers above a Spectrum of Moving Waves." Journal of the Atmospheric Sciences **71**(11): 4001-4027.

High-resolution simulations of surface wind climate, ocean currents and waves

Hálfdán Ágústsson[1], Oyvind Birkjedal[1],
Jon Albrecthsen[2] og Birgitte Furevik[3]

With contributions from Rolv Bredesen and Knut Harstveit

Meteorologisk institutt

HAVFORSKNINGSINSTITUTTET
INSTITUTE OF MARINE RESEARCH

Offshore structures

- Design loads:
  - Extreme winds,
  - Waves and currents.
- Wind-energy production
  - Pre- and post-construction.
- Planning of maintenance.
- Intra-windfarm interactions.

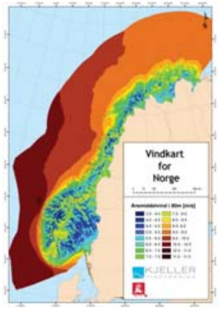

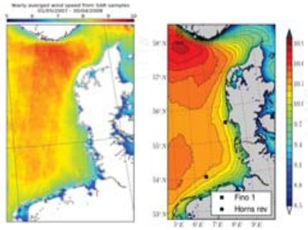

Experience from 'extreme' bridges

- The Norwegian road authorities shall bridge the remaining ferry crossings along the E39:
  - Fjord width 2-7.5 km.
  - Fjord depth 300-1300 m.
  - High and variable wind, wave and current loads.


Concept bridge across Halsafjorden (2km)

Design loads and climatic conditions

- Very high resolution (500 m) meso-scale atmospheric simulations (WRF).
  - Estimating wind climate and extreme winds.
  - Extrapolate observed winds to middle of fjord.
  - Input to high-res. wave (ROMS) and current (SWAN) models.
- Observations of wind for model verification and load estimates.


Concept bridge across Bjornafjorden (5km)

Atmospheric simulations

- WRF-ARW state-of-the-art numerical weather model.
- Down-scaling from global atmospheric analysis (FNL).
- ~10 years at 500 m resol.

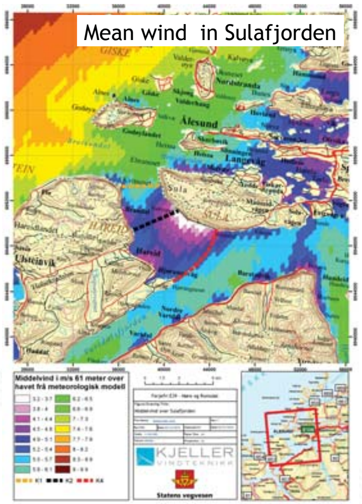

Setup of atmospheric simulations

- Model in Halsafjorden includes 177x183 grid points at 500 m.
- Complex orography but fjord is reasonably well resolved.
- Simulated data used as input to wave and current-models.

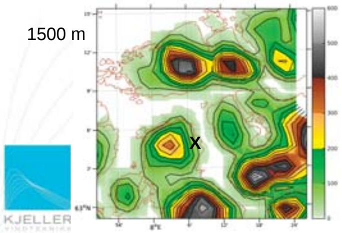

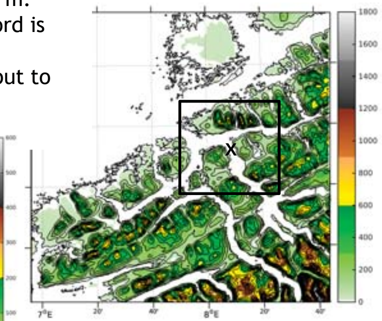

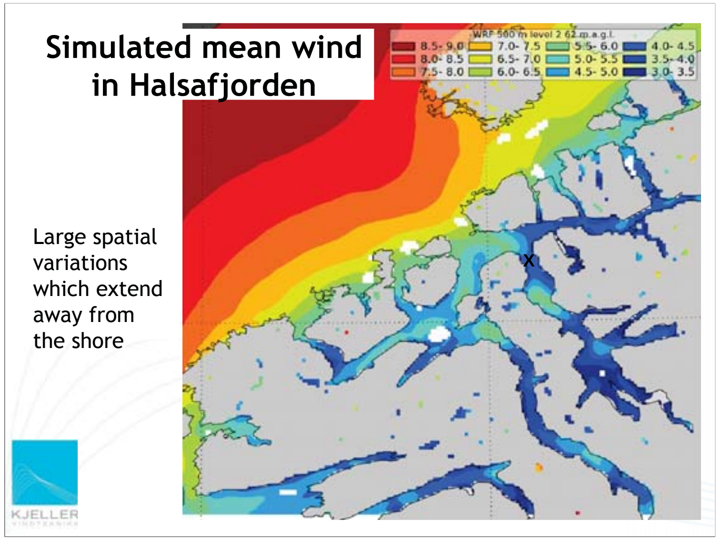
Simulated mean wind in Halsafjorden
Large spatial variations which extend away from the shore
KJELLER

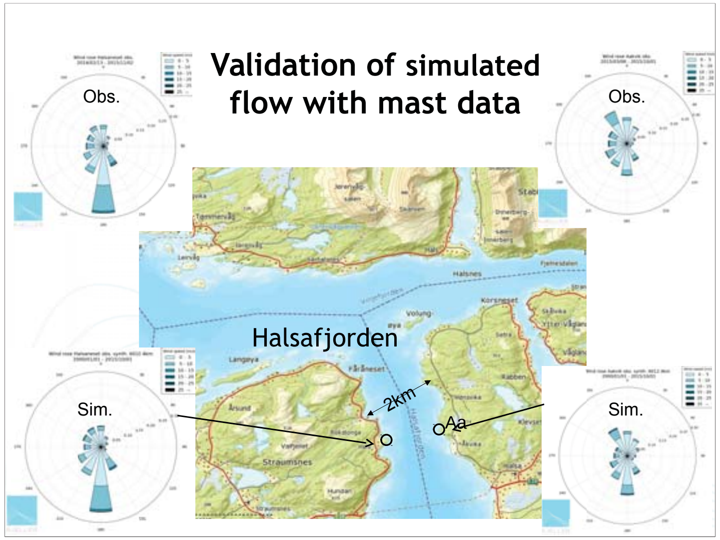
Validation of simulated flow with mast data
Obs.
Obs.
Halsafjorden
Sim.
Sim.
2km
Aa

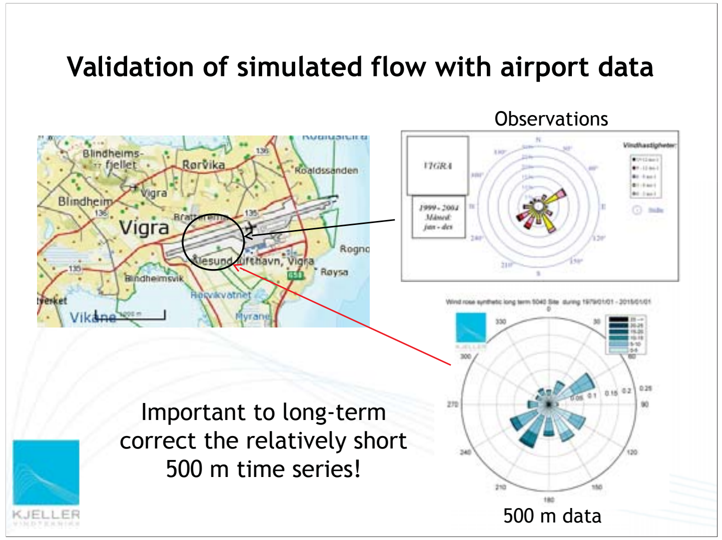
Validation of simulated flow with airport data
Observations
Vigra
Important to long-term correct the relatively short 500 m time series!
500 m data
KJELLER

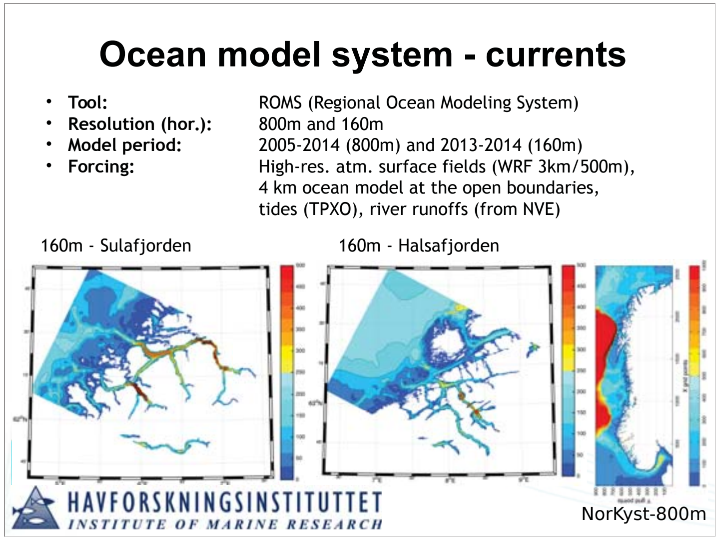
Ocean model system - currents
Tool: ROMS (Regional Ocean Modeling System)
Resolution (hor.): 800m and 160m
Model period: 2005-2014 (800m) and 2013-2014 (160m)
Forcing: High-res. atm. surface fields (WRF 3km/500m), 4 km ocean model at the open boundaries, tides (TPXO), river runoffs (from NVE)
160m - Sulafjorden
160m - Halsafjorden
NorKyst-800m
HAVFORSKNINGSINSTITUTTET
INSTITUTE OF MARINE RESEARCH

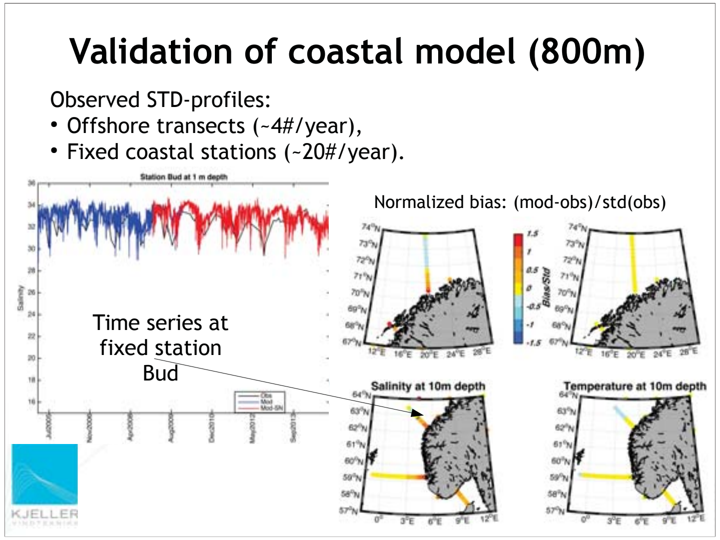
Validation of coastal model (800m)
Observed STD-profiles:
• Offshore transects (~4#/year),
• Fixed coastal stations (~20#/year).
Station Bud at 1 m depth
Normalized bias: (mod-obs)/std(obs)
Time series at fixed station Bud
Salinity at 10m depth
Temperature at 10m depth
KJELLER

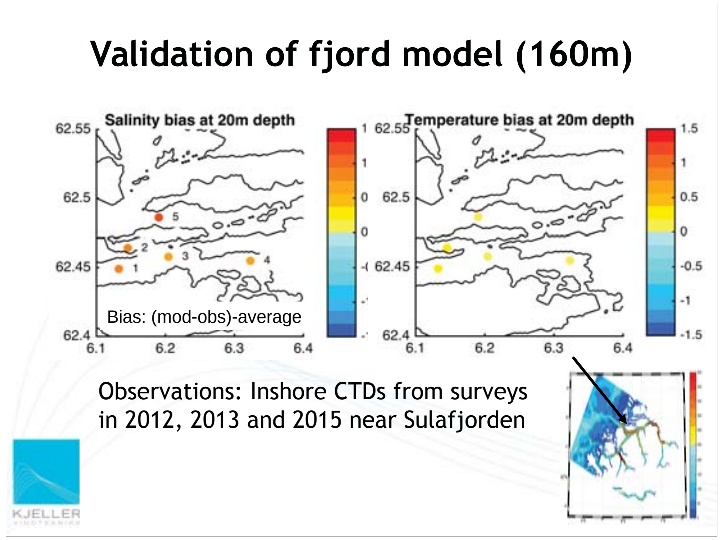
Validation of fjord model (160m)
Salinity bias at 20m depth
Temperature bias at 20m depth
Bias: (mod-obs)-average
Observations: Inshore CTDs from surveys in 2012, 2013 and 2015 near Sulafjorden
KJELLER

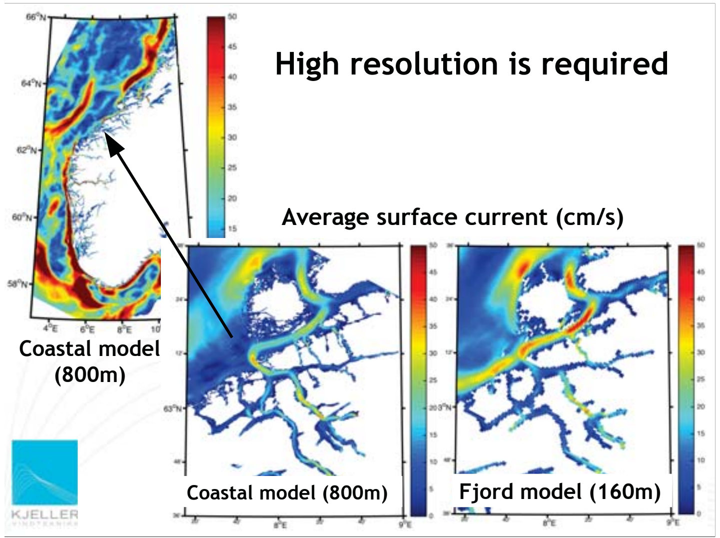
High resolution is required
Average surface current (cm/s)
Coastal model (800m)
Coastal model (800m)
Fjord model (160m)
KJELLER

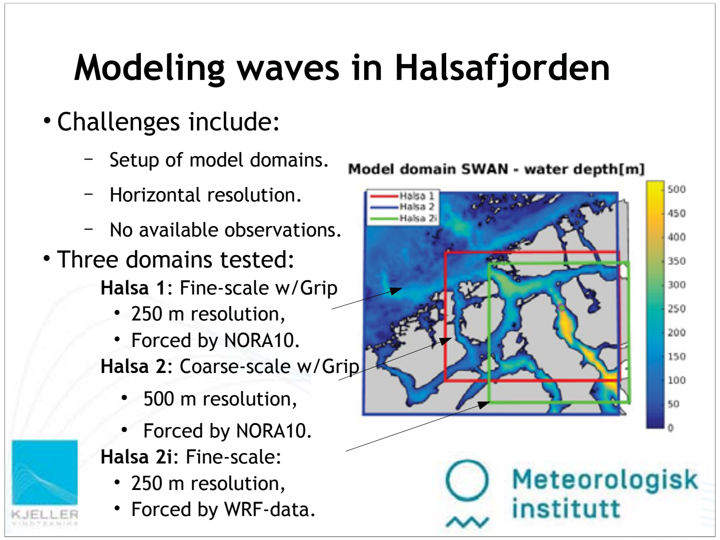
Modeling waves in Halsafjorden
• Challenges include:
– Setup of model domains.
– Horizontal resolution.
– No available observations.
• Three domains tested:
Halsa 1: Fine-scale w/Grip
• 250 m resolution,
• Forced by NORA10.
Halsa 2: Coarse-scale w/Grip
• 500 m resolution,
• Forced by NORA10.
Halsa 2i: Fine-scale:
• 250 m resolution,
• Forced by WRF-data.
Model domain SWAN - water depth[m]
Halsa 1
Halsa 2
Halsa 2i
Meteorologisk institutt
KJELLER

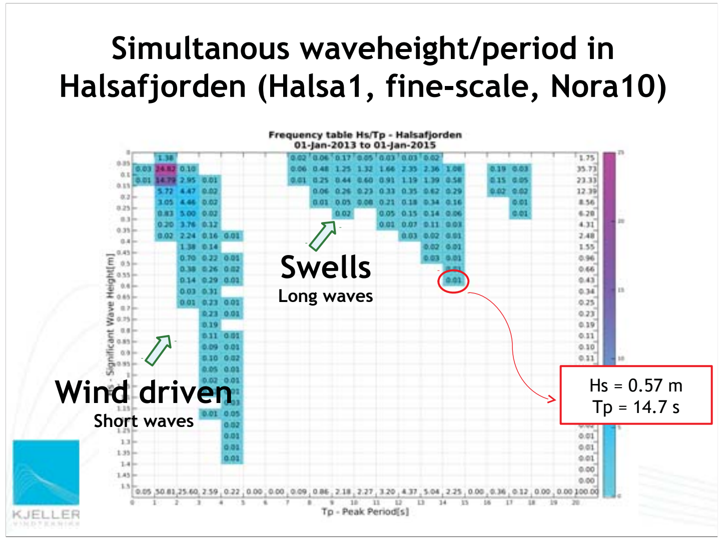
Simultanous waveheight/period in Halsafjorden (Halsa1, fine-scale, Nora10)
Frequency table Hs/Tp - Halsafjorden
01-Jan-2013 to 01-Jan-2015
Swells
Long waves
Wind driven
Short waves
Hs = 0.57 m
Tp = 14.7 s
Tp - Peak Period[s]
KJELLER

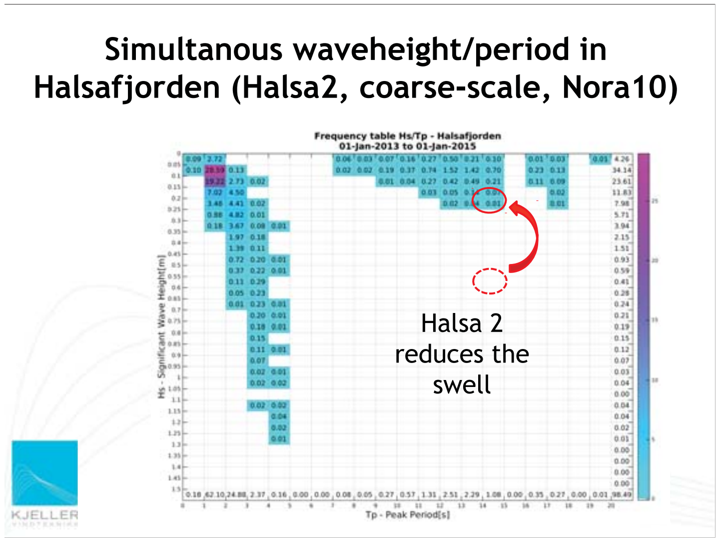
Simultanous waveheight/period in Halsafjorden (Halsa2, coarse-scale, Nora10)
Frequency table Hs/Tp - Halsafjorden
01-Jan-2013 to 01-Jan-2015
Halsa 2 reduces the swell
Hs - Significant Wave Height[m]
Tp - Peak Period[s]
KJELLER

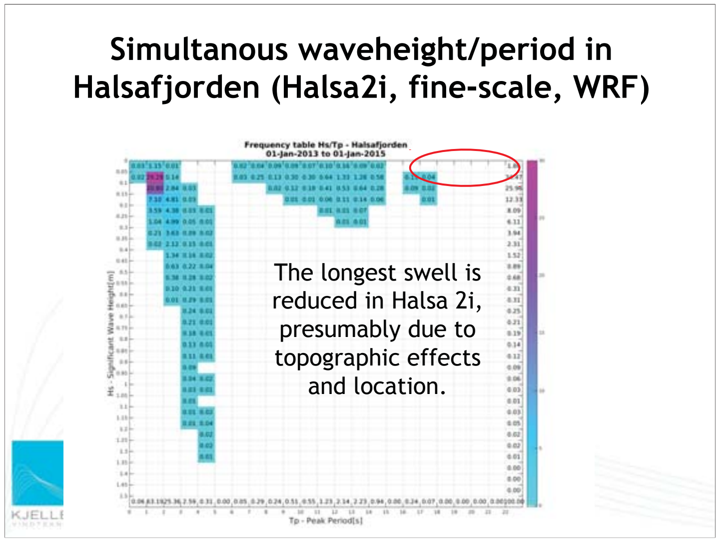
Simultanous waveheight/period in Halsafjorden (Halsa2i, fine-scale, WRF)
Frequency table Hs/Tp - Halsafjorden
01-Jan-2013 to 01-Jan-2015
The longest swell is reduced in Halsa 2i, presumably due to topographic effects and location.
Tp - Peak Period[s]

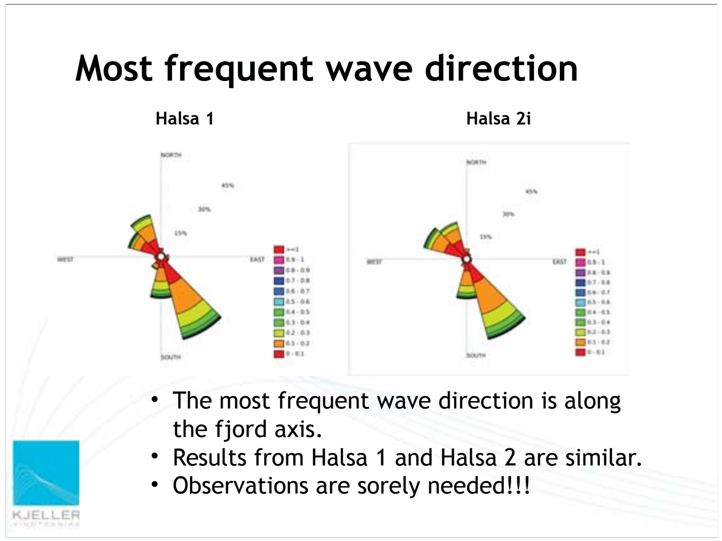
Most frequent wave direction
Halsa 1
Halsa 2i
• The most frequent wave direction is along the fjord axis.
• Results from Halsa 1 and Halsa 2 are similar.
• Observations are sorely needed!!!
KJELLER

What is simulated?

- Wind speed and direction at 500 m horizontal resolution and at many vertical levels.
  - Time series with 1 hour temporal resolution.
  - Wind climate and return periods of extreme winds.
- Ocean currents at 800 and 160 m resolution and at many depth levels.
  - Daily values and temporal behaviour.
- Wave height, period, direction and wave spectrum at 250 m resolution.
  - Mean values and temporal behaviour.
  - Max, mean, median, percentiles, variance, return periods, directional and frequence distribution.
- Observations are critically important to verify model results and help understand important processes.

Main conclusions and summary

- A high resolution atmospheric model coupled with wave and current-models is used to describe in detail the sea-state, wind- and wave climate.
- This study is focusing at in- and near-shore locations in complex orography.
  - → High resolution is also needed off-shore to accurately capture relevant atmospheric and oceanic phenomena.
  - Relevant for design and planning but also during operations.

We present results from high-resolution simulations of mesoscale atmospheric flow, sea currents and waves which are used to study large- and small-scale features of the surface wind climate and sea state in the Sula- and Halsafjords in West-Norway. The atmospheric simulations are performed with the state-of-the-art AR-WRF numerical weather prediction model at a resolution of 6 km for 1979-2015 and at 500 m for 2005-2014, and a temporal resolution of 1 hour. The coarse grid simulated dataset is used to long-term correct the high resolution simulated dataset so that both datasets represent the same period (1979-2015). The simulated flow from the final high-resolution dataset are compared with observations from weather stations in the region, including wind speed and direction observed at various heights in dedicated meteorological masts as well as with airport data.

The simulated atmospheric parameters, including winds, surface pressure, temperature, humidity, precipitation and radiative fluxes, are used as additional forcing for a fine scale wave model (SWAN) running at a horizontal resolution of 250 m and a the ROMS ocean current model running at a horizontal resolution of 800 and 160 m, producing hourly and daily values describing the sea state. Additional input to these models includes high resolution datasets describing the coastline and the bottom topography of the fjords.

The results of the study show that high-resolution atmospheric simulations and coupled current/wave models are a valuable tool that can be used to describe the wind and wave climate. The results are not only valid for the meteorological and ocean conditions near complex orography but they are also applicable for locations away from orography. This is in particular important in the context of reproducing and forecasting winds, waves and currents near offshore constructions such as wind turbines and platforms. Both during the building and planning period but also with regard to accessibility during the operation of the sites.

Eksempel på datauttak fra 500m modell

```
#SiteInformation:
Site Number            - 5050
Location               - Julsundet_W_500m_s1
Elevation              - 19.6 m
Latitude               - 62.729839
Longitude              -  6.939510
Landmask               - 0
Landuse                - 16
Distance from station  - 220 m
I pos in grid          - 178
J pos in grid          - 80
Displacement height    - 0 m

#SensorDescription: COL.NO; TYPE ; OPERATOR ; UNITS ; HEIGHT ; NAME; MODEL; ANEM TYPE; DESCRIPTION
 1; DATE; VAL; yyyy-mm-dd
 2; TIME; VAL; hh-min-ss
 3;   WS; AVG;  m/s;  20.0; WRF model; WRF model; FF; Wind speed - interpolated height value
 4;   WS; AVG;  m/s;  40.0; WRF model; WRF model; FF; Wind speed - interpolated height value
 5;   WS; AVG;  m/s;  60.0; WRF model; WRF model; FF; Wind speed - interpolated height value
 6;   WS; AVG;  m/s;  80.0; WRF model; WRF model; FF; Wind speed - interpolated height value
 7;   WS; AVG;  m/s; 100.0; WRF model; WRF model; FF; Wind speed - interpolated height value
 8;   WS; AVG;  m/s; 120.0; WRF model; WRF model; FF; Wind speed - interpolated height value
 9;   WS; AVG;  m/s; 140.0; WRF model; WRF model; FF; Wind speed - interpolated height value
10;   WS; AVG;  m/s; 160.0; WRF model; WRF model; FF; Wind speed - interpolated height value
11;   WS; AVG;  m/s; 200.0; WRF model; WRF model; FF; Wind speed - interpolated height value
12;   WS; AVG;  m/s; 250.0; WRF model; WRF model; FF; Wind speed - interpolated height value
13;   WS; AVG;  m/s; 300.0; WRF model; WRF model; FF; Wind speed - interpolated height value
14;   WS; AVG;  m/s; 350.0; WRF model; WRF model; FF; Wind speed - interpolated height value
15;   WS; AVG;  m/s; 400.0; WRF model; WRF model; FF; Wind speed - interpolated height value
16;   WS; AVG;  m/s; 450.0; WRF model; WRF model; FF; Wind speed - interpolated height value
17;   WS; AVG;  m/s; 500.0; WRF model; WRF model; FF; Wind speed - interpolated height value
18;   WD; AVG;  deg;  20.0; WRF model; WRF model; DD; Wind direction - interpolated height value
19;   WD; AVG;  deg;  40.0; WRF model; WRF model; DD; Wind direction - interpolated height value
20;   WD; AVG;  deg;  60.0; WRF model; WRF model; DD; Wind direction - interpolated height value
21;   WD; AVG;  deg;  80.0; WRF model; WRF model; DD; Wind direction - interpolated height value
22;   WD; AVG;  deg; 100.0; WRF model; WRF model; DD; Wind direction - interpolated height value
23;   WD; AVG;  deg; 120.0; WRF model; WRF model; DD; Wind direction - interpolated height value
24;   WD; AVG;  deg; 140.0; WRF model; WRF model; DD; Wind direction - interpolated height value
25;   WD; AVG;  deg; 160.0; WRF model; WRF model; DD; Wind direction - interpolated height value
26;   WD; AVG;  deg; 200.0; WRF model; WRF model; DD; Wind direction - interpolated height value
27;   WD; AVG;  deg; 250.0; WRF model; WRF model; DD; Wind direction - interpolated height value
28;   WD; AVG;  deg; 300.0; WRF model; WRF model; DD; Wind direction - interpolated height value
29;   WD; AVG;  deg; 350.0; WRF model; WRF model; DD; Wind direction - interpolated height value
30;   WD; AVG;  deg; 400.0; WRF model; WRF model; DD; Wind direction - interpolated height value
31;   WD; AVG;  deg; 450.0; WRF model; WRF model; DD; Wind direction - interpolated height value
32;   WD; AVG;  deg; 500.0; WRF model; WRF model; DD; Wind direction - interpolated height value
33;   WS; AVG; ms-1;  10.0; WRF model; WRF model; FF10; WIND SPEED AT 10 M - surface level
34;   WD; AVG;  deg;  10.0; WRF model; WRF model; DD10; WIND DIRECTION AT 10 M - surface level
```

Utvalgte resultater: Halsaneset

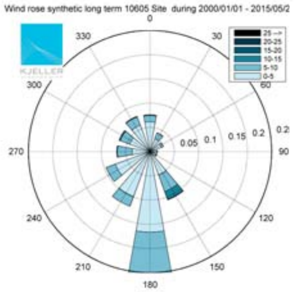

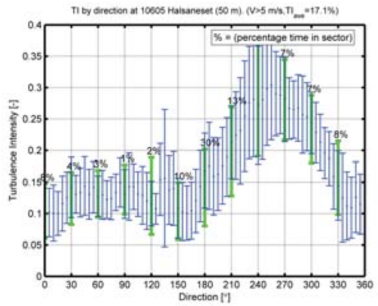

Utvalgte resultater

Tabell 1: Ekstremverdier med 10 min middelvind og 50 års returperiode hentet fra rapport KVT/TMW/2015/R052

	N	NE	E	SE	S	SW	W	NW	Omni
Midsund	25.5	18.6	19.0	23.9	26.4	19.4	15.8	23.6	27.2
Julbø	26.8	17.5	18.5	21.7	27.8	25.7	26.8	25.9	29.1
Halsaneset	22.3	17.9	22.6	28.2	25.6	19.8	21.7	21.1	28.4
Åkvik	20.1	20.4	16.8	25.3	24.6	22.5	23.6	23.2	26.3

Tabell 2: Ekstremverdier med 3 sec vindkast og 50 års returperiode hentet fra rapport KVT/TMW/2015/R052 [1]

	N	NE	E	SE	S	SW	W	NW	Omni
Midsund	36.5	25.1	25.4	30.8	35.3	32.4	35.2	39.2	40.0
Julbø	34.0	24.6	25.8	31.6	36.3	40.4	40.5	32.5	42.1
Halsaneset	32.1	23.8	29.3	36.8	30.6	33.5	38.0	32.7	39.0
Åkvik	30.3	30.6	27.2	30.5	30.6	33.8	36.3	30.0	36.7

Frekvensspekter- Halsaneset (171˚)

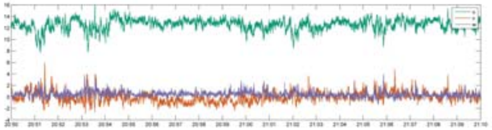

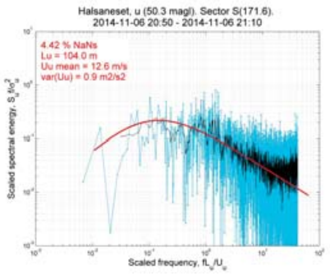

Koherens som funksjon av frekvens ved gitt vertikal separasjon

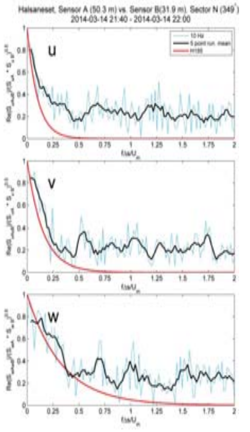

Med Um=10 m/s og Δs=50.3-31.9m=18.4 m, ser vi at fΔs/Um=0.2 svarer til 0.1 Hz (10 sek). Dvs at koherensen er sterkt til stede når tidsskala på virvlene overstiger 10 sekunder, mens den dør ut på kortere tidsskala.

Økes vindhastigheten til 20 m/s, fåes respons ned til 5 sekunder.

Analysis of offshore turbulence intensity – comparison with prediction models

Karolina Lamkowska
Piotr Domagalski
Lars Morten Bardal
Lars Roar Saetran

NTNU

Agenda

1. Site description and methodology
2. Atmospheric stability
3. Models in neutral conditions
4. Models in stable conditions
5. Models in unstable conditions
6. Conclusions
7. Bibliography

Site of Skipheia measurement station

Titran on Frøya island,
Sør-Trøndelag region in mid-Norway

100 m high Mast-2 is located
63.66638 N, 8.34251 E

Equipment and methodology

- Mast-2: six pairs of 2D ultrasonic wind sensors (Gill Wind Observer); seven temperature sensors
- Sampling frequency: 1Hz
- Investigated heights: 16, 25, 40, 70 and 100 m
- Pressure from Sula Weather Station, 20 km north from Mast-2
- Average surface roughness: 0.00308 m
- Most frequent wind velocity at 100 m: 9.05 m/s
- Observations time: 18.11.2009 — 31.12.2014
- Filter: 10 min. subsamples of wind data only with 100% covering 600 s interval
- Coverage: 44.2% i.e. 360 870 000 one-second-samples

Atmospheric stability class calculation

The Monin-Obukhov length (L) is computed from bulk Richardson number.

$$Ri_b = \frac{g}{\bar{\theta}_v} \frac{\frac{\Delta\theta_v}{\Delta z}}{\left(\frac{\Delta u}{\Delta z}\right)^2}$$

If bulk Richardson number is 0, assuming L=∞ [3]

$$L = \begin{cases} \frac{z_{ref}}{Ri_b}, & Ri_b \le 0 \\ \frac{z_{ref}(1-5Ri_b)}{Ri_b}, & 0 < x < 0.2 \end{cases}$$

where $z_{ref} = \frac{z_2 - z_1}{\log\left(\frac{z_2}{z_1}\right)}$

Three **atmospheric stability classes**

Stability classifications according to the Monin-Obukhov length:

Monin-Obukhov length [L]	Atmospheric stability class	
-200 m <L< 0 m	very unstable	unstable
-1000 m< L<-200 m	unstable	
|L| > 1000 m	neutral	
200 m < L< 1000 m	stable	stable
0 m < L < 200 m	very stable	

Stability **of the atmosphere**

Distribution of atmospheric stability for all investigated heights

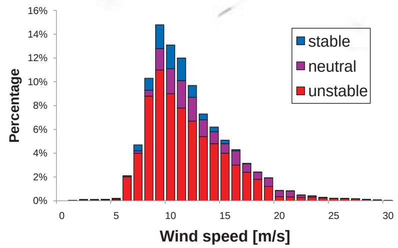

Stability class frequency in 16 sectors

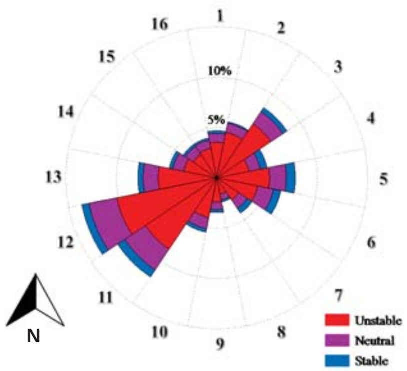

Longitudinal TI in neutral class

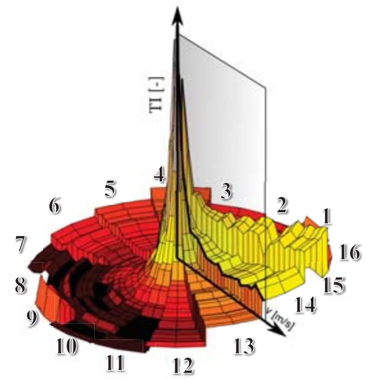

Neutral conditions

Source	Input	Output	Comments
ESDU 85020	f, z, u, z_0, u_*	std of u	u >10m/s, ESDU recommended formula for u_*
TIPEX, Zhou, Panofsky, Emeis et al.	u_*	std of u	models $\alpha \cdot u_*$, $\alpha \in (2;3.5)$
Wieringa	z, z_0	TI	
Hanna, Wyngaard	f, z, z_0	std of lateral wind speed	

Average TI from 5 years

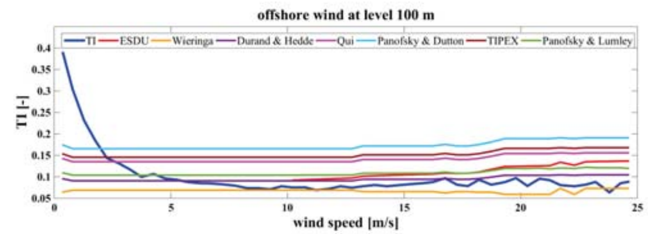

ESDU in equilibrium conditions, where $\eta = 1 - 6fz/u_*$ and h can be taken as $u_*/(6f)$. [7]

$$\frac{std(u)}{u_*} = \frac{7.5\eta[0.538 + 0.09\ln(\frac{z}{z_0})]^{\eta^{16}}}{1 + 0.156\ln(\frac{u_*}{f z_0})}$$

Zhou et al. (2000) [9] $std(u) = 3.4u_*$

Qi et al. (1996) [9] $std(u) = 2.98u_*$

Hedde & Durand [15] $std(u) = 2u_*$

TIPEX [9] $std(u) = 3.45u_*$

Panofsky & Dutton (1984) for surface layer only. [9] $std(u) = 2.65u_*$

Counihan [18], Emeis [4] $std(u) = 2.5u_*$

Wieringa (1973) [14] $TI = \frac{1}{\ln(z/z_0)}$

Accuracy change with altitude

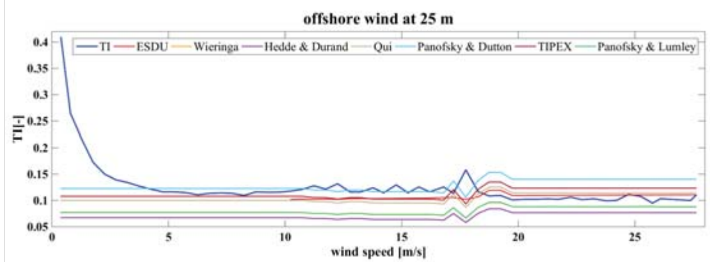

TI in normal direction

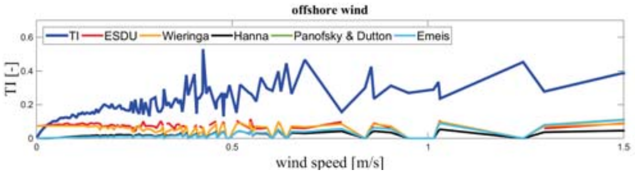

ESDU in equilibrium conditions [7]

$$\mathrm{std}(v) = \mathrm{std}(u)\left[1 - 0.22\cos^4\left(\frac{\pi}{2}\frac{z}{h}\right)\right]$$

Hanna(1982) based on Wyngaard (1974) for the surface layer only. [16]

$$\mathrm{std}(v) = 1.3u_* \exp(-2\frac{fz}{u_*})$$

Panofsky & Dutton (1984) for surface layer only. [9]

$$\mathrm{std}(v) = 1.92u_*$$

Counihan [18], Emeis [4]

$$\mathrm{std}(v) = 1.875u_*$$

Wieringa (1973) [14]

$$TI = \frac{1}{\ln(z/z_0)}$$

13

Stable conditions

Source	Input	Output	Comments
Gryning et al. Paumier	z, h, u_*	std of u	
Banta, De Bruin	u_*	std of u	
Pasquill, Luhar, Cirillo&Poli	std of wind direction, u	std of u	only for $u < 2$ m/s

14

Stable atmospheric class

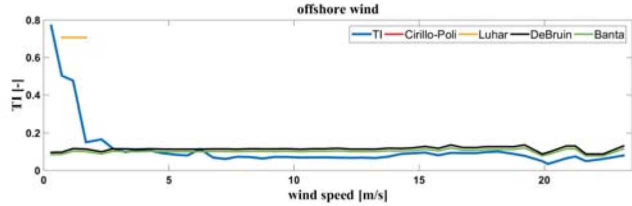

Average from 5 years for offshore wind at level 100 m

Banta et al. [11]

$$\mathrm{std}(u)^2 = 4.9u_*^2$$

De Bruin, Kohsiek, Van Den Hurk (1992) [5]

$$\mathrm{std}(u) = 2.5u_*$$

Formulas only for low wind ($u < 2\frac{m}{s}$):

Cirillo and Poli (1992)[17]

$$\mathrm{std}^2(u) = \overline{u}^2[\cosh(\sigma_\theta^2) - 1]$$

Luhar (2010) [10]

$$\mathrm{std}^2(u) = \overline{u}^2\exp(-\sigma_\theta^2)[\cosh(\sigma_\theta^2) - 1]$$

15

Diagrams of TI in normal direction during stable conditions

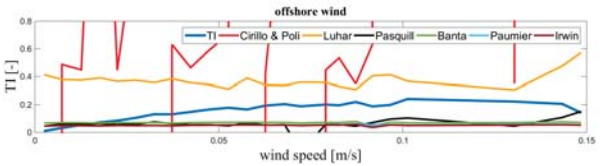

Offshore wind from 5 years at level 70 m

Gryning, Holtslag, Irwin and Sivertsen (1987) [8]

$$\frac{\mathrm{std}(v)}{u_*} = \left[2\left(1 - \frac{z}{h}\right)\right]^{1/2}$$

Banta et al. [11]

$$\mathrm{std}(v)^2 = 3.4u_*^2$$

Paumier. Formula from COST 710 [6]

$$\mathrm{std}(v) = 1.643u_*\frac{1 - \frac{z}{h}}{(1 + 2.8\frac{z}{h})^{\frac{1}{3}}}$$

Formulas only for low wind ($u < 2\frac{m}{s}$):

Pasquill (1974) (in article of Steven Hanna (1983)) [9]

$$\frac{\mathrm{std}(v)}{\overline{u}} = \mathrm{tg}\,\sigma_\theta$$

Cirillo and Poli (1992)[17]

$$\mathrm{std}^2(v) = \overline{u}^2\sinh(\sigma_\theta^2)$$

Luhar (2010) [10]

$$\mathrm{std}^2(v) = \overline{u}^2\exp(-\sigma_\theta^2)\sinh(\sigma_\theta^2)$$

16

Model's behavior in sector 9

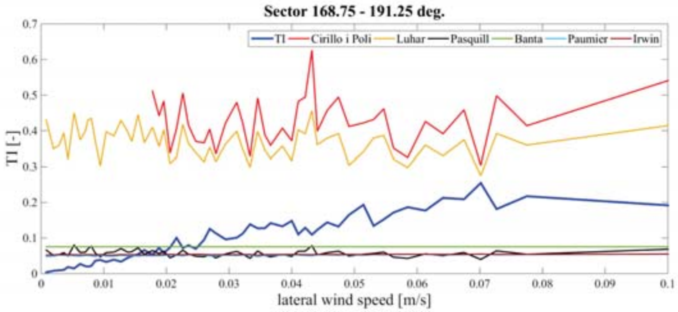

17

Normal TI in stable atmospheric class

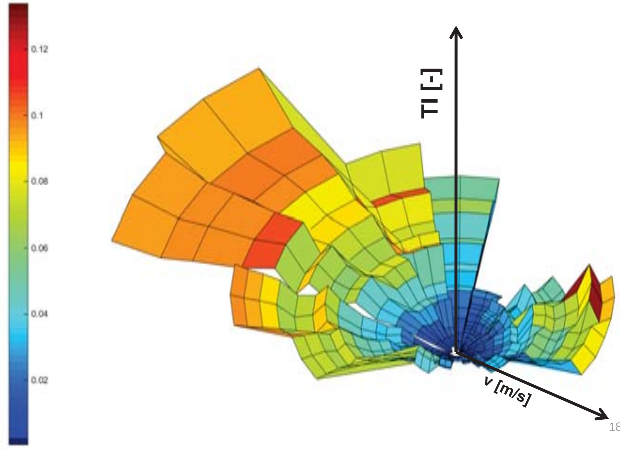

18

Unstable conditions

Source	Input	Output	Comments
Townsend	L, z, h, u_*, u	std of u	
Wilson	L, z, h, u_*, u	std of u	$z \ll h$
Wyngaard, Cote Panofsky, Arya	L, h, u_*	std of u	formulas good also for near neutral conditions
TIPEX De Bruin et al.	L, z, u_*	std of u	
Gryning et al.	L, z, h, u_*, k	std of u	k is von Karman constant

19

TI in longitudinal direction

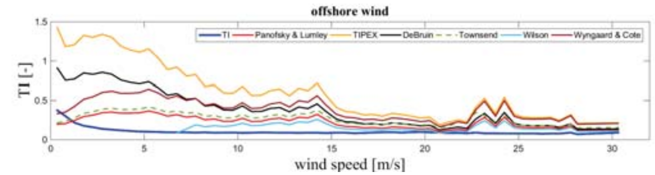

Offshore wind from 5 years at level 70 m

Models in use:

Townsend (1976), where Towsend & Perry recomended $A_1 = 1.26$ [12]

$$\frac{\mathrm{std}^2(u)}{u_*^2} = 4 + 0.6\left(\frac{h}{-L}\right)^{2/3} - A_1 \ln\left(\frac{z}{h}\right)$$

Wilson with parameters $b = 3/4 \quad c = 1/4,\ z \ll h$.[12]

$$\frac{\mathrm{std}^2(u)}{u_*^2} = \left[4 + b\left(\frac{h}{-L}\right)^{2/3}\right]\left[1 - \left(\frac{z}{h}\right)^c\right]$$

Wyngaard & Cote (1974) [13]

$$\frac{\mathrm{std}(u)}{u_*} = \left[4 + 0.6\left(\frac{h}{-L}\right)^{2/3}\right]^{1/2}$$

Panofsky & Lumley (1964) [13]

$$\frac{\mathrm{std}(u)}{u_*} = \left(12 + 0.5\frac{h}{-L}\right)^{1/3}$$

De Bruin, Kohsiek, Van Den Hurk (1992) [5]

$$\frac{\mathrm{std}(u)}{u_*} = 2.2\left(1 + 3\frac{z}{-L}\right)^{1/3}$$

Bian, Xu, Lu and others, TIPEX (2002) [9]

$$\frac{\mathrm{std}(u)}{u_*} = 3.45\left(1 + 3\frac{z}{-L}\right)^{1/3}$$

20

Only for the weak?

Crosswind components of wind velocity during unstable conditions

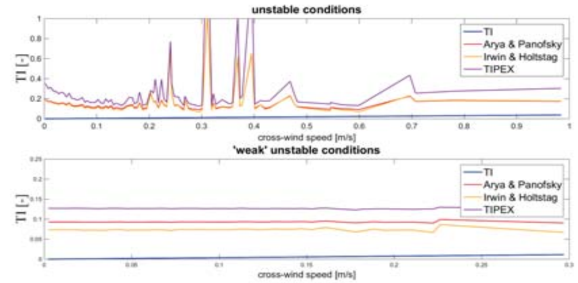

Panofsky (1977), Arya(1995) [6]

$$\frac{\mathrm{std}(v)}{u_*} = \left(12 + 0.5\frac{h}{-L}\right)^{1/3}$$

Bian, Xu, Lu and others, TIPEX, at Tibetan Plateau (2002) [9]

$$\frac{\mathrm{std}(v)}{u_*} = 3.15\left(1 + 3\frac{z}{-L}\right)^{1/3}$$

Gryning, Holtstag, Irwin and Sivertsen (1987) [8]

$$\frac{\mathrm{std}(v)}{u_*} = \left[2\left(1 - \frac{z}{h}\right)\right]^{1/2}$$

21

Weak unstable condition

Model's accuracy at level 16 m

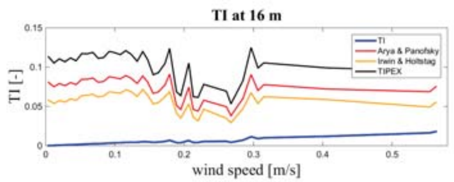

Model's accuracy at level 100 m

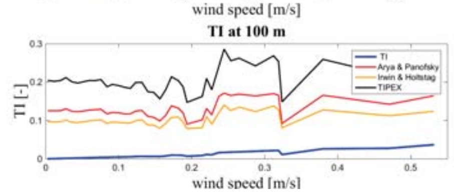

22

Conclusions

- **Neutral** atmospheric stability class**:** the strong influence of height on the models accuracy. Longitudinal TI at the level **100** m: **Wieringa, Hedde & Durand**, but with level the accuracy change.
  Best, regardless of the height: **ESDU**.
  Normal TI: **none**.
- **Stable** conditions, longitudinal TI: both **De Bruin et al.** and **Banta** models.
  Normal TI: model of **Luhar**.
- **Unstable** class of atmospheric stability, longitudinal TI: model of **Wilson.**
  TI in normal direction: **Irwin & Holstag** .

23

References
[1] Kalvig, Siri, Ove Tobias Gudmestad, and Nina Winther. "Exploring the gap between 'best knowledge' and 'best practice' in boundary layer meteorology for offshore wind energy." Wind Energy 17.1 (2014): 161-171.
[2] IEC 61400–1, Wind turbines – Part 1: Design requirements, Ed.3, 2005.
[3] J. Businger, Y. Izumi, E. Bradley and J. Wyngaard, Flux-Profile Relationships in the Atmospheric Surface Layer, Journal of Meteorology, 1971, p. 181–189.
[4] S. Emeis, ”Wind Energy Meteorology. Atmospheric Physics for Wind Power Generation”, Springer, 2012
[5] H.A.R. De Bruin, W. Kohsiek, B.J.J.M. Van Den Hurk,”A Verification of Some Methods to Determine the Fluxes of Momentum, Sensible Heat, and Water Vapour Using Standard Deviation and Structure Parameter of Scalar Meteorological Quantities”,1992
[6] A. Cenedese, G. Cosemans, H. Erbrink, R. Stubi, ”Vertical profiles of wind, temperature and turbulence”, COST Action 710, Preprocessing of Meteorological Data for Dispersion Modelling, 1998
[7] T.V. Lawson et al. ESDU 85020 ”Characteristics of atmospheric turbulence near the ground Part II: single point data for strong winds (neutral atmosphere)”, 1985
[8] S. E. Gryning, A. A. M. Holtstag, J. S. Irwin, B. Silvertsen, ” Applied Dispersion Modelling Bosed on Meteorological Scaling Parameters”, Atmospheric Environment, Vol. 21, pp. 79-89, 1987
[9] Bian L. et al., ”Analyses of Turbulence Parameters in the Near-Surface Layer at Qamdo of the Southeastern Tibetan Plateau”, Advances in Atmospheric Sciences, Vol. 20, No. 3, pp.369-378, 2003
[10] A. K. Luhar, ”Estimating Variances of Horizontal Wind Fluctuations in Stable Conditions”, Boundary-Layer Meteorol, Vol. 135, pp. 301–311, 2010
[11] R. M. Banta, Y. L. Pichugina, W. A. Brewer, ”Turbulent Velocity-Variance Profiles in the Stable Boundary Layer Generated by a Nocturnal Low-Level Jet”, Journal of the Atmospheric Sciences, Vol. 63, pp. 2700-2719, 2006
[12] J. D. Wilson, ”Monin-Obukhov Functions for Standard Deviations of Velocity”, Boundary-Layer Meteorology, Vol. 129, pp. 353–369, 2008
[13] H. A. Panofsky, H. Tennekes, D. H. Lenschow, J. C. Wyngaard, ”The Characteristics of Turbulent Velocity Components in the Surface Layer Under Convective Conditions”, 1977
[14] J. Wieringa, ”Gust Factors over Open Water and Built-up Country”, 1972
[15] T. Hedde, P. Durand, ”Turbulence intensities and bulk coefficients in the surface layer above the sea”, Boundary-Layer Meteorology Vol. 71, pp 415-432, 1994
[16] I. Korsakissok, V. Mallet, ”Comparative study of Gaussian dispersion formulas within the Polyphemus platform: evaluation with Prairie Grass and Kincaid experiments”, Journal of Applied Meteorology and Climatology, Vol. 48, 2459-2473, 2009
[17] M.C. Cirillo, A.A. Poli, ”An intercomparison of semiempirical diffusion models under low wind speed, stable conditions”, Atmospheric Environment Vol. 26A, No. 5, pp. 765-774, 1992
[18] J. Counihan, ”Adiabatic atmospheric boundary layers: a review and analysis of data from the period 1880-1972”, Atmospheric Environment, Vol. 9, pp. 871-905, 1975
[19] S. Fechner, ”Preprocessing of meteorological data for atmospheric theoretical/numerical models”, Master's Thesis, NTNU, 2015

24

C2) Met-ocean conditions

Coherence of turbulent wind under neutral wind conditions at FINO,
L. Eliassen, NTNU / Statkraft

Assessment of offshore wind coherence by pulsed Doppler lidars, J.B. Jakobsen, UiS

Turbulent Structure over Air-Sea Wavy Interface: Large-Eddy Simulation, M.B. Paskyabi, UiB

Coherence of turbulent wind under neutral wind condition at FINO1

Charlotte Obhrai, University of Stavanger, charlotte.obhrai@uis.no
Lene Eliassen, Norwegian Technical and Scientific University, lene.eliassen@ntnu.no

University of Stavanger
uis.no

1/26/2016

Overview

- Motivation
- Methods
- Results
- Conclusion

Overview

- Motivation
- Methods
- Results
- Conclusion

Turbulence models in the IEC 61400

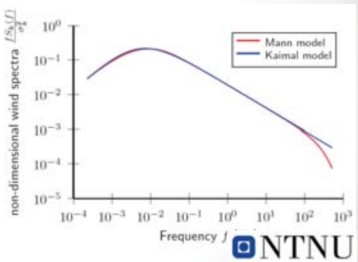

Simulated wind (app B.2 IEC 61400-1)

- Kaimal spectrum
- IEC coherence function:

$$\gamma(r,f) = e^{\left[-12\left(\left(f\cdot r/V_{hub}\right)^2+\left(0.12\cdot r/L_c\right)^2\right)^{0.5}\right]}$$

- Reduced frequency:

$$f\cdot r/V_{hub}$$

Simulated wind (app B.1 IEC 61400-1)

- Mann turbulence model:

$$\Phi_{11}(k_1,k_2,k_3) = \frac{E(k_0)}{4\pi k_0^4}\left(k_0^2 - k_1^2 - 2k_1(k_3+\beta(k)k_1)\zeta_1 + (k_1^2+k_2^2)\zeta_1^2\right) \quad (B.1)$$

$$\Phi_{22}(k_1,k_2,k_3) = \frac{E(k_0)}{4\pi k_0^4}\left(k_0^2 - k_2^2 - 2k_2(k_3+\beta(k)k_1)\zeta_2 + (k_1^2+k_2^2)\zeta_2^2\right) \quad (B.2)$$

$$\Phi_{33}(k_1,k_2,k_3) = \frac{E(k_0)}{4\pi k^4}\left(k_1^2+k_2^2\right) \quad (B.3)$$

$$\Phi_{12}(k_1,k_2,k_3) = \frac{E(k_0)}{4\pi k_0^4}\left(-k_1k_2 - k_1(k_3+\beta(k)k_1)\zeta_2 - k_2(k_3+\beta(k)k_1)\zeta_1 + (k_1^2+k_2^2)\zeta_1\zeta_2\right) \quad (B.4)$$

$$\Phi_{13}(k_1,k_2,k_3) = \frac{E(k_0)}{4\pi k_0^2k^2}\left(-k_1(k_3+\beta(k)k_1) + (k_1^2+k_2^2)\zeta_1\right) \quad (B.5)$$

$$\Phi_{23}(k_1,k_2,k_3) = \frac{E(k_0)}{4\pi k_0^2k^2}\left(-k_2(k_3+\beta(k)k_1) + (k_1^2+k_2^2)\zeta_2\right)$$

Overview

- Motivation
- Methods
- Results
- Conclusion

FINO 1

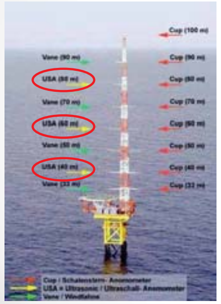

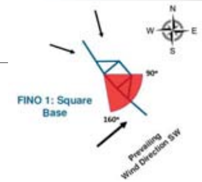

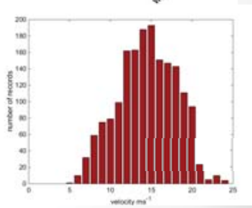

10 min averages

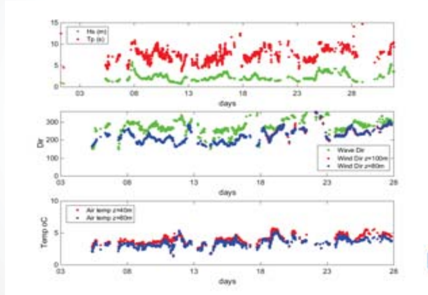

10 min averages

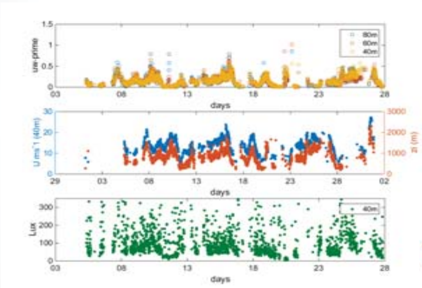

Overview

- Motivation
- Methods
- Results
- Conclusion

uu cocoherence 20 m seperation

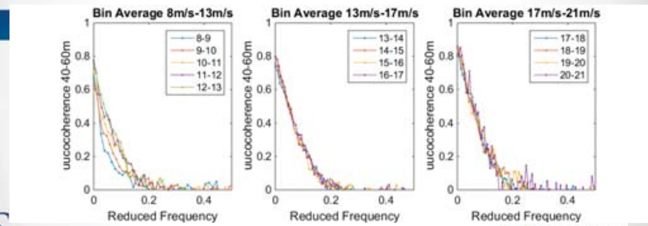

$f \cdot r / V_{hub}$

vv cocoherence 20 m seperation

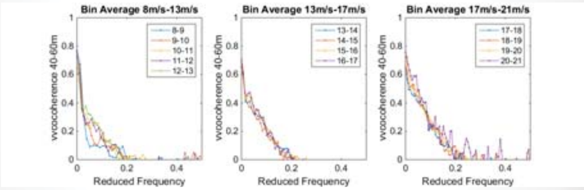

University of Stavanger
NTNU

ww cocoherence 20 m seperation

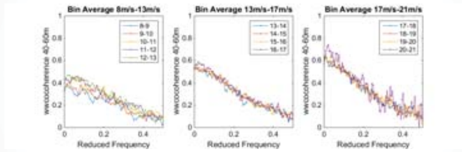

University of Stavanger
NTNU

40-60m and 60-80m (20 m separation)

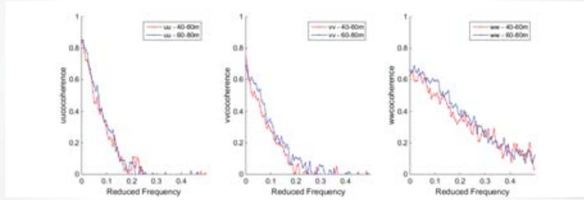

University of Stavanger
NTNU

Compare 40m and 20 m separation

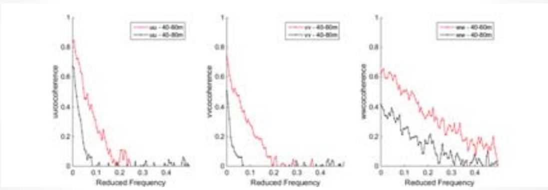

University of Stavanger
NTNU

Compare to the coherence in IEC 61400-1

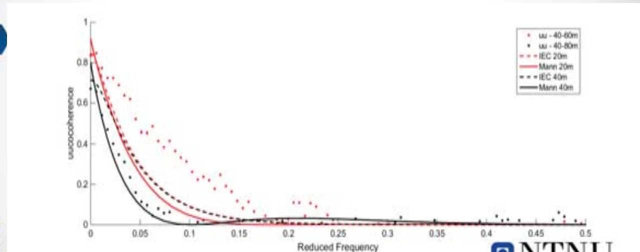

University of Stavanger
NTNU

Compare to the coherence in IEC 61400-1

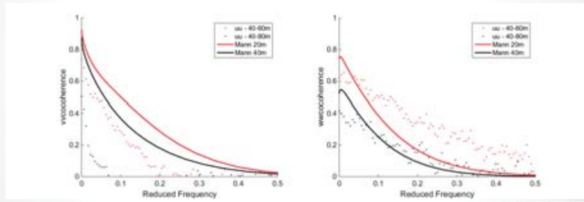

University of Stavanger
NTNU

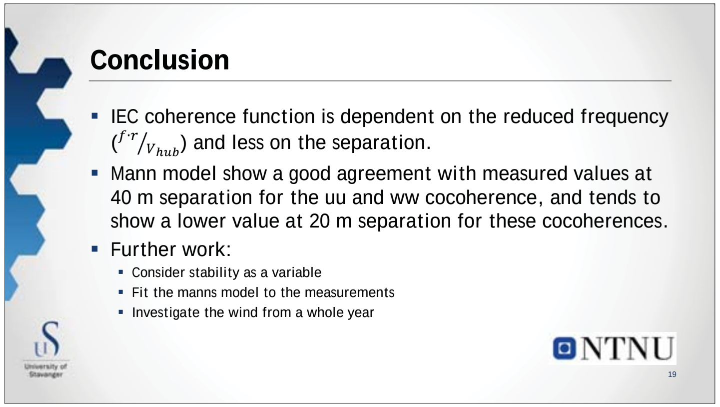
Conclusion
IEC coherence function is dependent on the reduced frequency ($^{f \cdot r}/_{V_{hub}}$) and less on the separation.
Mann model show a good agreement with measured values at 40 m separation for the uu and ww cocoherence, and tends to show a lower value at 20 m separation for these cocoherences.
Further work:
Consider stability as a variable
Fit the manns model to the measurements
Investigate the wind from a whole year
University of Stavanger
NTNU
19

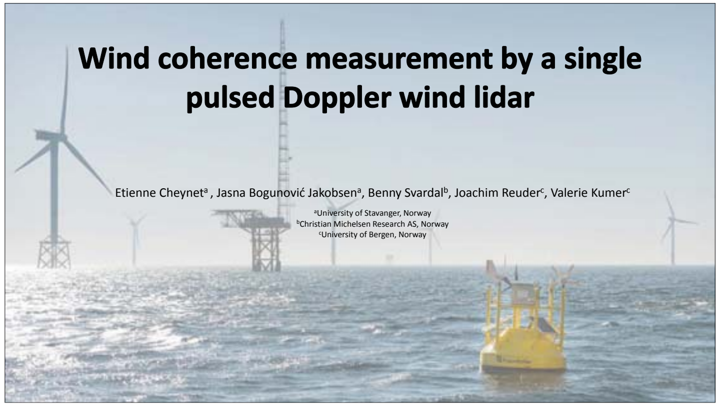
Wind coherence measurement by a single pulsed Doppler wind lidar
Etienne Cheynet[a] , Jasna Bogunović Jakobsen[a], Benny Svardal[b], Joachim Reuder[c], Valerie Kumer[c]
[a]University of Stavanger, Norway
[b]Christian Michelsen Research AS, Norway
[c]University of Bergen, Norway

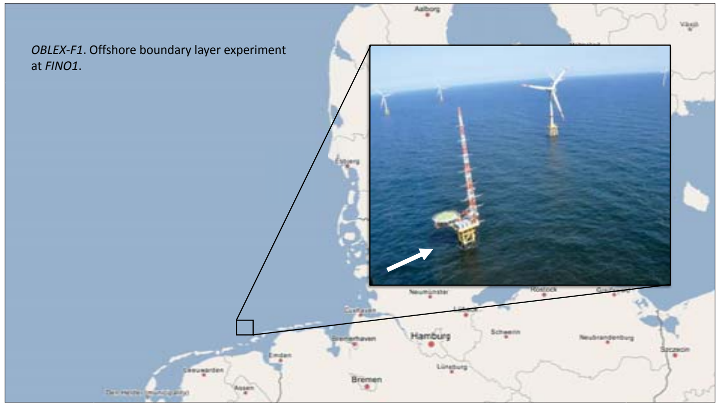
OBLEX-F1. Offshore boundary layer experiment at FINO1.
Aalborg
Hamburg
Bremen
Schwerin
Rostock

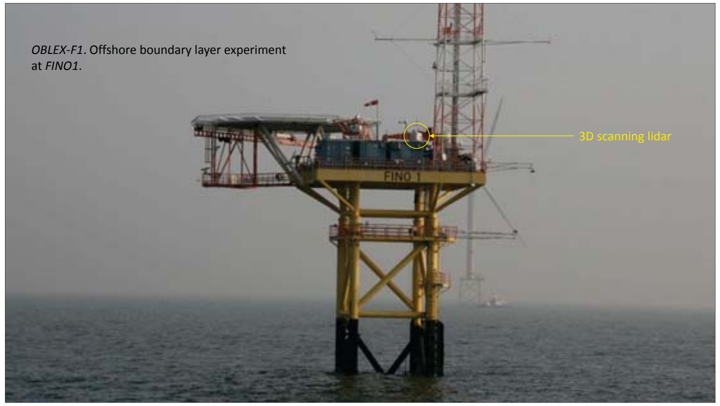
OBLEX-F1. Offshore boundary layer experiment at FINO1.
3D scanning lidar
FINO 1

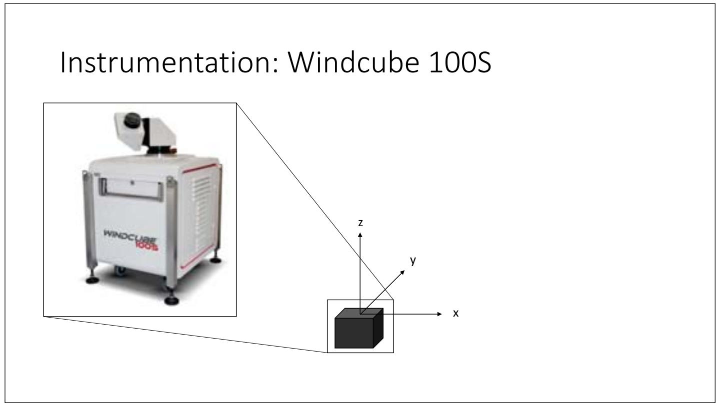
Instrumentation: Windcube 100S
z
y
x

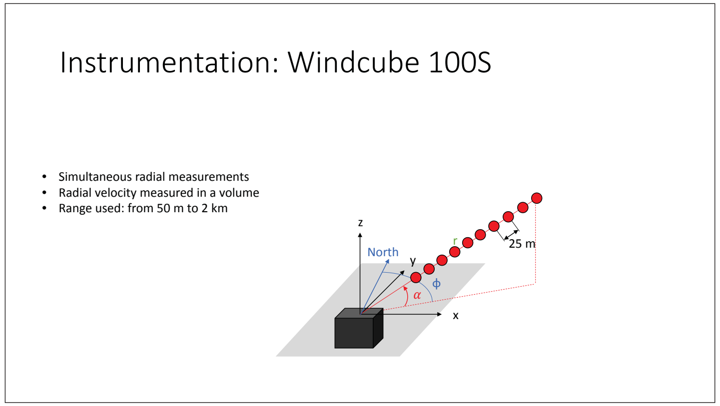
Instrumentation: Windcube 100S
• Simultaneous radial measurements
• Radial velocity measured in a volume
• Range used: from 50 m to 2 km
z
North
y
x
25 m
r
α
ϕ

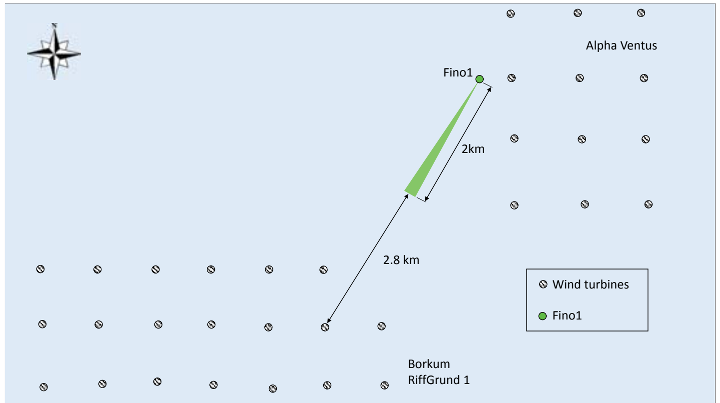
Alpha Ventus
Fino1
2km
2.8 km
Wind turbines
Fino1
Borkum
RiffGrund 1

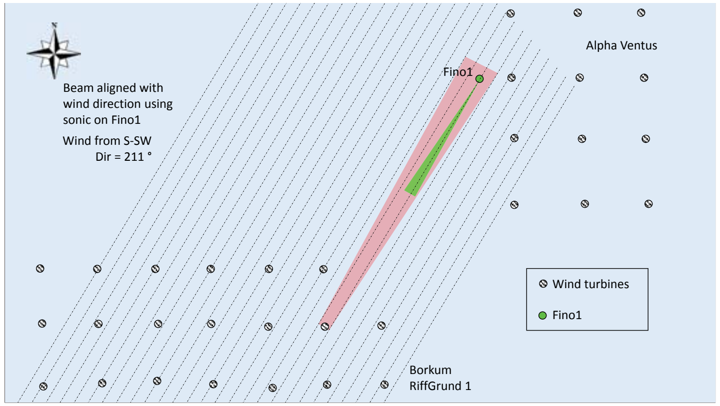
Alpha Ventus
Fino1
Beam aligned with wind direction using sonic on Fino1
Wind from S-SW
Dir = 211 °
Wind turbines
Fino1
Borkum RiffGrund 1

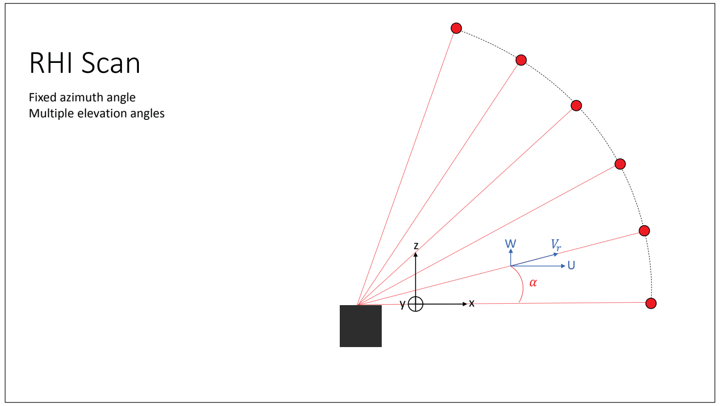
RHI Scan
Fixed azimuth angle
Multiple elevation angles
z
W
V_r
U
α
y
x

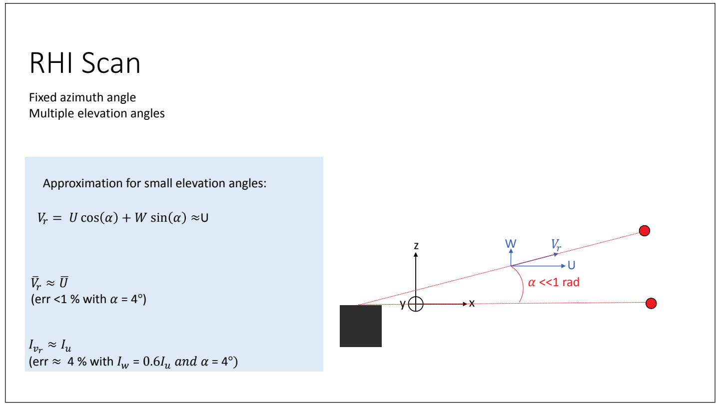
RHI Scan
Fixed azimuth angle
Multiple elevation angles
Approximation for small elevation angles:
$V_r = U\cos(\alpha) + W\sin(\alpha) \approx U$
$\bar{V}_r \approx \bar{U}$
(err <1 % with α = 4°)
$I_{v_r} \approx I_u$
(err ≈ 4 % with $I_w = 0.6 I_u$ and α = 4°)
z
W
V_r
U
α <<1 rad
y
x

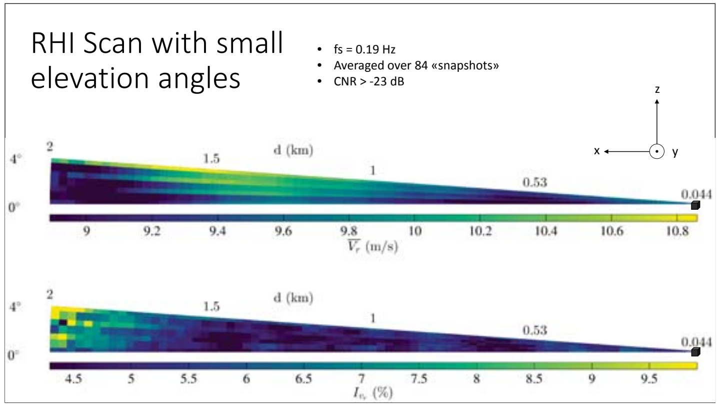
RHI Scan with small elevation angles
fs = 0.19 Hz
Averaged over 84 «snapshots»
CNR > -23 dB
z
x
y
d (km)
4°
0°
2
1.5
1
0.53
0.044
9
9.2
9.4
9.6
9.8
10
10.2
10.4
10.6
10.8
$\bar{V}_r$ (m/s)
4.5
5
5.5
6
6.5
7
7.5
8
8.5
9
9.5
I_{v_r} (%)

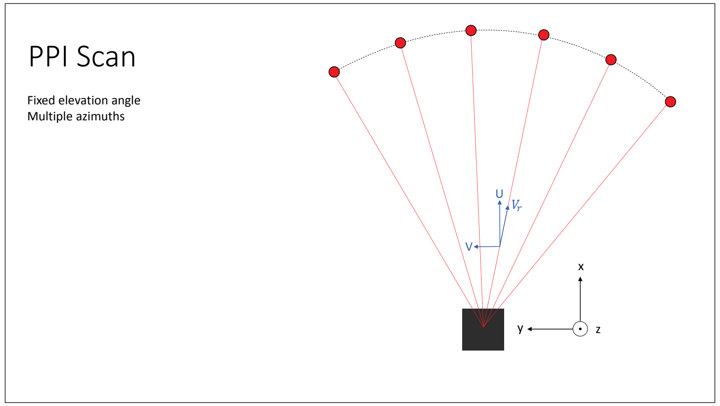
PPI Scan
Fixed elevation angle
Multiple azimuths
U
V_r
V
x
y
z

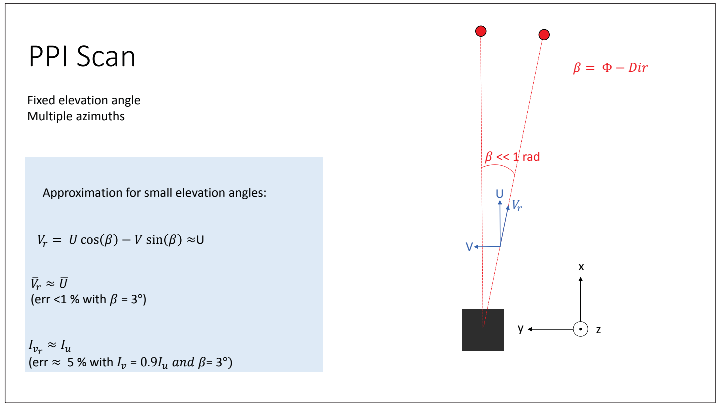
PPI Scan
Fixed elevation angle
Multiple azimuths
$\beta = \Phi - Dir$
β << 1 rad
Approximation for small elevation angles:
$V_r = U\cos(\beta) - V\sin(\beta) \approx U$
$\bar{V}_r \approx \bar{U}$
(err <1 % with β = 3°)
$I_{v_r} \approx I_u$
(err ≈ 5 % with $I_v = 0.9 I_u$ and β= 3°)
U
V_r
V
x
y
z

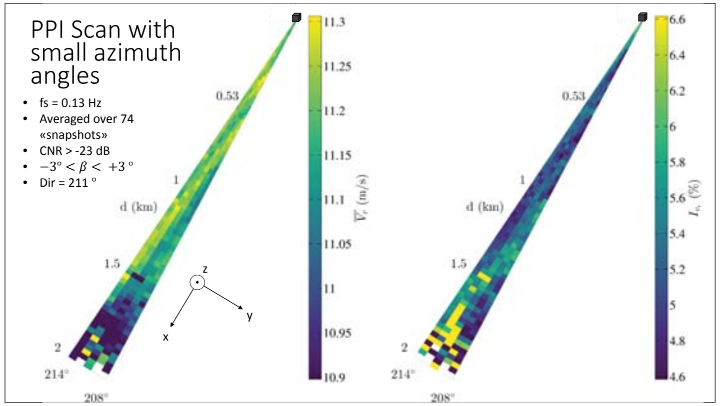
PPI Scan with small azimuth angles
fs = 0.13 Hz
Averaged over 74 «snapshots»
CNR > -23 dB
−3° < β < +3°
Dir = 211°
d (km)
214°
208°

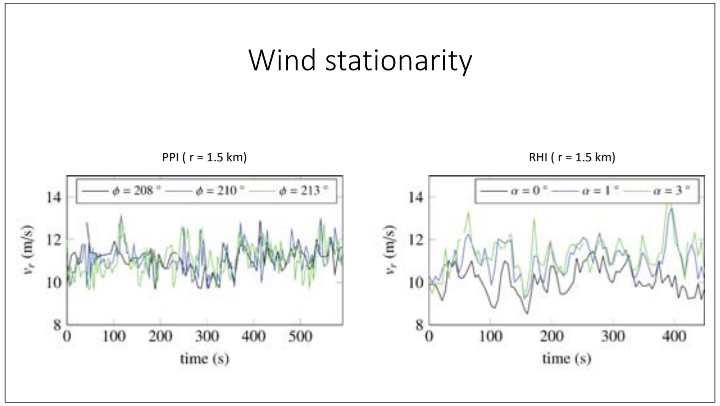
Wind stationarity
PPI (r = 1.5 km)
RHI (r = 1.5 km)
time (s)

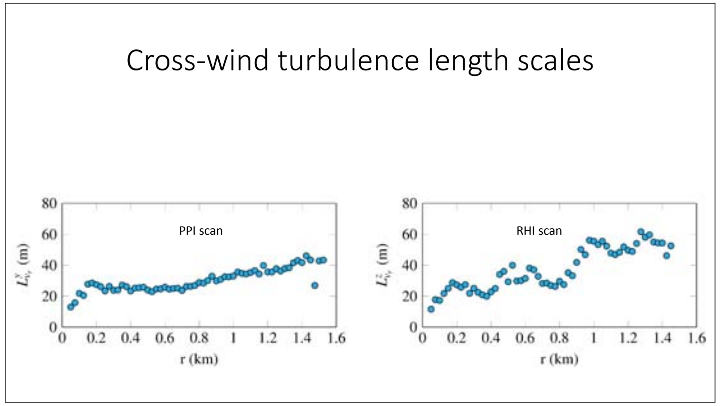
Cross-wind turbulence length scales
PPI scan
RHI scan
r (km)

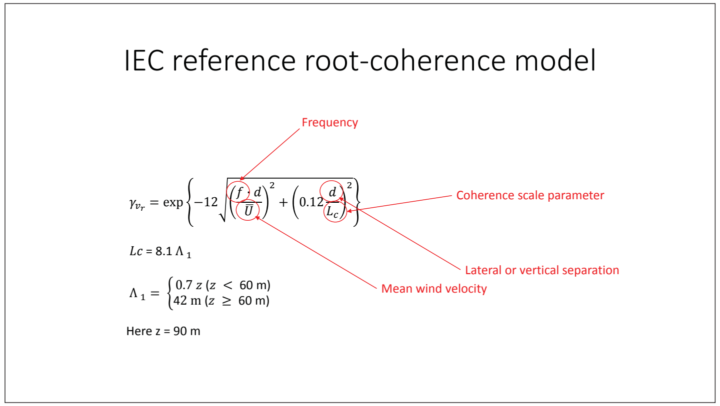
IEC reference root-coherence model
Frequency
Coherence scale parameter
Lateral or vertical separation
Mean wind velocity
Lc = 8.1 Λ1
Λ1 = 0.7 z (z < 60 m) ; 42 m (z ≥ 60 m)
Here z = 90 m

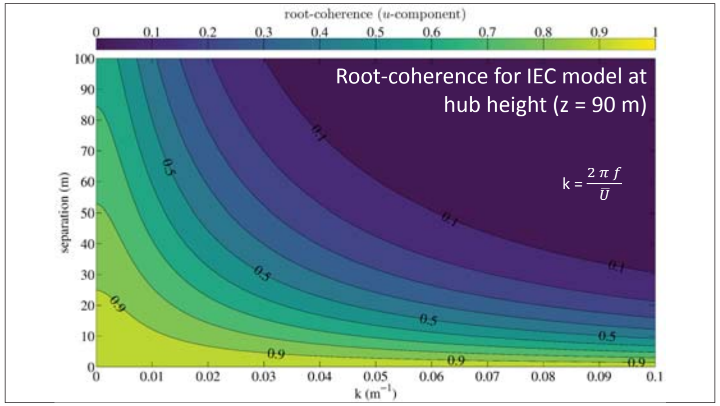
root-coherence (u-component)
Root-coherence for IEC model at hub height (z = 90 m)
k = 2 π f / Ū
separation (m)
k (m⁻¹)

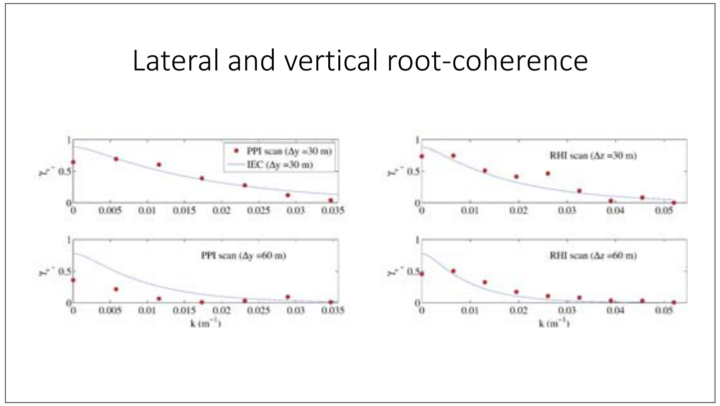
Lateral and vertical root-coherence

Lateral and vertical root-coherence

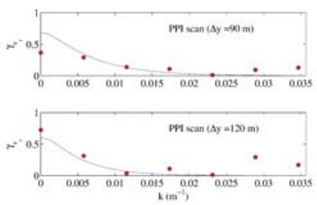

Conclusions

Summary:

- A single pulsed Doppler wind lidar is used to record wind time histories (PPI & RHI scan)
- This requires a particular configuration (small angles relative to mean wind direction)
- The measured coherence showed a rather good agreement with the IEC model

Challenges and prospects:

- The alignment of the lidar beam with the mean wind direction is done manually.
- Multiple samples should be used for coherence estimation.

Turbulent Structure underneath Air-Sea Wavy Interface: Large-Eddy Simulation

Mostafa Bakhoday Paskyabi
Geophysical Institute, University of Bergen
(Mostafa.Bakhoday@uib.no)

Introduction

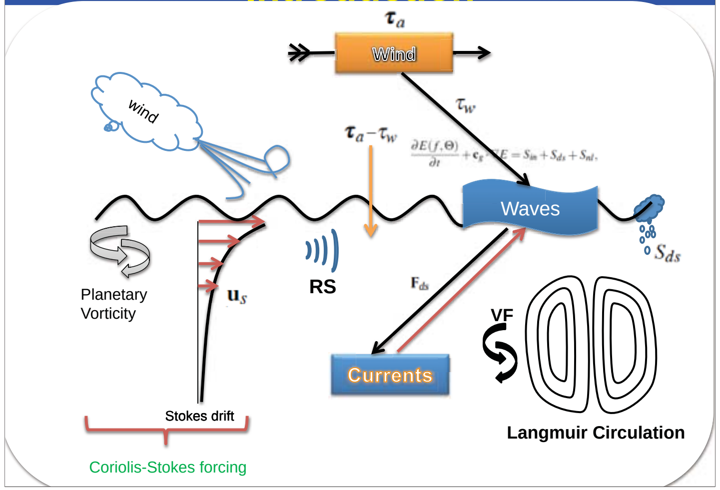

Stokes drift

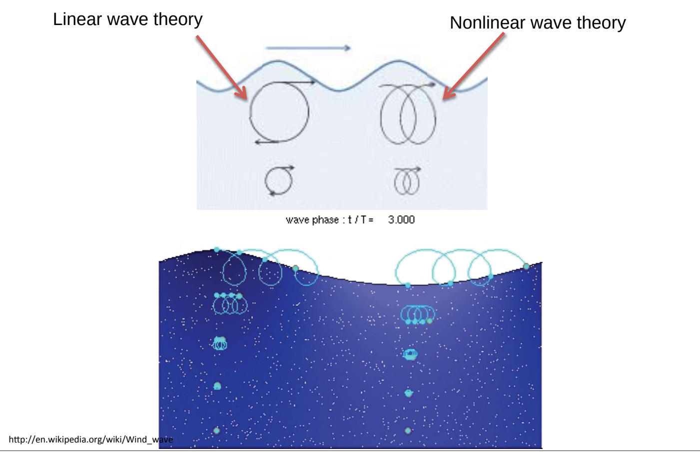

Stokes drift

1. Lagrangian description
2. Eulerian description

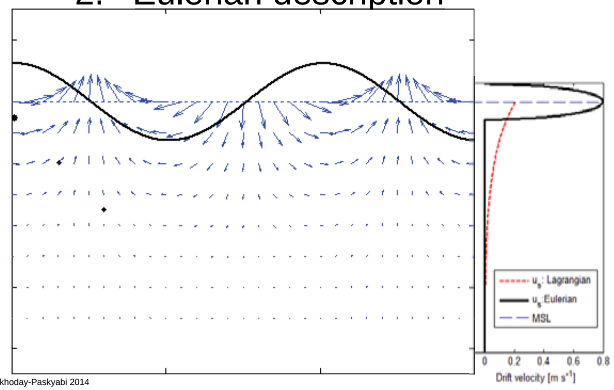

From Bakhoday-Paskyabi 2014

Turbulence (compressible flow)

- Reynolds Averaged modelling (RANS)
- capture only the ensemble statistics

- Direct numerical simulation (DNS) capture all eddies

- Large eddy simulation (LES) intermediate method

Eddies

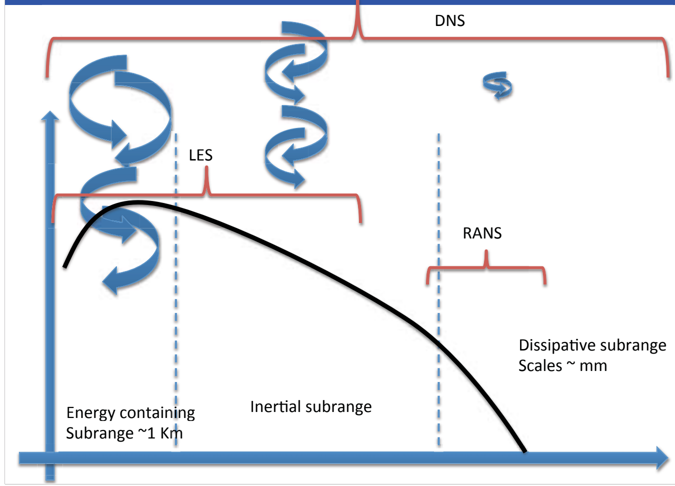

Wave-tubulence interaction (RANS)

Decomposition

Eulerian frame

$T' \ll \tilde{T} \ll \bar{T}$; and $X = X' + \tilde{X} + \bar{X}$,

$$u = \bar{u} + u'$$
$$p = \bar{p} + p'$$

$$\overline{u'} = 0$$
$$\frac{\partial \bar{u}}{\partial t} = \frac{1}{T}\int_0^T \frac{\partial u}{\partial t}dt = \frac{u(T)-u(0)}{T}$$

$$\frac{\partial u}{\partial t} = -\frac{\partial(\overline{u'w'})}{\partial z} + f_{cor}(v+v_s) + F_x,$$
$$\frac{\partial v}{\partial t} = -\frac{\partial(\overline{v'w'})}{\partial z} - f_{cor}(u+u_s) + F_y,$$

7

Bakhoday-Paskyabi 2014

LES

Turbulent flow → Large resolved eddies → Low pass filter $\tilde{f}(x) = \int f(x')G(x,x')dx'$

Turbulent flow → Small non-resolved eddies → Subgrid scales $f''(x) = f(x) - \tilde{f}(x)$

G-Filtering

$$\frac{\partial u_i}{\partial t} + u_j \frac{\partial u_i}{\partial x_j} = \frac{g_i}{T_0}\theta - \frac{1}{\rho}\frac{\partial p}{\partial x_i} + \upsilon \frac{\partial^2 u_i}{\partial x_j^2}$$

SGS

$$\frac{\partial \tilde{u}_i}{\partial t} + \tilde{u}_j \frac{\partial \tilde{u}_i}{\partial x_j} = \frac{g_i}{T_0}\tilde{\theta} - \frac{1}{\rho}\frac{\partial \tilde{p}}{\partial x_i} - \frac{\partial(\widetilde{u_i u_j} - \tilde{u}_i\tilde{u}_j)}{\partial x_j} + \upsilon \frac{\partial^2 \tilde{u}_i}{\partial x_j^2}$$

Wave-Averaged Large-Eddy Simulation

Spatially filtered and temporal filtration for wave decomposition

$$\frac{\partial \bar{u}_i}{\partial x_i} = 0$$

SGS / LC Vortex force

$$\frac{\partial \bar{u}_i}{\partial t} + \bar{u}_j \frac{\partial \bar{u}_i}{\partial x_j} = -\frac{\partial \bar{\Pi}}{\partial x_i} + \frac{1}{Re_\tau}\frac{\partial^2 \bar{u}_i}{\partial x_j^2} - \frac{\partial \tau_{ij}^{LES\,(d)}}{\partial x_j} + \frac{1}{La_t^2}\epsilon_{ijk}U_j^s \bar{\omega}_k$$

$$\overbrace{\frac{\partial k}{\partial t}}^{1} = \overbrace{\frac{\tau}{\rho_0}\cdot\frac{\partial \mathbf{u}}{\partial z}}^{2} + \overbrace{\frac{\tau}{\rho_0}\cdot\frac{\partial \mathbf{u}_s}{\partial z}}^{3} + \overbrace{\overline{b'w'}}^{4} - \varepsilon$$
$$+ \overbrace{\frac{\partial}{\partial z}\left[\frac{\nu_t}{\sigma_k}\frac{\partial k}{\partial z}\right]}^{5} - \overbrace{\frac{\partial T}{\partial z}}^{6},$$

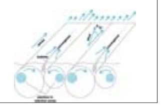

Wave-current-turbulence interaction

In coupled wave-turbulence system, Stokes drift introduces

1. **Coriolis-Stokes force and modification of momentum.**
2. **Langmuir turbulence** and enhanced/suppressed upper ocean mixing.
3. **near surface mass transport** and affecting the transport of materials and sediment transport in shallow water.

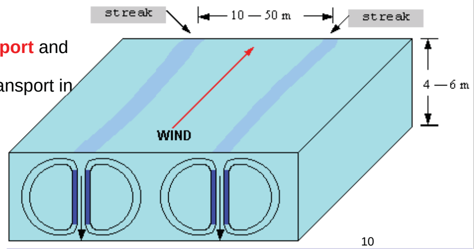

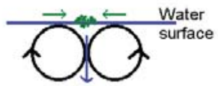

10

T. S. Bianchi

Figure 1 Diagram tracing water through Langmuir circulation cells.

Example og Mixed layer Evolution

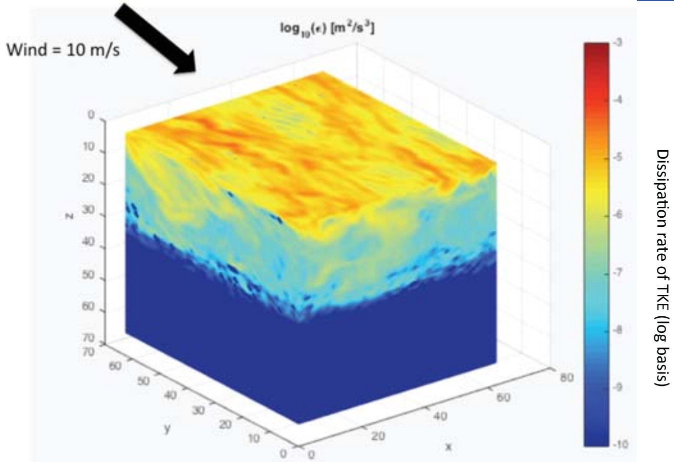

Model-Observation Assesment

Experiment site: Havsul

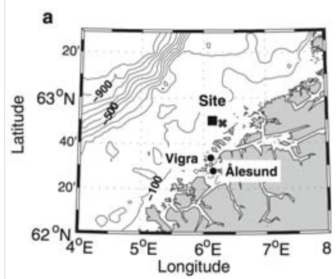

Forcing condition

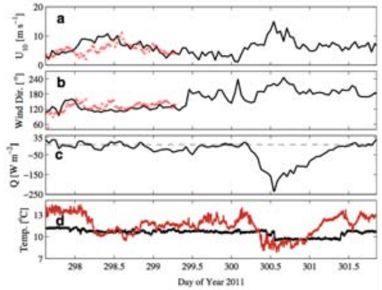

from October 25 to 30, 2011. During the field work, the wind speed ranged from 1 to 15 m s−1 with direction typically confined within from southeast and southwest from which the wind is emanating.

Model-Observation Assesment

MATS SHEAR PROBE

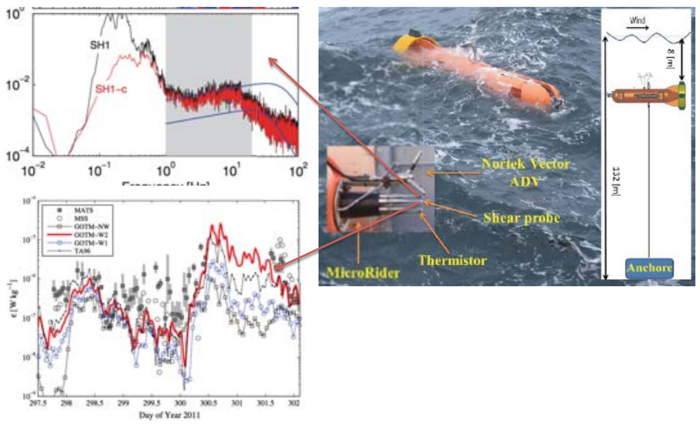

Model-Observation Assesment

General Ocean Turbulence Model (GOTM)

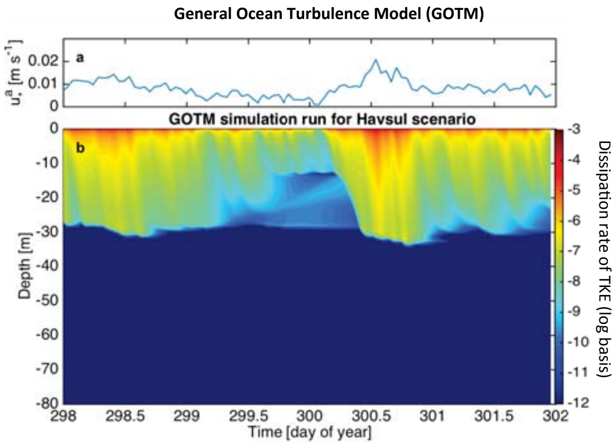

Model-Observation Assesment

LES result

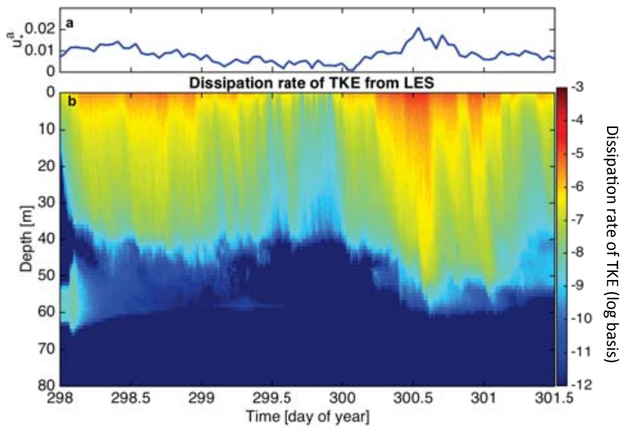

Model-Observation Assesment

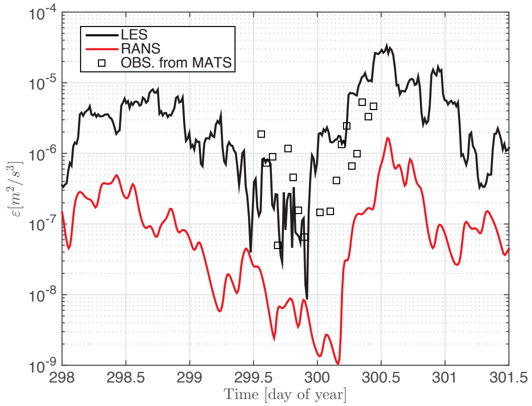

There is a slight time-lag between GOTM & LES in this fig.

Application: Langmuir Circulation

General characterestics:

- Although depth of Langmuir cells is about 4-6 m, it can be extended up to 200 m.
- Cells spatial separation is about 10-50 m.
- The length of cells is ranged from few meters long to many kilometers.
- The cell axes are typically aligned with wind, but may vary as much as 20 degrees.
- Clles try to be aligned with wind and in the case of wind change of direction, they need 15-20 minutes to be aligned in new direction.
- Downwelling velocitties are important for mixed layer implications, biological systems, and particle tracking.
- The mixed layer can be deepend (up to 200 m) in the presence of LC.
- The LC effects can be remained still strong from a few minutes to several hours after cells develop.
- To generate LC, Wind speeds must typically reach 3 m/s.

Conclusions

1. LES gives promising estimate of turbulent fluxes near the wavy surface.
2. The closure problem in LES needs further investigation.
3. Wave breaking inclusion using dissipation source term will be included.

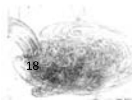

Acknowledgment

Author of this work is grateful of **Joachim Reuder**, **Alastair D. Jenkins**, **Ilker Fer**, **P. Sullivan**, **Ramsay Harcourt**, **J. Liang,** **and** **Martin Flugge** for all their supports and help throughout this investigation.

References

[1] Mostafa Bakhoday Paskyabi and Ilker Fer, Turbulence structure in the upper ocean: a comparative study of observations and modeling, Ocean Dyn., 64, 611-631, 2014. The article is available at: http://hdl.handle.net/1956/8684.
[2] Bakhoday Paskyabi M., S. Zieger, A.D. Jenkins, A.V. Babanin, and D. Chalikov: Sea Surface Gravity Wave-wind Interaction in the Marine Atmospheric Boundary Layer, Energy Proc., Volume 53, 2014, Pages 184-192.
[3] Mostafa Bakhoday Paskyabi and Ilker Fer, The influence of surface gravity waves on the injection of turbulence in the upper ocean, Nonlin. Proc. Geophys., 21, 713-733, 2014. The article is available at: http://hdl.handle.net/1956/8685
[4] Ilker Fer and Mostafa Bakhoday Paskyabi, Autonomous ocean turbulence measurements using shear probes on a moored instrument, J. Atmos. Ocean. Tech., 31, 474–490, 2014. The article is available at: http://hdl.handle.net/1956/8678
[5] M. Bakhoday Paskyabi, Small-scale turbulence dynamics under sea surface gravity waves, PhD dissertation, 2014.
[6] Harcourt, R. R., 2013: A second moment closure model of Langmuir turbulence. *J. Phys. Oceanogr.*, 43, 673–697.
[7] Sullivan, P. P., J. C. McWilliams, and W. K. Melville, 2004: The oceanic boundary layer driven by wave breaking with stochastic variability. Part i. direct numerical simulations. *J. Fluid Mech.*, 507.
[8] Sullivan, P. P., J. C. McWilliams, and W. K. Melville, 2007: Surface gravity wave effects in the oceanic boundary layer: large-eddy simulation with vortex force and stochastic breakers. *J. Fluid Mech.*, 593, 405–452.
[9] Sullivan, P. P., L. Romero, J. C. McWilliams, and W. K. Melville, 2012: Transient evolution of Langmuir turbulence in the ocean boundary layers driven by hurricane winds and waves. *J. Phys. Oceanogr.*, 42, 1959–1979.

D) Operations & maintenance

A Risk Based Inspection Methodology for Offshore Wind Jacket Structures,
M. Shafiee, Cranfield Univ

Effect of Tower-top Axial Acceleration on Monopile Offshore Wind Turbine Drivetrains,
A.R. Nejad, NTNU

Safety Indicators for the Marine Operations in the Installation and Operating Phase of an Offshore Wind Farm, H. Seyr, NTNU

Probabilistic assessment of floating wind turbine access by catamaran vessel,
M. Martini, Inst of Cantabria

EERA DeepWind'2016, 13th Deep Sea Offshore Wind R&D Conference

A Risk-Based Inspection Methodology for Offshore Wind Jacket Structures

Mahmood Shafiee
Lecturer in Engineering Risk, Reliability & Maintenance
Cranfield University, UK
m.shafiee@cranfield.ac.uk

Presentation outline

- Motivation of research
- Risk-Based Inspection (RBI)
- Wind Jacket Foundations
- RBI Planning Methodology
- Testing the Model
- Conclusion

Motivation

- NREL , EWEA Offshore wind energy has experienced an exponential growth worldwide over the past decade
- The installed offshore wind energy capacity continues to rise
- 2004: 622 MW → 2014: 8 GW (annual growth rate of around %30)

Cumulative installed capacity of offshore wind power in the European Union (EU)

Motivation

- ***Cost reduction*** is of increasing importance for all offshore wind energy players
- To make the electricity generated by offshore wind turbines more price-competitive
- The cost per kilowatt hour of electricity generated by offshore wind turbines is approximately 22 cents, but it should reduce to 7 ȼ/kwh by 2030

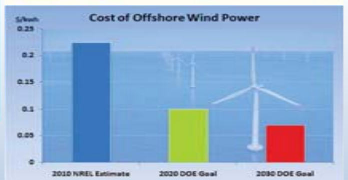

22 ȼ/kwh → 7 ȼ/kwh ?

Motivation

- operation and maintenance (O&M) costs account for about 25 to 40% of the overall energy generation cost
- A significant portion of annual maintenance budget is wasted due to insufficient or inefficient maintenance activities

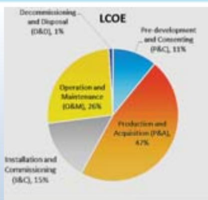

Cost drivers of a typical 5MW offshore wind turbine

- One of the most effective ways to minimize the inspection & repair costs is to apply risk-based inspection methods and tools

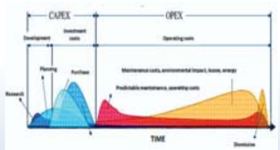

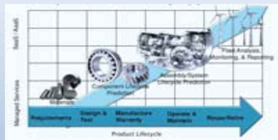

Risk-Based Inspection (RBI)

- Risk-based Inspection technique has been applied to a wide range of industries
- Many institutes and organizations (like HSE, API, DNVGL, ABB, TWI) have developed risk-based inspection solutions for different structures by taking into account the regulatory requirements and guidelines (e.g. API RP 580 ; DNVGL-RP-C210)
- The main aim of RBI tool is to achieve safe operating conditions at minimum inspection cost, and protect human life and the environment from any possible damage during operation

Risk-Based Inspection (RBI)

Risk is a combination of *likelihood* and *magnitude*

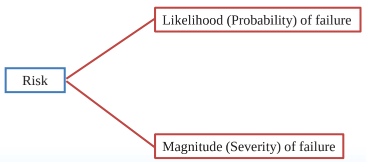

How could risk assessment information be used in making more cost-effective inspection decisions?

Is this cost-effective to choose same inspection strategy for high / medium / low risk assets?

Probability	Impact: Trivial	Minor	Moderate	Major	Extreme
Rare	Low	Low	Low	Medium	Medium
Unlikely	Low	Low	Medium	Medium	Medium
Moderate	Low	Medium	Medium	Medium	High
Likely	Medium	Medium	Medium	High	High
Very likely	Medium	Medium	High	High	High

M Shafiee

Risk-Based Inspection (RBI)

- RBI is a technique which prioritises inspection tasks according to the information provided by risk assessment procedure
- RBI is a technique which determines the frequency of inspection for different assets based on their criticality levels
- RBI is a technique which assists inspectors to find the most appropriate inspection method for assets

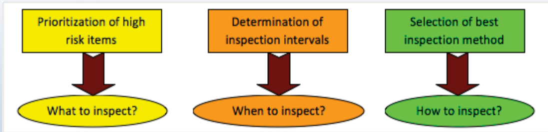

API RP 580 Methodology

There are several RBI methodologies available in energy industries

Topside facilities
Onshore Terminals
Subsea Pipeline

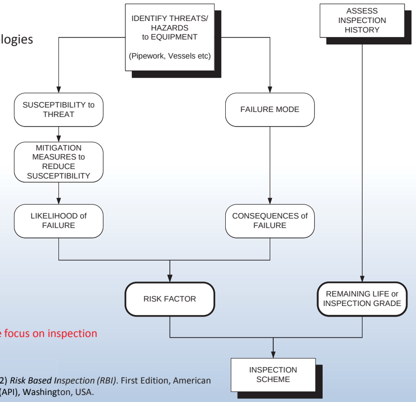

The larger the risk level, the more the focus on inspection

M Shafiee

Ref: API RP 580 (2002) *Risk Based Inspection (RBI)*. First Edition, American Petroleum Institute (API), Washington, USA.

RBI Applications to Wind Energy Structures

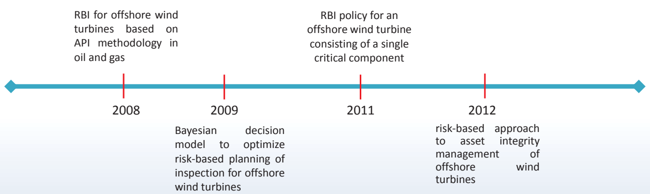

To the best of authors' knowledge, there have been few attempts made by researchers on developing RBI optimization methodologies for offshore wind jacket structures

M Shafiee

Offshore Wind Jacket Structures

- Jacket structures are one of the most common fixed structures used in the offshore oil and gas and wind energy industries. The number of installations is steadily increasing every year as the offshore energy market continues to rise
- A jacket support structure is a welded tubular space frame consisting of three or more near-vertical legs supported by a lateral bracing system

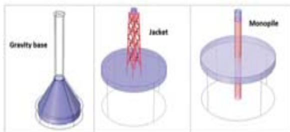

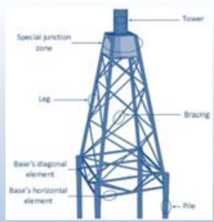

M Shafiee

Offshore Wind Jacket Structures

- The function of a jacket structure is to support the topside facilities or wind turbines and to serve as a template for the foundation system. These structures can transfer the loads from the topside to the seabed through the driven piles
- The offshore jacket structures should be designed with ***sufficient strength and*** stiffness to withstand the wind and wave forces, forces due to current acting on the sea, tides, temperature forces, ice forces, earthquakes, etc.

Wind turbine substructures (jackets)

M Shafiee

Aims and Objectives

- To review the RBI methodologies available in the Offshore Wind Energy industries
- To propose a generic RBI framework to apply to Offshore Wind Foundations
- To propose an Analytical framework to compare RBI performance with currently used constant-interval inspections
- To test and validate the proposed model on various foundation topologies

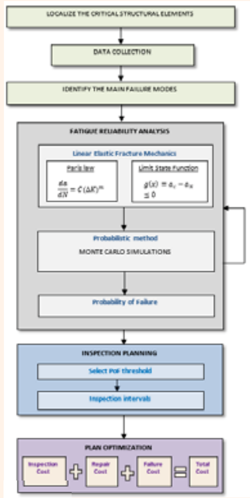

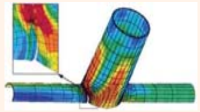

M Shafiee

A generic RBI planning methodology for Offshore Wind Jacket Structures

RBI Methodology

The condition assessment data (e.g., sea-state data, deterioration modes and causes, damage propagation, etc.) are collected from different condition monitoring solutions

Different damage mechanisms are identified and the associated root causes are investigated

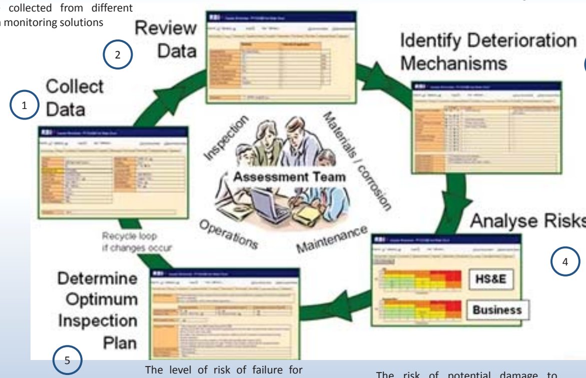

The level of risk of failure for wind foundations is used to schedule appropriate inspection and preventative repair tasks

The risk of potential damage to foundation is evaluated by combining the likelihood of structural damage and the magnitude of consequences

M Shafiee

RBI Methodology
Data collection & review

Collect data and populate the RBI document to include:

- Technical Specification – Type of Jacket, Design codes, etc.
- Operating Conditions – Temperature, pressure, weather conditions
- Construction – Material Specification, Thickness, Corrosion Allowance.
- Inspection History – Previous Reports, Repairs, Modifications.

Discussion and review of the data to agree, add and amend as necessary to form an accurate record of the jacket condition and operating parameters

Dr. Mahmood Shafiee

RBI Methodology
Identification of Damage Mechanisms and Root Causes

Dr. Mahmood Shafiee

RBI Methodology
Risk (Or PoF) Analysis

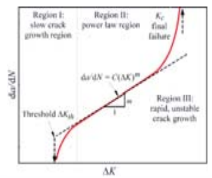

- Qualitative approach
  - Based on descriptive data using engineering judgement and experience

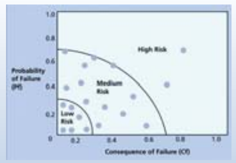

- Quantitative approach (Black box)
  - Based on probabilistic or statistical models

Dr. Mahmood Shafiee

RBI Methodology
Risk (Or PoF) Analysis

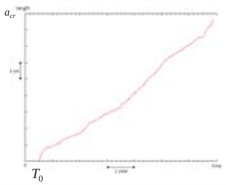

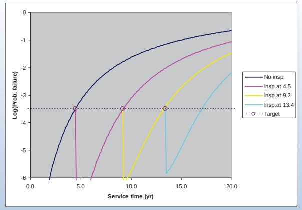

Time of failure | Specified time | Critical crack depth | Crack depth at time t

$$P[T_f \le t] = P[a_{cr} - A(t) < 0]$$
$$= P[T_0 + T_G(a_{cr}) - t < 0]$$

Time for crack initiation | Time for crack growth to critical depth

RBI Methodology
Failure Cost Analysis

Three cost factors are considered for this purpose:

C_I: cost of inspection
C_R: cost of imperfect repair
C_F: cost of failure

$$C_T = \Sigma[C_I(t) + C_R(t) + C_F(t)] \times (1+r)^t$$

RBI Methodology
Optimal Inspection Planning

Determine an Optimum Inspection Plan:

Min C_T
S.t. $R \ge R_0$

- Focus effort on high risk assets
- Choose appropriate inspection techniques for each identified deterioration mechanism
- Identify appropriate periodicities
- Consider ways to reduce risk (Inspection does not reduce consequence!)

Application

The proposed RBI planning methodology is being applied to two welded tubular joints of a steel jacket structure

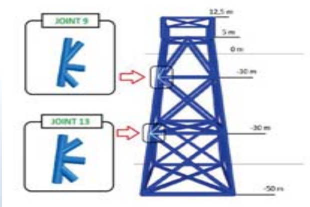

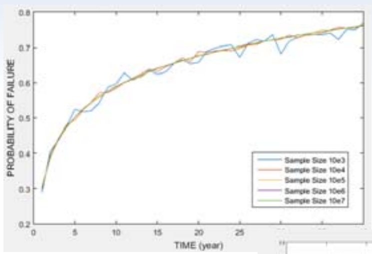

Likelihood of failure for joint 9 using MCS technique

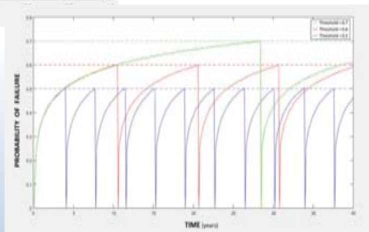

Inspection plan on the basis of likelihood of failure

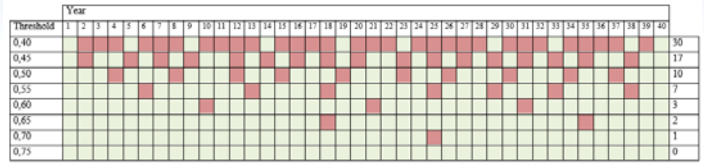

	Year																																							
Threshold	1	2	3	4	5	6	7	8	9	10	11	12	13	14	15	16	17	18	19	20	21	22	23	24	25	26	27	28	29	30	31	32	33	34	35	36	37	38	39	40	
0,40																																									30
0,45																																									17
0,50																																									10
0,55																																									7
0,60																																									3
0,65																																									2
0,70																																									1
0,75																																									0

Inspection schedule of joint 9 for different POF thresholds

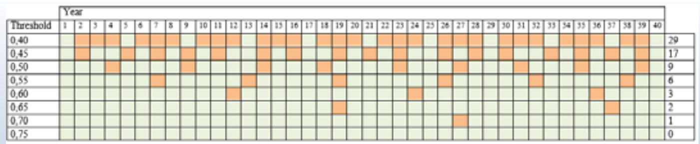

	Year																																							
Threshold	1	2	3	4	5	6	7	8	9	10	11	12	13	14	15	16	17	18	19	20	21	22	23	24	25	26	27	28	29	30	31	32	33	34	35	36	37	38	39	40	
0,40																																									29
0,45																																									17
0,50																																									9
0,55																																									6
0,60																																									3
0,65																																									2
0,70																																									1
0,75																																									0

Inspection schedule of joint 13 for different POF thresholds

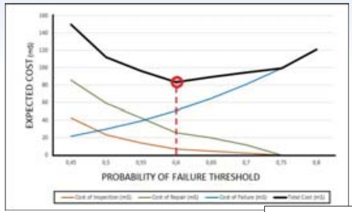

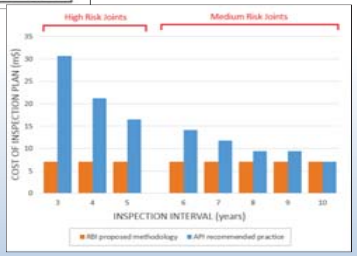

25

Conclusion

- The existing RBI methodologies in the wind energy industry were reviewed
- A generic RBI methodology for offshore wind jacket structures was proposed
- The performance of the proposed RBI methodology (in terms of cost) was compared with constant-interval inspections suggested by API

26

Correlation between Acceleration and Drivetrain Load Effects for Monopile Offshore Wind Turbines

Amir R. Nejad
Erin E. Bachynski, Lin Li, Torgeir Moan
NTNU
EERA DeepWind'2016,
Trondheim

Norwegian University of Science and Technology

Objectives

- There is a common practice in the wind industry to set a limit for the maximum axial acceleration on the tower-top in the range of 0.2g-0.3g (in particular for the floating wind turbines)
- Is this limit rational?
- What is the correlation between axial acceleration and responses in drivetrain?

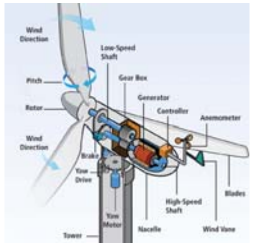

Method & Model

- Effect of tower-top maximum axial acceleration on the drivetrain installed on a monopile offshore wind turbine was investigated.
- Wind/ wave data from an actual shallow water site "North Sea Centre" site from the MARINA platform project with water depth of 29 m is selected. This is similar to the Dogger Bank wind farm.

Method & Model

Models:

- NREL 5 MW reference turbine, supported by the monopile foundation from the OC3 study.
- Nowitech/NREL 5 MW reference gearbox.

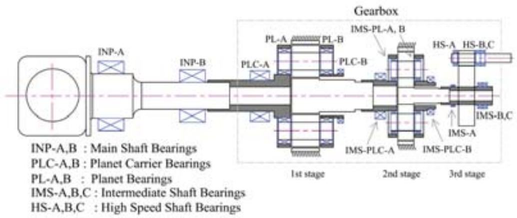

Method & Model

- De-coupled modelling approach:

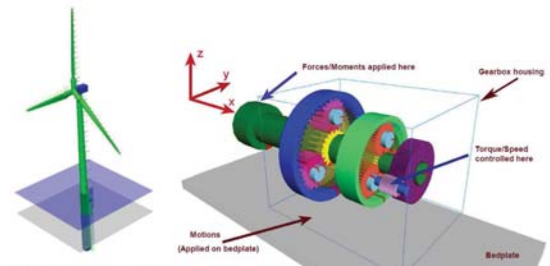

(a) 5MW wind turbine model in SIMO-RIFLEX-AeroDyn

(b) MBS model of 5 MW reference drivetrain [11]

Method & Model

- 24 EC were considered, from cut-in to cut-out:

EC	1	2	3	4	5	6	7	8	9	10	11	12
U_w (m/s)	3	4	5	6	7	8	9	10	11	11.4	12	13
H_s (m)	0.59	0.72	0.85	1	1.17	1.34	1.52	1.72	1.92	2	2.13	2.35
T_p (s)	6.38	6.32	6.28	6.27	6.31	6.35	6.41	6.5	6.59	6.62	6.69	6.81
used in MBS	√		√		√		√			√		√
EC	**13**	**14**	**15**	**16**	**17**	**18**	**19**	**20**	**21**	**22**	**23**	**24**
U_w (m/s)	14	15	16	17	18	19	20	21	22	23	24	25
H_s (m)	2.57	2.81	3.05	3.3	3.55	3.81	4.08	4.35	4.63	4.92	5.21	5.5
T_p (s)	6.92	7.06	7.19	7.33	7.47	7.62	7.78	7.93	8.09	8.27	8.43	8.6
used in MBS				√			√			√		√

- 10 min. simulation, 6 seeds
- Results from all EC were used for evaluating main shaft responses
- Results from selected EC were used for MBS analysis and calculating forces on bearings and gears

Results

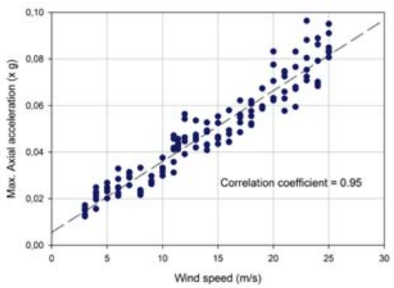

Max. axial acceleration vs. wind speed

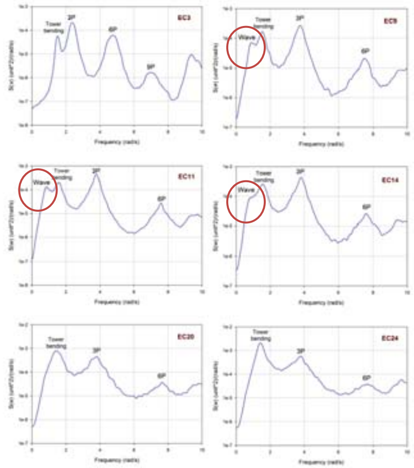

Spectrum of axial acceleration in different environmental conditions

Results

Axial force:

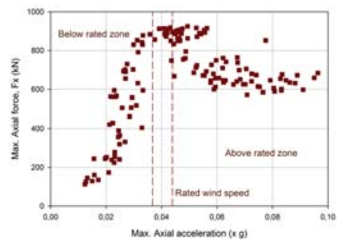

Max. Axial force on tower-top vs. max. axial acceleration

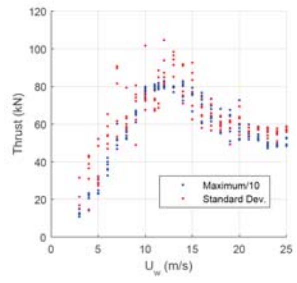

Thrust force vs. wind speed

Results

Bending moment:

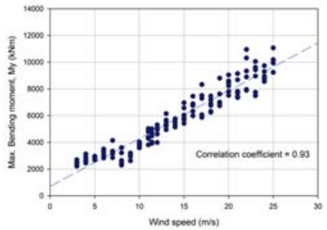

Max. bending moment vs. wind speed

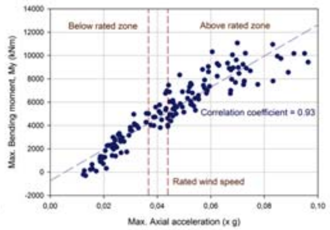

Max. bending moment on tower-top vs. max. axial acceleration

Results

Drivetrain components:

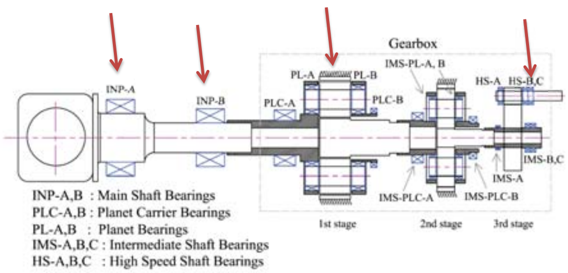

Nowitech/NREL 5 MW Reference Drivetrain

Results

Drivetrain components:

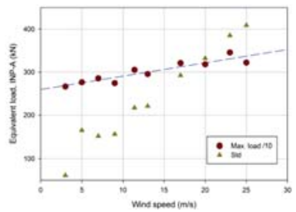

Main bearing: INP-A

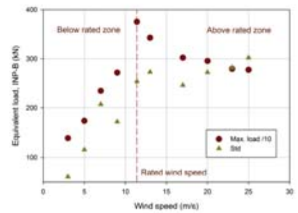

Main bearing: INP-B

Results

Drivetrain components:

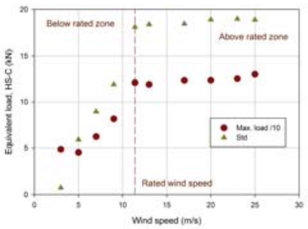

High speed stage bearing: HS-C

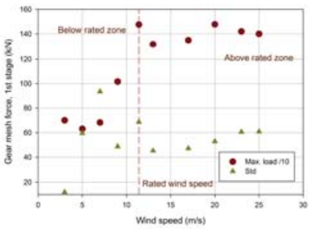

1st stage gear mesh force

Discussion & Conclusion

- The results showed that the maximum tower-top acceleration is about 0.1g for this case study monopile.
- The axial acceleration increases with the wind speed.
- No correlation was found between the maximum axial force on the tower-top and the maximum axial acceleration. The axial force follows the thrust force mainly. (In a 4-point support configuration, the axial force on the main shaft is the design driver for the second main bearing).

Discussion & Conclusion

- The tower-top bending moment was found to increase as the wind increase. (The bending moment is a design driver for the main shaft and the main bearing).
- The load effect of the components, gears and bearings, inside the gearbox were found to be not correlated with the axial acceleration. They mainly follow the torque and are influenced by the power control system.

References

- 5 MW reference offshore gearbox:

Nejad A.R., Guo Y., Gao Z., and Moan T. *Development of a 5 MW reference gearbox for offshore wind turbines*. **Wind Energy**, DOI:10.1002/we.1884, 2015.

- Environmental data:

Li L., Gao Z., and Moan T. *Joint long-term environmental conditions at five European offshore sites for design of combined wind and wave energy devices*. **Journal of Offshore Mechanics and Arctic Engineering**, 137(3), 2015.

Thank you

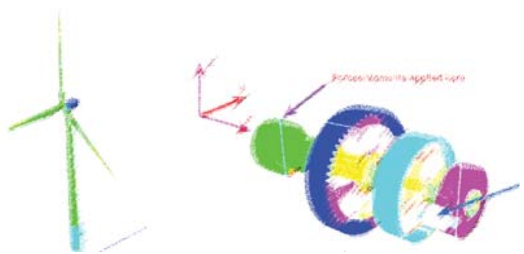

Safety Indicators for the Marine Operations in the Installation and Operating Phase of an Offshore Wind Farm

EERA DeepWind'2016 - Helene Seyr & Michael Muskulus

This project has received funding from the European Union's Horizon 2020 research and innovation programme under the Marie Sklodowska-Curie grant agreement No 642108

Agenda

- Introduction to Safety Indicators
- Methodology
- System "wind farm"
- Indicator analysis
- Incident data
- Conclusion and outlook

AWESOME

Introduction – Safety Indicators

- Measure of performance/system safety
- Enhance performance and productivity
- Ensure worker safety – Political discussions
- Complete, consistent, effective, traceable, minimal, improving, unbiased
- Drive improvement

AWESOME

Methodology

- System approach
- Review – Indicators
  - OWF analysis
  - Turbine analysis
  - Oil and Gas analysis
  - Risk of collision
- Review – Incidents
  - Incident data reports
  - Indicators

AWESOME

The system "wind farm"

- Phases
  - Installation and Commissioning
  - Operations and Maintenance
- System components
  - Turbine
  - Offshore Foundation (Monopile)
  - External influences

AWESOME

The system "wind farm" – turbine subsystems

- Electrical systems
- Electronic control
- Hydraulics
- Yaw system
- Pitch control
- Mechanical break
- Support and housing
- Generator
- Gearbox
- Rotor and blades
- Main shaft
- Sensors

AWESOME

Indicator Review – Offshore wind industry specific

- System properties – Work tasks
- Work at heights
- Marine/helicopter operations
- Dangerous work environment
- External influences
- Collisions

AWESOME

Indicator Review – Turbine

- Electrical system
- Electronic control
- Rotor assembly
- Differences between publications for other subsystems
- More detailed investigation

AWESOME

Indicator Review – Oil and gas

- Organizational structure
- Industry specific indicators
- Shut down preparedness – Weather windows

AWESOME

Incidents and Indicators

- G9 incident data report 2013 and 2014
- Reporting increased: 616 - 994
  Lost work days frequency decreased: by 34%
- Lifting operations: 9 LWD 2013, 3 in 2014
- Working at heights: 7%
- Falling objects: during lifting/work at heights
- Marine operations: over 20% of incidents

AWESOME

Incidents and Indicators

- Nacelle: 4 LWD, work activity
- Hub and blade assembly: 4%/2%
- Hazardous substances: 15/10 incidents - one category
- No incidents:
  - Organizational failures
  - Collisions
- No indicators:
  - Transition piece : 5% - 2 LWD
  - Substations: 3%

AWESOME

Conclusion

- Many useful indicators
- Merging of some indicators
- Grouping by area not favorable
- Focus on work process
- Future Research:
  - Validation by operators
  - Extend to additional structures (jackets, floating)
  - Continuous improvement

AWESOME

AWESOME
PhD's in Wind Power O&M

Thank you for your attention

Helene Seyr
PhD Candidate
helene.seyr@ntnu.no
+47 400 86 761

NTNU
Norwegian University of Science and Technology

Appendix: References

- Øien, K., Utne, I., Herrera, I.. Building Safety indicators: Part 1 Theoretical foundation. Safety Science 2011;49(2):148–161.
- Øien, K., Utne, I.B., Tinmannsvik, R.K., Massaiu, S.. Building Safety indicators: Part 2 - Application, practices and results. Safety Science 2011;49(2):162–171.
- Skogdalen, J.E., Utne, I.B., Vinnem, J.E.. Developing safety indicators for preventing offshore oil and gas deepwater drilling blowouts. Safety Science 2011;49(8-9):1187–1199.
- Utne, I., Thuestad, L., Finbak, K., Thorstensen, T.A.. Shutdown preparedness in oil and gas production. Journal of Quality in Maintenance Engineering 2012;18(2):154–170.
- Pasman, H.J., Rogers, W.J.. How can we use the information provided by process safety performance indicators? Possibilities and limitations. Journal of Loss Prevention in the Process Industries 2013;30:10.
- Leveson, N.. A systems approach to risk management through leading safety indicators. Reliability Engineering & System Safety 2015;136:17–34.
- Hopkins, A.. Thinking About Process Safety Indicators. Safety Science 2009;47(4):460–465.
- Feng, Y., Tavner, P., Long, H.. Early experience with uk round 1 offshore wind farms. In: Proceedings of the Institution of Civil Engineers. 2010
- Scheu, M., Matha, D., Hofmann, M., Muskulus, M.. Maintenance strategies for large offshore wind farms. Energy Procedia 2012
- Utne, I.B.. Systems engineering principles in fisheries management. Marine Policy 2006;30(6):624–634.

AWESOME

Appendix: References

- Arabian-Hoseynabadi, H., Oraee, H., Tavner, P.. Failure Modes and Effects Analysis (FMEA) for wind turbines. International Journal of Electrical Power & Energy Systems 2010;32(7):817–824.
- Faulstich, S., Hahn, B., Tavner, P.J.. Wind turbine downtime and its importance for offshore deployment. Wind Energy
- Tveiten, C.K., Albrechtsen, E., Hofmann, M., Jersin, E., Leira, B., Norddal, P.K.. Report HSE challenges related to offshore renewable energy. 2011.
- Committee on Offshore Wind Farm Worker Safety, . Transportation Research Board; 2013.
- G9 Offshore wind health and safety association, . 2013 annual incident data report. Energy Institute; 2014.
- G9 Offshore wind health and safety association, . 2014 incident data report. Energy Institute; 2015.
- Aneziris, O.N., Psinias, I.A.P.A., Psinias, A.. Occupational risk for wind farms 2014;(2010):1489–1496.
- Caithness Windfarm Information Forum, . Summary of Wind Turbine Accidents. 2012. URL: www.caithnesswindfarms.co.uk.
- Dai, L., Ehlers, S., Rausand, M., Utne, I.B.. Risk of collision between service vessels and offshore wind turbines. Reliability Engineering & System Safety 2013;109:18–31.

AWESOME

EERA DeepWind'2016 13th Deep Sea Offshore Wind R&D Conference

Probabilistic assessment of floating wind turbine access by catamaran vessel

Michele Martini*, Alfonso Jurado, Raul Guanche**, Iñigo Losada

*michele.martini@unican.es
**raul.guanche@unican.es

Environmental Hydraulics Institute "IH Cantabria"
C/Isabel Torres 15, 39011 Santander (Spain)

Trondheim, Norway, 20-22 January 2016

Friday, January 22, 2015
Operations and maintenance

Outline

- Motivation
  - Offshore wind energy trends
  - O&M challenges
- Methodology
  - Analysis of constrained multi-body system
  - Definition of access criteria
  - Calculation of short-term extreme response
- Case study: Aberdeen, Scotland
  - Evaluation of long-term accessibility
- Conclusions

Motivation

Motivation/1

TRENDS
- Offshore wind market is rapidly increasing (EWEA 2015)
- **+111%/+70%** capacity/average investment in 2012-2014

LIMITATIONS
- Maximum water depth for fixed structures is **50 m** (EWEA 2013)
- Limited amount of available sites

ALTERNATIVES
- **Floating systems** for deeper waters (Hywind, WindFloat, Fukushima)
- Vast **potential market**

Water depth: 100-700 m

Source: Statoil

Motivation/2

CHALLENGES
- **Availability** (% of time wind turbine produces electricity)
- Reducing **downtimes**
- Inspection and maintenance has high cost **(25% of LCOE, GL 2015)**

ACCESS STRATEGIES
- Helicopter
- Relatively large access vessels with motion compensated gangway
- **Small and fast CTVs with fender**

Source: NOS, Windcat Workboats

QUESTIONS
- What is the **combined response** of floating platform/access vessel?
- What is the **long-term accessibility** for a chosen spot?

OBJECTIVES
- **Model the catamaran walk-to-work access of floating wind turbine**
- **Evaluate long-term accessibility in Aberdeen, Scotland**

Methodology

Methodology/1

Landing procedure on a floating platform

- The catamaran lands on the bumpers mounted on the platform. The platform displaces until the system reaches equilibrium
- The bow-mounted fender helps in:
  - Absorbing the impact energy
  - Providing friction at the contact surface
- O&M technicians step-over from the vessel to a platform mounted ladder
- Access is possible when:
  - No-slip conditions occur at the fender
  - Relative rotations are below tolerance limits

Source: Windcat Workboats

Methodology/2

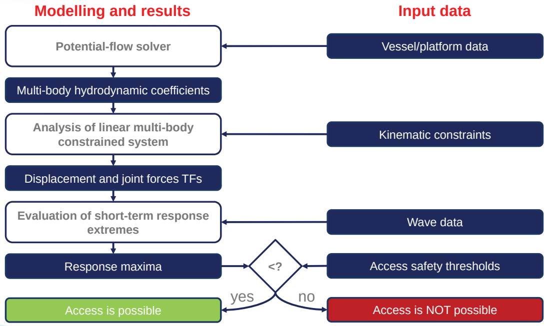

Methodology/3

Analysis of constrained multi-body system: approach

- Floating body equation of motion in frequency domain
  - Multibody hydrodynamic coefficients from DNV SESAM
  - Linearization of mooring and quadratic damping

$$G(j\omega)\zeta(j\omega) = f(j\omega,\theta)$$

$$G(j\omega) = -\omega^2[M + A(\omega)] + j\omega[B(\omega) + B_l] + [C + C_l]$$

- The fender acts as a joint between the two bodies
  - Motion is constrained: equation has to be rewritten
  - Relative translations at contact point are impeded

$$\begin{bmatrix} G & D^T \\ D & 0 \end{bmatrix} \begin{Bmatrix} \zeta \\ \lambda \end{Bmatrix} = \begin{Bmatrix} f \\ 0 \end{Bmatrix}$$

Displacements (ζ), Reaction forces (λ), Constraint matrix (D)

$$D = \begin{bmatrix} 1 & 0 & 0 & 0 & +z_C^v & -y_C^v & 1 & 0 & 0 & 0 & +z_C^p & -y_C^p \\ 0 & 1 & 0 & -z_C^v & 0 & +x_C^v & 0 & 1 & 0 & -z_C^p & 0 & +x_C^p \\ 0 & 0 & 1 & +y_C^v & -x_C^v & 0 & 0 & 0 & -1 & -y_C^p & +x_C^p & 0 \end{bmatrix}$$

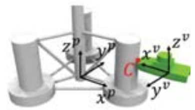

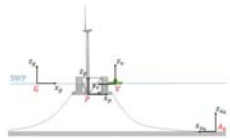

L. Sun, R. Eatock Taylor, and Y. S. Choo, "Response of interconnected floating bodies," IES J. Part A Civ. Struct. Eng., vol. 4, no. 3, pp. 143–156, 2011

Methodology/5

Analysis of constrained multi-body system: access criteria

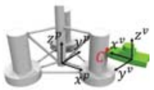

Condition 1

- No-slip at fender

$$|\lambda_3(t)| \le \mu_s[F_b + \lambda_1(t)]$$

$$\alpha(t) = +\lambda_3(t) - \mu_s\lambda_1(t) \le \mu_s F_b \rightarrow \alpha(j\omega) = +\lambda_3(j\omega) - \mu_s\lambda_1(j\omega)$$

$$\beta(t) = -\lambda_3(t) - \mu_s\lambda_1(t) \le \mu_s F_b \rightarrow \beta(j\omega) = -\lambda_3(j\omega) - \mu_s\lambda_1(j\omega)$$

Condition 2

- Small relative rotations at fender

$$|\Delta\rho(t)| \le \Delta\rho_{\lim} \rightarrow \Delta\rho(j\omega) = \zeta_4(j\omega) + \zeta_{10}(j\omega)$$

$$|\Delta\psi(t)| \le \Delta\psi_{\lim} \rightarrow \Delta\psi(j\omega) = \zeta_6(j\omega) - \zeta_{12}(j\omega)$$

(Transfer functions)

Methodology/6

Calculation of short-term response extremes

- Wave directional spectrum
- Response transfer functions α, β, Δρ, Δψ
- Variance of linear response

$$\sigma_x = \int_0^{2\pi}\int_0^{\infty} |H_{\eta x}(j\omega,\theta)|^2 S_{\eta\eta}(\omega,\theta)\, d\omega\, d\theta$$

- Distribution of response crests

$$F(x_c) = 1 - e^{-(x_c/2\sigma_x)^2}$$

- Distribution of response extremes

$$F_E(x_c) = F(x_c)^N = \left[1 - e^{-(x_c/2\sigma_x)^2}\right]^N$$

- Extreme response (with exc. prob.)

$$x_c = \sqrt{2\sigma_x^2}\left[-\ln\left(1 - F_E^{1/N}\right)\right]^{1/2}$$

F_E = 0.95 in this work

- Comparison with access thresholds and evaluation of accessibility

L. H. Holthuijsen, Waves in Oceanic and Coastal Waters. New York: Cambridge University Press, 2007.
Det Norske Veritas, Environmental conditions and loads, DNV-RP-C205, 2014.

Case study

Case study/1

Floating platform and vessel data

Catamaran CTV

CTV		
Displacement	102	t
Length/Beam/Draft	24/10/1.37	m
Water plane area	94.45	m^2
Fender friction coefficient	1.2	-
Bollard push force	135	kN
Heave/roll/pitch natural period	3.0/3.5/4.5	s

OC4 floating platform

OC4		
Displacement	13473	t
Total draft	20	m
Diameter of central/offset col.	6.5/12.0	m
Diameter of heave plates	24	m
Spacing between offset columns	50	m
Heave/roll/pitch natural period	18/27.5/27.5	s

Case study/2

System transfer functions – Joint forces (α and β)

$$\alpha(j\omega) = +\lambda_3(j\omega) - \mu_s\lambda_1(j\omega)$$ (upward slip)

$$\beta(j\omega) = -\lambda_3(j\omega) - \mu_s\lambda_1(j\omega)$$ (downward slip)

- Short (5-12 s) and very long (20-25 s) waves
  - Upward slip is more probable than downward
  - Head seas give higher contact forces than in beam seas
- Medium length/long waves (12-20 s)
  - Upward and downward slip are equally probable
  - Beam seas give higher contact forces than in head seas
- Slip is highly probable at 16.5 s and 24 s
  - Shifted from platform natural periods (18 s, 27.5 s)!
  - Relative motion drives contact forces!

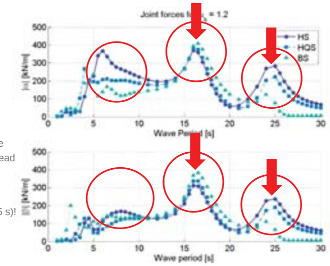

"HS" = "Head Sea", "HQS" = "Head Quartering Sea", "BS" = "Beam sea"

Case study/3

System transfer functions – Catamaran displacements

- When free to move, bodies respond to:
  - Catamaran: short waves (small inertia)
  - Floating platform: long waves (high inertia)
- When constrained, bodies exchange forces through the joint
  - Catamaran: response also to longer waves, when contact forces are higher

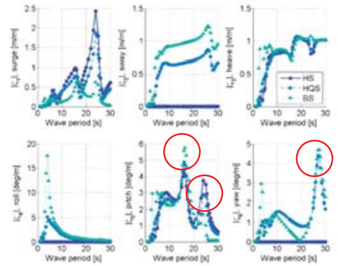

"HS" = "Head Sea", "HQS" = "Head Quartering Sea", "BS" = "Beam sea"

Case study/4

System transfer functions – Limiting wave height in regular waves

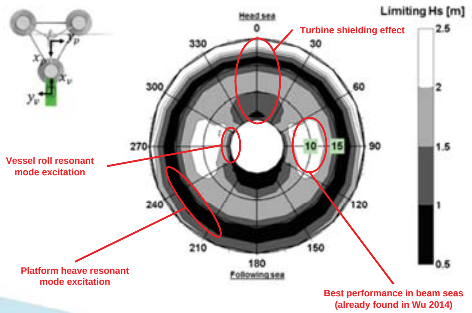

M. Wu, "Numerical analysis of docking operation between service vessels and offshore wind turbines," Ocean Eng., vol. 91, pp. 379–388, 2014

Case study/5

Offshore location and data – Aberdeen, Scotland

Coordinates: 57.000º N, 1.875º W
Distance from the coast: 10 km
Water depth: 90 m

Reanalysis data: IH Cantabria

- GOW: Global Ocean Waves
  - 0.125º spatial resolution (lat/lon)
  - 1 hour time resolution
  - 1980-2013 spanned period
- Time series of:
  - Hs, significant wave height
  - Tp, wave peak period
  - θm, mean wave direction
  - σθ, mean directional spreading

Case study/6

Offshore location and data – Aberdeen, Scotland

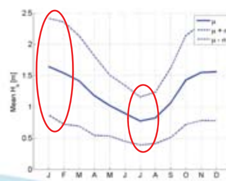

Wave peak period [s]	0.5	1.5	2.5	3.5	4.5	5.5	6.5	
2	0.1%	0.0%	0.0%	0.0%	0.0%	0.0%	0.0%	0.1%
3	1.6%	0.0%	0.0%	0.0%	0.0%	0.0%	0.0%	1.6%
4	6.9%	0.4%	0.0%	0.0%	0.0%	0.0%	0.0%	7.3%
5	9.1%	4.5%	0.0%	0.0%	0.0%	0.0%	0.0%	13.6%
6	7.5%	9.1%	0.6%	0.0%	0.0%	0.0%	0.0%	17.1%
7	5.5%	7.8%	2.0%	0.0%	0.0%	0.0%	0.0%	15.4%
8	4.9%	7.3%	3.0%	0.5%	0.0%	0.0%	0.0%	15.7%
9	3.5%	4.4%	2.3%	1.0%	0.1%	0.0%	0.0%	11.4%
10	2.2%	2.9%	1.2%	0.6%	0.3%	0.1%	0.0%	7.3%
11	1.5%	2.1%	0.6%	0.3%	0.1%	0.1%	0.0%	4.6%
12	0.9%	1.3%	0.4%	0.2%	0.0%	0.0%	0.0%	2.7%
13	0.5%	0.6%	0.2%	0.1%	0.0%	0.0%	0.0%	1.3%
14	0.4%	0.3%	0.1%	0.0%	0.0%	0.0%	0.0%	0.9%
15	0.4%	0.2%	0.0%	0.0%	0.0%	0.0%	0.0%	0.6%
16	0.2%	0.0%	0.0%	0.0%	0.0%	0.0%	0.0%	0.3%
17	0.1%	0.0%	0.0%	0.0%	0.0%	0.0%	0.0%	0.1%
	45.3%	40.8%	10.2%	2.7%	0.6%	0.1%	0.0%	100.0%

Wave significant height [m]

Wave mean direction [deg]	0.5	1.5	2.5	3.5	4.5	5.5	6.5	
E	1.5%	1.5%	0.6%	0.3%	0.1%	0.0%	0.0%	3.9%
ESE	3.8%	3.2%	1.1%	0.4%	0.2%	0.1%	0.0%	8.8%
SE	5.1%	4.5%	1.3%	0.4%	0.1%	0.0%	0.0%	11.3%
SSE	3.7%	4.3%	1.5%	0.4%	0.1%	0.0%	0.0%	10.0%
S	3.0%	3.1%	0.8%	0.1%	0.0%	0.0%	0.0%	7.0%
SSW	3.9%	3.5%	0.5%	0.1%	0.0%	0.0%	0.0%	7.9%
SW	1.3%	1.1%	0.1%	0.0%	0.0%	0.0%	0.0%	2.5%
WSW	0.4%	0.3%	0.0%	0.0%	0.0%	0.0%	0.0%	0.8%
W	0.3%	0.2%	0.0%	0.0%	0.0%	0.0%	0.0%	0.5%
WNW	0.3%	0.1%	0.0%	0.0%	0.0%	0.0%	0.0%	0.4%
NW	0.3%	0.2%	0.0%	0.0%	0.0%	0.0%	0.0%	0.5%
NNW	0.6%	0.4%	0.0%	0.0%	0.0%	0.0%	0.0%	1.0%
N	1.9%	1.5%	0.2%	0.0%	0.0%	0.0%	0.0%	3.6%
NNE	9.9%	9.9%	2.4%	0.6%	0.1%	0.0%	0.0%	22.9%
NE	5.0%	3.2%	0.5%	0.1%	0.0%	0.0%	0.0%	8.9%
ENE	3.0%	2.3%	0.5%	0.2%	0.0%	0.0%	0.0%	6.0%
	45.4%	40.9%	10.2%	2.7%	0.6%	0.1%	0.0%	100.0%

- 86.1% of Hs less than 2 m — 41.1% of θm between E and S
- 80.4% of Tp between 4.5 and 10.5 s — 41.4% of θm between N and E

IHcantabria

Case study/7

Long-term accessibility – Aberdeen, Scotland

Average 1980-2013 accessibility: 23.7 % (87 days/year)

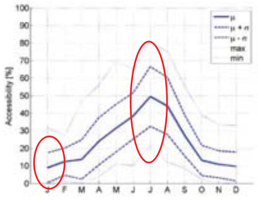

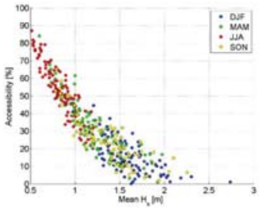

- Large monthly variation
- More variability in summer than in winter

- Small spreading for small (<1 m) and large Hs (>2 m)
- Intermediate region indicates sensitivity to Tp and θm

Need for reliable and long-term metocean data

IH UC

IHcantabria

Conclusions

IH UC

IHcantabria

Conclusions

- Developed methodology to evaluate walk-to-work accessibility of floating turbine
  - Frequency domain approach: linearization of non-linear actions
  - Definition of access criteria
    - No-slip conditions at fender
    - Small relative rotations at fender
  - Calculation of short-term extreme responses
- Evaluated combined response of CTV and OC4 floating platform
  - Largest forces shifted from natural periods
  - Vessel response affected by platform response
- Evaluated long-term accessibility at Kincardine
  - Hindcast data 1980-2013: large climate variability (seasonal, year-by-year), mostly winter.
  - Average accessibility: 23.7 %. Large variability (seasonal, year-by-year), mostly summer.
  - Influence of wave period and direction for Hs between 1 m and 2 m

IH UC

IHcantabria

THANKS FOR YOUR ATTENTION!

Probabilistic assessment of floating wind turbine access by catamaran vessel

Michele Martini*, Alfonso Jurado, Raul Guanche**, Iñigo Losada

*michele.martini@unican.es
**raul.guanche@unican.es

Environmental Hydraulics Institute "IH Cantabria"
C/Isabel Torres 15, 39011 Santander (Spain)

IH UC

E1) Installation and sub-structures

Accurate frequency domain method for monopiles K. Merz, SINTEF Energi

Crack growth fatigue modeling for monopiles, L. Ziegler, Rambøll/NTNU

The effect of slamming on a one degree of freedom model of an offshore wind turbine: experimental results, L. Suja-Thauvin, Statkraft/NTNU

Towards a risk-based decision support for offshore wind turbine installation and operation & maintenance, T. Gintautas, Aalborg Univ.

Frequency-domain methods for the analysis of offshore wind turbine foundations

Karl Merz
SINTEF Energy Research

With contributions from
Lene Eliassen
NTNU/Statkraft

January 21, 2016

Additional thanks to Sebastian Schafhirt and Jason Jonkman for providing simulation results for verification.

A linear state-space model

$$\mathbf{L}\frac{d\mathbf{x}}{dt} = \mathbf{A}\mathbf{x} + \mathbf{B}\mathbf{u}$$

$$\mathbf{y} = \mathbf{C}\mathbf{x} + \mathbf{D}\mathbf{u}$$

L, A, B, C, D: sparse
$\mathbf{L}^{-1}$: full

Motto:
"If we can put it into state space then we can solve it.
If we can put it into linear state space then we can understand it."

Outline of a frequency domain calculation

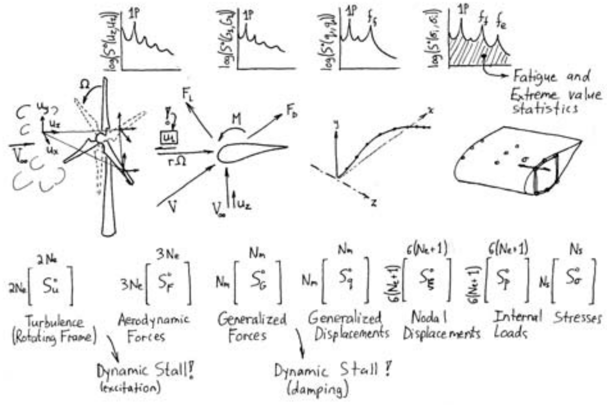

Why frequency-domain analysis?

Linear, superposition applies.
- Linear time-invariant matrix equations can be partitioned, and examined piece-by-piece.

Modal frequencies and damping.
- Stability properties of the system can be computed directly.

Stochastic cycle counts and estimates of extremes can be obtained without the use of random numbers.
- Numerically smooth, nice for optimization.

Analysis of high-frequency dynamics is straightforward.

Speed of calculation.
- Within a given load case, each frequency can be considered independently, computed in parallel.

Control gain tuning, recipes for "optimal" control.
- Well-designed control systems are robust against (small) inaccuracies in modelling.

Why *not* frequency-domain analysis?

Transient load cases

Accuracy.
- Hypotheses, results, designs generated using frequency-domain analysis should in the later stages be verified with nonlinear time-domain simulations.

Rotationally-sampled isotropic turbulence, axial and tangential components

$$s = \sqrt{(V_\infty \tau)^2 + r_1^2 + r_2^2 - 2r_1 r_2 \cos\Omega\tau}$$

$$Q_{ss} = \frac{2\sigma_u^2}{\Gamma(1/3)}\left(\frac{s}{2.68L_u}\right)^{1/3} K_{1/3}\left(\frac{s}{1.34L_u}\right)$$

$$\frac{dQ_{ss}}{ds} = -\frac{2\sigma_u^2}{\Gamma(1/3)}\left(\frac{1}{1.34L_u}\right)\left(\frac{s}{2.68L_u}\right)^{1/3} K_{-2/3}\left(\frac{s}{1.34L_u}\right)$$

$$Q_{zz} = Q_{ss} + \frac{s}{2}\frac{dQ_{ss}}{ds} - \frac{s_z^2}{2s}\frac{dQ_{ss}}{ds}$$

$$\boxed{Q_{tt} = (\sin\Omega\tau)\frac{s_x s_y}{2s}\frac{dQ_{ss}}{ds} + (\cos\Omega\tau)\left(Q_{ss} + \frac{s}{2}\frac{dQ_{ss}}{ds} - \frac{s_y^2}{2s}\frac{dQ_{ss}}{ds}\right)}$$

$$Q_{zt}, Q_{tz} \approx 0$$

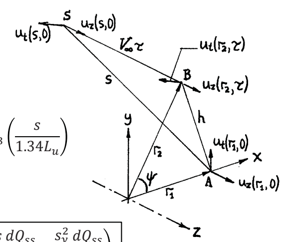

$$Q_{ij} \equiv E\left[u_i(r_1)\, u_j(r_1 + s)\right] = E\left[u_i(r_1, t)\, u_j(r_2, t + \tau)\right]$$

Rotationally-sampled turbulence correlation functions, single blade, near tip

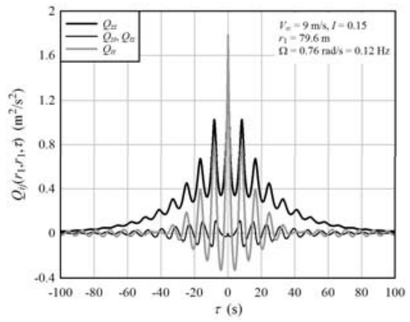

Rotationally-sampled turbulence spectrum near blade tip

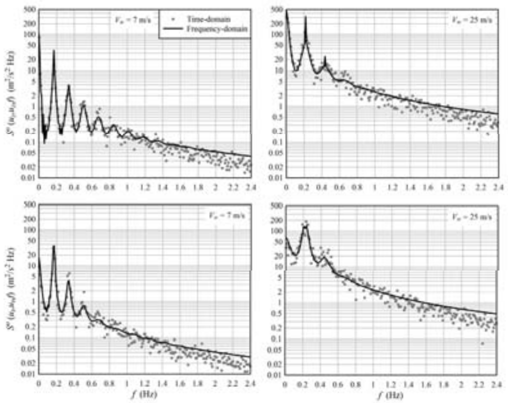

Note: not the DTU turbine. Stall-regulated blades.

Multi-blade coordinate transform of rotationally-sampled turbulence

$$\mathbf{Q}^{\psi}(r_1, r_2, \tau) = \mathbf{T}^{\psi}_{B,p}(0)\ \mathbf{Q}_{ij}(s_{pq}(\tau), 0)\ \left[\mathbf{T}^{\psi}_{B,q}(\tau)\right]^T$$

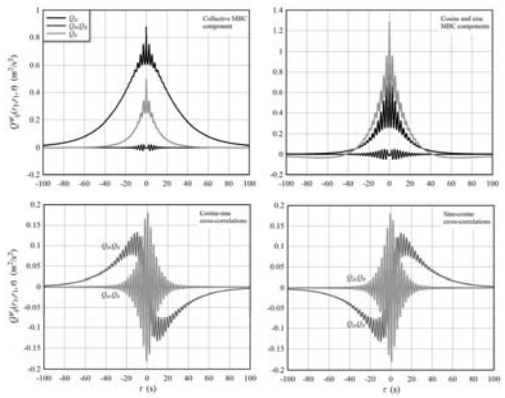

Multi-blade coordinate transform of rotationally-sampled turbulence

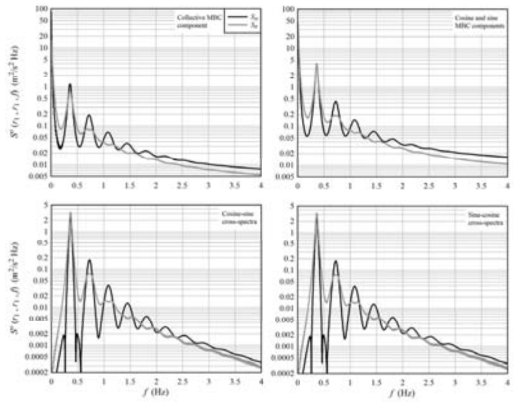

Wave loads: "MacCamy-Fuchs plus Morison drag plus Wheeler stretching"

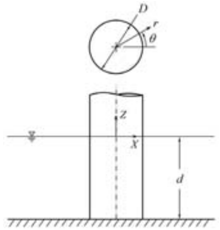

$$\Phi = \frac{g\zeta_0}{\omega}\exp(i\omega t)\frac{\cosh k_r(z+d)}{\cosh k_r d}$$

$$\times \sum_{m=0}^{\infty} i^{m+1}(-1)^m \epsilon_m \left(J_m(k_r r) - f_m(R)\left[J_m(k_r r) - iY_m(k_r r)\right]\right)\cos m\theta,$$

$$f_m(R) := \frac{-k_r J_{m+1}(k_r R) + \frac{m}{R}J_m(k_r R)}{-k_r J_{m+1}(k_r R) + \frac{m}{R}J_m(k_r R) - i\left(-k_r Y_{m+1}(k_r R) + \frac{m}{R}Y_m(k_r R)\right)}$$

Wheeler stretching, mapping to finite element nodes, pressure integration

$$z + d = (z' + d)\frac{d}{d+\zeta}$$

$$dz = dz'\frac{d}{d+\zeta}$$

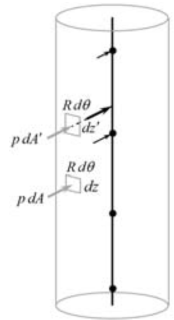

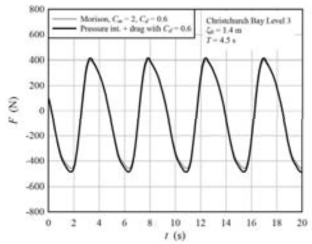

Wave loads in the splash zone

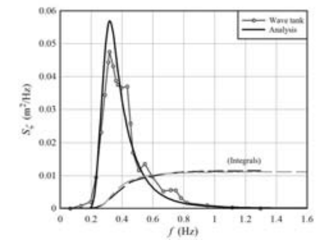

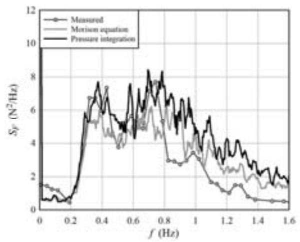

Wave tank data from: Isaacson M, Baldwin J. Measured and predicted random wave forces near the free surface. Applied Ocean Research 12 (1990) 188-199.

Nodal wave force spectra

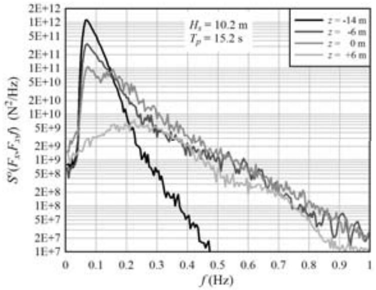

Some second-order effects are accounted for.
Not a true second-order method. Second-order frequency-domain methods are available and could be implemented.

Commercial codes can also be used to generate the input time series.

Linearized DTU Basic Wind Energy Controller

4 - 7 m/s

8 - 11 m/s

12 - 25 m/s

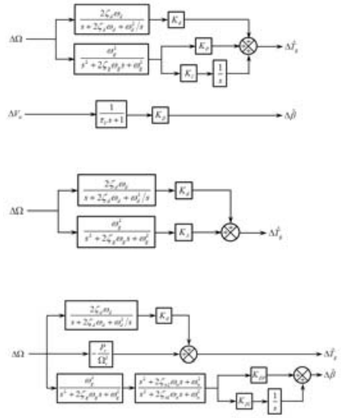

Generator model

Mean:

$$\left(\omega_0 \mathbf{T}_a^\theta \boldsymbol{\Lambda} \frac{d\mathbf{T}_\theta^a}{d\theta} + \mathbf{T}_a^\theta \mathbf{R} \mathbf{T}_\theta^a\right)\mathbf{i}_0^\theta = -\mathbf{v}_0^\theta - \omega_0 \mathbf{T}_a^\theta \frac{d\mathbf{T}_\theta^a}{d\theta}\boldsymbol{\lambda}_r^\theta$$

Fluctuations:

$$\mathbf{T}_a^\theta \boldsymbol{\Lambda} \mathbf{T}_\theta^a \frac{d\Delta\mathbf{i}^\theta}{dt} = -\left(\omega_0 \mathbf{T}_a^\theta \boldsymbol{\Lambda} \frac{d\mathbf{T}_\theta^a}{d\theta} + \mathbf{T}_a^\theta \mathbf{R} \mathbf{T}_\theta^a\right)\Delta\mathbf{i}^\theta - \Delta\mathbf{v}^\theta$$

Control:

$$\mathbf{v}^\theta = -\overline{\omega}\mathbf{T}_a^\theta \boldsymbol{\Lambda} \frac{d\mathbf{T}_\theta^a}{d\theta}\overline{\mathbf{i}}^\theta - \overline{\omega}\mathbf{T}_a^\theta \frac{d\mathbf{T}_\theta^a}{d\theta}\boldsymbol{\lambda}_r^\theta - \mathbf{K}_P\left(\hat{\mathbf{i}}^\theta - \overline{\mathbf{i}}^\theta\right) - \int_0^t \mathbf{K}_I\left(\hat{\mathbf{i}}^\theta - \overline{\mathbf{i}}^\theta\right)dt$$

State-space:

$$\begin{bmatrix} \mathbf{T}_a^\theta \boldsymbol{\Lambda} \mathbf{T}_\theta^a & \mathbf{0} \\ \mathbf{0} & \mathbf{I} \end{bmatrix} \frac{d}{dt} \begin{bmatrix} \Delta\mathbf{i}^\theta \\ \int \Delta\overline{\mathbf{i}}^\theta \\ \Delta\overline{\mathbf{i}}^\theta \\ \Delta\overline{\omega} \\ \int \Delta\hat{\mathbf{i}}_q^\theta \end{bmatrix} = \begin{bmatrix} \mathbf{A}_{11} & -\mathbf{K}_I & \mathbf{A}_{13} & \mathbf{A}_{14} & \mathbf{A}_{15} \\ \mathbf{0} & \mathbf{0} & \mathbf{I} & \mathbf{0} & \mathbf{0} \\ \mathbf{A}_{31} & \mathbf{0} & -\mathbf{A}_{31} & \mathbf{0} & \mathbf{0} \\ \mathbf{0} & \mathbf{0} & \mathbf{0} & -\omega_s & 0 \\ \mathbf{0} & \mathbf{0} & \mathbf{0} & 0 & 0 \end{bmatrix} \begin{bmatrix} \Delta\mathbf{i}^\theta \\ \int \Delta\overline{\mathbf{i}}^\theta \\ \Delta\overline{\mathbf{i}}^\theta \\ \Delta\overline{\omega} \\ \int \Delta\hat{\mathbf{i}}_q^\theta \end{bmatrix} + \begin{bmatrix} \mathbf{B}_{11} & \mathbf{B}_{12} \\ \mathbf{0} & \mathbf{0} \\ \mathbf{0} & \mathbf{0} \\ 0 & \omega_s \\ \overline{\Omega}/E_q & 0 \end{bmatrix} \begin{bmatrix} \Delta\hat{T} \\ \Delta\omega \end{bmatrix}$$

Merz KO. Pitch actuator and generator models for wind turbine control system studies. Memo AN 15.12.35, SINTEF Energy Research, 2015.

Linear and nonlinear components of foundation loading

OC3 monopile
V_∞ = 7 m/s

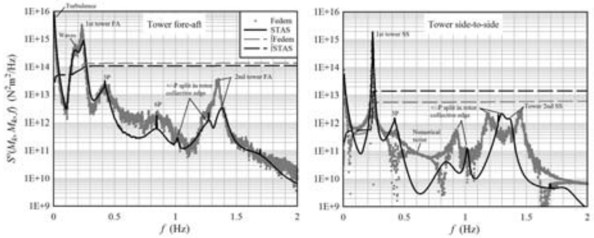

Approximate calibration to parked turbine frequencies and control gains tuned. Not a blind comparison.

Linear and nonlinear components of foundation loading

V_∞ = 11 m/s

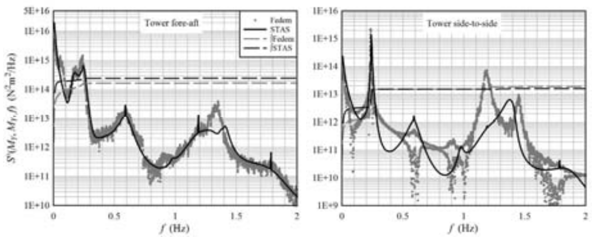

Linear and nonlinear components of foundation loading

V_∞ = 15 m/s

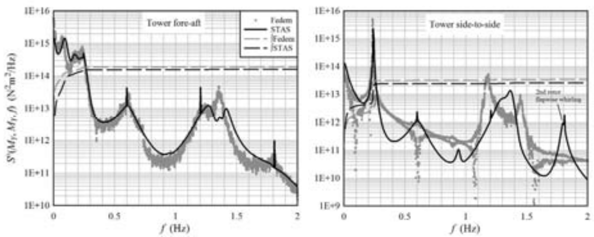

DTU 10 MW wind turbine (+ NOWITECH 10 MW nacelle), offshore foundation

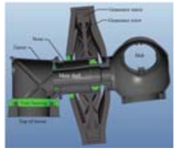

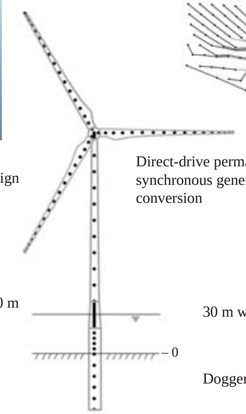

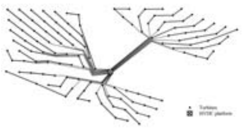

Tower +40 to +145 m
Stiffened w.r.t. onshore design
approx. 900 tonnes

Direct-drive permanent-magnet synchronous generator, full power conversion

Transition piece +20 to +40 m
approx. 600 tonnes

30 m water depth

Monopile, -42 m to +20 m
9 m diameter
approx. 1500 tonnes

Dogger Bank seabed profile

Transverse vibrations under wave loading

Transfer functions between waterline wave force and tower mudline bending moments

Shut down in storm

Operating at 10 m/s

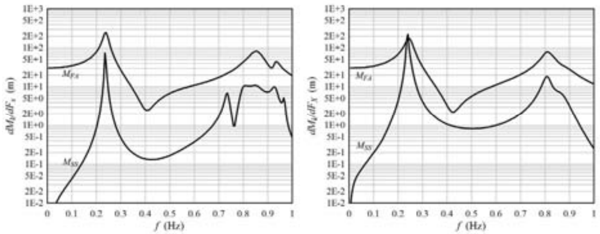

Transverse vibrations under wave loading

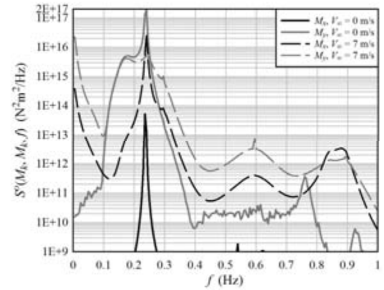

The transverse vibrations are attributed to the operating rotor.

Transverse vibrations under wave loading

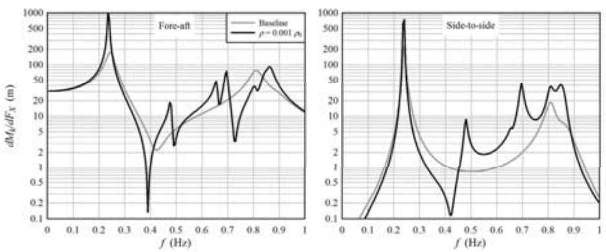

... but the interaction is nonetheless present when the rotor is spinning in a vacuum.

Hypothesis: Gyroscopic effects coupling with a rotor "nodding" component of the first tower fore-aft mode.

Fatigue of the monopile foundation

Load case ID	Turbine state	V_∞	θ_V	I	H_s	T_p	θ_w	V_c	θ_c
7.1-0-V	Pitch fault	1-yr	0	NTM	50-yr(1)	$E[T_p\|H_s]$	0	1-yr	0
7.1-90-V	Pitch fault	1-yr	0	NTM	50-yr(1)	$E[T_p\|H_s]$	90	1-yr	90
6.1-0-W	Parked	10-yr	0	NTM	50-yr	50-yr	0	1-yr	0
6.1-90-W	Parked	10-yr	0	NTM	50-yr	50-yr	90	1-yr	90
1.3-0-V	Operating	V_r	0	ETM	10-yr	$E[T_p\|H_s]$	0	1-yr	0
1.3-90-V	Operating	V_r	0	ETM	10-yr	$E[T_p\|H_s]$	90	1-yr	90
1.3-0-W	Operating	$\approx V_r$	0	NTM	50-yr	50-yr	0	1-yr	0
1.3-90-W	Operating	$\approx V_r$	0	NTM	50-yr	50-yr	90	1-yr	90
1.2	Operating	4...25	0(2)	NTM	$f(V_\infty)$	$f(V_\infty, H_s)$	0,45,90	$E[V_c]$	0,45,90

Environmental load probabilities

$$P\left(V_\infty, \theta_V^E, H_s, T_p, \theta_w^E\right) = P(\theta_V^E)\, P_V(V_\infty \mid \theta_V^E)\, P_H(H_s \mid V_\infty)\, P_T(T_p \mid H_s)\, P(\theta_w^E \mid \theta_V^E)$$

Table XX: Windspeed and direction bin probability

	-180	-150	-120	-90	-60	-30	0	30	60	90	120	150
7	0.0261	0.0220	0.0268	0.0356	0.0365	0.0394	0.0403	0.0461	0.0464	0.0378	0.0311	0.0280
11	0.0113	0.0092	0.0098	0.0152	0.0192	0.0208	0.0237	0.0280	0.0276	0.0208	0.0142	0.0124
14	0.0078	0.0061	0.0054	0.0103	0.0167	0.0181	0.0239	0.0294	0.0280	0.0191	0.0103	0.0087
18	0.0027	0.0019	0.0012	0.0034	0.0094	0.0102	0.0186	0.0254	0.0224	0.0121	0.0040	0.0031

H_s \ V_∞	0	7	11	14	18
0	0.0260	0.0000	0.0000	0.0000	0.0000
1	0.8600	0.8355	0.4600	0.3800	0.2000
2	0.1095	0.1391	0.4400	0.4000	0.2500
3	0.0042	0.0240	0.0890	0.1600	0.2600
4	0.0003	0.0014	0.0090	0.0390	0.2000
5	0.0000	0.0000	0.0020	0.0170	0.0600
6	0.0000	0.0000	0.0000	0.0040	0.0211
7	0.0000	0.0000	0.0000	0.0000	0.0081
8	0.0000	0.0000	0.0000	0.0000	0.0008

H_s \ $T_p \mid H_s$	2	4	6	8	10	12	14	16
1	0.0007	0.2406	0.4658	0.2172	0.0598	0.0129	0.0026	0.0005
2	0.0000	0.0183	0.3650	0.4203	0.1565	0.0337	0.0055	0.0007
3	0.0000	0.0000	0.0947	0.4979	0.3221	0.0747	0.0105	0.0000
4	0.0000	0.0000	0.0057	0.2877	0.5157	0.1709	0.0199	0.0000
5	0.0000	0.0000	0.0000	0.0531	0.5575	0.3451	0.0442	0.0000
6	0.0000	0.0000	0.0000	0.0000	0.2941	0.5882	0.1176	0.0000
7	0.0000	0.0000	0.0000	0.0000	0.1000	0.6000	0.3000	0.0000
8	0.0000	0.0000	0.0000	0.0000	0.0000	0.0000	1.0000	0.0000

waves \ wind	-180	-150	-120	-90	-60	-30	0	30	60	90	120	150
-180	0.2424	0.1848	0.0799	0.0196	0.0057	0.0048	0.0048	0.0048	0.0057	0.0196	0.0799	0.1848
-150	0.1848	0.2424	0.1848	0.0799	0.0196	0.0057	0.0048	0.0048	0.0048	0.0057	0.0196	0.0799
-120	0.0799	0.1848	0.2424	0.1848	0.0799	0.0196	0.0057	0.0048	0.0048	0.0048	0.0057	0.0196
-90	**0.1368**	**0.1971**	**0.3020**	**0.3596**	**0.3020**	**0.1971**	**0.1368**	**0.1228**	**0.1219**	**0.1219**	**0.1219**	**0.1228**
-60	**0.0517**	**0.0656**	**0.1260**	**0.2309**	**0.2884**	**0.2309**	**0.1260**	**0.0656**	**0.0517**	**0.0508**	**0.0508**	**0.0508**
-30	0.0048	0.0057	0.0196	0.0799	0.1848	0.2424	0.1848	0.0799	0.0196	0.0057	0.0048	0.0048
0	0.0048	0.0048	0.0057	0.0196	0.0799	0.1848	0.2424	0.1848	0.0799	0.0196	0.0057	0.0048
30	0.0048	0.0048	0.0048	0.0057	0.0196	0.0799	0.1848	0.2424	0.1848	0.0799	0.0196	0.0057
60	0.0057	0.0048	0.0048	0.0048	0.0057	0.0196	0.0799	0.1848	0.2424	0.1848	0.0799	0.0196
90	0.0196	0.0057	0.0048	0.0048	0.0048	0.0057	0.0196	0.0799	0.1848	0.2424	0.1848	0.0799
120	0.0799	0.0196	0.0057	0.0048	0.0048	0.0048	0.0057	0.0196	0.0799	0.1848	0.2424	0.1848
150	0.1848	0.0799	0.0196	0.0057	0.0048	0.0048	0.0048	0.0057	0.0196	0.0799	0.1848	0.2424

All permutations:
25,920 load cases

Moment and stress spectra

$$S_{VM} = S_{\sigma\sigma} + 3S_{\tau\tau}$$

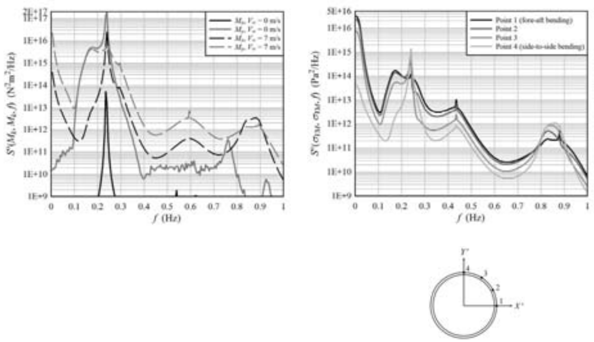

Fatigue cycle exceedance rate

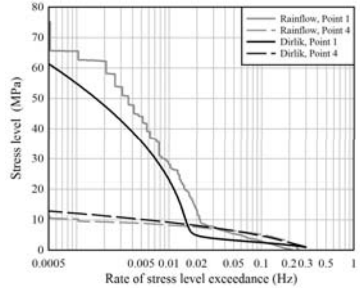

Lifetime stress cycles

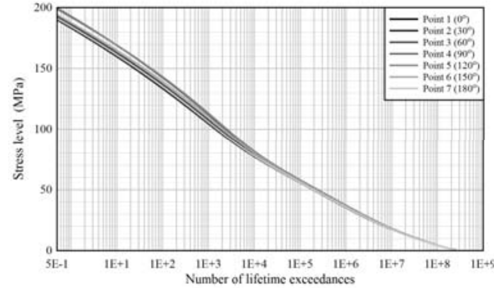

Lifetime fatigue analysis: trends with met-ocean conditions

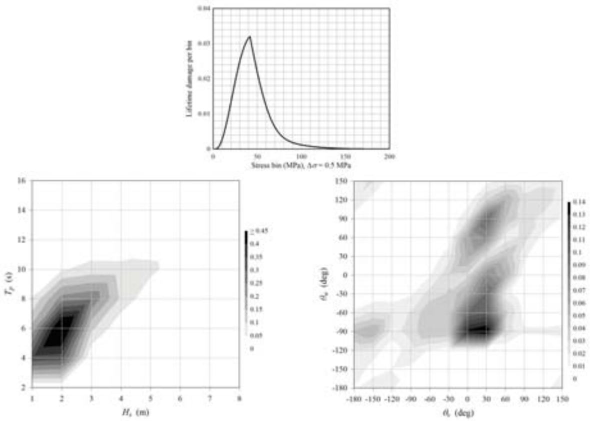

STAS program: "a wind power plant in a matrix"

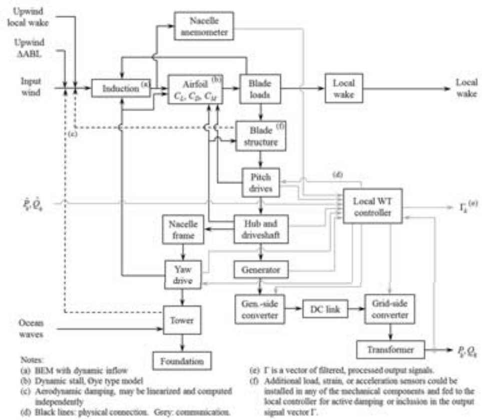

STAS program: "a wind power plant in a matrix"

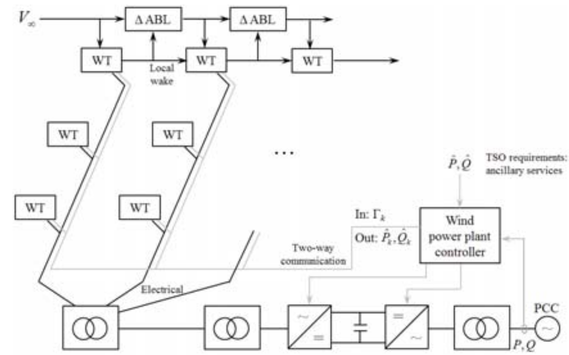

(End of presentation.)

RAMBØLL

EERA DeepWind'2016
Trondheim, 21.01.2016

AWESOME
PhD'S IN WIND POWER O&M

Fatigue crack growth for monopiles

Lisa Ziegler[1,2], Sebastian Schafhirt[2], Matti Scheu[1] & Michael Muskulus[2]

[1] Rambøll Wind, Germany
[2] Norwegian University of Science and Technology

This project has received funding from the European Union's Horizon 2020 research and innovation programme under the Marie Sklodowska-Curie grant agreement No 642108

Does load sequence and weather seasonality influence fatigue crack growth?

Why should we model fatigue crack propagation?

Trend: Aging offshore wind farms

Needs:

- Optimize maintenance and inspection scheduling
- Reassess fatigue lifetime
- Decide about lifetime extension

Challenges:

- Uncertainties in loading, material resistance, design models
- Design lifetime differs from reality
- Update lifetime prediction through monitoring and inspections

→ Fatigue crack propagation

3

Fatigue design in offshore wind today

- SN-curve approach
- Linear damage accumulation
- Does not describe crack propagation
- Neglects sequence effects

$$D = \sum_i \frac{n_i}{N_i}$$

D: damage [-]
n_i: number of occurred stress cycles [-]
N_i: number of stress cycles until failure [-]

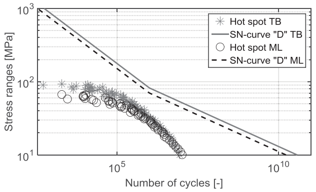

Fig 1. SN-curves and number of stress cycles during 20 years.

4

Agenda

- Methods
  - Fatigue crack propagation
  - Markov weather model
- Results
  - Load sequence
  - Weather seasonality
- Conclusion

AWESOME

5

Fatigue crack propagation

- Paris law

$$\frac{da}{dN} = C(\Delta K_I)^m$$

$$\Delta K_I = \Delta S \cdot Y \sqrt{\pi \cdot a}$$

a : crack depth [mm]
N : number of cycles [-]
ΔK_I : stress intensity factor [...]
ΔS : stress range [MPa]
Y : geometry factor [-]
C, m : material constants [-]

- Physical and mathematical sequence effect
- Calibration of C with SN-curve results

Tab 1. Damage, extrapolated lifetime and calibrated C.

Location	20 year damage [-]	$T_{failure}$ [years]	ln(C) [-]
TB	1.21	16.48	-28.52
ML	0.61	32.89	-28.36

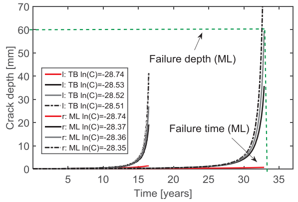

Fig 2. Crack growth at tower bottom (TB) and mudline (ML) for various C parameter.

6

Markov weather model

- Requirements:
  - Wind distribution
  - Seasonal trend
  - Weather persistence
- Stochastic process with finite memory
- Transition matrix T_M from historical data (22-years of wind speed in 6h resolution)

$$T_M = \begin{bmatrix} p_{11} & p_{12} & \cdots & p_{1s} \\ p_{21} & p_{22} & \cdots & p_{2s} \\ \cdots & \cdots & \cdots & \cdots \\ p_{s1} & p_{s2} & \cdots & p_{ss} \end{bmatrix}$$

with
T_M: transition matrix [-]
p: transition probability [-]

- Discrete time series for wind speed: 2 – 30 m/s with 6h time steps

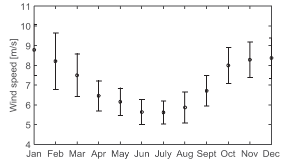

Fig 3. Monthly wind speed variation.

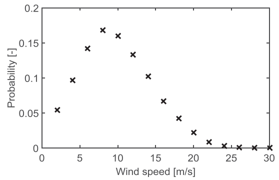

Fig 4. Wind speed distribution.

AWESOME

Does load sequence and weather seasonality influence fatigue crack growth?

Case study

- NREL 5MW and monopile from OC3 project (Nichols et al. 2009)
- Met-ocean data from Upwind project (Fischer et al. 2010)
- 15 fatigue load cases: power production, idling
- Structural response (1h time series) to aerodynamic and hydrodynamic loading with impulse-based substructuring

⟹ Analysis of *mathematical effect* of load sequence only

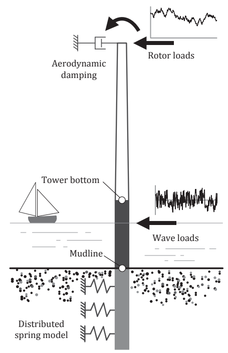

Fig 5. Model of offshore wind monopile.

Results: load sequence

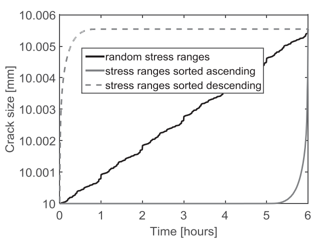

Fig 6. Crack growth for 6h time interval assuming 10mm initial crack size.

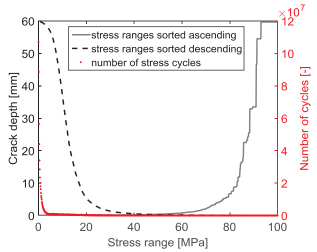

Fig 7. Crack growth during structural lifetime as a function of stress ranges. Red line gives number of stress cycles.

AWESOME

Results: weather seasonality

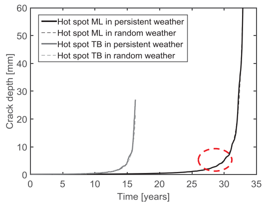

Fig 8. Comparison of crack growths in persistent weather and random weather.

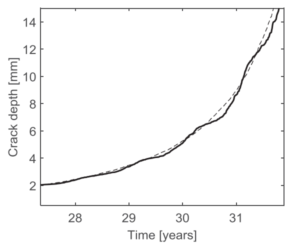

Fig 9. Zoom into Figure 8.

Conclusion

Under the assumptions made in this study…

1. Not necessary to reassess lifetimes regarding history of load sequence
2. Inspection and repair planning of aging wind turbines should account for weather seasonality
3. Interesting for future: What is the impact of ultimate loads on fatigue lifetime?

AWESOME

Thanks for your attention

Lisa Ziegler
PhD researcher
lisa.ziegler@ramboll.com
+49 (0) 151 44 006 445

Rambøll Wind
Hamburg, Germany
www.ramboll.com/wind

RAMBØLL

Appx. 1: Parameters of crack growth model

Tab 2. Parameters applied in crack growth model.

Parameter	Unit	Value	Source
a_0	mm	0.1	DNV 2014
a_C	mm	60/27	Li et al 2011, Dong et al 2012
m	-	3.1	DNV 2014
ln(C)	[…]	-28.36/-28.52	calibrated
Y	-	1	Kirkemo 1998

Appx. 2: AWESOME

- AWESOME = Advanced wind energy systems operation and maintenance expertise
- Marie Skłodowska-Curie Innovative Training Networks
- 11 PhD's
- O&M
  - Failure diagnostic and prognostic
  - Maintenance scheduling
  - Strategy optimization

www.awesome-h2020.eu

Appx. 3: References

DNV. 2014. Design of offshore wind turbine structures. Offshore standard DNV-OS-J101. Høvik: Det Norske Veritas.

Dong W, Moan T, & Gao, Z. 2012. Fatigue reliability analysis of the jacket support structure for offshore wind turbine considering the effect of corrosion and inspection. *Reliability Engineering and System Safety, 106*: 11-27.

Fischer T, De Vries WE, & Schmidt B. 2010. *UpWind design basis (WP4: Offshore foundations and support structures)*. Upwind.

Li Y, Lence BJ, Shi-Liang Z, & Wu Q. 2011. Stochastic Fatigue Assessment for Berthing Monopiles in Inland Waterways. *J. Waterway, Port, Coastal, Ocean Eng, 137* (2): 43–53. DOI: 10.1061/(ASCE)WW.1943-5460.0000063.

Nichols J, et al. 2009. Offshore code comparison collaboration within IEA Wind Annex XXIII: phase III results regarding tripod support structure modeling. 47th AIAA Aerospace Sciences Meeting and Exhibit, 5–8 January 2008, Orlando, Florida, *AIAA Meeting Papers on Disc 14* (1).

Kirkemo F. 1988. Applications of probabilistic fracture mechanics to offshore structures. *Applied Mechanics Reviews, 41*(2), 61-84.

AWESOME

MAXIMUM LOADS ON A 1-DOF MODEL-SCALE OFFSHORE WIND TURBINE

Loup Suja-Thauvin (Industry PhD)
Jørgen Krokstad (prof II)
Joakim Fürst Frimann-Dahl (DNV-GL)

Statkraft | NTNU – Trondheim Norwegian University of Science and Technology

Table of contents

Table of contents

1. Motivation

- Increasing rotor diameter

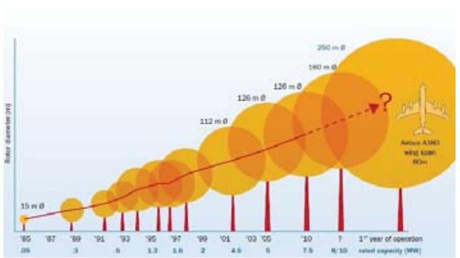

1. Motivation

- Focus on
  - Large diameter monopiles
  - Shallow waters

➔ increase of non-linearities (frequent breaking)

ULS: what is the design driver?

Table of contents

2. Experiments

Responding model

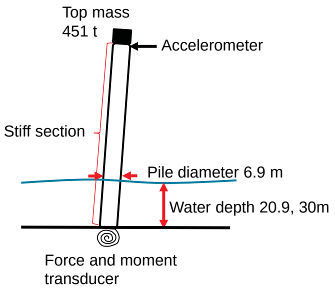

2. Experiments

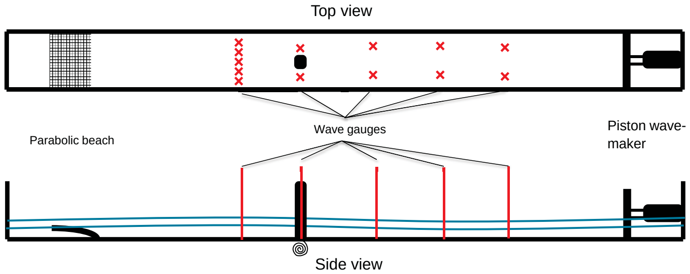

2. Experiments

- Sea states:
  - JONSWAP spectra
  - Storms with different return periods
  - 20 seeds per sea state

H_s (m)	T_p (s)	g
6.71	11.25	2.32
7.69	“	2.61
8.22	“	2.76
9.04	“	3
6.71	15	1.42
7.69	“	1.59
8.22	“	1.69
9.04	“	1.83

Table of contents

3. Numerical model

- Representation of the model: 1 degree of freedom equation

$$M_{hydro} = (I_P + I_A)\ddot{\theta} + C\dot{\theta} + K\theta$$

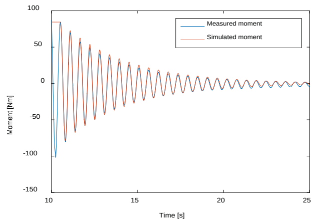

3. Numerical model

- Input hydrodynamic loads from FNV formulation

$$
\begin{aligned}
F_{FNV} = \quad & 2\pi\rho R^2 \int_{-h}^{0} u_t(z)dz && O(\epsilon) \\
& + 2\pi\rho R^2 u_t\big|_{z=0} \zeta^{(1)} + \pi\rho R^2 \int_{-h}^{0} [2w(z)w_x(z) + u(z)u_x(z)]dz && O(\epsilon^2) \\
& + \pi\rho R^2 \left[\zeta^{(1)} \left(u_{tz}\zeta^{(1)} + 2ww_x + uu_x - \frac{2}{g} u_t w_t \right) - \left(\frac{u_t}{g} \right) (u^2 + v^2)\Big|_{z=0} \right] && O(\epsilon^3) \\
& + \pi\rho \frac{R^2}{g} u^2 u_t\big|_{z=0} \beta \left({}^{h}/_{R} \right) && O(\epsilon^3)
\end{aligned}
$$

Finite water depth formulation

Table of contents

4. Analysis of the results

- Focus on maximum responses
  - Very long and steep waves hit the structure
  - Frequent breaking waves
  - 1st eigenperiod of the structure is excited

4. Analysis of the results

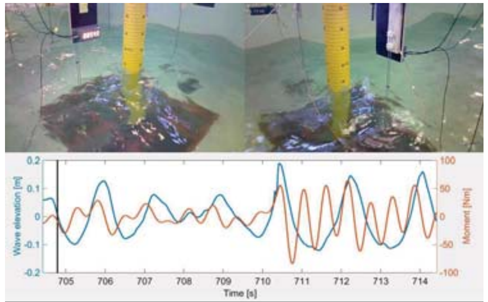

4. Analysis of the results

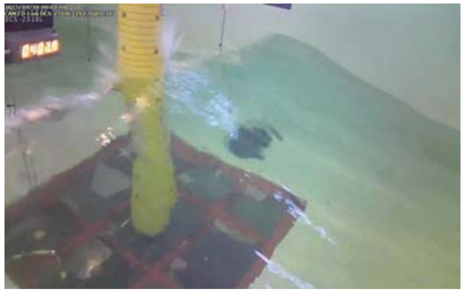

4. Analysis of the results

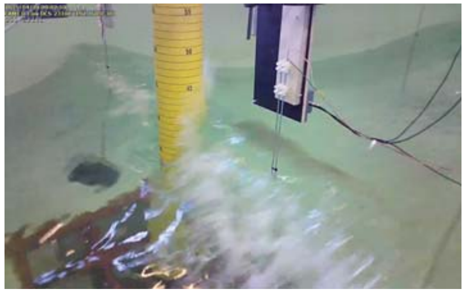

4. Analysis of the results

- FNV matches the maximum load

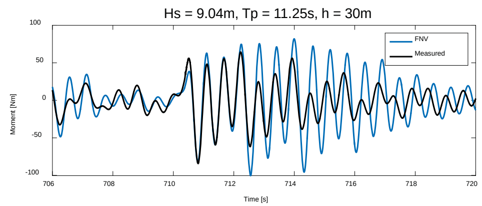

4. Analysis of the results

How does the 1st mode get triggered?

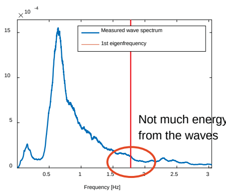

Not much energy from the waves

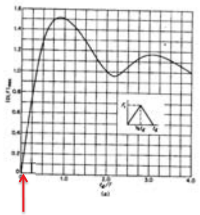

$$t_d = \frac{13R}{32c}$$

NTNU – Trondheim
Norwegian University of Science and Technology

4. Analysis of the results

- Input hydrodynamic loads from FNV formulation

$$F_{FNV} = 2\pi\rho R^2 \int_{-h}^{0} u_t(z)dz \qquad O(\epsilon)$$

$$+ 2\pi\rho R^2 u_t\big|_{z=0} \zeta^{(1)} + \pi\rho R^2 \int_{-h}^{0} [2w(z)w_x(z) + u(z)u_x(z)]dz \qquad O(\epsilon^2)$$

$$+\pi\rho R^2 \left[\zeta^{(1)}\left(u_{tz}\zeta^{(1)} + 2ww_x + uu_x - \frac{2}{g}u_t w_t\right) - \left(\frac{u_t}{g}\right)(u^2+v^2)\Big|_{z=0}\right] \qquad O(\epsilon^3)$$

$$+\pi\rho \frac{R^2}{g} u^2 u_t\big|_{z=0} \beta\left({}^{h}/_{R}\right) \qquad O(\epsilon^3)$$

Contribution of linear potential at the free surface

4. Analysis of the results

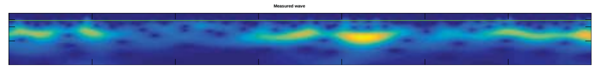

4. Analysis of the results

- Decomposition of the response into different modes

For all cases, there is a hump in the 2nd order excitation load

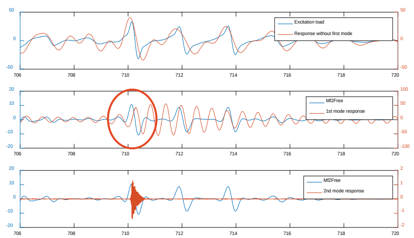

(artificial second mode is triggered by slamming)

4. Analysis of the results

- Simple approximation: trying to match the 2nd order load with an impulse load of sinusoidal shape

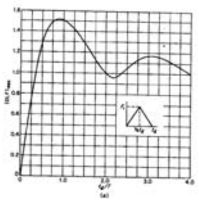

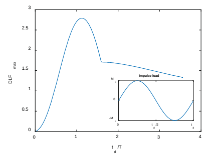

4. Analysis of the results

- Simple approximation: trying to match the 2nd order load with an impulse load of sinusoidal shape

The free surface 2nd order load has a high energy content around the eigenfrequency of the structure

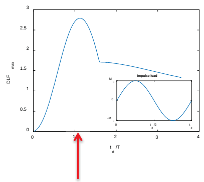

4. Analysis of the results

- Decomposition of the response into different modes

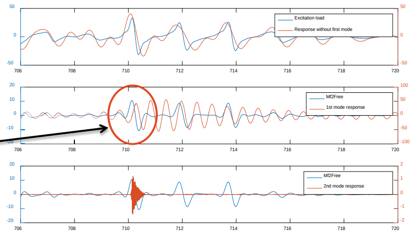

Phase difference

4. Analysis of the results

- Analytical formula for the response

$$M(t) = M_0\cos(\omega t) + \frac{\dot{M}_0}{\omega}\sin(\omega t) + \omega M_a \int_0^t f(\tau)\sin[\omega(t-\tau)]d\tau$$

with
- M the response moment of the structure
- M_0 moment at initial state
- M_a load amplitude
- f load shape function
- ω eigenperiod of the system

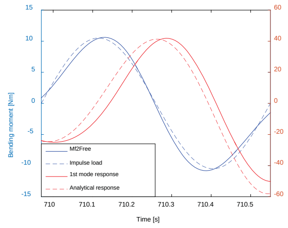

4. Analysis of the results

- Analytical formula for the response

$$M(t) = M_0\cos(\omega t) + \frac{\dot{M}_0}{\omega}\sin(\omega t) + \omega M_a \int_0^t f(\tau)\sin[\omega(t-\tau)]d\tau$$

Initial conditions are necessary to match the maximum value and phase

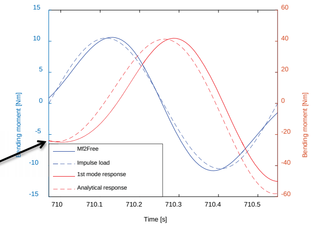

4. Analysis of the results

- Input hydrodynamic loads from FNV formulation

$$
\begin{aligned}
F_{FNV} = \; & 2\pi\rho R^2 \int_{-h}^{0} u_t(z)dz & O(\epsilon) \\
& + 2\pi\rho R^2 u_t\big|_{z=0}\zeta^{(1)} + \pi\rho R^2 \int_{-h}^{0}[2w(z)w_x(z) + u(z)u_x(z)]dz & O(\epsilon^2) \\
& + \pi\rho R^2\left[\zeta^{(1)}\left(u_{tz}\zeta^{(1)} + 2ww_x + uu_x - \frac{2}{g}u_t w_t\right) - \left(\frac{u_t}{g}\right)(u^2+v^2)\Big|_{z=0}\right] & O(\epsilon^3) \\
& + \pi\rho\frac{R^2}{g}u^2 u_t\big|_{z=0}\beta\left(h/R\right) & O(\epsilon^3)
\end{aligned}
$$

4. Analysis of the results

$$
\begin{aligned}
F_{FNV} = \; & 2\pi\rho R^2 \int_{-h}^{0} u_t(z)dz & O(\epsilon) \\
& + 2\pi\rho R^2 u_t\big|_{z=0}\zeta^{(1)} + \pi\rho R^2 \int_{-h}^{0}[2w(z)w_x(z) + u(z)u_x(z)]dz & O(\epsilon^2) \\
& + \pi\rho R^2\left[\zeta^{(1)}\left(u_{tz}\zeta^{(1)} + 2ww_x + uu_x - \frac{2}{g}u_t w_t\right) - \left(\frac{u_t}{g}\right)(u^2+v^2)\Big|_{z=0}\right] & O(\epsilon^3) \\
& + \pi\rho\frac{R^2}{g}u^2 u_t\big|_{z=0}\beta\left(h/R\right) & O(\epsilon^3)
\end{aligned}
$$

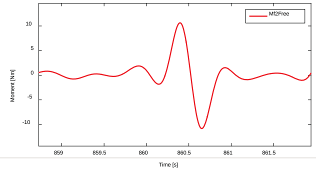

4. Analysis of the results

$$
\begin{aligned}
F_{FNV} = \; & 2\pi\rho R^2 \int_{-h}^{0} u_t(z)dz & O(\epsilon) \\
& + 2\pi\rho R^2 u_t\big|_{z=0}\zeta^{(1)} + \pi\rho R^2 \int_{-h}^{0}[2w(z)w_x(z) + u(z)u_x(z)]dz & O(\epsilon^2) \\
& + \pi\rho R^2\left[\zeta^{(1)}\left(u_{tz}\zeta^{(1)} + 2ww_x + uu_x - \frac{2}{g}u_t w_t\right) - \left(\frac{u_t}{g}\right)(u^2+v^2)\Big|_{z=0}\right] & O(\epsilon^3) \\
& + \pi\rho\frac{R^2}{g}u^2 u_t\big|_{z=0}\beta\left(h/R\right) & O(\epsilon^3)
\end{aligned}
$$

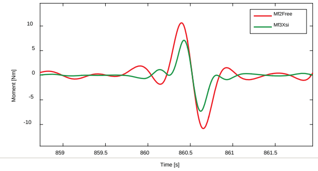

4. Analysis of the results

$$F_{FNV} = 2\pi\rho R^2 \int_{-h}^{0} u_t(z)dz \qquad O(\epsilon)$$
$$+\, 2\pi\rho R^2 u_t\big|_{z=0}\zeta^{(1)} + \pi\rho R^2 \int_{-h}^{0}[2w(z)w_x(z) + u(z)u_x(z)]dz \qquad O(\epsilon^2)$$
$$+\pi\rho R^2\left[\zeta^{(1)}\left(u_{tz}\zeta^{(1)} + 2ww_x + uu_x - \frac{2}{g}u_t w_t\right) - \left(\frac{u_t}{g}\right)(u^2+v^2)\right]\Bigg|_{z=0} \qquad O(\epsilon^3)$$
$$+\pi\rho\frac{R^2}{g}u^2 u_t\big|_{z=0}\beta\left({}^{h}/_{R}\right) \qquad O(\epsilon^3)$$

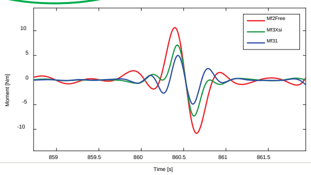

Statkraft

4. Analysis of the results

- Input hydrodynamic loads from FNV formulation

$$F_{FNV} = 2\pi\rho R^2 \int_{-h}^{0} u_t(z)dz \qquad O(\epsilon)$$
$$+\, 2\pi\rho R^2 u_t\big|_{z=0}\zeta^{(1)} + \pi\rho R^2 \int_{-h}^{0}[2w(z)w_x(z) + u(z)u_x(z)]dz \qquad O(\epsilon^2)$$
$$+\pi\rho R^2\left[\zeta^{(1)}\left(u_{tz}\zeta^{(1)} + 2ww_x + uu_x - \frac{2}{g}u_t w_t\right) - \left(\frac{u_t}{g}\right)(u^2+v^2)\right]\Bigg|_{z=0} \qquad O(\epsilon^3)$$
$$+\pi\rho\frac{R^2}{g}u^2 u_t\big|_{z=0}\beta\left({}^{h}/_{R}\right) \qquad O(\epsilon^3)$$

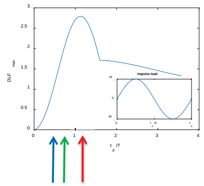

Statkraft

4. Analysis of the results

$$F_{FNV} = 2\pi\rho R^2 \int_{-h}^{0} u_t(z)dz \qquad O(\epsilon)$$
$$+\, 2\pi\rho R^2 u_t\big|_{z=0}\zeta^{(1)} + \pi\rho R^2 \int_{-h}^{0}[2w(z)w_x(z) + u(z)u_x(z)]dz \qquad O(\epsilon^2)$$
$$+\pi\rho R^2\left[\zeta^{(1)}\left(u_{tz}\zeta^{(1)} + 2ww_x + uu_x - \frac{2}{g}u_t w_t\right) - \left(\frac{u_t}{g}\right)(u^2+v^2)\right]\Bigg|_{z=0} \qquad O(\epsilon^3)$$
$$+\pi\rho\frac{R^2}{g}u^2 u_t\big|_{z=0}\beta\left({}^{h}/_{R}\right) \qquad O(\epsilon^3)$$

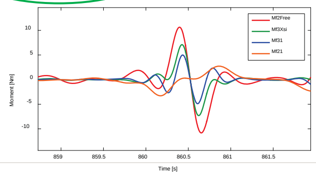

Statkraft

4. Analysis of the results

- Damping considerations:
  - Low damping due to idling turbine (here 2.4%)
  - If the turbine is already oscillating, maximum load can be amplified or decreased depending on initial conditions

Statkraft

Table of contents

NTNU – Trondheim
Norwegian University of Science and Technology

Statkraft

5. Conclusion

- Simple model to explain qualitatively maximum loads observed during experiments with high frequency of breaking waves
- Impulsive slamming has shown not to induce 1st mode shape response
- The maximum load can be explained as the transient response to an impulse load caused by higher order hydrodynamic loads components
- Low damping can potentially increase the maximum load by changing the initial conditions
- 2nd mode of the structure is triggered by breaking and should be taken into consideration when assessing maximum loads

Statkraft

Acknowledgments

The experiments were done using the set-up developed by Statoil for the Dudgeon project

Statkraft

NTNU – Trondheim
Norwegian University of Science and Technology

Statkraft
REN ENERGI

www.statkraft.no

RISK-BASED DECISION SUPPORT FOR OFFSHORE WIND TURBINE INSTALLATION AND OPERATION & MAINTENANCE

TOMAS GINTAUTAS*, AAU (tg@civil.aau.dk)

PROFESSOR JOHN DALSGAARD SØRENSEN, AAU

SIGRID RINGDALEN VATNE, MARINTEK

AALBORG UNIVERSITY
DENMARK

Agenda

- **Research Motivation**
- **Description of the software tool in question.**
- **Short term validation input.** Weather and vessel model**.**
    - Position
    - Input variables
    - Hywind Rotor-Lift installation phases
    - Limit states under consideration
- Types of limit states
- Procedure for estimating **Probabilities of Failed Operations**
- **Proof of concept. DEMO**
- **Probability based Decision Making.**
    - Limit State Probabilities of Failure
    - Operation Failure rate
    - Weather window estimation
- **Long term validation for summer 2014.**
- Risk Based Decision Making
- **Conclusions and discussion**

Motivation

State-of-the-art in assessing whether a weather sensitive offshore operation is safe to commence is only based on significant wave height Hs and wind speed at the location in question.

The actual limitations of installation are mostly physical:

- strength of the installation equipment used - crane cable loads, tug wire tensions, etc.
- Limits on the equipment being installed – maximum acceleration limits on wind turbine nacelle/rotor components.
- safe working environment conditions – motions and accelerations at the height/location of the installation limiting or prohibiting the installation crews work.

Transition from limits on weather conditions to limits on physical response criteria in decision making would improve the predictions of weather windows for installation and potentially reduce the cost of energy.

DECOFF method and Topology Expected Software Tool

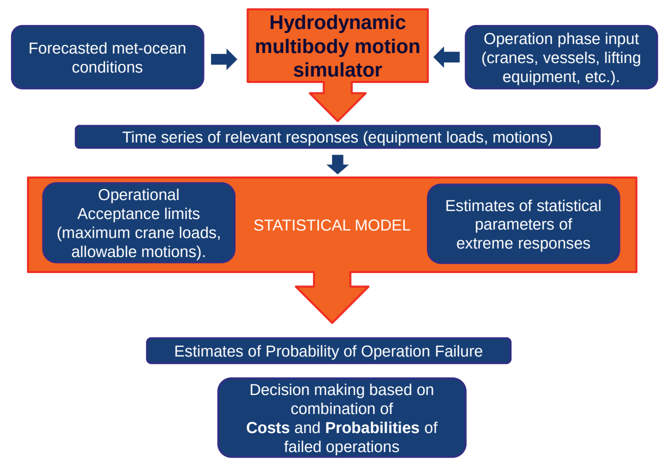

DECOFF – Example test case

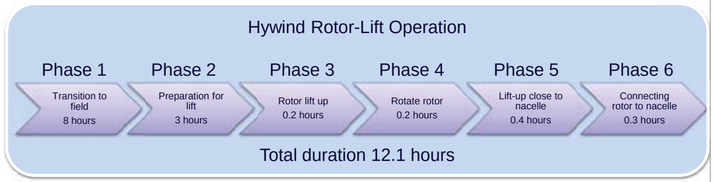

Test case:

- Phases 3-6 – barge is at the installation position, rotor is lifted up and bolted to the nacelle.

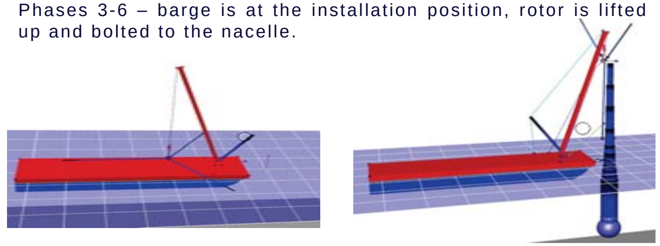

Limiting operational parameters

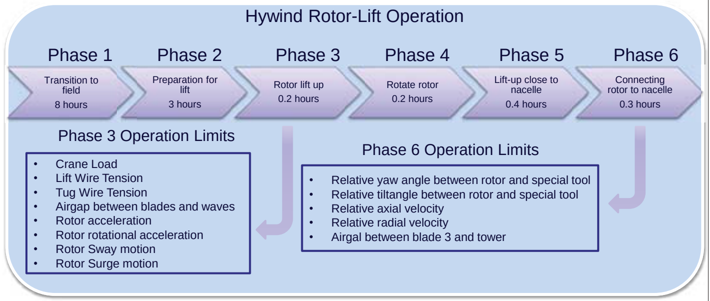

Short term Validation. Simulation input - weather

Location: 7 ° W 55.25 ° N

FINO 3 site

Forecast: ECMWF 2013

2013-08-06

51 ensemble members containing up to **250 hours lead time** forecast**.**

- Wind speed and direction.
- Sig wave height and peak and direction.
- Swell sig wave height and mean period and direction.

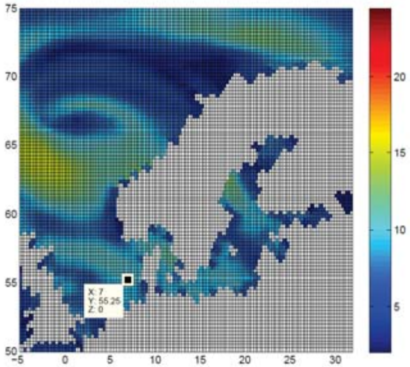

DEPARTAMENT OF CIVIL ENGINEERING
AALBORG UNIVERSITET

Short term Validation. Simulation input - weather

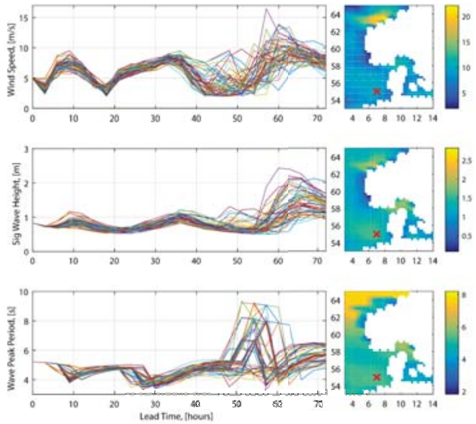

Types of limit states

Non-exceedance limit state. The response has to be above the acceptance limit (no slack in lifting cables, tug wires, tower clearance etc.)

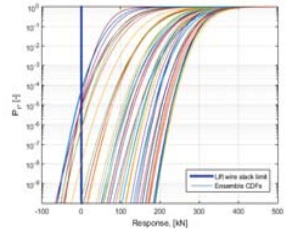

Evaluation of non-exceedance function at acceptance limit R_{max}.

$$P_{F,ens} = F_{non-exc,ens}(R_{max})$$

Exceedance limit state. The response has to be below a certain acceptance limit (maximum motions, loads on lifting equipment etc.)

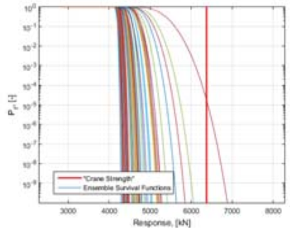

Evaluation of exceedance function at acceptance limit R_{max}.

$$P_{F,ens} = P_{exc,ens}(R_{max})$$

Types of limit states continued

Deterministic limit state. Defined by a single value of acceptance/ failure limit.

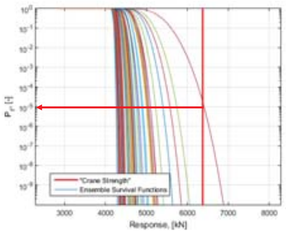

Evaluation of CDF at the acceptance limit R_{max}.

$$P_{F,ens} = P_{F,exc,ens}(R_{max})$$

Non-deterministic limit state. Defined by a distribution of the acceptance limit.

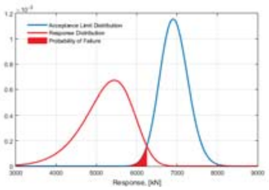

Inegral of response CDF multiplied with „stregth" PDF within acceptance limit range.

$$P_{F,ens} = \int P_{exc,ens}(R) \cdot f(R|\mu_{ln}, \sigma_{ln})dR$$

DEPARTMENT OF CIVIL ENGINEERING
AALBORG UNIVERSITET

Types of limit states continued

Deterministic limit state. Defined by a single value of acceptance/ failure limit.

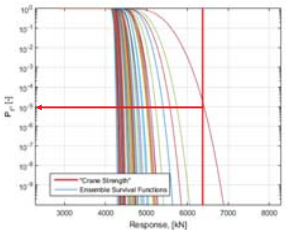

Evaluation of CDF at the acceptance limit R_{max}.

$$P_{F,ens} = P_{F,exc,ens}(R_{max})$$

Non-deterministic limit state. Defined by a distribution of the acceptance limit.

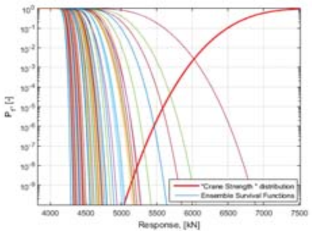

Inegral of response CDF multiplied with „stregth" PDF within acceptance limit range.

$$P_{F,ens} = \int P_{exc,ens}(R) \cdot f(R|\mu_{ln}, \sigma_{ln})dR$$

DEPARTMENT OF CIVIL ENGINEERING
AALBORG UNIVERSITET

Procedure of Failure Probability estimation

Weather forecasts are passed through hydro-elastic simulator and response time series are analysed statistically in order to obtain Probabilities of Failed operations:

1. Peak Over Threshold method is applied to extract extreme values of relevant responses (R) (with $E(R) + 1.4 \cdot \sqrt{VAR(R)}$ threshold and 5 response cycles time separation).

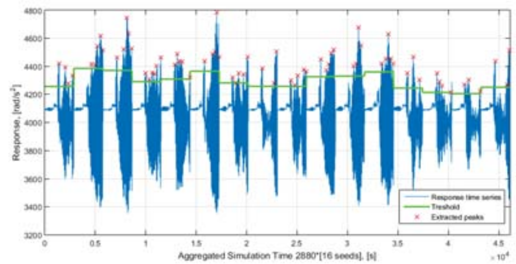

Procedure of Failure Probability estimation

2. Weibull or Normal distribution (adjusted for number of peaks after POT) is fitted to the extremes using Maximum Likelihood parameter estimation.

3. Steps 1-2 are repeated for 51 forecast ensembles.

4. The Probability of Failure for one limit state is an average over 51 ensembles. Combining up all the limits states in one phase gives Probability of failure within an operation phase.

$$P_{F,Lim\ State} = \frac{\sum_{i=1}^{N} P_{F,Ensemble}}{number\ of\ ens}$$

$$P_{F,Operation} = 1 - \prod_{i=1}^{N_{Lim\ States}} (1 - P_{F,\text{Lim}\ State,i})$$

$$P_{F,Operation} = 1 - \prod_{i=1}^{N_{Phases}} (1 - P_{F,Phase,i})$$

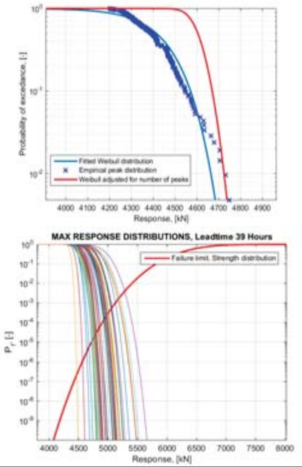

Proof of Concept. Short Term Validation

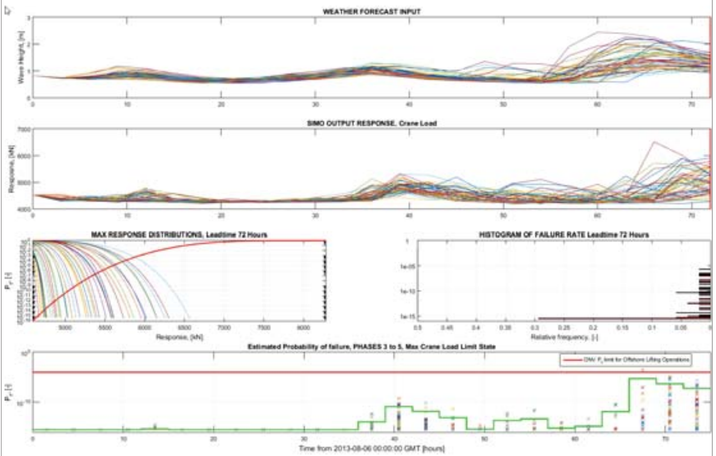

Combination of Limit state Probabilites of Failure

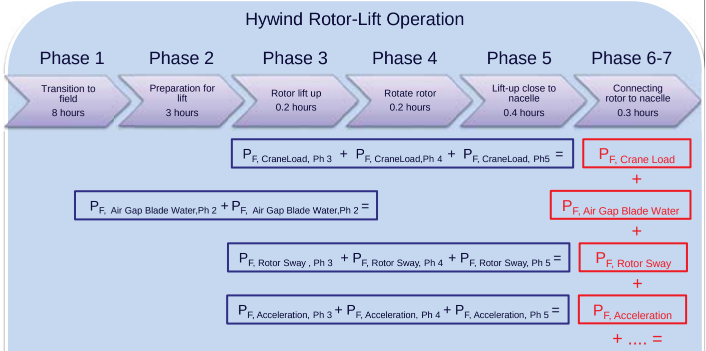

$$P_{F,Operation} = 1 - \prod_{i=1}^{N_{Lim\ States}} (1 - P_{F,\text{Lim}\ State,i})$$

Limit state Probabilities of Failure

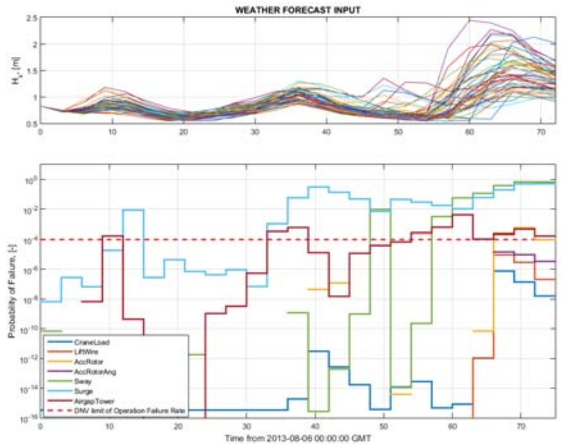

Operation Failure Rate

$$P_{F,Operation} = 1 - \prod_{i=1}^{N_{Lim\ States}} (1 - P_{F,\text{Lim}\ State,i})$$

5. A sum over all the phases gives the total Operation failure rate. Based on $P_{F,Op}$ weather windows, suitable for installation, could be found.

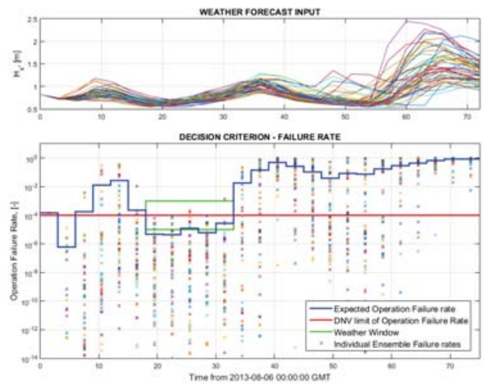

Risk based decision making

$$C_{total} = C_{waiting} + C_{equipment} + \sum_{i=1}^{N_{phases}} \left(\sum_{j=1}^{N_{LS}} P_{LS,i,j} C_{LS,i,j} \right)$$

Having Probabilities of Failure related to a particular limit state and combining those with monetary consequences of failure with particular limit state Risk Based decision making is possible.

What is needed:

- Cost in NOK (€) related to Operation Failure with a particular limit state.
- Cost in NOK (€) of complete Operation Failure for less detailed analysis (one failure results in loss of all equipment and complete Operation Failure).

Long term validation. Input

- **Location**: *7 º W 55.25 º* N **FINO 3 site.**
- **Forecast**: *ECMWF* **May 1st to August 1st 2014.**
  measurements **@FINO3.**
- **Parameters used:**
  - Wind speed and direction.
  - Significant wave height and peak and direction.
  - Swell sig wave height and mean period and direction.
- **Hydrodynamic model:** Hywind Rotor Lift operation.
- **Benchmarking:** The proposed method is validated against a standard "***Alpha-Factor***" from DNV-HS-101.
- **Different benchmarking cases:**
  - Tabulated ***Alpha-Factors*** from DNV-HS-10.
  - Site specific ***Alpha-Factors*** for FINO3 site according to DNV-HS-10.
  - **DECOFF** method with **ECMWF forecasts @FINO3**.
  - **DECOFF** method with **measurements @FINO3**.

Long term validation. Alpha-Factor method

Weather limits for Hywind Rotor Lift operation:

- H_s=1.5m, T_p=5s, W_s=7m/s.

Case	α_{Hs} for H_s = 1.5m	α_{Tp} for T_p = 5s			α_{Ws} for W_s = 7m/s	Quantile
T 4-1. WFQ = C	0.705	inf	0.78	1	0.8	mean
T 4-2. WFQ = B	0.740	inf	0.78	1	0.8	maximum
T 4-3. WFQ = A+M	0.780	inf	0.78	1	0.8	maximum
T 4-4. WFQ = A+C	0.925	inf	0.78	1	0.8	maximum
T 4-5. WFQ = A+M+C	0.925	inf	0.78	1	0.8	maximum
FINO3 measurements	0.810	inf	0.78	1	0.8	maximum

T x-y – table indicator for reference in DNV-HS-10;
WFQ – weather forecast quality class **A, B** or **C**.
+M – meteorologist on site, **+C** – calibrated based on measurement data.

Long term validation. Alpha-Factor method

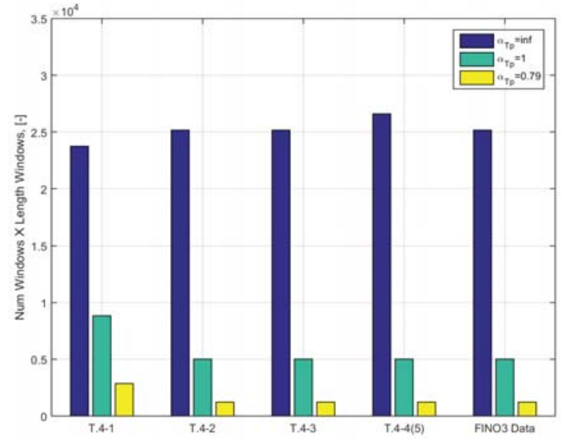

Long term validation. Results

Alpha-Factor method

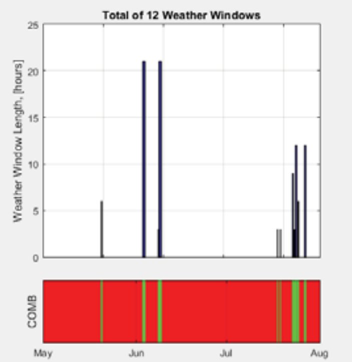

DECOFF method with ECMWF

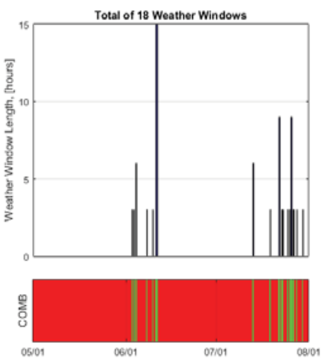

Long term validation. Results

Alpha-Factor method

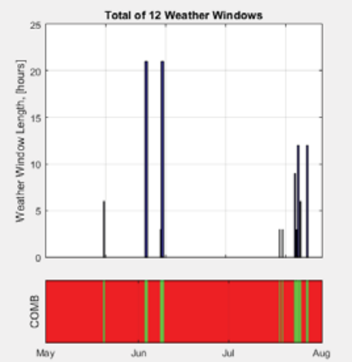

DECOFF method with FINO3 measurements

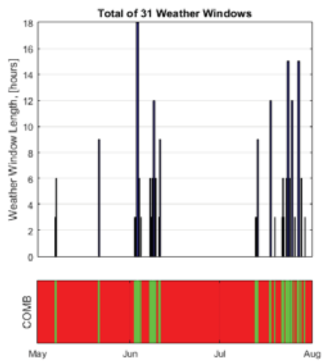

Long term validation. Results

Number of weather windows

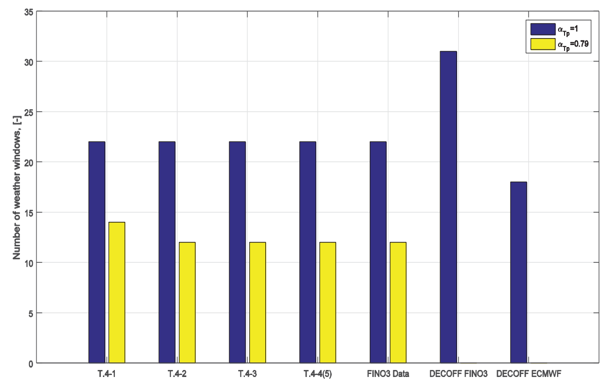

Long term validation. Results

Total Length of weather windows

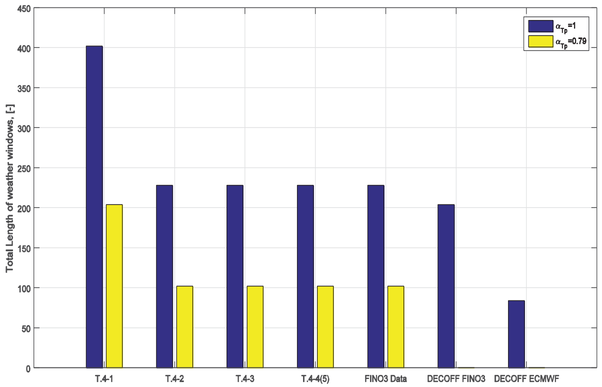

Long term validation. Results

Length X Number of weather windows

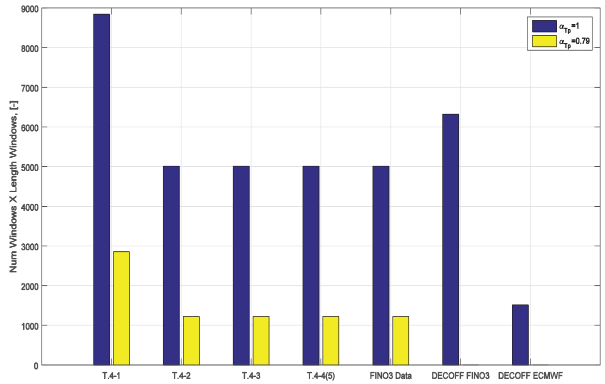

Conclusions and discussion

- After extensive testing it can be concluded that the procedure for estimation of Probability of Failed Operations produces consistent results and could be used to assist in decision making for Offshore Wind Turbine installation.
- The proposed new ***DECOFF method*** performs better or at least as good as the standard "***Alpha-factor"*** *method (when* ***number of windows x total window length*** *measure is used).*
- Weather forecast uncertainty plays a central role in predicting weather windows. With increasing uncertainty the length and number of weather windows decreases. This is on par with the standard "***Alpha-factor"*** *method.*
- Using better, less uncertain, weather forecasts (calibrated weather forecasts, downscaling etc.) would be very beneficial in the performance of ***DECOFF method***.
- Easy extension to Oil and Gas an other relevant industries.

Future work

Possible future work would include but should not be limited to:

- Updating the model with Structural Reliability techniques in order to reduce the demand on a lot of simulations necessary to obtained reliable results.
- Splitting the limit states in Serviceability and Ultimate.
- Including Costs of Failure to produce a "Risk-Based" aspect allowing to evaluate different weather windows in terms of expected Risk rather than just Probability of Failure.
- Improving the accuracy of weather forecasts.
- Extending the methodology to more general Offshore Operations (Oil and Gas, Wind turbine installation on monopoles/jackets etc.).

Acknowledgements

The research is funded by The Research Council of Norway, project No. 225231/070 - Decision support for offshore wind turbine installation.

The authors also acknowledge for their valuable inputs and support:

- Christian Michelsen Research
- STATOIL
- Meteorologisk Institut (Norway)
- MARINTEK
- Uni Research,
- University of Bergen (UiB)

THANK YOU FOR YOUR ATTENTION!

ANY QUESTIONS? COMMENTS?

TOMAS GINTAUTAS*, AAU
tg@civil.aau.dk

JOHN DALSGAARD SØRENSEN, AAU
jds@civil.aau.dk

SIGRID RINGDALEN VATNE, MARINTEK
Sigrid.Ringdalen.Vatne@marintek.sintef.no

AALBORG UNIVERSITY
DENMARK

E2) Installation and sub-structures

SATH platform concept study, Carrascosa, Saitec

Methodology for risk assessment of floating wind substructures, R.Proskovics, ORE Catapult

Scaling up floating wind – investigating the potential for platform cost reductions, M.I. Kvittem, DNVGL


saitec
engineering


David Carrascosa
Head of Offshore Wind
davidcarrascosa@saitec.es
www.saitec.es


saitec


SATH®
Swinging
Around
Twin
Hull
s a t h
saitec
engineering

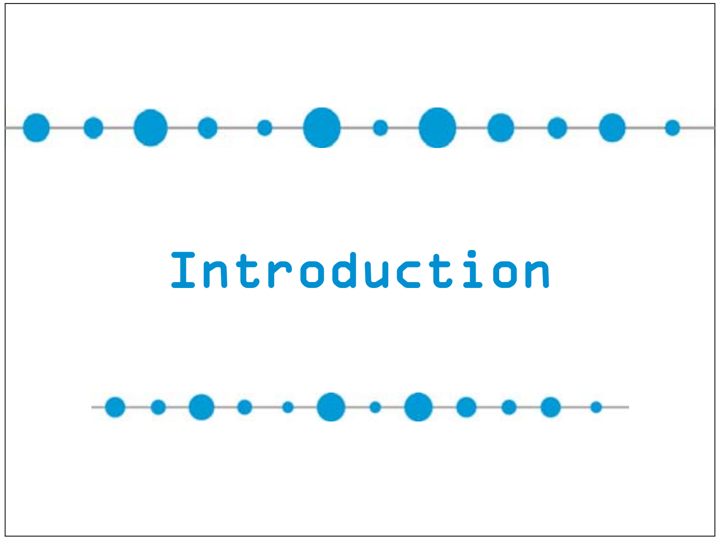
Introduction

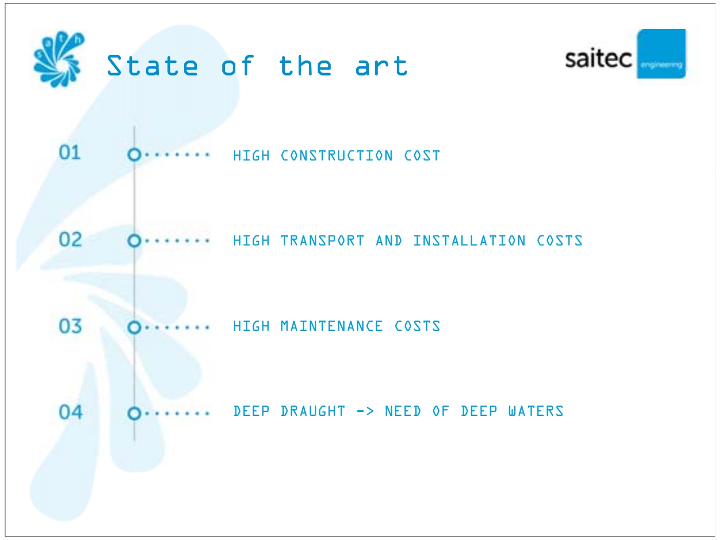
State of the art
saitec
01 HIGH CONSTRUCTION COST
02 HIGH TRANSPORT AND INSTALLATION COSTS
03 HIGH MAINTENANCE COSTS
04 DEEP DRAUGHT -> NEED OF DEEP WATERS

Challenges

saitec

- Providing a competitive solution in terms of both capital expenditures (CAPEX) and operational expenditures (OPEX).
- Providing a solution suitable for any kind of seabed whose mooring system has as low an impact on cost as possible.

Solution

saitec

HIGH CONSTRUCTION COST

Low construction cost

No maintenance cost

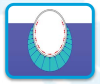

GEOMETRY OF FLOATERS: CYLINDRICAL WITH OVOIDAL CROSS-SECTION

Compression stresses

LAYOUT: TWIN HULL

Low construction cost

Concept

Platform Concept

saitec

Platform Concept

saitec

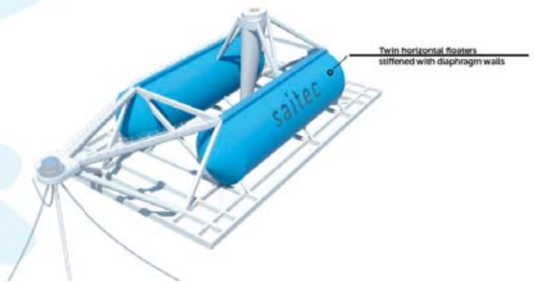

Platform Concept

saitec

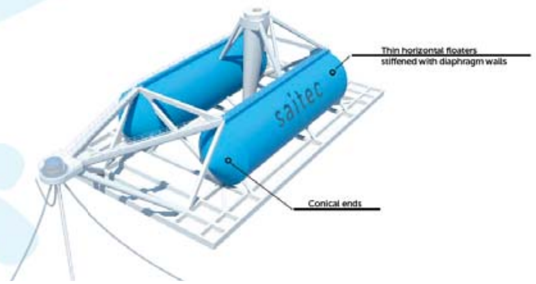

Platform Concept

saitec engineering

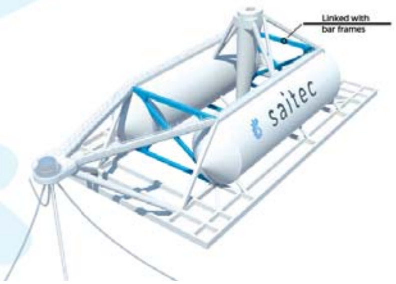

Platform Concept

saitec engineering

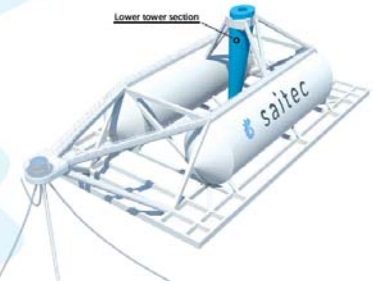

Platform Concept

saitec engineering

Platform Concept

saitec engineering

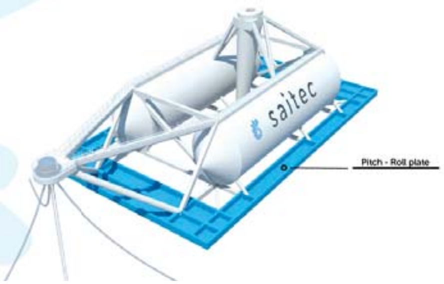

Platform Concept

saitec engineering

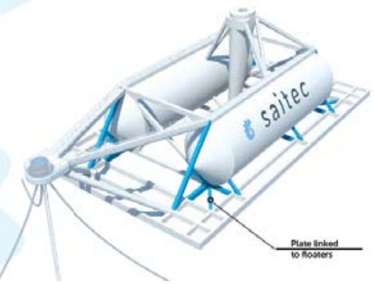

Platform Concept

saitec engineering

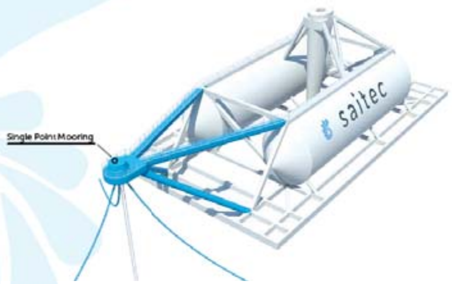

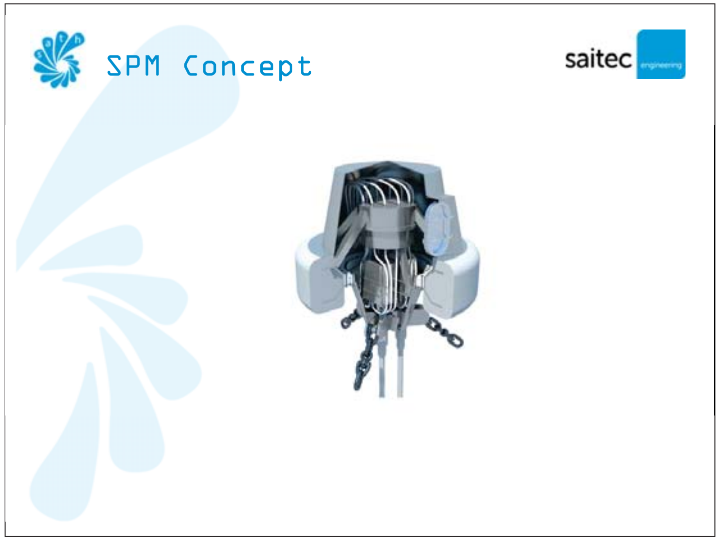
SPM Concept
saitec

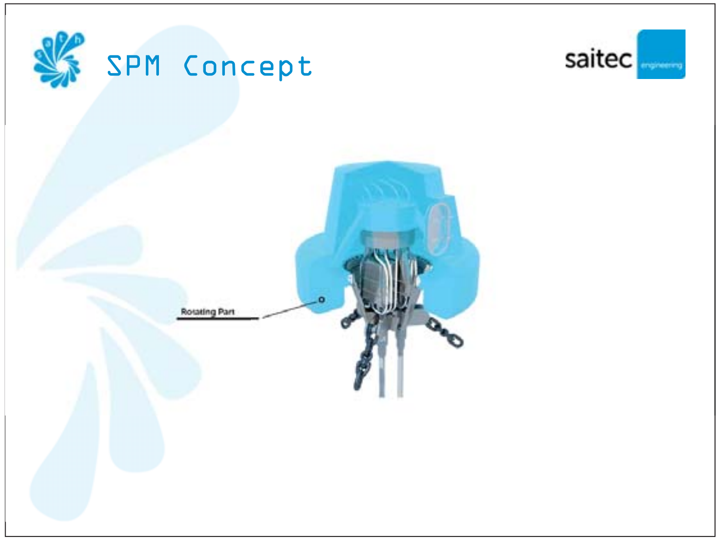
SPM Concept
saitec
Rotating Part

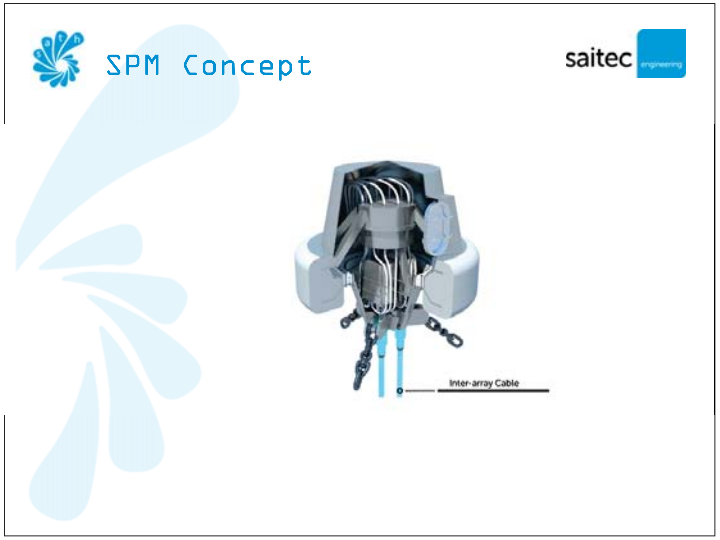
SPM Concept
saitec
Inter-array Cable

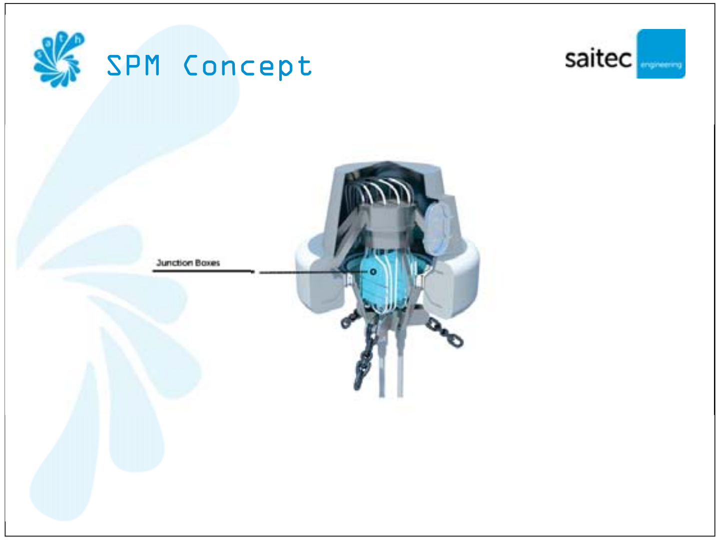
SPM Concept
saitec
Junction Boxes

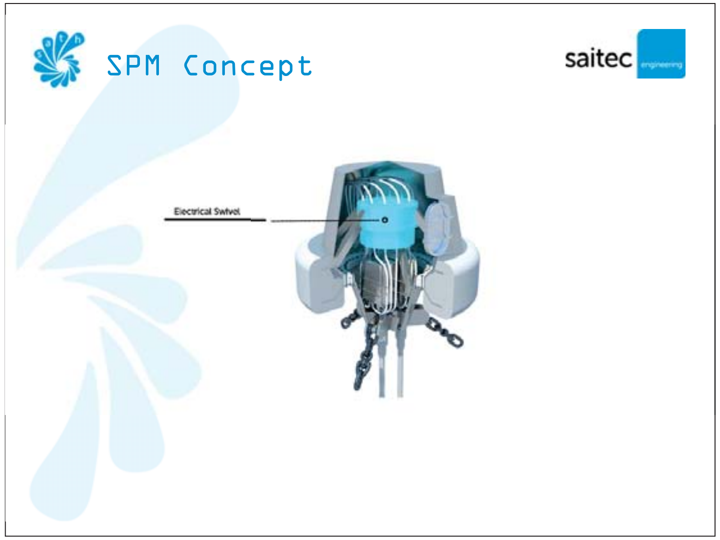
SPM Concept
saitec
Electrical Swivel

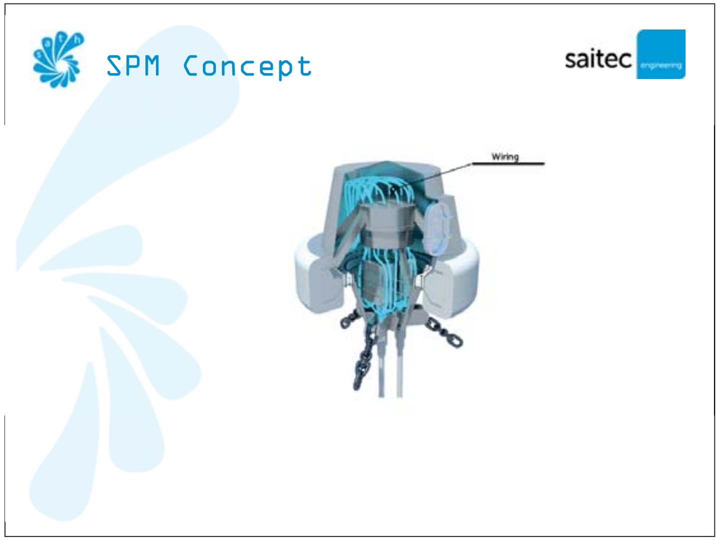
SPM Concept
saitec
Wiring

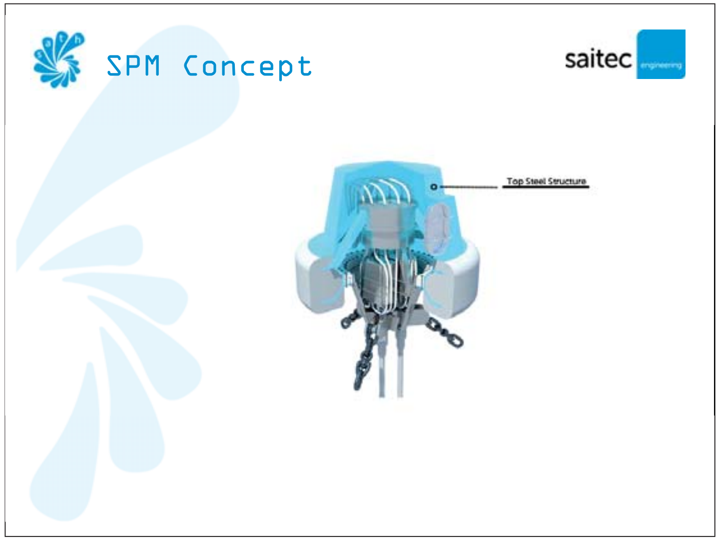
SPM Concept
saitec
Top Steel Structure

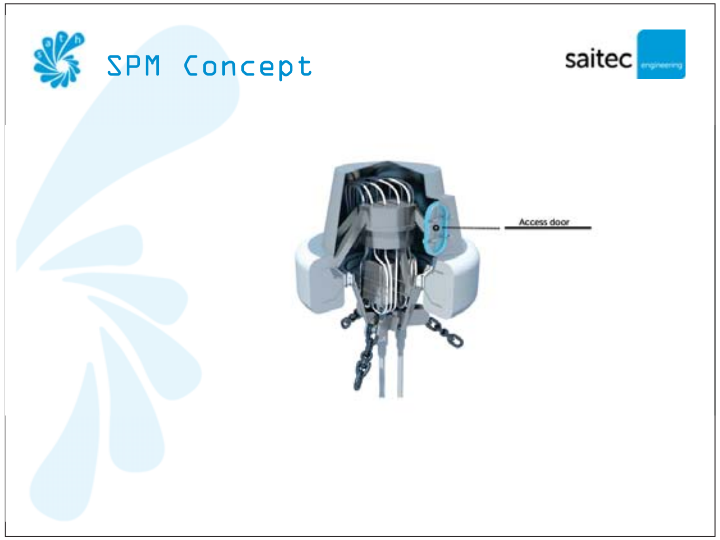
SPM Concept
saitec
Access door

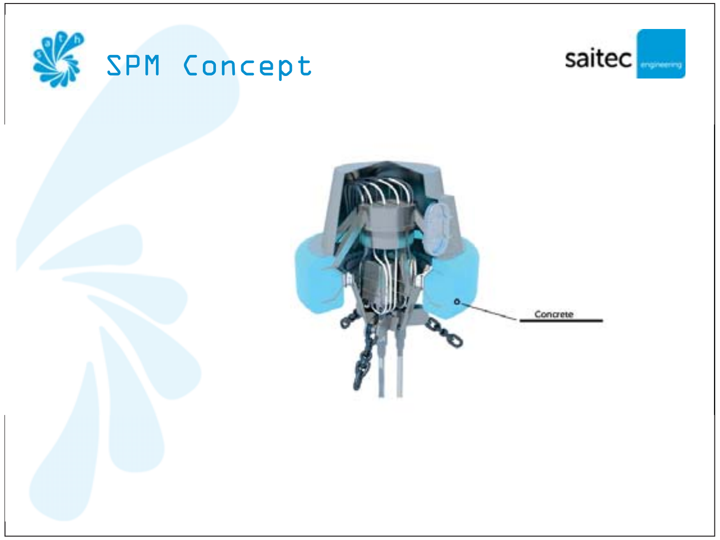
SPM Concept
saitec
Concrete

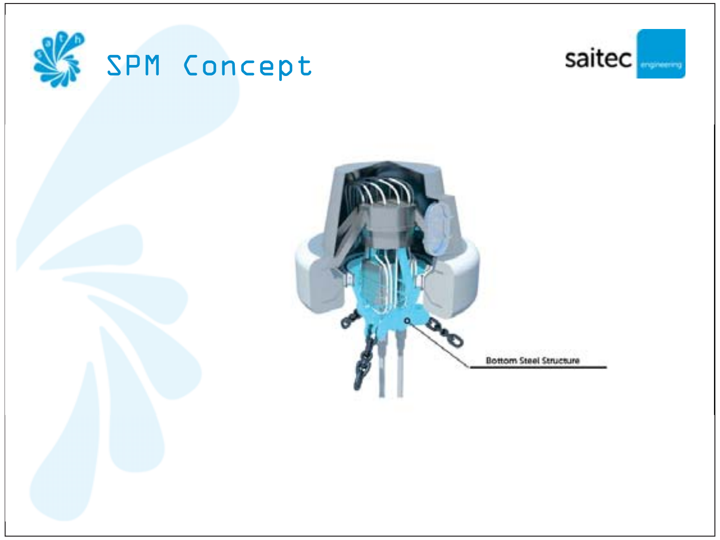
SPM Concept
saitec
Bottom Steel Structure

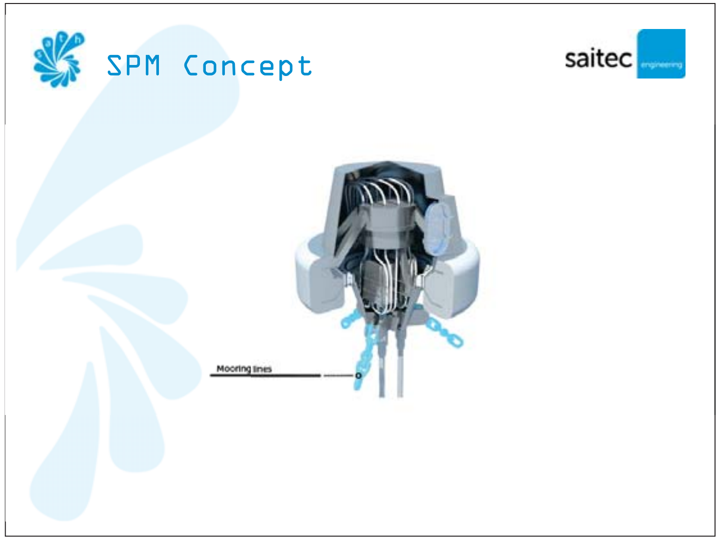
SPM Concept
saitec
Mooring lines

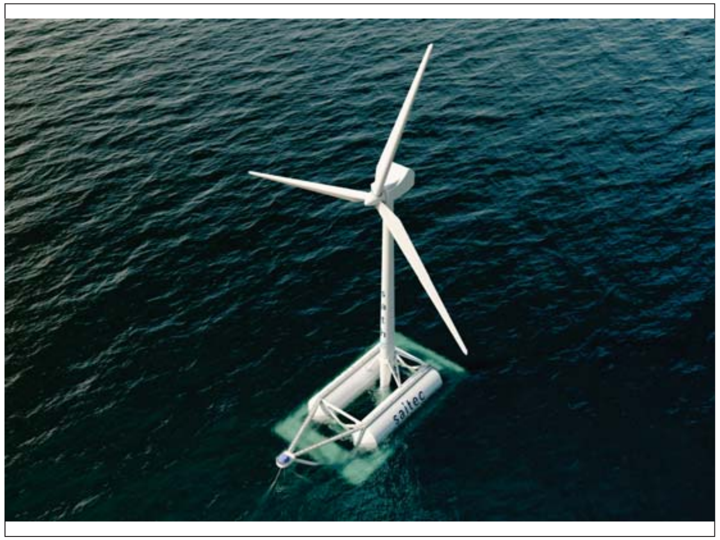

Sath design for a hawt of 5 mw

Introduction

saitec

- The design has been tailored to support a 5MW wind turbine and its performance has been proved in operational and extreme environmental conditions by numerical calculations and through intensive testing with a scale model in the water tanks at I.H. University of Cantabria.

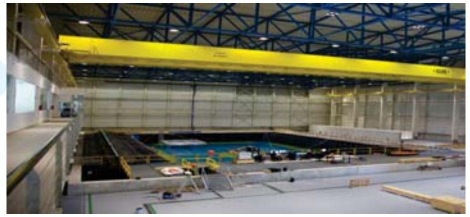

Enviromental conditions

saitec

- Operating scenario :
  - Wind velocity:
    V=3 m/s (Cut-in)
    V=11,4 m/s (Rated)
    V=25 m/s (Cut-out)
    Expected Significant Height: Hs=6,0 m.

Enviromental conditions

saitec

- Extreme scenario :
  - T=1 year
    V1 (Zhub)=40 m/s (10min)
    Ve1 (Zhub)=56 m/s (3sec)
    Hs1 =11 m (spectral significant wave)
    H1=20 m (deterministic wave)
  - T=50 year
    V50 (Zhub)=50 m/s (10min)
    Ve50 (Zhub)=70 m/s (3sec)
    Hs50 =14 m (spectral significant wave)
    H50=26 m (deterministic wave)

Basic requirements

saitec

- Stability
  The area under the ringhting moemnt curve to the second intercept or down-flooding angle,whichever is less, shall be equal to or greater than 140 % of the area under the wind heelingmoment curve to the same limiting angle.

- Maximum pitch/roll inclination (OC) ≤ 15º
- Maximum hub acceleration (OC-EC) ≤ 0,3g

Analysis Process

Analysis stages

saitec engineering

01 SOFTWARE ANALYSIS & PRE-DIMENSIONING

02 SCALE MODEL TEST

03 SOFTWARE CALIBRATION & MODEL OPTIMIZATION

Scale model testing

saitec engineering

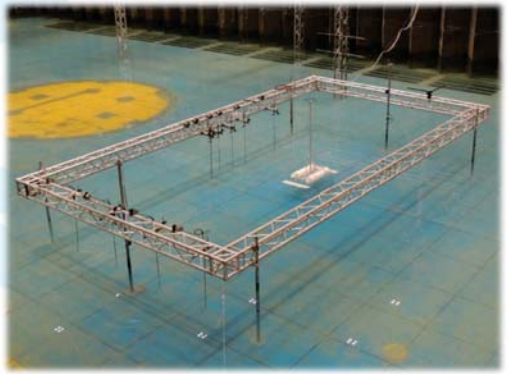

Scale model testing (Results)

saitec engineering

- Stability

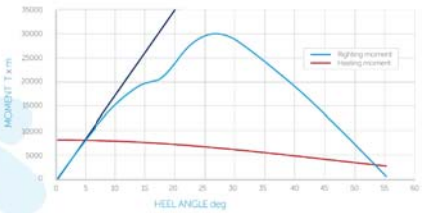

Heeling area > 334.268 T*m

Righting area > 941.215 T*m

SF > 2,82

Scale model testing (Results)

saitec engineering

- Natural Periods :

  Pitch: T=25,22 s

  Roll: T=21,94 s

  Heave: T=9,18 s

- Oscillations and Accelerations :

	Cut-in	Cut-out	Rated	Extreme
V(m/s)	3.00	25.00	11.40	50.00
Hs(m)	2.85	6.04	2.85	14.00
T(s)	6.90	17.63	6.90	17.63
Max_A(deg)	0.33	2.98	0.33	6.63
Max_a(m/s2)	0.28	1.02	0.28	2.48
Static_α(deg)	0.58	1.78	5.09	1.76

Software calibration & model optimization

saitec engineering

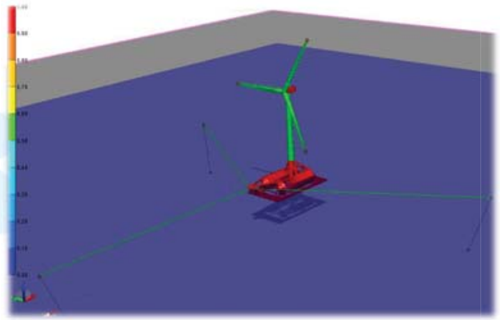

Construction

Cost analysis

Industrial production CAPEX

	INDUSTRIAL PRODUCTION	
	Cost [€/MW]	Cost [€]
Balance of the System	**1 631 790**	**8 158 952**
Development	120 000	600 000
Engineering & Management	80 000	400 000
Platform	541 254	2 706 272
Site access staging & Port	100 000	500 000
Electrical infrastructure	367 202	1 836 010
Assembly & Installation	423 334	2 116 670
Financial costs	**621 419**	**3 119 987**
Insurance	74 064	370 321
Decommissioning	111 096	555 481
Contingency	325 162	1 625 811
Construction finance	111 096	555 481
Turbine costs	**1 450 000**	**7 250 000**
TOTAL	**3 703 209**	**18 516 046**

On a 500 MW Wind Farm (50m deep) basis and 5 MW WTG

Industrial production CAPEX Sath dependent

	INDUSTRIAL PRODUCTION	
	Cost [€/MW]	Cost [€]
Development	**120 000**	**600 000**
Engineering & Management	**80 000**	**400 000**
Platform	**541 254**	**2 706 272**
Platform material & labour	231 099	1 155 496
Construction yard and	121 615	608 076
Mooring	130 390	651 950
Electrical swivel	50 000	250 000
SPM Bearing	5 000	25 000
SPM Steel Structure	3 150	15 750
Assembly & Installation	**100 158**	**500 790**
Installation of Mooring	28 158	140 790
Platform´s Transport &	72 000	360 000
TOTAL	**841 412**	**4 207 062**

On a 500 MW Wind Farm (50m deep) basis and 5 MW WTG

Offshore Wind OPEX Cost Reduction

Considering average values :

11.1 m€/year x 20 years= 222.0 m€reduction of more than 20 % OPEX

ACTIVITY	Base 5 MW Monopile (20 - 30 m) Average (€/year)	Base 5 MW SATH (40 m) Average (€/year)
Onshore logistic	778 227,49	778 227,49
Workboats	3 537 397,70	3 537 397,70
Aviation	3 183 657,93	3 183 657,93
Crane barge services	11 319 672,64	0,00
Offshore accommodation / base	21 224 386,20	21 224 386,20
Turbine maintenance	7 074 795,40	7 074 795,40
Turbine spare parts	6 367 315,86	6 367 315,86
Offshore substation maintenance	176 869,89	176 869,89
Export cable surveys and repairs	176 869,89	176 869,89
Onshore electrical	84 897,54	84 897,54
Array cable surveys and repairs	495 235,68	495 235,68
Scour and structural surveys	565 983,63	188 661,21
Foundation repairs	495 235,68	247 617,84
Lifting, climbing & safety equipment inspections	212 243,86	212 243,86
SCADA adn condition monitoring	848 975,45	848 975,45
SAP and arine co-coordination	848 975,45	848 975,45
Weather forecasting	91 972,34	91 972,34
Administration	495 235,68	495 235,68
Total Cost (€/Mw)	57 977 948,30	46 033 335,40
Cost Reduction (%)	20,60 %	

On site dependent

Source : IHS EER; Project Finance; Erneuerbare Energien; Handelsblatt; Roland Berger

SATH vs Monopile

Saitec made a comparison between a 500 MW monopile wind farm (20m depth) vs a 500 MW SATH® wind farm (40 to 50 m depth):

- CAPEX -> Overall cost reduction: 10.12 %
  -> Foundation related: 33.59 %
- OPEX -> more than 20 % cost reduction
- **LCOE -> cost reduction of about 13 %**

Conclusions

Conclusions

Saitec has developed a floating platform solution made of prestressed concrete that responds to the challenges brought :

- Low draught (<10m)
- Plug & Play solution.
- Low mooring stresses.
- Low movements and accelerations
- Reduced costs

Conclusions

- SATH is a competitive solution with offshore fixed-bottom wind turbines in shallow waters (30-40 m)
- SATH's performance has also been proved for both 8 & 10 MW wind turbines

This project has also been financed by E.E.A. Grants

Iceland Liechtenstein Norway eea grants

David Carrascosa
Head of Offshore Wind
davidcarrascosa@saitec.es

www.sath-platform.com

Methodology for Risk Assessment of Floating Wind Substructures

Roberts Proskovics, Offshore Renewable Energy Catapult

13th Deep Sea Offshore Wind R&D Conference

21st of January 2016

Qualification of innovative floating substructures for 10MW wind turbines and water depths greater than 50m

The research leading to these results has received funding from the European Union Horizon2020 programme under the agreement H2020-LCE-2014-1-640741.

Contents

- Introduction
- Risk assessment and management
- Methodology developed
  - 4 risk areas
- Conclusions

Introduction

- A Horizon2020 project – LIFES50+
  - Qualification of innovative floating substructures for 10MW wind turbines and water depths greater than 50m
  - 40 months duration
  - 7.3M€
  - 12 partners
- Work package 6 – Uncertainty and risk management
- Developed for LIFES50+, but applicable outside

Introduction

- LIFES50+ Consortium

DTU, Universität Stuttgart, MARINTEK, CATAPULT, tecnalia, DR. TECHN. OLAV OLSEN, IBERDROLA, ideol, IREC, RAMBOLL, DNV·GL

Risk Assessment and Management

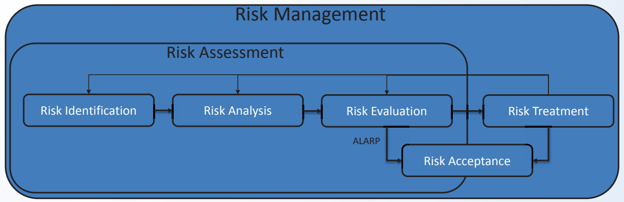

Methodology – Introduction

- Why?
  - No dedicated risk assessment methodology for floating wind
- How?
  - Risk areas considered
    - Technology
    - Health, Safety and Environment (HSE)
    - Manufacture
    - Commercialisation
  - Covers all life cycle phases
  - Based on common techniques, but updated to meet specific requirements
  - Mostly qualitative

Methodology – Technology Composition

- Floating substructure is integration of multiple element technologies
- Technology composition analysis allows for:
  - Improved understanding of the system being analysed
    - Identify its elements
    - Identify interdependencies
  - Early risk identification
- Split into
  - Functions (e.g. stability, structural integrity)
  - System and sub-systems (e.g. crew transfer system, mooring system)
  - Components/elements (e.g. anchors, transition piece)

Methodology – Technology Composition

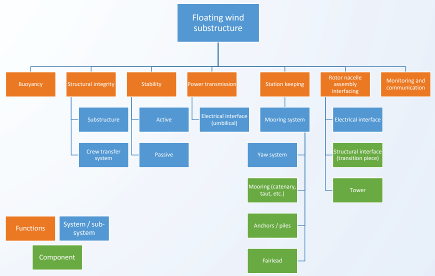

(Example functional hierarchy from LIFES50+ 'Risk Management for Deep Water Substructures')

Methodology – Technology Categorisation

- Advances in technology are generally evolutionary
- Only some elements of technology are typically novel
- Dimensions of uncertainty of technology
  - Novelty
  - Application
- Technology categorisation prioritises areas of most uncertainty/risk

Application Area	Degree of Novelty of Technology		
	Proven	Limited Field History	New or Unproven
Known	1	2	3
Limited Knowledge	2	3	4
New	3	4	4

Technology Category	Indicator
1	No new technical uncertainties (proven technology)
2	New technical uncertainties
3	New technical challenges
4	Demanding new technical challenges

(DNV GL, DNV-RP-A203 'Qualification of New Technology', July 2011.)

Methodology – HSE

- Split into
  - Health and Safety
  - Environment
- Health and Safety
  - No dedicated H&S standards for floating wind or even offshore wind
  - RenewableUK risk categories (24) + some specific FOWT categories
- Environment
  - Source-Pathway-Receptor
- 4 dimensions of risk
  - Risk to personal injury
  - Potential pollution/societal losses
  - Potential economic consequence
  - Risk to human life

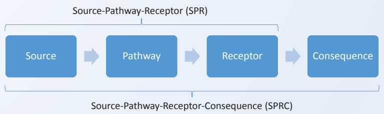

Methodology – Manufacturing

- Proposed to use Manufacturing Readiness Levels (MRLs)
  - MRLs vs TRLs
  - Manufacturing risk areas (9 threads, 22 sub-threads)
  - 3 dimensions of risk
    - Cost
    - Schedule
    - Quality
- Risk treatment
  - Manufacturing Maturation Plan (MMP)

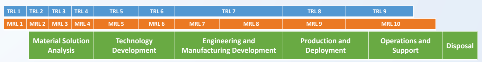

Methodology – Commercialisation

- Proposed to use Commercial Readiness Index (CRI)
  - 6 levels (hypothetical commercial proposition to bankable asset class)
  - CRI vs TRL
- Dimensions derived to judge commercial readiness:
  - 8 dimensions
  - 18 sub-categories

Methodology – Commercialisation

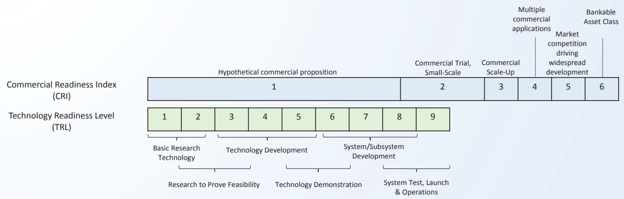

(ARENA, 'Commercial Readiness Index for Renewable Energy Sector', 2014)

Conclusion

- Developed a bespoke methodology
  - Will be tested in the following months
  - Reduce risk
  - Make FOWTs more attractive to investment
  - Reduce LCoE (main aim we all are striving for)
  - Applicable outside of floating substructures for floating wind
- D6.1 publicly available from 02/2016

Thank You!

DNV·GL

ENERGY

Scaling up floating wind

Investigating the potential for platform cost reductions

M. Kvittem, A. Steinert (TUHH), M. Ebbesen, D. Merino

21 January 2016

Ungraded

Agenda

- Introduction
- Optimisation tool
- Case studies
- Results: Costs
- Results: Optimisation
- Conclusions

Ungraded

Introduction

Ungraded

Cost Reduction for Offshore Wind

Our promise to the industry:

- Do things RIGHT
- Do things BETTER
- Do things DIFFERENTLY
- "DNV GL is committed to help drive the commercialisation of floating wind power technology"

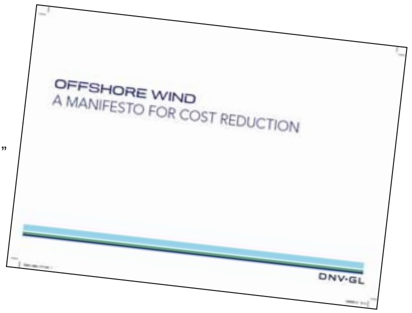

Ungraded

Technically ready does not mean it's commercial

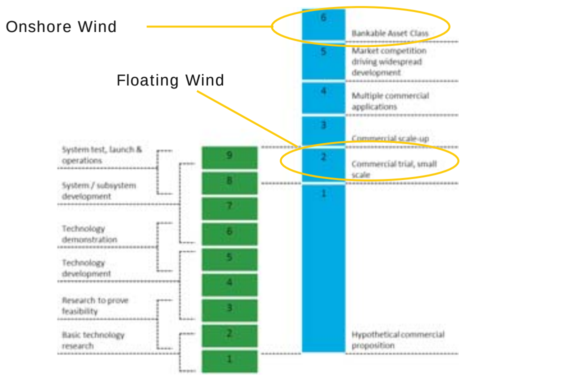

Source: http://arena.gov.au/files/2014/02/Commercial-Readiness-Index.pdf

Ungraded

Optimisation tool

Ungraded

Motivation

- What are the cost drivers for floating wind turbines?
- How does a platform scale with larger turbines?
- What is the impact of various turbine parameters on the platform design?
  - Tower top mass
  - Maximum thrust force
  - Hub height
- How to change the geometry of the platform to obtain a cost-optimized structure?

Semi-submersible optimisation

- Iterates through a large space of variables:
  - Column diameter
  - Column spacing
  - Draught
  - Heave plate size
- Constraints for the design:
  - Surge, heave and pitch periods
  - Maximum static tilt in operation
  - Maximum dynamic tilt in survival
  - Maximum tower base bending moment
  - Nacelle acceleration
- Cost rates per steel mass unit based on type of structural element



Optimisation tool

- Developed in collaboration with master student Alexander Steinert
- Optimisation with respect to unit cost
- Parameter influences
- Turbine rating influence

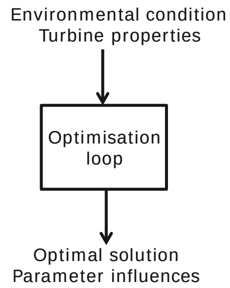

Particle Swarm Optimisation (PSO)

- Find: Optimal solution (✖)
  - Minimise cost (objective function)
  - Satisfy design criteria (constraints)
- Stochastic process
- 1 swarm particle = 1 Platform

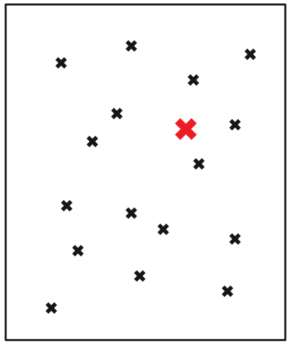

Current limitations

- Currently only tested for a semi-submersible type floater
- Linear or linearized theory
- Limited structural check
- No fatigue limit state

Case studies

Scaling up platforms for 10 and 20 MW turbines

- Extreme wind speed: 50 m/s
- 50 year significant wave height: 18 m

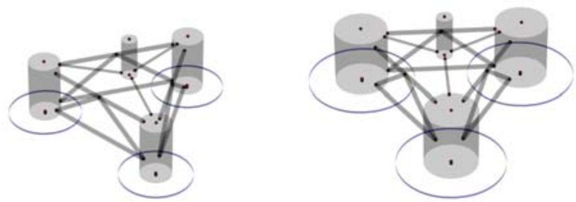

Ungraded

Platform optimisation for different turbines

	NREL	FORCE	DTU
Rating	5 MW	7 MW	10 MW

Environmental Condition

- 50-year event
- Location: West of Norway
  - $H_s = 10.96\,m$
  - $T_p = 11.06\,s$
  - $U_{10} = 39.49\,\frac{m}{s}$

Turbines

- Adapted for floating support structure
  - Reinforced tower base
- Scaled thrust force, based on NREL turbine using rotor swept area

Ungraded

Results: Cost

Ungraded

Support structure cost

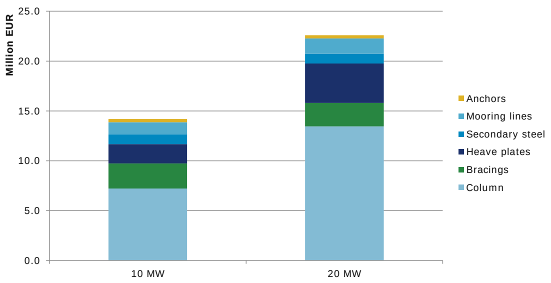

- 60% increase in cost from 10 to 20 MW.

Ungraded

Cost development

Steinert, 2015, Master thesis TUHH

With slenderness ratio **Without slenderness ratio**

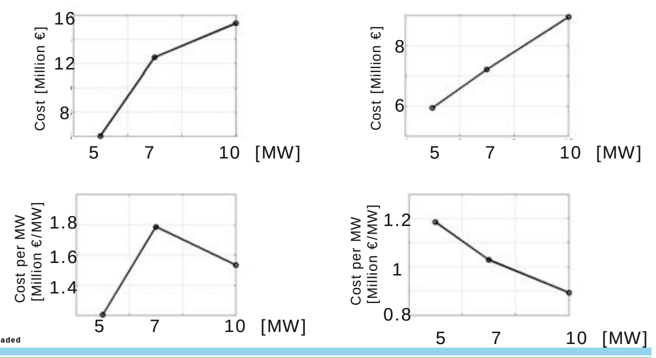

Ungraded

Results: Optimisation

Ungraded

Optimisation progression

Steinert, 2015, Master thesis TUHH

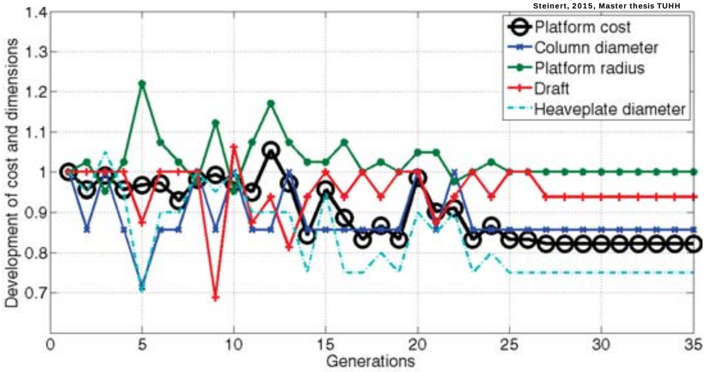

Ungraded

Resulting optimal solutions

Steinert, 2015, Master thesis TUHH

	NREL 5 MW	FORCE 7 MW	DTU 10 MW
Column diameter [m] (D_C)	6	9	11
Heave plate diameter [m] (D_{HP})	15	22	25
Draft [m]	15	22	29
Platform radius [m] (R)	41	60	62
$\mathbf{D_{HP}/D_C}$	2.5	2.4	2.3
$\mathbf{R/D_C}$	6.8	6.7	5.6

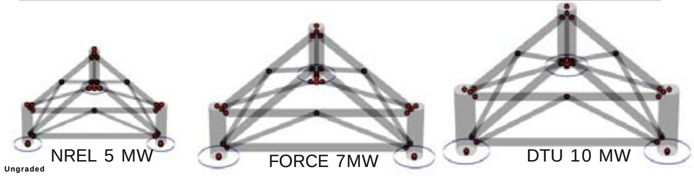

Ungraded

Conclusions

Ungraded

Observations

- Numerical optimisation is a useful tool for initial assessments
- Column spacing prevailing parameter
- Sensitive to structural component type prices
- Structural design should be included in the optimisation loop
- Will the cost per MW go down with increasing turbine size?

Ungraded

Ungraded

Email:
marit.irene.kvittem@dnvgl.com

www.dnvgl.com

SAFER, SMARTER, GREENER

Ungraded

F) Wind farm optimization

A parametric investigation into the effect of low induction rotor (LIR) wind turbines on the LCoE of a 1GW offshore wind farm in a North Sea wind climate, G. Scheepers, ECN Wind Energy

ProdBase: Theoretical power production in the time domain using Wind Farm Simulator, M.S. Grønsleth, Kjeller Vindteknikk

A continuously differentiable turbine layout optimization model for offshore wind farms, A. Klein, UiB

Experimental testing of axial induction based control strategies for wind farm power optimization, J. Bartl, NTNU

EUROPEAN MASTER in RENEWABLE ENERGY
Coordinated by EUREC

ECN Your energy. Our passion.

An investigation into the effect of low induction rotors on the levelised cost of electricity for a 1GW offshore wind farm

Rory Quinn, Bernard Bulder, Gerard Schepers
EERA DeepWind Conference
Trondheim 22nd Jan 2016

www.ecn.nl

ECN

List of Contents

ECN

Goal:

To optimise the LCOE of Low Induction Rotors versus Conventional Rotors for a 1GW off-shore wind farm with different values of Wind Farm Power Density using state of the art wake modelling, electrical modelling and cost modelling

ECN

List of Contents

ECN

Introduction

Classical Approach versus Low Induction

- Power Coefficient flat around Betz maximum (a = 1/3)

$$C_P = \frac{P}{\frac{1}{2}\rho A U_\infty^{\ 3}} = 4a(1-a)^2$$

- Aerodynamic load coefficient strongly dependant on a

$$C_{D.ax} = \frac{D.ax}{\frac{1}{2}\rho A U_\infty^{\ 2}} = 4a(1-a)$$

- Increase diameter→ maintain aerodynamic loads→ increase power

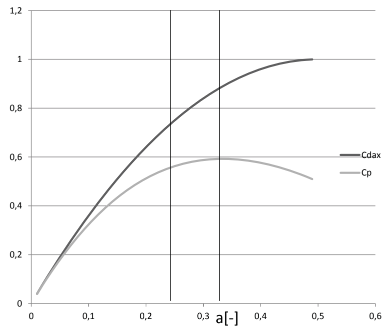

ECN

Introduction

Low Induction Rotors

- Low induction Rotors (LIR's) are sometimes seen as an option to reduce LCOE
- Literature finds justification for LIR's for isolated operation, e.g. [1])
- Wake effects are known to depend on C_{Dax} (induction)
- LIR's are expected to reduce the wake effects

[1]) Chaviaropoulos, Beurskens & Voutsinas 2013

Introduction
No clear trend on Wind Farm Power Density (WFPD)

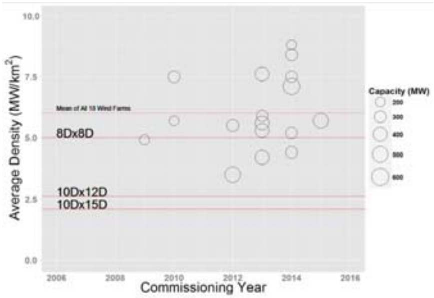

List of Contents

- Goal
- Context
  - Low Induction Rotors (LIR's)
  - Wind Farm Power Density
- *Methodology*
  - Target wind farm
  - Target turbines
  - Modelling: Wake effects, electrical infrastructure, turbine costs
- Results

Methodology
The Approach

- Theoretical 1GW wind farm (10x10 grid)
- Range of Turbine Spacings
  - Fixed spacing ratios (PWD/CWD)
  - Range of CWDs

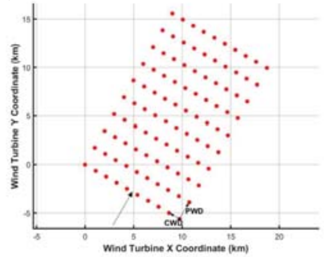

Methodology
The Approach

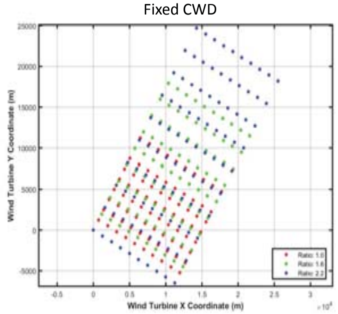

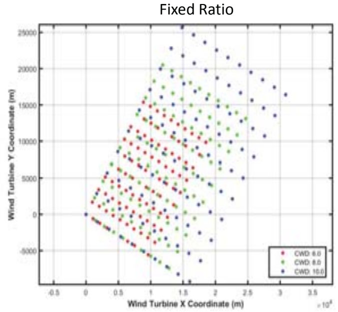

Methodology
The Approach

- Theoretical 1GW wind farm (10x10 grid)
- Range of Turbine Spacings
  - Fixed spacing ratios (PWD/CWD)
  - Range of CWDs
- Either conventional or LIR turbines

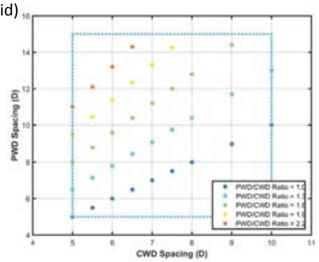

INNWIND.EU and AVATAR RWT *)

	INNWIND.EU	AVATAR
Power:	10 MW	10 MW
Rotor diameter:	178.3m	205.8m
WTPD:	400 W/m²	300 W/m²
Axial induction:	0.3	0.24
RPM→ Tip speed	9.8rpm→ 90m/s	9.8 rpm→ 103.4 m/s
Hub height:	119m	132.7m

www.innwind.eu and http://www.eera-avatar.eu/

AVATAR RWT vs. INNWIND.EU RWT

http://www.eera-avatar.eu/publications-results-and-links/

- 5% Increase in energy production due to larger diameter
- Key rotor load levels are maintained but:
  - Non-rotor loads and mass slightly exceeded
  - Use of carbon fibre
  - →
  - Does increased AEP compensate increased costs?

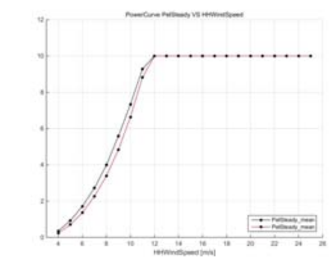

Methodology
The Approach

- Theoretical 1GW wind farm (10x10 grid)
- Range of Turbine Spacings
  - Fixed spacing ratios (PWD/CWD)
  - Range of CWDs
- Either conventional or LIR turbines
- Typical North Sea wind climate

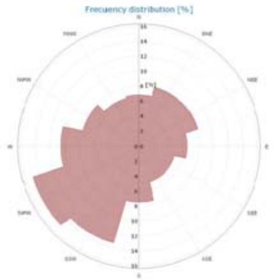

Methodology
Process

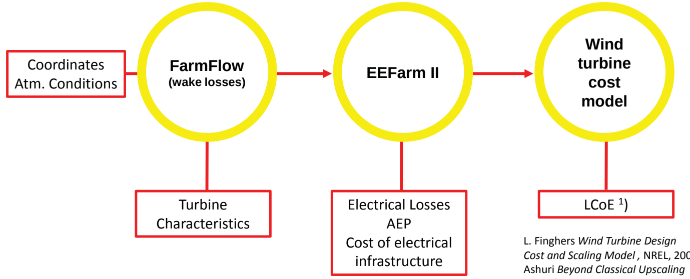

L. Finghers *Wind Turbine Design Cost and Scaling Model*, NREL, 2006
Ashuri *Beyond Classical Upscaling* TUDelft 2014

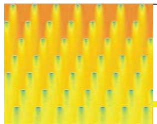
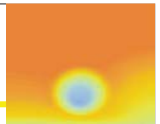

What is FARMFLOW?

- Calculates:
  - Losses and added turbulence due to wakes
  - Annual energy production (AEP)
- The model is based on UPMWAKE [1])/WAKEFARM/FARMFLOW
  - Modified by ECN since 1993
  - Extensively validated with results from ECN's research farms and measurements from EU projects (e.g. ENDOW, Upwind, EERA-DTOC)

[1]) Crespo et al. 1988

FARMFLOW: Theory and model description

- Solves the Parabolized Navier-Stokes equation
- Turbines modelled as actuator disc, prescribed by C_{Dax}
- Wake modelled with a k-ε turbulence model

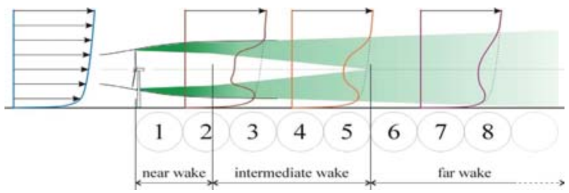

FARMFLOW: Advanced Model

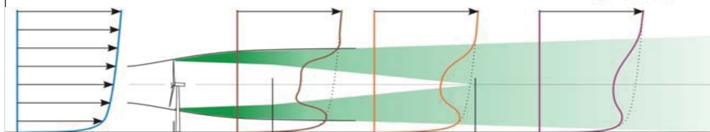

- Parabolisation: Fast, but how to solve the near wake where axial pressure gradients are significant?
- Solution:
  - Prescribe axial pressure gradients from free vortex wake method!
  - Fast database approach
- Adjusted k-ε turbulence model parameters in near wake based on:
  - Measurements from ECN's research farms and Horns Rev farm
  - Detailed wake measurements in TUDelft wind tunnel

ECN

What is EEFARM?

- Program to study and optimise the electrical performance of wind farms.
- Program is used to determine the:
  - Energy production,
  - Electrical losses,
  - Component failure losses
  - Price of the produced electric power

ECN

EeFarm-II linked to FarmFlow!

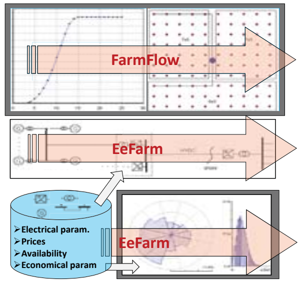

Aerodynamic power:
$P_{WT1} \ldots P_{WTN} = f(Vw, Vdir)$

Investments
P_{loss}
P_{fail}
per component

LCOE

ECN

List of Contents

- Goal
- Context
  - Low Induction Rotors
  - Wind Farm Power Density
- Methodology
  - Target turbines
  - Target wind farm
  - Modelling: Wake effects, electrical effects, costs
- *Results*

ECN

Results

Capacity Factor

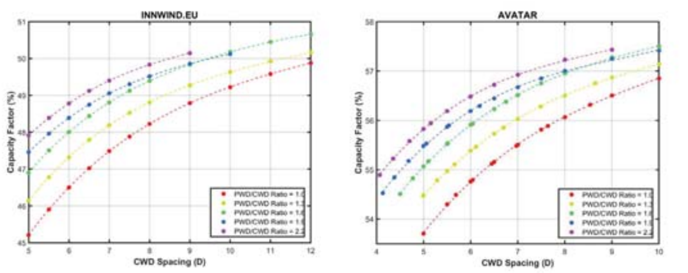

ECN

Results

Power Performance (7Dx11.2D)

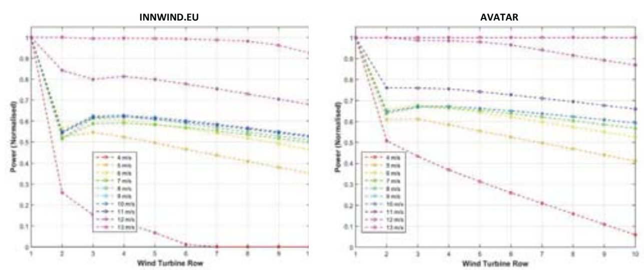

ECN

Results

LCoE

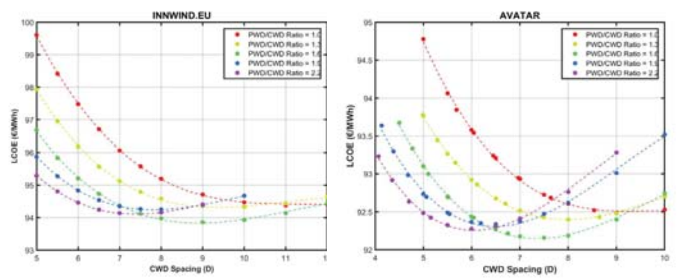

Results

LCoE

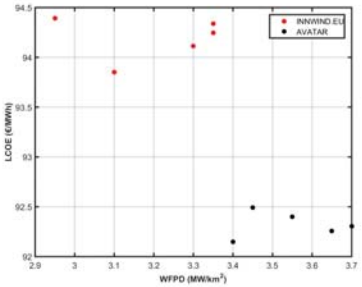

Conclusions

- LIR could offer a lower LCoE than conventional turbines
  - Sensitive to cost model
  - Sensitive to atmospheric conditions
  - How representative is AVATAR LIR?
- LIR requires less area than conventional turbine for optimum LCoE
  - Indicates LIR turbines offer more efficient use of sea area
- Alternative layouts (not in presentation, but in paper)
  - Staggered offered no improvement
  - Aligned offered marginal cost reduction

Questions?

ProdBase

Theoretical power production in the time domain using Wind Farm Simulator

Martin S. Grønsleth, PhD
Kjeller Vindteknikk AS (KVT)

Co-authors: Ove Undheim, Øyvind Byrkjedal, Finn Nyhammer (KVT) and Erik Berge (Civitas)

EERA DeepWind'2016, Trondheim
2016-01-22

Outline

- What is ProdBase?
- What is Wind Farm Simulator (WFS)?
- Examples/results
- Possibilities

KVT ProdBase

- **ProdBase** is an interactive web interface
- Presentation of up-to-date wind farm conditions
  - Actual production
  - Estimated / potential / theoretical production
  - Wind speed/direction
- Monitor wind farm health, statistics, *uncover problems early*
- Presented visually (graphs) + data (time series) for download
- *In operational use for 11 wind farms, including offshore*

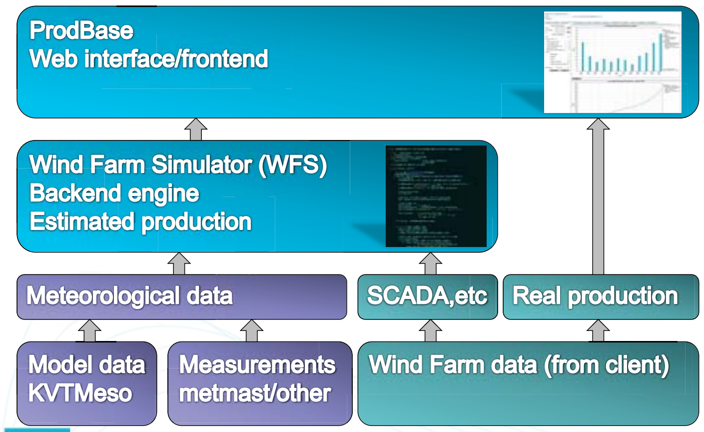

Wind Farm Simulator (WFS)

- Developed by Statkraft, UiO and Kjeller Vindteknikk
- Simulates meteorological conditions at individual turbines
- Driven by measured data or model data (KVT Meso) (or both)
- Estimate production each time step
- Modules for
  - Wake effects (N. O. Jensen (NOJ), Dynamic Wake Meandering (DWM))
  - Fine scale transfer coefficients between reference point, turbine positions
  - Air density correction
  - High wind hysteresis
  - Rotor equivalent wind speed, REWS (Gryning wind profile)
  - IceLoss (icing conditions, optionally for individual turbines)
  - SCADA data interpreter
  - Downrating/curtailment of individual turbines
  - WFS v1.0 released 2014.

Statkraft Forskningsrådet

REWS: Rotor Equivalent Wind Speed

- Take into account wind shear / wind profile when calculating power output of turbine
- REWS to be included in IEC 61400-12-1. *Definition, Wagner et al. (2014)*

$$U_{eq} = \left(\sum_{i=1}^{N_h} U_i^3 \frac{A_i}{A}\right)^{1/3}$$

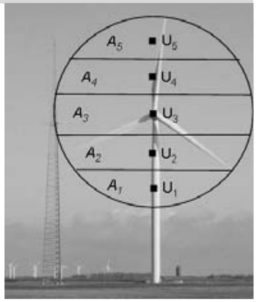

From Ioannis et al. 2013.

- In **Wind Farm Simulator** (**WFS**):
  - Gryning profile (Gryning et al. (2007))
  - For each individual turbine, each time step:
    - Estimate profile
    - Compute REWS
  - Use calculated REWS in wake and power calculations

Theoretical production: Wind Farm Simulator

- Model data as input
  - Wind speed, wind direction, Turbulence Intensity (TI), +++
- Density correction (each timestep), correct use of power curve
- Scaling free wind at each turbine (WAsP; 12 or 36 sectors)
- REWS (Rotor Equivalent Wind Speed), account for wind shear.
- Wake model, loop all turbines downwind, each time step
- Time dependent IceLoss, scaled to match target percentage
- Production at individual turbines *(only the grand total is presented currently)*
- *Scale model wind speed so target AEP (Annual Energy Production) is reached, iteration for reference period (14 years).*

KJELLER

ProdBase

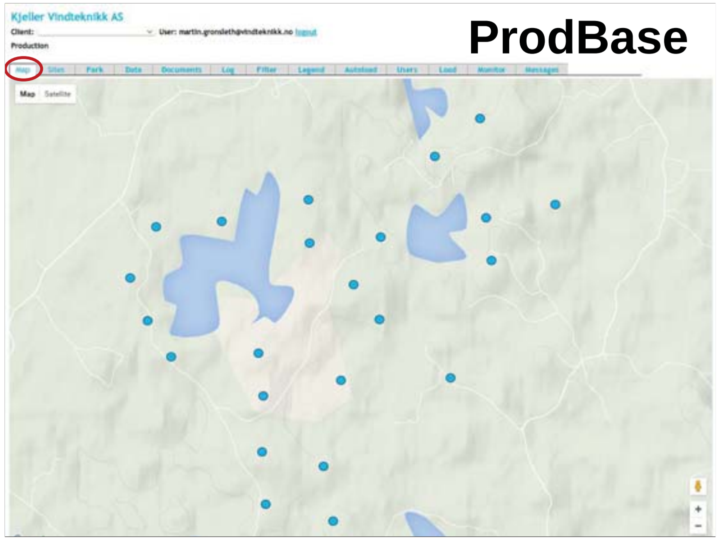

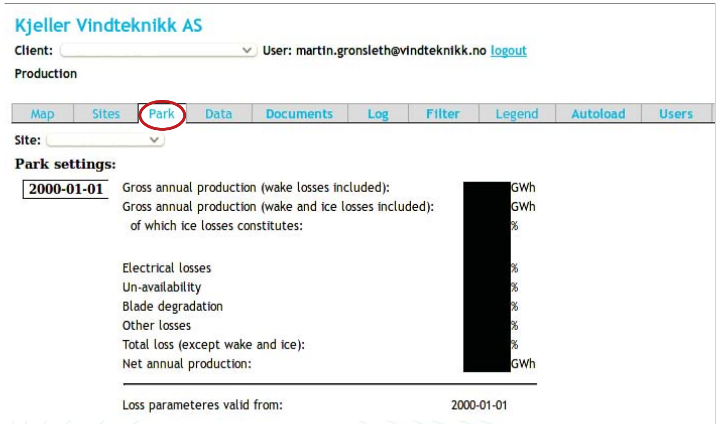

KJELLER

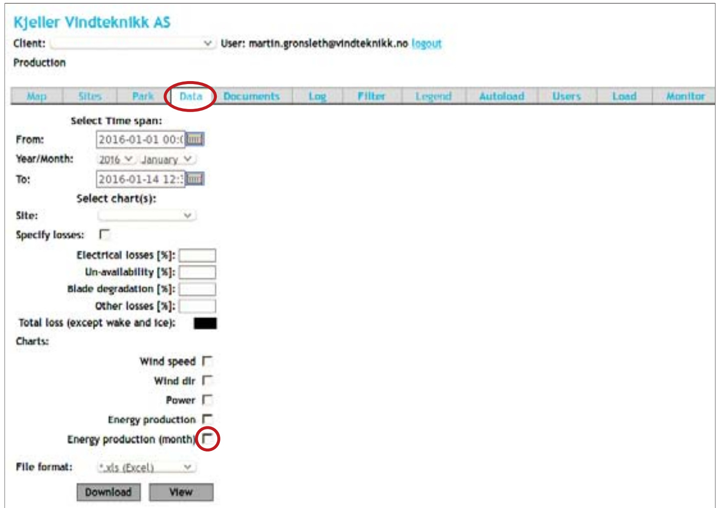

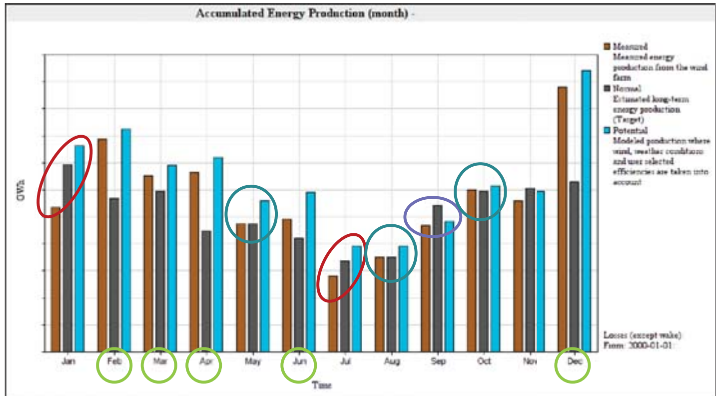

1. Underperformance (icing/maintenance/other?)
2. Performance as normal year, OK?
3. Overperformance? No
4. Problems? No!

KJELLER

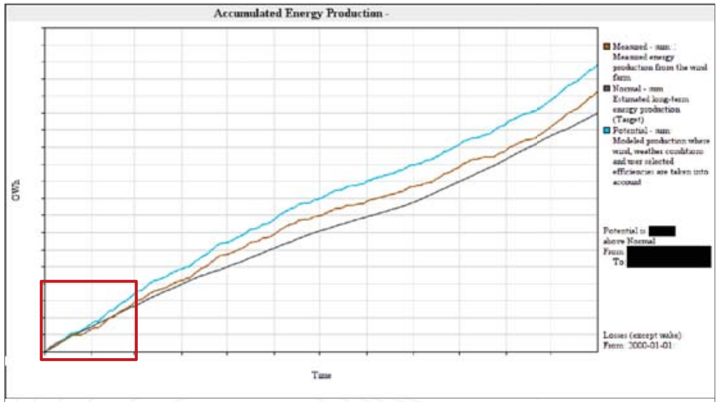

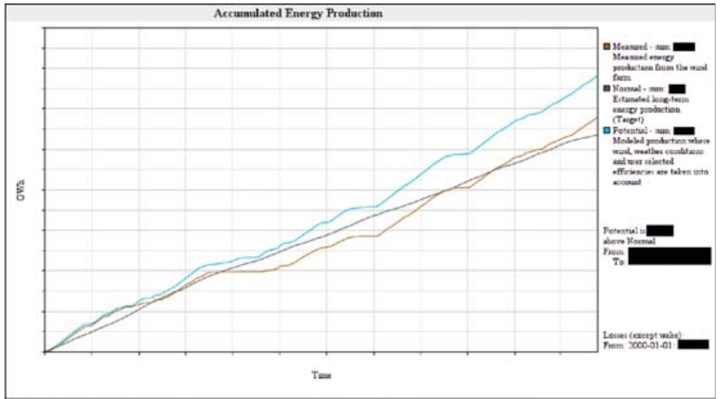

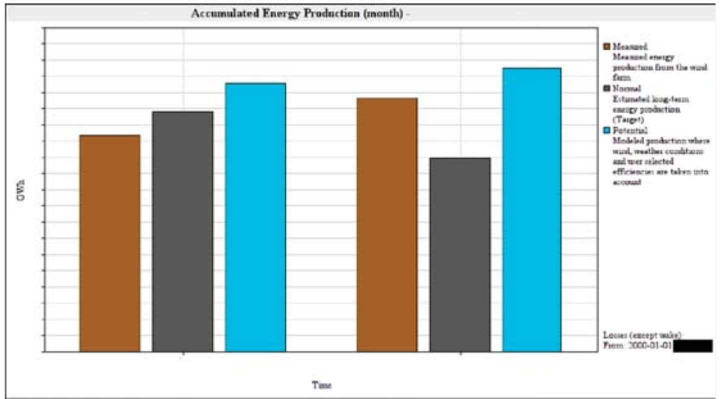

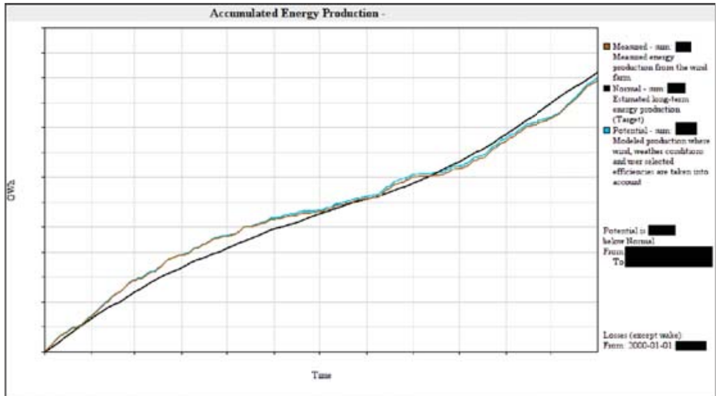

- Offshore farm, Year A
- Real production <1 % under potential / theoretical production

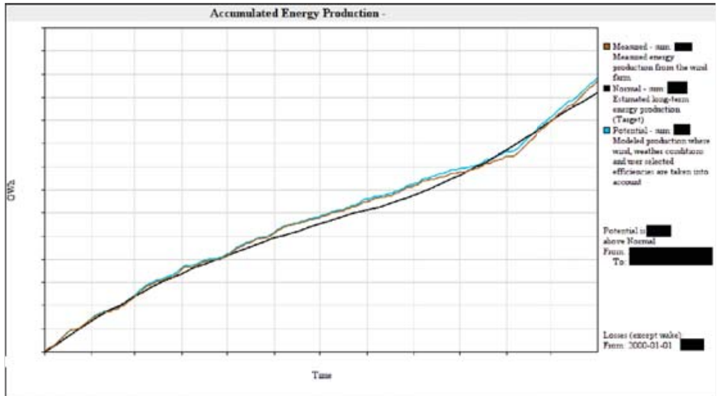

- Offshore farm, Year B
- Real production ~1% under potential / theoretical production

OLD Method (park power curve)

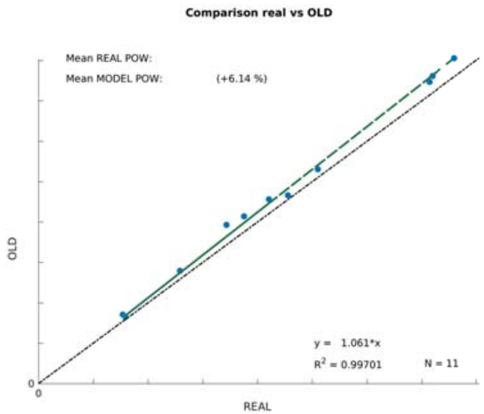

WFS without Rotor Equiv. Wind Speed (REWS)

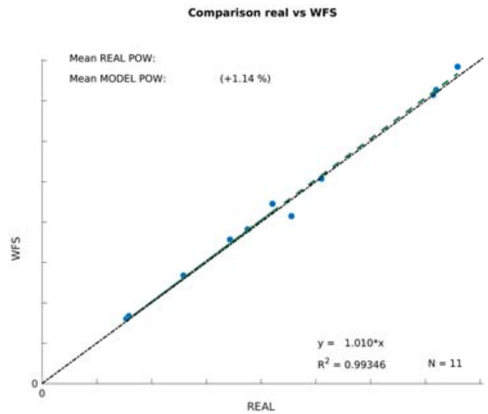

WFS with Rotor Equiv. Wind Speed (REWS)

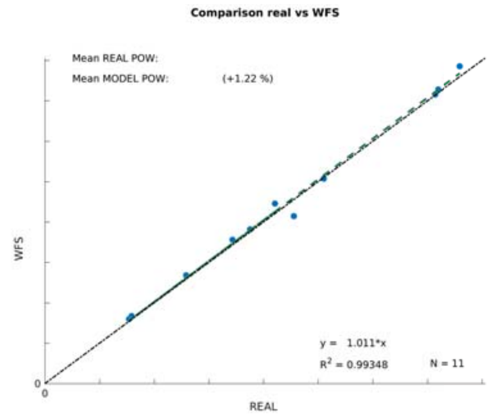

Effect of Rotor Equiv. Wind Speed (REWS) on potential production Offshore

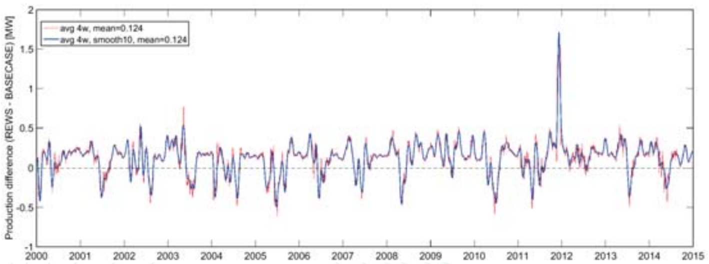

Possibilities with WFS and ProdBase

- Currently only historical, total production presented in ProdBase

Future:

- Present data from individual turbines
- Forecast of power production
  - Next hour(s)
  - Next day(s)
- Optimize operation <- simulate scenarios
- Maintenance planning. Minimize loss during downtime.
- Include observations within wind farm as input to WFS
- Take operational status into account (*SCADA*)
- Use individual power curves, conditional curtailment
- Extend ProdBase to other platforms, mobile, app.
- More…

KJELLER VINDTEKNIKK

Thank you!

Martin S. Grønsleth

martin.gronsleth@vindteknikk.no

Example on results from Gryning et al. (2007):

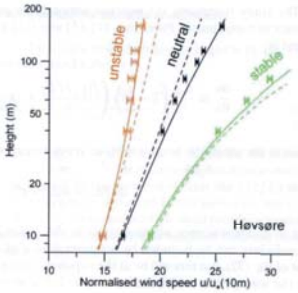

Fig. 7 Comparison between surface layer theory with Monin-Obukhov scaling for the stability according to Dyer (1974) (dashed lines) and the wind profile expressions suggested here (full lines). The stability ranges of L are: unstable (−50 to −100 m), neutral (−500 to 500 m) and stable (50 to 200 m). Measurements from Høvsøre site are shown by symbols and bars indicate the standard deviation of the mean wind speed. The values of L and z_0 that are used in the wind profile calculations are given in Table 3, and those of z_i in Table 2

A continuously differentiable turbine layout optimization model for offshore wind farms

Arne Klein
Supervisor: Dag Haugland
Collaboration: Mario Mommer, Modellierung und Systemoptimierung Mommer GmbH

Department of Informatics, University of Bergen, Norway

EERA DeepWind 2016, January 22, 2016

www.uib.no

Wind farm layout design / turbine micro-siting

- Layout problem
- Optimal placement of turbines within an offshore wind farm
- Wind slows down behind (in the “wake” of) a wind turbine
- Other turbines in the wake experience lower wind speeds and thus produce less power

www.uib.no

Outline

- Problem definition
- Optimization model
- Preliminary experimental results
- Open problems

www.uib.no

Problem definition

Aim

- Model suitable for gradient based optimization methods
- Maximize power production
- Investigate model with different wind data

Approach

- Set up of optimization model
  - continuous variables
  - differentiable
  - non-convex
- Computations with wind data of real wind farm sites

www.uib.no

Wind turbine locations

- Given parameters
  - Number of turbines
  - Allowed convex area for turbine placement
  - Wind rose
  - Turbine parameters
- Set of turbines T with Turbine locations as independent decision variables $r_t = \begin{pmatrix} x_t \\ y_t \end{pmatrix} \in \mathbb{R}^2$, $t \in T$
- All turbine locations have the same polyhedral constraint

$$Ar_t \leq b \quad \forall t \in T$$

www.uib.no

Wind information

- Wind rose
- Discretized set W of wind data, $w \in W$
  - undisturbed wind velocity v_w
  - direction ϕ_w
  - frequency of occurrence f_w

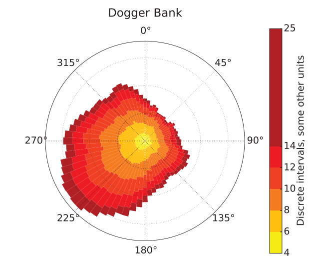

www.uib.no

Basis for wake model

- Calculates wind velocity deficit in wake of a turbine
- Based on widely used Jensen wake model (Jensen 1986)
  - only defined in wake of turbine
  - non-differentiable
- Extension by Haugland (2012), Park and Law (2015)
- Differentiable in lateral direction by application of Gauss function
- Still non-smooth in downstream direction

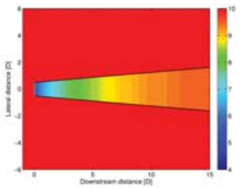

(Credit: Renkema 2007)

Extension of wake model

- Application of an approximation of the Heaviside step function in downstream direction
- Wake function g continuously differentiable on $\mathbb{R}^2$
- g_{ijw} velocity deficit from turbine $i \in T$ on turbine $j \in T$ for wind vector $w \in W$
  - d_{ijw} downwind and s_{ijw} normal to wind projection of distance

$$g_{ijw} = \frac{\frac{2}{3}\left(\frac{R}{R+\kappa d_{ijw}}\right)^2 \exp\left(-\left(\frac{s_{ijw}}{R+\kappa d_{ijw}}\right)^2\right)}{1+\exp\left(-1.75\left(\frac{d_{ijw}}{R}+1.7\right)\right)}$$

Extension of wake model II

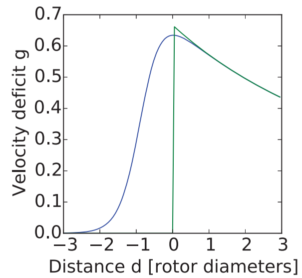

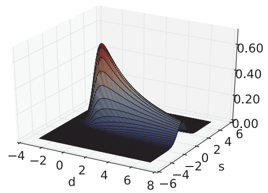

Left: Jensen (green) and our model (blue) on $s = 0$.
Right: Visualization of model in 3d

Wake combination model

- Effective wind velocity u_{tw} for a turbine $t \in T$ with undisturbed wind vector v_w, $w \in W$.
- Combination of all wake deficits for a given wind vector

$$u_{tw} = v_w\left(1 - \sqrt{\sum_{k\in T, k\neq t}(g_{ktw})^2}\right)$$

Power curve

- Power production of turbine as function of wind velocity
- Characteristic of turbine
- Rated power P^{rated} and wind speed u^{rated}, cut-in wind speed $u^{\text{cut-in}}$, cut-off wind speed $u^{\text{cut-off}}$

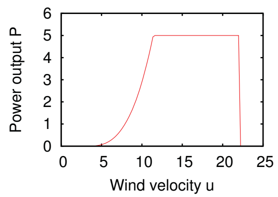

$$C(u) = \begin{cases} 0 & \text{if } u < u^{\text{cut-in}} \\ a(u - u^{\text{cut-in}})^3 & \text{if } u^{\text{cut-in}} \le u < u^{\text{rated}} \\ P^{\text{rated}} & \text{if } u^{\text{rated}} \le u < u^{\text{cut-off}} \\ 0 & \text{if } u^{\text{cut-off}} \le u \end{cases}$$

Power curve

- Remove wind velocities above $u^{\text{cut-off}}$ and below $u^{\text{cut-in}}$ from set W
- Add additional constraints to remove non-differentiable function
- For each turbine $t \in T$ and wind vector $w \in W$

$$P_{tw} \le \begin{cases} 0 & \text{if } u_{tw} \le u^{cut-in} \\ (u_{tw} - u^{cut-in})^3 & \text{if } u_{tw} \ge u^{cut-in} \end{cases}$$

$$P_{tw} \le P^{\text{rated}}$$

Total power production

- Objective function is total power production
- Sum over turbines and wind vectors, weighted with frequencies

$$\max \sum_{w \in W} \left(f_w \sum_{t \in T} P_{tw} \right)$$

Solution method

- Model formulated in AMPL
- Solver Ipopt (Interior Point OPTimizer)
- Multistart with grid and random initial turbine locations
- Computations on Intel Xeon E5-2699, 72 logical cores, 256 GB Ram
  - Each optimization runs on a single core, parallel computations possible

Wind data

- Simulated wind data from 07/1999 to 12/2009
  - Lorenz and Barstad, 2015 (Uni Research, NORCOWE)
- 5-10 minute time resolution
- Aggregated in $2m/s$ and $1°$ and $5°$ bins
- Locations
  - Dogger Bank
  - Dudgeon
  - Greater Gabbard
  - Gunfleet Sands
  - Horns Rev
  - Race Bank
  - Sheringham Shoal

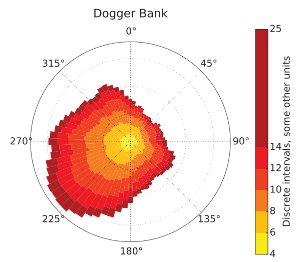

Data for experiments

- Reference 5MW wind turbine (Jonkman 2009, NREL)
  - $u^{cut-in} = 3m/s$
  - $u^{rated} = 11.4m/s$
  - $u^{cut-off} = 25m/s$
  - $P^{rated} = 5MW$
- 9, 16, 25 turbines with rotor diameter $D = 126m$
- Minimal turbine spacing $3D$
- Grid turbine spacing $5D$ to $20D$

Preliminary experimental results

- Quadratic farm boundaries
  - grid layout is within 0.5% to optimum for wind data of all farms, for 9, 16 turbines, for $5d$ and $7d$ turbine spacing
  - multistart with 400 random initial locations for 9 turbines, 32 for 16 turbines.
- Algorithm behaves well placing turbines in other shapes

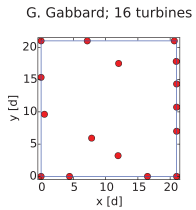

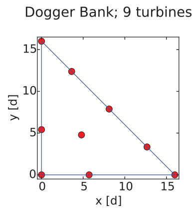

Open problems

- Speed of model/solver
  - Approximation of power curve with splines
- Validation of results
  - Applying other wake models
- Optimizing shape of farm, number of turbines
- Investigating uncertainty in wind information

Thank you!

Norwegian University of Science and Technology

Experimental testing of induction based control strategies for wind farm optimization

PhD cand. Jan Bartl
Prof. Lars Sætran

Fluid Mechanics Group
Department of Energy and Process Engineering (EPT)
Norwegian University of Science and Technology (NTNU)

EERA DEEPWIND R&D SEMINAR –
22 JANUARY 2016 – TRONDHEIM, NORWAY

NOWITECH

Outline

1. Motivation
2. Methods
3. Theory: *wake control*
4. Results
5. Discussion & future work

Motivation

Wake effects in a wind farm

Picture source: Hasager et al., "Wind Farm Wake: The Horns Rev Photo Case", Energies 2013, Picture courtesy: Vattenfall

Motivation

Normalized power at Horns Rev and Nysted for wind directions of full wake interaction

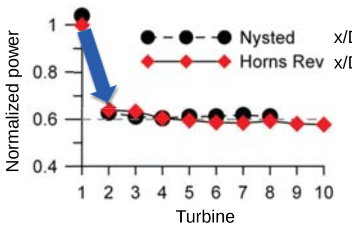

Graph reproduced from: Barthelmie et al. "Modelling the impact of wakes on power output at Nysted and Horns Rev." EWEC, 2009.

⇨ Biggest power drop (~35%) between first and second row

Methods: wind tunnel experiments

Full-scale measurements

Alpha ventus, Picture: Martina Nolte, Licence: Creative Commons by-sa-3.0 de

PREDICTION

SCALING?? BLOCKAGE??

Simulations

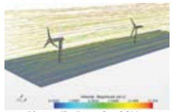

Picture: Jim Ryan, StarCCM+

VALIDATION & CALIBRATION

Wind tunnel experiments

Picture: Geir Mogen, NTNU

Low speed wind tunnel at NTNU

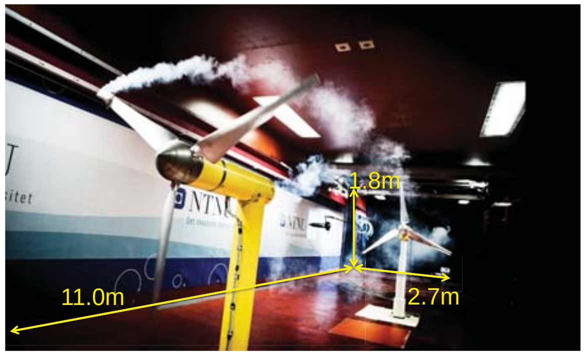

Picture credit: Geir Mogen/NTNU

Grid generated inlet turbulence

Simulation of background turblence
TI ≈ 10% at upstream turbine, TI ≈ 5% at downstream turbine

7

Background

Basic strategies for wake control

Axial induction based control
- **λ: torque (TSR) control**
- **β: blade pitch angle control**

Wake deflection control
- **ϒ: turbine yaw angle control**

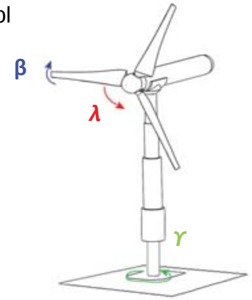

⇨ *Reduce energy capture of upstream turbine to the benefit of the downstream turbines*

8

Axial induction based wake control

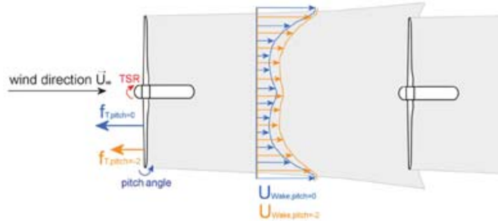

Variation of upstream turbine tip speed ratio λ or pitch angle β
⇨ assessment of mean and turbulent wake flow
⇨ assessment of downstream turbine performance (C_P, C_T)

9

Axial induction based wake control

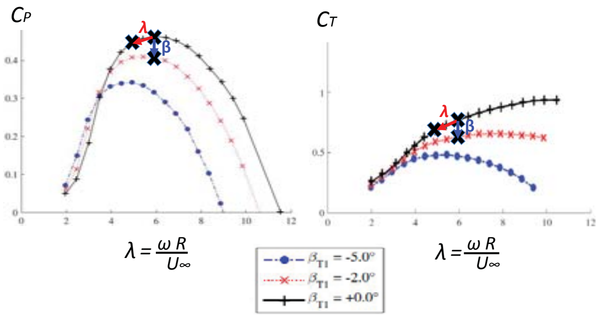

10

Results

λ-variations:
Selected results of Master thesis by
C. Ceccotti, *A. Spiga*, *P. Wiklak* and *S. Luczynski*

β-variations
Selected results of Master thesis by *M. Löther*

11

Results: λ-control of upstream turbine

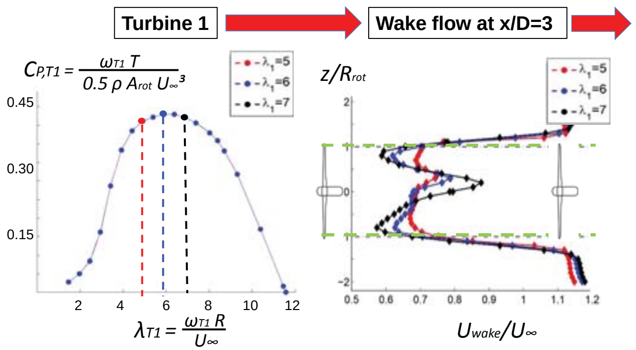

12

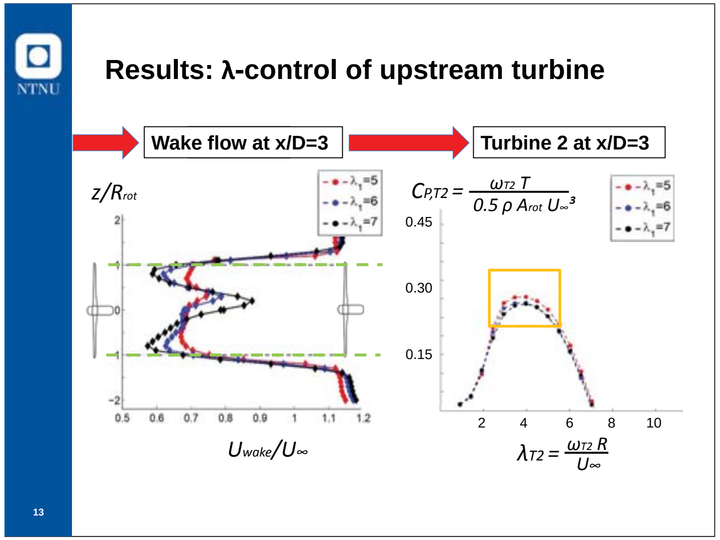
Results: λ-control of upstream turbine
Wake flow at x/D=3
Turbine 2 at x/D=3
z/R_rot
U_wake/U∞
C_P,T2 = ω_T2 T / 0.5 ρ A_rot U∞³
λ_T2 = ω_T2 R / U∞
λ1=5
λ1=6
λ1=7
13

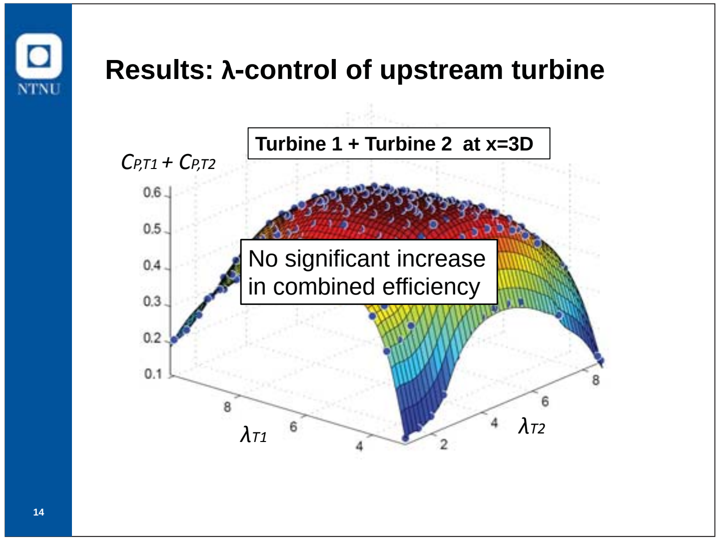
Results: λ-control of upstream turbine
Turbine 1 + Turbine 2 at x=3D
C_P,T1 + C_P,T2
No significant increase
in combined efficiency
λ_T1
λ_T2
14

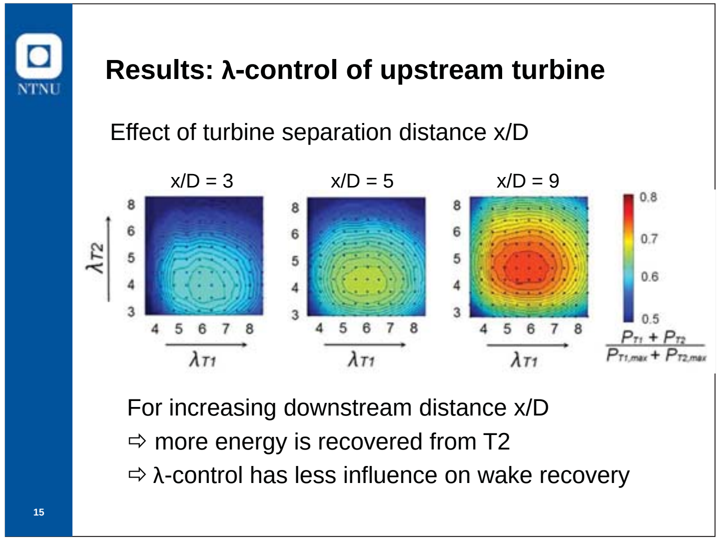
Results: λ-control of upstream turbine
Effect of turbine separation distance x/D
x/D = 3
x/D = 5
x/D = 9
λ_T2
λ_T1
P_T1 + P_T2 / P_T1,max + P_T2,max
For increasing downstream distance x/D
⇨ more energy is recovered from T2
⇨ λ-control has less influence on wake recovery
15

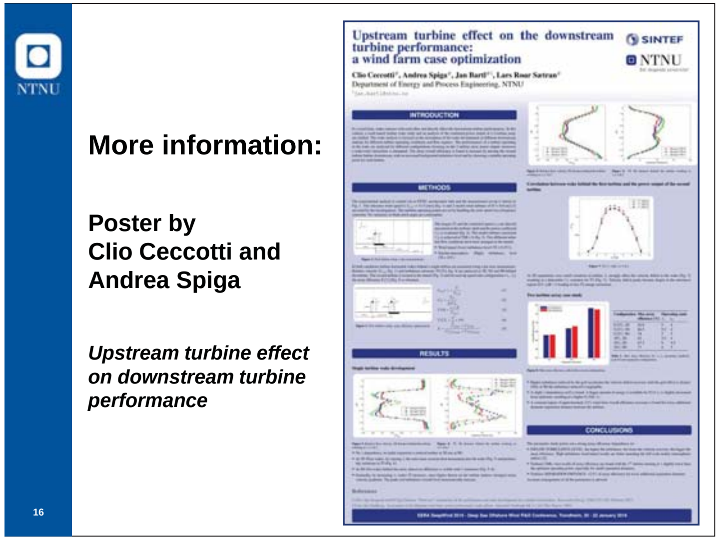
More information:
Poster by
Clio Ceccotti and
Andrea Spiga
Upstream turbine effect
on downstream turbine
performance
Upstream turbine effect on the downstream turbine performance:
a wind farm case optimization
Clio Ceccotti, Andrea Spiga, Jan Bartl, Lars Roar Sætran
Department of Energy and Process Engineering, NTNU
SINTEF
NTNU
INTRODUCTION
METHODS
RESULTS
CONCLUSIONS
16

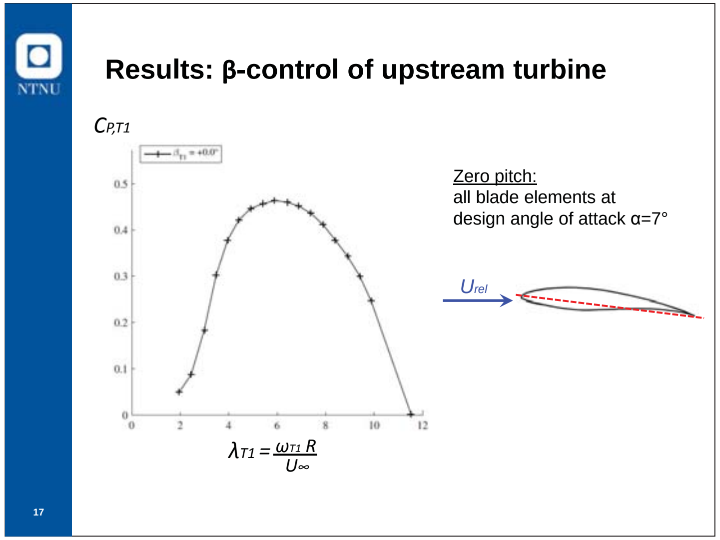
Results: β-control of upstream turbine
C_P,T1
Zero pitch:
all blade elements at
design angle of attack α=7°
U_rel
λ_T1 = ω_T1 R / U∞
17

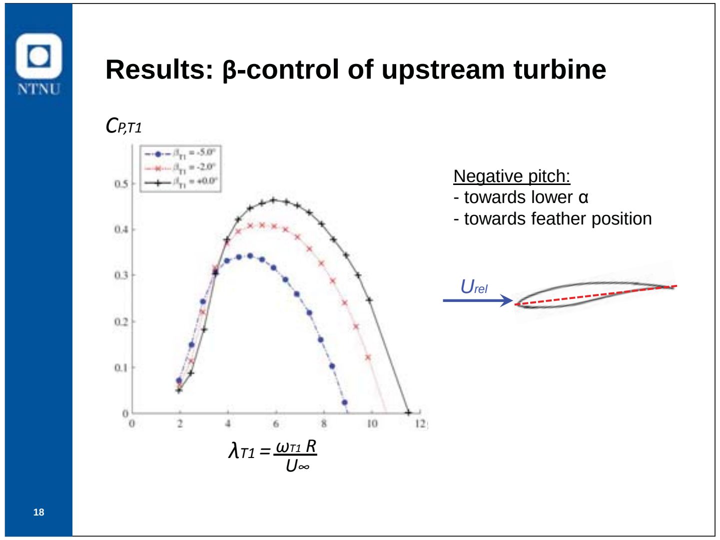
Results: β-control of upstream turbine
C_P,T1
Negative pitch:
- towards lower α
- towards feather position
U_rel
λ_T1 = ω_T1 R / U∞
18

Results: β-control of upstream turbine

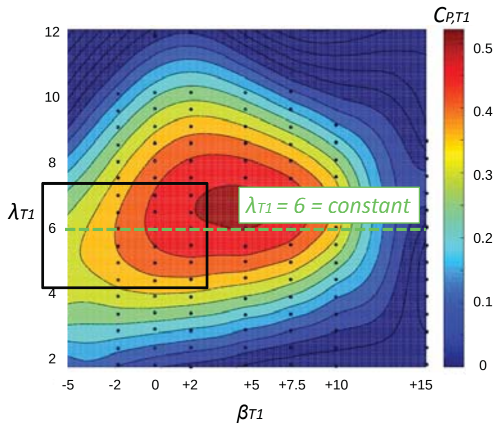

Results: β-control of upstream turbine

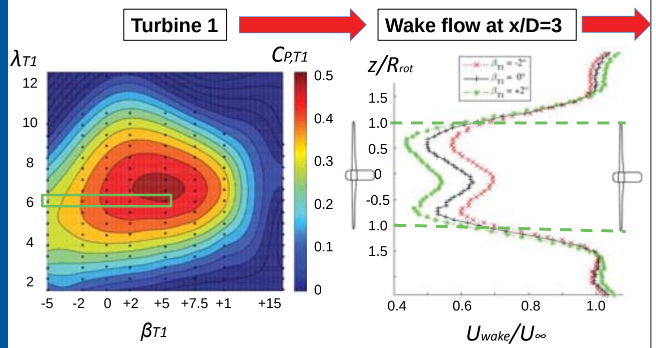

Results: β-control of upstream turbine

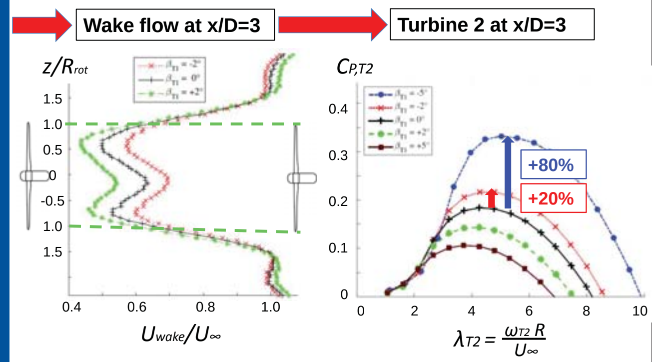

Results: β-control of upstream turbine

Combined wind farm efficiency $P_{T1} + P_{T2}$, x/D=3

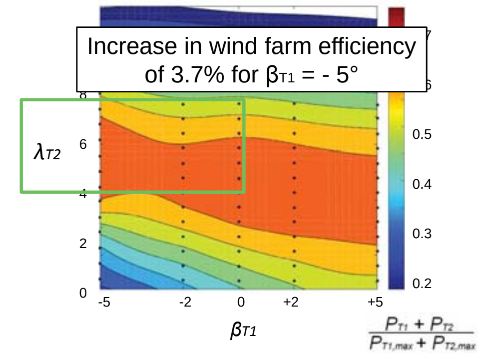

Results: β-control of upstream turbine

Effect of turbine separation distance x/D

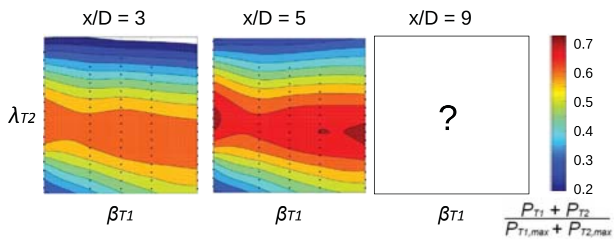

⇨ More energy can be recovered by downstream turbine

Results: β-control of upstream turbine

Where is the added kinetic energy located in the wake?

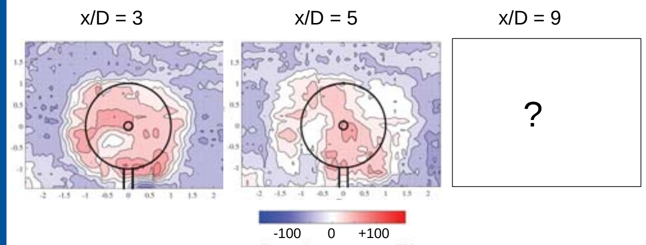

$$\frac{P}{A} = \frac{1}{2} \cdot \rho \cdot U_M^3 \left[\frac{W}{m^2}\right]$$

⇨ Added kinetic energy is diffusing outside the downstream rotor area

Some concluding remarks

λ-control:
- Insignificant effect on total power output from slight variations around the design tip speed ratio
- power lost on the upstream turbine is recovered by the downstream turbine

⇨ total power production is stable around design TSR

β-control:
- Higher potential for wind farm efficiency increase
- Pitch angle of β=-5° gives highest combined efficiency

⇨ more pitch angles to be analysed
⇨ more thorough wake analysis needed

25

Further work

- Wake analysis for pitch angles β_{T1}
- 3rd turbine?
- *Υ*-control

26

Thank you for your attention!

27

Model wind turbines & blade geometry

Two model turbines

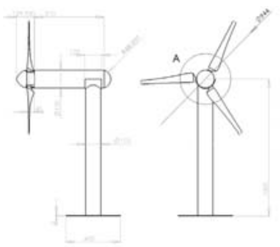

$D_{Rotor,T1}$ ≈ 0.90 m

Solid blockage $\sigma = \frac{A_{Rotor}}{A_{Tunnel}}$ = 12%

Blade: NREL S826 airfoil

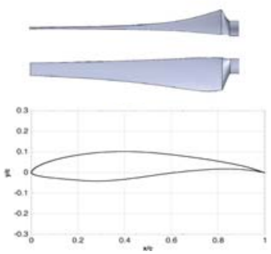

- designed for Re = 10^6
- operated at Re ≈ 10^5

28

Power measurements

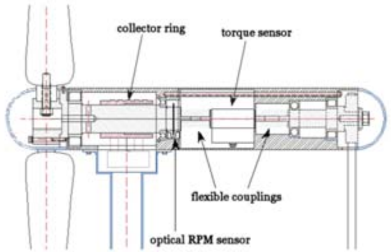

$P = \omega * T$

29

Wake flow measurements

Constant Temperature Anemometry (CTA) Hot-wire

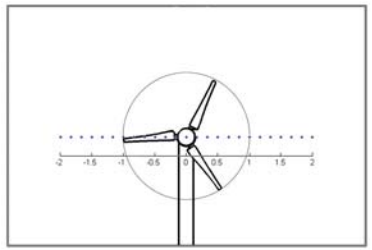

41 measurement points in the wake z/R = -2 to z/R = +2

30

NTNU

NREL S826 airfoil characteristics

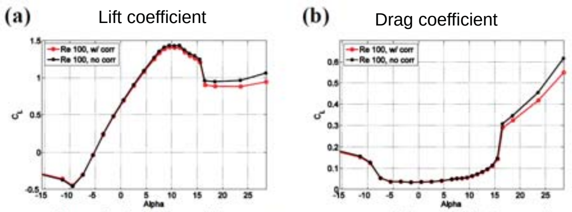

Figure 7 a-b: Lift- and drag measurements corrected for solid blockage, wake blockage and streamline curvatures. $Re = 1.0 \times 10^5$, $TI = 0.71\%$

Source: Initial measurements on S826 wing, N.Aksnes & J.Bartl, NTNU

31

NTNU

Full-area wake measurements, β= -2, 0, +2

x/D=3

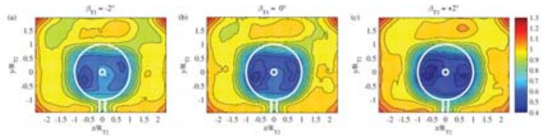

x/D=5

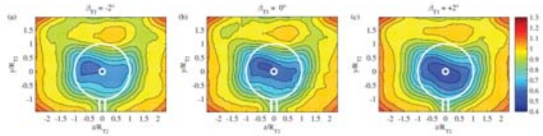

32

NTNU

Background

Basic ***individual*** wind turbine control

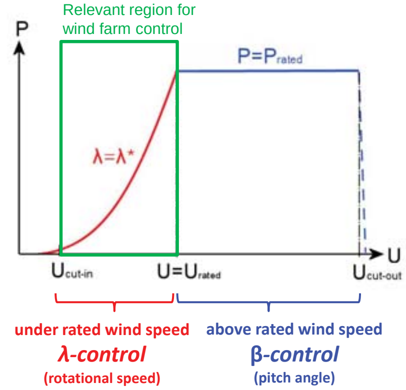

33

NTNU

Background

Concepts of **wind farm control** / **wake control**

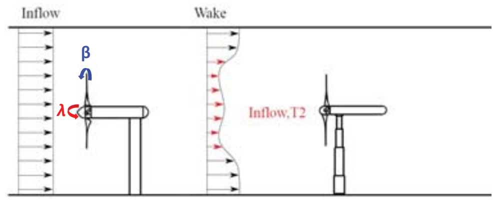

⇨ Reduce energy capture of upstream turbine to the benefit of the downstream turbines

34

NTNU

Background

Further wind turbine control goals

- Fatigue load reduction
- Resonance avoidance
- Gust load alleviation
  (extreme loads)
- Periodic disturbance reduction
  (wind shear, tower shadow effect)
- Actuator duty cycles reduction
- …

*(**Source:** C.L. Bottasso, «Wind turbine control – short course»; http://www.aero.polimi.it/~bottasso/DownloadArea.htm)*

35

G1) Experimental Testing and Validation

Key note: Introduction to the OC5 Project, an IEA Task Focused on Validating Offshore Wind Modeling Tools, Amy Robertson, NREL

Recent Developments of FAST for Modelling Offshore Wind Turbines, Jason Jonkman, NREL

CFD predictions of NREL Phase VI Rotor Experiments in operational and parked conditions, Luca Oggiano, IFE

Verification of the Second-Order Wave Loads on the OC4-Semisubmersible, Sébastien Gueydon, Maritime Inst. Netherlands

Study of the effect of water depth on potential flow solution of the OC4-semisubmersible Floating Offshore Wind Turbine, Ilmas Bayati, Politecnico di Milano

NREL NATIONAL RENEWABLE ENERGY LABORATORY

Statoil

Validation of a FAST Model of the Statoil-Hywind Demo Floating Wind Turbine

EERA DeepWind'2016

20-22 January, 2016

Frederick Driscoll, NREL
Jason Jonkman, NREL
Amy Robertson, NREL
Senu Sirnivas, NREL
Bjørn Skaare, Statoil
Finn Gunnar Nielsen, Statoil

Project Overview & Objectives

- **FAST** is DOE/NREL's premier open-source wind turbine multi-physics engineering tool:
  - Turbine capability validated for land-based applications
  - FOWT capability verified in IEA Wind OC3 & OC4 projects
  - FOWT capability validated against model-scale wave-tank data
- This presentation uses Hywind Demo field data to validate & assess accuracy of **FAST** under realistic full-scale open-ocean conditions

Project Methodology

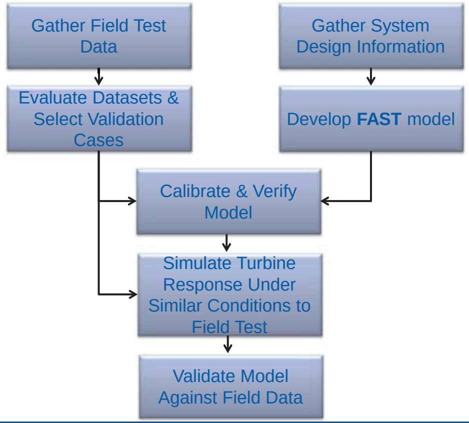

Field Data

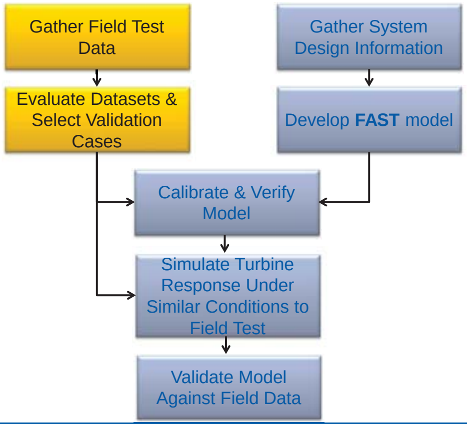

Field Data

Datasets Used for Validation: Statoil provided 8 time series w/ turbine operating (nothing parked/idling), each 30-60-min long, in roughly stationary environmental conditions

Case no.	Duration (min)	Mean wind speed (m/s)	Wind direction (coming from) (deg)	Significant wave height (m)	Peak-spectral wave period (s)	Peak-shape parameter (-)	Wave propagation direction (deg)	Mean current speed (m/s)	Current direction (deg)	Turbine status
1	60	4.7	151	0.88	7.0	2.2	4	0.40	138	Producing power
2	60	9.1	36	1.3	6.9	1	144	0.31	68	Producing power
3	60	9.7	15	1.4	8.6	2	146	0.32	316	Producing power
4	35	12.8	227	3.3	9.7	1.1	25	0.29	50	Producing power
5	35	13.4	252	5.2	10.3	1.74	79	0.52	89	Producing power
6	35	17.5	147	4.0	10.0	1.2	355	0.43	337	Producing power
7	35	18.3	165	2.0	6.8	2.2	353	0.38	316	Producing power
8	35	21.7	152	2.3	7.1	2	358	0.30	336	Producing power

Field Data

Measurements:

Metocean	Turbine	Tower	Platform
• Wind speed & direction • Current speed & direction profiles • Wave height & direction spectral moments	• Generator speed • LSS moments & torque • Blade pitch • Blade root moments • Nacelle yaw • Export power	• Accelerations @ tower top • Bending moments @ stations along tower	• 6 DOF motion • Geodetic position

Data QA (in addition to previous QA by Statoil):

- Reviewed each measurement for continuity/gaps, noise, spikes, strange values/obvious errors, range/thresholds, etc.
- Spot-checked measured values against specifications/expected values
- Verified sample rates for consistency & against specifications
- Cross-compared similar measurements & performed correlation tests

Several channels were rejected, but majority of data was good

Measurement calibrations & uncertainties not provided (limits extent of validation possible)

Model Data

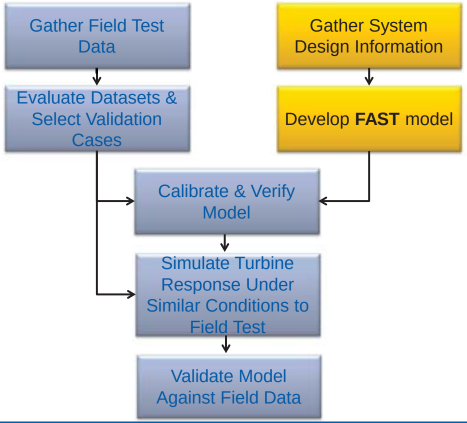

Model Data – Simplifications/Differences

FAST model built by data provided by Siemens & Statoil

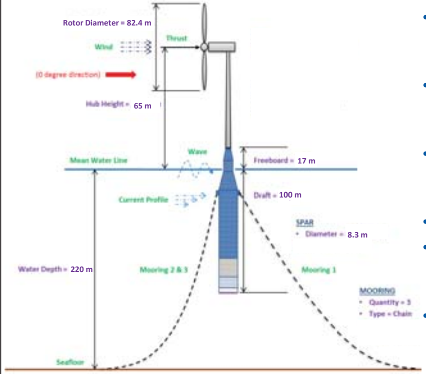

- Blades simplified as straight beams
- Moorings simplified as uniform catenaries w/ equivalent mass/stiffness
- Linear yaw stiffness used to approximate restoring of mooring delta
- Approximate offshore controller mimics 2-layer Siemens-Statoil controller deployed in field
- No nacelle-yaw control
- Wind time series accurate @ hub-height; other points in field derived (**TurbSim**)
- Unidirectional wave time series developed from limited wave statistics

Calibration & Verification

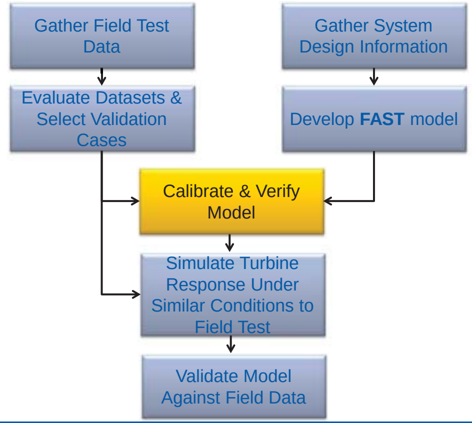

Calibration – Methodology

Parameter	Change	Rationale
Blade mass	Scaled to match total mass	Simplified beam model
Tower mass	Scaled to match total mass	Simplified beam model
Mooring mass/length	Scaled to match surge/sway natural frequencies	Simplified mooring model & provided mooring details were approximate
Yaw spring	Selected to match yaw natural frequency	Simplified mooring model & provided mooring details were approximate
Spar vertical CG	Shifted to match pith/roll natural frequencies	CG not provided

Calibration – Results

Masses & Inertias (Normalized)

Parameter	Specified	Simulated
Blade Mass	1	1
Blade CoG	1	1.007
Second Mass Moment	1	0.9954
Tower-top Mass	1	1.0002
Tower Mass	1	0.993

Blade & Tower Frequencies (Normalized, Fixed/Nonspinning)

Parameter	Specified	Simulated
Flap Blade Mode 1	1	1.008
Flap Blade Mode 2	1	1.03
Edge Blade Mode 1	1	1.006
Tower Mode 1	1	0.91
Tower Mode 2	1	0.99

Spar Natural Periods (with Nonoperating Turbine)

Parameter	Measured (s)	Simulated (s)
Surge	125.0	120.0
Sway	125.0	119.5
Heave	27.5	27.8
Roll	23.9	25.6
Pitch	23.9	25.1
Yaw	6.2	7.36

Verification – Power Curve & Rotor Speed

- Excellent agreement between fixed & floating model
- Good agreement between Siemens simulated land-based power curve

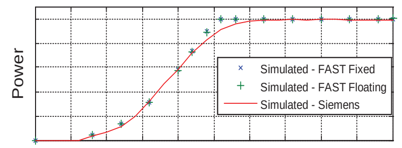

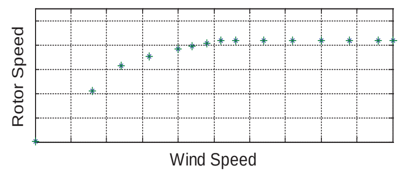

*Fixed **FAST** model uses Siemens' land-based controller*

*Floating **FAST** model uses approximate offshore controller*

Validation

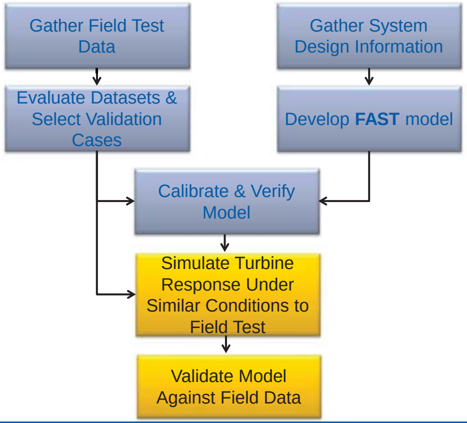

Validation – Control

- Excellent agreement between measured & simulated blade pitch:
  - In response to rapid changes to wind speed
  - @ different mean wind speeds
  - Even though wave time series differ

*The use of **TurbSim** to reproduce measured wind time series @ hub height & statistically equivalent wind field allowed comparison of time series*

Being able to do same for waves would be useful

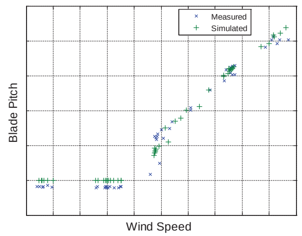

5-Min Averages

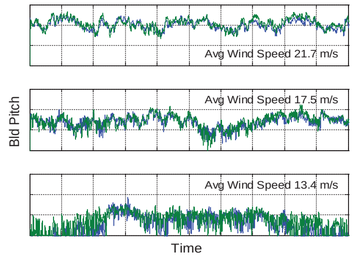

Validation – Drivetrain

- Excellent agreement in power & torque above rated
- Model slightly over-predicts power & torque below rated, expected because:
  - Simplifications in blade model
  - Use of approximate controller
  - Use of nacelle-based wind measurements

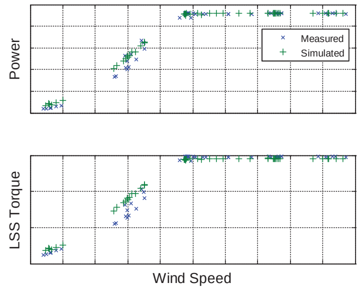

No scale factors were provided to convert measured strain to torque; a scale factor & offset (to remove signal bias) were chosen to fit measured torque with simulated values

Validation – Blade Loads

- Mean flap moments agree well
- Mean edge moments agree up until rated power, but diverge when blade is pitched:
  - Flap moment >> edge moment & difference may be due to slight misalignment of strain gauges from principle edge & flap axes

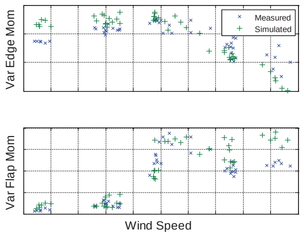

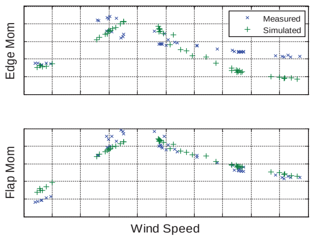

No scaling factors were provided; a scale factor & offset were chosen to fit measured & simulated 5-min average variance & mean

Only a comparison of general response can be made, not a direct comparisons of signal magnitude

Validation – Platform Response @ H_s = 4 m, T_p = 10 s

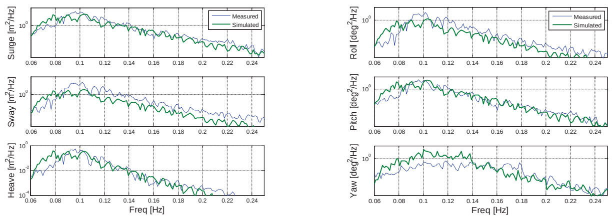

- Good agreement in surge, sway, heave, roll & pitch over all frequencies within wave-band
- More variation outside wave-band & in yaw response, likely caused by:
  - Mooring simplification
  - Spread seas
  - Different wind variation across disk

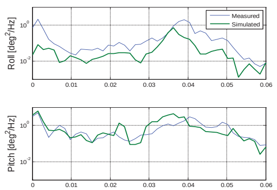

Conclusions & Outlook

- Good agreement found between measured & simulated responses
- Validation presents solid first step in checking **FAST** accuracy to model coupled FOWT response under realistic open-ocean conditions
- Next steps could involve:
  - Improvement of blade (**BeamDyn**) & mooring models (**MoorDyn**)
  - Measured wave time series
  - Measurement uncertainty quantification & model sensitivity analysis
  - Analysis of additional cases, including parked/idling under extreme conditions

NREL
NATIONAL RENEWABLE ENERGY LABORATORY

Statoil

Carpe Ventum!

Jason Jonkman, Ph.D.
+1 (303) 384 – 7026
jason.jonkman@nrel.gov

Real-time hybrid testing of a braceless semi-submersible wind turbine

Erin Bachynski, MARINTEK
Valentin Chabaud, NTNU
Maxime Thys, MARINTEK

MARINTEK
Norsk Marinteknisk Forskningsinstitutt
SINTEF

Outline

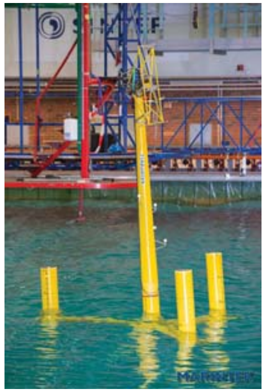

- How to Perform Model Test with a Floating Wind Turbine (FWT)
- Objectives of the Model Tests
- The Experimental Setup
- The Hybrid System
- Results of the Model Tests
- Conclusions about the Hybrid Model Tests

MARINTEK SINTEF

How to Perform Model Tests with a FWT?

Fowler et al. (2013

Approach 1: Install a wind tunnel in the basin

Use Froude scaling for waves, current, and floater.

What about wind and rotor scaling?

- Geometrical or performance-based scaling.

Approach 2: Real-Time Hybrid Model Tests

Use Froude scaling for waves, current, and floater and aerodynamic loads!

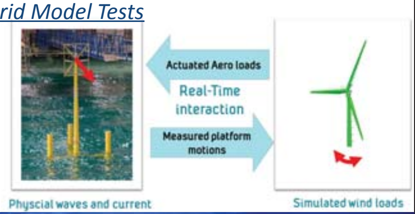

MARINTEK SINTEF

Objectives of the Model Tests

- Quantify the system behavior in environmental conditions representative of the Northern North Sea
- Prove the applicability of the hybrid test method

MARINTEK SINTEF

Experimental Setup

- The FWT:
  - 5MW CSC turbine
  - Floater designed by C. Luan for the NOWITECH project
  - 5 MW NREL rotor-nacelle-assembly
- Froude Scale 1/30
- Water depth: 200m
- Mooring: Chain-chain catenary mooring system

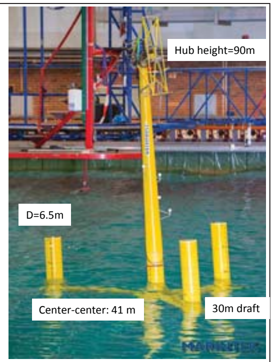

MARINTEK SINTEF

Experimental Setup: Instrumentation

- Position of model by optical positioning system
- Measure linear accelerations and rate of rotation at hub
- "Wind line" and mooring line tensions
- Overturning moment X and Y at base of tower
- Overturning moment X and Y at base of column 3
- Ultra thin instrumentation cable under the model

MARINTEK SINTEF

The Hybrid System

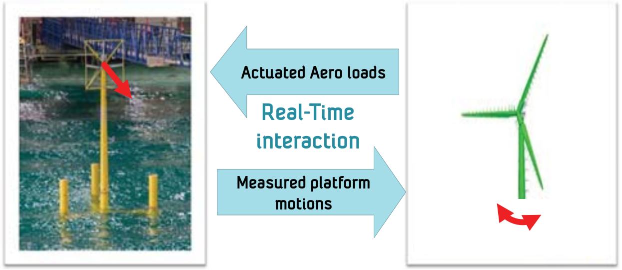

Physcial waves and current

Simulated aerodynamic loads

- Thrust
- Aerodynamic sway force
- Aerodynamic pitch and yaw moment
- Generator torque

MARINTEK SINTEF

The Hybrid System

How do we apply the aerodynamic loads in 5DOF on the model?

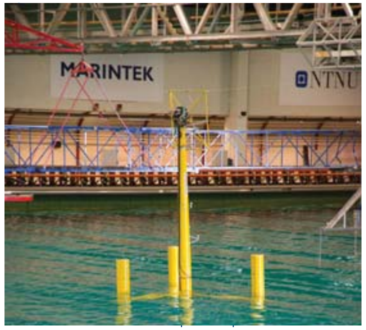

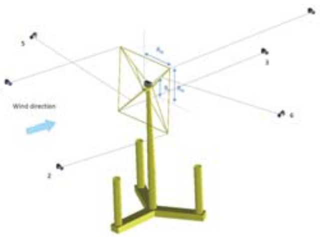

MARINTEK SINTEF

Model Test program

- Tests without hybrid system
  - Decay, Regular waves, Irregular waves
- Tests with zero wind
  - Decay, Regular waves, Irregular waves
- Tests with constant wind
  - Decay and Regular waves
- Tests with turbulent wind
  - Wind-only
  - Irregular waves
    - Below rated, rated, above rated
    - One test with current
    - Misaligned waves
  - Fault conditions

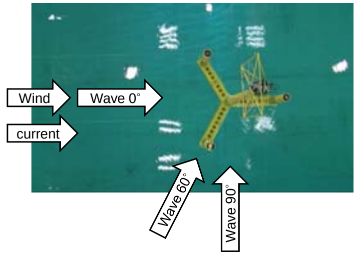

Step by step increase in complexity with repetitions and decomposed conditions

MARINTEK SINTEF

Conclusions about the Hybrid Model Tests

- Performed model tests with a FWT in the Ocean Basin at MARINTEK:
  - with physical waves and current
  - simulated aerodynamic and generator loads on the wind turbine
- The hybrid system was found to perform well
  - Damping and irregular wave tests without the system and with the system in following mode showed little influence
- The wind turbine (including the control system) was found to have significant effects on the natural periods and damping of the system
- Interaction between aerodynamic and hydrodynamic loads was observed primarily at low frequencies
- Studied two fault conditions for the wind turbine
- Step forward toward commercialization of hybrid testing
- Further publications planned for OMAE 2016

MARINTEK SINTEF

MARINTEK
Norwegian Marine Technology Research Institute

NOWITECH

NTNU

This research is part of FME NOWITECH (Norwegian Research Centre for Offshore Wind Technology) which is funded by the Research Council of Norway, industrial companies and participating research organizations

Thank you for your attention.

SINTEF

OC5 Project Phase Ib: Validation of Hydrodynamic Loading on a Fixed, Flexible Cylinder for Offshore Wind Applications

DeepWind Conference – Trondheim, Norway

Amy Robertson

January 21, 2016

Co-Authors

- ***Fabian F. Wendt*** - National Renewable Energy Laboratory, Colorado, USA
- ***Jason M. Jonkman*** - National Renewable Energy Laboratory, Colorado, USA
- ***Wojciech Popko*** - Fraunhofer IWES, Germany
- ***Henrik Bredmose*** – Technical University of Denmark, Denmark
- ***Michael Borg*** - Technical University of Denmark, Denmark
- ***Flemming Schlutter*** - Technical University of Denmark, Denmark
- ***Jacob Qvist*** - 4Subsea, Norway
- ***Roger Bergua*** - Alstom Wind, Spain
- ***Rob Harries*** - DNV GL, England
- ***Anders Yde*** - Technical University of Denmark, Denmark
- ***Tor Anders Nygaard*** - Institute for Energy Technology, Norway
- ***Luca Oggiano*** - Institute for Energy Technology, Norway
- ***Pauline Bozonnet*** - IFP Energies nouvelles, France
- ***Ludovic Bouy*** - PRINCIPIA, France
- ***Carlos Barrera Sanchez*** - Universidad de Cantabria – IH Cantabria, Spain
- ***Raul Guanche García*** - Universidad de Cantabria – IH Cantabria, Spain
- ***Erin E. Bachynski*** - MARINTEK, Norway
- ***Ying Tu*** - Norwegian University of Science and Technology, Norway
- ***Ilmas Bayati*** - Politecnico di Milano, Italy
- ***Friedemann Beyer*** - Stuttgart Wind Energy, University of Stuttgart, Germany
- ***Hyunkyoung Shin*** - University of Ulsan, Korea
- ***Matthieu Guerinel*** - WavEC Offshore Renewables, Portugal
- ***Tjeerd van der Zee*** - Knowledge Centre WMC, the Netherlands

IEA Wind Tasks 23 and 30 (OC3/OC4/OC5)

- Verification and validation of offshore wind modeling tools are need to ensure their accuracy, and give confidence in their usefulness to users.
- Three research projects were initiated under IEA Wind to address this need:

OC3 = Offshore Code Comparison Collaboration (2005-2009)

OC4 = Offshore Code Comparison Collaboration, Continuation (2010-2013)

OC5 = Offshore Code Comparison Collaboration, Continuation, with Correlation (2014-2017)

OC5 Project Phases

- OC3 and OC4 focused on ***verifying*** tools (tool-to-tool comparisons)
- OC5 focuses on ***validating*** tools (code-to-data comparisons)

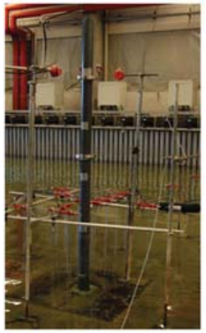

Phase I:
Monopile - Tank Testing

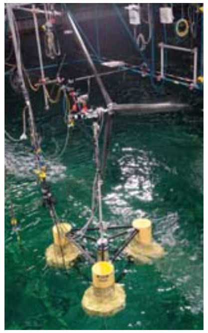

Phase II:
Semi - Tank Testing

Phase III:
Jacket/Tripod – Open Ocean

OC5 Phase Ib

- **Objective**: validate hydrodynamic loads and acceleration response for a fixed, flexible cylinder
- Test Data from **Wave Loads Project:**
  - 3-year project with goal of improving numerical models for wave loads on offshore wind turbines
  - Carried out collaboratively by DTU Wind Energy, DTU Mechanical Engineering, and DHI
  - Performed at shallow-water basin at DHI
  - **Thank you to:** Ole Petersen at DHI and Henrik Bredmose and Michael Borg at DTU for graciously supplying the data and information needed for this phase of the OC5 project.

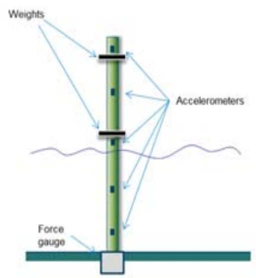

Test Set-Up

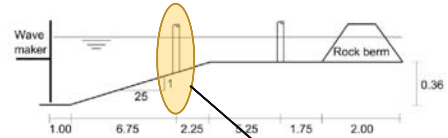

- 1:80 scale, flexible cylinder
- On slope – to create steep waves
- Tests done at two water depths: 0.51 m and 0.26 m (40 and 20 m full scale)
- Measurements used:
  - Wave elevation
  - Acceleration at top mass of cylinder
  - Total hydrodynamic force on cylinder

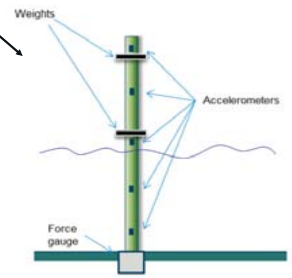

Tests Simulated

Test #	Wave Type	Water Depth (m)	H/Hs (m)	T/Tp (s)	Gamma	C_A	C_D
1	Regular	0.51	0.090	1.5655		1.22	1.0
2	Regular	0.51	0.118	1.5655		1.22	1.0
3	Irregular	0.51	0.104	1.40	3.3	1.0	1.0
4	Irregular	0.51	0.140	1.55	3.3	1.0	1.0
5	Regular	0.26	0.086	1.565		1.22	1.0
6	Regular	0.26	0.121	1.565		1.22	1.0
7	Irregular	0.26	0.133	1.560	3.3	1.0	1.0

- **7 Datasets were examined:**
  - 4 regular cases
    - 2 water depths
    - 2 wave heights
  - 3 irregular cases
    - 2 water depths
    - 2 wave heights
- **First regular wave case used for calibration**

Summary of Tools and Modeling Approach

Participant	Code	Wave Model (Reg/Irr)	Wave Elevation	Hydro Model	Structural Model	Number DOFs
4Subsea	OrcaFlex	FNPF kinematics	FNPF kinematics	ME	FE, RDS	160 elements 960 DOFs
GE	SAMCEF Wind Turbines (S4WT)	5th Order Stokes/ Linear Airy	Stretching	ME	FE (TS), RD	13 elements 84 DOF
DNV GL-ME	Bladed 4.6	6th and 8th Order SF/ Linear Airy	Measured	ME	FE (TS), MD	8 (CB)
DNV GL-PF	Bladed 4.6	Linear Airy	Measured	1st Order PF	Rigid	N/A
DTU-HAWC2	HAWC2	6th and 8th Order SF/L. Airy & FNPF kinematics	Stretching & FNPF kin.	ME	FE (TS), RDS	20 elements, 126 DOF
DTU-HAWC2-PF	HAWC2	6th and 8th Order SF/L. Airy	Stretching	1st Order PF	FE (TS), RDS	31 elements, 192 DOF
DTU-BEAM	OceanWave3D	FNPF kinematics	FNPF kinematics	ME+Rainey	FE (EB), RD	160 DOFs
IFE	3Dfloat	FNPF kinematics	FNPF kinematics	ME	FE (EB), RDS	62 elements, 378 DOF
IFE-CFD	STAR CCM	CFD	CFD-derived	CFD	Rigid	N/A
IFP-PRI	DeeplinesWind	3rd Ord. SF/ Linear Airy	Measured	ME	FE	200 elements
UC-IHC	IH2VOF	FNPF kinematics	FNPF kinematics	ME	Rigid	N/A
MARINTEK	RIFLEX	2nd Order Stokes & FNPF kinematics	Measured & FNPF kin.	ME	FE(E-B), RDS, FS	167 elements, 1002 DOF
NREL-ME	FAST	2nd Order Stokes & FNPF kinematics	Measured & FNPF kin.	ME	FE (TS), MD	4 (CB)
NREL-PF	FAST	2nd Order Stokes	Measured	2nd Order PF	Rigid	N/A
NTNU-Lin	FEDEM 7.1	Linear Airy	None	ME	FE (EB), RD	13 elements, 84 DOF
NTNU-Stokes5	FEDEM 7.1	5th Order Stokes	None	ME	FE (EB), RD	13 elements, 84 DOF
NTNU-Stream	FEDEM 7.1	Stream Function	None	ME	FE (EB), RD	13 elements, 84 DOF
PoliMi	POLI-HydroWind	2nd Order Stokes	None	ME	FE (EB), RD	23 elements, 69 DOF
SWE	SIMPACK +HydroDyn	2nd Order Stokes	None	ME	FE (TS), MD	50
UOU	UOU + FAST	2nd Order Stokes	None	ME	Rigid	N/A
WavEC	Wavec2Wire	2nd Order Stokes /Linear Airy	Measured	2nd/1st Order PF	Rigid	N/A
WMC	FOCUS6 (PHATAS)	FNPF kinematics	FNPF kinematics	ME	FE (TS), MD	12 (CB)

Calibration

- **Group calibrated C_A and C_D coefficients based on Test 1, to get appropriate levels of force**
  - All participants used same values to have consistency in model parameters – to better see differences in modeling approach
- **A C_A value of 1.22 was required, which is larger than expected**
  - Suspect the higher measured loads might be due to reflected waves that were not modeled in the simulation

$$F = \frac{1}{2} C_D \rho D u|u| + C_M \rho \frac{\pi D^2}{4} \dot{u}$$

Morison's Equation

Test 1 – Regular Wave – Deeper Water - Force Results

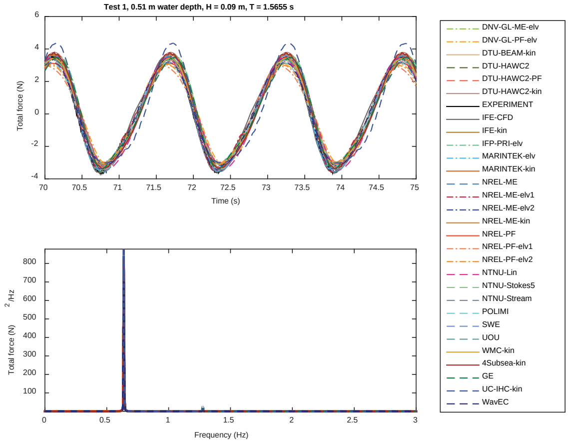

Test 6 – Regular Wave – Shallower Water - Force Results

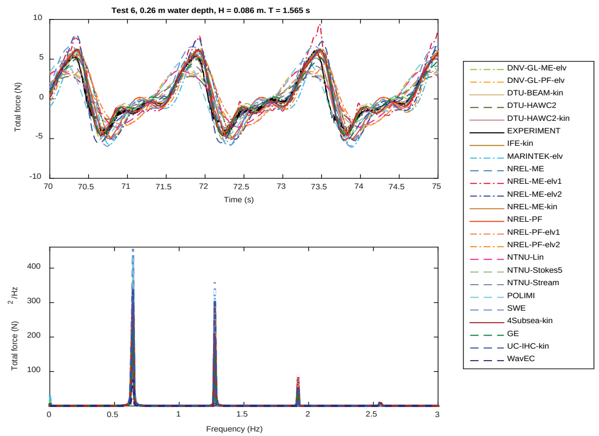

1st Peak Force Component

Deeper Water Depth

Shallower Water Depth

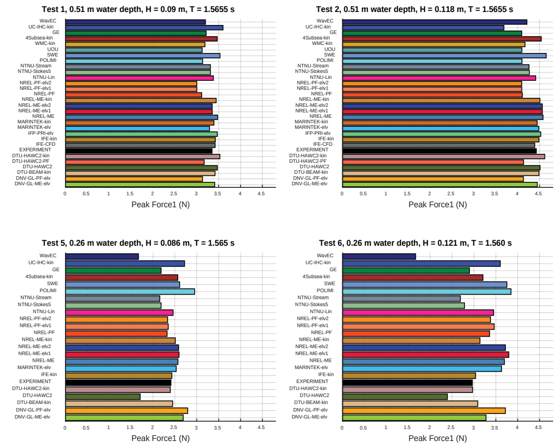

2nd Peak Force Component

Deeper Water Depth

Shallower Water Depth

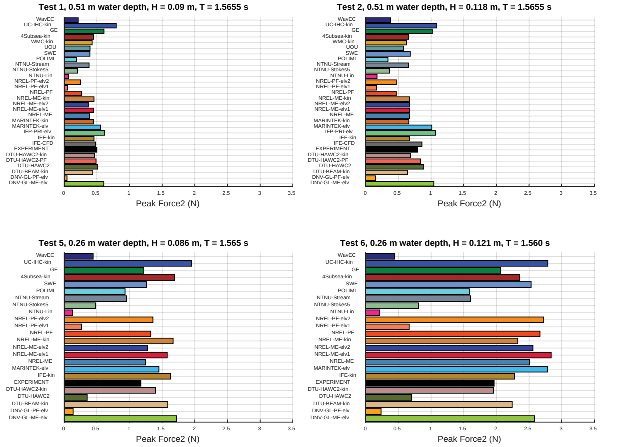

3rd Peak Force Component

Deeper Water Depth

Shallower Water Depth

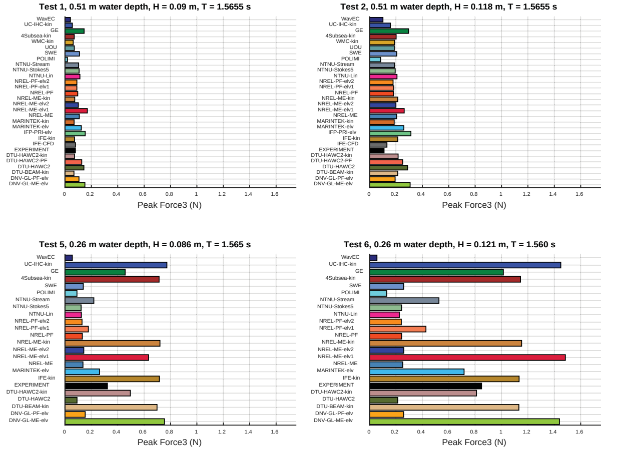

Test 7 – Irregular Wave – Shallower Water

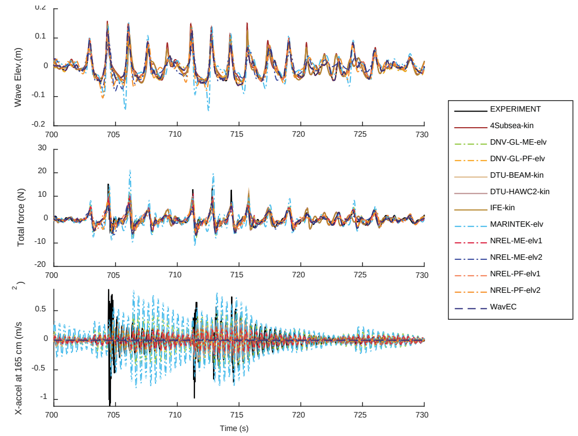

Irregular Waves – Exceedance Probability Plots

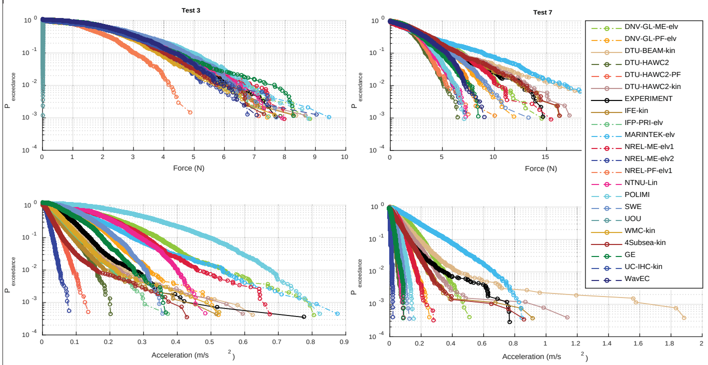

Conclusions

- **Higher-order wave theory important in capturing higher-order components of hydrodynamic force**
  - Extreme loads
  - Excitation of structural frequencies
  - Most important in shallow water
- **Sloped seabed creates complex wave kinematics**
  - Standard wave theories cannot account for slope
  - CFD-type analysis might be needed to create wave kinematics for non-flat seabed conditions
- **Majority of offshore wind modeling tools do not presently address breaking waves**
  - Complex wave theories and CFD can accurately model steep waves that will break
  - Need to model the impulsive load that a breaking wave will impart on the structure
  - Some codes are seeking to include this

AMOS

NTNU
Norwegian University of
Science and Technology

Hydro-Elastic Contributions to Fatigue Damage on a Large Monopile

Jan-Tore H. Horn[a,b], Jørgen R. Krokstad[b,c] and Jørgen Amdahl[a,b]

[a]Centre for Autonomous Marine Operations and Systems - AMOS
[b]Department of Marine Technology, NTNU
[c]Statkraft

January 21, 2016

Motivation

Motivation

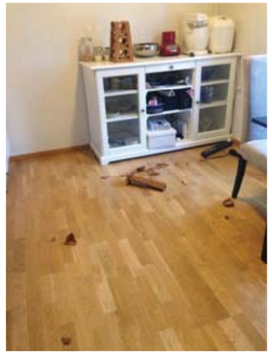

Motivation

Overview

Hydrodynamic Modeling

Motivation:

- Need accurate and realistic load models to evaluate control strategies
- Upscaling of monopiles will give new response characteristics
- Load theory validation and relative impact on lifetime estimation

Hydrodynamic Modeling

Motivation:

- Need accurate and realistic load models to evaluate control strategies
- Upscaling of monopiles will give new response characteristics
- Load theory validation and relative impact on lifetime estimation

NTNU Norwegian University of Science and Technology

Hydrodynamic Modeling

Motivation:

- Need accurate and realistic load models to evaluate control strategies
- Upscaling of monopiles will give new response characteristics
- Load theory validation and relative impact on lifetime estimation

NTNU Norwegian University of Science and Technology

Hydrodynamic Modeling

Motivation:

- Need accurate and realistic load models to evaluate control strategies
- Upscaling of monopiles will give new response characteristics
- Load theory validation and relative impact on lifetime estimation

Findings:

- Significant higher order contributions to fatigue damage in sea-states with $H_S > D/2$
- Necessary to include diffraction effects on second order inertia forces
- Higher order loads more prominent at low damping levels

NTNU Norwegian University of Science and Technology

Hydrodynamic Modeling

Motivation:

- Need accurate and realistic load models to evaluate control strategies
- Upscaling of monopiles will give new response characteristics
- Load theory validation and relative impact on lifetime estimation

Findings:

- Significant higher order contributions to fatigue damage in sea-states with $H_S > D/2$
- Necessary to include diffraction effects on second order inertia forces
- Higher order loads more prominent at low damping levels

NTNU Norwegian University of Science and Technology

Hydrodynamic Modeling

Motivation:

- Need accurate and realistic load models to evaluate control strategies
- Upscaling of monopiles will give new response characteristics
- Load theory validation and relative impact on lifetime estimation

Findings:

- Significant higher order contributions to fatigue damage in sea-states with $H_S > D/2$
- Necessary to include diffraction effects on second order inertia forces
- Higher order loads more prominent at low damping levels

NTNU Norwegian University of Science and Technology

Model

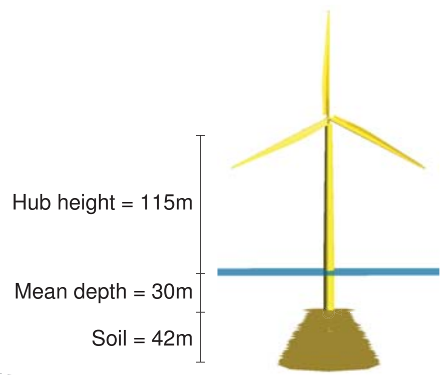

NTNU Norwegian University of Science and Technology

Model

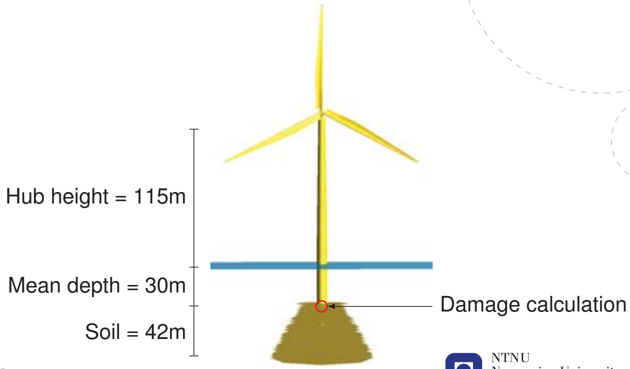

NTNU
Norwegian University of Science and Technology

Model

Parameters:

Diameter	9m
Depth	30m
Structural damping	3% of critical damping (Rayleigh)
Aerodynamic damping	Constant Rayleigh included in structural
Soil	Non-linear springs for sand and clay
Natural periods	Mode 1: 4.2s, Mode 2: 1.0s
Sea-states	FLS

NTNU
Norwegian University of Science and Technology

Modal analysis

Mode 1: 4.1 seconds
Mode 2: 1.0 seconds

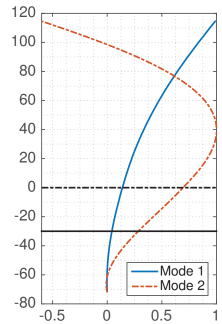

NTNU
Norwegian University of Science and Technology

Wave load models

O1	Linear waves
O1D	Linear waves with diffraction (MacCamy and Fuchs)
O2	Second order contribution from kinematics stretching
O3	Third+fourth order contribution from kinematics stretching
FNV3	Third order FNV - direct implementation
O1P	First order distributed pressure from panel code
O2P	Second order total force from panel code

NTNU
Norwegian University of Science and Technology

Diffraction - MacCamy and Fuchs

Correction of wave load due to interaction with large-volume structure. a_{eq} = equivalent water particle acceleration.

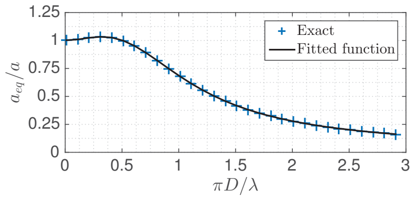

NTNU
Norwegian University of Science and Technology

Diffraction - MacCamy and Fuchs

Correction of wave load due to interaction with large-volume structure. a_{eq} = equivalent water particle acceleration.

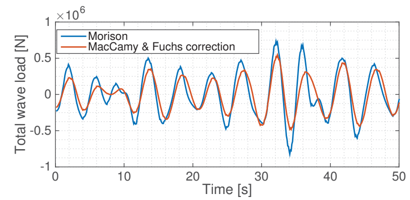

NTNU
Norwegian University of Science and Technology

Second order wave elevation

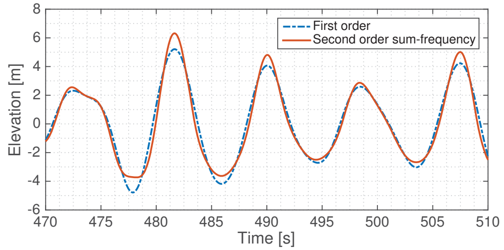

NTNU Norwegian University of Science and Technology

Second order sum-frequency from panel code

HydroD - Wadam

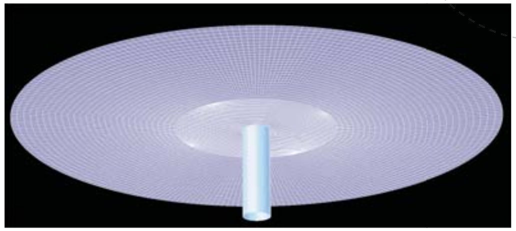

NTNU Norwegian University of Science and Technology

Second order sum-frequency from panel code

Non-dimensional resulting pressure in x-direction over the column as a function of ω_1, ω_2 and z.

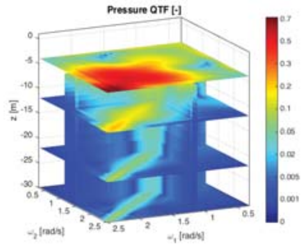

NTNU Norwegian University of Science and Technology

Second order sum-frequency from panel code

The second-order pressures are lumped to $z = 0$ and act as a point force.

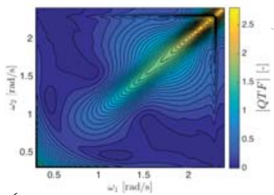

$$\bar{F} = \Re\left\{\sum_{n=1}^{N}\sum_{m=1}^{M} \zeta_{a,n}\cdot\zeta_{a,m}\cdot QTF\cdot e^{-i(\phi_m+\phi_n)}\right\}$$

NTNU Norwegian University of Science and Technology

Load application

Distrubuted, point force or moment?

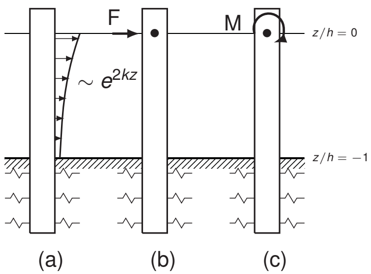

NTNU Norwegian University of Science and Technology

Load application

Distrubuted, point force or moment?

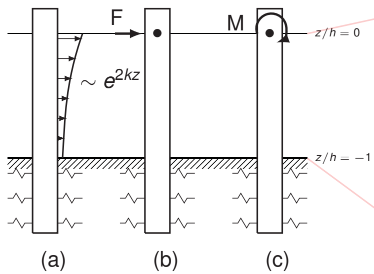

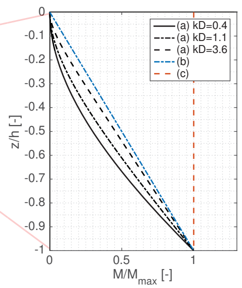

NTNU Norwegian University of Science and Technology

Third Order FNV

Third order horizontal force from linear elevation and diffraction potential assuming deep water:

$$F_x^{FNV(3)} = \rho\pi r^2 \left[\zeta_1\left(\zeta_1 u_{tz} + 2ww_x + uu_x - \frac{2}{g}u_t w_t\right) - \left(\frac{u_t}{g}\right)(u^2+w^2) + \frac{\beta}{g}u^2 u_t\right]_{z=0}$$

NTNU Norwegian University of Science and Technology

Kinematics models

Assuming
$k\zeta_a = O(\epsilon)$
$kD = O(\delta)$
where $\epsilon \ll 1$ and $\epsilon \approx \delta$

NTNU Norwegian University of Science and Technology

Kinematics models

Assuming
$k\zeta_a = O(\epsilon)$
$kD = O(\delta)$

Order of horizontal inertia forces:

— A: $\epsilon^1\delta^2$

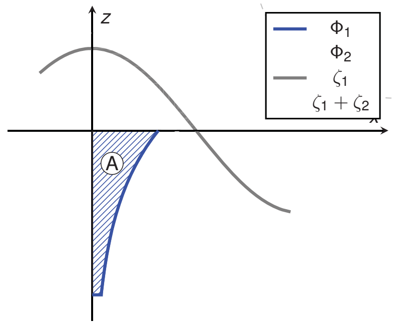

NTNU Norwegian University of Science and Technology

Kinematics models

Assuming
$k\zeta_a = O(\epsilon)$
$kD = O(\delta)$

Order of horizontal inertia forces:

— A: $\epsilon^1\delta^2$
— B+C: $\epsilon^2\delta^2$

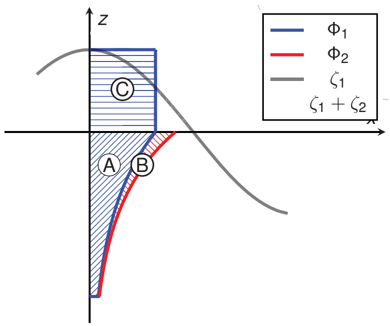

NTNU Norwegian University of Science and Technology

Kinematics models

Assuming
$k\zeta_a = O(\epsilon)$
$kD = O(\delta)$

Order of horizontal inertia forces:

— A: $\epsilon^1\delta^2$
— B+C: $\epsilon^2\delta^2$
— D+E+F: $\epsilon^3\delta^2$

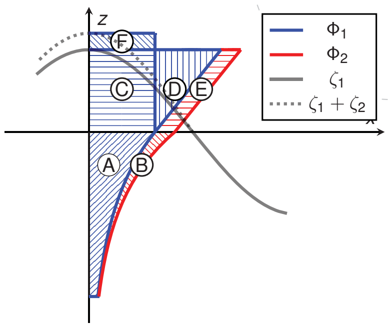

NTNU Norwegian University of Science and Technology

Kinematics models

Assuming
$k\zeta_a = O(\epsilon)$
$kD = O(\delta)$

Order of horizontal inertia forces:

— A: $\epsilon^1\delta^2$
— B+C: $\epsilon^2\delta^2$
— D+E+F: $\epsilon^3\delta^2$
— G+H: $\epsilon^4\delta^2$

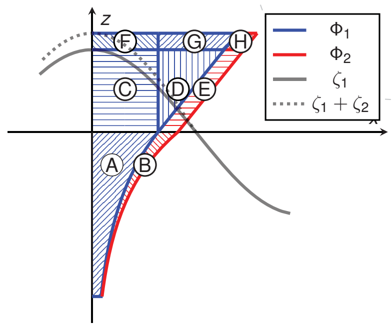

NTNU Norwegian University of Science and Technology

Kinematics models

	$F_x/(0.5\pi\rho D^2)$	$O(F_x)$	$F_x \propto$	Frequency
A	$\int_{-h}^{0} u_{1,t}(z)dz$	$\epsilon\delta^2$	ζ_a	1ω
B	$\int_{-h}^{0} u_{2,t}(z)dz$	$\epsilon^2\delta^2$	ζ_a^2	2ω
C	$\int_{0}^{\max(0,\zeta_1)} u_{1,t}(0)dz$	$\epsilon^2\delta^2$	ζ_a^2	2ω
D	$\int_{0}^{\max(0,\zeta_1)} zu_{1,tz}dz$	$\epsilon^3\delta^2$	ζ_a^3	$1\omega + 3\omega$
E	$\int_{0}^{\max(0,\zeta_1)} u_{2,t}(0)dz$	$\epsilon^3\delta^2$	ζ_a^3	$1\omega + 3\omega$
F	$\int_{\max(0,\zeta_1)}^{\max(0,\zeta_1+\zeta_2)} u_{1,t}(0)dz$	$\epsilon^3\delta^2$	ζ_a^3	$1\omega + 3\omega$
G	$\int_{\max(0,\zeta_1)}^{\max(0,\zeta_1+\zeta_2)} zu_{1,tz}(0)dz$	$\epsilon^4\delta^2$	ζ_a^4	4ω
H	$\int_{\max(0,\zeta_1)}^{\max(0,\zeta_1+\zeta_2)} u_{2,t}(0)dz$	$\epsilon^4\delta^2$	ζ_a^4	4ω

NTNU Norwegian University of Science and Technology

Third order forces

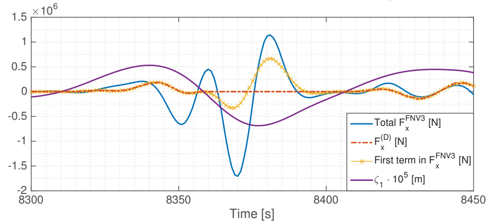

$$F_x^{FNV(3)} = \rho\pi r^2 \left[\zeta_1^2 u_{tz} + 2\zeta_1 w w_x + \zeta_1 u u_x - \frac{2}{g}\zeta_1 u_t w_t - \left(\frac{u_t}{g}\right)(u^2 + w^2) + \frac{\beta}{g}u^2 u_t\right]_{z=0}$$

NTNU Norwegian University of Science and Technology

Third order forces

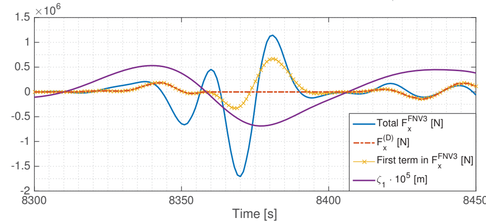

$$F_x^{FNV(3)} = \rho\pi r^2 \left[\zeta_1^2 u_{tz} + 2\zeta_1 w w_x + \zeta_1 u u_x - \frac{2}{g}\zeta_1 u_t w_t - \left(\frac{u_t}{g}\right)(u^2 + w^2) + \frac{\beta}{g}u^2 u_t\right]_{z=0}$$

NTNU Norwegian University of Science and Technology

Kinematics models

Notation	Fields	Description
O1	A	First order incident wave potential
O1D	A	First order incident wave potential w/diffraction
O2	B+C	Second order incident wave potential and stretched first order potential
O3	D+E+F+G+H	Third and fourth order force from stretched first and second order potential
O1P	A	First order diffraction pressure from panel code modeled as acceleration
O2P	B+C	Total second order diffraction force from panel code
FNV3	N/A	Third order FNV ringing force based on first order incident potential

NTNU Norwegian University of Science and Technology

Wave kinematics grid

- Logarithmically distributed in z-direction to increase accuracy in wave-zone
- 4.3 million points for 30 minute simulation with $dt = 0.1$ and $N_Z = 40$, $\rightarrow$ large files!

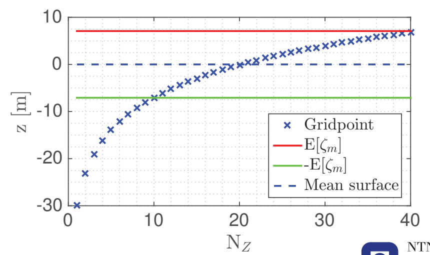

NTNU Norwegian University of Science and Technology

Sea-states

Chosen sea-states for Dogger Bank conditions. JONSWAP spectrum with peak parameter 3.3 is used.

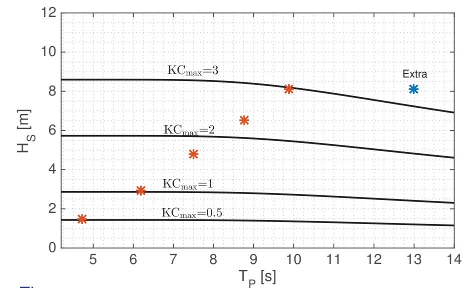

Figure: Sea-states with finite depth KC number for h=30m.

NTNU Norwegian University of Science and Technology

Sea-states

AMOS

Chosen sea-states for Dogger Bank conditions. JONSWAP spectrum with peak parameter 3.3 is used.

No.	H_S [m]	T_P [s]	f_{H_S,T_P}[-]	KC_{max}[-]	$\pi D/\lambda$ [-]
1	1.46	4.72	0.1002	0.5	1.28
2	2.95	6.18	0.0314	1.0	0.75
3	4.79	7.50	0.0092	1.7	0.50
4	6.54	8.76	0.0016	2.3	0.37
5	8.13	9.88	0.0002	3.0	0.29
6*	8.13	13.00	0.0000	3.5	0.17

NTNU Norwegian University of Science and Technology

Results

AMOS

— For each sea-state and hydrodynamic model, 3×30 minute simulations have been run without wind
— Average findings presented
— Small variances between the seeds

NTNU Norwegian University of Science and Technology

Results

AMOS

Baseline maximum moment

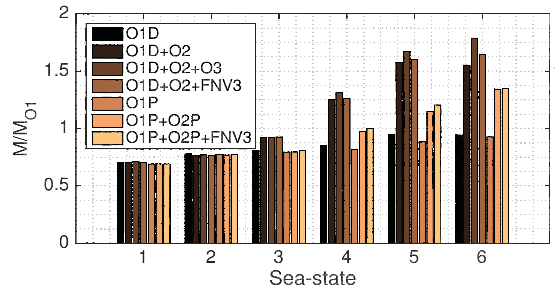

NTNU Norwegian University of Science and Technology

Results

AMOS

Fatigue damage relative to first order incident wave

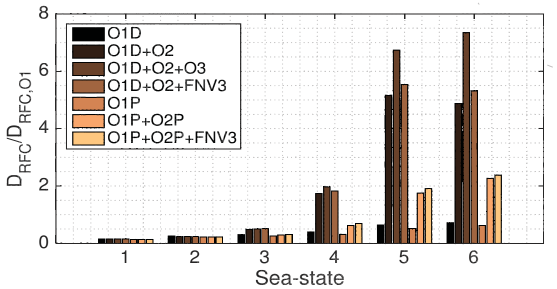

NTNU Norwegian University of Science and Technology

Results

AMOS

Relative fatigue damage accounting for probability of occurrence

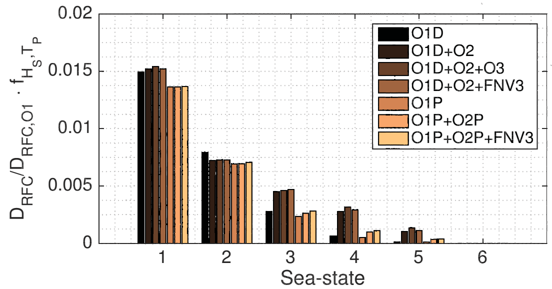

NTNU Norwegian University of Science and Technology

Results

AMOS

Relative fatigue damage accounting for probability of occurrence

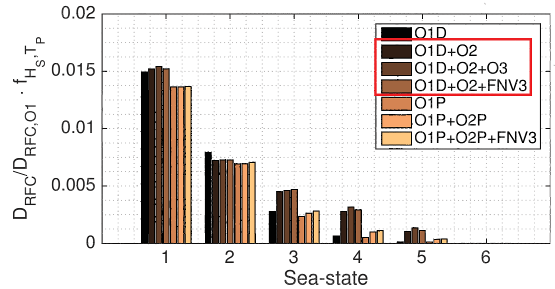

NTNU Norwegian University of Science and Technology

Results

Increased fatigue damage for lightly damped system: 3% → 1%

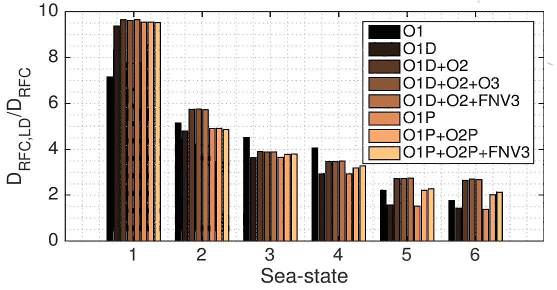

Results

Drag force contribution due to wave elevation and increasing KC-number

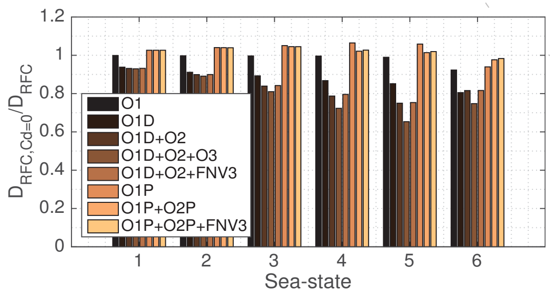

Time-frequency analysis

Wavelet analysis revealing most dominating oscillation periods.

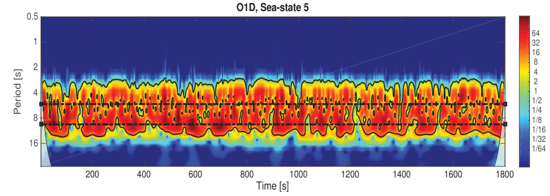

Time-frequency analysis

Wavelet analysis revealing most dominating oscillation periods.

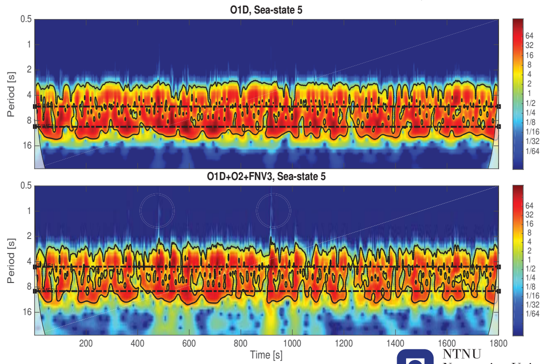

Time-frequency analysis

Wavelet analysis revealing most dominating oscillation periods.

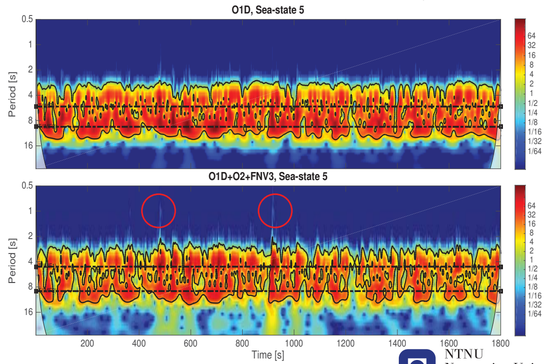

Conclusions

- When $H_S > D/2$, significant contributions to fatigue damage from higher order loads are observed
- Higher order effects not important for smaller sea-states - overall small contributions when frequency of occurrence is accounted for
- Lower damping level results in more prominent contributions from higher order forces
- Drag forces still important when wave elevation is accounted for - need sensitivity study of C_D
- A Morison type loading for second order load seems to be predicting very large responses and fatigue damage for large sea-states - elevation important
- Important to include diffraction effects - both first and second order

Conclusions

AMOS

- When $H_S > D/2$, significant contributions to fatigue damage from higher order loads are observed
- Higher order effects not important for smaller sea-states - overall small contributions when frequency of occurrence is accounted for
- Lower damping level results in more prominent contributions from higher order forces
- Drag forces still important when wave elevation is accounted for - need sensitivity study of C_D
- A Morison type loading for second order load seems to be predicting very large responses and fatigue damage for large sea-states - elevation important
- Important to include diffraction effects - both first and second order

NTNU
Norwegian University of Science and Technology

Conclusions

AMOS

- When $H_S > D/2$, significant contributions to fatigue damage from higher order loads are observed
- Higher order effects not important for smaller sea-states - overall small contributions when frequency of occurrence is accounted for
- Lower damping level results in more prominent contributions from higher order forces
- Drag forces still important when wave elevation is accounted for - need sensitivity study of C_D
- A Morison type loading for second order load seems to be predicting very large responses and fatigue damage for large sea-states - elevation important
- Important to include diffraction effects - both first and second order

NTNU
Norwegian University of Science and Technology

www.ntnu.edu/amos EERA DeepWind'2016 24

Conclusions

AMOS

- When $H_S > D/2$, significant contributions to fatigue damage from higher order loads are observed
- Higher order effects not important for smaller sea-states - overall small contributions when frequency of occurrence is accounted for
- Lower damping level results in more prominent contributions from higher order forces
- Drag forces still important when wave elevation is accounted for - need sensitivity study of C_D
- A Morison type loading for second order load seems to be predicting very large responses and fatigue damage for large sea-states - elevation important
- Important to include diffraction effects - both first and second order

NTNU
Norwegian University of Science and Technology

www.ntnu.edu/amos EERA DeepWind'2016 24

Conclusions

AMOS

- When $H_S > D/2$, significant contributions to fatigue damage from higher order loads are observed
- Higher order effects not important for smaller sea-states - overall small contributions when frequency of occurrence is accounted for
- Lower damping level results in more prominent contributions from higher order forces
- Drag forces still important when wave elevation is accounted for - need sensitivity study of C_D
- A Morison type loading for second order load seems to be predicting very large responses and fatigue damage for large sea-states - elevation important
- Important to include diffraction effects - both first and second order

NTNU
Norwegian University of Science and Technology

www.ntnu.edu/amos EERA DeepWind'2016 24

Conclusions

AMOS

- When $H_S > D/2$, significant contributions to fatigue damage from higher order loads are observed
- Higher order effects not important for smaller sea-states - overall small contributions when frequency of occurrence is accounted for
- Lower damping level results in more prominent contributions from higher order forces
- Drag forces still important when wave elevation is accounted for - need sensitivity study of C_D
- A Morison type loading for second order load seems to be predicting very large responses and fatigue damage for large sea-states - elevation important
- Important to include diffraction effects - both first and second order

NTNU
Norwegian University of Science and Technology

www.ntnu.edu/amos EERA DeepWind'2016 24

Thank you for your attention.
- Questions?

NTNU
Norwegian University of Science and Technology

G2) Experimental Testing and Validation

Validation of uncertainty in IEC damage calculations based on measurements from alpha ventus, K. Müller, Univ of Stuttgart

Experimental Validation of the W2Power Hybrid Floating Platform, P. Mayorga, W2Power

Unsteady aerodynamics of floating offshore wind turbines: toward experimental validation of equivalent lumped-element models, A. Zasso, Politecnico di Milano

Aerodynamic damping of a HAWT on a Semisubmersible, S. Gueydon, Maritime Institute of The Netherlands

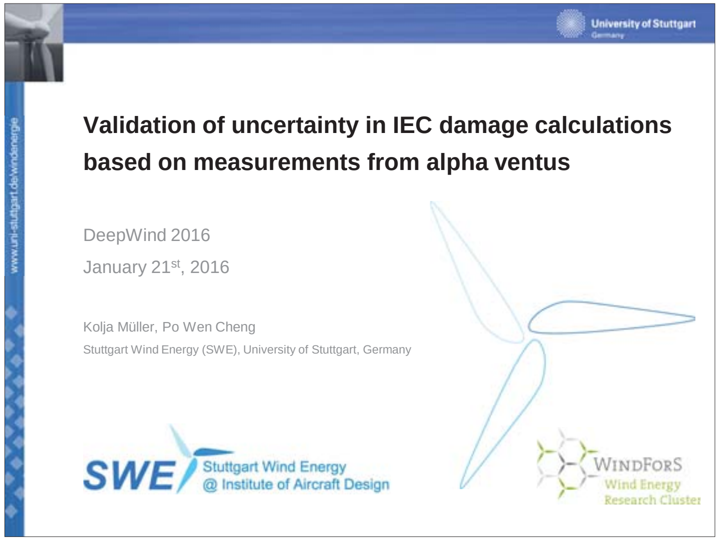
University of Stuttgart
Germany
www.uni-stuttgart.de/windenergie
Validation of uncertainty in IEC damage calculations based on measurements from alpha ventus
DeepWind 2016
January 21st, 2016
Kolja Müller, Po Wen Cheng
Stuttgart Wind Energy (SWE), University of Stuttgart, Germany
SWE
Stuttgart Wind Energy
@ Institute of Aircraft Design
WINDFORS
Wind Energy
Research Cluster

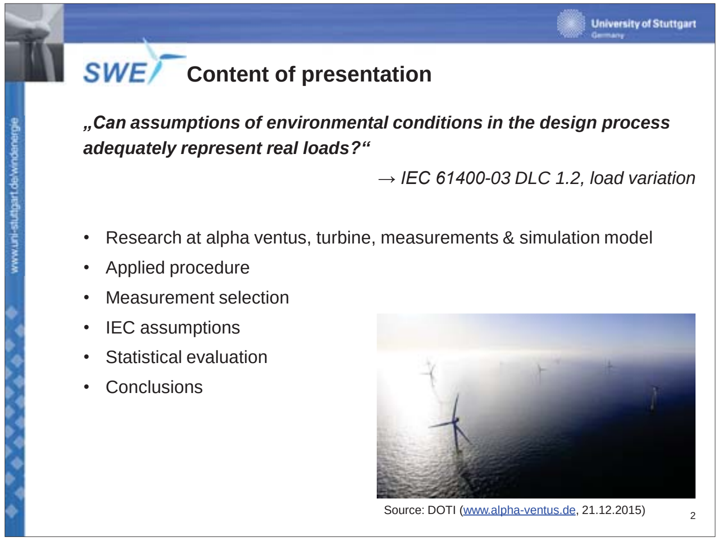
University of Stuttgart
SWE
Content of presentation
„Can assumptions of environmental conditions in the design process adequately represent real loads?“
→ IEC 61400-03 DLC 1.2, load variation
Research at alpha ventus, turbine, measurements & simulation model
Applied procedure
Measurement selection
IEC assumptions
Statistical evaluation
Conclusions
Source: DOTI (www.alpha-ventus.de, 21.12.2015)
2

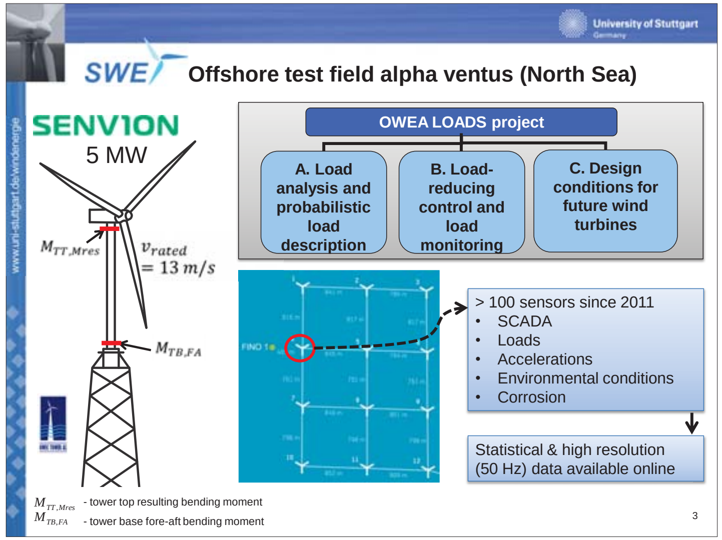
University of Stuttgart
SWE
Offshore test field alpha ventus (North Sea)
SENV1ON
5 MW
$M_{TT,Mres}$
$v_{rated} = 13\,m/s$
$M_{TB,FA}$
OWEA LOADS project
A. Load analysis and probabilistic load description
B. Load-reducing control and load monitoring
C. Design conditions for future wind turbines
FINO 1
> 100 sensors since 2011
SCADA
Loads
Accelerations
Environmental conditions
Corrosion
Statistical & high resolution (50 Hz) data available online
$M_{TT,Mres}$ - tower top resulting bending moment
$M_{TB,FA}$ - tower base fore-aft bending moment
3

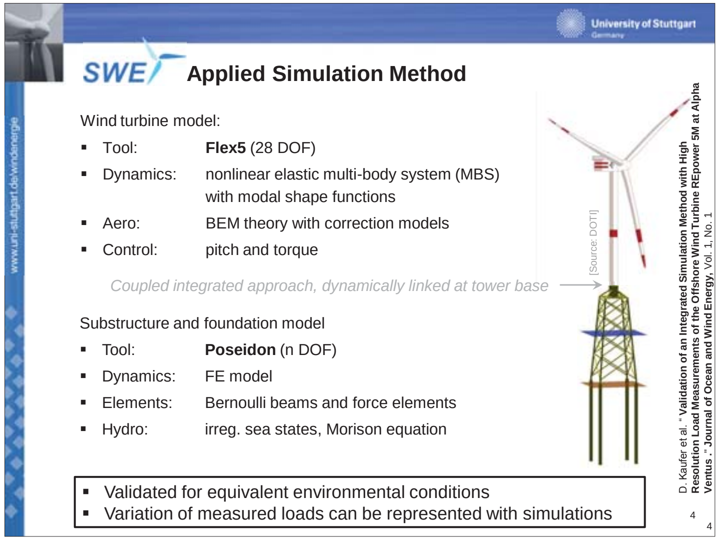
University of Stuttgart
SWE
Applied Simulation Method
Wind turbine model:
Tool: Flex5 (28 DOF)
Dynamics: nonlinear elastic multi-body system (MBS) with modal shape functions
Aero: BEM theory with correction models
Control: pitch and torque
Coupled integrated approach, dynamically linked at tower base
[Source: DOTI]
Substructure and foundation model
Tool: Poseidon (n DOF)
Dynamics: FE model
Elements: Bernoulli beams and force elements
Hydro: irreg. sea states, Morison equation
Validated for equivalent environmental conditions
Variation of measured loads can be represented with simulations
D. Kaufer et al. " Validation of an Integrated Simulation Method with High Resolution Load Measurements of the Offshore Wind Turbine REpower 5M at Alpha Ventus," Journal of Ocean and Wind Energy, Vol. 1, No. 1
4

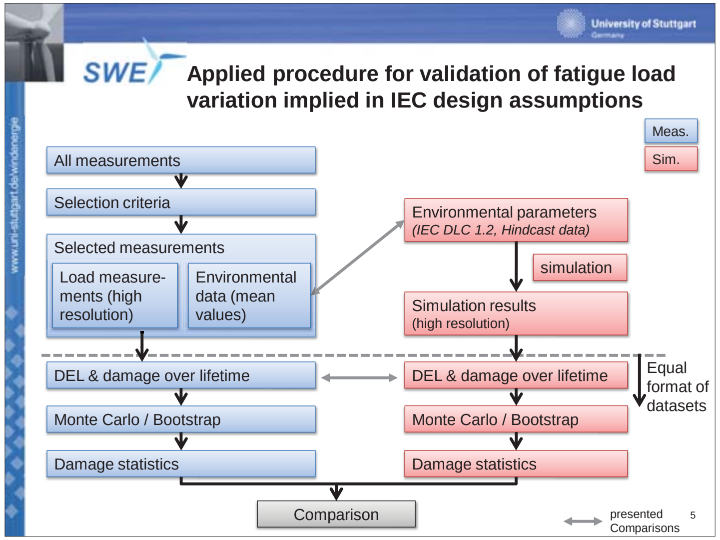
University of Stuttgart
SWE
Applied procedure for validation of fatigue load variation implied in IEC design assumptions
Meas.
Sim.
All measurements
Selection criteria
Selected measurements
Load measurements (high resolution)
Environmental data (mean values)
Environmental parameters
(IEC DLC 1.2, Hindcast data)
simulation
Simulation results
(high resolution)
DEL & damage over lifetime
DEL & damage over lifetime
Equal format of datasets
Monte Carlo / Bootstrap
Monte Carlo / Bootstrap
Damage statistics
Damage statistics
Comparison
presented Comparisons
5

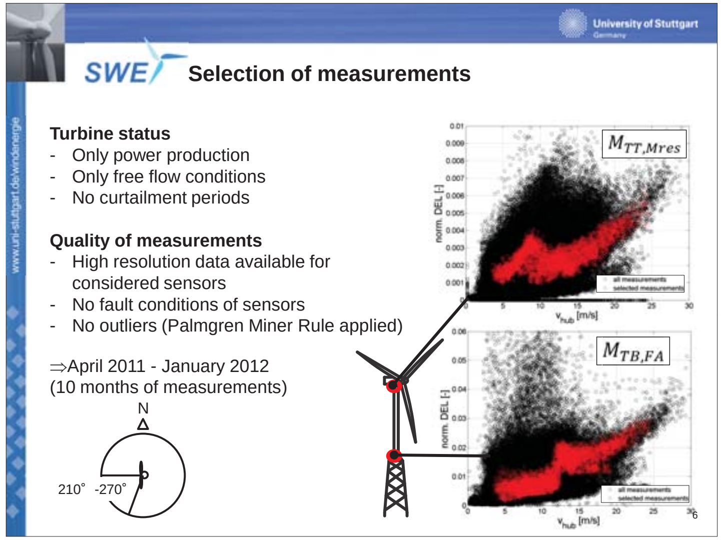
University of Stuttgart
SWE
Selection of measurements
Turbine status
- Only power production
- Only free flow conditions
- No curtailment periods
Quality of measurements
- High resolution data available for considered sensors
- No fault conditions of sensors
- No outliers (Palmgren Miner Rule applied)
⇒April 2011 - January 2012
(10 months of measurements)
N
210° -270°
$M_{TT,Mres}$
$M_{TB,FA}$
norm. DEL [-]
v_{hub} [m/s]
6

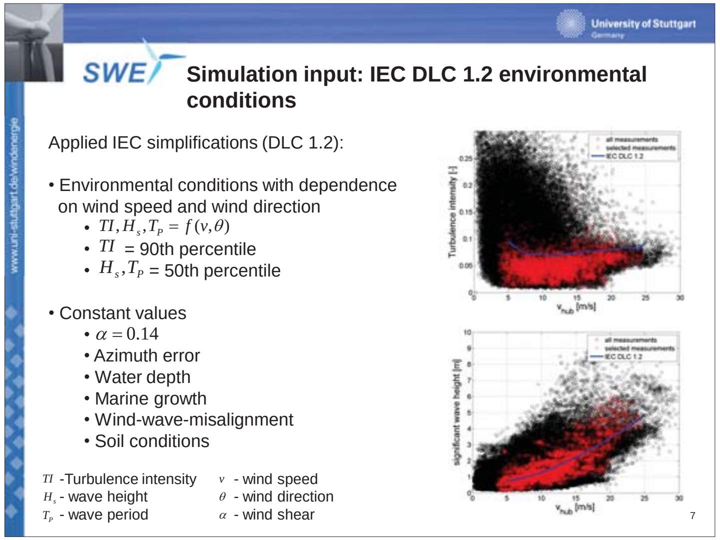
University of Stuttgart
Germany
SWE
Simulation input: IEC DLC 1.2 environmental conditions
Applied IEC simplifications (DLC 1.2):
• Environmental conditions with dependence on wind speed and wind direction
• $TI, H_s, T_P = f(v, \theta)$
• TI = 90th percentile
• H_s, T_P = 50th percentile
• Constant values
• $\alpha = 0.14$
• Azimuth error
• Water depth
• Marine growth
• Wind-wave-misalignment
• Soil conditions
TI -Turbulence intensity
H_s - wave height
T_P - wave period
v - wind speed
θ - wind direction
α - wind shear
Turbulence intensity [-]
significant wave height [m]
v_{hub} [m/s]
all measurements
selected measurements
IEC DLC 1.2
www.uni-stuttgart.de/windenergie
7

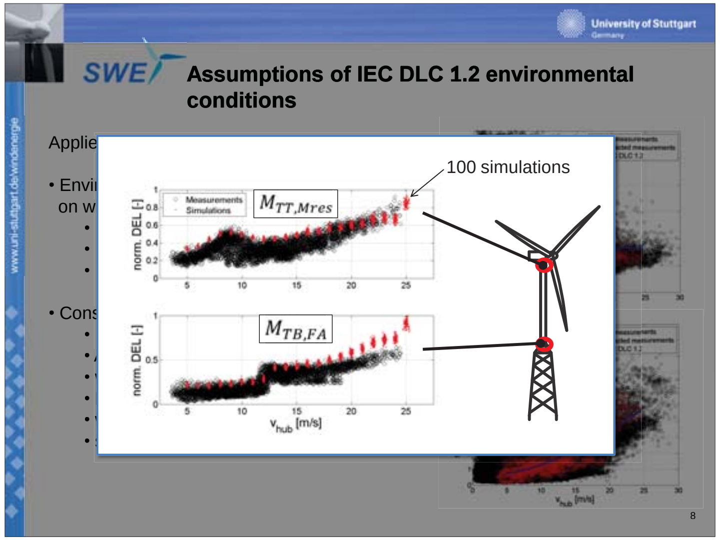
University of Stuttgart
Germany
SWE
Assumptions of IEC DLC 1.2 environmental conditions
Applie
• Envi
on w
• Cons
100 simulations
Measurements
Simulations
$M_{TT,Mres}$
$M_{TB,FA}$
norm. DEL [-]
v_{hub} [m/s]
www.uni-stuttgart.de/windenergie
8

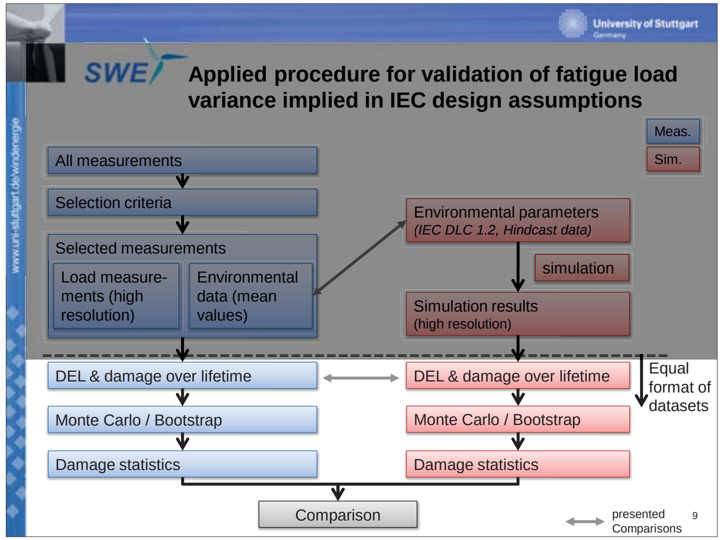
University of Stuttgart
Germany
SWE
Applied procedure for validation of fatigue load variance implied in IEC design assumptions
Meas.
Sim.
All measurements
Selection criteria
Selected measurements
Load measurements (high resolution)
Environmental data (mean values)
Environmental parameters
(IEC DLC 1.2, Hindcast data)
simulation
Simulation results
(high resolution)
DEL & damage over lifetime
DEL & damage over lifetime
Equal format of datasets
Monte Carlo / Bootstrap
Monte Carlo / Bootstrap
Damage statistics
Damage statistics
Comparison
presented Comparisons
www.uni-stuttgart.de/windenergie
9

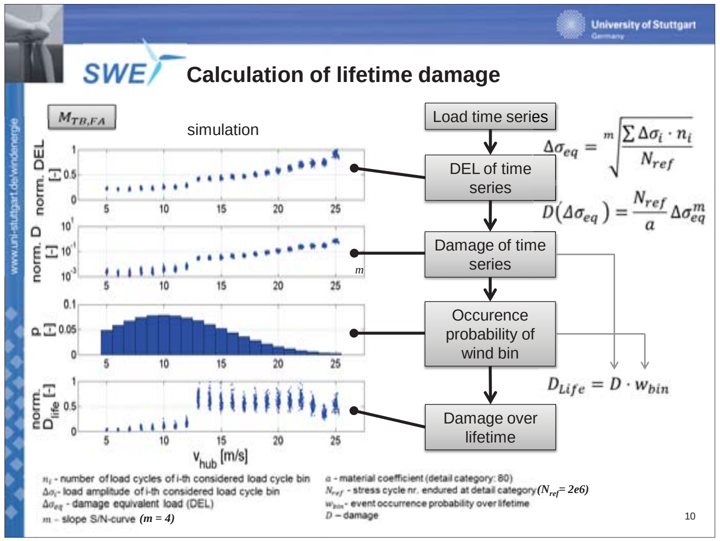
University of Stuttgart
Germany
SWE
Calculation of lifetime damage
$M_{TB,FA}$
simulation
norm. DEL [-]
norm. D [-]
p [-]
norm. D_{life} [-]
v_{hub} [m/s]
Load time series
DEL of time series
Damage of time series
Occurence probability of wind bin
Damage over lifetime
$\Delta\sigma_{eq} = \sqrt[m]{\frac{\sum \Delta\sigma_i \cdot n_i}{N_{ref}}}$
$D(\Delta\sigma_{eq}) = \frac{N_{ref}}{a} \Delta\sigma_{eq}^m$
$D_{Life} = D \cdot w_{bin}$
n_i - number of load cycles of i-th considered load cycle bin
$\Delta\sigma_i$ - load amplitude of i-th considered load cycle bin
$\Delta\sigma_{eq}$ - damage equivalent load (DEL)
m - slope S/N-curve ($m = 4$)
a - material coefficient (detail category: 80)
N_{ref} - stress cycle nr. endured at detail category (N_{ref}= 2e6)
w_{bin} - event occurrence probability over lifetime
D – damage
www.uni-stuttgart.de/windenergie
10

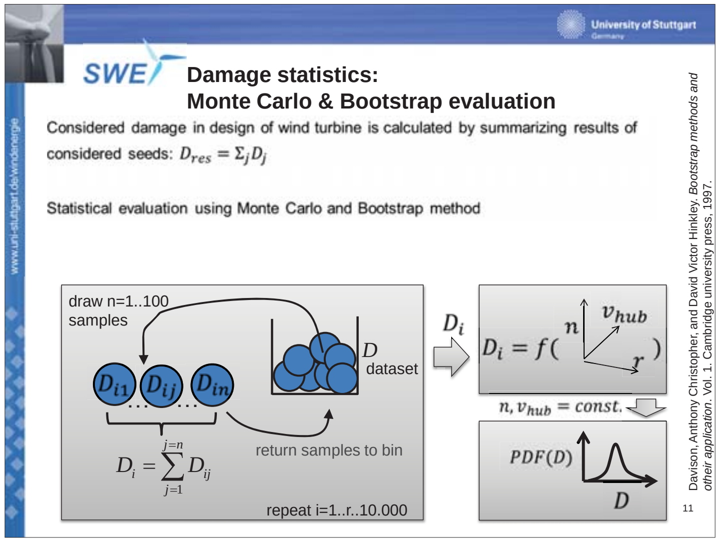
University of Stuttgart
Germany
SWE
Damage statistics:
Monte Carlo & Bootstrap evaluation
Considered damage in design of wind turbine is calculated by summarizing results of considered seeds: $D_{res} = \Sigma_j D_j$
Statistical evaluation using Monte Carlo and Bootstrap method
draw n=1..100 samples
D_{i1} D_{ij} D_{in}
D dataset
$D_i = \sum_{j=1}^{j=n} D_{ij}$
return samples to bin
repeat i=1..r..10.000
D_i
$D_i = f(n, v_{hub}, r)$
$n, v_{hub} = const.$
$PDF(D)$
D
Davison, Anthony Christopher, and David Victor Hinkley. Bootstrap methods and their application. Vol. 1. Cambridge university press, 1997.
www.uni-stuttgart.de/windenergie
11

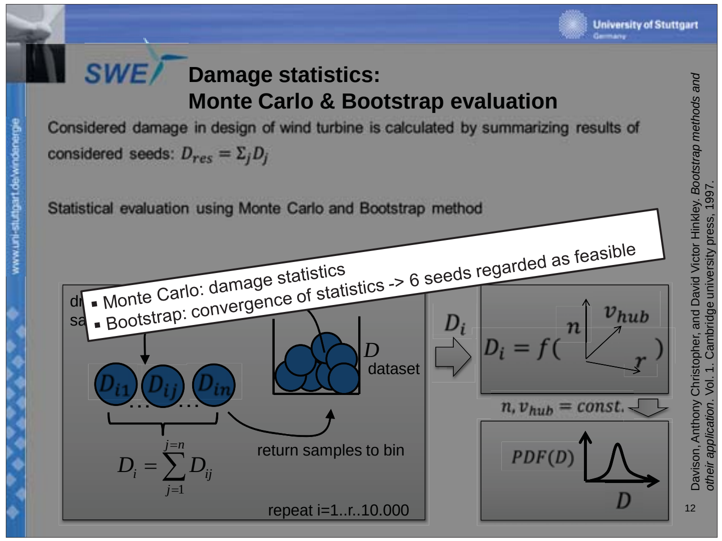
University of Stuttgart
Germany
SWE
Damage statistics:
Monte Carlo & Bootstrap evaluation
Considered damage in design of wind turbine is calculated by summarizing results of considered seeds: $D_{res} = \Sigma_j D_j$
Statistical evaluation using Monte Carlo and Bootstrap method
▪ Monte Carlo: damage statistics
▪ Bootstrap: convergence of statistics -> 6 seeds regarded as feasible
D_{i1} D_{ij} D_{in}
D dataset
$D_i = \sum_{j=1}^{j=n} D_{ij}$
return samples to bin
repeat i=1..r..10.000
D_i
$D_i = f(n, v_{hub}, r)$
$n, v_{hub} = const.$
$PDF(D)$
D
Davison, Anthony Christopher, and David Victor Hinkley. Bootstrap methods and their application. Vol. 1. Cambridge university press, 1997.
www.uni-stuttgart.de/windenergie
12

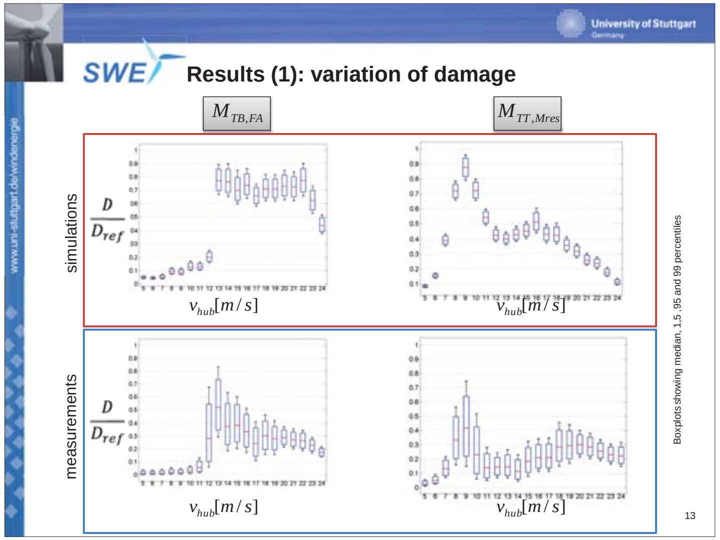
University of Stuttgart
Germany
SWE
Results (1): variation of damage
$M_{TB,FA}$
$M_{TT,Mres}$
simulations
measurements
$\frac{D}{D_{ref}}$
$v_{hub}[m/s]$
Boxplots showing median, 1,5, 95 and 99 percentiles
www.uni-stuttgart.de/windenergie
13

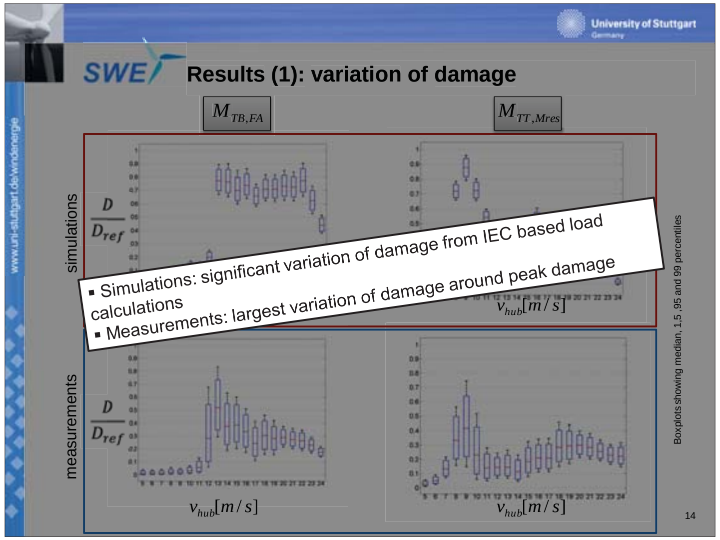
University of Stuttgart
Germany
SWE
Results (1): variation of damage
$M_{TB,FA}$
$M_{TT,Mres}$
simulations
measurements
$\frac{D}{D_{ref}}$
$v_{hub}[m/s]$
▪ Simulations: significant variation of damage from IEC based load calculations
▪ Measurements: largest variation of damage around peak damage
Boxplots showing median, 1,5, 95 and 99 percentiles
www.uni-stuttgart.de/windenergie
14

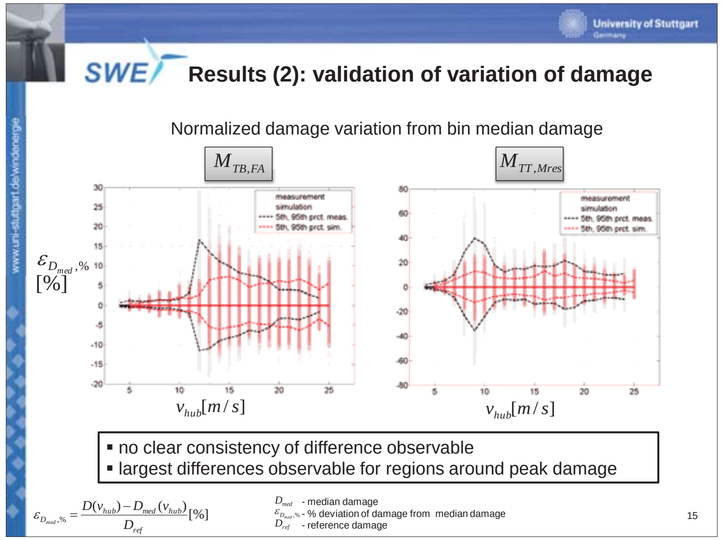
University of Stuttgart
Germany
SWE
Results (2): validation of variation of damage
Normalized damage variation from bin median damage
$M_{TB,FA}$
$M_{TT,Mres}$
$\varepsilon_{D_{med},\%}$ [%]
measurement
simulation
5th, 95th prct. meas.
5th, 95th prct. sim.
$v_{hub}[m/s]$
▪ no clear consistency of difference observable
▪ largest differences observable for regions around peak damage
$\varepsilon_{D_{med},\%} = \frac{D(v_{hub}) - D_{med}(v_{hub})}{D_{ref}}[\%]$
D_{med} - median damage
$\varepsilon_{D_{med},\%}$ - % deviation of damage from median damage
D_{ref} - reference damage
www.uni-stuttgart.de/windenergie
15

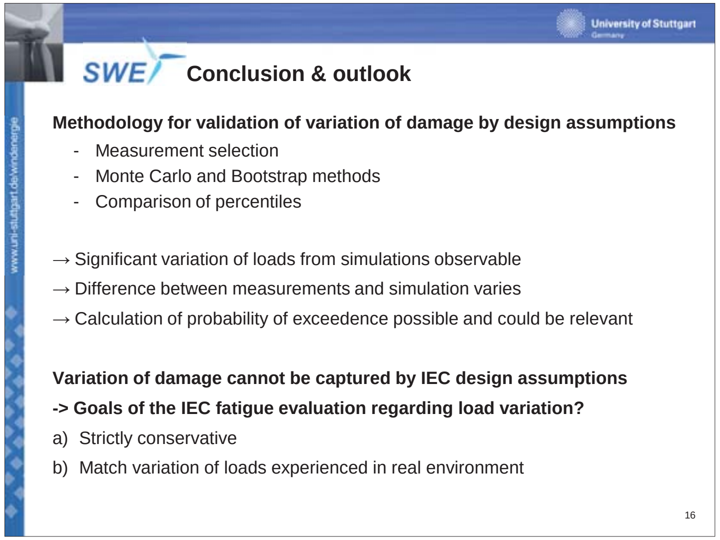
University of Stuttgart
Germany
SWE
Conclusion & outlook
Methodology for validation of variation of damage by design assumptions
- Measurement selection
- Monte Carlo and Bootstrap methods
- Comparison of percentiles
→ Significant variation of loads from simulations observable
→ Difference between measurements and simulation varies
→ Calculation of probability of exceedence possible and could be relevant
Variation of damage cannot be captured by IEC design assumptions
-> Goals of the IEC fatigue evaluation regarding load variation?
a) Strictly conservative
b) Match variation of loads experienced in real environment
www.uni-stuttgart.de/windenergie
16


University of Stuttgart
Germany
SWE
Acknowledgement
Thank you for your attention
This research is part of the RAVE projects OWEA - "Verification of offshore wind turbines" and OWEA Loads.
It is funded by the Federal Ministry for the Economic Affairs and Energy (BMWi).
[wikipedia.org/wiki/Windmessmast]
RAVE
RESEARCH AT ALPHA VENTUS
Federal Ministry for Economic Affairs and Energy
WindForS
Wind Energy Research Alliance
www.uni-stuttgart.de/windenergie
17

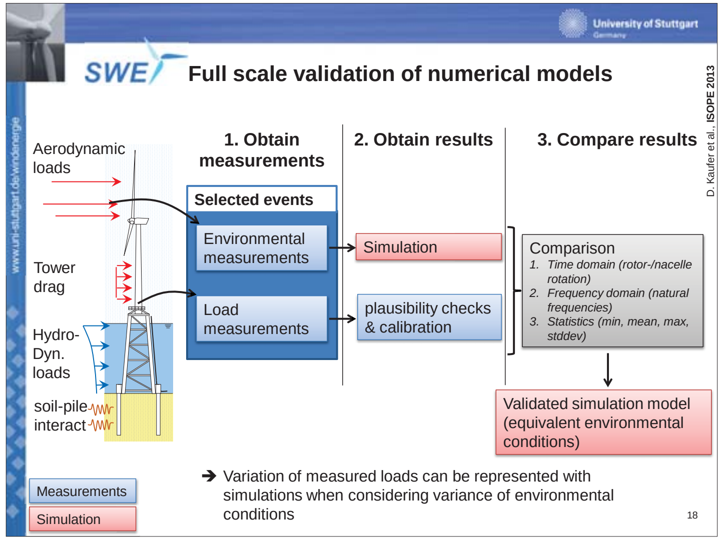
University of Stuttgart
Germany
SWE
Full scale validation of numerical models
D. Kaufer et al., ISOPE 2013
Aerodynamic loads
Tower drag
Hydro-Dyn. loads
soil-pile interact
1. Obtain measurements
2. Obtain results
3. Compare results
Selected events
Environmental measurements
Load measurements
Simulation
plausibility checks & calibration
Comparison
1. Time domain (rotor-/nacelle rotation)
2. Frequency domain (natural frequencies)
3. Statistics (min, mean, max, stddev)
Validated simulation model (equivalent environmental conditions)
Measurements
Simulation
➔ Variation of measured loads can be represented with simulations when considering variance of environmental conditions
www.uni-stuttgart.de/windenergie
18

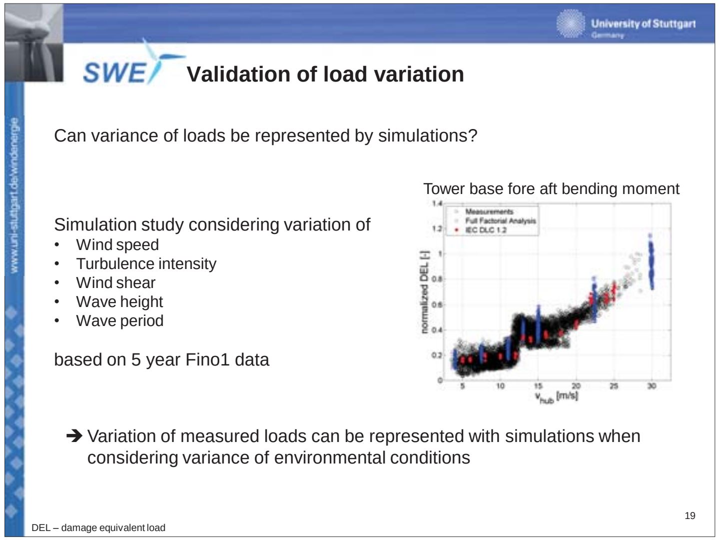
University of Stuttgart
Germany
SWE
Validation of load variation
www.uni-stuttgart.de/windenergie
Can variance of loads be represented by simulations?
Tower base fore aft bending moment
Simulation study considering variation of
Wind speed
Turbulence intensity
Wind shear
Wave height
Wave period
based on 5 year Fino1 data
Measurements
Full Factorial Analysis
IEC DLC 1.2
normalized DEL [-]
v_hub [m/s]
➔ Variation of measured loads can be represented with simulations when considering variance of environmental conditions
19
DEL – damage equivalent load

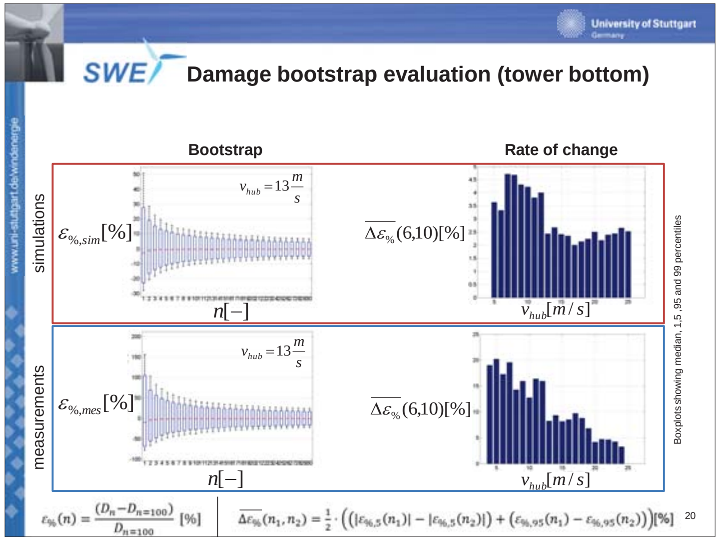
University of Stuttgart
Germany
SWE
Damage bootstrap evaluation (tower bottom)
www.uni-stuttgart.de/windenergie
Bootstrap
Rate of change
simulations
measurements
$\varepsilon_{\%,sim}[\%]$
$\varepsilon_{\%,mes}[\%]$
$v_{hub} = 13\frac{m}{s}$
$n[-]$
$\overline{\Delta\varepsilon_{\%}}(6,10)[\%]$
$v_{hub}[m/s]$
Boxplots showing median, 1,5 ,95 and 99 percentiles
$\varepsilon_{\%}(n) = \frac{(D_n - D_{n=100})}{D_{n=100}}[\%]$
$\overline{\Delta\varepsilon_{\%}}(n_1,n_2) = \frac{1}{2}\cdot\left(\left(|\varepsilon_{\%,5}(n_1)| - |\varepsilon_{\%,5}(n_2)|\right) + \left(\varepsilon_{\%,95}(n_1) - \varepsilon_{\%,95}(n_2)\right)\right)[\%]$
20

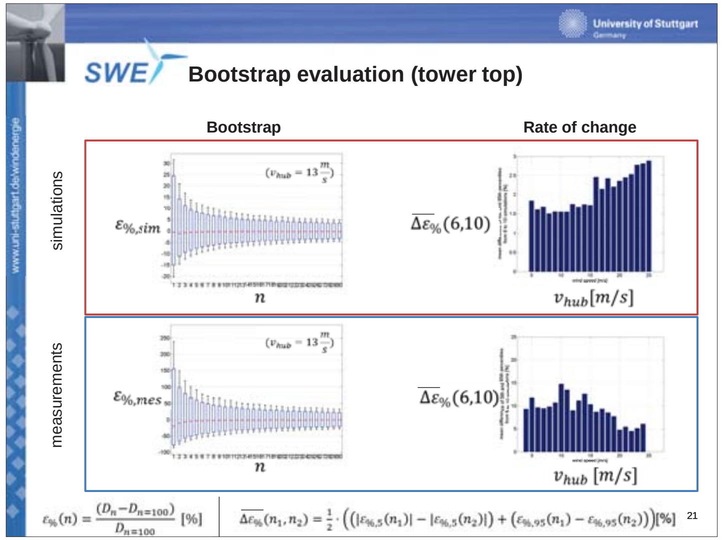
University of Stuttgart
Germany
SWE
Bootstrap evaluation (tower top)
www.uni-stuttgart.de/windenergie
Bootstrap
Rate of change
simulations
measurements
$\varepsilon_{\%,sim}$
$\varepsilon_{\%,mes}$
$(v_{hub} = 13\frac{m}{s})$
n
$\overline{\Delta\varepsilon_{\%}}(6,10)$
$v_{hub}[m/s]$
$\varepsilon_{\%}(n) = \frac{(D_n - D_{n=100})}{D_{n=100}}[\%]$
$\overline{\Delta\varepsilon_{\%}}(n_1,n_2) = \frac{1}{2}\cdot\left(\left(|\varepsilon_{\%,5}(n_1)| - |\varepsilon_{\%,5}(n_2)|\right) + \left(\varepsilon_{\%,95}(n_1) - \varepsilon_{\%,95}(n_2)\right)\right)[\%]$
21

W2POWER enerOCEAN

EERA DeepWind 2016

Pedro Mayorga – President & CTO
EnerOcean S.L. (Málaga, Spain)

Experimental validation of the
W2Power Hybrid Floating Platform

Paper presented at EERA DeepWind 2016,
13th Deep Sea Offshore Wind R&D Conference, Trondheim (Norway), January 20th - 22nd 2016

W2POWER enerOCEAN

Outline
- EnerOcean introduction
- Future of offshore wind
- W2Power Technology Development:
  - MARINET Testing
  - W2Power Technology Development: Achieved TRL 3 and 4 in 2012-14 Validated TRL 5 at FloWave 2015
  - Video impressions from tank tests
- W2Power Advantages
- Ongoing developments

enerOCEAN **Future of offshore wind**

- Offshore wind will move to deep waters and worldwide deployment
- Floaters are the logical solution, as the oil & gas industry discovered
- Combined utilisation of wind & wave energy is an attractive prospect if done properly:
  - Large wave resource in many ocean areas
  - More hours of renewable energy production and better price (wind and wave are not always simultaneous, swell)
  - Better use of marine space (MSP)

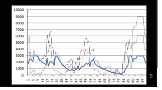

W2POWER enerOCEAN

Co-Authors:
- Jan HANSSEN, 1-Tech SPRL
- Reza HEZARI, Pelagic Power AS
- Tom DAVEY, Flowave TT;
- Jeff STEYNOR, Flowave TT;
- David INGRAM, The University of Edinburgh

Paper presented at EERA DeepWind 2016,
13th Deep Sea Offshore Wind R&D Conference, Trondheim (Norway), January 20th - 22nd 2016

enerOCEAN

- Lean R&D SME
- Specialised in Marine Energy Engineering
- Business scope:
  - from resource & feasibility studies to commercial exploitation
- Winner of numerous awards, tenders and funded projects
- Developer of W2Power hybrid offshore solution, together with Pelagic Power AS

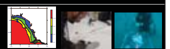

Competences:
- Offshore wind, wave and tidal energy
- Floating platform design
- Structural health/Condition monitoring
- Techno-economic modelling and financial viability assessment
- Integration into grid of offshore renewable energy and energy storage solutions
- Commercialisation of innovative solutions

MARINET

W2Power Technology development:
Sequential progress to TRL 3, 2012 – 2013 enerOCEAN

FP7 MARINET testing project: "W2P Sea States Tests 1 and 2",
- Facility: University of Edinburgh. Curved wave tank
- Tank testing in multi-directional sea states for design verification at 1:100 scale
- WEC's characterization and global behavior in operational and survival modes
- From TRL 2 ("Stage 1") to TRL 3 ("Stage 2") upon completion of all tests

MARINET

W2Power Technology: to TRL 4 enerOCEAN

FP7 Marinet testing project "W2P Mooring and wind" (2014)
- Facility: UCC-Beaufort (HMRC) – Cork, Ireland
- Tank testing in multi-directional sea states for performance validation at 1:100 scale with scaled-down full design of the mooring and wind force simulation.
- Compatibility with other economic activities on the platform (aquaculture).
- Specific test campaign on the validation of the WEC's (wave energy converters) and a new innovative control system developed, validated at 1:30 scale.
- TRL 4 achieved after validation of the main components individually

MARINET

W2Power Technology: to TRL 5 enerOCEAN

FP7 Marinet project: "W2P TRL5 Validation" (2015)
Facility: Univ. Edinburgh - FloWave TT: Current and Wave Test Tank
- 25 m diameter, 2 m deep. Allows testing W2Power at full 1:40 scale
- 168 force feedback wave makers, 28 reversible flow drive units
- 360º wave and current generation capability

MARINET

W2Power Technology: to TRL 5 enerOCEAN

- Flowave allows acurate reproduction of sea states, e.g. from EMEC site

Reproduction of sea states in the Tank

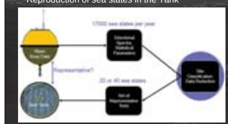

Desired Measured

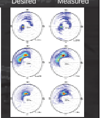

RESULTS

W2Power Technology: to TRL 5 enerOCEAN

Test programme Objectives:
- Fully achieve a Technology Readiness Level (TRL) of 5 for the W2Power platform
- Validation at 1:40 scale the full scale design, mooring and wind force simulation (thrust and gyroscopic effects). Corresponds to 80 m depth.
- Regular and irregular waves (based on real-sea data for Cabo Silleiro off NW Spain), currents (low-speed tidal, to 1 m/s) and wave spreading.
- Specific test campaign on the validation of wave converters' influence on the platform in the worst conditions, operational and survival modes limits.

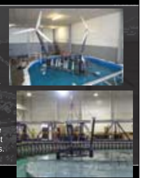

MARINET

W2Power Technology: to TRL 5 enerOCEAN

Configurations:
- Full platform with wind force, without Wave Energy Converters (WEC's)
- Full platform without wind force, without WEC's
- Full platform with max. wind force and WEC arrays in two configurations

Total 20 hours of test data collection, covering 77 regular wave tests and 36 irregular wave tests (normal and survival modes)

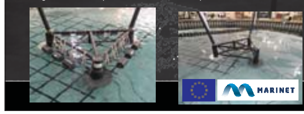

MARINET

W2Power Technology Development enerOCEAN

- EnerOcean introduction
- Future of offshore wind
- W2Power Technology Development:
  - MARINET Testing
  - W2Power Video: some scenes from the tank
- W2Power: Advantages
- Next stages

W2POWER 12

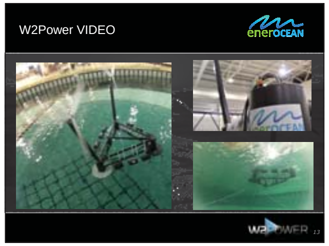
W2Power VIDEO
enerOCEAN
13

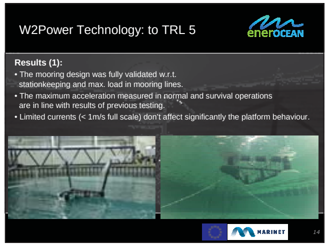
W2Power Technology: to TRL 5
enerOCEAN
Results (1):
• The mooring design was fully validated w.r.t. stationkeeping and max. load in mooring lines.
• The maximum acceleration measured in normal and survival operations are in line with results of previous testing.
• Limited currents (< 1m/s full scale) don't affect significantly the platform behaviour.
MARINET
14


W2Power Technology: to TRL 5
enerOCEAN
Results (2):
• The tests provided FloWave with an opportunity to test a large scale floating wind turbine model and to investigate wind systems for incorporating wind forces into the tests (motion control using system of lines and pulleys is an effective method).
• When the wind blows in a different direction than the wave angle, this does not significantly affect the wind power production.
15

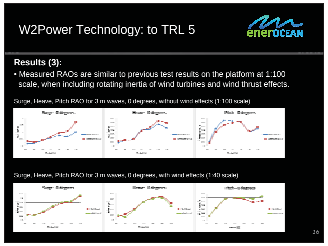
W2Power Technology: to TRL 5
enerOCEAN
Results (3):
• Measured RAOs are similar to previous test results on the platform at 1:100 scale, when including rotating inertia of wind turbines and wind thrust effects.
Surge, Heave, Pitch RAO for 3 m waves, 0 degrees, without wind effects (1:100 scale)
Surge, Heave, Pitch RAO for 3 m waves, 0 degrees, with wind effects (1:40 scale)
16

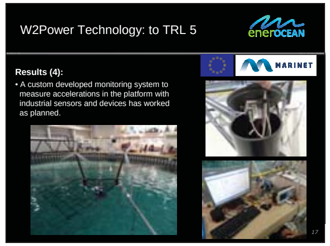
W2Power Technology: to TRL 5
enerOCEAN
MARINET
Results (4):
• A custom developed monitoring system to measure accelerations in the platform with industrial sensors and devices has worked as planned.
17


W2Power Technology Development
enerOCEAN
• MARINET Ambassador Users
– EnerOcean: Winner of Prize Category "Combined / Hybrid Technologies"
MARINET
MARINET
18

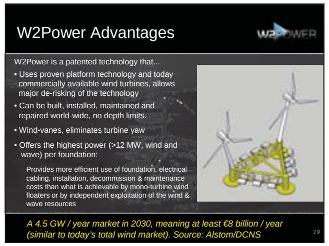
W2Power Advantages
W2Power is a patented technology that...
• Uses proven platform technology and today commercially available wind turbines, allows major de-risking of the technology
• Can be built, installed, maintained and repaired world-wide, no depth limits.
• Wind-vanes, eliminates turbine yaw
• Offers the highest power (>12 MW, wind and wave) per foundation:
Provides more efficient use of foundation, electrical cabling, installation, decommission & maintenance costs than what is achievable by mono-turbine wind floaters or by independent exploitation of the wind & wave resources
A 4.5 GW / year market in 2030, meaning at least €8 billion / year (similar to today's total wind market). Source: Alstom/DCNS
19

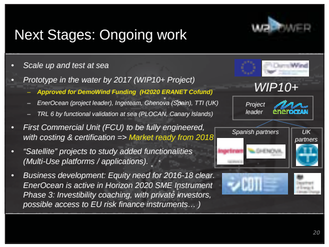
Next Stages: Ongoing work
• Scale up and test at sea
• Prototype in the water by 2017 (WIP10+ Project)
– Approved for DemoWind Funding (H2020 ERANET Cofund)
– EnerOcean (project leader), Ingeteam, Ghenova (Spain), TTI (UK)
– TRL 6 by functional validation at sea (PLOCAN, Canary Islands)
• First Commercial Unit (FCU) to be fully engineered, with costing & certification => Market ready from 2018
• "Satellite" projects to study added functionalities (Multi-Use platforms / applications).
• Business development: Equity need for 2016-18 clear. EnerOcean is active in Horizon 2020 SME Instrument Phase 3: Investibility coaching, with private investors, possible access to EU risk finance instruments…)
WIP10+
Project leader
enerOCEAN
Spanish partners
UK partners
20

POLITECNICO MILANO 1863

mecc

Unsteady Aerodynamics Of FOWT: Toward Experimental Validation Of Equivalent Lumped-element Models

Ilmas Bayati, Luca Bernini, Alberto Zasso

Department of Mechanical Engineering

2DoF Setup

- Polimi WT 2011 Test of Vestas V52 (may 2011)
- Surge imposed motion
- 1/25 geometric blade scale D=2.1m Ω=2.5Hz

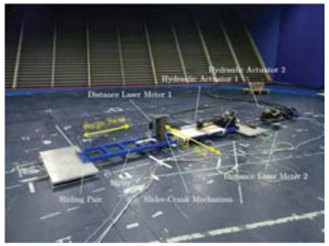

2DoF Setup experimental Session

- **Steady** configuration
- **Unsteady** configuration:
  Surge and Pitch Sine waves
  - **Wind/No Wind** measurements
  - Inertial Forces **subtraction**

Frequency (f)	[Hz]	0.2	0.4	0.6	1
Amplitude (A)	[mm]	10	20	40	80
Wind Speed (W)	[m/s]	4.5	5	5.5	6

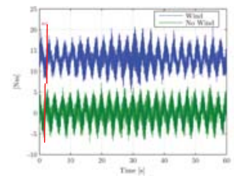

2DoF Setup Previous Experimental Session

- Aerodynamic Histeresis registered
- Dimension and shape of cycle depends on dynamic conditions
- **Does FAST/Aerodyn predict this behaviour?**

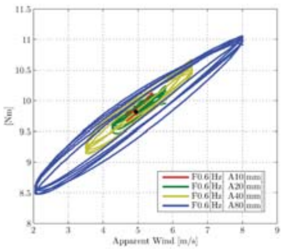

Example of histeretic cycles: aerodynamic pitch moment

Modelling Imposed Motion In FAST

User Input File

- Platform Dof: Surge and Pitch
- Additional Damping and Stiffness matrices

HydroDyn.dat

FAST 8 custom version
Definition of a control force at the tower's base to get an imposed motion

FORCE = K_add · (PtfmDisp − X) + C_add· (PtfmVel − XD)

HydroDyn_input.f90
HydroDyn_Types.f90
HydroDyn.f90

K_add and *C_add* :
parameters of the **oscillator**
f >10*f imposed motion
h =1

K_add and C_add (see FAST7/Seismic module)

FAST 8 Simulations

DYNIN

Generalized **D**ynamic **W**ake **(GDW)** = acceleration potential method

- Does not require iterative process
  - More **general pressure distribution** accross rotor
  - Fully nonlinear implementation: **turbulence and spatial variation of inflow**
  - **Inherent modelling** of:
    - Dynamic wake effect
    - Tip losses
    - Skewed wake

Accounting for **time lag** in the **induced velocity** created by vorticity shed from blades and convected downstream

Nomeclature

Experimental/Numerical test scheme

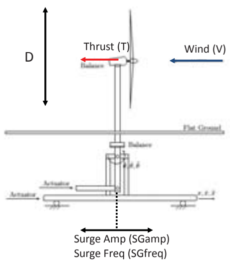

Variable definition

x → surge motion displacement

$\dot{x}$ → surge motion velocity

$V_A = V + \dot{x}$ → Apparent wind

$Ct = \dfrac{T}{0{,}5\rho V_a (\frac{\pi D^2}{4})}$ → Thrust coefficient

$TSR = \dfrac{\Omega D/2}{V}$ → Nominal tip speed ratio

tsr= $\dfrac{\Omega D/2}{V_A}$ → Effective tip speed ratio

Experimental vs Numerical results

Static thrust

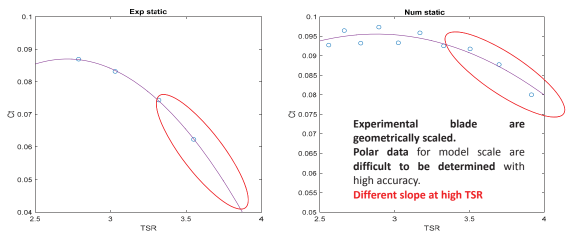

I.Bayati, L.Bernini, A.Zasso – Department of Mechanical Engineering POLITECNICO MILANO 1863

Experimental vs Numerical results

Dynamic results

- Surge motion frequency 0.4Hz
- Various amplitude

- Agreement Experimental & Numerical
  → Dissipative Hysteresis cycles
- Disagreement in the time delay value i.e.
  → amplitude of hysteresis cycles

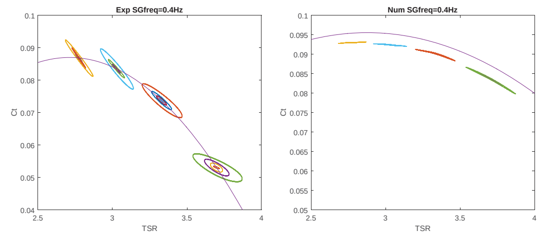

I.Bayati, L.Bernini, A.Zasso – Department of Mechanical Engineering POLITECNICO MILANO 1863

Experimental vs Numerical results

Dynamic results

- Surge motion frequency 0.6Hz
- Various amplitude

- Agreement Experimental & Numerical → Larger Hysteresis cycles
- GDW underestimates the hysteresis effects

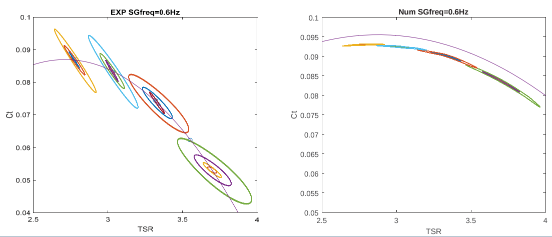

I.Bayati, L.Bernini, A.Zasso – Department of Mechanical Engineering POLITECNICO MILANO 1863

Lumped-element model: advantages

- SS model aero (control, integrated with hydro)
- Different parameters (wt verification) relationship with wind/sea states (nominal condition for simulations)
- Large wind farms control

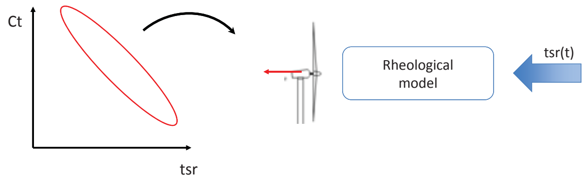

I.Bayati, L.Bernini, A.Zasso – Department of Mechanical Engineering POLITECNICO MILANO 1863

Proposed lumped model

Objective:
Model the unsteady turbine response to platform motion

Maxwell + Voigt

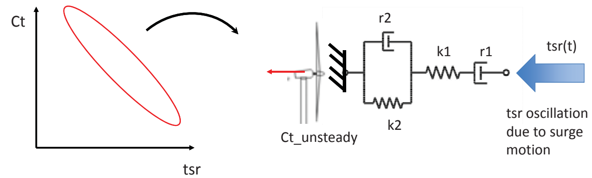

Ct=Ct_static(TSR)+Ct_unsteady(tsr)

I.Bayati, L.Bernini, A.Zasso – Department of Mechanical Engineering POLITECNICO MILANO 1863

Proposed lumped model

Good results for turbine thrust unsteady modelling both for numerical and experimental data.
Parameters identification is required

Example of experimental data prediction

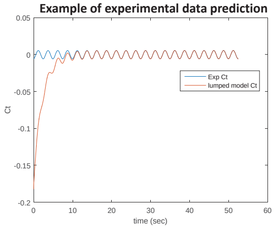

Example of numerical data prediction

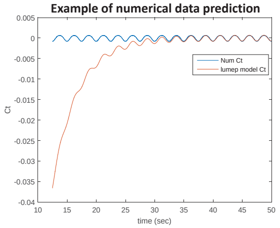

Lumped model identification

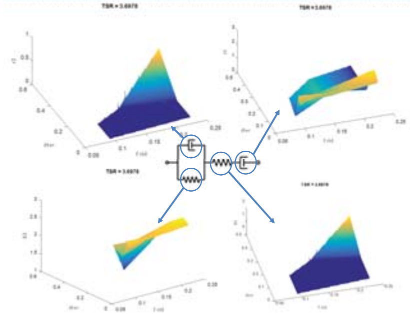

Lumped model parameter
Are identified via **quadratic error minimization** for each nominal TSR working condition.
Model parameters function of **reduced frequency and amplitude** of the surge motion

$$f_{rid} = \frac{SGfreq \cdot D/2}{V}$$

$$Amp_{tsr} = \frac{\Delta(tsr)}{2}$$

LIFES 50+ Project

2011 PoliMi tests

2016-17 PoliMi LIFES50+ tests

1st LIFES50+ deliverable for Polimi
is the validation of **steady/unsteady** AeroDyn for FOWT

The 2011 Polimi wind tunnel tests were used as preliminary set of data for the numerical and experimental comparison

LIFES50+ A novel hybrid real time approach (Hardware-In-The-Loop)

Aerodynamics (real) + Hydrodinamics (computed)

Aerodynamics (Computed) + Hydrodinamics (Real)

Force Input through controlled cables

- Less constrictive scaling issues
- Exploiting the advantages of each test facility

LIFES50+ Aeroelastic Model Blade Design: DTU 10 MW

PoliMi &DTU Airfoil Characterization
LowRe Wind Tunnel

Selig SD7032 Airfoil

LIFES50+ Aeroelastic Model Blade Design: DTU 10 MW

Aerodynamic Scaling

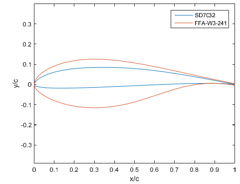

Different airfoil used in WT

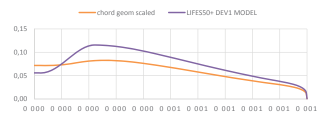

Model chord is different from the geometrically scaled.
Account for polar Reynolds dependency

LIFES50+

Design and verification Tools

Since LIFES50+ will be a multidisciplinary project (Aero, Hydro, Structural, Control,…). Advanced simulation tools both for design and verification are actually under implementation at Polimi.

- Fast (aero-servo-hydro)
- Adams (Multibody)
- AdWimo (AeroDyn+Adams)

Figure 1: Coupled flexible multibody model the robot and the FOWT.

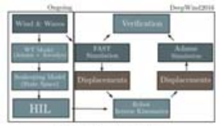

Figure 3: Numerical methodology.

A design support multibody tool for assessing the dynamic capabilities of a wind tunnel 6DoF/HIL setup ***. Belloli-Giberti-Fiore DeepWind Poster***

MARIN

Challenging wind and waves

Linking hydrodynamic research to the maritime industry

AERODYNAMIC DAMPING OF A HAWT ON A SEMISUBMERSIBLE

Effect of aerodynamic loading on the motions of the OC4-semi in waves

Sebastien Gueydon

EERA DeepWind'2016 conference, Trondheim

OUTLINE

- How MARIN is helping developers of floating wind turbines?
  - Model-tests
  - Simulations
- From 'concept design' to validated model 'Model of the model'
  - Example of the OC4-semisubmersible
  - Sensitivity to change in inertia
  - Sensitivity of the model to rotor force coefficients
- Conclusions
- Further work

FLOATING WIND AT MARIN

Model tests

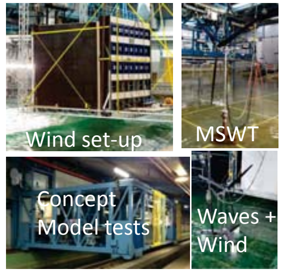

Scaled wind

Scaled thrust

Model of the model

Numerical studies

CFD for wind set-up, blades

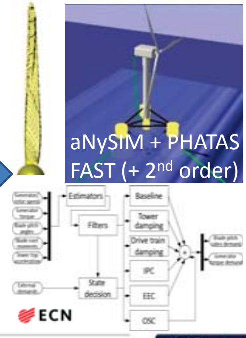

My objectives:
- R&D: What does matter for the floater?
- BU: Verification => Concept study

'MODEL OF A MODEL'

- A concept design evolves before and after the model-tests (different mass distribution, different turbine, etc…)
- A turbine is available for model-testing in wave and wind (but the actual wind turbine may be slightly different)
- While modeling wind & waves, a new scaling approach is followed ('performance scaling for the rotor'). This has an impact an the aerodynamic performance of the turbine.

⇒ Use model-test data to calibrate a numerical model = 'Model of the model'

⇒ What is the influence on the motions of a OFWT of all these differences?

MODEL OF THE OC4 SEMISUBMERSIBLE

- Differences?
  - (Design) OC4-SEMI
  - (Built) OC5-SEMI

⇒ "Model of the model"

Designation	Symbol	Unit	Values OC4 Calculated	Values OC5 As-built
Draft	T	m	20.0	20.0
Mass	M	ton	14,260	13,958
Centre of Gravity above keel	KG	m	9.96	11.93
Longitudinal metacentric height	GM_L	m	7.34	5.29
Roll radius of gyration in air	k_{xx}	m	32.07	32.63
Pitch radius of gyration in air	k_{yy}	m	32.94	33.38
Yaw radius of gyration in air	k_{zz}	m	31.83	31.32
Natural pitch period (moored)	T_θ	s	25.1	32.1
Natural heave period (moored)	T_z	s	17.0	17.2

CALCULATION PROCESS & POST-PROCESSING

Potential Flow | Equation of motions | Post-processing

- Mesh → DIFFRAC OC4 → aNySIM OC4-semi → Time-series
- Damping estimates
- Damping decay tests → aNySIM OC5-semi → Time-series
- Quadratic transfer functions
- Added-mass, Potential dpg, Wave load RAOs
- Time-series Plots
- Spectral Plots

POTENTIAL THEORY RESULTS IN WAVES

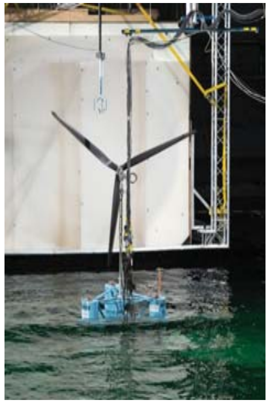

Load case:

- Long-crested waves
- JONSWAP Hs = 7.1 m Tp = 12.1 s

Comparison of simulations for:

A. *OC5 = calibrated model*
B. *OC4 = original 5MW*
C. *Measurements*

VERIFICATION OF HYDRODYNAMIC RESPONSE

- Operational sea, head waves

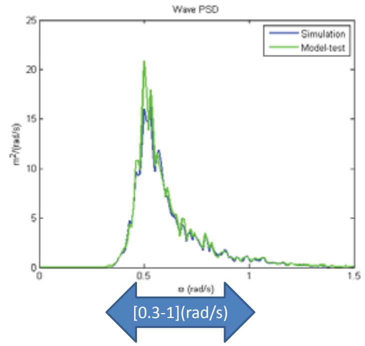

VERIFICATION OF HYDRODYNAMIC RESPONSE

- Operational sea, head waves

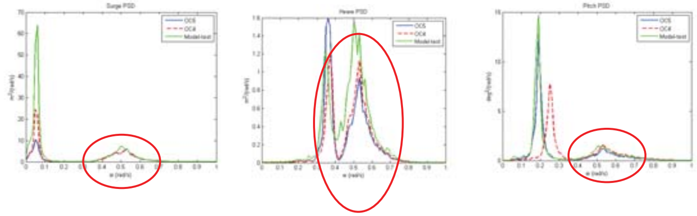

- Response in wave energy range (1st order) are similar

VERIFICATION OF HYDRODYNAMIC RESPONSE

- Operational sea, head waves

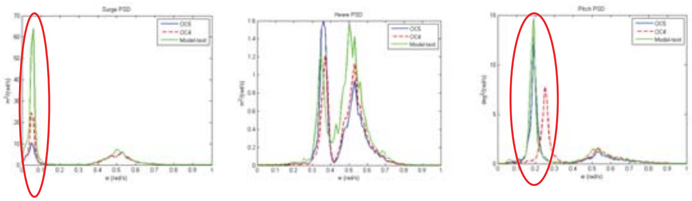

- Response in low frequency range (2nd order) are different
- Difference at resonance (surge, heave & pitch)

COMPARISON: MODEL OF THE MODEL

- OC5 Calibrated / OC4 Design / Model-test data

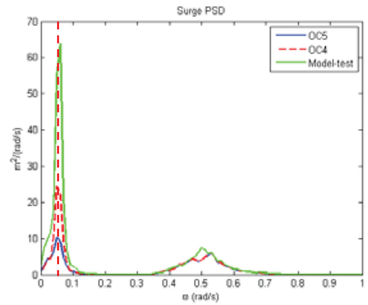

- Surge resonance peak of simulations are different and much smaller than in the model-test data.

COMPARISON: MODEL OF THE MODEL

- OC5 Calibrated / OC4 Design / Model-test data

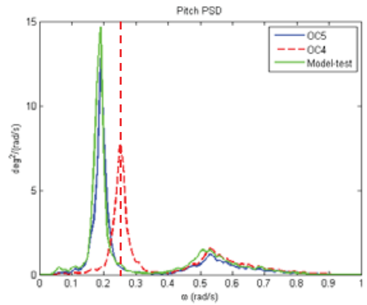

- Pitch resonance peak are different:
  - OC4 < model-test

BEMT RESULTS IN WAVES & WIND

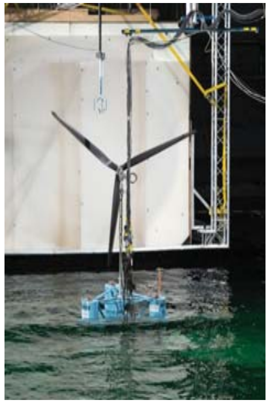

Load case:
- Co-linear waves and wind
- JONSWAP Hs = 7.1 m Tp = 12.1 s
- Wind speed V = 13 m/s
- Rotor fixed rpm = 12.1
- Blade pitch angle = 1 deg
  => TSR = 6.156

Comparison of simulations for:

A. OC4 design (XFOIL @ FS)
B. OC5 model (UMaine @ MS)
C. OC5 model (ECN RFOIL @ MS)

VERIFICATION OF RESPONSE IN WIND & WAVES

- Operational sea + steady wind, head waves

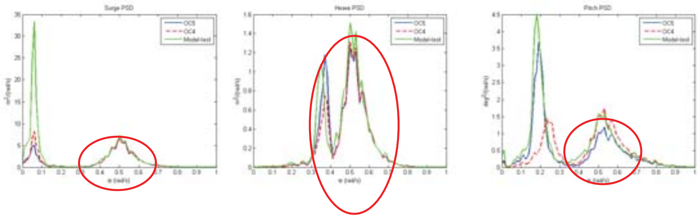

- Response in wave energy range (1st order)

VERIFICATION OF RESPONSE IN WIND & WAVES

- Operational sea + steady wind, head waves

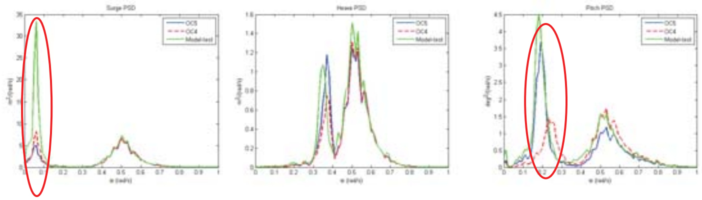

- Response in low frequency range (2nd order)

COMPARISON: MODEL OF THE MODEL

- OC5 Calibrated / OC4 Design / Model-test data

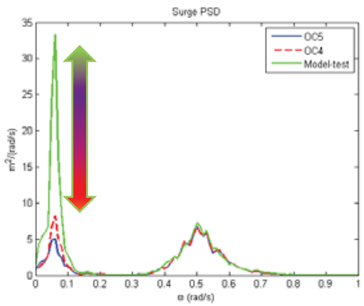

⇒ Less damping for the model-tests than the simulations

⇒ Effect mainly visible at resonance (slow drift 2nd order response)

COMPARISON: MODEL OF THE MODEL

- OC5 Calibrated / OC4 Design / Model-test data

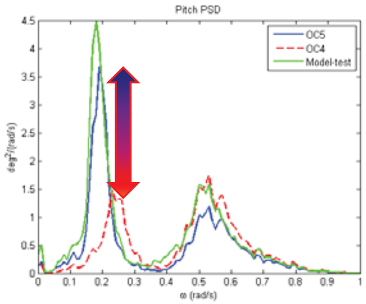

=> Less damping for the 'Model of the model' than the 'Design' case

COMPARISON: MODEL OF THE MODEL

- OC5 Calibrated / OC4 Design / Model-test data

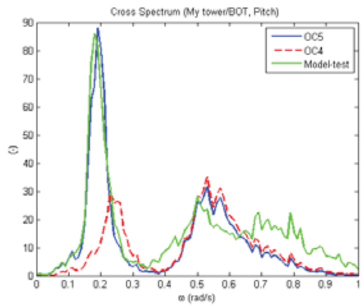

⇒ Correlation of pitch moment at tower foot and pitch motion

CALIBRATION OF THE ROTOR OF THE WIND TURBINE

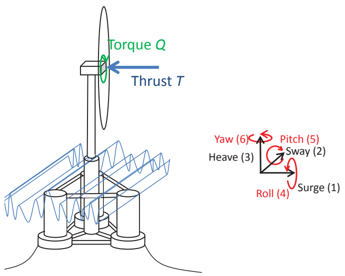

- Parallel wind and wave, no yaw
- Thrust acts mainly on
  - Surge
  - Pitch
- Test in a basin at scale 1/50 with a re-designed rotor that mimics the full scale rotor {Ct, (Cp)} for a range of TSR
- What are the {Cl, Cd}?

MARIN

CALIBRATION OF AERODYNAMIC LOAD COEFFICIENTS

- Optimization = vary {Cl, Cd} to match measured {Ct, Cp}

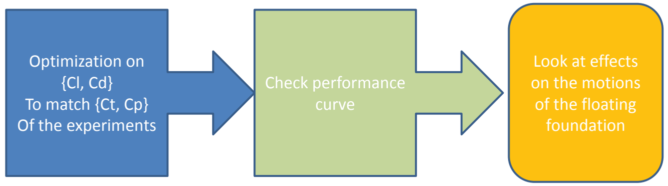

MARIN

LOOK AT THE DYNAMIC RESPONSE

- Simulation of a pitch decay test in steady wind (13 m/s)

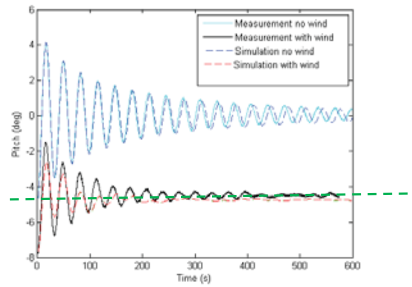

=> More damping for the 'Model of the model' than the model-test

MARIN

LOOK AT EFFECT OF {CL,CD} ON THE RESPONSE

- Simulation of a pitch decay test in steady wind (13 m/s) with other {Cl, Cd}

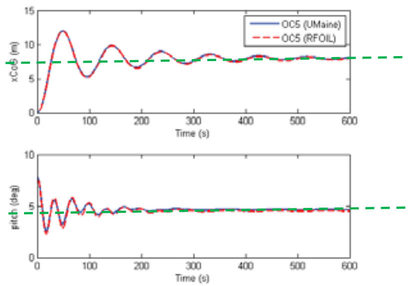

- Surge (and heave) are identical
- Less damping with **RFOIL** than **UMaine**

MARIN

LOOK AT EFFECT OF {CL,CD} ON THE RESPONSE

- Operational sea + steady wind (13 m/s), head waves
- **RFOIL** versus **UMaine** coefficients

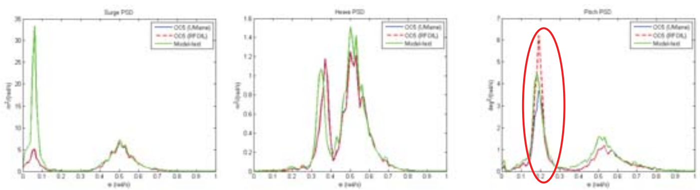

- Surge and heave are identical
- Different amplitudes of pitch resonance peak
- Less damping with **RFOIL** than **UMaine**

MARIN

CONCLUSIONS

Lessons learnt:

- OC5 and OC4 behave in similar ways (small differences)
- 'Model of the model' => learn about main physics at play
- Response to 2nd order wave loads in surge and pitch
- Rotor loads acts primarily on resonance peaks
- Aerodynamic damping is mainly effective on surge and **PITCH**
- Level of damping (aero + hydro) is important to know if a numeric model is conservative or not
- Further work necessary on the determination of the damping:
- Horizontal (hydrodynamics)
- Pitch (aerodynamics)
- Also on the wave loads (surge)

MARIN

THANK YOU

Acknowledgments:
Andrew Goupee (UMaine)
Feike Savenije (ECN) for the rotor coefficients
Umaine, NREL, DOE, Joop Helder (MARIN) for the OC5 model-tests
Dutch Economics Affairs for TO2 subsidies

MARIN
P.O. Box 28
6700 AA Wageningen
The Netherlands
T +31 317 49 39 11
F +31 317 49 32 45
E info@marin.nl
I www.marin.nl

X1) Online technology transfer network for wind energy research

No presentations available

X2) Numerical reference wind farms

NORCOWE Reference Wind Farm, Kristin Guldbrandsen Frøysa, director NORCOWE

NOWITECH Dogger Bank Reference Wind Farm, Karl Merz, SINTEF Energy Research

NORCOWE Reference Wind Farm

Kristin Guldbrandsen Frøysa, director NORCOWE
kristin@cmr.no

Main contributions to presentation: Angus Graham, Alla Sapronova, Thomas Bak, John Dalsgaard Sørensen, Mihai Florian and Masoud Asgarpour

Why NORCOWE Reference Wind Farm?

- In order to link the work in WP3 **- Design, installation and operation of offshore wind turbines**
- Better integration of the work in WP3 was a request from RCN after their mid-term evaluation of NORCOWE
- Idea: John Dalsgaard Sørensen, Aalborg University
- Development and use of NORCOWE RWF is integrated in NORCOWE's annual work plans
- NORCOWE RWF will be used in case studies in 2016 in NORCOWE
- NORCOWE RWF to be used in IEA Wind task 37 - **Wind Energy Systems Engineering: Integrated RD&D**

NORCOWE reference wind farm

- Developmental work on NORCOWE's reference wind farm (RWF) has taken place at Aalborg University and Uni Research.
- The RWF comprises a fictitious 800 MW wind farm at the location of the FINO3 met mast, 80 km west of the island of Sylt at the Danish-German border.
- The farm involves a set of 80 reference wind turbines and two substations.
- DTU's 10 MW reference wind turbine is the chosen turbine type, a variable-speed rotor of diameter 178 m and hub height 119 m.
- Foundations are monopiles: mean water depth at FINO3 is 22.5 m, soil type comprises medium dense to very dense sand deposits with gravel and silt constituents.
- There is a real wind farm at FINO3, DanTysk, owned by Vattenfall.

Development drivers

- Output from consultation
  - **Open**ly available / **realistic** / **challenging** / **neutral**
  - **Spacing:**
    - Along wind, 8D
    - Cross wind, 6-7D
    - Perimeter: 5D
  - The availability of relevant measurement data
  - The use of publicly available **ambitious** turbine model to simplify the use and increase the impact
  - **Quick** rather than optimal
  - Rule based

Baseline turbine layouts of the NORCOWE reference wind farm

- The main wind and wave climatology at the FINO3 site for use in the reference wind farm will follow from met-ocean reanalysis over an 11 yr period 2000-2010, with the final year also serving as a year for calibrating to wind and wave measurements at the site.
- A wind rose has been established from a co-distribution of wind speed and direction, essentially at hub height.

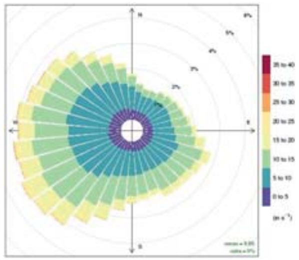

Baseline turbine layouts of the NORCOWE reference wind farm

- The co-distribution has been used to calculate the directional capacity factor.
- This is the expected power at some arbitrarily-picked moment from winds from within a sector of unit angle, as a function of sector centre-line angle, and expressed as a fraction of rated power.
- Integration of the directional capacity factor over 360° yields an overall capacity factor at FINO3 for a DTU reference turbine of 0.45.

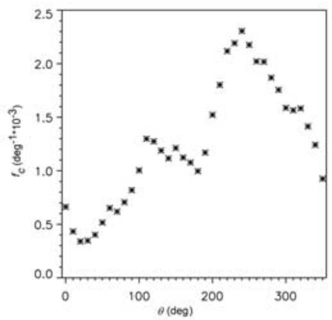

Baseline turbine layouts

- As the reference wind farm is fictitious, it does not have a defining zone associated with the licensing and site concession.
- We have decided not to use real bathymetry in the vicinity of FINO3, but to take the seabed there as flat, so bathymetry will not play a role in determining the shape or area of the farm.
- Instead we have used the directional capacity factor to arrive at a shape for the reference wind farm.
- The width of the shape along a line through the centroid scales with the expected power from winds blowing normally to this.The shape is thus periodic over 180°.

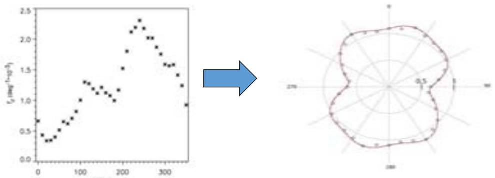

Baseline turbine layouts

- The shape is then filled with turbines spaced 5-8 rotor diameters apart, and the smallest area containing 82 installations is obtained.
- Along the perimeter, turbines are spaced 5 rotor diameters apart – there is thus “perimeter weighting”.
- Within the shape, turbines lie on a spiral (the involute of a circle).
- The centre of the spiral is offset from the shape centre normally to the leading axis of the shape, by a distance which depends on the elongation of the shape.
- Successive spiral arms are spaced 8 rotor diameters apart.
- Along the spiral, turbines are separated by a distance which depends on the elongation of the shape, working out at FINO3 at 6.5 rotor diameters.

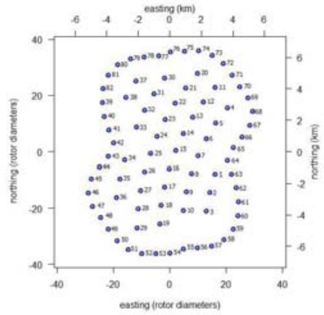

Baseline turbine layouts

Advantages of the baseline layout scheme:

- It follows rationally with a minimum of ad-hoc parameters from rules.
- The methodology is generic: it can be applied with an arbitrary wind climatology to arrive at the corresponding layout at any location of interest.
- Wake effects are implicitly taken into account.

Disadvantages

- Real-world considerations reflecting zone limits established in the licencing process, and site bathymetry, are not taken into account.
- The shape does not resemble that of any current offshore wind farm.

Baseline turbine layouts

It was decided to also determine a conventional, rectilinear, baseline layout.

- It has the same number of installations (82), within the same square area (a factor, 4105, times the rotor area).
- It is a symmetric arrangement of installations about the centroid of its enclosed area, a set of five rows aligned normally to the direction from which most power is available (the direction of the prevailing wind).
- Installation spacing along the minor axis (in the prevailing wind direction) is 8 rotor diameters, spacing along the major axis 6.7 rotor diameters.
- Spacings are thus very close to the corresponding values in the curvilinear case.

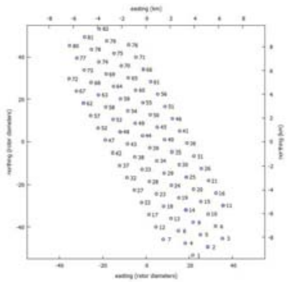

Use of the reference wind farm

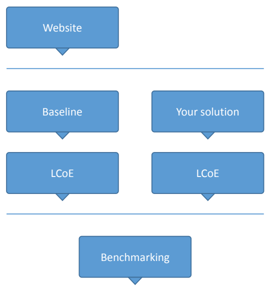

Overview, models and data

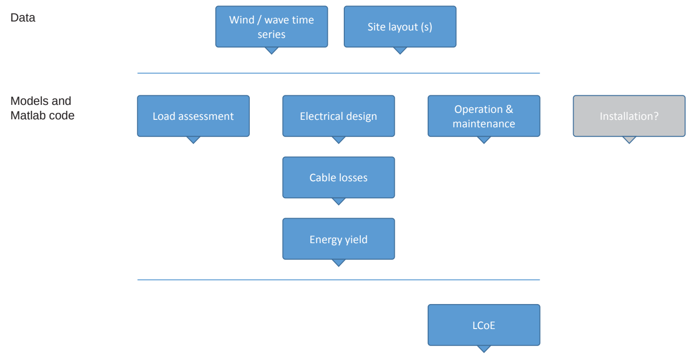

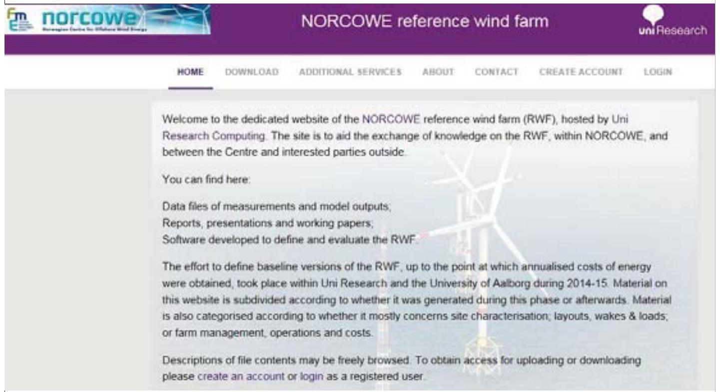

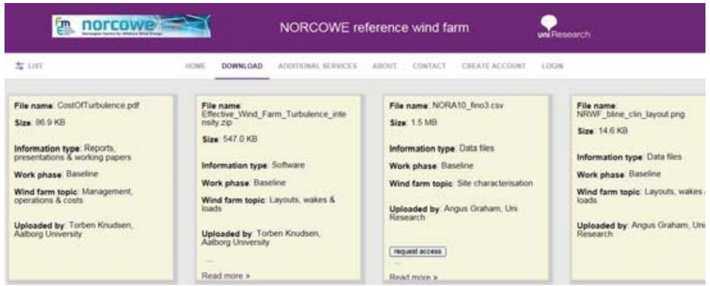

Operation and Maintenance Strategies for NORCOWE Wind Farm

Mihai Florian, Masoud Asgarpour, John Dalsgaard Sørensen
Aalborg University, Denmark

Photo: wallconvert.com

NORCOWE RWF – Baseline O&M model

AALBORG UNIVERSITY

Weather:
- FINO3 - 3 h wind and wave time series
  - Limiting factor for farm access

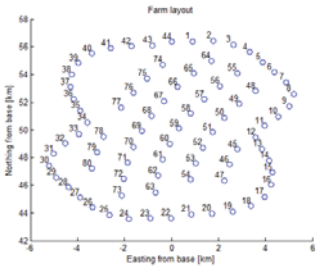

Failures:
- Generated from exponential distributions

Simulations:
- 11 years simulation with 3h resolution – 20 year design lifetime

NORCOWE RWF – Baseline O&M model

AALBORG UNIVERSITY

Corrective maintenance policy based partly on *

Failures in 3 categories and regular annual service :

	Minor Repair	Major Repair	Major Replacement	Annual Service
Frequency	6	1	0.1	1
Vessel	Crew transfer vessel	Crew transfer vessel	Heavy lift vessel	Heavy lift vessel
No. Technicians	3	3	6	3
Duration	6 [h]	18 [h]	48 [h]	35 [h]
Cost	61.200 [€]	530.000 [€]	3.000.000 [€]	140.000 [€]

- Spare parts available in stock
- 24 hired technicians working 12 h shifts a day
- Major replacements carried out in two 12 h shifts
- Failures lead to turbine shutdown
- Annual service carried out at start of each June

* Iain Dinwoodie, Ole-Erik V. Endrerud, Matthias Hofmann, Rebecca Martin, Iver Bakken Sperstad. 2014. "Reference cases for verification of offshore operation and maintenance simulation models for offshore wind farms".

NORCOWE RWF – Baseline O&M model

- 2 hired work boats (CTVs)
- HLV chartered for major replacements

	Crew Transfer Vessel (CTV)	Heavy-Lift Vessel (HLV)
Number	2	1
Limiting weather criteria	Wave 1.5 [m]	Wind / Wave 20 [m/s] / 2[m]
Mobilisation time	0	40 [days]
Mobilisation cost	0	680.000 [€]
Speed	20 [knots]	11 [knots]
Technician capacity	12	100
Day rate	3200 [€]	320000 [€]
Maximum offshore time	1 shift	Unlimited

NORCOWE RWF – LCoE – preliminary results

O&M cost	Availability
0.020 [€/kWh]	90.01[%]

Table 2.4.1: O&M cost and availability

Cost of Energy:

Component	Value
Turnkey	3300 [€/kW]
OPEX	0.022 [€/kW]
AEP	3981.3 [GWh]
r_c	8 [%]
r_p	6 [%]
T	20 [years]

Table 3: LCoE input

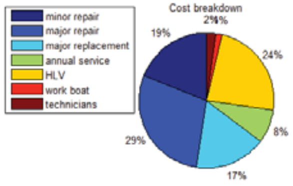

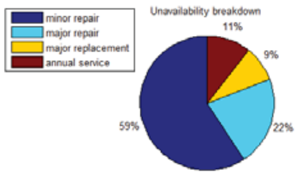

LCoE = 0.098 [€/kWh]

NORCOWE RWF – alternative Rectilinear layout

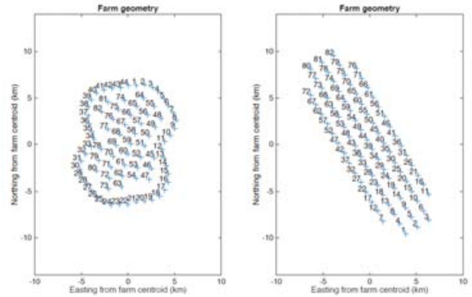

- slight difference in availability from vessel access – 0.2%

Results:

Layout	Annual O&M cost	Availability
Curvilinear	1.0564 10^8 [€]	90.01[%]
Rectilinear	1.0553 10^8 [€]	90.21[%]

Table 2.4.1: O&M cost and availability

NORCOWE RWF – Blade O&M

- Maintenance strategies:
  - Corrective maintenance
  - Preventive maintenance – incl. inspections
- Damage model
  - Example: bondline failures
  - Calibrated to observed failure rates
- Inspection reliability model

Blade O&M model for wind turbine blades Results

	Without inspections	With inspections
O&M cost [€/kWh]	0.020	0.0188
Availability [%]	90.01	90.45

Table 4.1: O&M cost

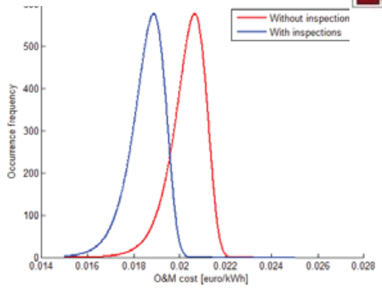

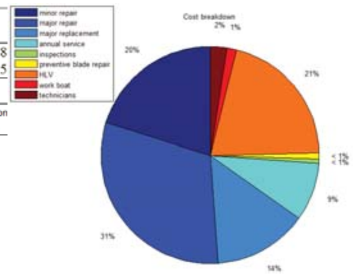

Key parameters and more information

- Reference zone: FINO3
- Installed capacity: 800 MW
- Number of turbines: 80
- Turbine: DTU 10 MW turbine, rotor* 178m, hub height 119m
- Water depth / foundations is not in the initial focus – 22 meter, monopole
- More information
  - NORCOWE 2014 annual report
  - Science meets industry (SMI) Bergen 2015
  - https://rwf.computing.uni.no/

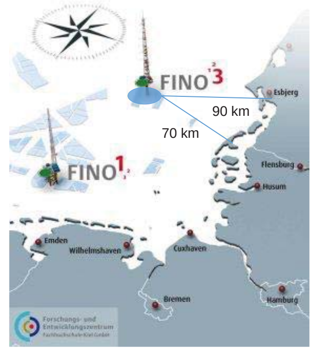

Upcoming NORCOWE events

- Science meets industry , Stavanger 6th April
  - At the conference the main focus areas will be turbulence and Hywind Scotland, with presentations from the University of Stavanger, Statkraft, Statoil and MacGregor. In addition we will have two presentations regarding decision support software, including the award winning Endrerud who started the company Shoreline in 2014. The conference is free of charge.
- NORCOWE 2016, Bergen 14-15 September
  - The conference will take place in Bergen on September 14-15, 2016. The first day of the conference aims to showcase the highlights of NORCOWE's research and to look at the impact of the FME centre. Day two will delve more into technical details, with two parallel sessions exploring themes like turbulence, wind farm layout and operation and maintenance. Poster sessions will take place on both days. The concluding conference is free of charge and open to the public.
  - On Friday September 16 NORCOWE organizes a trip to visit Midtfjellet wind farm and the ship yard Fjellstrand.

Dogger Bank Reference Wind Power Plant: Layout, Electrical Design, and Wind Turbine Specification

Karl O. Merz
SINTEF Energy Research
January 21, 2016

Acknowledgements:
JOG Tande (SINTEF), OG Dahlhaug (NTNU), R Nilssen (NTNU),
B Haugen (NTNU), H Kirkeby (SINTEF), L Eliassen (Statkraft/NTNU)

Documentation

Dogger Bank wind power plant

Merz KO. Turbine placement in the NOWITECH Reference Windfarm. Memo AN 14.12.09, SINTEF Energy Research, 2014.

Kirkeby H. NOWITECH Reference Windfarm electrical design. Memo AN 14.12.15, SINTEF Energy Research, 2014.

Brantsæter H, Årdal AR. Dogger Bank Reference Windfarm AC design. Memo AN 14.12.42, SINTEF Energy Research, 2014.

Direct-drive 10 MW wind turbine

Bak C, *et al*. Description of the DTU 10 MW Reference Wind Turbine. DTU Wind Energy Report-I-0092, 2013.

Hansen MH, Henriksen LC. Basic DTU Wind Energy Controller. DTU Wind Energy Report E-0028, 2013.

Merz KO. Pitch actuator and generator models for wind turbine control system studies. Memo AN 15.12.35, SINTEF Energy Research, 2015.

Merz KO. Design verification of the drivetrain, support structure, and controller for a direct-drive version of the DTU 10 MW Reference Wind Turbine. Memo AN 15.12.68, SINTEF Energy Research, 2015.

DTU 10 MW wind turbine (+ NOWITECH 10 MW nacelle), offshore foundation

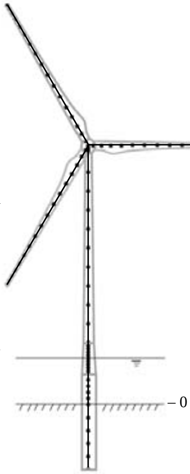

Tower +40 to +145 m
Stiffened w.r.t. onshore design
approx. 900 tonnes

Transition piece +20 to +40 m
approx. 600 tonnes

30 m water depth

Monopile, -42 m to +20 m
9 m diameter
approx. 1500 tonnes

Dogger Bank seabed profile

Direct-drive nacelle assembly

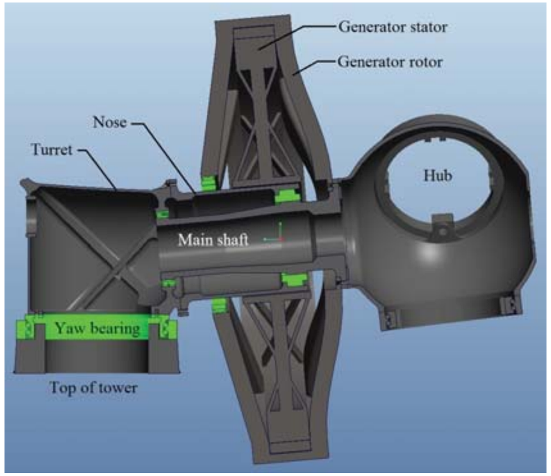

Generator

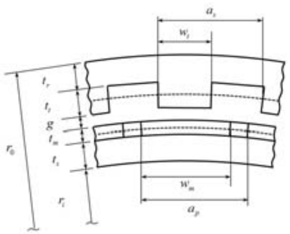

r_0	6030.2
r_i	5843.2
g	10.0
t_s	59.9
t_m	20.0
t_t	43.3
t_r	53.8
w_t	86.3
w_m	169.2
a_s	172.6
a_p	188.0

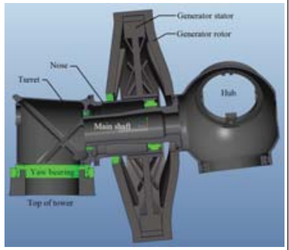

Generator

Parameter	Value	Units	Comments
P_r	10	MW	Rated power at generator terminals. Increased from 9.6 MW.
Ω_r	1.005	rad/s	Rated speed of the wind turbine and generator.
$\Omega_{cut\text{-}in}$	0.628	rad/s	Cut-in speed of the wind turbine and generator.
f_e	9.9-15.8	Hz	Electrical frequency range. Modified from 6.6-21.4 Hz.
V_r	3500	V	Nominal RMS line voltage. Increased from 3235 V.
i_a	1926	A	Nominal RMS phase current. Reduced from 2025 A.
	321	A	Nominal RMS winding current; 6 parallel current paths.
	3.97	A/mm^2	Nominal RMS copper current density.
b	1.770	m	Stack length. Increased from 1.218 m.
g	0.010	m	Air gap width.
n_p	198		Number of poles.
n_s	216		Number of slots.
N	23		Number of turns per winding.
	0.5		Copper fill factor = copper area/winding area of the cross-section.
R	0.0366	Ω	Phase resistance.[5] Increased from 0.0260 Ω.
L_a	5.29	mH	Phase inductance. Increased from 3.64 mH.
B_m	1.2	T	Residual magnetic field strength in magnets.
λ_k	4.47	Wb	Amplitude of winding flux due to magnets. Increased from 3.08 Wb.
	0.18		Fraction of rated resistive losses assumed for no-load losses.[6]
m_g	240	tonnes	Estimated total generator mass.[7] Increased from 200 tonnes.
η	0.954		Efficiency at rated power and speed.

Control: DTU Basic Wind Energy Controller

$V_\infty \le 7$ m/s

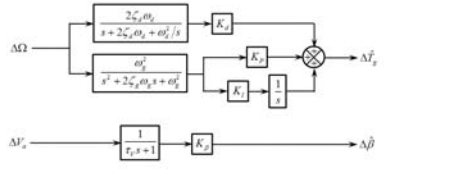

Variable-speed regime

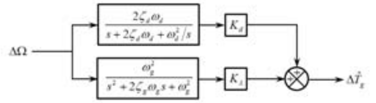

Above-rated

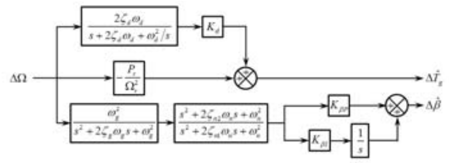

Dynamic verification of the 10 MW wind turbine

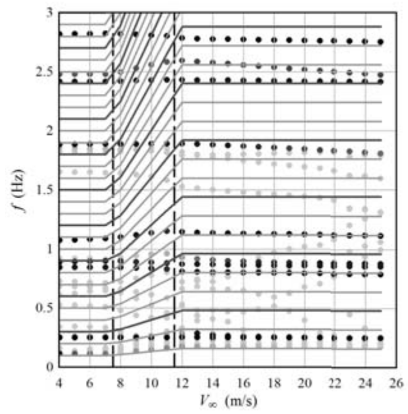

Dogger Bank Wind Power Plant

Dogger Bank – Creyke Beck A

Base case for further trade studies

1.2 GW, 120 10 MW turbines, DTU rotor, 178.3 m diameter

Electrical designs:

Baseline: 33 kV collection grid, three MV/HV substations, HVDC to shore

Upcoming technology: 66 kV collection grid, eliminate substations, HVDC to shore

Alternative: 66kV/220kV HVAC transmission

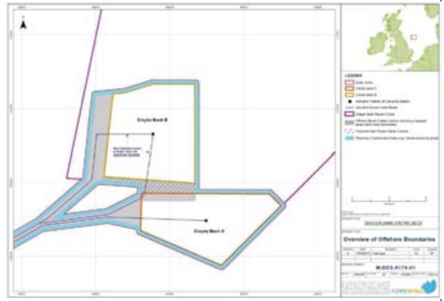

Forewind Consortium; *Dogger Bank Creyke Beck Environmental Statement: Chapter 5, Project Description.* 2013.

Creyke Beck A depth and cost trends

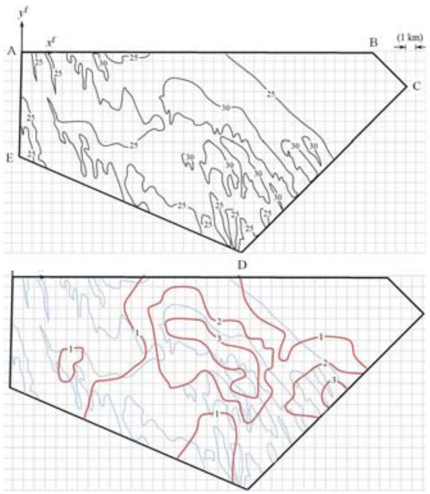

Creyke Beck A constraints

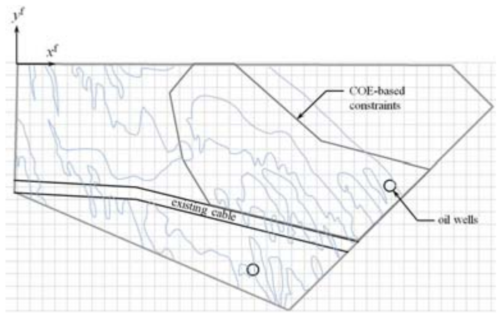

DRW Layout

Roughly 10*D* spacing

Curved rows/columns to reduce sensitivity to wind direction

Electrical: Three blocks of 40 turbines, substations "in-pattern" for ease of navigation

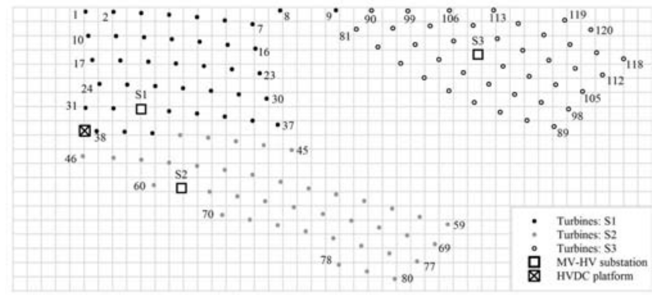

A comparison of layouts

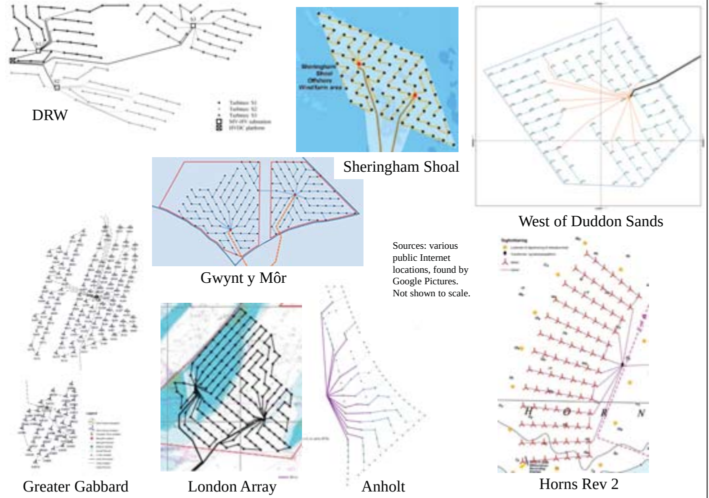

Hub-height windspeeds computed with Viper 2D boundary-layer analysis

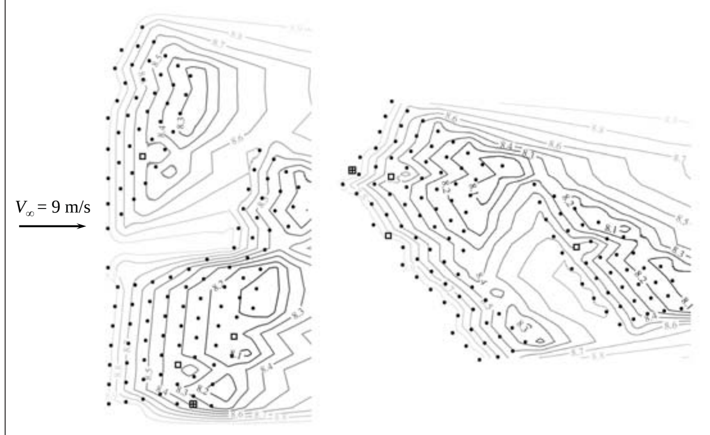

AEP computed by Viper

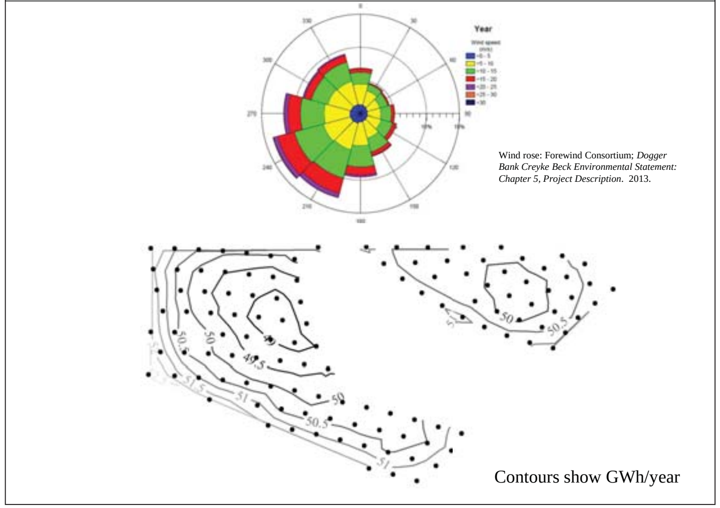

Wind rose: Forewind Consortium; *Dogger Bank Creyke Beck Environmental Statement: Chapter 5, Project Description*. 2013.

AEP versus spacing

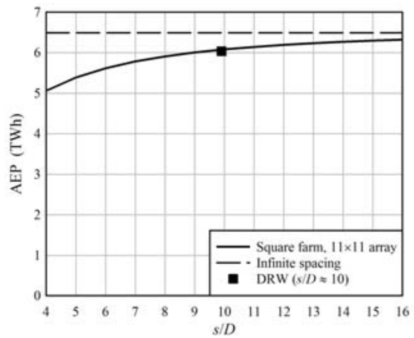

Hypothesis: For wind farms with relatively uniform spacing, AEP depends primarily upon the spacing and not the shape of the outer boundary.

Have we chosen a good turbine spacing?

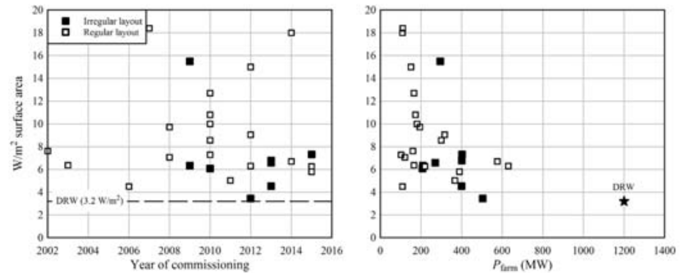

Hypothesis: Global (atmospheric boundary-layer) wake effects drive up the characteristic *s/D* spacing between turbines in very large wind farms, if area is not the primary constraint.

Hypothesis: Diminishing per-turbine costs of marine operations make higher turbine densities economical in "small" wind farms.

What effect does the areal cost of the offshore sector have on the optimal turbine density? Are coastal waters worth more than those far offshore like Dogger Bank?

It is relatively easy to rescale the existing pattern (depart from the "actual" Creyke Beck case).

Turbines per string selected by a parametric study

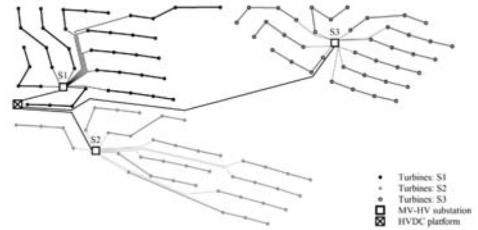

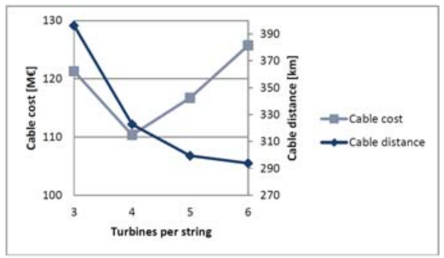

Kirkeby H; NOWITECH Reference Wind Farm Electrical Design; Memo AN 14.12.15, Sintef Energy Research, 2014

66kV AC to HVDC, eliminate substations

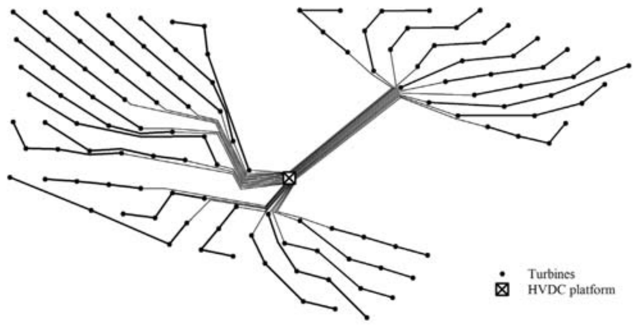

Kirkeby H; NOWITECH Reference Wind Farm Electrical Design; Memo AN 14.12.15, Sintef Energy Research, 2014

Electrical: Voltage and substations

Internal grid lifecycle costs

Infrastructure		33 kV Specification	33 kV Price [M€]	66 kV Specification	66 kV Price [M€]
WTG	Switchgear	120x	7,87	120x	10,88
Cables	Cables LV	396 km 33kV	130,37	328 km 66kV	91,55
	Cables HV	128,67 km 132 kV	128,70	128,67 km 132 kV	128,70
	Deployment	MV & HV	19,20	MV & HV	17,90
Substation	Platform	3x 66/132 kV	92,40	3x 66/132 kV	92,40
	Installation	18 days, 2 vessels	12,00	18 days, 2 vessels	12,00
Converter station	Switchgear	3x 132kV	2,76	3x 132kV	2,76
Energy losses	Losses	1 - 98.42 %	138,00	1 - 98.68 %	115,29
Total			531,30		471,48

Internal grid lifecycle costs

Infrastructure		With substation Specification	With substation Price [M€]	Without substation Specification	Without substation Price [M€]
WTG	Switchgear	120x	10,88	120x 66kV	10,88
Cables	Cables LV	328 km 66kV	91,55	490 km 66kV	154,22
	Cables HV	128,67 km 132 kV	128,70		
	Deployment	MV & HV	17,90	MV	16,65
Substation	Platform	3x 66/132 kV	92,40		
	Installation	18 days, 2 vessels	12,00		
Converter station	LV switchgear	3x 132kV	2,76	24x 66kV	2,18
Energy losses	Losses	1 - 98.68 %	115,29	1 - 99.34 %	57,65
Total			471,48		241,58

Kirkeby H; NOWITECH Reference Wind Farm Electrical Design; Memo AN 14.12.15, Sintef Energy Research, 2014

Link to IEA Task 37 on Wind Energy Systems Engineering

Task 2.1: Reference wind turbines
- Task 2.1.0: Specify a common data format for exchanging aeroelastic/control/electrical descriptions of onshore and offshore wind turbines, suitable for building models in typical wind turbine simulation programs.
- Task 2.1.1: 3 MW Low-wind Onshore Reference Turbine Development
  - Task 2.1.1.1: Design specifications for a 3.x MW reference wind turbine with a geared drivetrain, targeting the onshore/Class III market segment.
  - Task 2.1.1.2 Upscale an existing 2.4 MW direct-drive wind turbine design to the 3.x MW range using established procedures.
  - Task 2.1.1.3 Design the reference 3.x MW Class III geared wind turbine.
  - Task 2.1.1.4 Design review and approval by OEM industry participants (Nordex, Vestas, Siemens, GE and DNV GL)
- Task 2.1.2 10 MW offshore reference turbine with a direct-drive generator. (lead: SINTEF)
  - Task 2.1.2.1 ...

Task 2.2: Reference wind plants
- Task 2.2.0 Catalogue offshore and onshore wind plants where we know we have data and identify what types of data are available for each
- ...
- Task 2.2.4 Select and establish plant design criteria for a series of reference wind plants
- Task 2.2.5 Develop reference wind plant 1 (low-wind onshore site)
- Task 2.2.6 Develop reference wind plant 2 (high-wind offshore site)

Deliverables:
D2.1.1 Specifications document for the 3.x and 10 MW reference wind turbines
D2.1.2 Publication of the refined 3.x MW geared wind turbine design
D2.1.3 Publication of the refined 10 MW direct-drive wind turbine design
D2.2.1 Specifications document for the reference wind plants
D2.2.2 Publication of reference onshore plant 1
D2.2.3 Publication of reference offshore plant 2

Link to IEA Task 37 on Wind Energy Systems Engineering

Task 3.1: Benchmarking MDAO for wind turbines
- Task 3.1.1: Phase 1 benchmarks: Rotor only
  - 3.1.1a: Benchmarking of rotor aero only
  - 3.1.1b: Benchmarking of rotor aero and structure
- Task 3.1.2: Phase 2 benchmarks: full turbine
  - 3.1.2a Benchmarking of full turbine TBD

Task 3.2: Benchmarking MDAO for wind plants
- Task 3.2.1 Layout optimization onshore
- Task 3.2.2 Layout optimization offshore

(Tentative) Controls optimization
(Tentative) Electrical analysis and optimization
(Tentative) LCOE analysis and optimization (O&M)

Deliverables
D3.0.1: Online portal / information clearinghouse for MDAO research and software
D3.0.2: Report on benchmarking scope, process and evaluation criteria
D3.1.1: First turbine benchmark finalized and reported
D3.1.2: First plant benchmark finalized and reported
D3.2.1: Second turbine benchmark finalized and reported
D3.2.2: Second plant benchmark finalized and reported

Closing session – Strategic Outlook

DeRisk project on extreme wave loads, H. Bredmose, DTU

Type Validation for the SeaWatch Wind Lidar Buoy, V. Neshaug, Fugro OCEANOR

Increasing wind farm profit through integrated condition monitoring and control, Berit Floor Lund, Kongsberg Renewables

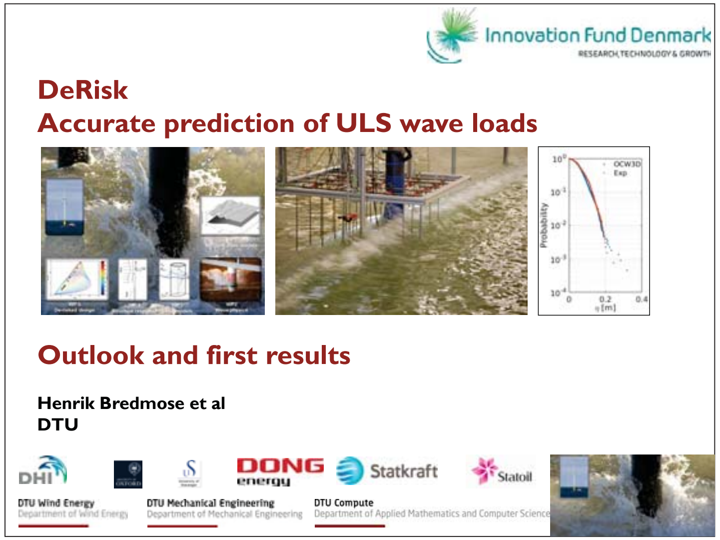
Innovation Fund Denmark
RESEARCH, TECHNOLOGY & GROWTH
DeRisk
Accurate prediction of ULS wave loads
Outlook and first results
Henrik Bredmose et al
DTU
DHI
DONG energy
Statkraft
Statoil
DTU Wind Energy
Department of Wind Energy
DTU Mechanical Engineering
Department of Mechanical Engineering
DTU Compute
Department of Applied Mathematics and Computer Science

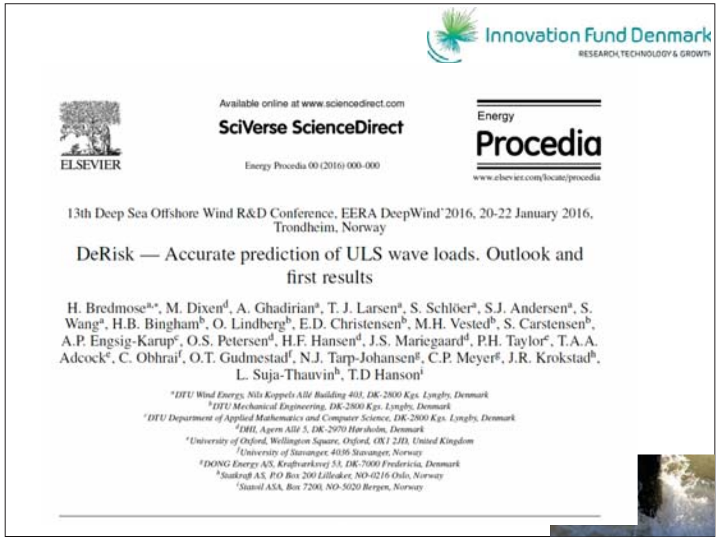
Innovation Fund Denmark
RESEARCH, TECHNOLOGY & GROWTH
ELSEVIER
Available online at www.sciencedirect.com
SciVerse ScienceDirect
Energy Procedia 00 (2016) 000-000
Energy
Procedia
www.elsevier.com/locate/procedia
13th Deep Sea Offshore Wind R&D Conference, EERA DeepWind'2016, 20-22 January 2016, Trondheim, Norway
DeRisk — Accurate prediction of ULS wave loads. Outlook and first results
H. Bredmose[a,*], M. Dixen[d], A. Ghadirian[a], T. J. Larsen[a], S. Schlöer[a], S.J. Andersen[a], S. Wang[a], H.B. Bingham[b], O. Lindberg[b], E.D. Christensen[b], M.H. Vested[b], S. Carstensen[b], A.P. Engsig-Karup[c], O.S. Petersen[d], H.F. Hansen[d], J.S. Mariegaard[d], P.H. Taylor[e], T.A.A. Adcock[e], C. Obhrai[f], O.T. Gudmestad[f], N.J. Tarp-Johansen[g], C.P. Meyer[g], J.R. Krokstad[h], L. Suja-Thauvin[h], T.D Hanson[i]
[a]DTU Wind Energy, Nils Koppels Allé Building 403, DK-2800 Kgs. Lyngby, Denmark
[b]DTU Mechanical Engineering, DK-2800 Kgs. Lyngby, Denmark
[c]DTU Department of Applied Mathematics and Computer Science, DK-2800 Kgs. Lyngby, Denmark
[d]DHI, Agern Allé 5, DK-2970 Hørsholm, Denmark
[e]University of Oxford, Wellington Square, Oxford, OX1 2JD, United Kingdom
[f]University of Stavanger, 4036 Stavanger, Norway
[g]DONG Energy A/S, Kraftværksvej 53, DK-7000 Fredericia, Denmark
[h]Statkraft AS, P.O Box 200 Lilleaker, NO-0216 Oslo, Norway
[i]Statoil ASA, Box 7200, NO-5020 Bergen, Norway


Innovation Fund Denmark
RESEARCH, TECHNOLOGY & GROWTH
H. Bredmose[a,*], M. Dixen[d], A. Ghadirian[a], T. J. Larsen[a], S. Schlöer[a], S.J. Andersen[a], S. Wang[a], H.B. Bingham[b], O. Lindberg[b], E.D. Christensen[b], M.H. Vested[b], S. Carstensen[b], A.P. Engsig-Karup[c], O.S. Petersen[d], H.F. Hansen[d], J.S. Mariegaard[d], P.H. Taylor[e], T.A.A. Adcock[e], C. Obhrai[f], O.T. Gudmestad[f], N.J. Tarp-Johansen[g], C.P. Meyer[g], J.R. Krokstad[h], L. Suja-Thauvin[h], T.D Hanson[i]
DHI
DONG energy
Statkraft
Statoil
DTU Wind Energy
Department of Wind Energy
DTU Mechanical Engineering
Department of Mechanical Engineering
DTU Compute
Department of Applied Mathematics and Computer Science


Innovation Fund Denmark
RESEARCH, TECHNOLOGY & GROWTH
4 years (2015-2019)
9 Partners
DHI
DONG energy
Statkraft
Statoil
DTU Wind Energy
Department of Wind Energy
DTU Mechanical Engineering
Department of Mechanical Engineering
DTU Compute
Department of Applied Mathematics and Computer Science
7 Advisory Board members
DNV·GL
RAMBØLL
DTU Wind Energy
Department of Wind Energy
DONG energy
Statkraft
Statoil
Funded by Innovation Fund Denmark, Statoil and in-kind
DeRisk – De-risking of ULS wave loads on offshore wind turbine structures

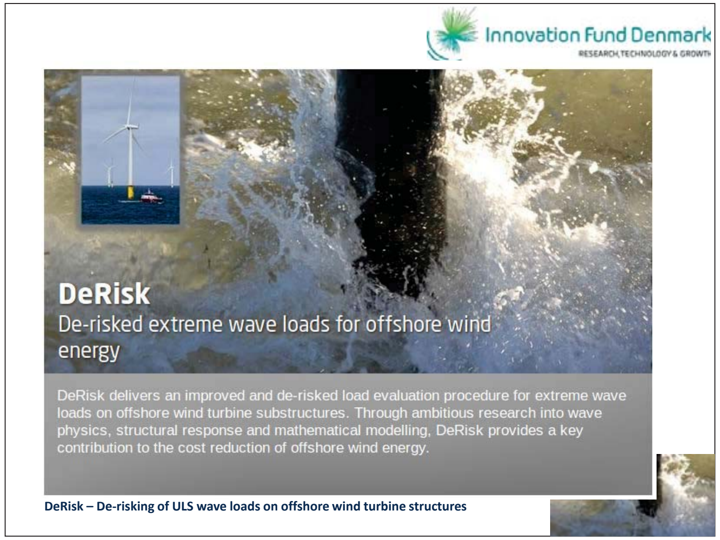
Innovation Fund Denmark
RESEARCH, TECHNOLOGY & GROWTH
DeRisk
De-risked extreme wave loads for offshore wind energy
DeRisk delivers an improved and de-risked load evaluation procedure for extreme wave loads on offshore wind turbine substructures. Through ambitious research into wave physics, structural response and mathematical modelling, DeRisk provides a key contribution to the cost reduction of offshore wind energy.
DeRisk – De-risking of ULS wave loads on offshore wind turbine structures


Outline
Innovation Fund Denmark
RESEARCH, TECHNOLOGY & GROWTH
Background
Opportunities
Elements of DeRisk
First results
DeRisk – De-risking of ULS wave loads on offshore wind turbine structures

Offshore wind energy

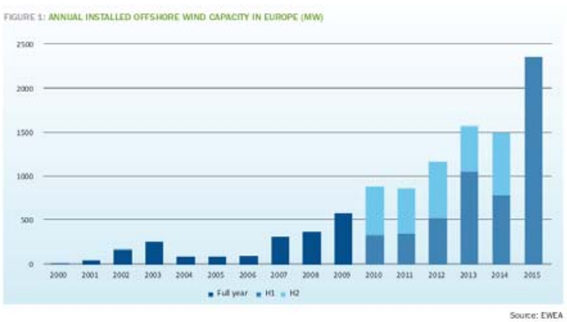

Graphics from www.ewea.com

Offshore wind energy

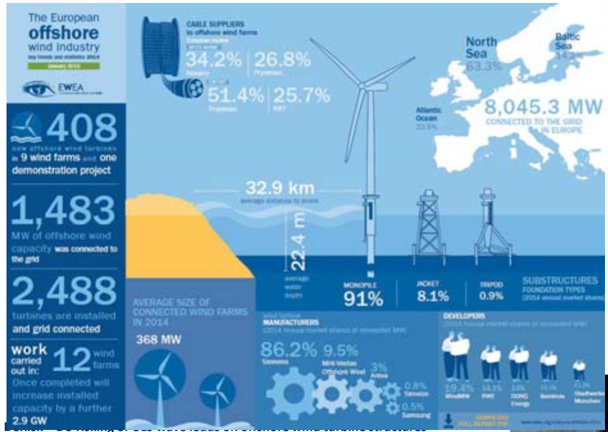

Graphics from www.ewea.com

How deep do we go?

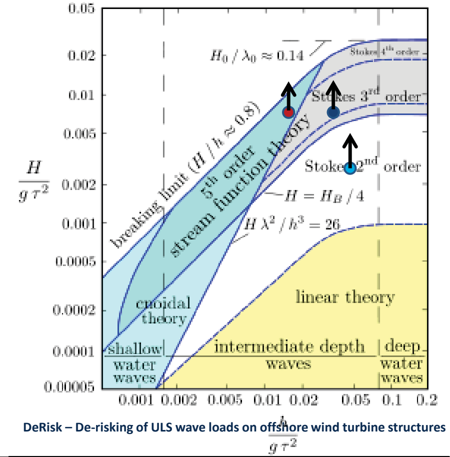

At h=22m depth

Operational
- Hs=1m; Tp=6s
- Hs=6m; Tp=9.5s

ULS
- Hs=9.5; Tp=12s
- 1.86 x Hs

Stream function theory waves

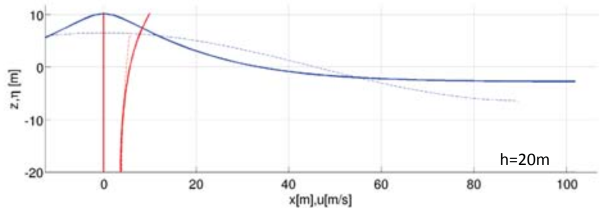

Fully nonlinear
Easily computed (e.g. Fenton 1988)
Can be embedded into background state
But: flat bed theory; periodic; 2D
What about wave transformation, transient group nature, current, 3D effects?

Opportunities

Can we improve the design methods?

Hydrodynamic loads

Simplest: Linear wave kinematics and Morison equation

$$F = \frac{1}{2}\rho C_D D|U|U + \rho C_M A \frac{dU}{dt}$$

Better: Fully nonlinear wave kinematics and Morison-type force model

Advanced: CFD and coupled CFD

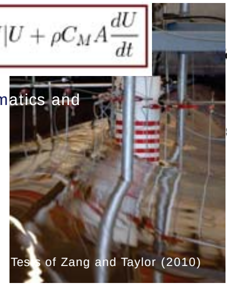

Tests of Zang and Taylor (2010)

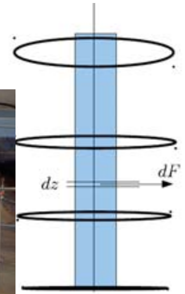

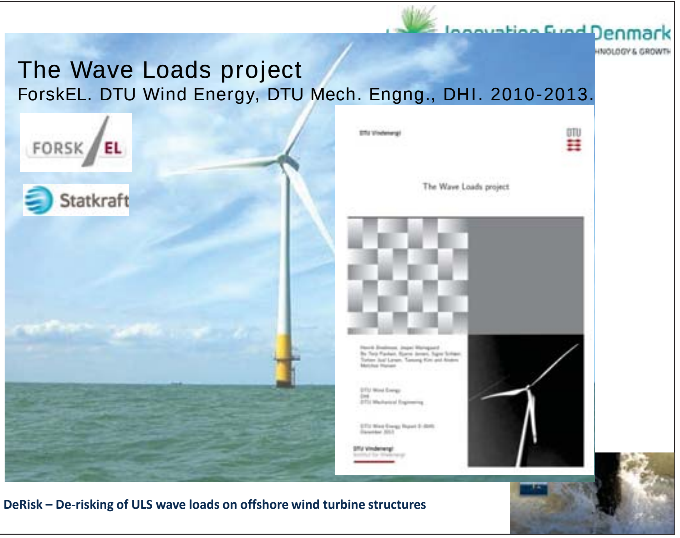

DeRisk – De-risking of ULS wave loads on offshore wind turbine structures

Kinematics from a fully nonlinear potential flow solver

'OceanWave3D', Engsig-Karup et al (2009)
Allan Engsig-Karup, Harry Bingham and Ole Lindberg

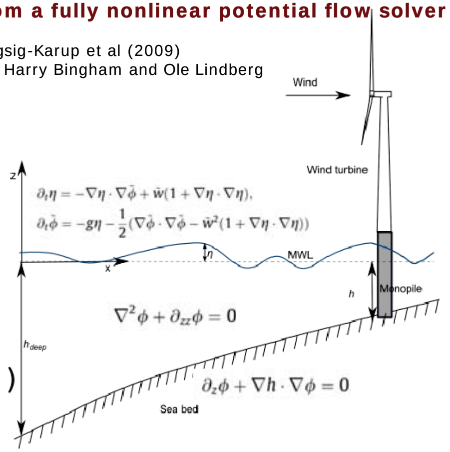

$$\partial_t \eta = -\nabla\eta \cdot \nabla\tilde{\phi} + \tilde{w}(1 + \nabla\eta \cdot \nabla\eta),$$
$$\partial_t \tilde{\phi} = -g\eta - \frac{1}{2}(\nabla\tilde{\phi} \cdot \nabla\tilde{\phi} - \tilde{w}^2(1 + \nabla\eta \cdot \nabla\eta))$$
$$\nabla^2\phi + \partial_{zz}\phi = 0$$
$$\partial_z\phi + \nabla h \cdot \nabla\phi = 0$$

Study of nonlinear wave load effects

Response calculations with Flex5 aero-elastic model, NREL 5MW turbine

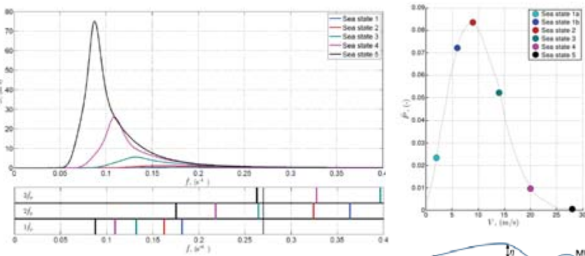

Signe Schløer (2013)

Statkraft

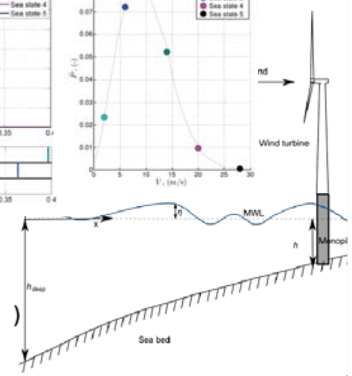

Static load analysis, h=30m

crest elevations

force peaks
depth integrated
force

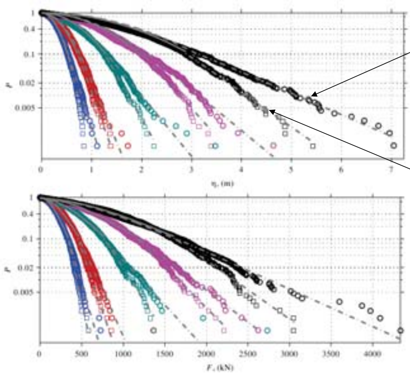

nonlinear

linear

CFD for multi-directional waves
Coupled solver

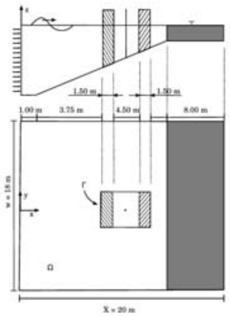

Bo Terp Paulsen
Paulsen, Bredmose & Bingham (2014)

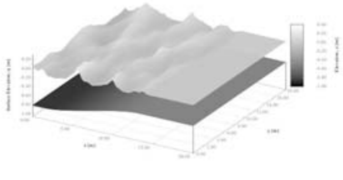

Figure 3.27: Snapshot of the free surface elevation computed by the potential flow solver at time $t = 15$ s.

Figure 3.28: Snapshot of the free surface elevation computed by the Navier-Stokes solver at time $t = 15$ s.

Study of regular steep wave forcing of circular cylinders

J. Fluid Mech. (2014), vol. 755, pp. 1–34. © Cambridge University Press 2014 doi:10.1017/jfm.2014.386 1

Forcing of a bottom-mounted circular cylinder by steep regular water waves at finite depth

Bo T. Paulsen[1,2,†], H. Bredmose[3], H. B. Bingham[1] and N. G. Jacobsen[1,2]
[1]Department of Mechanical Engineering, Technical University of Denmark, Kgs. Lyngby, 2800, Denmark
[2]Deltares, Rotterdamseweg 185, 2629HD Delft, The Netherlands
[3]Department of Wind Energy, Technical University of Denmark, Kgs. Lyngby, 2800, Denmark

(Received 22 March 2013; revised 13 June 2014; accepted 28 June 2014; first published online 14 August 2014)

Forcing by steep regular water waves on a vertical circular cylinder at finite depth was investigated numerically by solving the two-phase incompressible Navier–Stokes equations. Consistently with potential flow theory, boundary layer effects were neglected at the sea bed and at the cylinder surface, but the strong nonlinear motion of the free surface was included. The numerical model was verified and validated by grid convergence and by comparison to relevant experimental measurements. First-order convergence towards an analytical solution was demonstrated and an excellent agreement with the experimental data was found. Time-domain computations of the normalized inline force history on the cylinder were analysed as a function

Validation for propagation of nonlinear waves

Force validation

Parameter study

The flow of the secondary load cycle

How about the forces? II

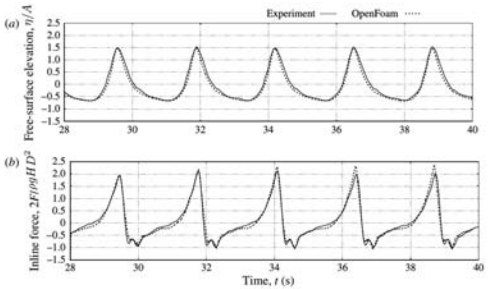

Comparison to experiments of Wave Loads project (DTU-DHI)

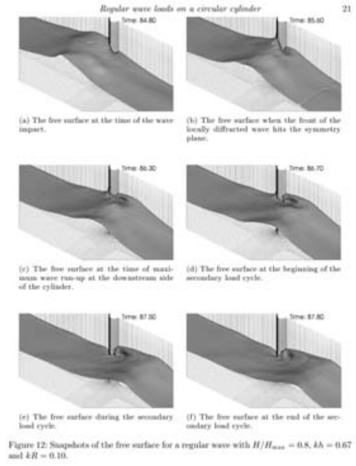

Innovation Fund Denmark

Physical model test with a flexible cylinder at DHI

Bredmose et al OMAE 2013
Inspiration from de Ridder et al OMAE 2011
Data used in OC5 (Robertson et al yesterday)

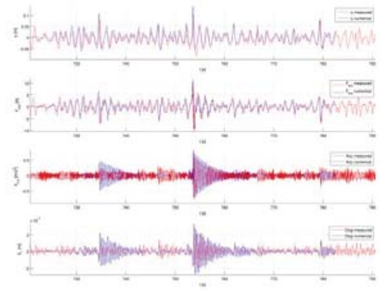

DeRisk – De-risking of ULS wave loads on offshore wind turbine structures

Innovation Fund Denmark

DeRisk – De-risking of ULS wave loads on offshore wind turbine structures

Innovation Fund Denmark

Mission

Bring tools for realistic ULS wave loads into engineering!
Apply to reduce risk and uncertainty. Thereby reduce LCOE.

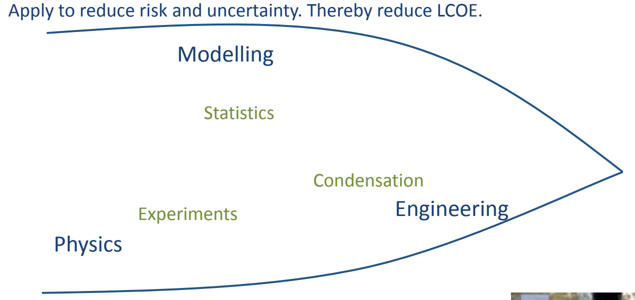

DeRisk – De-risking of ULS wave loads on offshore wind turbine structures

Innovation Fund Denmark

Elements of DeRisk

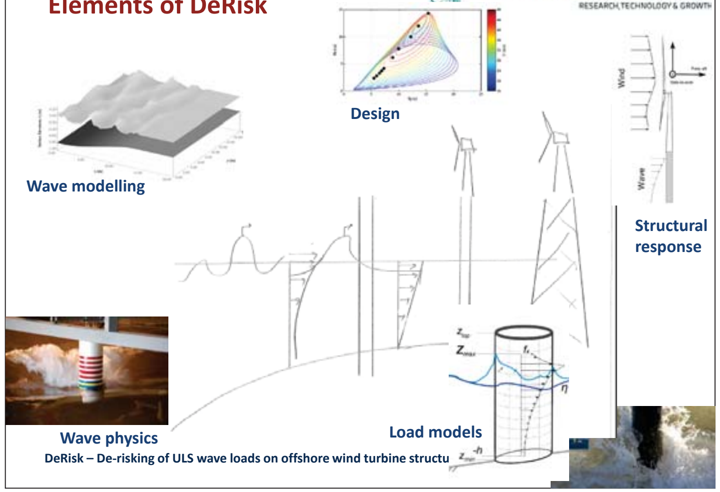

DeRisk – De-risking of ULS wave loads on offshore wind turbine structu

Efficient wave models

Innovation Fund Denmark
RESEARCH, TECHNOLOGY & GROWTH

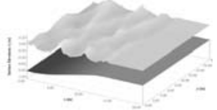

- Operational GPU wave model with wave generation.
- Improved breaking.
- Kinematics library for use by the other work packages.
- Proof of concept for DHI wave model for flows with vorticity.

WP leader: Harry Bingham, DTU Mechanical Engineering.
Partners: DTU Mechanical Engineering, DTU Compute and DHI.

Wave physics

Innovation Fund Denmark
RESEARCH, TECHNOLOGY & GROWTH

- Experiments with steep/breaking wave impacts
- Derivation of a slope reduction factor for extreme loads.
- Quantification of current effect on loads.
- Kinematics and corresponding forces
- Mathematical uncertainty quantification for wave kinematics and loads.
- Numerical study of 3D wave formation and effects on crest height distribution and load distribution.

WP leader: Henrik Bredmose, DTU Wind Energy.
Partners: DTU Wind Energy, DTU Mechanical Engineering, DTU Compute, DHI and University of Oxford.

DeRisk – De-risking of ULS wave loads on offshore wind turbine structures

Validated load models

Innovation Fund Denmark
RESEARCH, TECHNOLOGY & GROWTH

- Validated force model for steep and highly nonlinear waves.
- Validated force model for breaking wave loads.
- DES strategy for monopile CFD with inclusion of structural boundary layer.
- Load computations for drag-dominated wave impacts.

WP leader: Henrik Bredmose, DTU Wind Energy.
Partners: DTU Wind Energy, University of Oxford, University of Stavanger and Statkraft.

DeRisk – De-risking of ULS wave loads on offshore wind turbine structures

Response of wind turbine structures

Innovation Fund Denmark
RESEARCH, TECHNOLOGY & GROWTH

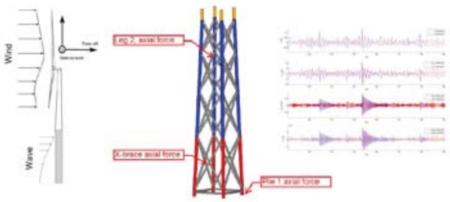

- Identification of critical load cases for jacket response to extreme waves.
- Analysis of the WaveSlam data set (NTNU, Stavanger University)
- Study of load effects from cyclic degradation of soil properties.
- Analysis of full scale data to identify the extent of ringing loads.
- Analysis and model formulation of current blockage effect for jackets

WP leader: Torben Juul Larsen, DTU Wind Energy.
Partners: DTU Wind, University of Oxford, University of Stavanger, DONG.

DeRisk – De-risking of ULS wave loads on offshore wind turbine structures

De-risked design

Innovation Fund Denmark
RESEARCH, TECHNOLOGY & GROWTH

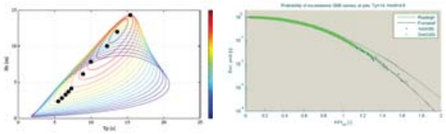

- White paper on the design chain from met-ocean data to design stress with discussion of the uncertainty.
- Uncertainty reduction for the statistical combination of extreme wind, sea and current data.
- Joint probability analysis methods that include structural response.
- A new load evaluation procedure based on fully nonlinear wave kinematics and the validated load models and an n¬-dimensional joint probability model of sea state parameters.

WP leader: Hans Fabricius Hansen, DHI.
Partners: DHI, DONG and DTU Compute.

DeRisk – De-risking of ULS wave loads on offshore wind turbine structures

Elements of DeRisk

Innovation Fund Denmark
RESEARCH, TECHNOLOGY & GROWTH

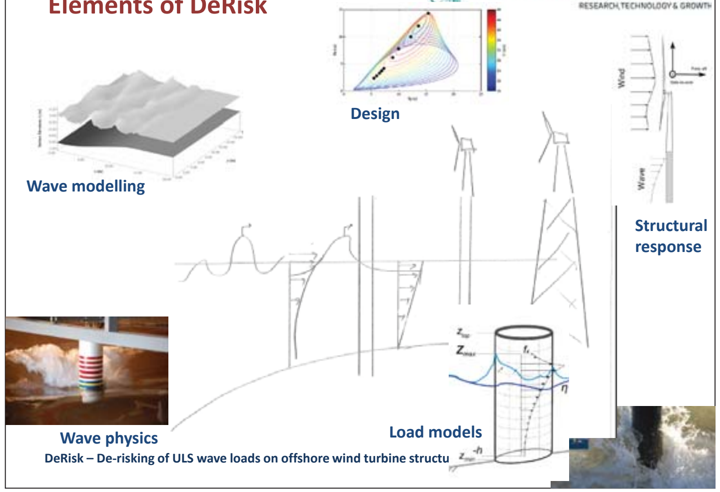

First results: Model tests at DHI

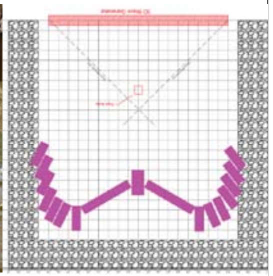

Led by Martin Dixen, DHI

First results: Model tests at DHI

Purpose:
- Tests of 10, 100 and 1000 year sea states of LONG duration (72 h full scale)
- Focus on 3D spread waves
- Force and moment
- Stiff structure
- 7m mono pile and 1.8m drag column
- 2D reference tests (6 h full scale)
- Focused groups and selected events

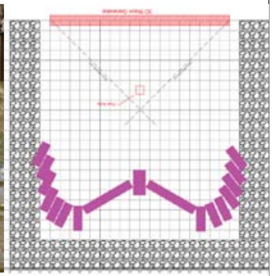

Focused wave groups

Innovation Fund Denmark
RESEARCH, TECHNOLOGY & GROWTH

The New Wave Theory
Lindgren (1970), Boccotti (1983), Tromans et al (1991)
Taylor et al (1995), Jensen (2005)

The most likely realization of a peak in a Gaussian process is the auto-correlation function of the free surface elevation

$$\eta(x,t) = \frac{\alpha}{\sigma^2}\sum_{j=1}^{N} S_\eta(f_j)\cos\left(\omega_j(t-t_0) - k_j(x-x_0)\right)\Delta f$$

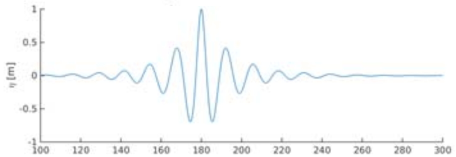

Focused wave groups

Innovation Fund Denmark
RESEARCH, TECHNOLOGY & GROWTH

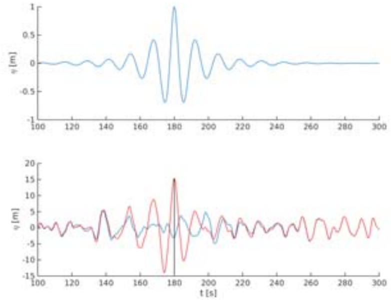

Can be embedded into background process
Directional focused version can be made too

DeRisk – De-risking of ULS wave loads on offshore wind turbine structures

Video

Innovation Fund Denmark
RESEARCH, TECHNOLOGY & GROWTH

DeRisk – De-risking of ULS wave loads on offshore wind turbine structures

Numerical reproduction in OceanWave3D

Innovation Fund Denmark
RESEARCH, TECHNOLOGY & GROWTH

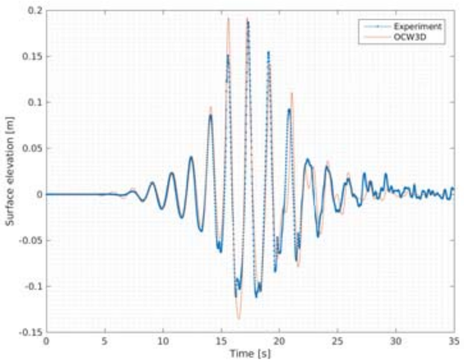

Computations by Amin Ghadirian

2D focused group

Corresponds to
Hs=9.5m
Tp=12s

DeRisk – De-risking of ULS wave loads on offshore wind turbine structures

Reproduction of 3D group

Innovation Fund Denmark
RESEARCH, TECHNOLOGY & GROWTH

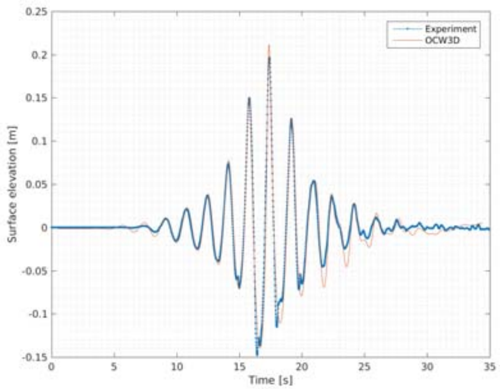

3D focused group

DeRisk – De-risking of ULS wave loads on offshore wind turbine structures

3D reproduction

Innovation Fund Denmark
RESEARCH, TECHNOLOGY & GROWTH

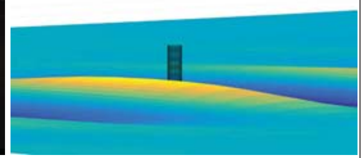

DeRisk – De-risking of ULS wave loads on offshore wind turbine structures

2D vs 3D dynamics

Innovation Fund Denmark
RESEARCH, TECHNOLOGY & GROWTH

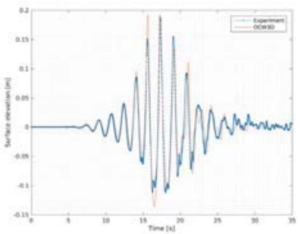

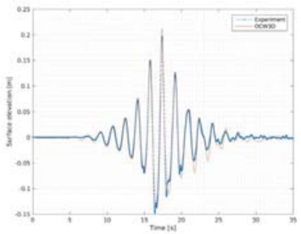

3D group can build up more rapidly
2D can only focus through dispersion

DeRisk – De-risking of ULS wave loads on offshore wind turbine structures

6 hour time series

Innovation Fund Denmark
RESEARCH, TECHNOLOGY & GROWTH

Can we reproduce crest statistics of a 6 h time series?

Hs=9.5m
Tp=12s

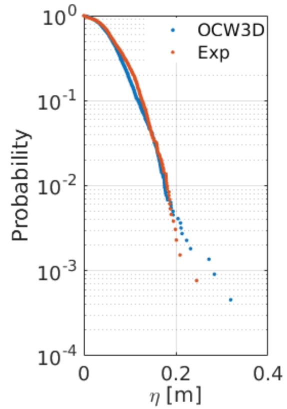

DeRisk – De-risking of ULS wave loads on offshore wind turbine structures

Elements of DeRisk

Innovation Fund Denmark
RESEARCH, TECHNOLOGY & GROWTH

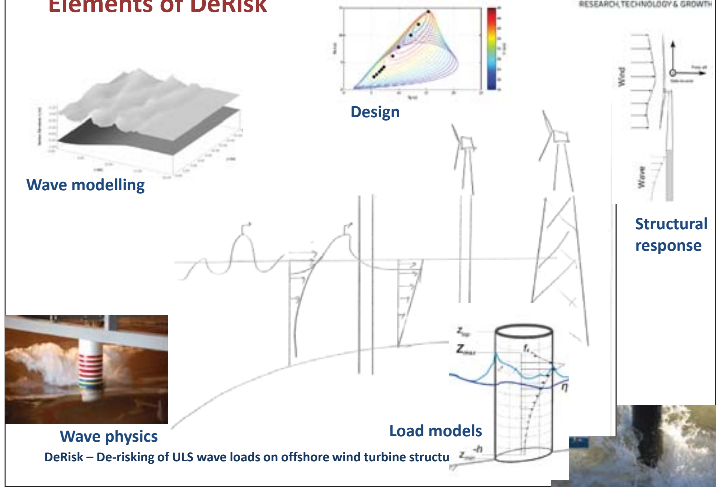

DeRisk – De-risking of ULS wave loads on offshore wind turbine structu

Summary

Innovation Fund Denmark
RESEARCH, TECHNOLOGY & GROWTH

Opportunities for better description of ULS wave loads
Can contribute to reduced LCOE
9 partners, 4 years, 2015-2019

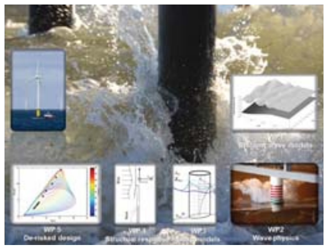

3D wave basin experiments at DHI – long duration
Succesful reproduction with fully nonlinear wave solver

DeRisk – De-risking of ULS wave loads on offshore wind turbine structures

Innovation Fund Denmark
RESEARCH, TECHNOLOGY & GROWTH

Follow us at
www.derisk.dk

ULS wave load symposium
August 2017 DTU

DeRisk
De-risked extreme wave loads for offshore wind energy

DeRisk delivers an improved and de-risked load evaluation procedure for extreme wave loads on offshore wind turbine substructures. Through ambitious research into wave physics, structural response and mathematical modelling, DeRisk provides a key contribution to the cost reduction of offshore wind energy.

DeRisk – De-risking of ULS wave loads on offshore wind turbine structures


Increasing wind farm profit through integrated condition monitoring and control
Principal Engineer Berit Floor Lund, Dr.ing.
Kongsberg Renewables Technology
KONGSBERG


Outline
1. Kongsberg Renewables Technology
2. Kongsberg EmPower
3. «Integrated»– not just a buzzword.
RENEWABLE ENERGY?
I'M A BIG FAN
KONGSBERG
22.01.2016
WORLD CLASS - through people, technology and dedication
Page 2

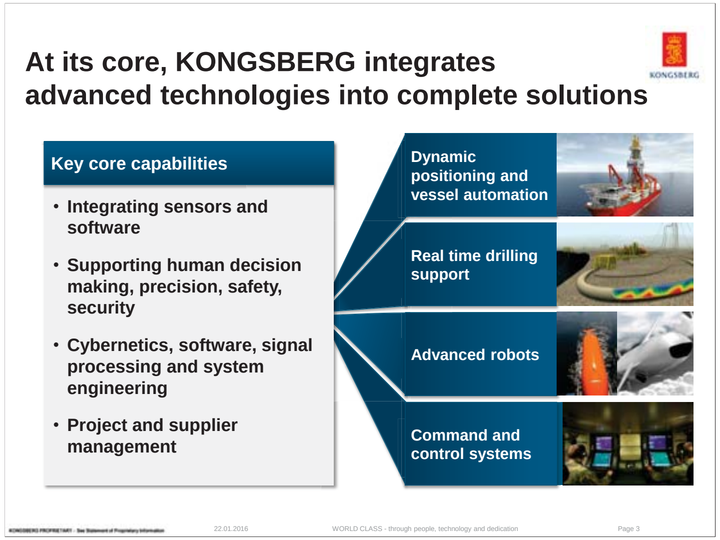
At its core, KONGSBERG integrates advanced technologies into complete solutions
Key core capabilities
• Integrating sensors and software
• Supporting human decision making, precision, safety, security
• Cybernetics, software, signal processing and system engineering
• Project and supplier management
Dynamic positioning and vessel automation
Real time drilling support
Advanced robots
Command and control systems
KONGSBERG
22.01.2016
WORLD CLASS - through people, technology and dedication
Page 3

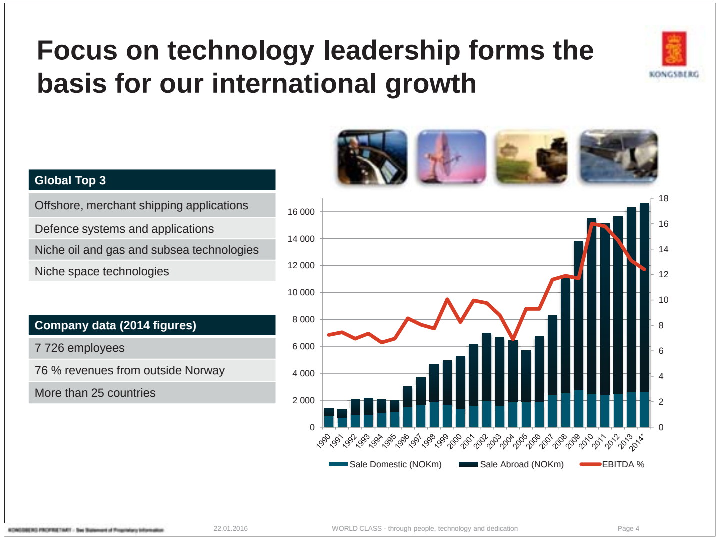
Focus on technology leadership forms the basis for our international growth
Global Top 3
Offshore, merchant shipping applications
Defence systems and applications
Niche oil and gas and subsea technologies
Niche space technologies
Company data (2014 figures)
7 726 employees
76 % revenues from outside Norway
More than 25 countries
Sale Domestic (NOKm)
Sale Abroad (NOKm)
EBITDA %
KONGSBERG
22.01.2016
WORLD CLASS - through people, technology and dedication
Page 4

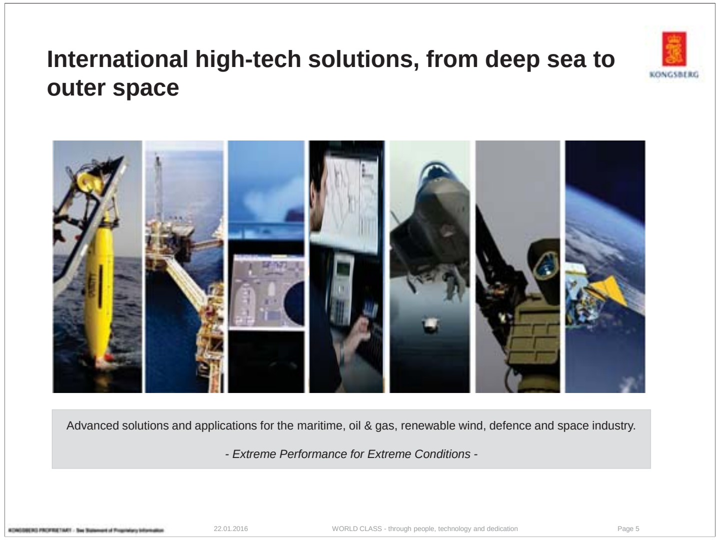
International high-tech solutions, from deep sea to outer space
Advanced solutions and applications for the maritime, oil & gas, renewable wind, defence and space industry.
- Extreme Performance for Extreme Conditions -
KONGSBERG
22.01.2016
WORLD CLASS - through people, technology and dedication
Page 5


World Wide Life Cycle Support
• KM - equipment on more than 17 000 vessels – comprehensive service network
• KONGSBERG's life cycle services is a key differentiator in the market
Kongsberg Maritime's "follow the sun" support centers, located in Norway, Singapore and New Orleans, ensure service 24/7 around the globe
KONGSBERG
22.01.2016
WORLD CLASS - through people, technology and dedication
Page 6

Kongsberg Renewables Technology

(Innovation – Execution – Acquisition)

TIMELINE

- **2010**: Kongsberg Maritime (KM Trondheim) activities linked to NCE Instrumentation. Participation in NowiTech, Wind Cluster Mid-Norway.
- **2011**: RCN project WindSense. Seminar held by «EcoSystem» on «Operation and maintenance of offshore wind turbines»
- **2012:** Kongsberg hires InTurbine/Scandinavian Wind as consultants
- **2012:** Strategic decision to enter wind power market and establish a department for this at KM Trondheim, 4 persons employed.
- **2012:** Kongsberg aquires InTurbine (4 persons)
- **2013**: Development of new product starts.
- **2013:** Support from Innovation Norway, Miljøteknologiordningen
- **2014:** 14 persons + consultants
- **2015**: From Kongsberg Maritime to Kongsberg Renewables Technology
- **2015**: Official product launch June 15, 2015.
- **2015**: **First contract on Kongsberg EmPower, June 2015.**

http://www.kongsberg.com/en/kongsberg-renewables/news/2015/june/arctic-wind-chooses-kongsberg-empower/

The KONGSBERG ambition

- ***Reduced O&M costs –*** *through improved overview and improved negotiation position*
- ***Yield optimization –*** *through increased production time and decreased wake issues*
- ***Reduced downtime –*** *through understanding the challenges in your wind farm*

Kongsberg EmPower → **Objective: 5-8% reduction in CoE**

Common challenges for wind farm owners

- Often no access to primary turbine signals, only aggregated values delivered by turbine manufacturer to wind farm owner.
- Difficult to extract valuable information from primary signals (multivariable, dynamic relationships)
- Different turbine types– different systems
- Different functionality – different systems with no/little integration

Kongsberg EmPower

-One portfolio, one system

Kongsberg EmPower

-Smart monitoring & control of wind farms

- **Conditioning Monitoring** with enhanced analysis of turbine data
- **Production Forecasting** through improved weather analysing tools/ algorithms
- **Wind Farm Control** reducing wake and turbine loads with dynamic production optimizer
- **Performance Monitoring;** reporting, fault analysis, trending and benchmarking of wind turbines and wind farms

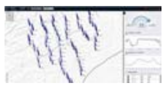

Production optimizer, load and wake control

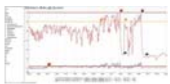

Reduced down time and operational cost

Reduced imbalance Improved maintenance planning

Identify deviations Improved benchmarking

→ **Potential of 5-8% reduction in CoE** ←

Kongsberg EmPower – Wind Farm Control

Increased yield – reduced operating costs

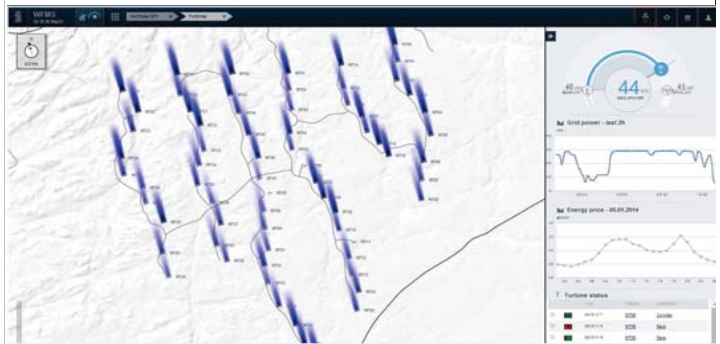

Production Forecasting

- *Correction of weather forecast based on historic data*
- *Correction based on wind observations*
- *Production forecasting based on several methods, taking turbine states, site specific issues, grid condtition, and maintenance plans into consideration.*

Kongsberg EmPower Performance monitoring, farm level.

Kongsberg EmPower Turbine view, condition monitoring.

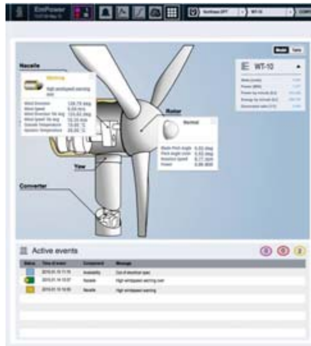

- ***Condition Monitoring***
  - *Early detection of failure*
  - *Advanced analysis methods of*
    - *Scada signals*
    - *Add-on sensors*
  - *Failure classification - RUL estimation*
  - *CM results used by many other EmPower modules*

Virtual («soft») sensors help interpreting multivariable, dynamic relationships

«Friction» in same type of bearing, all turbines.

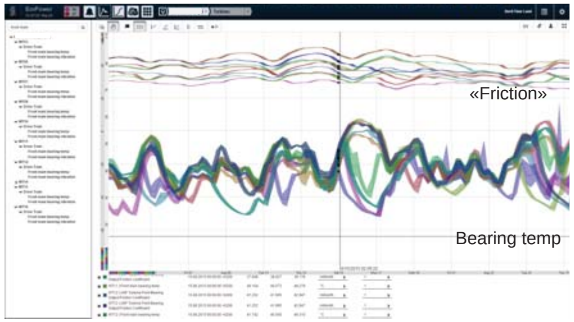

Developing bearing wear

- Model (ANN) temperature deviation and vibration – same trend.

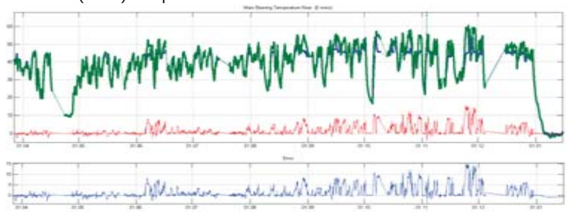

- RMS vibration – increasing trend

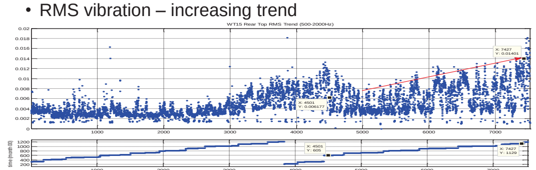

Failure Model of Rolling Element Bearing

- **Stage 1**
  - Noise level normal
  - Temperature normal
  - Earliest indications in the ultrasonic range (35000 Hz)
- **Stage 2**
  - Slight increase in noise level
  - Temperature normal
  - Slight bearing defects begin to excite **natural frequencies** of bearing components (500 to 2000 Hz).
- **Stage 3**
  - Noise level quite audible
  - Slight increase in temperature
  - Bearing frequencies with harmonics and sidebands (**BPFI, BPFO, 2xBSF and FTF**) clearly visible in linear scale with a noticeable increase in floor noise.
- **Stage 4**
  - High level of audible noise
  - Significant temperature increase
  - Discreet bearing defect frequencies disappear and are replaced by random broad band vibration in the form of a noise floor

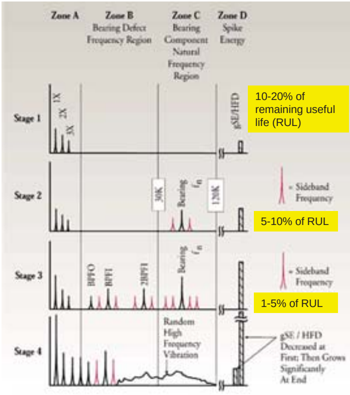

Why condition monitoring?

- **Cost** of planned repair is **< 30%** of unplanned replacement (DEWI report, onshore)

+

- **Lost Production (time and timing)**
  - Component lead-time
  - Waiting for vessel and personnel availability
  - Waiting for weather
  - Transport to farm
  - Enter Turbine
  - Perform repair
  - Exit Turbine

Planned

Corrective

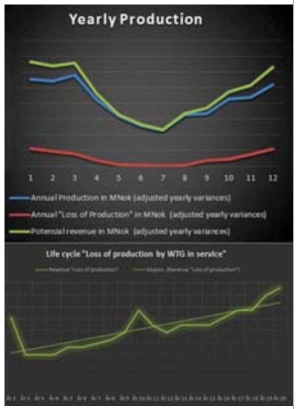

Sheringham Shoal data collected from the web

Kongsberg EmPower, integration

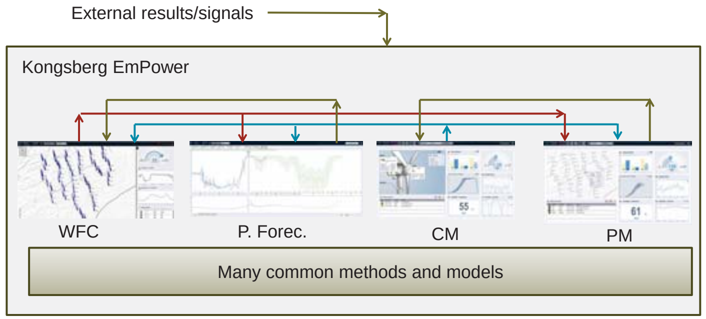

Condition and production based maintenance

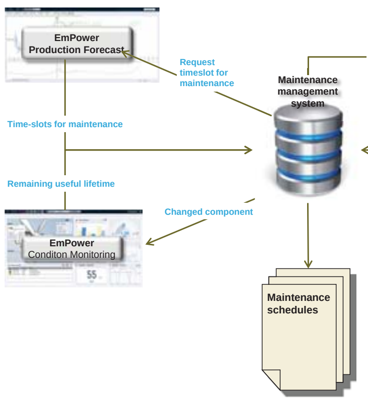

Maximizing performance by providing THE FULL PICTURE

Berit Floor Lund, Dr.Ing.
Principal Engineer
Wind Farm Management Systems
Kongsberg Renewables Technology AS
Haakon VII's gate 4
N-7041 Trondheim, Norway

Mobile phone: +47 9305 9302
Switchboard : +47 815 73 700
berit.floor.lund@kongsberg.com

WORLD CLASS – through people, technology and dedication

Poster session

1. *Development of a FAST model for a floating 10MW wind turbine, M. Borg, DTU Wind Energy*
2. *Investigation on Fault-ride Through Method for VSC-HVDC Connected Offshore Wind Farms, W. Sun, NTNU*
3. *Design and Modelling of a LFAC transmission system for offshore wind, J. Ruddy, Univ College Dublin*
4. *A Review on Wind Power Plant Control and Modelling Requirements, O. Anaya-Lara, Univ of Strathclyde*
5. *Synthetic inertia from wind power plant: Investigation of practical issues based on laboratory-based studies, O. Anaya-Lara, Univ of Strathclyde*
6. *Provision of Ancillary Services from Large Offshore Wind Farms, W. Ross, Univ of Strathclyde*
7. *Analysis of cyclone Xaver (2013) for offshore wind energy, K. Christakos, Uni Research Polytec AS*
8. *OBLO instrumentation at FINO1, M. Flügge, CMR*
9. *Energy systems on autonomous offshore measurement stations, T.K. Løken, NTNU*
10. *A Site Assessment of the Hywind Floating Wind Turbine location, L. Sætran, NTNU*
11. *Gust factors in gale and storm conditions at Frøya, L.M. Bardal, NTNU*
12. *Proof of concept for wind turbine wake investigations with the RPAS SUMO, J. Reuder, UiB*
13. *Development of a TLP substructure for a 6MW wind turbine – use of steel concrete composite material, F. Adam, Wind Power Construction GMBH*
14. *First results from an offshore 40m high TLP met. mast at 65m deep waters in the Aegean Sea, D. Foussekis, Centre for Renewable Energy Sources (CRES)*
15. *Project schedule assessment with a focus on different input weather data sources, G. Wolken-Möhlmann, Fraunhofer IWES*
16. *Nonlinear wave propagation and breaking in the coastal area, M.B. Paskyabi, UiB*
17. *Lagrangian Study of Turbulence Structure Near the Sea Surface, M.B. Paskyabi, UiB*
18. *Evaluation of ensemble prediction forecasts for estimating weather windows, B.R. Furevik, MET*
19. *A surrogate model for simulations – finding optimal operation & maintenance strategies for offshore wind farms, M.R. Gallala, NTNU*
20. *Risk and reliability based maintenance planning for offshore wind farms using Bayesian statistics, M. Florian, Aalborg Univ.*
21. *The operation and maintenance planning based on reliability analysis of fatigue fracture of a wind turbine drivetrain components. A. Beržonskis, Aalborg Univ.*
22. *Operation and maintenance and logistics strategy optimisation for offshore wind farms, I.B. Sperstad, SINTEF Energi*
23. *Vessel fleet optimization for maintenance operations at offshore wind farms under uncertainty, M. Stålhane, NTNU*
24. *Maintenance polar and marine traffic validation on existing wind farm, Colone, L., DTU*
25. *Assessment of the dynamic responses and operational sea states of a novel OWT tower and rotor nacelle assembly installation concept based on the inverted pendulum principle, W. G. Acero, NTNU*
26. *Multi-level hydrodynamic modelling of a 10MW TLP wind turbine, A.P. Jurado, DTU*
27. *A model for jacket optimization in Matlab, K. Sandal, DTU*
28. *Strategy and costs of installing floating offshore wind farms, L.B. Savenije, ECN*
29. *Analysis of second order effects on a floating concrete structure for FOWT's, Prof. Climent Molins, Universitat Politecnica de Catalunya*
30. *Vibration-based identification of hydrodynamic loads and system parameters for offshore wind turbine support structures, D. Fallais, Delft University of Technology*
31. *Improved Simulation of Wave Loads on Offshore Structures in Integral Design Load Case Simulations, M.J. de Ruiter, Knowledge Centre WMC*
32. *Adaptation of Control Concepts for the Support Structure Load Mitigation of Offshore Wind Turbines, B. Shrestha, ForWind*
33. *Comparison of experiments and CFD simulations of a braceless concrete semi-submersible platform, L. Oggiano, IFE*
34. *Parametric Wave Excitation Model for Floating Wind Turbines, F.Lemmer, né Sandner, University of Stuttgart*
35. *On Fatigue Damage Assessment for Offshore Support Structures with tubular Joints B. Hammerstad, NTNU*
36. *Influence of Soil Parameters on Fatigue Lifetime for Offshore Wind Turbines with Monopile Support Structure, S. Schafhirt, NTNU*
37. *Mooring Line Dynamics Experiments and Computations. Effects on Floating Wind Turbine Fatigue Life and Extreme Loads, J. Azcona, CENER*
38. *Semisubmersible floater design for a 10MW wind turbine, J. Azcona, CENER*
39. *Sizing optimization of a jacket under many dynamic loads, A. Verbart, DTU Wind Energy*
40. *Rational upscaling of a semi-submersible floating platform, M. Leimeister, NTNU*
41. *Numerical and experimental investigation of breaking wave impact forces on a vertical cylinder in shallow waters, M.A. Chella, NTNU*
42. *Irregular Wave Forces on Circular Cylinders placed in Tandem, A. Aggarawal, NTNU*
43. *New design concepts of an upwind turbine rotor and their impact on wake characteristics, F. Mühle, NMBU*
44. *Wake modelling: the actuator disc concept in PHOENICS, N. Simisiroglou, WindSim AS*

45. *Wind farm control applications for Windscanner infrastructure, T.I. Reigstad, SINTEF Energi AS*
46. *Real-Time Hybrid Model Testing of a Floating Wind Turbine: Numerical validation of the setup, V. Chabaud, NTNU*
47. *Experimental Wind Turbine Wake Investigation towards Offshore Wind Farm Performance Validation, Y. Kim, LSTM, FAU*
48. *Validation of a Semi-Submersible Offshore Wind Platform through tank test, G. Aguirre, Tecnalia R&I*
49. *Field site experimental analysis of a 1:30 scaled model of a spar floating offshore wind turbine, M. Collu, Mediterranea University*
50. *A Review and Comparison of Floating Offshore Wind Turbine Model Experiments, G. Stewart, NTNU*
51. *Wind Model for Simulation of Thrust Variations on a Wind Turbine, E. Smilden, NTNU*
52. *Numerical simulations of the NREL S826 aerofoil performance characteristics – A CFD validation and simulation of 3D effects in wind tunnel testing, K. Sagmo, NTNU*
53. *A Single-Axis Hybrid Modelling System for Floating Wind Turbine Basin Testing, M. Hall, University of Maine*
54. *A design support multibody tool for assessing the dynamic capabilities of a wind tunnel 6DoF/HIL setup, M. Belloli, Politecnico di Milano*
55. *Assessment and evaluation of a wind turbine condition using a time-frequency signal processing method, P. McKeever, Offshore Renewable Energy Catapult*
56. *Development, Verification and Validation of 3DFloat; Aero-Servo-Hydro-Elastic Computations of Offshore Structures, T.A. Nygaard, IFE*
57. *Effect of upstream turbine tip speed variations on downstream turbine performance: a wind farm case optimization, J. Bartl, NTNU*
58. *Droplet Erosion Protection Coatings for Offshore Wind Turbine Blades, A. Brink, SINTEF M&C*
59. *Design of an airfoil insensitive to leading edge roughness, T. Bracchi, HIST*
60. *Socio-economic evaluation of floating substructures within LIFES 50+ project, M. de Prada, IREC*
61. *Coordinated control of DFIG-based offshore wind power plant connected to a single VSC-HVDC operated at variable frequency, M. de Prada , IREC*
62. *Implications of different regulatory approaches for offshore wind in Europe, L. Kitzing, DTU Management Engineering*
63. *Fiskarstrand Verft AS tooling up for renewable energy, Einar Kjerstad, Fiskerstrand Verft AS*
64. *LIFES50+: Innovative floating offshore wind energy .P.A.Berthelsen, Marintek*
65. *Aerodynamic modeling of offshore floating vertical axis wind turbines, Z. Cheng, NTNU*
66. *Scalability of floating Vertical Axis Wind Turbines, E. Andersen, UiS*
67. *Advanced Wind Energy Systems Operation and Maintenance Expertise, J. Melero, CIRCE*

DTU Wind Energy
Department of Wind Energy

DTU

Development of a FAST model for a floating 10MW wind turbine

Michael Borg, Mahmood Mirzaei, Morten H. Hansen, Henrik Bredmose

Motivation

The motivation for this work is the *LIFES50+* project [1] that focuses on the qualification of innovative floating substructures for the next generation of 10MW wind turbines. As part of this project there is a need to establish a reference 10MW turbine model for designing floating substructures. The DTU 10MW Reference Wind Turbine [2] was selected for this task by the consortium. A common numerical tool available to all partners, as well as the public, was desired for this reference model, and FAST v8.12 was selected [3].

Control	Variable speed Collective pitch
Cut in wind speed [m/s]	4
Cut out wind speed [m/s]	25
Rated wind speed [m/s]	11.4
Rated power [MW]	10.0
Rotor diameter [m]	178.3
Hub diameter [m]	5.6
Hub height [m]	119.0
Minimum rotor speed [rpm]	6.0
Maximum rotor speed [rpm]	9.6
Hub overhang [m]	7.1
Shaft tilt angle [deg]	5.0
Rotor precone angle [deg]	-2.5
Blade prebend [m]	3.332
Rotor mass [kg]	227,962
Nacelle mass [kg]	446,036
Tower mass [kg]	628,442

Model Development

Developed ***onshore*** aero-elastic model in FAST v8.12 [3]

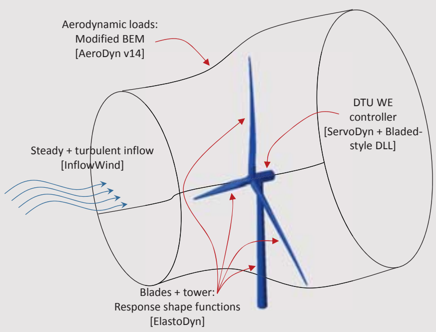

Structural Model

Natural frequencies comparison against HAWC2

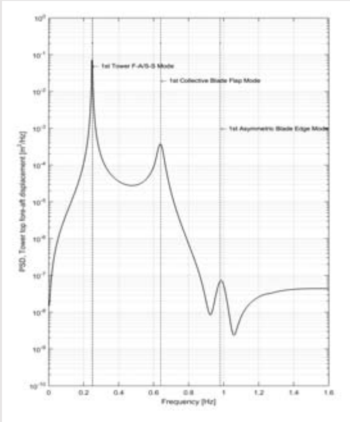

Steady State Performance

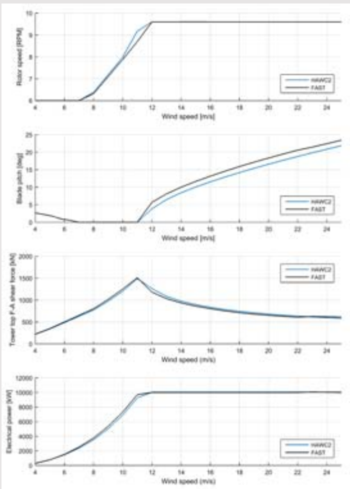

Challenges

Initially the BeamDyn FEM blade structural module within FAST was considered to capture the dynamic response of the large, flexible blades. However the BeamDyn module proved to be too computationally intensive for the purposes of floating substructure optimization, and hence the blade model was reverted back to the modal-based ElastoDyn module. As HAWC2 uses a multibody formulation and a different aerodynamic BEM implementation, there were expected differences in loads predicted by FAST and HAWC2 that were mitigated by the controller adjusting the blade pitch setting.

The FAST model implementation of the DTU 10MW Reference Wind Turbine is publicly available [4].

Scan this QR code for more information:

Controller Performance

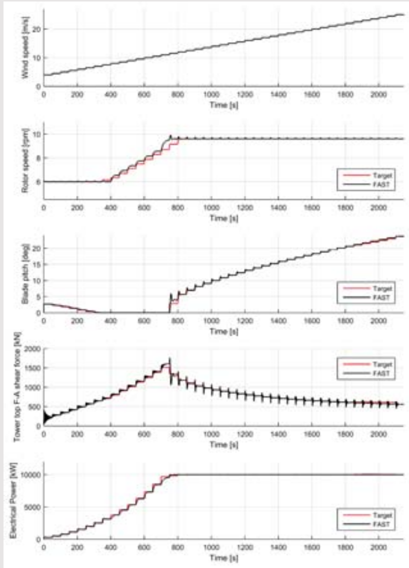

Ongoing & Future Work

Developing framework for adapting controller to floating foundations in LIFES50+:

Develop & verify FAST implementation of *onshore* controller against HAWC2

↓

Establish methodology for adapting controller

↓

Develop & verify baseline floating wind turbine controller in FAST with generic floater against HAWC2

↓

Interact with LIFES50+ floating platform concept developers to develop controller tuned to each floating substructure concept

INNWIND.EU Triple Spar floating platform concept [5] as basis for generic controller tuning

References

[1] http://www.lifes50plus.eu
[2] C. Bak, F. Zahle, R. Bitsche, T. Kim, A. Yde, L.C. Henriksen, A. Natarajan, M.H. Hansen (2013). *Description of the DTU 10 MW Reference Wind Turbine,* DTU Wind Energy Report-I-0092, Roskilde, Denmark.
[3] B.J. Jonkman, J.M. Jonkman (2015). *Guide to changes in FAST v8: v8.12.00a-bjj.* National Renewable Energy Laboratory, Golden, Colorado
[4] M. Borg, M. Mirzaei, H. Bredmose (2015). *Wind turbine models for the design,* LIFES50+ Deliverable 1.2, DTU Wind Energy E-101, Lyngby, Denmark.
[5] F. Amann, F. Lemmer (2016). *Design solutions for 10MW floating offshore wind turbines,* INNWIND.EU Deliverable 4.37, University of Stuttgart.

Acknowledgements

The authors would like to acknowledge the assistance of Frank Lemmer (University of Stuttgart) and José Azcona Armendariz (CENER) in providing the design of the INNWIND Triple Spar floating platform, which was developed in the INNWIND.EU project.

The authors also acknowledge that this project has received funding from the European Union's Horizon 2020 research and innovation programme under grant agreement No 640741.

13th Deep Sea Offshore Wind R&D Conference
EERA DeepWind 2016
20 – 22 January 2016
Trondheim, Norway

LIFES50+

Investigation on Fault-ride Through Method for VSC-HVDC Connected Offshore Wind Farms: New Proposal

Wenye Sun*, Raymundo Enrique Torres-Olguin*+ & Olimpo Anaya-Lara*+

Norwegian University of Science and Technology* and SINTEF Energy Research+

NTNU

Objective

This work proposes a novel fault-ride through method for VSC-HVDC connected to offshore wind farms. The proposed method initiates a controlled voltage drop at offshore grid to achieve a fast power reduction when an onshore fault occurs. Almost simultaneously, the individual wind turbine detects the voltage drop of offshore grid, then its controller decreases the power set-point to reduce the power output from each wind turbine.

Introduction

When a fault occurs at the ac grid, the onshore converter is unable to transmit all the active power to the ac grid, however OWF still inject active power to offshore converter. This results in power imbalance that will charge the capacitance in the dc-link. Without any actions, this will result in a fast increase of the dc voltage, which may damage the HVDC equipment.

Test System

Two OWFs with capacity of 300 MW and 200 MW connected to the onshore grid via VSC-HVDC is considered as the test system, shown in Figure 1.

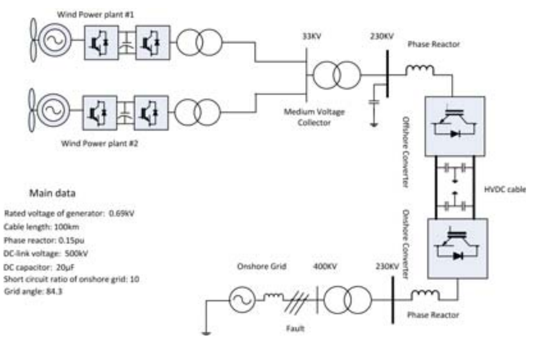

Figure 1: Figure caption

Control design for VSC-based HVDC

Since the wind turbines can control active power and reactive power by themselves, the basic function of the offshore converter controller is to maintain the ac voltage and frequency in the OWF grid. The block diagram of the controller is shown in Figure 2.

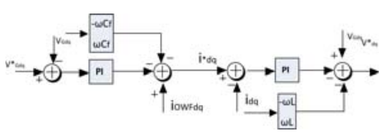

Figure 2: Figure caption

The control objective of onshore converter is to regulate the dc-link voltage. Additionally, the onshore converter can regulate the reactive power to provide voltage support. The controller is shown in Figure 3.

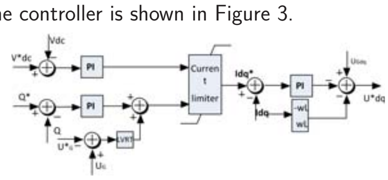

Figure 3: Figure caption

Proposed Fault Ride through Method

The overall control structure is shown in Figure 4. When an onshore fault occurs, the dc voltage at the offshore converter will increase. When the dc-link voltage exceeds its threshold value, it will activate the offshore converter controller to control offshore ac voltage magnitude based on (1). Almost at the same time, wind turbines detect the offshore ac voltage magnitude reduction. A power droop factor is generated and sent to wind turbine to de-load active power based on (2).

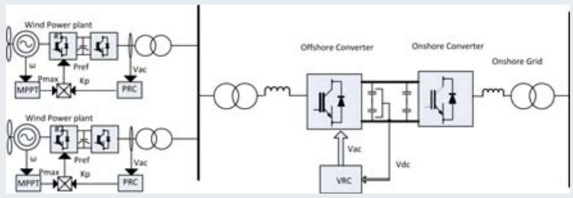

Figure 4: Control structure of the novel fault-ride through method

$$V_{ac} = V_{ac_{ref}} - k_v(V_{dc_{ref}} - V_{dc}) \quad (1)$$

$$K_p = \frac{V_{reduce}}{V_{rated}} \quad (2)$$

Simulation Results

The effectiveness of this method is verified by simulation in PSCAD. A three-phase-to-ground fault occurs at 10.5 s and last for 200 ms, and a small ground fault resistance is used.

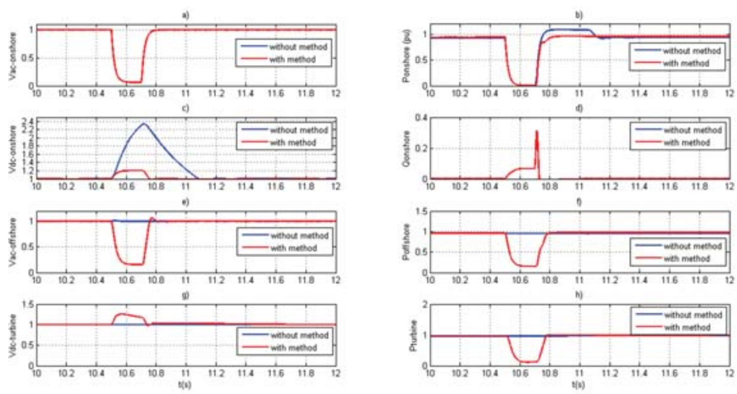

Figure 5: Three phase-to-ground fault without and with FRT

Conclusions

This paper proposed a novel FRT method for VSC-HVDC connected OWF system. There are four main advantages of this novel FRT method:

- Fast OWF power reduction by decreasing the offshore grid voltage and the output power from each wind turbine is also reduced.
- There is no communication delay.
- The wind turbine drive train does not suffer from large electrical stress.
- This method largely improves the control ability of HVDC over voltage and limits the dc voltage within safety value.

Contact email: wenye.sun@cn.abb.com

Design and Modelling of a LFAC Transmission System for Offshore Wind

Jonathan Ruddy (jonathan.ruddy@ucdconnect.ie), **Dr. Ronan Meere** (ronan.meere@ucd.ie), **Dr. Terence O'Donnell** (terence.odonnell@ucd.ie)

Introduction

Low Frequency AC (LFAC) transmission has recently been suggested by industry and academia as a competitor to HVDC transmission for the interconnection of offshore wind [1]. Offshore cables operated at low frequencies, (16.7 Hz), extend the maximum power transmission distance of the cable from 60-80 km for 50 Hz to 180-200 km for 16.7 Hz [2].

Advantages of LFAC

- No offshore converter station reduces complexity offshore
- Uses AC technology (lots of experience onshore)
- No DC breakers required – 16.7 Hz AC breakers available
- Economic analysis - LFAC viable competitor to HVDC [3]
- Low frequency experience in railway

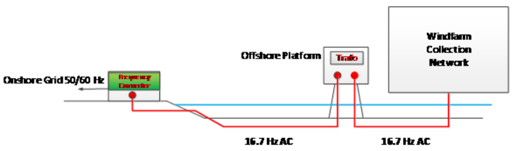

Fig 1: Overview of LFAC transmission system for offshore wind

Objective

This work aims to develop the design and modelling of the Low Frequency AC offshore transmission system in particular the 16.7 Hz offshore grid frequency and voltage controlled by the Voltage Sourced Converter.

Techno Economic Analysis [4]

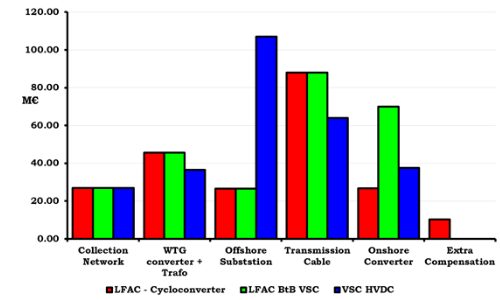

Fig 2: Cost Comparison between LFAC and HVDC

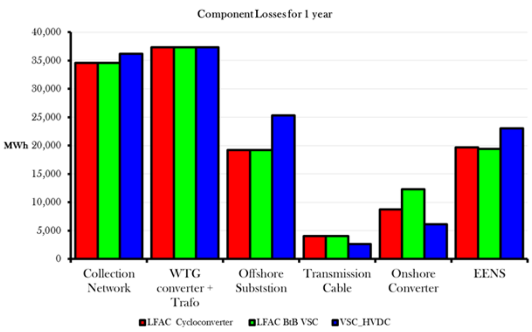

Fig 2: Loss Comparison between LFAC and HVDC

Summary	Capital Cost (M€)	Losses (MWh)
LFAC Cycloconverter	224.27	123,455
LFAC Btb	**257.17**	**126,785**
VSC – HVDC	272.03	130,639

Acknowledgement

This work was conducted in the Electricity Research Centre, University College Dublin, Ireland, which is supported by the Electricity Research Centre's Industry Affiliates Programme (http://erc.ucd.ie/industry/). Jonathan Ruddy and Terence O'Donnell are funded through the Sustainable Electrical Energy Systems Strategic Research Cluster (SEES Cluster) under grant number 09/SRC/E1780.

Ronan Meere is funded under Programme for Research in Third Level Institutions and co-funded under the European Regional Development Fund (ERDF).

Onshore Converter Comparison [5]

Cycloconverter

- Thyristor based
- High Harmonic content
- Pf (~ 0.78 lagging)
- Less expensive than BtB
- Frequency step up issues
  Inter-harmonics and sub-harmonics
- Compact converter station

Back to Back VSC converter

- Small Harmonic content
- IGBT power switches
- Independent control over P&Q
- Large converter stations
- Any output frequency possible

Techno Economic Conclusion– LFAC comparable to HVDC & Use Back to Back VSC converter onshore instead of Cycloconverter [4]

LFAC System Modelling

Parameters

DC link Voltage	400 kV
Nominal Power	200 MVA
Dc Link Capacitance	100 µF
LFAC voltage	150 kV
Offshore Frequency	16.7 Hz
C_{f_LF}	40 µF

Phase Reactor Design at LFAC

$$L = \frac{0.15 * Zbase}{100\pi} \text{ @ 50 Hz} = 0.0537\ H$$

$$L_{LF} = \frac{0.15 * Zbase}{33.4\pi} \text{ @ 16.7 Hz} = 0.1608\ H$$

Keeping X/R ratio constant: $R = R_{LF} = 0.3375\ \Omega$

Grid forming VSC control

The grid forming control is developed using a controlled frequency VSC. The control is adapted from Chapter 9 of Yazdani [6]. The objective is to regulate the amplitude and frequency of the offshore voltage (V_{abc}) in response to changes in the offshore current (I_{oabc}). The capacitance C_f is required as part of the RLC filter to ensure voltage support and to filter switching current harmonics. The controlled frequency is controlled in dq mode similar to the grid imposed frequency converter (VSC 2).

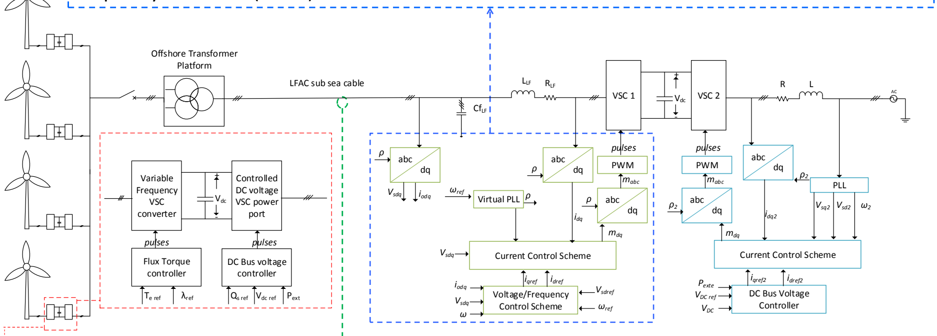

Fig 4: Control scheme for Offshore wind turbine and onshore Back to Back converter for LFAC

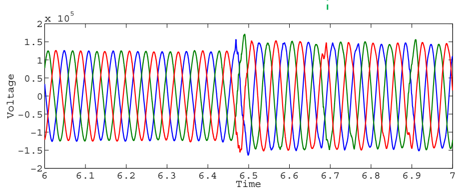

Fig 5: LFAC offshore voltage at 16.7 Hz responding to increase in reference voltage from 120 kV to 150 kV

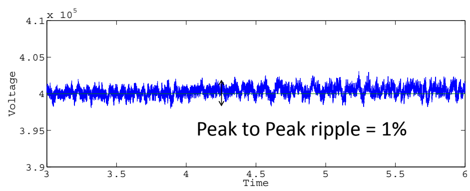

Fig 6: DC link voltage between VSC 1 and VSC 1. DC voltage controller maintains voltage with less than 1% peak to peak ripple.

Full conversion wind turbine control at 16.7 Hz has been verified and demonstrated in paper by Dr. Ronan Meere, "*Scaled Hardware Implementation of a Full Conversion Wind Turbine for Low Frequency AC transmission*" presented at EERA DeepWind 2016

Future work:

- Synchronisation of offshore converters to power electronically formed LFAC grid
- Scaled Model + hardware verification of entire LFAC system incorporating work by Dr. Meere
- Development of control mechanisms for system services i.e. frequency support, voltage support
- Testing of grid code compliance i.e. faults offshore and onshore

References

[1] **W. Fischer**, R. Braun, and I. Erlich, "Low frequency high voltage offshore grid for transmission of renewable power," in *3rd IEEE PES Innovative Smart Grid Technologies Europe*, 2012.

[2] **E. Olsen**, U. Axelsson, and A. Canelhas, "Low Frequency AC Transmission on large scale Offshore Wind Power Plants, Achieivng the best from two worlds?," in *13th Wind Integration Workshop*, 2014.

[3] **J. Ruddy**, R. Meere, and T. O'Donnell, "A Comparison of VSC-HVDC with Low Frequency AC for Offshore Wind Farm Design and Interconnection," in *EERA DeepWind'2015Deep Sea Offshore Wind R&D Conference, 04-06 Feburary*, 2015.

[4] **J. Ruddy**, R. Meere, and T. O'Donnell, "Low Frequency AC transmission as an alternative to VSC-HVDC for grid interconnection of offshore wind," in PowerTech, 2015 IEEE Eindhoven , vol., no., pp.1-6, June 29 2015-July 2 2015

[5] **J. Ruddy**, R. Meere, and T. O'Donnell, "Low Frequency AC transmission for offshore wind power: A review", Renewable and Sustainable Energy Reviews, Volume 56, April 2016, Pages 75-86, ISSN 1364-0321

[6] **A. Yazdani** and R. Iravani "Voltage-Sourced Converters in Power Systems, Modeling, Control and Applications"

Synthetic inertia from wind power plant: Investigation of practical issues based on laboratory studies

Olimpo Anaya-Lara[1], Atle Rygg Årdal[2], Kjell Ljøkelsøy[2], Salvattore D'Arco[2], John Olav Tande[2]

Abstract

- In addition to the impacts on network operation, provision of short-term frequency support has implications on the turbines themselves. In essence, the control implementation to deliver the 'synthetic inertia' response required for the power system will introduce additional and possibly significant torque demands on the turbine.
- It is therefore necessary to conduct experimental tests that shed light and provide understanding of the impact that different control strategies have on sensitive components of the turbines such as the power electronics.
- The impact of the sudden release of kinetic energy in the form of active power from the generators has be assessed for the partial-power back-to-back converter of the DFIG and the full-scale back-to-back converter of the FRC.

Fig. 1. Frequency event

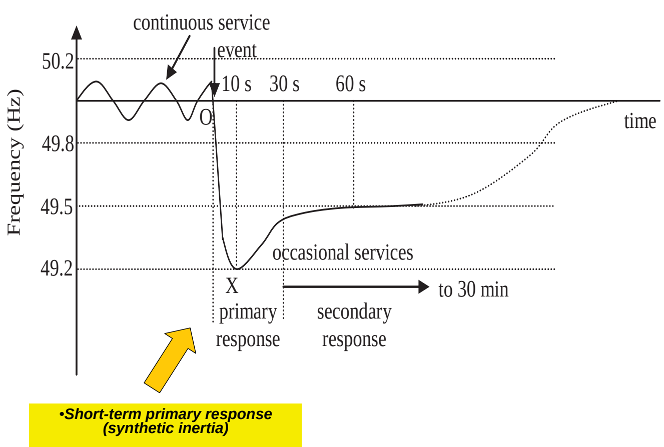

Frequency event fundamentals

- The kinetic energy stored in the rotating masses of generators and loads, i.e. the power system inertia, determines the sensitivity of the change in system frequnecy. The higher the power system inertia, the lower the rate-of-change of frequency in case of an imbalance between generation and demand.
- In the event of a suddent failure in generation or connection of a large load the system frequency starts dropping (region OX in Figure 1) at a rate mainly determined by the total angular momentum of the system (addition of the angular momentum of all generators and spinning loads connected to the system).
- The extracted power from variable-speed wind turbines is controlled by power electronic converters and there is no inherent relation between frequency of the system and the rotational speed of the tubrine. Hence, modern wind turbines cannot naturally provide an instantaneous power boost in response to a system frequency fall and thus contribute to power system inertia.

The block diagram of the control loop implemented in the laboratory to enable the FRC wind turbine to provide synthetic inertia is illustrated in figure 2. It can be observed that the control concept is simple, and works on modifying the torque set point.

The lab implementation is shown in Fig. 3 for the FRC wind turbine.

Fig. 3. FRC implementation in the lab

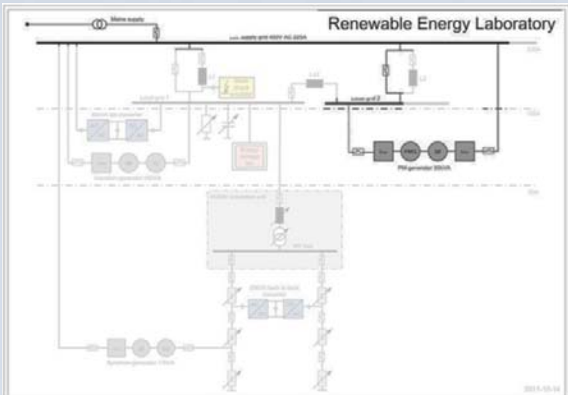

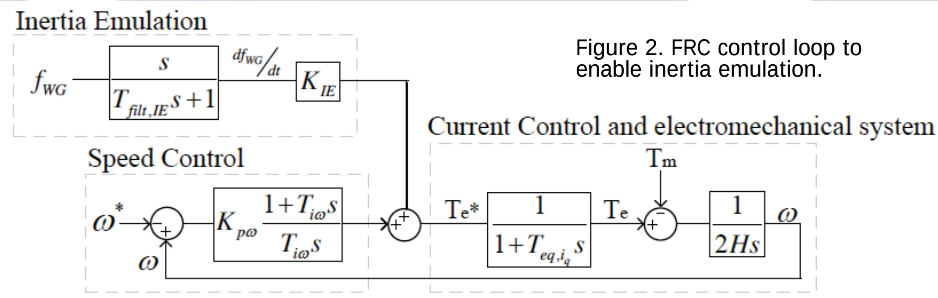

Figure 2. FRC control loop to enable inertia emulation.

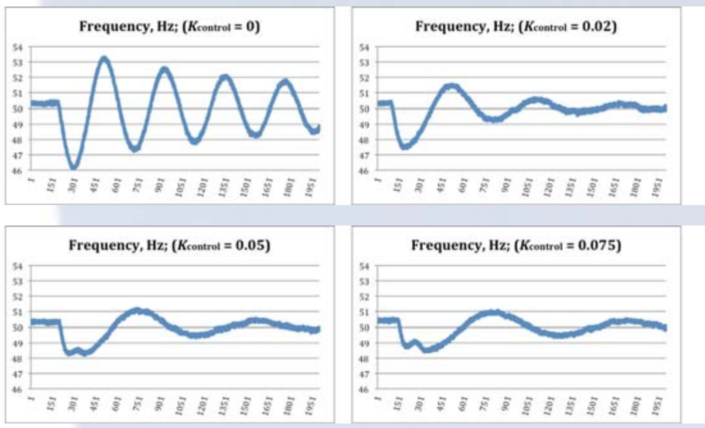

Fig.4 Results for Near-rated wind speed: In this scenario, the speed of the wind generator was set 1000 rpm.

Fig. 5. Working in the lab.

Conclusions

- No drastic variations were observed in the currents or dc voltage in the power electronics. However, it is not possible to generalise at this stage that it will be the case in every case as further tests may be necessary.
- Of importance when considering the provision of synthetic inertia may no be in the sense of magnitudes but duration of the service provision.

[1] Institute for Energy and Environment, University of Strathclyde, Glasgow, UK
[2]SINTEF Energy Research, Trondheim, Norway
Contact: olimpo.anaya-lara@strath.ac.uk

The research presented in this paper was conducted at the SINTEF Renewable Energy Lab - SmartGrids sponsored by the EU FP7 MARINET project. The authors acknowledge the support provided by Hanne Stoeylen.

Provision of Ancillary Services from Large Offshore Wind Farms

William Ross[1], Dr Olimpo Anaya-Lara[2],
Prof. Stephen Finney[3], Prof. Aurelio Medina-Rios[4]

1 - Department of Electronic & Electrical Engineering, University of Strathclyde, Glasgow, G1 4EP, UK (william.g.ross@strath.ac.uk)

2, 3 - Department of Electronic & Electrical Engineering, University of Strathclyde, 4 - Universidad Michoacana de San Nicolas de Hidalgo, Mexico

Wind power has adopted a significant role in the rise of renewable power systems, however high wind penetration brings with it technical, economic and regulatory issues. One of the primary concerns for large scale connection of wind power is network operators' ability to maintain desired frequency and voltage for the network consumers. During faults and outages, operators must rely on spinning reserve and ancillary services from various generators to maintain frequency and prevent cascading loss of load. To enable high levels of wind penetration, it is imperative that wind farms be operated, where possible, as conventional power plants in order to provide their dynamic characteristics and network support features. This can be expensive however, and there is great need for cost effective solutions to better enable higher penetration of wind and all renewables.

1. Connection of Wind Farm using HVDC

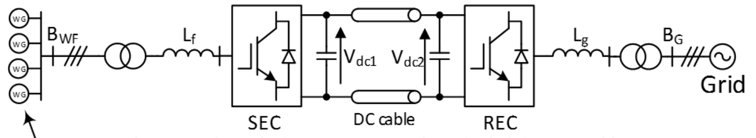

Fig 1. – Schematic for HVDC connection of wind farm to grid showing Sending-End Converter and Receiving-End Converter

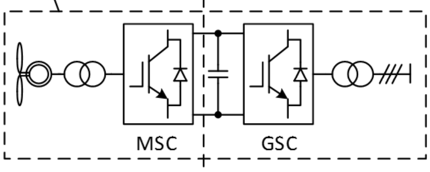

Fig 2. – Schematic for wind turbines showing back-to-back converter with decoupling capacitor

Due to the decoupling effect of capacitor in the back-to-back converter, wind turbines may be modelled as DC source connected to Grid-Side Converter in order to simplify the model.

For further simplicity, the entire offshore wind farm is represented by one equivalent unit.

2. Control of HVDC link

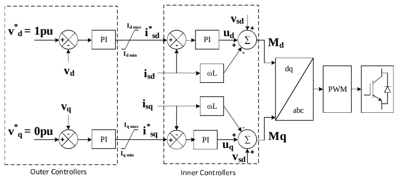

Fig 3. – Control Diagram for SEC

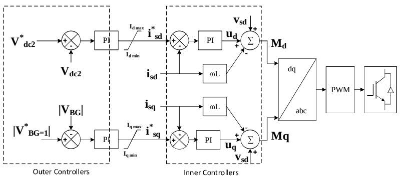

Fig 4. – Control Diagram for REC

The Sending-End Converter of the VSC-HVDC keeps a stiff ac bus at the wind farm main platform (B_{WF}). This is important to ensure stable control of wind turbine GSCs which used the voltage set by SEC as a reference.

The Receiving End Converter of the VSC-HVDC is configured to regulate the DC link voltage level at $640\,kV$ and the AC voltage at the PCC (B_G).

This control scheme allows independent control of P and Q which enables it to perform Fault Ride Through behaviour.

3. Simulation Results

Simulations were run with wind farm output initially set to $300MW\ (0.3\,pu)$, with a ramp up in power output beginning at $t = 2s$. Different magnitudes of ramp were tested as shown in Figures 5a-5f below.

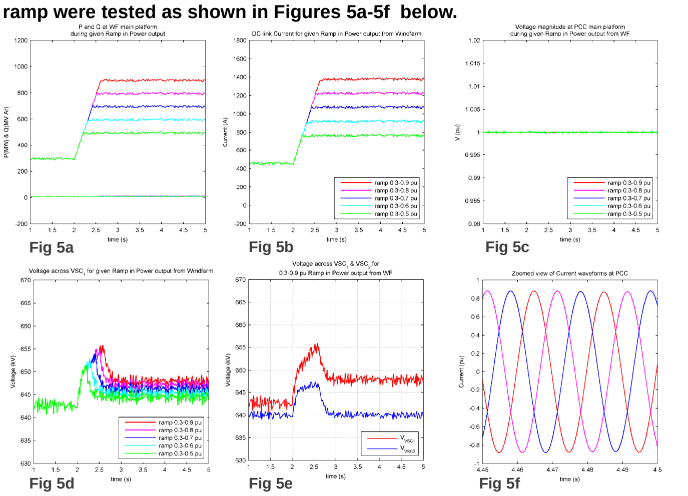

Fig 5a, Fig 5b, Fig 5c, Fig 5d, Fig 5e, Fig 5f

To illustrate the improved ac fault ride-through behaviour of the wind farm when integrated into the mainland grid using a VSC-HVDC link, a symmetrical ac three-phase fault to ground was applied to one of the tie lines that connects bus B_G to the grid as shown in Figures 6a - 6c below.

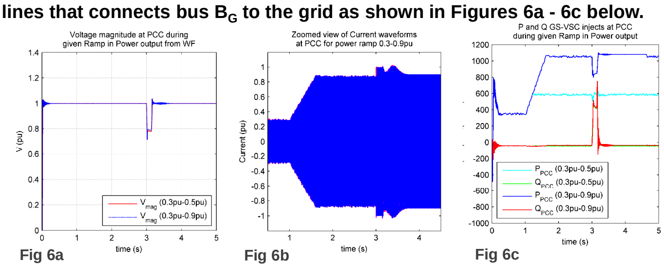

Fig 6a, Fig 6b, Fig 6c

4. Preliminary Study on Hybrid Converter for SEC

The SEC VSC can be reduced to 1/3 of original rating and connected with two equally rated 12-Pulse Diode Rectifiers in a hybrid topology as shown in Figure 7. This reduces the number of IGBTs used, replacing them with Diodes resulting in a lower cost converter with lower losses.

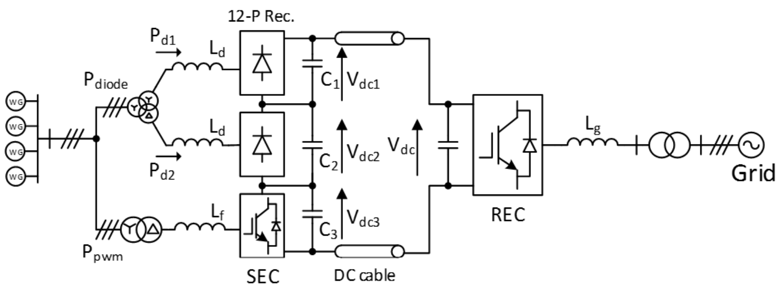

Fig 7. – Schematic for HVDC link with Hybrid Sending End Converter

Simulation was run with ramp up in power output from wind farm of $0.5\,pu\ to\ 0.9\,pu$, starting at $t = 2s$.

For this brief preliminary investigation into the described hybrid converter design, control of the SEC VSC was as before.

It can be seen from Figure 8 that Voltages across capacitors in the SEC of the DC link do not remain balanced with different magnitudes of power flow from the wind farm and additional control is required to achieve this.

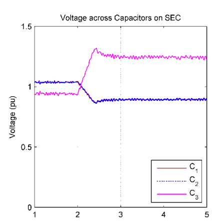

Fig 8. – Voltage across capacitors C_1, C_2 & C_3

5. Conclusion from Results

Figures 6a – 6c illustrate current HVDC technologies ability provide Low Voltage Ride Through (LVRT) support to the network while other ancillary services, such as frequency support, may also be demonstrated.

Since the REC converter, which governs HVDC link voltage, and its controller design remained the same for hybrid design, the DC link dynamics are similar to those seen in Figure 5b.

Therefore it should demonstrate LVRT capabilities but this is yet to be tested through simulations.

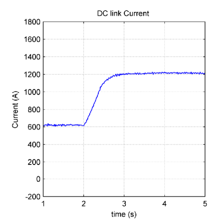

Fig 9. – Current through HVDC link

It is of high importance that the hybrid design for SEC be able to keep a stiff bus for the offshore AC network while also balancing the capacitor voltages in the SEC.

This will require additional control of power injected though the VSC into the DC link, thus controlling the balance of power injected by 12-P rectifiers and VSC allowing balancing of the capacitor voltages on the DC link.

With robust control over this, followed by demonstration of the models LVRT capabilities, investigations into frequency restoration services from the low cost hybrid converter may begin.

Future Work

- **Improve SEC control loop for voltage regulation both for offshore AC network and balancing C_1,C_2,C_3.**
- **Demonstrate LVRT for HVDC link with hybrid converter and investigate capability for participating in frequency restoration services.**
- **Investigate optimised solution for low cost, high support capability HVDC link for large offshore wind farms.**

ACKNOWLEDGMENTS - The authors would like to thank ETP, DNV and the NEWTON Institutional Links Project 247099 (CONACYT-British Council), for the funding and support provided in the preparation of this research work

Analysis of cyclone Xaver (2013) for offshore wind energy

Konstantinos Christakos[1], Ioannis Cheliotis[2], George Varlas[3,4], Gert-Jan Steeneveld[2]

[1]Metocean Group, Uni Research Polytec AS, Norway
[2]Meteorology and Air Quality Section, Wageningen University, The Netherlands
[3]Department of Geography, Harokopion University of Athens (HUA), Greece
[4]Institute of Marine Biological Resources and Inland Waters, Hellenic Centre for Marine Research (HCMR), Greece

Introduction

Cyclone Xaver (December 2013) was an extreme weather event which affected northern Europe, yielding a record of wind power generation. On 4 December, 2013 Xaver was initiated southeasterly of Greenland. During its formation, the upper air conditions intensified the cyclonic circulation and the system progressed southeasterly. The cyclone was continuously deepening during its movement towards Scandinavian Peninsula. In total, Xaver influenced an extensive region of North Europe, moving gradually from southeastern Greenland to the Baltic Sea, passing over the northern shore of United Kingdom, the North Sea and Scandinavia. The cyclone was accompanied by gale-force winds over North Sea and exceptionally low values of the core mean sea level pressure.

Weather Conditions

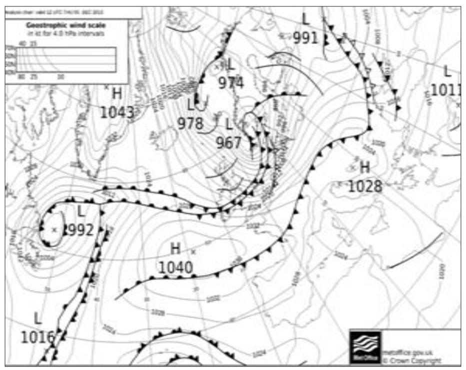

Figure 1. Surface pressure analysis map (hPa) on 5 December at 12:00 UTC, derived from UK Metoffice surface analyses archive. Cyclone Xaver is the low pressure system with its centre at 967 hPa.

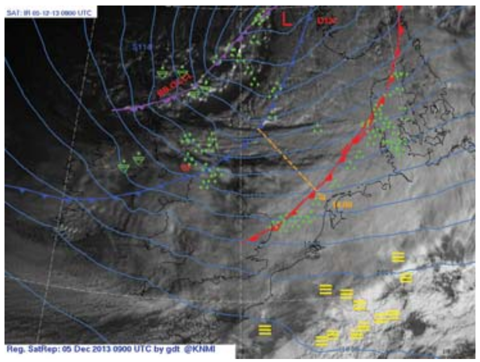

Figure 2. Regional SatRep over the North Sea on 5 December at 09:00 UTC, archived by http://www.knmi.nl/satrep

Energy Prices

Wind turbines set energy production records higher than 26000 MW, decreasing the power spot prices lower than 25 €/MWh. However in Denmark the shut down of wind turbines led to increase of the power spot prices up to 580 DKK/MWh.

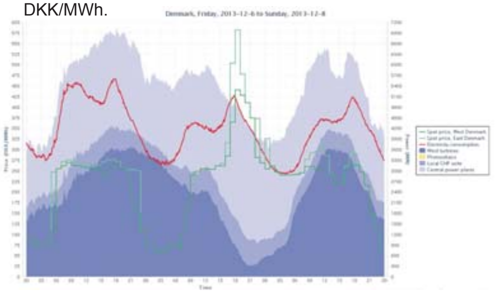

Figure 3. Energy spot prices and production during Cyclone Xaver in Denmark (source: EMD International A/S)

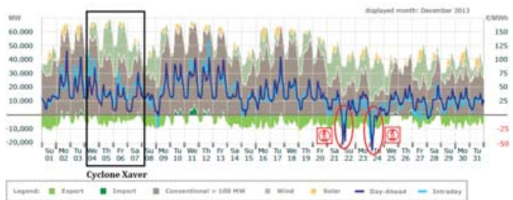

Figure 4. Energy spot prices and production, December 2013 in Germany [1]

Model & Evaluation

The Weather Research & Forecasting Model (WRF) ARW version 3.5 [2] was utilized for the simulation of cyclone Xaver. The numerical experiment used a 822 × 626 horizontal grid mesh, with horizontal resolution 5 km × 5 km, time step of 30 s and 50 vertical levels stretching from surface to 50 hPa. The simulation period was 84 hours, from 4 December, 2013 at 00:00 UTC to 7 December, 2013 at 12:00 UTC. Figure 5 illustrates the evaluation of the modelled wind speed with observations at 100 m at FINO 1, 2 and 3 [3].

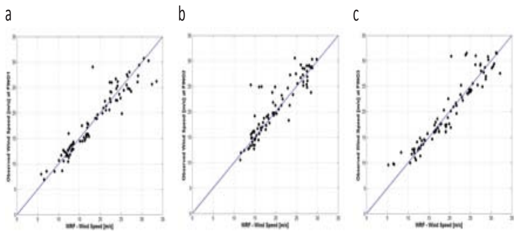

Figure 5. Scatter plots of model and observed wind speed (a-c) at FINO1-3 during 4 December, 2013 to 7 December, 2013

Cyclone Track

Figure 6. Mean sea level pressure in hPa (yellow) and maximum wind power density in W/m ^{2} at 100 m (red) tracks for cyclone Xaver as simulated by WRF model.

Wind Power

Figure 7 reveals information for the entire period under simulation. Figure 7 (a) presents the sum of hours that modelled wind speed at 100 m resides within the range 11-25 m/s (rated output wind speed). On the other hand Figure 7 (b) shows the sum of hours for extreme modelled wind speeds at 100 m, higher than 25 m/s (cut out wind speed). Figure 7 (a) shows the modelled wind speed ranging within 11-25 m/s approximately for 35 hours over the North Sea while the Baltic Sea displays higher frequencies, reaching up to 70 hours at some regions.

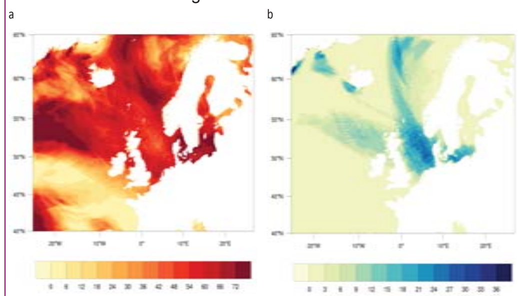

Figure 7 Sum of hours for wind speed at 100 m within the range 11-25 m/s (a), exceeding 25 m/s (b) for the period 4 December, 2013 at 00:00 UTC to 7 December, 2013 at 12:00 UTC as simulated by WRF model.

Figure 8 presents the simulated average wind power density for the period 5 December, 2013 06:00 UTC – 5 December, 2013 12:00 UTC for two 100 m (a) and 200 m (b). North Sea region is characterized by relatively high average wind power density. Especially for areas far away from the shore, wind power density exceeds 8000 W/m² at 100 m, ten times higher than the typical annual mean WPD for the area, and reaches 10000 W/m ^{2} at 200 m. On the contrary for regions outside the North Sea the values are equivalent to 4000 W/m².

Figure 8 (c) showcases the percentage increase of the wind power density between 200 m and 100 m. For the largest part of the North Sea the percentage increase ranges within 15% to 20%. Some regions of the North Sea, such as easterly of UK, display an increase that exceeds 25%.

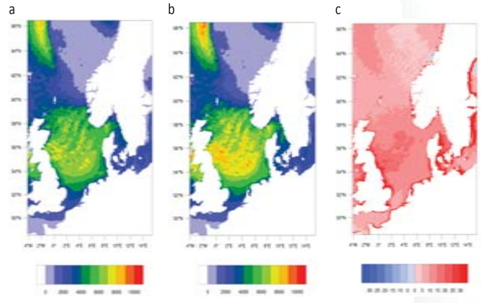

Figure 8. Average wind power density (W/m²) for the period 5 December, 2013 06:00 UTC – 5 December, 2013 12:00 UTC at 100 m (a), and 200 m (b) and the percentage increase (%) of the wind power density between 200 m and 100 m (c).

Conclusions

The current study presented an analysis of a severe cyclone, namely Xaver, with respect to the offshore wind energy as simulated by the WRF model.

- The focus of the study is on the extended region of the North Sea and the Baltic Sea.
- High values of wind power density at 100 m and 200 m occurred over the North Sea, surpassing 18000 W/m ^{2}, twenty two times higher than the typical annual mean WPD for the North Sea.
- The sum of hours for which the wind turbines perform to their utmost capacity (11-25 m/s) is ca 40 over the North Sea and ca 70 over the Baltic Sea.
- The sum of hours with wind speed at 100 m, exceeding 25 m/s, is more than 30 over the North Sea.
- A comparison of average wind power density between the height levels 100 m and 200 m showcased 15% to 20% increase at 200 m for the largest part of the North Sea with particular regions exceeding 25%.

Acknowledgements

1.Wind data from FINO 1, 2 and 3 platforms provided by BMWi (Bundesministerium fuer Wirtschaft und Energie, Federal Ministry for Economic Affairs and Energy) and the PTJ (Projekttraeger Juelich, project executing organisation).
2. The ACDG of Harokopio University of Athens is gratefully acknowledged for the provision of the numerical model WRF and the computer infrastructure to perform the simulations.

References

1. Mayer J., (2014), Electricity spot-prices and production data in Germany 2013, Fraunhofer Institute for Solar Energy Systems ISE
2. Skamarock, W. C., et al. A Description of the Advanced Research WRF Version 3, NCAR Technical Note, TN-468+STR, 113 pp., 2008
3.Forschungsplattformen in Nord- und Ostsee Nr. 1,2,3, http://www.fino-offshore.de

OBLO instrumentation at FINO1

Martin Flügge[1,3], Benny Svardal[1,3], Mostafa Bakhoday Paskyabi[2,3], Ilker Fer[2,3], Joachim Reuder[2,3], Stian Stavland[1] and Stephan Kral[2]

[1] Christian Michelsen Research AS, Bergen, Norway
[2] University of Bergen, Bergen, Norway
[3] Norwegian Centre for Offshore Wind Energy (NORCOWE)

Background

The Offshore Boundary-Layer Observatory (OBLO) operates state-of-the-art instrumentation and provides measurement capabilities for a wide range of atmospheric and oceanographic parameters relevant for offshore wind energy applications. As part of a measurement campaign performed by the Norwegian Centre for Offshore Wind Energy (NORCOWE), two scanning LiDAR systems and a passive microwave radiometer are deployed at the German research platform FINO1 in close vicinity to the Alpha Ventus wind farm. Simultaneous measurements of both wind speed, air temperature and humidity are performed up to an altitude of 1000 m, between May 2015 and June 2016. The oceanographic conditions, including sea temperature, salinity and current profiles, directional surface wave properties and turbulence levels in the water column were sampled from several submerged moorings, deployed between June and October 2015 in close vicinity to Alpha Ventus. The gathered data provides information on the interaction between the waves and the lower 200 m of the marine atmospheric boundary-layer. Such a combination of both meteorological and oceanographic instruments provide researchers with a unique data set that is highly relevant for offshore wind energy, e.g. wake propagation effects, boundary-layer stability and numerical model validation.

Meteorological OBLO instrumentation deployed at the German research platform FINO1 in the North Sea.

Measurement of the radial wind speed by scanning LiDAR systems

Two WindCube 100s systems perform measurements of the radial wind speed. The gathered data provide information on the wind conditions inside and around Alpha Ventus. This allows studies such as turbine inflow and turbine wake effects.

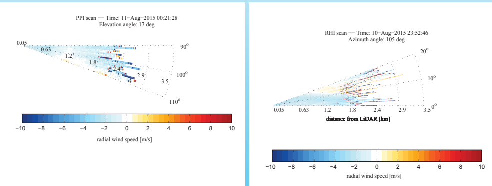

Example of an PPI (left) and RHI (right) scan directed into the Alpha Ventus wind farm. The changes in the wind speed due to the presence of a wind turbine is clearly visible

Measurement temperature- and humidity profiles

A passive microwave radiometer provides vertical profiles of atmospheric temperature and humidity up to more than 1000 m. These measurements are combined with the wind LiDAR measurements to obtain information on dynamic stability conditions at FINO1. This is the first time that such measurements are performed continuously nearby an offshore wind farm.

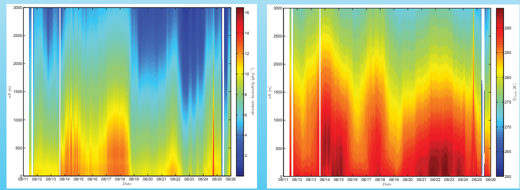

Example of Hovmøller diagrams for humidity (left) and temperature (right) obtained from radiometer data.

High frequency wind measurements

Two Gill-R3 ultra sonic anemometers (USA) have been installed at 15 and 20 masl, in addition to the already installed FINO1 USA at 40, 60 and 80 masl. The array of USA provide profiles of high-frequency 3D wind vector measurements. In addition, the USA installed at the lower levels provide information on heat- and momentum fluxes which is highly needed for the characterization of the marine atmospheric boundary-layer.

FINO1 mast measurements

Measurements of wind speed and direction are performed from cup anemometers and wind vanes installed in the FINO1 100 m met-mast since its construction in 2003. Time series of air and water temperature, relative humidity and precipitation are also recorded at FINO1 at selected heights. In addition, wave parameters are recorded from a Datawell Directional Waverider Buoy moored nearby the platform.

Oceanographic measurements

The overall aim of the oceanographic deployment is to gain a better understanding of environmentally significant interactions between the atmosphere, the ocean and offshore structures. This research focuses on the upper ocean turbulence characteristics in the presence of surface gravity wave-related processes such as wave breaking, non-breaking waves and coherent large-scale Langmuir circulations. This study intents to increase our knowledge about the interactions between offshore wind farms and upper ocean processes and to improve the understanding of single turbine and wind farm wake characteristics in the presence of combined wind and wave effects.

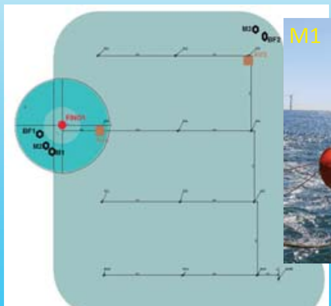

Several moorings have been deployed in close vicinity to FINO1 and the northeast side of the Alpah Ventus wind farm. The bottom frames (BF1 and BF2) and the submerged moorings (M2 and M3) were equipped with ADCP and ADV which provided current profiles and directional wave properties, in addition to turbulence statistics within the water column. The mooring M1 was equipped with airfoil shear probes and fast response thermistors in order to assess the Reynolds stresses.

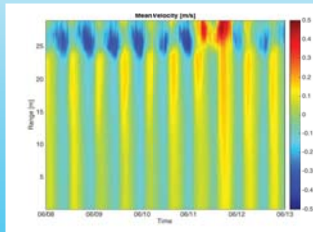

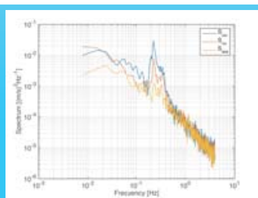

Example of a Hovmøller diagram for current speed obtained from ADCP measurements (upper figure) and example of a power spectra obtained from ADV measurements (lower figure).

SailBuoy

In addition to the oceanographic equipment, the Sailbuoy "SB Wave" was deployed at FINO1. The Sailbuoy was equipped with a motion sensor to provide an additional source of wave properties during the measurement campaign.

This platform is a surface vehicle with autonomous navigation. It is able to stay at sea for several months and can be used for a variety of ocean applications. For more information, visit http://www.sailbuoy.no/ .

Infrastructure access

The presented instrumentation is available for public and private research institutions dealing with wind energy. The OBLO project offers services for planning and execution of field deployments and post-analysis of the gathered data through the University of Bergen and Christian Michelsen Research AS.

For more information and access to the infrastructure, please contact Joachim.Reuder@uib.no, University of Bergen or Martin.Flugge@cmr.no , Christian Michelsen Research AS.

Energy systems on autonomous offshore measurement stations

T.K. Løken, Norwegian University of Science and Technology (NTNU) (trygve.loken@gmail.com), L.R. Sætran, NTNU, V. Neshaug, Fugro OCEANOR AS

Fluid Engineering Department, NTNU, Kolbjørn Hejes v 1 B, Trondheim 7491, Norway

Abstract

In this study, a performance test has been performed on a 200 W marine wind turbine, both in a wind tunnel, and mounted on a Wavescan ocean buoy in a coastal location near Trondheim. Long term wind data satisfying the DNV-RP-C205 [1] recommended practice for describing environmental conditions and environmental loads have been extracted from the Eklima database subordinated the Norwegian Meteorological Institute for a selected location called Sula weather station outside of the Norwegian coast. 10 years of data from Sula and a one-month performance test near Trondheim formed the basis for monthly wind energy estimates at the Sula site. Energy estimates for solar production on the Wavescan has been carried out at the same site utilizing the solar engineering software Meteonorm. The motivation of the study is to ensure continuous energy supply on remote measurement station enabling one-year autonomous operation.

Introduction

Wind speed varies with time and height above the sea surface. Elevation correction is especially important close to the sea surface, even for small elevation differences, due to the sharp gradient of the wind profile close to the surface. In this study, the commonly used logarithmic profile is used for correction:

$$U(z) = U(H)\left(1 + \frac{\ln(z/H)}{\ln(H/z_0)}\right)$$

where z_0 is a roughness parameter that depends on the wave height [2]. Regular Wavescan buoys have one mast with a sensor carrier assembly on top, supporting the ultrasonic wind sensor 4.0 m above the sea surface. The Air Breeze turbine was mounted on top of a second mast, with a resultant hub height of 2.6 m above the sea surface as seen in Fig. 1.

Fig. 1: Turbine on buoy

Methods

The experimental set-up presented in Fig. 2 resembled the planned buoy configuration, where the wind turbine was wired to a battery bank and a thermal load that dissipated produced energy.

It turned out more convenient to measure electrical power compared to mechanical power as the turbine drive shaft was sealed in the turbine house casing, making it impossible to connect it to a torque gauge. Additionally, this solution made the lab test and the field test compatible since the buoy configuration would log current consumption and production, which is directly proportional to electric power.

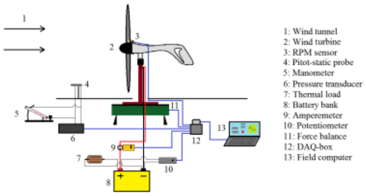

Fig. 2: Wind tunnel test-setup

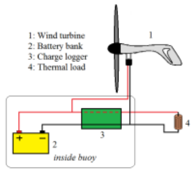

Fig. 3: Electrical configuration on buoy

The wind turbine and its complementary electrical system shown in Fig. 3 was wired isolated from the rest of the buoy in order to reduce sources of error that could disturb the measurements. The turbine was connected to a battery bank and a charge logger was used to monitor current flowing to and from the battery.

Results

The wind turbine was tested in a 2x3 sq. meter cross section wind tunnel and on the buoy located outside of Munkholmen in the Trondheim fjord. The field test period spanned from April 13th till May 25th 2015, with a gap of 10 days from May 8th, due to a malfunction on the wind sensor.

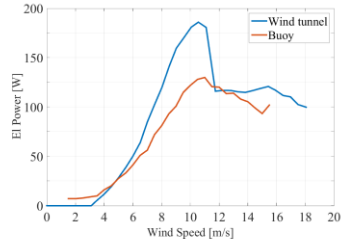

Fig. 4: Electric power-output in the wind tunnel (blue) and in the field (red)

Fig. 4 show a qualitative consistence between the electric power output from the wind tunnel test (blue) compared with the results from the test period on the buoy (red). Wind speeds below 1.5 m/s were discarded due to higher uncertainties associated to standard deviation in these bins relative to the other bins. The power output from the buoy peaked at 128 W. From cut-in speed up to rated wind speed, the output was approximately 35% lower than expected during ideal conditions.

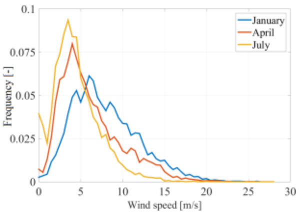

Fig. 5: Wind distributions

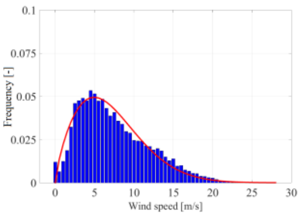

Fig. 6: Weibull fit for average March

Fig. 5 shows the ten year averaged, monthly wind distributions from Sula lighthouse outside the Norwegian coast for three selected months. As an example, the wind distribution and the fitted Weibull distribution for March are plotted in Fig. 6. The two distributions were quite consistent, thus the Weibull distribution was a reasonable assumption.

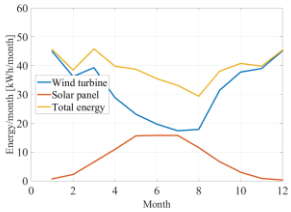

Fig. 7: Wind distributions

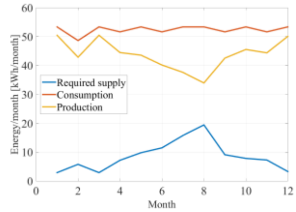

Fig. 8: Weibull fit for average March

Average wind power production on a monthly base at Sula was estimated with the extracted wind data. Solar production on the buoy was estimated with irradiation data from the Meteonorm solar engineering software for the same site. The results are presented in Fig. 7 along with solar and wind combined. When comparing total renewable energy production with energy consumption on board the buoy, presented in Fig. 8, the outcome was not a balanced energy budget. The figure shows a monthly additional energy requirement of 13 kWh on average, less in the winter and more in the summer.

References

[1] "Environmental Conditions and Environmental Loads," DNV-RP-C205, 2014.
[2] H. Bredemose, S. E. Larsen, D. Matha, A. Rettenmeier, E. Marino, and L. R. Sætran, "Offshore wind-wave climates and their scaling to lab conditions," MARINET, pp. 11-15, 2012.

Conclusion

- The solar panels and fuel cells already installed on the standard Wavescan buoys combined with an Air Breeze wind turbine would ensure autonomous operation for 24 months at the selected site, which is a significant improvement compared to the current 6 months operation capacity.
- To ensure a supply system based solely on renewable energy, the turbine area would have to be increased by 85% in order to balance the energy budget throughout the year.
- Alternatively, a second turbine could be introduced. In that case, it is recommended to mount the turbines at different elevations to avoid wake losses when the turbines are aligned with the wind speed direction, and to consider thrust data imparted on the buoy.

Site Assessment of the floating wind turbine Hywind

Marit Stokke, Anja Eide Onstad, Lars Sætran*
Norwegian University of Science and Technology
Department of Energy and Process Engineering
*lars.satran@ntnu.no

Abstract
In order to predict the environmental conditions at a wind turbine site it is essential to perform a Site Assessment at the specific site. In this work, 2 years of data from a Seawatch buoy at the Hywind site have been evaluated and results for wind, waves and ocean currents are presented and evaluated. A long term extrapolation of wind data has been performed to ensure that results are not based on inter-annual trends. Seasonal variations with maximum values for wind, waves and ocean current occurring during winter are found, with the prevailing flow directions parallel to the coastline.

The site

In 2009 Statoil installed the world's first full-scale floating wind turbine off the coast of Karmøy in the North Sea. This work is based on data from 2009 to 2011 measured by a Seawatch buoy located 200 m west of the floating turbine, Hywind. The depth at the site is 210 m.

Figure 1 : **Map of positions of Seawatch buoy, Hywind turbine and meteorological stations from Google Maps**

Wind

Wind data are measured at 3.5 m height as 10-minute means. The buoy data are long term extrapolated (LTE) utilizing the Matrix Time Series method with the data from Utsira as reference data, see Figure 1. Figure 2 displays the results for the LTE data, Figure 2 a showing the direction of the approaching wind. The LTE data display

- A near constant diurnal wind speed profile
- Seasonal variations with stronger wind speeds during winter
- A mean wind speed of 10.0 m/s at hub height, vertically extrapolated using the power law with $\alpha = 0.11$

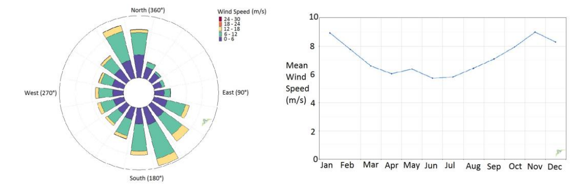

(a) Wind direction distribution for the LTE data **(b) Monthly Wind Speed Profile for the LTE data**

Figure 2 : **Wind results for the LTE data at the Hywind site.**

Wave

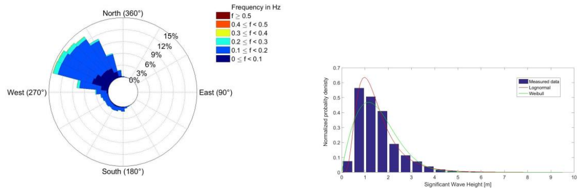

(a) Distribution of frequency vs direction **(b) Normalized distribution of significant wave height**

Figure 3 : **Results for estimated significant wave height.**

The time series from the Seawatch buoy contains several parameters, among them are the estimated significant wave height, the period and the flow direction, these are represented by Figure 3. Direction is in degree measured clockwise from True North and describes the direction the wave comes from. Most of the waves have

- Frequency between 0.05 and 0.30 Hz
- Direction between 250° and 350°

Ocean current

As depth increases the flow direction of the ocean current gets more evenly distributed as Figure 4 shows. 0° represent north and the direction describes where the ocean current flows towards.

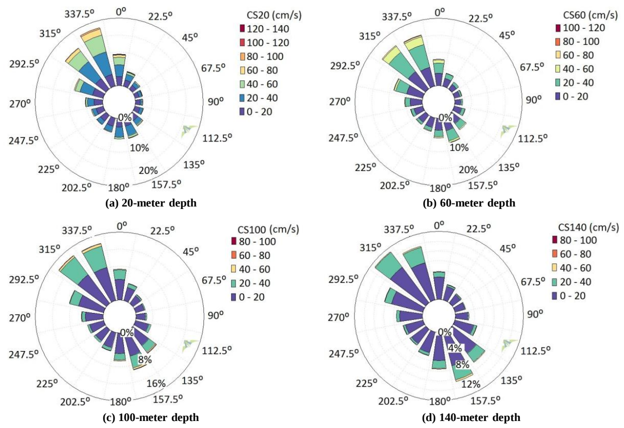

Figure 4 : **The frequency vs direction at different depths.**

The ocean current are measured with 10 m intervals down to 180 m, the mean speed at these depths in addition to the no-slip condition at the bottom result in the velocity profile in Figure 5.

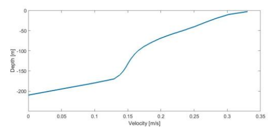

[ht]

Figure 5 : **Velocity profile for the ocean current**

Conclusions

- Constant mean diurnal wind speed profile
- Seasonal trends. Higher wind during winter and extremes of both waves and current observed in late winter as result of sudden increases in wind speed.
- Vertical extrapolation using the power law with α=0.11 results in a mean wind speed of 10 m/s at hub height.
- Combination of lognormal and Weibull distributions are preferable to describe waves.
- Weibull distribution gives a good description of the ocean current.

References

[1] Measnet - Evaluation of site-specific wind condition. Measuring Network of Wind Energy Institute, November (2009).

[2] DIAZ, P., MIKKELSEN, A., GRYNING, T., HASAGER, S.-E., BAY, C., HAHMANN, A. N., BADGER, M., KARAGALI, I., AND COURTNEY, M. Offshore vertical wind shear: Final report on NORSEWInD's work task 3.1. DTU Wind Energy E; No. 0005 (2012), 116.

[3] FUGRO OCEANOR. Seawatch buoy, (2016).

[4] MASSEL, S. R. Ocean surface waves: their physics and prediction, vol. 11. World Scientific, Toh Tuck Link, Singapore, (2005).

[5] TUCKER, M. J. Waves in Ocean Engineering - Measurement, Analysis, Interpretation. Ellis Horwood Limited, Chichester, England, (1991).

Acknowledgements

The authors would like to thank Statoil, Fugro OCEANOR and NOWITECH for providing them with material of the Seawatch buoy.

Analysis of gust factors from Frøya

Lars Morten Bardal[1], Lars Roar Sætran[1]

[1]Norwegian University of Science and Technology, Dept. Energy and Process Engineering, 7491 Trondheim, Norway

Introduction

A wind turbine is harvesting the energy in the wind, but must also withstand the large dynamic forces imposed by the turbulent wind field. Ideally we would like the wind to be stable with no fluctuations, both from a design and operation point of view, but the reality is far from ideal. The atmospheric wind is very turbulent over a large range of scales and wind gusts of the scale of a wind turbine become important for load calculation and wind turbine control. The wind velocity gust factor is a parameter used for extreme load calculations and is defined as the ratio between maximum and mean wind speed:

$$G_{T,\tau} = \frac{U_{max,\tau}}{\overline{U}_T}$$

where $U_{max,\tau}$ is the maximum τ second moving average wind speed during a T-second averaging period. Another gust parameter often used is the "peak factor" which is defined as the relative gust amplitude divided by the standard deviation of the longitudinal wind speed:

$$k_{pT,\tau} = \frac{U_{max,\tau} - \overline{U}_T}{\sigma_U} = \frac{G-1}{I_U}$$

Many models and standards exist for gust factor for engineering applications. In this study measurements will be compared to an analytical model by Greenway [1] based on a Von Karman turbulence spectrum and a Gaussian wind speed distribution and a simple formulation for peak factor by Wieringa [2]:

$$G_{T,\tau} = 1 + I_U\left(1.42 + 0.3013\ln\left(\frac{T}{\tau} - 4\right)\right)$$

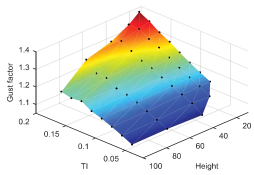

Fig. 1 Measured mean gust factor vs. Turbulence intensity and height

The Frøya site

- Location: Skipheia, near the village Titran at the island Frøya on the coast of Mid-Norway. (Fig. 2)

Fig. 2 The measurement site and mast at Frøya

- Facilities: 2 100m masts, 1 45m mast and house for instrumentation and accommodation
- Instrumentation:
  - 16 Gill WindObserver ultrasonic 2D anemometers
  - 1 Gill WindMaster 3D ultrasonic anemometer
  - 6 PT100 temperature sensors
  - pressure and humidity sensor
- Wind climate:
  - Mean wind speed at 10m: 6.5m/s
  - Mean power law exponent α: 0.108
  - Roughness length: 0.0005-0.02

Methods

Gust factor and peak factor have been calculated for 6 heights between 10 and 100 meters from 100000 10-min time series. A running average filter with a time window τ of 1, 3 and 10 seconds was applied to the time series. In order to remove low frequency trends and reduce influence of non-stationarity, linear de-trending was applied prior to analysis. The horizontal wind speed and wind direction were measured at a sampling rate of 1Hz using Gill WindObserver 2D ultrasonic anemometers. The Obukhov length have been estimated from the measured bulk Richarson number.

Results

The gust factor increases with turbulence intensity and deceases with gust averaging time. A linear model by Wieringa based on these two parameters is compared with measurements in Fig. 3 and shows a good fit for low and moderate turbulence intensities, but not I_U > ~0.2. The reason for this might be that the high turbulence intensity conditions are associated with low wind speeds and therefore the assumption of a Gaussian wind speed distribution is broken.

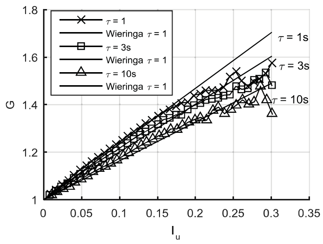

Fig. 3 Gust factor $G_{600,\tau}$ as a function of turbulence intensity I_U and gust averaging time τ.

Comparing the measured gust factors to the model of Greenway [1] we use only data from narrow bins for wind speed and turbulence intensity. For a detailed derivation of the model see [1]. The results shown in Figure 4 shows a discrepancy between the measurements and the model, the model giving a mode value 1.24 compared to a mode of 1.20 from the data. A length scale of 300 meters is used, but it could be noted that the analytical model is not very sensitive to the integral length scale used. The error increases with increasing turbulence intensity and systematically overestimates the gust factors from the Frøya .

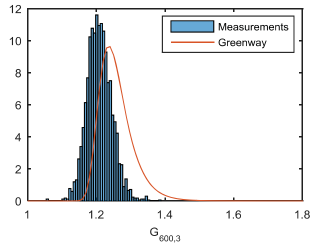

Fig. 4 Measurements of G600,3 compared to the analytical model from [1] for U=10m/s, I_U=0.1 and L_U=300. Measurements include 14m/s < U < 16m/s and 0.09 < I_U < 0.11.

The mean peak factor measured at Frøya is independent of wind speed and height, but decreases with increasing turbulence intensity (Fig. 5) . The ISO 4352 standard for wind action on structures recommends a constant peak factor of 3.9, 3.0 and 2.4 for 1, 3 and 10 second gust averaging respectively. Compared to the measured data (Fig. 5 and Fig. 6) this appears very conservative.

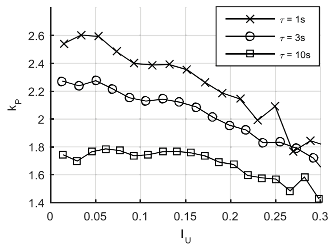

Fig. 5 Peak factor k_P vs. Turbulence intensity and gust averaging time, τ

The peak factor (Fig. 6) is less sensitive to atmospheric stability, but shows a slightly deceasing trend with increased stability. This variation might be due to the larger scale and intensity of turbulence associated with unstable conditions[13].

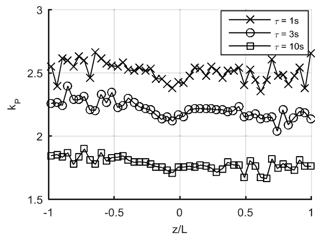

Fig. 6 Peak factor k_P vs. atmospheric stability z/L

Conclusion

The dependence of measured gust factors on various parameters of the atmospheric wind field is presented based on a 5 year dataset from Frøya.

- The gust factor mainly depends on turbulence intensity, height and gust averaging time
- The simple linear model by Wieringa [2] fits the measurements well for low and intermediate turbulence.
- The model from Greenway [1] for the distribution of gust factors shows an overall overestimations compared to the measured data., but a good fit of the scale parameter.
- The peak factor which includes the turbulence intensity has a small dependence on turbulence intensity and atmospheric stability.

References

[1] M.E. Greenway, An analytical approach to wind velocity gust factors, Journal of Wind Engineering and Industrial Aerodynamics, 5 (1979) 61-91.

[2] J. Wieringa, Gust factors over open water and built-up country, Boundary-Layer Meteorol, 3 (1973) 424-441.

[3] S. Frandsen, H.E. Jørgensen, J.D. Sørensen, Relevant criteria for testing the quality of turbulence models, in: The European Wind Energy Conference and Exhibition, EWEC 2007, Milan, 2007.

NTNU
Norwegian University of Technology

Universität Rostock Traditio et Innovatio

LWET Stiftungslehrstuhl Windenergietechnik

ESG

DR.-ING. FRANK ADAM

USE OF REINFORCED CONCRETE COMPOSITE MATERIAL

Development of a TLP substructure for a 6 MW wind turbine

PATH OF DEVELOPMENT – TLP SUBSTRUCTURE

The challenging work for the research project called 'Floating platform for offshore wind turbines' started in 2009. The GICON®-Group and their key partners, e.g. University of Rostock and fabrication partner ESG GmbH have been developing a TLP solution for offshore wind turbines with vertical and angled ten-sioned ropes. Based on the fundamental experience from experimental and numerical studies, the current design was established.

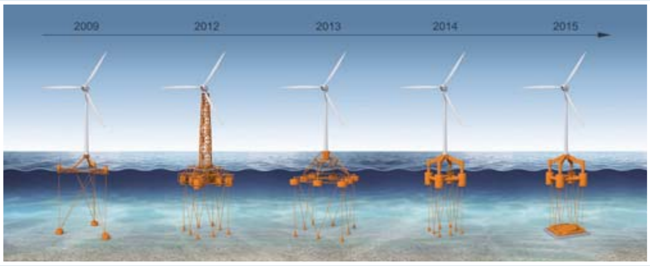

KEY PARAMETER COMPARISON OF THE STRUCTURE'S DESIGN PHASES:

Year / Parameter	2009	2012	2013	2014	**2016**
TLP Mass in t	≈ 2000	2214	1790	742	**1356**
Width in m	70	68	50	32	**32**
Height in m	25	24	39	28	**40**
Max. righting arm in m	N/A	5.30	7.60	2.50	**2.10**
CoG	N/A	8.90	10.50	10.91	**13.60**
# of anchor points	3	4	4	4	**4**
Wind turbine capacity	2.0 MW	2.0 MW	2.0 MW	2.3 MW	**6.0 MW**

ADVANTAGES:

- Deployable from 20 meters to 350 meters and more
- Portside assembly and transport of the entire structure to the deployme location
- Modular construction resulting in more flexibility in the supply chain
- Several anchoring technology options
- Reduced impact on site subsoil via gravity anchor plate foundation
- Ease of maintenance
- If needed, entire structure can be completely replaced

SCIENCE & RESEARCH

Currently ongoing research includes the comparison of calculated data with actual experimental data obtained through wind & wave tank experiments with the scaled models. These tests have provided insights regarding the dynamic characteristics of the GICON®-TLP by analyzing the measured time series RAO´s or decay test results.

Research insights from the various experiments have been published:

- The added mass coefficients belonging to the comparison of measured results compared with simulated ones yielded to C_{a_pipe} = 0.6 and C_{a_bb} = 0.2 > published by *Adam, F., Steinke, C., Dahlhaus, F. and Großmann, J.*, 2013. **„GICON-TLP for wind turbines – Validation of calculated results"**. Proc. ISOPE 2013 An chorage, vol. 1, pp. p: 421–427.
- Validation of the calculation model via decay test results and confirmation of the added mass coefficients > published by *Adam, F., Myland, T., Dahlhaus, F. and Großmann, J.*, 2014. **„Scale tests of the GICON®-TLP for wind turbines"**. Proc. OMAE 2014, Paper-No. 23216, San Francisco.
- Evaluation of internal force superposition on a TLP for wind turbines > published by *Adam, F., Myland, T., Schuldt, B., Großmann, J. and Dahlhaus, F.*, 2014. **„Evaluation of internal force superposition on a TLP for wind turbines"**. Renewable Energy
- Comparison of three different TLPs for wind turbines > published by *Adam, F., Myland, T., Dahlhaus, F. and Großmann, J.*, 2015. **„Comparison of three different TLPs for wind turbines by tank tests and calculated results"**. Proc. OMAE 2015, Paper-No. 41018, St. Johns.

DEVELOPMENT OF A TLP SUBSTRUCTURE FOR A 6 MW WIND TURBINE

The preliminary scaling up of the system will comprise initially a geometrical re-design, utilizing past experience to implement design improvements. Analysis will then be carried out re. three critical areas:

- Hydrodynamic stability, during both installation and operation
- Eigen Analysis
- Structural Resistance

Initially analyzing these areas will give a good overview of the feasibility of the system and highlight which areas of the design should be optimized for future development.

HYDRODYNAMIC STABILITY

The hydrodynamic stability is an important part of the design as it is beneficial to keep the wind turbine at its optimal height and orientation. It is also vital to keep the movement and acceleration of the structure to a minimum in order to prevent damage to and potential failure of the components. Initially, the floating stability of the structure (Anchor + TLP + RNA + Tower) is analyzed to determine how the system would react independently.

Angle of Attack in deg	Maximum Deviation				
	Acceleration in m/s²			Rotation in deg	
	x	y	z	rx	ry
180	0.616	0.155	3.014	0.058	0.716
135	0.385	0.495	2.799	0.078	0.854
90	0.017	0.661	2.716	0.164	7.970
45	0.384	0.496	2.801	0.040	0.736
0	0.617	0.155	3.017	0.100	0.735

EIGEN ANALYSIS

A modal analysis was then conducted on the entire TLP system, including: Mooring lines, Tower and SOF structure, with the RNA being modeled as a signal mass point. The results are presented for the following four systems:

- 50 meters water depth; 4 vertical mooring lines
- 50 meters water depth; 4 vertical mooring lines, 8 angled mooring lines

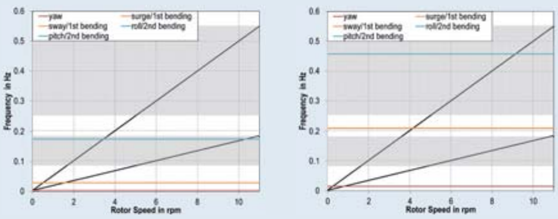

STRUCTURAL RESISTANCE

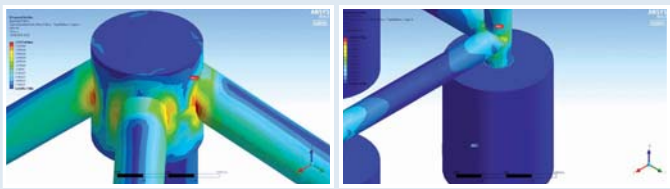

ACKNOWLEDGMENT

We like to express our sincere gratitude to the German Federal State of Mecklenburg-Vorpommern, for the financial support provided to the ESG GmbH, a member of the GICON Group (Project number: V-630-1-260-2012/103).

CONTACT

STIFTUNGSLEHRSTUHL WINDENERGIETECHNIK | Universität Rostock | Albert-Einstein-Strasse 2 | 18051 Rostock, Germany
ESG EDELSTAHL UND UMWELTTECHNIK GMBH | GICON Group | Ziegelstrasse 8 | 18439 Stralsund, Germany

AN OFFSHORE 40M HIGH TLP MET. MAST AT 65M DEEP WATERS IN THE AEGEAN SEA

FloatMast® Ltd.

ΚΑΠΕ CRES

Dimitri FOUSSEKIS[1], Antonios PEPPAS[2], Theodore PAPATHEODOROU[3]

1 Research Engineer, Centre for Renewable Energy Sources (CRES), 19th km Marathon Avenue, GR-19009, Pikermi, Greece, **dfousek@cres.gr**

2 Civil Engineer, FloatMast® Ltd, 156A Burnt Oak Broadway, Edgware, Middlesex, HA8 0AX, **peppas@floatmast.com**

3 Naval Engineer, Streamlined Naval Architects Ltd, 98 Neorion St,188 63 Perama, Greece, **papatheodorou@streamlined.gr**

INTRODUCTION

Reliable and Bankable Wind Resource Assessment in offshore wind farms, presents a huge challenge, as only fixed met-masts are, at the moment, IEC/MEASNET compliant measuring devices.

With the FloatMast platform, IEC/MEASNET compliant data can be acquired, at a much lower cost, at any depth and distance from the shore. As a result, a wider range of capabilities become available to developers (from wind resource assessment to environmental -marine and atmospheric- data monitoring), increasing thus the project value, the data credibility and bankability.

At the end of a campaign, the platform can be redeployed at another site. The adaptation consists mainly in modifying the anchorage to adapt at the new water depth and sea tide.

DESIGN PARAMETERS

- Comply with the IEC / MEASNET Guidelines
- Conform with the proven methodology applied for onshore complex topographies (low met mast+Lidar)
- Adopt existing mature solutions from the mature Oil & Gas Industry
- Re-deployable platform
- Optimize the ratio `P90/Cost´ for offshore wind resource assessment

	Cost	Wind Speed uncertainty 1	
Fixed HH Mast	~ 8.0M€	~ 2.2%	
Fixed HH Mast + Lidar	~ 8.5M€	~ 2.1%	
Floating Lidar	~ 1.2M€	~ 4.0%	
FloatMast	~ 3.0M€	~ 2.4%	(expected)

KEY ADVANTAGES VS FIXED MASTS AND FLOATING LIDARS

Extremely low mean wind speed deviation compared to a Fixed Met Mast

Analysis of real offshore 10min-wind data2 using a 5MW HAWT shows that, using the measured wind shear, the deviation between the annual average wind speed at hub-height (100m asl) and the extrapolated one from a lower anemometer is only 0.4%. Similarly, the deviation of the WT's annual energy yield is 1.3% and capacity factor deviation result is 0.7%.

Superior data availability based on cup anemometer.

Contrary to LIDARs, cup anemometers are expected to approach 100% data availability. For an annual availability of 80%3, then the above mentioned offshore dataset, run for 14 different scenarios, yields average deviations for the annual wind speed of 1.4% and for the annual energy yield of 1.7%.

Avoid wind speed uncertainties due to wave motions

Results from recent publications with wind speed comparisons between stable and wave-influenced platforms, for various types of LIDARs, converge to similar deviations: 1.6%[4] 1.5%[5] 1.4% 1.0%[6] 1.4%[7]

Although no energy yield deviations are given, the above result is an additional uncertainty to be accounted, further decreasing the bankability of an offshore project.

MODEL TANK TESTS

The small (unavoidable) motions of the TLP platform are monitored by high-precision marine motion and orientation sensors. Naval Design calculations, together with CFD simulations and model tank tests of a 1:25 prototype, showed practically no heave motion, very low translations (<0.1Hz) and tilt angles below 3deg, even in storm conditions. The above, when confirmed in the real model, will render motion compensation unnecessary.

Naval Design Calculations | CFD Simulations | Model Tank Tests | Platform Translation Behavior | Platform Rotation Behavior

DEPLOYMENT PHASE STARTED

The prototype is ready for deployment off the coast of Makronisos island at a sea depth of 65m, in the Aegean sea, known for its severe sea state conditions and its high wind potential (9m/s annual average wind speed).

CONCLUSIONS

The project demonstrates that TLP platforms are very well suited to wind energy applications and practically no motion compensation is required for the wind speed measuring devices.

Lidars are known to have lower data availabilities than cup anemometers, mainly due to atmospheric conditions, but also because they are sophisticated opticoelectronic devices, requiring also power autonomy. With the FloatMast platform, lidar unavoidable data losses are recovered from cup anemometers, with much lower uncertainties than correlating with faraway met masts. The high data availability assured by the reliable cup anemometers, lowers the results uncertainties, the investment cost of the offshore wind farm and increases bankability.

1. John Slater , Charles Pearce "The benefits and uncertainties of floating lidar", RWE Innogy UK, EWEA 2015
2. CRES Technical note: "Sensitivity analysis of 5-year wind data from the FINO1 offshore platform", EERA-DTOC project, 2014.
3. Latest revision of the German TR6 guideline for Wind Resource Assessment, requiring for LIDAR standalone operation, 12 consecutive months of measurement, with a minimum data availability of 80%.
4. CMR publication: "Effect of wave motion on wind lidar measurements - Comparison testing with controlled motion applied", DeepWind 2013 Conference, Norway
5. DNV publication: "Remote Sensing on Moving Offshore Platforms", Tony Rogers, Katy Briggs, Gordon Randall, Holly Hughes, EWEA 2011
6. ZephIR Lidar publication: "The effect of motion on continuous wave lidar wind measurements", A. Rutherford, M. Pitter, C Slinger, etc, WINDPOWER 2013, Chicago
7. GL-GH publication: "Investigating the Efficacy of Floating LIDAR Motion Compensation Algorithms for Offshore Wind Resource Assessment Applications", Daniel W. Jaynes, EWEA 2011.

SPONSORS

HUTCHINSON® TITAN BUREAU VERITAS TPW THEBES PIPEWORKS S.A.

A project co-founded by: EUROPEAN UNION EUROPEAN REGIONAL DEVELOPMENT FUND

Evaluation of ensemble prediction forecasts for estimating weather windows

Norwegian Meteorological Institute

B. R. Furevik, J. B. Bremnes, M. Reistad
Contact: *Allégaten 70, 5007 Bergen.*
Telephone: 5523 6600
birgitte.furevik@met.no

Introduction

The chaotic nature of the weather system was early pointed out by Edward Lorenz (1917-2008) :

"…two states differing by imperceptible amounts may eventually evolve into two considerably different states. If, then, there is any error whatever in observing the present state — and in any real system such errors seem inevitable — an acceptable prediction of an instantaneous state in the distant future may well be impossible….In view of the inevitable inaccuracy and incompleteness of weather observations, precise very-long-range forecasting would seem to be nonexistent." Lorentz (1963).

Running the same numerical model several times using nearly identical initial conditions and comparing the results, gives an indication of the uncertainty of the weather situation. The 51 ensemble members of wave height shown in Figure 1 indicate that forecasting skills are greatly reduced after day 4.

The European Center for Medium Range Weather Forecast ensemble system (ENS) is global and needs calibration before it can be used to estimate uncertainties of forecasts at specific locations. Some challenges are illustrated in figure1-3.

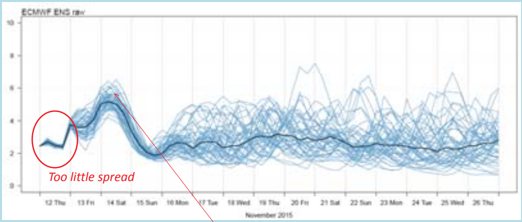

Figure 1: Example of significant wave height forecast from ECMWF ensemble model system with 51 members. Black line is the median. North Sea location.

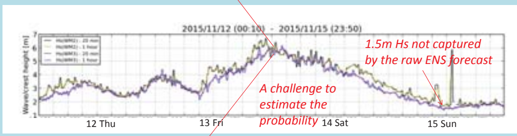

Figure 2: Observed wave height over the three first days of the forecast from two different wave sensors.

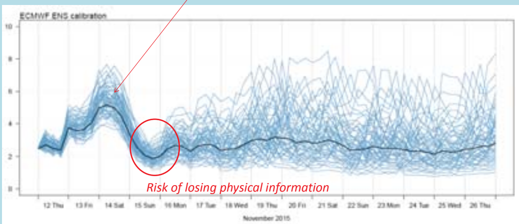

Figure 3: Example of calibrated forecast.

We further look into the possibility of using calibrated ensembles as an alternative to the alpha – factor method when predicting weather windows.

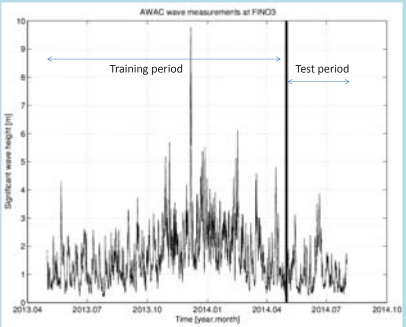

Figure 4: Training and test data set from the FINO-3 Acoustic Wave and Current Profiler.

Using reliable observations over one year from the AWAC (figure 4) at FINO3 (see location in figure 5) the ENS forecasts of significant wave height (Hs) and mean wave period (Tz) are calibrated to give probability forecasts over the 3 months test period. Results on the right part of poster are from the test period.

In locations where there are no observations an alternative is to use the Norwegian Reanalysis of wind and waves (NORA10) (figure 5). NORA10 is a downscaling to 10 km of the ERA-40 dataset and ECMWF forecasts for 1958-2015, which verify well against observations in Norwegian areas (Reistad et al., 2015).

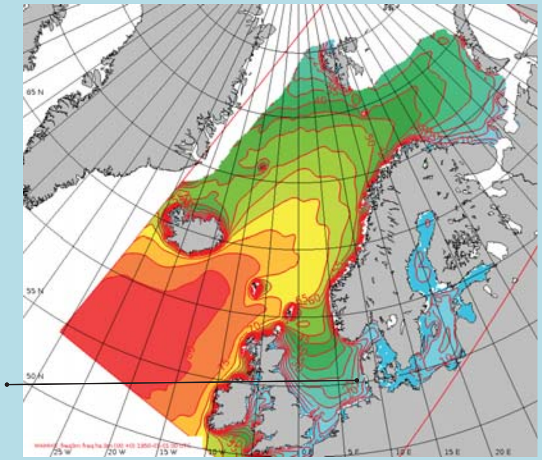

Figure 5: % of the time when significant wave height is above 3m in January. Based on NORA10 data.

norcowe
Norwegian Centre for Offshore Wind Energy

Validation results

The validation of the forecasts of Hs and Tz over the test period is shown in figures below. Continued rank probability skill score (CRPSS) show a 40% improvement in wave height and 60% improvement in mean period from the calibration. Mean absolute error (MAE) is reduced for wave period and the mean error (ME) in both parameters is strongly reduced.

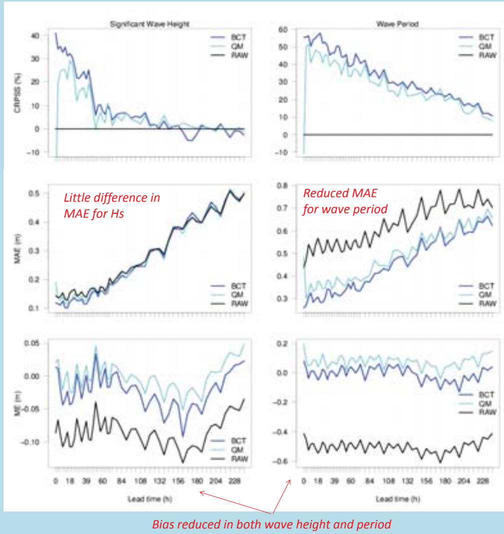

Ranking the observation with the 51 forecasts, the rank of the observation should over time be uniformly distributed if the forecast is reliable, given by the reliability index.

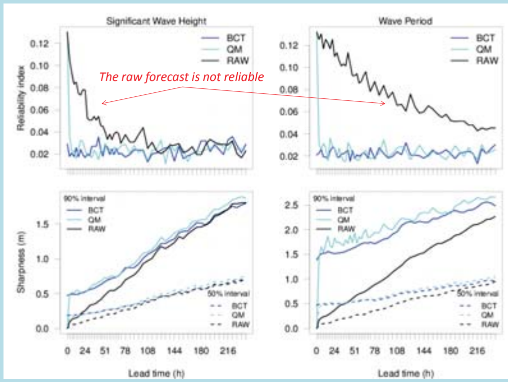

Sharpness is a measure of the width of the 90% and 50% interval in meter for Hs and seconds for Tz. The raw forecast has no spread at analysis time, and therefore 0 sharpness.

Alpha-factor

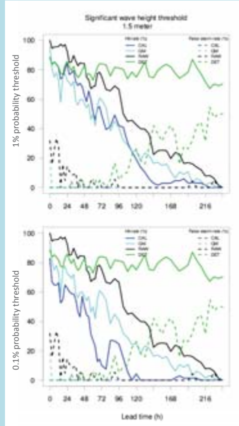

Figure 6: Hit and false alarm rate probabilities of 1 and 0.1 % for Hs<1.5m.

RAW: raw ECMWF ENS forecast
BCT : calibrated forecast
QM : bias corrected forecast
DET : deterministic forecast (α-factor 0.71)

Hit and false alarm rate (Figure 6) at 1% threshold for EPS and 1hr window is not improved compared to α-factor method (green line). The Box-Cox t-distribution (BCT) used for calibration is very flexible (four parameters) and if there is high variability in the observations during the training period this may result in a heavy upper tail in the statistical model. That may be the reason for the conservative result with the BCT in figure 6 and may be improved.

In the tables we've counted the number of 24-hours weather windows for design wave height 1.5m over the test period.

Based on the observations there are 67 forecasts with weather windows and 39 forecasts without. ENS50 of the raw ensemble predicts 4 false weather windows.

	Obs	Forecast	Ctrl	Med.	Mean
BCT	Yes	Yes	44	45	46
	Yes	No	23	22	21
	No	Yes	0	0	0
	No	No	39	39	39
RAW	Yes	Yes	53	53	53
	Yes	No	14	14	14
	No	Yes	0	0	0
	No	No	39	39	39

Table 1: Number of 24 hours weather windows using deterministic forecast and α-factor according to level A – meteorologist on site.

Calibrated ENS – best forecast?

	Obs	Forecast	Ctrl	Med.	Mean	ENS50	ENS49	ENS48	ENS47	ENS46	ENS45
BCT	Yes	Yes	39	40	40	49	51	53	54	54	54
	Yes	No	28	27	27	18	16	14	13	13	13
	No	Yes	0	0	0	0	0	0	0	0	0
	No	No	39	39	39	39	39	39	39	39	39
RAW	Yes	Yes	44	44	44	60	63	64	64	64	64
	Yes	No	23	23	23	7	4	3	3	3	3
	No	Yes	0	0	0	4	4	4	4	6	7
	No	No	39	39	39	35	35	35	35	33	32

Table 2: Number of 24 hours weather windows using deterministic forecast and α-factor according to level C – base case. ENS50 is the uppermost ensemble member at any time, representing approximately 2% probability. ENS49 is the 2nd from the top etc.

Acknowledgements

The work is part of the project "Decision support for offshore wind turbine installation" funded by the Norwegian Research Council and Statoil ASA. The wave measurements from FINO3 are obtained from Bundesministerium für Umwelt, Federal Ministry for the Environment, Nature Conservation and Nuclear Safety, Germany. Ensemble forecasts are obtained from European Center for Medium-Range Weather Forecasts, Reading, UK.

References

- Bremnes, J.B., M. Reistad and B.R. Furevik (2016) Statistical calibration of wave ensembles – a Box-Cox t-distribution approach, MET report 1/2016.
- DNV (2011) Marine operations, General. DNV-OS-H101 .
- Lorenz, E. N., (1963) Deterministic nonperiodic flow, Journal of the atmospheric sciences, vol. 20. Citations from page 133 & 141.
- Reistad, M., H. Haakenstad, B. R. Furevik, J. E. Haugen, Ø. Breivik and O. J. Aarnes (2015) Validation of the Norwegian wind and wave hindcast – NORA10, MET report 28/2015.

Assessment of profitable operation and maintenance strategies

Adaptive surrogate model fitting for the NOWIcob model

Marius Rise Gallala

Department of Mathematical Sciences, NTNU. Contact: marius.gallala@gmail.com

NTNU

Introduction

Reducing the operation and maintenance (O&M) cost is essential in order to reduce the cost of energy from wind farms. Finding good O&M strategies are a complex problem: the strategies involve many decisions that interacts and develop over time. Simulation models enable us to evaluate the performance of different O&M strategies. The set of all possible strategies is very large, so we can only explore small parts of it.

In the following, a method that effectively explore and identify favorable O&M strategies is presented. The method guides the search of optimum towards regions with high predicted performance and/or regions with little knowledge. The method iteratively performs simulations and select the next input point for simulation.

Main Objectives

Identify O&M strategies which ensures a high amount of produced energy compared to the associated O&M cost. The trade off between these and other performance measures is specified by the user and represented with an objective function to be maximized. The process should be applicable to any well-defined wind farm and choice of decision variables.

Setting - stochastic simulation model

The NOWIcob model is used to simulate the failure of turbines and the related maintenance and logistic operations. The associated output is typically a measure of produced energy and related O&M costs.

Input ($\mathbf{x}$)	Description
Weather	Time series for wave height and wind speed.
Turbine type	Properties as power curve, physical dimensions, cut-in and cut-off speed etc.
Distance to location	The shortest distance from to the location(s) with personnel accommodation.
Simulation horizon	The simulated lifetime of the wind farm-.
Failure rates	The different failure types are assumed to occur randomly with some intensity.
Personnel available	The average number of technicians available each shift.
Vessel fleet	Vessels are used in the various O&M tasks.

Table 1: Examples of input parameters.

The observed output y of the objective, e.g. profit or another perfomance measure, may be viewed as a realization of

$$y = f(\mathbf{x}) + \epsilon(\mathbf{x}) \tag{1}$$

where $f(\mathbf{x})$ may be interpreted as the true input-output relation. The noise term $\epsilon(\mathbf{x})$ is due to stochastic treatment of time between failures and weather.

Method

We use an adaptive approach for exploring favorable O&M strategies. The procedure is called adaptive since an input point for simulation is selected based on existing information, and new information is obtained through simulation. This is repeated iteratively.

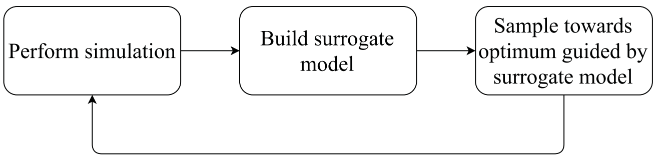

Figure 1: Adaptive fitting of surrogate model.

Perform simulation

Any O&M strategy may be represented by a set of input parameters $\mathbf{x}_{new}$. The resulting output y_{new} gives us information of the performance of the strategy. The new information is appended to previous simulation data, e.g. $\mathbf{D} = \{\mathbf{D}, (\mathbf{x}, y)_{new}\}$

Fit surrogate model - Prediction and quantification of uncertainty

A surrogate model $\hat{f}(\mathbf{x})$ mimics the input-output relation $f(\mathbf{x})$. We model the relation as a two layer feedforward neural network fitted to all available simulation data $\mathbf{D}$.

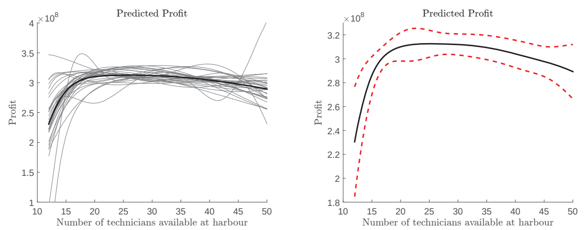

(a) 30 single neural network predictions varies around the surrogate model prediction.

(b) Surrogate model prediction and a measure prediction uncertainty $\epsilon(\mathbf{x})$.

Figure 2: Surrogate model prediction and a measure of uncertainty.

A more stable and accurate surrogate model is formed by combining the prediction of several neural networks, each fitted to a bootstrap sample of $\mathbf{D}$. Moreover, this technique enables us to quantify the uncertainty $\epsilon(\mathbf{x})$.

Sample towards optimum: balance exploitation and exploration

We want to gain knowledge of O&M strategies which are likely to maximize the objective. To avoid finding local optimums, we aid the search towards regions with high uncertainty as well as high predicted objective. The two aspects

1. exploitation - high predicted objective

2. exploration - high predicted variance

are balanced by an acquisition function $u(\mathbf{x})$.

$$\mathbf{x}_{new} = \underset{\mathbf{x}\in\Omega}{\text{argmax}} \quad \{u(\mathbf{x}) \mid \mathbf{D}\} \tag{2}$$

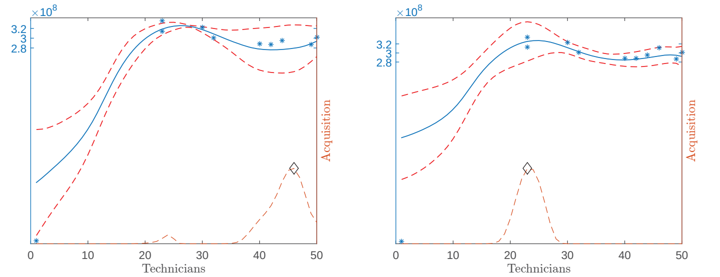

(a) 6. iteration $\mathbf{x}_{new} = 46$

(b) 7. iteration $\mathbf{x}_{new} = 23$

Figure 3: Balancing exploitation and exploration.

Results

The method for finding optimal strategies should ideally converge to approximately the same solution, regardless of sampling path. By starting with initial samples in opposite regions, the method is able to identify the same favorable region in less than 20 iterations.

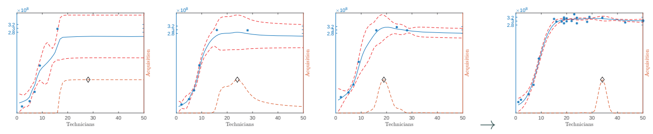

(a) 1. iteration $\mathbf{x}_{new} = 28$ **(b)** 2. iteration $\mathbf{x}_{new} = 24$ **(c)** 3. iteration $\mathbf{x}_{new} = 19$ **(d)** 20. iteration

Figure 4: Starting with samples in left region (few technicians).

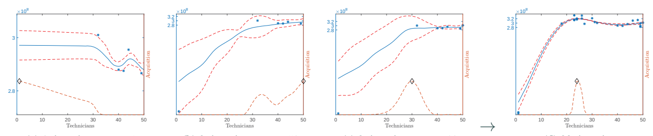

(a) 1. iteration $\mathbf{x}_{new} = 1$ **(b)** 2. iteration $\mathbf{x}_{new} = 50$ **(c)** 3. iteration $\mathbf{x}_{new} = 30$ **(d)** 20. iteration

Figure 5: Starting with samples in right region (many technicians).

Conclusions

The adaptive method of iteratively performing simulation, fitting surrogate model and selecting the next point for simulation has been tested for cases with a low number of decision parameters.

- The adaptive approach is able to identify reasonable strategies for the test cases.
- By balancing exploitation and exploration the method avoids getting stuck in local optimums.
- The process of simulating, fitting and selecting is performed automatically. This reduces the need of manually initialize and analyze a large number of simulations.

Forthcoming Research

The adaptive approach is further studied in a Master's thesis during the spring of 2016. The thesis aims at giving a deeper understanding of the abilities of the suggested approach.

Risk and Reliability based O&M Planning of Offshore Wind Farms

M. Florian[1], M. Asgarpour[1,2], J.D. Sørensen[1]

1) Aalborg University (AAU), Department of Civil Engineering, Denmark

2) Energy Research Centre of the Netherlands (ECN), Unit Wind Energy, the Netherlands

Introduction

Operational costs of offshore wind farms are one of the main contributors to the high cost of energy and can be significantly reduced by using an optimal maintenance strategy to support the wind farm operator in short-term decision making and long-term O&M planning.

During two PhD projects an optimal risk and reliability O&M model is being developed to minimize the total operational costs by balancing the amount of corrective and preventive maintenance efforts, considering all system effects.

The developed O&M model consists of a risk based decision and cost model, which are using deterioration models, inspection results, SCADA data, condition monitoring data and climate data as inputs.

The model output is the long-term O&M planning of the wind farm and decision support to the wind farm operator in daily wind farm operation.

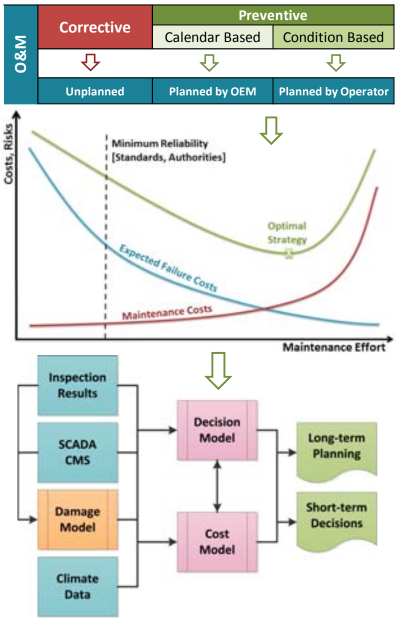

Developing and Updating the Decision Model

By having all the input data and the cost model it's possible to develop a decision model including decision rules and criteria. The following figure shows a life cycle decision tree for optimal O&M planning of a wind turbine or a wind farm with multiple critical components.

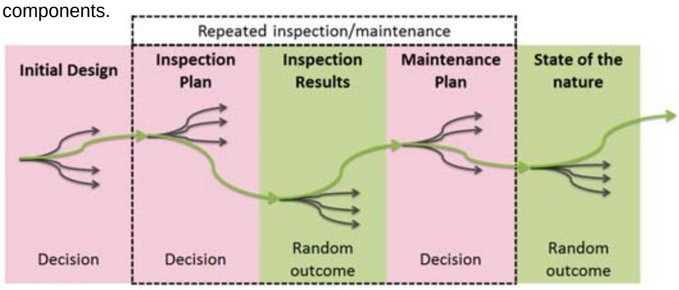

Decision of initial design is made by the designer as it should maximize the total expected benefits minus costs during the whole lifetime such that safety requirement are fulfilled at any time. The 'repeated inspection/maintenance' box includes continuous decisions and observation of uncertain parameters during the whole lifetime.

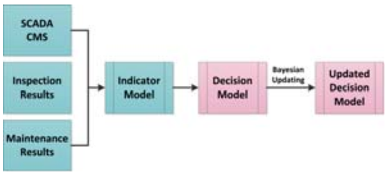

Risk based O&M planning of offshore wind turbines it's a process where there is continuous feedback of information from the system. Therefore, it's necessary to update the decision rules and criteria whenever new information is being available.

Developing the Deterioration Models

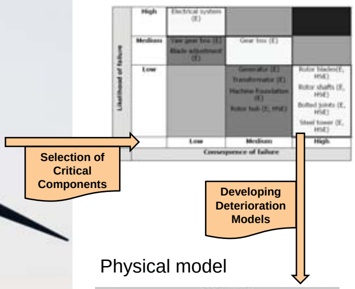

Within this project four deterioration models for selected critical components are being considered:

- ➢ Steel welded
- ➢ Steel non-welded
- ➢ Electrical systems
- ➢ Composite materials

Physical model

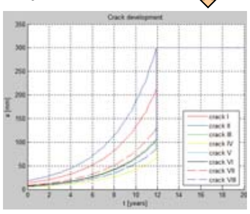

Statistical model

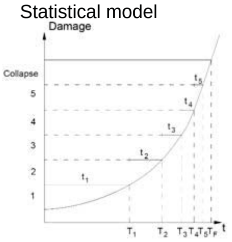

Application on NORCOWE wind farm

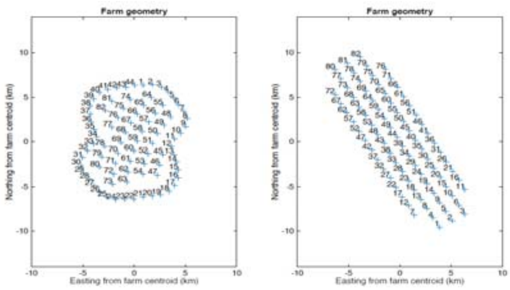

A baseline O&M strategy is developed and applied to the NORCOWE wind farm. The analysis is made on two different layouts and serves as a reference point for comparison of cost of energy between traditional O&M strategies, and a risk and reliability based approach

Layout	Annual O&M cost	Availability
Curvilinear	1.0564 10^8 [€]	90.01[%]
Rectilinear	1.0553 10^8 [€]	90.21[%]

Updating the Deterioration Models

Since deterioration mechanisms such as fatigue, corrosion, wear and erosion are associated with significant uncertainty, the developed deterioration models should be updated using direct and indirect information from indicators and Bayesian statistical techniques.

As illustrated in the following figure, damage model at time T1 has been updated based on the observations from the inspection and associated maintenance actions. Therefore, the expected damage level at time T2 will be smaller in this example.

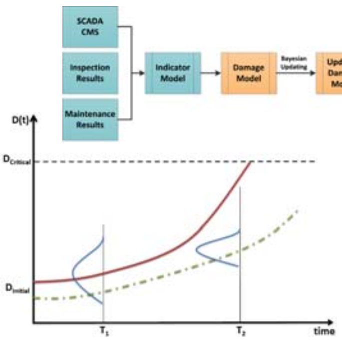

Demonstration of the risk-based O&M Model

By developing all required data blocks, an optimal risk and reliability based O&M model will be developed. Then, the component based approach will be extended to a system based approach to consider all system effects.

At the end of the project, the developed optimal risk and reliability based O&M approach will be demonstrated using the NORCOWE reference wind farm, which is a 800MW offshore wind farm consisting of 80 NREL 10MW reference wind turbine.

Acknowledgments

The work presented here is supported by Aalborg University, ECN and NORCOWE.

EERA DeepWind'2016
Radisson Blu Royal Garden Hotel, Trondheim
January 20-22, 2016

The Operation and Maintenance Planning Based on Reliability Analysis of Fatigue Fracture of a Wind Turbine Drivetrain Components

Arvydas Beržonskis(P), John Dalsgaard Sørensen
Aalborg University

Abstract

Offshore wind turbines located in deep waters are exposed to harsh environmental conditions including extreme winds, temperatures, waves and lightning storms. These severe conditions significantly increases the cost of offshore wind project installation, operation and maintenance (O&M) and reduces the reliability of the wind turbines. Therefore, the levelized cost of energy (LCOE) produced by offshore wind turbines is relatively high. The increased energy costs are due to the fact that the offshore O&M is quite expensive and contributes up to 30% of the COE.

The cost of offshore O&M is caused by the dependency on the weather condition, vessel availability in addition to the energy loses due to the down time of the turbine. Eventual failures in the wind turbine drivetrain module result in around 25% of the total down time, hence resulting in significant lost revenue.

The following research addresses the influence of the pre-existing defects on the reliability of the wind turbine drive train and the utilization of developed methods for O&M planning and quality control. The wind turbine main shaft is regarded as a main component of interest. Crack propagation models are developed with the assumption that the pre-existing defects are located in the main shaft and consequently subjected to lifetime loading history of the component.

Probabilistic models, based on Paris and Walker crack propagation laws, are developed and applied to estimate the probability of failure. The reliability analysis was conducted by the use of first order reliability method (FORM). The results gained form the probabilistic reliability analysis, provide a basis for O&M inspections and repair planning methods with additional potential for new quality control methods for casted iron components.

Graphical representation of the model

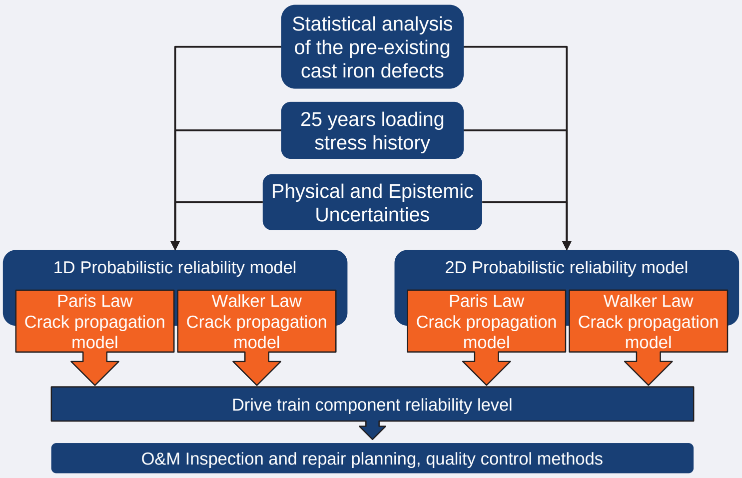

Objectives

- Present a general framework for the probabilistic reliability models.
- Present the results gained.
- Discuss model utilization for O&M and quality control.

Methods

- **Statistical analysis of the pre-existing cast iron defects**

The statistical analysis was performed on the defects gained by scanning the sand casted specimens of cast iron. An Weibull distribution was fitted to the defects data, which was evaluated in 10 quantiles.

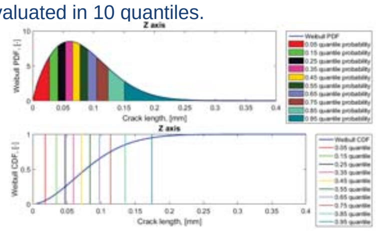

The values gained were used as deterministic values in combination with stochastic a_0/c_0 ratio of initial crack sizes for the probabilistic reliability models.

- **25 years loading stress history**

The internal reaction moments gained from the HAWC2 in combination with the wind speed distribution, was utilized as the basis to create the 25 years loading stress history of the main shaft. In this research the main shaft is subjected exclusively to torsional stresses.

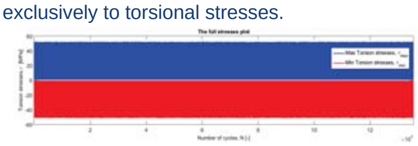

Probabilistic reliability models and results

- **Crack propagation models**

Two crack propagation models were utilized for the probabilistic reliability models, namely Paris and Walker laws. $\frac{da}{dN} = C(\Delta K)^m$; $\frac{da}{dN} = \frac{C(\Delta K)^m}{(1-R)^{m(1-\lambda)}}$;

- **1D Probabilistic reliability model**

The one dimensional reliability model is formulated around the stress intensity factor ΔK exceeding the fracture toughness value K_{IC}. The model limit state equation:

$$g(t) = K_{IC} - X_{dyn}X_{exp}X_{aero}X_{str}X_{sif}K_I(t)$$

- **2D Probabilistic reliability model**

The two dimensional reliability model is based on the ultimate limit state, investigating the reduced cross-section ability to resist the loading stresses. The model limit state equation:

$$g(t) = \sigma_y X_R A_{reduced}(t) - X_{dyn}X_{exp}X_{aero}X_{str}X_{sif}\tau A(t)$$

- **Total reliability index**

The reliability index in a critical volume part V_C is approximately by:

$$P_F(t) = \sum_i P(g(t)|c_0 = x_i)P_{Existence}P_{orientation}$$

$$\beta = -\Phi^{-1}(P_F(t))$$

- **1D accumulated reliability index**

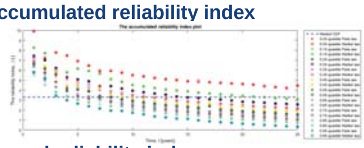

- **1D annual reliability index**

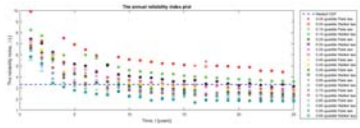

- **2D accumulated reliability index**

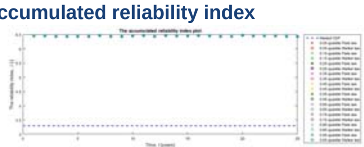

- **2D annual reliability index**

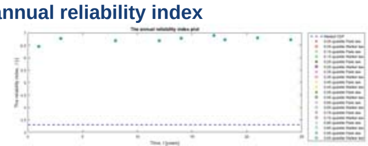

- **Total reliability index**

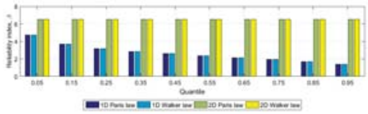

Acknowledgments

The research is supported by the Strategic Research Center "REWIND – Knowledge based engineering for improved reliability of critical wind turbine components", Danish research Council for Strategic Research.

Conclusions and future work

Based on the results gained via the one dimensional probabilistic reliability simulation, it can be observed that 60% of the simulated models fall under the design reliability index value of 3.3 after 10 years. Hence, the O&M inspections should be planned around this time. Additionally, the total reliability indexes reveal that seven largest of quantiles analyzed fails the design reliability requirement β=3.3 over the 25 year lifetime. It can be noticed from the two dimensional model that the crack growth does not reduce the reliability of the main shaft significantly throughout the lifetime of the component. Future work will include expanding the reliability models to incorporate the Failure Assessment Diagram model. In addition, expanding the probabilistic models to contain stochastic variables regarded to material properties of the considered casted component.

O&M decision problems

Investigating key decision problems to optimise the operation and maintenance strategy of offshore wind farms

Overview

- Investigates 3 decision problems with potential to optimise O&M and logistics strategies for offshore wind farms:
  1. What is the optimal composition of annual pre-determined jack-up vessel campaign periods for heavy maintenance ?
  2. What is the optimal crew transfer vessel (CTVs) fleet for smaller corrective and preventive maintenance tasks?
  3. What is the optimal start month for annual preventive maintenance services?
- Compares problems in terms of potential cost reduction and the variability and associated uncertainty in results.
- Demonstrates the benefits and difficulties of considering problems together rather than solving them in isolation.

Conclusions

a) Predetermined jack-up vessel campaigns could be a competitive strategy

b) Larger uncertainty for jack-up vessel decision problem

c) Not advantageous to consider jack-up vessel problem together with CTV fleet selection

d) Important of seeing the timing of annual service campaigns together with the selection of the CTV fleet

Acknowledgements:
This project has received funding from the European Union's Seventh Programme for research, technological development and demonstration under grant agreement No. 614020 (LEANWIND).

Iver Bakken Sperstad
Magne Kolstad
Severin Sjømark
SINTEF Energy Research, Trondheim, Norway

Fiona Devoy McAuliffe
MaREI, ERI, University College Cork, Ireland

Contact: iver.bakken.sperstad@sintef.no

Motivation and background

The offshore wind industry needs to reduce costs and turbine downtime to make it competitive with other forms of energy production. The O&M phase of an offshore wind farm is subject to a vast range of decisions and, therefore, opportunities to improve efficiency and reduce costs. The objective of the EU FP7 project LEANWIND is to improve efficiency and reduce costs across all life cycle phases, including O&M.

Comparison of decision problems

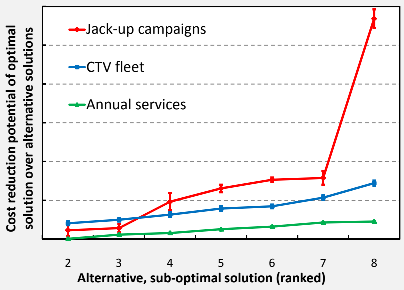

Jack-up vessel decisions have high potential for cost reduction but are associated with high uncertainties (failures requiring jack-up vessels happen rarely but each failure has large cost implications)

Better ↑ / Worse ↓

1	MarJulOct	1 SCTV + 2 ACTV	May
2	MarJunSepDec	2 SCTV + 2 ACTV	Apr
3	JanAprJulOct	3 ACTV	Jun
4	MarSep	2 SCTV + 1 ACTV	Mar
5	AprSepOct	2 ACTV	Feb
6	MarAugSep	1 SCTV + 3 ACTV	Jul
7	AprJunAugOct	3 SCTV + 1 ACTV	Jan
8	AugSepOct	1 SCTV + 1 ACTV	Aug

(SCTV = Standard CTV; ACTV = Advanced CTV)

Co-optimising decision problems

Difficulties: Although the optimal CTV fleet and jack-up vessel campaign composition remains the same when co-optimising , including the jack-up-vessels increases the stochastic variability. This introduces "noise" making it more challenging to solve the CTV fleet selection problem.

Advantages: Considering the CTV fleet and annual service start month problems together, it is found that with a larger fleet the start month could begin later in the year, potentially further reducing downtime and revenue losses.

Methodology

- The NOWIcob O&M model, a Monte Carlo discrete-event simulation model developed by SINTEF Energy Research, was applied for the study
- LEANWIND 125 x 8 MW reference wind farm with representative failure data:
  - 3 corrective maintenance tasks requiring crew transfer vessels
  - 1 corrective maintenance task requiring a jack-up vessel
  - 1 preventive maintenance task (annual service)
- For each decision problem, a selection of possible strategy solutions are defined
- To find the "optimal" solution, the sums of direct O&M costs and downtime costs are compared
- First each decision problems (1, 2 and 3) was studied in isolation for a relevant subset of maintenance tasks
- Then the decision problems (1+2 and 2+3) were co-optimised including all maintenance tasks

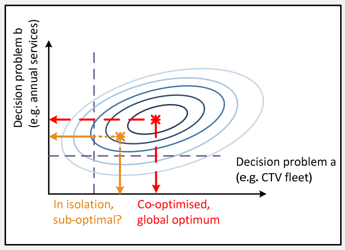

Jack-up vessel campaigns

- Compositions of 2-4 month-long heavy maintenance campaigns are considered
- Campaign periods spread relative evenly over the year are better
- Comparison with conventional fix-on-failure charter strategies indicate that predetermined campaign periods can be advantageous for large wind farms

Better ↑ / Worse ↓

Campaign composition	Spring			Summer			Autumn			Winter		
MarJulOct	Mar				Jul			Oct				
MarJunSepDec	Mar			Jun			Sep			Dec		
JanAprJulOct		Apr			Jul			Oct			Jan	
MarSep	Mar						Sep					
AprSepOct		Apr					Sep	Oct				
MarAugSep	Mar					Aug	Sep					
AprJunAugOct		Apr		Jun		Aug		Oct				
AugSepOct						Aug	Sep	Oct				

University College Cork, Ireland
Coláiste na hOllscoile Corcaigh

leanwind

Vessel fleet optimization for maintenance operations at offshore wind farms under uncertainty

Magnus Stålhane[a] (magnus.stalhane@iot.ntnu.no), Hanne Vefsnmo[a], Elin Halvorsen-Weare[b],
Lars Magnus Hvattum[c], Lars Magne[a] Nonås[b],
a) Department of Industrial Economics and Technology Management, NTNU
b) Department of Maritime Transport Systems, MARINTEK
c) Faculty of Logistics, Molde University College

Abstract

We study the problem of determining the optimal fleet size and mix of vessels to support maintenance activities at offshore wind farms. A two-stage stochastic programming model is proposed where uncertainty in demand and weather conditions are taken into account. The model aims to consider the whole life span of an offshore wind farm, and should at the same time remain solvable for realistically sized problem instances. The results from a computational study based on realistic data is provided.

Problem description

Today, the offshore wind energy industry needs financial support to be profitable, and producers in the United Kingdom receive a subsidy of approximately EUR 100 per MWh produced . Following the initial investment, the largest cost component is the cost of operations and maintenance (O&M) activities, which may constitute between 20--25 % of the life-cycle costs of an offshore wind turbine. The cost of vessels, helicopters and infrastructure used to support O&M activities is one of the largest cost elements during the operational phase of an offshore wind farm. With a many different vessels available, all with their strengths and weaknesses, the question then becomes which vessel fleet is the most cost effective for any given offshore wind farm(s)?

In addition, we also consider different base options, such as a normal onshore base, mother vessel concepts, artificial islands and offshore platforms. While offshore base concepts probably are too expensive for small wind farms, they may be useful if they are able to serve several wind farms in close proximity to each other.

Mathematical model

The problem is formulated as a two-stage stochastic mathematical model. The key elements of this model are:

- the goal is to minimize total costs
- more than one wind farm may be considered
- the wind farm(s) are built in several steps, spanning several years
- the vessels may be purchased and sold at different points in time
- there is uncertainty in the amount of maintenance to perform
- there is uncertainty in the time available for maintenance work
- uncertainty is captured through scenarios in a two-stage model

The first stage decisions are:

- Which vessels to buy, sell, charter in, and charter out each year
- Which base(s) to use

The second stage decisions for a given scenario with a given weather and failure realization ensure that all maintenance tasks are performed with the fleet decided in stage one, and calculates the estimated downtime costs.

Results

When testing the model we have considered one or several offshore wind farm(s) located in the North Sea. Initial testing showed that it was sufficient to use 50 scenarios to achieve good in-sample stability, while out-of-sample stability required fewer scenarios. The computational experiments show that the mathematical model provide close to optimal fleet size and mix decisions within short CPU times. The model provides significant added value compared with the deterministic counterpart in some instances. Closer inspection reveals that much of the Value of stochastic solution comes from the costly investments in a jack-up rig. The stochastic model is more reluctant to purchase such a rig, preferring to charter in whenever needed for small wind farms. The deterministic expected value problem is eager to invest in a rig, not being able to see that the special demand for the rig will be irregularly distributed.

Furthermore, the computational study showed that for some instances it is valuable to take uncertainty in demand and weather conditions into account. However, it is surprising that the value decreases for larger wind farms, and it is possible that for this particular problem a more detailed representation of the tactical planning is needed. However, the model will quickly become impractical to solve, and this appears to be a challenging prospect for future research.

Conclusions

- Model is most valuable for relatively small wind farms
- Stability tests show that at least 50 scenarios is needed to get stable results that are independent of the scenario tree
- Computing times are low (as long as 1% cut off)

NTNU

DTU Wind Energy
Department of Wind Energy

Maintenance polar and marine traffic analysis on an existing wind farm

Authors: Lorenzo Colone*, Anand Natarajan*, Nikolay Dimitrov* and Thomas Buhl*

***Technical University of Denmark Department of Wind Energy, Risø Campus Frederiksborgvej 399, 4000 Roskilde, Denmark**

Introduction

– Maintenance activities are based on short term and long term weather forecasts whose derivation relies on historical site-specific data analysis, typically supplied by meteorological masts installed in the area before the construction phase is initiated. Wind-wave statistical correlation is used to predict weather windows both on an annual scale and a monthly scale where the sea state is here represented by wind speed, direction and significant wave height. The objective of this work is a static prediction of weather windows based on the statistics typically available to operators when planning maintenance. Results are compared with real site measurements from two nacelle anemometers and utilized together with the past history of marine traffic analysis within an offshore wind farm.

Problem

– Known parameters : 1. Annual wind speed statistics conditional to wind direction $P(u \mid \theta)$ and marginal wind direction probability $P(\theta)$; 2. Distribution of the wind speed conditional on the month of the year represented by quantiles (percentage of time the wind speed is below a given value $P(U < u)$; 3. Annual and monthly wave statistical distributions for each direction as a function of mean wind speed. The aim is to define a measure of site accessibility conditional to wind speed and direction as driving parameter.

Annual analysis

– The aim is to derive a probability of maintenance $P_{m,\theta}(\theta)$ on an annual scale as the probability of having significant wave height conditional to wind speed below a certain threshold $h_{s0} = 2\,m$. The wind speed range is $u = [0,12]\,m/s$. Using statistical data described together with Figure 1 the information needed can be extracted. The probability of maintenance is a measure of the chances to visit the wind farm when knowledge about wind direction is provided. The site accessibility is total percentage of hours the sea state is below the thresholds defined.

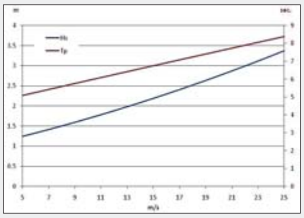

Figure 1 : Significant wave height $h_s(u)$ and wave period $T(u)$ as functions of mean wind speed u

$$P_{m,\theta}(\theta) = P(h_s(u) \le h_{s_0} \mid \theta) = \int_{u_0}^{u_1} p(u \mid \theta)\, p(h_s(u) \le h_{s_0} \mid u, \theta)\, du$$

$$a_\theta(\theta) = P(\theta)\, P_{m,\theta}(\theta) \qquad a = \int_0^{2\pi} a_\theta(\theta)\, d\theta$$

Definition of probability of maintenance $P_{m,\theta}(\theta)$, site accessibility $a_\theta(\theta)$ and the total accessibility as percentage of hours a as a function of wind direction

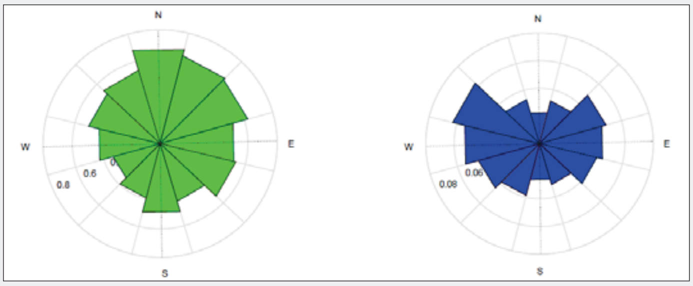

Figure 2 : On the left the probability of maintenance conditional to each direction (green) and on the right (blue) the site accessibility expressed in terms of fraction of hours over one year reference period

Monthly analysis

The transition annual to monthly is performed by combining annual and monthly statistics. From annual data is possible to infer a marginal wind direction distribution for each month $P_i(\theta)$ where i indicates the month. In order to account for a seasonal dependence, monthly wind roses are generated by introducing a random seasonal directional wind speed variability and a distribution $P_i(u \mid \theta)$ is generated for each month. Both $P_i(\theta)$ and $P_i(u \mid \theta)$ satisfy the annual constraints. This is achieved by setting up a non linear constrained system and assuming $P_i(u \mid \theta)$ to be Weibull distributed for each direction for each month. Similarities in the wind speed distribution and directional dependence are encountered between predicted wind roses and real measurements recorded in 2012 and 2013 from two cup anemometers installed on two different turbine nacelle.

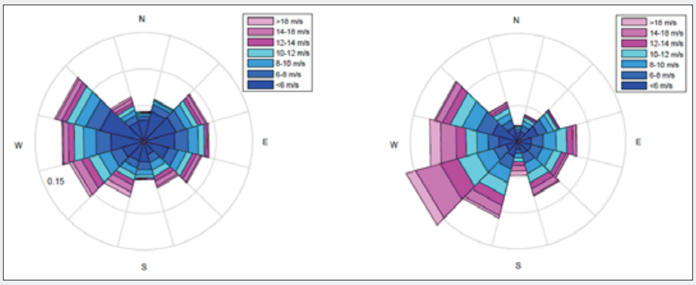

Figure 3 : Example of predicted from historical data wind roses in June and November assuming a random seasonal wind speed variation for each month and direction to match the annual data available.

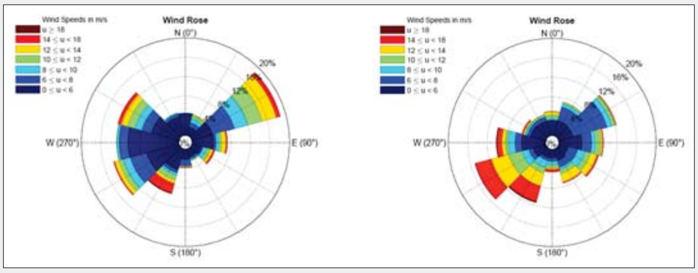

Figure 4 : Example of wind roses in June and November from cup anemometer installed on a turbine nacelle during 2013

Marine Traffic

Marine vessels analysis is used to verify the correspondence between the period of maintenance activity and site accessibility derived from predicted weather windows. Only transport data from heavy vessel activity is considered. Heavy vessels are assumed to be solely deployed for maintenance scope. An analysis is carried out to determine the frequency of visits and the duration of stay for each wind turbine. A vessel is considered to carry out maintenance activity if it is positioned in a radius around the turbine $r < 150\,m$ and the navigation speed $v < 1\,knot$. Cases where the stationary time is less than $2\,hrs$ have not been accounted as such. The effective hours of maintenance are exponentially distributed, meaning that serious activities are performed less frequently than ordinary minor repairs which, however, require medium large sized vessels to be deployed. The analysis allows the estimation of possible maintenance conditions and expected annual turbine downtime.

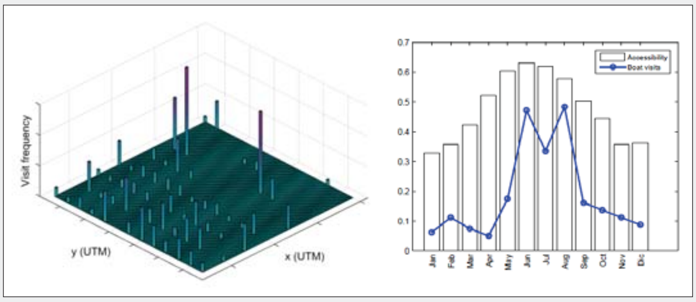

Figure 5 : Left - boat visits frequency histogram wind farm layout. Coordinates in UTM. Right – monthly total site accessibility from predicted roses and histogram real maintenance activity (boat visits s.f. = 2)

Conclusion

In this work historical metocean data measured by a met mast is processed to extract information utilized for planning maintenance. The mean wind speed and significant wave height are used herein to obtain a statistical description and define directional probabilities of maintenance over a certain reference period. The monthly site accessibility is then used to validate actual vessel deployment in the area. The activity is finalized comparing predicted favorable weather period occurrences against heavy vessel visits, showing that the highest probability maintenance corresponds to the period where visits are intensified. Predicted wind roses and measured mean wind speeds show statistical variations which turn into a statistical uncertainty when planning maintenance activities. This procedure is useful when planning long term maintenance activities within a wind farm and historical sea state information is limited.

References

[1] Hagen Brede, Simonsen Ingve, Hofmann Matthias, Muskulus Michael. A multivariate Markov weather model for O&M simulation of Oshore wind parks. Energy Procedia; 2013. p. 137-147.
[2] Scheu Matti, Matha Denis, Hofmann Matthias, Muskulus Michael. Maintenance strategies for large oshore wind farm. Energy Procedia; 2012. p. 281-288.
[3] Anastasiou K., Tsekos C. Persistence statistics of marine environmental parameters from Markov theory, Part 1: Analysis in discrete time; 1996. p. 187-199
[4] Koukoura Christina, Validated Loads Prediction Models for Oshore Wind Turbines for Enhanced Component Reliability, DTU Wind Energy PhD Thesis, 2014
[5] Jose A. Carta, Penelope Ramirez, Celia Bueno. A joint probability density function of wind speed and direction for wind energy analysis; Science Direct; 2008. p. 1309-1320
[6] Eunshin B., Yu Ding, Season-dependend condition based maintenance for a wind turbine using partially osberved Markof observed decision process. IEEE transactions on power systems; 2010
[7] Danish Marittime Authority, http://www.dma.dk/Sider/Home.aspx
[8] Marine Trac, http://www.marinetrac.com/
[10]Johannessen Kenneth, Meling Trond Stokka, Hayer Sverre. Joint Distribution forWind andWaves in the Northern North Sea. Statoil, Stavanger Norway; International Oshore and Polar Engineering Conference; 2001. ISBN 1880653516

Aknowledgment

This project has received funding from the European Unions Horizon 2020 research and innovation program under the Marie Sklodowska- Curie grant agreement No 642108.

DTU Wind Energy
Department of Wind Energy

Assessment of the dynamic responses and allowable sea states for a novel offshore wind turbine installation concept based on the inverted pendulum principle

Wilson Guachamin Acero (*wilson.i.g.acero@ntnu.no*), Zhen Gao and Torgeir Moan
Centre for Ships and Ocean Structures (CeSOS), Centre for Autonomous Marine Operations and Systems (AMOS), Department of Marine Technology, NTNU

ABSTRACT

A novel OWT and RNA installatin concept was introduced in [1], where it was shown to be feasible and an attractive alternative for procedures using jack-up vessels. For the critical installation activities and corresponsing limiting parameters it is necessary to assess their dynamic responses with the aim of establishing the operational limits and providing information for cost-effective design of structural components. Non-stationary time domain simulations are used to compute response statistics of limiting parameters for various installation phases and sensitivity to key modeling parameters is also investigated.

METHODOLOGY

Limiting parameters (for the critical installation activities)

Assessment of dynamic responses (for limiting parameters)
- TD simulations
- Upcrossing rate

Assessment of allowable sea states
Limit state for the limiting parameters: R allow=S charact.

INSTALLATION ACTIVITIES AND LIMITING PARAMETERS

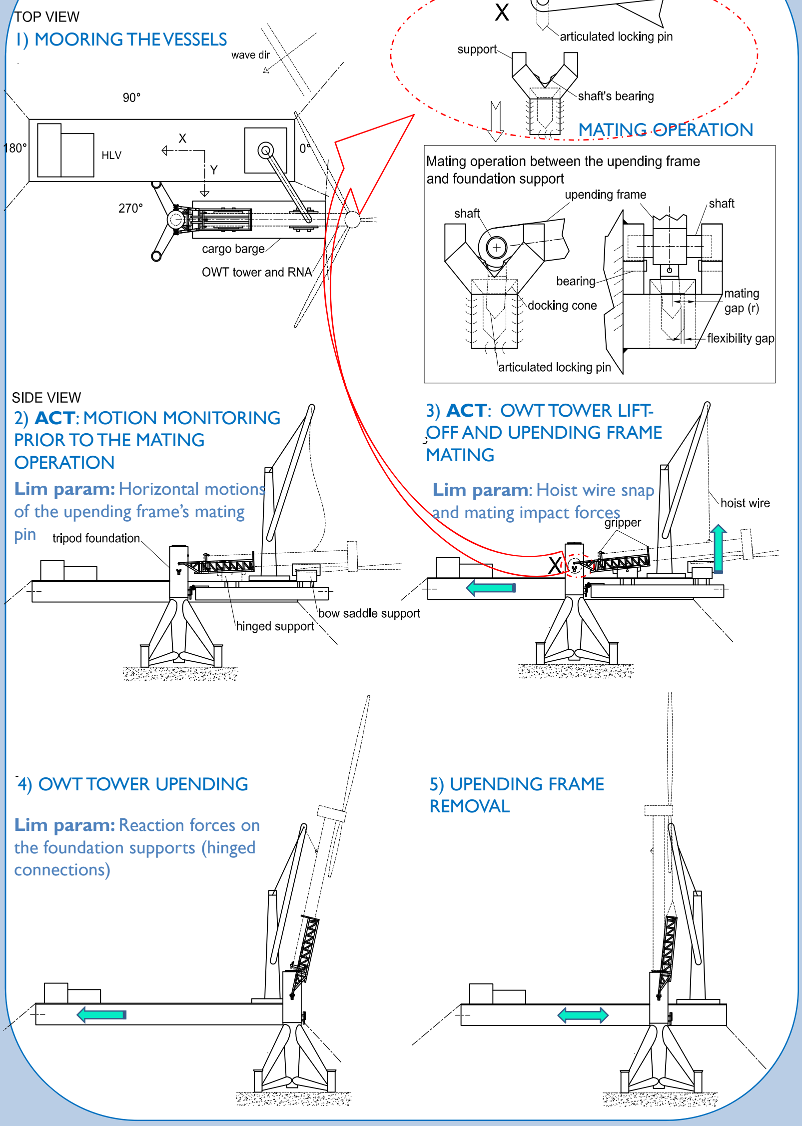

RESULTS

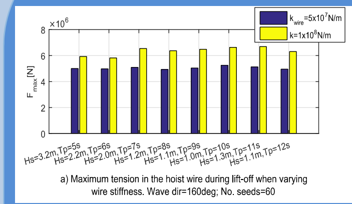

Maximum hoist wire snap forces during lift-off

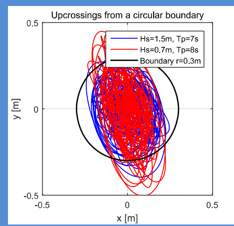

Upending frame´s pin crossings from a circular boundary

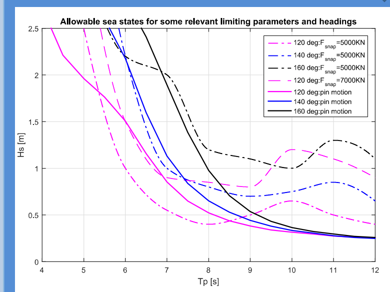

Allowable sea statates

Allowable sea states are established for the OWT tower lift-off and monitoring phase of the upending frame pin (prior to the mating phase) because the allowable limits (of the limiting parameters) are known explicitly

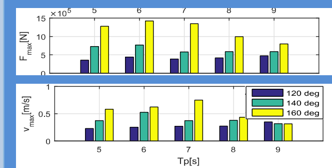

Maximum impact forces and velocities during the mating phase

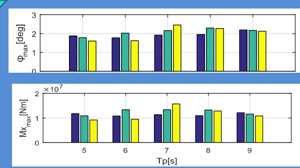

Maximum out of plane reaction moment and tower inclination during the final upending stage

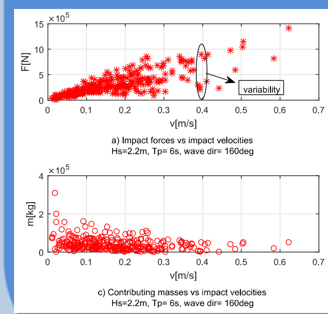

Contributing impact mass during impact events

Impact forces during the mating phase and reaction forces on the foundation support (docking cone) are computed for the allowable sea states corresponding to the lift-off and mating operation (conservative approach).

Impact velocities and contributing masses are provided (after balancing the kinetic and elastic energy of the contact elements) for future FEM of structural components

CONCLUSIONS AND FUTURE WORK

- A preliminary assessment of the dynamic responses (for the limiting parameters) and allowable sea states (for installation activities) for a novel OWT tower and RNA has been presented
- A crane with at least 700tons at 32m outreach radius is required to lift a 5MW NREL offshore wind turbine
- If the capacity of the crane is increased, the snap force on the hoist wires will not longer limit the operation
- Impact velocities and contributing masses are provided for cost-effective design of structural components of the foundation support (docking cone) and locking pin (of the upending frame)
- The foundation support and locking pins of the upending frame should have a rotational spring coefficient larger than $5x10^9$Nm/rad in order to achieve acceptable OWT tower inclinations at the final upending stage
- FEM of structural components should be carried out in a cost effective manner

EERA DeepWind's 2016, 13th Deep Sea Offshore Wind R&D Conference

[1] Guachamin Acero W., Gao Z. and Moan T. Feasibility study of a novel concept for the installation of the tower and rotor nacelle assembly of offshore wind turbines based on the inverted pendulum principle. Submitted for review to the Journal of Ocean Engineering

Multi-level hydrodynamic modelling of a 10MW TLP wind turbine

Antonio Pegalajar-Jurado, Henrik Bredmose and Michael Borg
DTU Wind Energy, Nils Koppels Allé, Building 403, DK-2800 Kgs. Lyngby, Denmark

Introduction

The design of floaters for offshore wind turbines relies on aero-hydro-servo-elastic numerical models, which must be validated against tests. In these models there is a trade-off between accuracy and computational cost.

In the present work three numerical models are applied to a scaled version of the DTU 10MW wind turbine mounted on a Tension Leg Platform (TLP). The results for a set of load cases are benchmarked against test data. Finally, the advanced models are employed to enhance the performance of the simple model.

Loads acting on a TLP WT

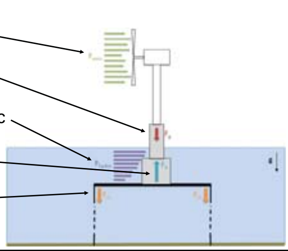

Results

Response to irregular waves

Full-size: H_s = 4.68m, T_p = 7.36s

The *Matlab* model underpredicts the surge motion and predicts well the nacelle acceleration. The first-order *Flex5* model is similar to the *Matlab* model in surge, while the second-order *Flex5* model shows larger surge response. The nacelle acceleration is well predicted by both *Flex5* models.

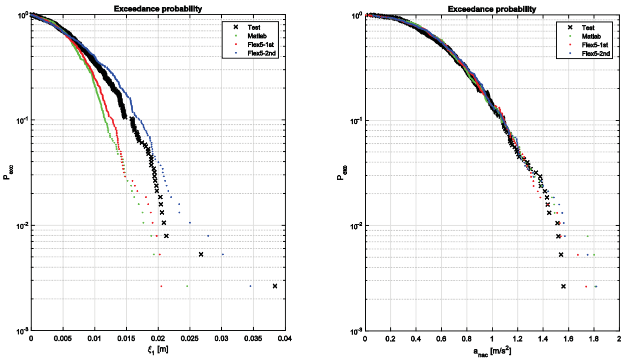

Response to focused waves

Full-size: H_{max} = 18.84m

Surge motion is influenced by its natural frequency (0.19 Hz). The second-order wave kinematics introduce subharmonic forcing at the surge frequency, perhaps due to the difference between second-order theory and test conditions. The *Matlab* and first-order *Flex5* models agree better with the test in surge. Nacelle acceleration is well predicted by all models.

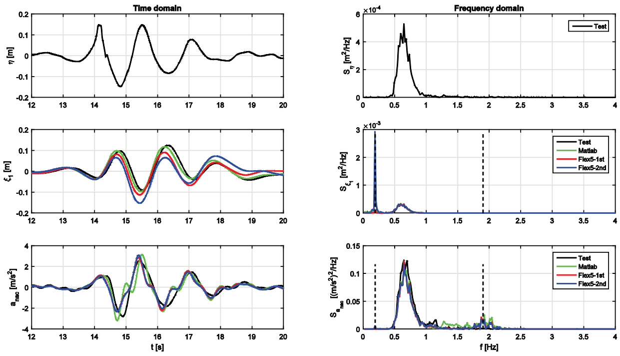

Models and load cases

The three numerical models are developed based on an experimental, Froude-scaled 1:60 TLP wind turbine:

Model	*Matlab*	*Flex5*-1st	*Flex5*-2nd
Domain	Frequency	Time	Time
DoF (total, floater)	2, 1	28, 6	28, 6
Wave kinematics	1st order	1st order	2nd order
Wave forcing	Morison	Morison	Morison
Mooring	Linear	Nonlinear	Nonlinear

A set of load cases without wind is chosen including irregular and focused waves, and corresponding to rated operation and storm condition. The wave loads are integrated by stretching up to $z=\eta$. The models are compared to the tests in terms of surge ξ_1 and nacelle fore-aft acceleration a_{nac}.

The calibration is done by comparison of the surge decay response. The nacelle damping in the *Matlab* model is further calibrated using the *Flex5* models.

The 1:60 scaled TLP WT that inspired the models

Conclusions

The *Matlab* model underpredicts surge in some cases, but often matches nacelle acceleration.

The second-order wave kinematics did not affect the nacelle acceleration significantly (due to large inertia of the TLP wind turbine). However, it induces an important subharmonic forcing at surge frequency (which leads to overprediction).

The *Matlab* model was enhanced by compensating the absent pitch motion with tower flexibility. After enhancement, its performance is comparable to that of more advanced models.

Further information

You can contact the main author via:

ampj@dtu.dk
https://dk.linkedin.com/in/antoniopegalajar

A full paper has been sent to *Energy Procedia* for publication in summer 2016.

Literature cited

Bak C, Zahle F, Bitsche R, Kim T, Yde A, Henriksen LC, Andersen PB, Natarajan A, Hansen MH. Description of the DTU 10MW Reference Wind Turbine. DTU Wind Energy Report-I-0092, Roskilde, Denmark, 2013.

Hansen AM, Laugesen R. Experimental study of the dynamic response of the DTU 10MW wind turbine on a tension leg platform. MSc thesis, DTU Wind Energy. Kgs. Lyngby, Denmark, 2015.

Bredmose H, Mikkelsen RF, Hansen AM, Laugesen R, Heilskov N, Jensen B, Kirkegaard J. Experimental study of the DTU 10MW wind turbine on a TLP floater in waves and wind. Presented at EWEA Offshore 2015 Conference. Copenhagen, Denmark, 2015.

Pegalajar-Jurado A. Numerical reproduction of laboratory experiments for a TLP wind turbine. MSc thesis, DTU Wind Energy. Kgs. Lyngby, Denmark, 2015.

Sharma JN, Dean RG. Second-order directional seas and associated wave forces. *Society of petroleum engineers journal*, 1981; p. 129-140.

Acknowledgments

This work is part of the project LIFES50+. The research leading to these results has received funding from the European Union's Horizon 2020 research and innovation programme under grant agreement H2020-LCE-2014-1-640741. The experimental results were obtained as part of the INNWIND.EU project.

DTU Wind Energy
Department of Wind Energy

LIFES50+

Analysis of second order effects on a floating concrete structure for FOWT's

Alexis Campos; **Climent Molins**; Pau Trubat; Daniel Alarcón
Universitat Politècnica de Catalunya. Escola de Camins
UPC BARCELONATECH

Dynamic co-rotational FE analysis for FOWT's

With the aim of improving the tools for the **analysis of floating spar type structures for offshore wind turbines**, a model which includes the **nonlinear FEA for large displacements based on a co-rotational formulation** is under development at the UPC-BarcelonaTech. The model is able to take into account the wind loads, hydrodynamic loads, the elasticity of the full structure and the mooring response. All forces integrated in the time domain. In its present stage, the model is working in 2D.

Formulation

A nonlinear dynamic finite element numerical model has been developed to analyze the structural behavior of the spar type structure using beam elements in 2D for its discretization. The model assumes small strains but considers large displacements. The FE are implemented with cubic shape functions in combination with the elasticity theory and the Euler beams theory. To deal with the **large displacements**, a **co-rotational formulation** is considered [1] [2].

$$\vec{X}_e = [u_1 \quad w_1 \quad \vartheta_1 \quad u_2 \quad w_2 \quad \vartheta_2]^T$$

$$\vec{x}_e = [0 \quad 0 \quad \vartheta_{l1} \quad u_l \quad 0 \quad \vartheta_{l2}]^T$$

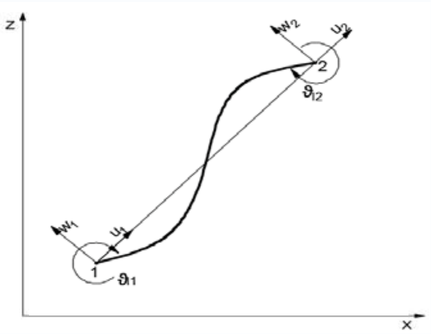

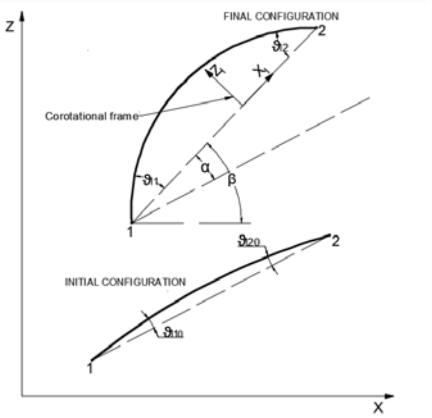

Loads

The external forces considered in the model include the effects of the environmental loads (buoyancy and waves), the mooring system, the wind turbine and the self-weight.

The equivalent **buoyancy forces** acting over the structure are computed by the **3D integration of the pressures over the structure**. A 3D mesh of the external face of the structure is used to obtain at each time step the global position of the mesh elements centroids to finally compute the hydrostatic pressures to compute the resultant force at each element.

The **drag forces** and the **wave loads** are computed with the **Morison's equation**, which was validated during the test campaign of the WindCrete scaled model in the AFOSP project [3]. The water particle kinematics are computed wit the **Stokes 5th order** non-linear wave theory.

The **mooring system** loads are computed in a **quasi static** way, combining it with the dynamic time-domain analysis of the structure.

The loads exerted by the **wind turbine** at the yaw bearing are computed with **FAST** software from NREL

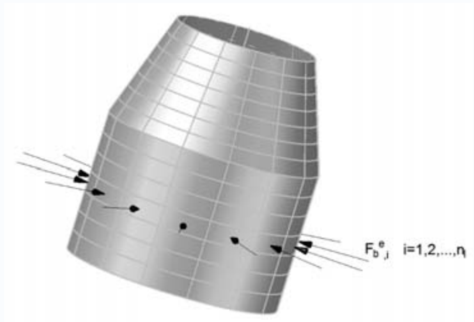

Numerical studies

A **sensitivity study** of the 2nd order effects to the **Young modulus (E)** of the structural material has been performed. Three different assumptions for E, are considered:

- Case 1: Standard concrete structure (E_c=3.7E4 MPa)
- Case 2: Rigid body assumption (E=3.7E6 MPa
- Case 3: Flexible structure (E=3.7E3 MPa)

The selected structure for the study is the **WindCrete** concept [4], a full concrete monolithic SPAR structure for FOWTs, subjected to aligned wind and waves.

Results

The FFT of the nacelle global X motion detects the peaks corresponding to heave motion (30s), the first structural frequency (0.7Hz) and the wave period (14s).

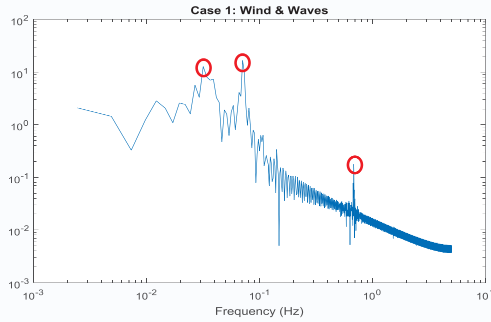

Due to the significant differences in the inertial terms, the computation of the internal forces for the structural assessment seems to be reasonable to be based in a dynamic FE analysis considering the 2nd order displacements, especially for the fatigue limit state.

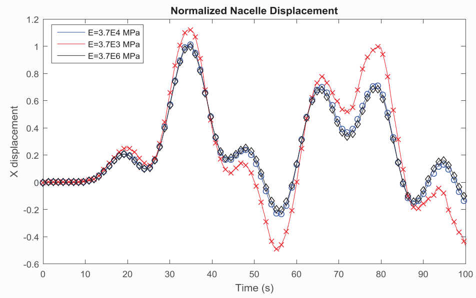

Acknowledgements

We would like to express our gratitude for the financial support obtained from the Catalan government, Generalitat de Catalunya, through its AGAUR agency and from the KIC InnoEnergy.

References

[1] Crisfield,M. A., Non-linear finite element analysis of solids and structures, vol. 1. John Wiley & Sons Inc, 1991.

[2] Behdinan,K.;Stylianou,M. C.;and Tabarrok,B., "Co-rotational dynamic analysis of flexible beams," Comput. Methods Appl. Mech. Eng., vol. 154, no. 3–4, pp. 151–161, 1998.

[3] Campos,A.;Molins,C.;Gironella,X.;Trubat,P.;and Alarcón,D., "Experimental rao's analysis of a monolithic concrete spar structure for offshore floating wind turbines," in Proceedings of the 34th International Conference on Ocean, Offshore and Arctic Engineering OMAE2015, 2015.

[4] Molins,C.;Campos,A.;Sandner,F.;and Matha,D., "Monolithic concrete off-shore floating structure for wind turbines," in Proceedings of the EWEA 2014 Barcelona, 2014, pp. 107–111.

Improved Simulation of Wave Loads on Offshore Structures in Integral Design Load Case Simulations

M.J. de Ruiter, T.J.J. van der Zee
m.j.deruiter@wmc.eu, T. +31 227 504941

Motivation

Integrated wind turbine design benefits from rapid load case evaluation since it allows faster design iterations. This is achieved by reduced model simulation. The model reduction focuses on global wind turbine behaviour, omitting details. These details are significant for e.g. member response in offshore support structures. This project obtains improved accuracy at limited calculation costs.

Approach

The Craig Bampton method reduces the model size by using modal amplitudes, and truncating the number of modal amplitudes used in the simulation. This project recovers the truncated forces for correction.

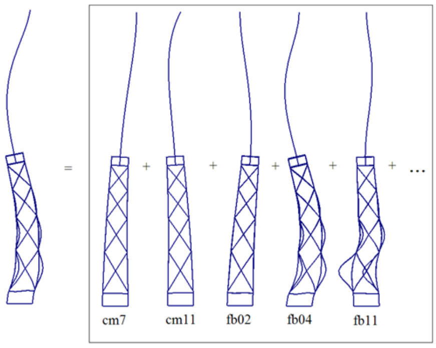

Finite Element evaluation

↓

Wave load = modal forces + surplus forces

↓ Efficient simulation using reduced number of modes

↓ Finite Element solution using the support structure model

Deformation = modal displacements + surplus displacements

↓ Finite Element solution using the support structure model

↓

Time series of the desired member response

Wave loads

The wave loads are evaluated using Morison's equation:

$$F = \rho\, V\, \dot{w} + \rho\, C_a\, V\, (\dot{w} - \ddot{u}) + \tfrac{1}{2}\rho\, C_d\, A\, (w - \dot{u})|w - \dot{u}|$$

involving data available at different stages of the solution

Wave loads are evaluated using FE.

Tower motion is evaluated at simulation time.

The evaluation can be postponed to simulation time by rewriting Morison's equation in modal form and separating water motion w and tower motion $\dot{u}$ and evaluating the coefficients, writing

$$F_{modal} = R_{(w)} + S_{(w)}\, \ddot{u}_{modal} + wT_{(w)}\, \dot{u}_{modal} + \dot{u}_{modal}^{T}\, T_{(w)}\, \dot{u}_{modal}$$

where

$$R_{(w)} \sim \rho\, V\, \dot{w} + \rho\, C_a\, V \dot{w} + \tfrac{1}{2}\rho\, C_d\, A\, |w|^2$$
$$S_{(w)} \sim -\rho\, C_a\, V$$
$$wT_{(w)} \sim \tfrac{1}{2}\rho\, C_d\, A\, |w|$$
$$T_w \sim \tfrac{1}{2}\rho\, C_d\, A$$

Application

The new method has been applied to a model of the XEMC Darwind XD115 5 MW wind turbine on top of the OC4 jacket experiencing North Sea 50 m deep water conditions.

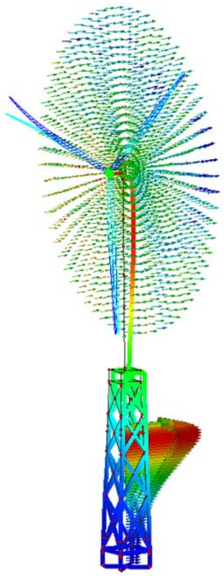

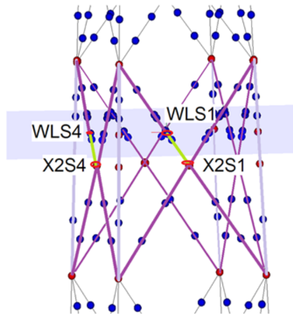

Response sensors

The response has been evaluated at water level (WL) and X-joint in bay 2 (X2), at side 1 (S1, lateral) and side 4 (S4, downstream).

Fatigue loads

Using Palmgren-Miner's hypothesis, the damage is calculated for in-plane (ip) and out-of-plane (oop) bending of the member. Locations and load cases are put in classes based on the damage ratios.

	Cumulative	WLS4		WLS1		X2S4		X2S1	
	damage	oop	ip	oop	ip	oop	ip	oop	ip
Grid loss	0 %	4	1	-1	-1	4	0	1	1
Normal operation	99 %	1	0	0	0	2	0	0	1
Yaw or pitch issues	0.4 %	1	0	0	0	2	0	0	1
Start	0 %	4	1	-1	-2	4	1	1	4
Stop	0 %	4	1	-1	-2	4	1	1	4
Idling	0.3 %	4	1	0	0	4	0	1	3

Damage ratio New/Trad	0.70	0.80	0.90	1.10	1.25	1.60	3	more
Class	-2	-1	0	1	2	3	4	

Extreme loads

The maximum stresses are calculated for in-plane and out-of-plane bending. Locations and load cases are put in classes based on the stress ratios.

	WLS4		WLS1		X2S4		X2S1	
	oop	ip	oop	ip	oop	ip	oop	ip
NTM, power production, SSS	0	0	0	0	0	0	0	0
NTM, power production, SWH	1	0	0	0	0	0	0	0
EWM50, idling upwind, SSS	2	0	1	0	2	0	2	0
RWM50, idling upwind, EWH	2	1	2	0	2	0	2	0
EWM50, idling, failed yaw,EWH	2	0	1	0	2	0	2	0

Maximum stress ratio New/Trad	0.90	1.20	1.4	more
Class	0	1	2	

Conclusions

- The new method can be used to obtain more accurate member results.
- The most fatigue damage occurs in normal operation, where the new method finds 32% more damage.
- The highest extreme load case stresses occur in the 50 year recurrence period, with up to 57% more stress.
- The new method performs efficiently. The additional time requirement is 80% of the reduced modal system simulation time.

FLOW Far and Large Offshore Wind innovation program

XEMC DARWIND

Knowledge Centre WMC

Adaptation of Control Concepts for the Support Structure Load Mitigation of Offshore Wind Turbines

B. Shrestha*, M. Kuehn
Research Group Wind Energy Systems
ForWind - Center for Wind Energy Research, University of Oldenburg, Germany

Objective

- To develop an adaptive control that selects the most effective individual control concept for the given load event in consideration of its respective collateral effect.
- To take advantage of controller concepts without having considerable collateral effect.

Methodology

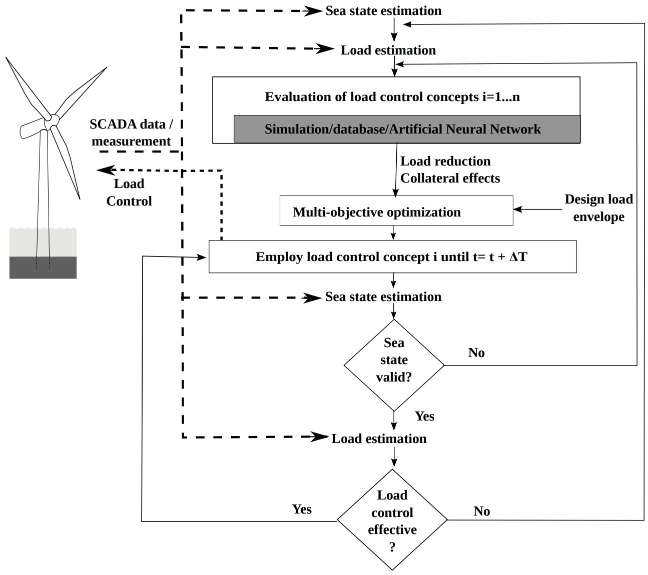

Fig 1: Flowchart of the steps followed for the selection of the most effective controllers

Analysis

Controllers used for NREL 5MW offshore turbine at 25 m water depth (MSL) at North Sea site founded on a monopile (f = 0.28 Hz):

1. Baseline controller (BLC)
2. Tower foreaft (TFA) controller - to reduce fore-aft bending moment
3. Active Generator Torque (AGT) controller- to reduce tower side to side bending moment

Collateral effects:

TFA : increased pitch activity given by pitch Actuator Duty cycle (ADC)

AGT : varying generator torque and hence increased power fluctuation

Load cases selected: mean wind speed of 14 m/s; IT = 14.2 %; wind-wave misalignment of 0°, 45°, 90° and 135°; 3 to 4 different wave heights per case; 6 seeds.

The optimization result of trade-off between tower fore-aft damage equivalent load (DEL_TMy) reduction and the increase in ADC is shown in Fig 2a.

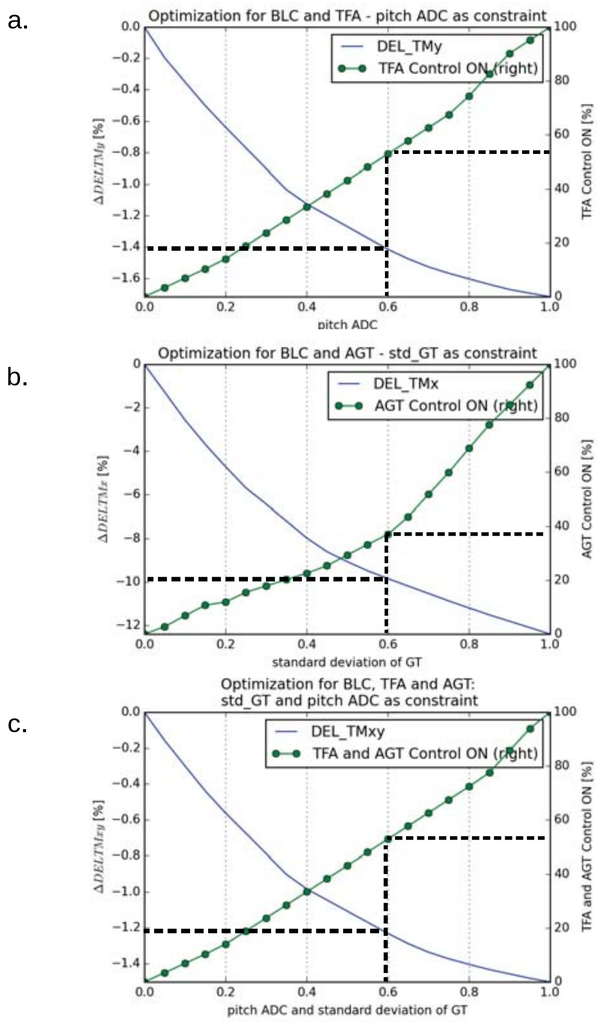

Fig 2: Optimization results for different controller settings and constraining factors for mitigation of a) pile fore/aft, b) pile side to side, c) pile Mxy bending moment at mudline

If 60 % of the total possible increase in pitch ADC is the constraint, the DEL_TMy is reduced by 1.5 % which is 78 % of the total achievable load reduction by operating the TFA for 53 % of time. The similar results in Fig 2b and Fig 2c shows that it is possible to considerably reduce the load when limiting the collateral effect for the given sea state.

Acknowledgement

This work was partially funded by the German Federal Ministry for Economic Affairs and Energy (BMWi) in the scope of the RAVE (Research at Alpha Ventus) - OWEALoads project (contract No. 0325577B).
Acknowledgement is given to David Schlipf, University of Stuttgart for providing the controller for NREL 5MW turbine and Adrian Jimenez for assisting in data handling.

Binita Shrestha
Tel: +49 441 798 5067
binita.shrestha@uni-oldenburg.de

University of Stuttgart
Germany

www.uni-stuttgart.de/windenergie

Parametric Wave Excitation Model for Floating Wind Turbines

Frank Lemmer (né Sandner), Steffen Raach, David Schlipf and Po Wen Cheng

Stuttgart Wind Energy (SWE), University of Stuttgart, Germany

Problem description

A state-space model is fitted to the wave-excitation force coefficient from panel-codes for two floating wind turbine (FOWT) models. As shown on the right the wave excitation transfer function (step 1) allows the derivation of a complete, "unified" linear description of the FOWT model (step 2) together with existing radiation force models. The transfer function to structural FOWT states has been set up and verified successfully.

The motivation for this work is:

- Derive a parametric wave-disturbance model for FOWT time-domain simulations
- Generate a "unified" linear FOWT model for controller design & optimization
- Set up a transfer function necessary for a wave-feedforward controller

Keywords: State-space modeling, wave excitation force, disturbance model, integrated floating wind turbine model, radiation force model.

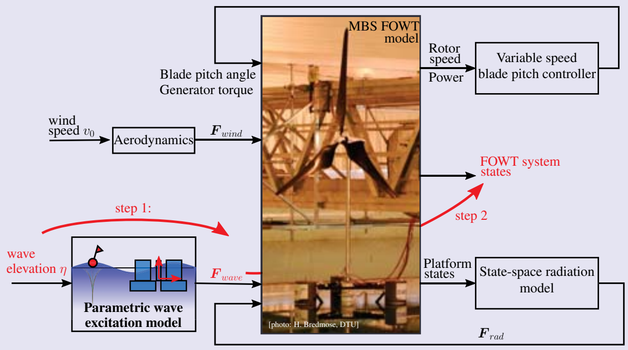

Figure 1: State-space FOWT model: Wave excitation transfer function is subject to this work.

Introduction

Panel codes provide the first-order wave excitation force coefficient $\boldsymbol{X}(\omega)$. For time-domain simulations an inverse Fourier transform prior to a simulation is usually necessary. Here, a linear model shall be fitted in order to obtain the wave forces $\boldsymbol{F}_{wave}(t)$ directly from a time-domain wave height input $\eta(t)$:

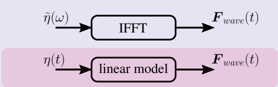

As proposed by [1] a state-space model is fitted to the impulse response of the wave-excitation force transfer function (e.g. the force response to a wave height impulse). Before this is done a causalization is necessary.

Causalization

The transfer function from wave height η to the forces and moments on the floating body $\boldsymbol{F}_{wave}$ is not always causal, depending on the position of the wave height measurement. Forces might arrive at the hull prior to the corresponding free-surface elevation. Figure 2 (grey line) shows that the wave force impulse response has a response at negative times, which proves the non-causality.

However, if the wave height is measured at a sufficient distance from the platform, against wave direction, the problem is causal. Therefore, prior to the model fit the impulse response is shifted in time by $\tau_c = 6\,\text{s}$, see the red line in Fig. 2.

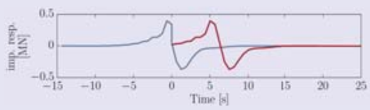

Figure 2: Non-causal (grey) and causalized (red) wave excitation impulse response of the OC3 spar in surge.

In frequency-domain the time-delay is represented by a frequency-dependent phase-lag $\varphi_c(\omega)$

$$\varphi_c(\omega) = \omega\ \tau_c \qquad (1)$$

Wave excitation model fit

A state-space model is now fitted to the causalized time-domain impulse response: Two hull shapes have been used for an assessment of the method: The cylindrical OC3-spar shape as well as the more complex OC4-semi submersible. Figure 3 shows the frequency-domain transfer function as well as the impulse response for the phase-shifted panel-code results with the model fit of $n_{states} = [4, 6, 8]$ in surge and pitch direction. Figure 4 shows the time-response of the 6-state model to a linear irregular wave input with peak period $T_p = [10, 15]s$.

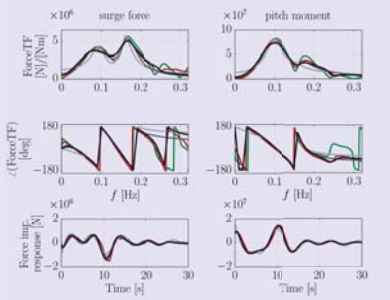

Figure 3: Panel code (green), causalized (red), model fit for OC4 semi-submersible with $n_{states} = [4, 6, 8]$ (grey, increasing darkness): 6-state model selected.

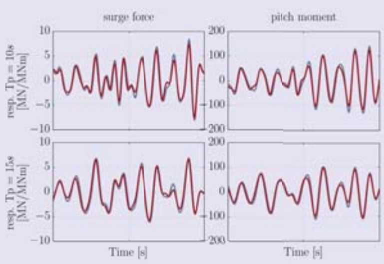

Figure 4: Wave force response by inverse Fourier transform (grey) and 6-state fitted model (red) for $T_p = [10, 15]$s, OC4 semi-submersible.

The model with 6 states shows a good agreement to the IFFT method in frequency and time-domain for the surge and pitch response of the OC4 semi-submersible. While the 6-state-OC4 model fits with 74.9 % the simpler OC3-model with 6 states shows a 87.9 % agreement.

Coupled transfer function

Now, the transfer function from wave height to tower-top displacement can be calculated and verified: A coupled nonlinear FOWT model of the OC4 semi-submersible is run with regular unit-amplitude wave force timeseries as input until it reaches a steady state.

Figure 5 shows for each frequency the amplitude and phase towards the wave input (red) and compares it to the linear wave transfer function of Fig. 3 in series with the linearized structural model (grey). The model is a 2D model with the degrees of freedom surge, pitch, tower-top displacement and rotor speed. It is run here without aerodynamic forces.

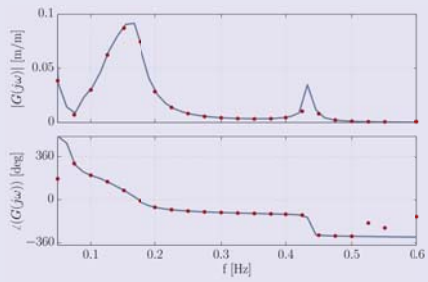

Figure 5: Transfer function from wave height η to tower-top displacement x_t for OC4 semi-submersible. Linear model (grey), nonlinear model (red).

Conclusions

A state-space model has been fitted to the linear wave excitation force coefficient from a panel-code. The results for two hull shapes of different complexity show that with few states it is possible to obtain a good agreement with the panel code for realistic ocean wave frequencies.

The overall transfer function from wave height to the wind turbine tower-top displacement has been calculated and verified through a comparison with the nonlinear FOWT model.

In future works the model will be used for the design of advanced FOWT controllers for improved power production and load reduction. A wave-feedforward control of a scaled model in a wind-wave basin is scheduled for March 2016.

SWE Stuttgart Wind Energy @ Institute of Aircraft Design

The research leading to these results has received partial funding from both, the European Community's Seventh Framework Programme under grant agreement No. 308974 (INNWIND.EU) and the European Union's Horizon 2020 research and innovation programme under grant agreement No. 640741 (LIFES50+).

[1] Yu, Z., Falnes, J. (1995) State-space modelling of a vertical cylinder in heave. *Applied Ocean Research;* 17(5):265-275.

Mooring Line Dynamics Experiments and Computations. Effects on Floating Wind Turbine Fatigue Life and Extreme Loads.

CENER
ADItech

José Azcona[1] and Tor Anders Nygaard[2]
[1]Renewable Energy National Center, CENER, Spain
[2]Institute for Energy Technology, IFE, Norway

Institute for Energy Technology

Introduction

The OPASS code [1] is a dynamic mooring lines simulation tool based on the Finite Element Method (FEM), that considers the hydrodynamic drag, the added mass, the axial stiffness, the structural damping and the seabed contact and friction. 3DFloat is an aero-servo-hydro-elastic FEM code by IFE that also includes bending and torsion of the mooring lines [2].

The objective of this work is to quantify the effect of mooring line dynamics on offshore wind turbine fatigue and ultimate loads with high-fidelity simulation tools validated against wave tank experiments.

Experimental validation

A chain was submerged into the water basin (see Figure 1), forming a catenary shape with the bottom end anchored to the tank floor and the fairlead connected to a mechanical actuator that excites the line with a harmonic motion with three different frequencies (1.58s, 3.16s and 4.74s).

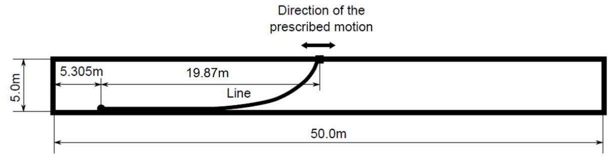

Figure 1. Experimental setup of the line at ECN, Nantes

Equivalent simulations of the chain setup were launched with OPASS and 3DFloat to compare against the experimental results. Figure 2 compares the chain fairlead tension with computations for the three excitation frequencies. The black lines represent the computations using the values for the chain drag coefficients provided by DNV [3]. The gray lines are the same computations with OPASS but increasing and decreasing the drag values in 20%, to evaluate the sensitivity of computations to this parameter.

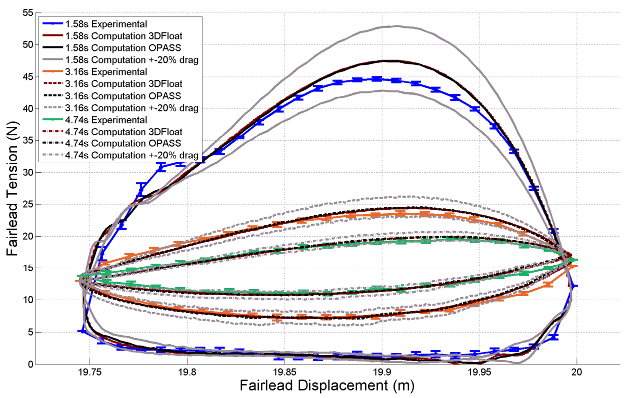

Figure 2. isometric view of the design

The agreement of computations with experiments is very good for the three frequencies, particularly when the reference DNV drag coefficients values are used. For the lowest excitation period, the chain totally loses tension. The agreement for this case is also good although the maximum tension provided by DNV drag coefficients is 4.5% higher than the experiments. This suggests that for high frequency motions, the drag coefficients are slightly conservative.

References

[1] Azcona, J., Munduate, X., Nygaard, T.A. and Merino, D. "Development of OPASS Code for Dynamic Simulation of Mooring Lines in Contact with Seabed". EWEA Offshore 2011. Amsterdam, The Netherlands, 2011.

[2] De Vaal, J. and Nygaard, T.A. "3DFloat User Manual". Report IFE/KR/E-2015-001. Institute for Energy Technology, Norway , 2015.

[3] Det Norske Veritas. Offshore Standard DNV-OS-E301. Position Mooring. Høvik, Norway, 2010.

[4] Robertson, A.N. and Jonkman, J.M. "Loads Analysis of Several Offshore Floating Wind Turbine Concepts". In: 21st International Offshore and Polar Engineering Conference, ISOPE. Maui, Hawaii, United States, 2011.

Effect of mooring dynamics on loads

The fatigue and ultimate loads of three different floating wind turbines (Figure 3) have been computed using the OPASS dynamic mooring model and a quasi-static approach to evaluate the effect on the results. The load calculations included all the case groups defined by the IEC 61400-3 guideline.

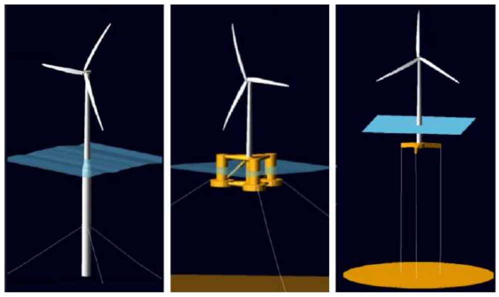

Figure 3. Platform concepts considered in this study [4]

In general, the influence of mooring dynamics both on fatigue and ultimate loads increases as elements located closer to the platform are evaluated. The blade and the shaft loads are only slightly modified by the mooring dynamics. Figure 4 shows that mooring dynamics significantly decrease the tower loads for the semisubmersible and the TLP concepts when compared with results using quasi-static mooring model..

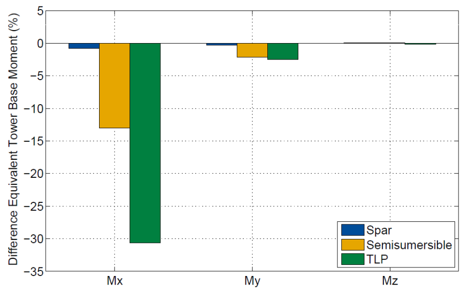

Figure 4. Relative difference of the tower base fatigue loads computed with dynamic mooring lines, with respect to quasi-static

Figure 5 reveals that the mooring dynamics have a significant effect (decrease around 30%) on the computation of the TLP's tower base extreme loads in comparison with quasi-static.

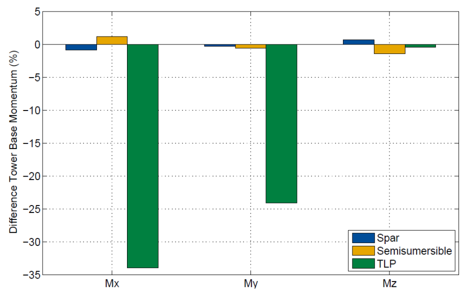

Figure 5. Relative difference in the tower base extreme loads computed dynamic mooring lines, with respect to quasi-static

Results also show that mooring lines tension strongly depends on the lines dynamics both in fatigue and extreme loads for all the platforms.

Acknowledgements

This project has received funding from the European Union's Seventh Framework Programme under grant agreements No.308974 (INNWIND.EU) and No.609795 (IRPWind), and the Norwegian Research Centre for Offshore Wind Technology (NOWITECH). Free access to the Ecole Centrale de Nantes water tank was provided by the MARINET European Community research programme.

Semisubmersible floater design for a 10MW wind turbine

José Azcona, Enrique Grela and Xabier Munduate
Wind Energy Department
Renewable Energy National Center, CENER, Spain

Introduction

A floating platform concept has been developed for the INNWIND 10MW reference wind turbine [1] located at a 200m sea depth location.

The platform is designed in steel and consists of an equilateral triangle with three stabilizing columns, one in each vertex, joined by pontoons. The function of the pontoons is not only structural, but also hydrodynamic, damping the motion of the system. The wind turbine is located in one of the columns, to avoid the use of an additional central column. The number of elements in the water plane is reduced, minimizing the hull cross section area at the sea surface where wave energy is located. The material and construction cost is reduced avoiding bracings and other connecting structural elements. The center of gravity is lowered to increase stability through the use of sea water as ballast.

Figure 1. isometric view of the design

Main platform properties

The main dimensions of the platform are summarized in Table 1.

Main characteristics	
Distance between columns	66 m
Draft	25.5 m
Freeboard	12 m
Column diameter	14.5 m
Pontoon transversal dimensions	7 x 10.875 m
Buoyancy volume	24907 m^3
Center of buoyancy (below SWL)	17.32 m
Center of gravity (below SWL)	13.46 m
Pitch displacement at rated wind speed	3.5º

Table 1: main dimensions of the platform design

The resulting natural heave and pitch periods are higher than 20 s to avoid the periods with more energy of the typical wave spectra. The motion and forces RAO's present low excitation within the wave frequency range.

Structural dimensioning

The platform steel structure has been designed according to the DNV guidelines ([2], [3] and [4]). The configuration is based in frames with tanks and decks. The dimensioning considered all relevant elements as shells, webs, stiffeners, weldings or reinforcements. This calculation allowed to estimate the system mass as it is summarized in Table 2.

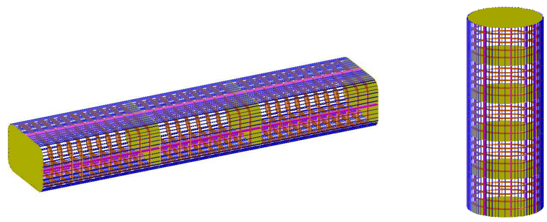

Figure 2. CAD models of the pontoon and column structures

System mass	
Wind turbine	$1.144 \cdot 10^6$ Kg
Unballasted platform	$3.745 \cdot 10^6$ Kg
Ballast	$1.829 \cdot 10^7$ Kg
Mooring system	$2.841 \cdot 10^5$ Kg
Total mass (m_{FOWT})	$2.346 \cdot 10^7$ Kg

Table 2: estimation of the system mass

Cost estimation

Based on the previous mass calculation, the CAPEX of the platform is estimated, assuming a cost of 3,000€ per ton of steel including manufacture and welding. The cost of each of the three anchors is estimated in 150,000€.

CAPEX estimation	
Cost of platform	11,235,000 €
Cost of mooring lines	852,300 €
Cost of anchors	450,000 €
Total cost	12,537,300 €

Table 3: CAPEX estimation

Summary

A new conceptual design of a floating platform for a 10MW wind turbine has been proposed. The motion and force RAO's show a good performance of the platform with moderate excitation in all the range of wave frequencies considered.

A structural design and calculation of the platform has been performed based in DNV's guidelines. Based on the calculation of the steel mass, a cost of 12.5MM€ has been estimated.

The performance of the design is promising and we plan to further develop it within the INNWIND.EU project and validate the concept with wave tank tests.

References

[1] C. Bak, F. Zahle, R. Bitsche, T. Kim, A. Yde, L. Henriksen, P. Andersen, A. Natarajan and M. Hansen, "Description of the DTU 10 MW Reference Wind Turbine," D1.21 INNWIND.EU, 2013.
[2] DNV, "DNV OS c103 Structural Design of Column Stabilised Units", 2012.
[3] DNV, "DNV OS j101 Design of Offshore Wind Turbines Structures" 2010.
[4] DNV, "DNV-OS-J103 Design of Floating Wind Turbine Structures" 2013.

Acknowledgements

This project has received funding from the European Union's Seventh Framework Programme for research, technological development and demonstration under grant agreement No.308974 (INNWIND.EU).

DTU Wind Energy
Department of Wind Energy

Sizing optimization of jacket structures under time-dependent stress constraints

Alexander Verbart, Postdoc, alev@dtu.dk

Kasper Sandal, Mathias Stolpe

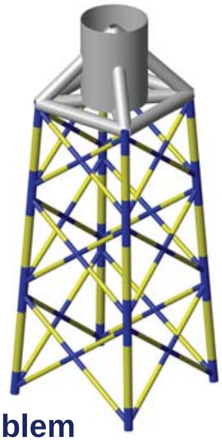

Introduction

Design optimization of offshore jackets is a challenge due to several reasons:

- **Prohibitive number of dynamic constraints on structural criteria such as stress, displacement and fatigue.**
- **Calculating the design sensitivities of these constraints is computationally very expensive.**
- **The required memory storage is very large.**

Aim

The aim of our research is to develop special purpose numerical optimization techniques that can effectively handle the vast number of dynamic constraints.

Model

- **Timoshenko beam elements**
- **Axial stresses: $\boldsymbol{\sigma}(\mathbf{u}(\mathbf{t}))$, obtained after solving:**

  $\mathbf{Ma}(t) + \mathbf{Cv}(t) + \mathbf{Ku}(t) = \boldsymbol{f}(t).$
- **Newmark-β**

Preliminary optimization problem

- **Minimize mass subjected to axial stress constraints that should be satisfied at all point at all times.**
- **Design variables: diameters and thicknesses of the members. After variable linking 18 independent variables.**

Result

Preliminary result of optimizing a jacket under time-dependent axial stress constraints.

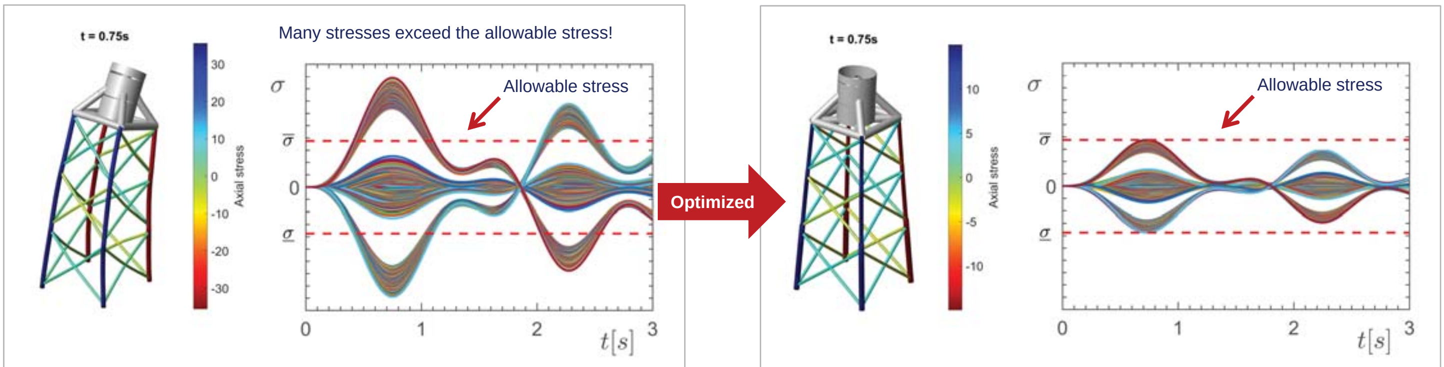

Initial design — ***All* axial stresses over time**

Optimized design — ***All* axial stresses over time**

- **3136 stress responses considered over 151 time steps; i.e. ~1 million constraints vs. 18 design variables.**
- **Interior-point solver Ipopt [2] found an optimized jacket design after 100 iterations.**
- **Axial stresses of the optimized design satisfy the allowable stress at *all points* in the structure at *all times.***
- **Current capabilities limited by computationally expensive design sensitivities and corresponding memory storage.**

Conclusions

Preliminary results indicate that we can successfully obtain optimized designs which satisfy dynamic stress constraints. However, the large number of constraints makes calculating design sensitivities computationally expensive and requires large memory storage.

Future work focusses on reduction techniques of both optimization problem and analysis.

References

[1] M. Muskulus and S. Schafhirt, Design Optimization of Wind Turbine Support Structures – A Review, Journal of Ocean and Wind Energy, 2014.
[2] A. Wächter and L. T. Biegler, On the Implementation of a Primal-Dual Interior Point Filter Line Search Algorithm for Large-Scale Nonlinear Programming, Mathematical Programming, 2006.

This work is part of ABYSS: 2014-2017

Fraunhofer IWES

NTNU Norwegian University of Science and Technology

Rational upscaling of a semi-submersible floating platform

Mareike Leimeister[1,2] (mareike-leimeister@gmx.de), Erin E. Bachynski[1], Michael Muskulus[1], Philipp Thomas[2]

[1] Norwegian University of Science and Technology, Trondheim, Norway

[2] Fraunhofer Institute for Wind Energy and Energy System Technology, Bremerhaven, Germany

Abstract: Technological progress, design changes and additional factors that floating structures have to deal with - like large motions and motion coupling, low frequency modes, radiation and diffraction, mooring system and damping interaction - make basic scaling based on the turbine rating insufficient. Thus, the objective of this work is to develop a rational upscaling process for a semi-submersible structure in order to find a reasonable design of a platform, which would fit a predefined wind turbine, is producible, and represents realistic dynamic behavior.

Methodology

Original design	→	Upscaled design
NREL 5MW	→	Fraunhofer IWT-7.5-164
DeepCwind semi-submersible	→	Rational upscaled semi-submersible

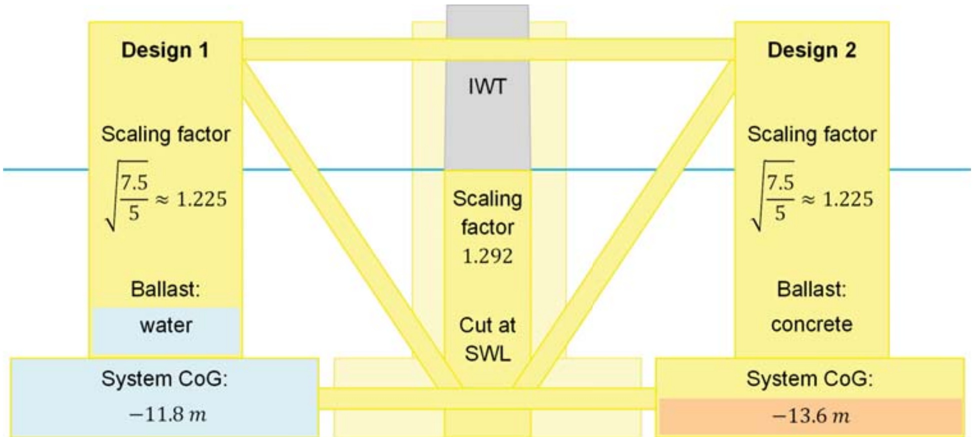

Upscaling procedure and main criteria:

- Main scaling based on power rating
- Main column has to fit tower base
- Unchanged hub height
- Ballasting with main focus on floatability and stability
- Unchanged water depth
- Unchanged mooring parameters

Platform performance analysis:

- Based on hand and HydroD computations
- Focus on stability limit in pitch, natural periods in heave and pitch, nominal pitch at rated power, frequency-dependent hydrodynamic behavior

Results

- **Design 1:** less stiff
  → higher pitch natural period
- **Design 2:** stiffer
  → higher stability
  → less nominal pitch

	Design 1	Design 2	Upscaled
$T_{\text{n,heave}}$	$19.12\ s$	$19.12\ s$	$21.12\ s$
$T_{\text{n,pitch}}$	$42.20\ s$	$38.71\ s$	$33.11\ s$
$\theta_{nominal}$	$3.67°$	$3.03°$	$2.31°$

Added mass limits:

- Equation-based approximation [1,2] gives poor results

$$\widetilde{A_{33}} = \frac{\rho}{3}D_d^3 - \left[\frac{\pi\rho}{8}D_c^2\left(D_d - \sqrt{D_d^2 - D_c^2}\right) + \frac{\pi\rho}{24}\left(D_d - \sqrt{D_d^2 - D_c^2}\right)^2\left(2D_d - \sqrt{D_d^2 - D_c^2}\right)\right]$$

$$\widetilde{A_{55}} = C_a\rho\pi r^2\left[\frac{(d-h)^3}{3} + \overline{KG}^2(d-h) + \overline{KG}(d-h)^2\right]$$

- Better approximation by upscaling of original added mass matrix with main scaling factor (1.225^3 for heave, 1.225^5 for pitch)

Ballast-independent added mass and damping terms

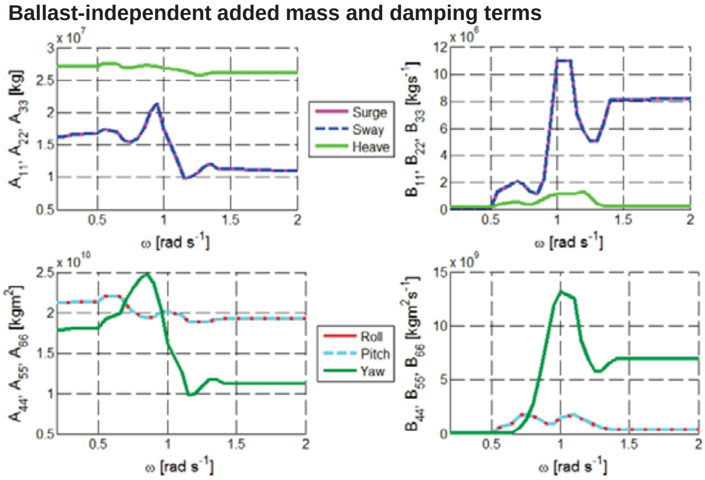

Diagonal added mass matrix terms

Diagonal damping matrix terms

Response amplitude operators:

- Main response in surge, heave and pitch (without mooring)
- Design 1 and 2 show different peaks in RAOs for rotational DoFs due to sampling frequencies

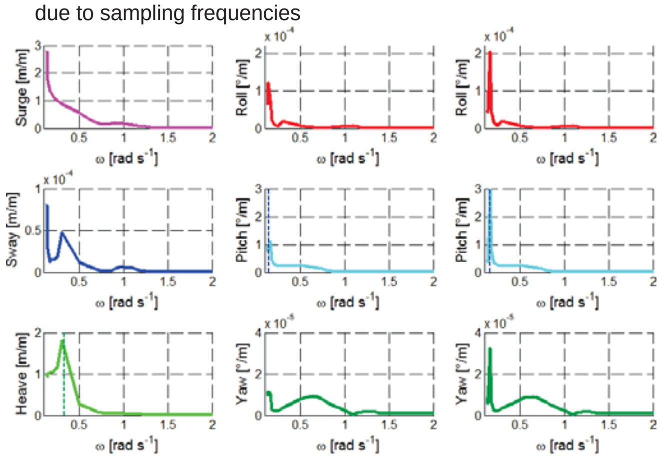

RAOs in translational DoFs Design 1 and 2

RAOs in rotational DoFs Design 1

RAOs in rotational DoFs Design 2

Standard deviations:

- Based on FD-analysis of 15 representative sea states
- Similar for both designs
- Main dynamic response in surge, heave and pitch
- Increasing dynamic response with more severe sea states
- Dynamic pitch motion up to 10% of nominal mean displacement

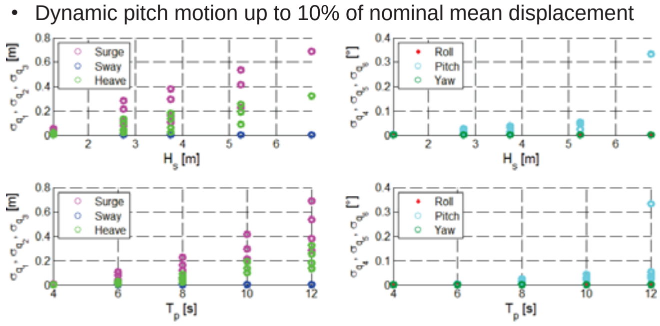

References:

[1] L. Tao, S. Cai. Heave motion suppression of a Spar with a heave plate. Ocean Engineering, 31:669-692, 2004.

[2] P. Ghadimi, H.P. Bandari, A.B. Rostami. Determination of the Heave and Pitch Motions of a Floating Cylinder by Analytical Solution of its Diffraction Problem and Examination of the Effects of Geometric Parameters on its Dynamics in Regular Waves. International Journal of Applied Mathematical Research, 1(4):611-633, 2012.

Outlook

- Detailed stability analysis needed, for example in Modelica
- Higher natural periods by allowing different geometrical upscaling (e.g. smaller upper column diameter, larger base column diameter)
- Optimized balance between stability and natural frequencies by adjustment of ballasting
- Inclusion of mooring system stiffness and mooring line tension

Irregular Wave Forces on a Large Vertical Circular Cylinder

Ankit Aggarwal[1], Mayilvahanan Alagan Chella[1], Arun Kamath[1], Hans Bihs[1], Øivind Asgeir Arnsten[1]
[1]Department of Civil and Transport Engineering
Norwegian University of Science and Technology
Trondheim 7491, Norway

Introduction

- The real sea state can not be defined by the regular waves.
- Fast fourier transformation (FFT) can be used to simplify the random sea surface into a summation of simple sine waves.
- Present study employs the open-source CFD model REEF3D to study the regular and irregular wave forces

Numerical Model

- Reynolds Averaged Navier-Stokes (RANS) equations are the governing equations of computational fluid dynamics (CFD).
- Explicit TVD third-order Runge-kutta scheme and fifth-order finite difference WENO scheme in multi-space dimensions are used.
- k-w model is used to model the turbulence.
- Level set method (LSM) is used for modelling the free surface
- The relaxation method is used in the present numerical model to generate and
- absorb the waves.
- First-order irregular waves are used which are obtained by the summation of linear regular wave components. JONSWAP spectrum is used for the wave generation.

Validation with regular waves

- Two cases with different wave steepness are tested in an empty wave tank. Grid refinement study is performed for one of them.
  Case 1: H = 0.005m, T=1.2s (linear waves)
  Case 2: H: 0.05m, T = 1.2s (2nd-order Stokes waves)
- For grid refinement study, different grid sizes dx = 0.10m,0.05m and 0.025m are tested for case 1. Figure below shows the comparison with theory for two different wave gauge locations.

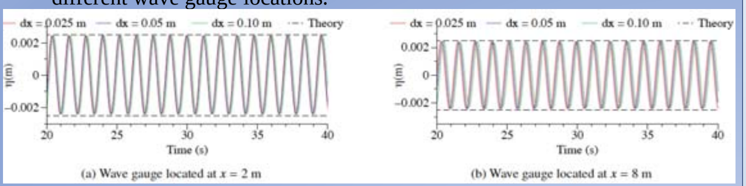

- Grid size dx = 0.025m is chosen for further simulations.
- Figure below presents the results for the case 2.

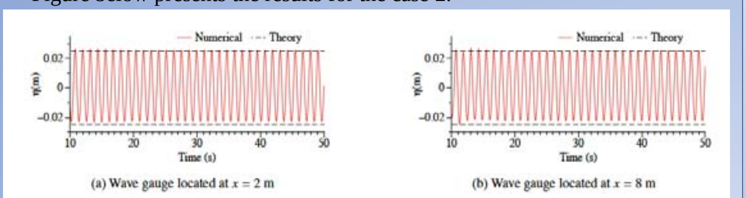

- Simulations are performed with a vertical cylinder of diameter D = 0.50m in a NWT 15m long, 5m wide and 1m deep. Water depth is 0.5m.
- Numerical forces are compared with the analytical forces calculated using MacCamyFuschs equation. Figure below shows the comparison.

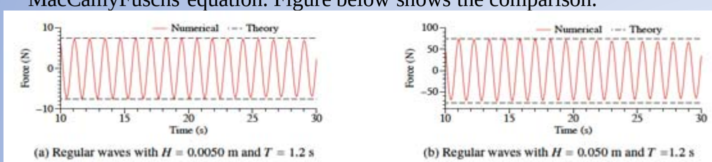

- A very good match is observed between the numerical and analytical results.

Next figure shows the free surface features around the cylinder for case2. Diffraction around the cylinder can be noticed.

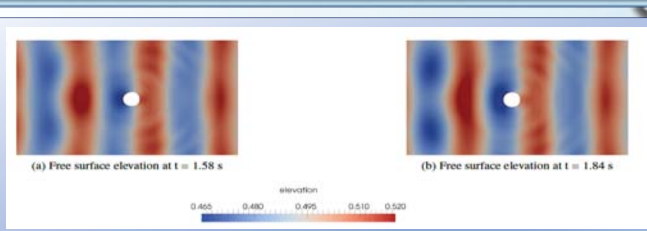

Testing with irregular waves

- Irregular wave generation is validated by comparing the numerical wave spectrum with the theoretical spectrum. Grid refinement study is also performed. Wave parameters are: H_s = 0.03m, T_p=1.0s
- For grid refinement study, different grid sizes dx = 0.10m,0.05m and 0.025m are tested. The figure below shows the results for dx =0.025m.

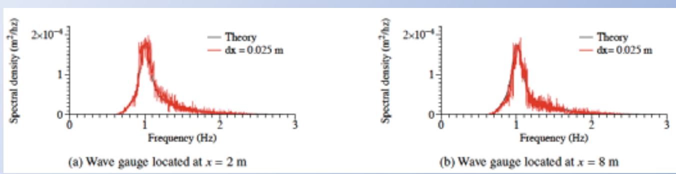

- Interaction of irregular waves of H_s: 0.05m, T_p = 1.2s with a vertical cylinder of diameter D = 0.50m in a NWT 15m long, 5m wide and 1m deep is studied. Water depth is 0.5m.
- Figure below presents the results numerical force results for this case.

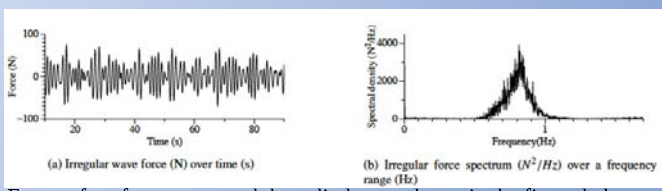

- Free surface features around the cylinder are shown in the figure below. Irregular wave surface can clearly be noticed. Diffraction is less clear as compared to the regular waves because H_s signifies only the highest of one--third of wave heights in an irregular wave terrain.

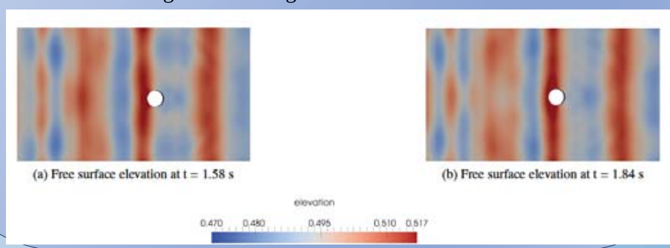

Conclusions

- Diffraction becomes more visible as the wave steepness increases.
- Irregular waves with the same significant wave height as the wave height of regular waves do not necessarily show the similar diffraction pattern.
- The numerical model REEF3D can be used as a good tool to study the regular and irregular wave forces on a vertical cylinder.

Acknowledgments

The research work has been funded by the Research Council of Norway through the project "Hydrodynamic Loads on Oshore Wind Turbine Substructures" (project number: 246810). The authors gratefully acknowledge the computing time granted by NOTUR (project number: NN2620).

The effect of the number of blades on wind turbine wake

A comparison between 2- and 3- bladed Rotors

Franz Mühle[1,*], Muyiwa S Adaramola[1] and Lars Sætran[2]
[1]Norwegian University of Life Science (NMBU), Ås, Norway
[2]Norwegian University of Science and Technology (NTNU), Trondheim, Norway

INTRODUCTION

In order to improve the performance of a wind farm, several aerodynamic concepts have been investigated and discussed [1]. Even though, these concepts have led to improved wind turbine arrangements in a farm park, there is still potential for further improvement in wind parks performance. Herein the rotor design of the turbines is offering various interesting possibilities.

In the present work, the effect of the number of blades on wind turbine wake is investigated. Therefore a three bladed rotor is compared with two different concepts for 2-bladed rotors. Herein the performance characteristics as well as the wake are analyzed.

In the wind power industry the development and research focused mostly on 3-bladed turbines. This is due to the disadvantages of two bladed turbines compared to 3-bladed rotors, such as the higher noise emissions, the distracting visual effects and the unfavorable dynamic behavior. As the offshore wind energy marked is gaining importance, the 2-bladed turbines are getting more significant again, this is due to the fact, that the drawbacks are not as relevant offshore and the big advantage of one rotor less is strongly decreasing the costs of the wind turbine[2].

OBJECTIVE

The objective of the work is, to show how rotors, showing the same performance characteristics, with different number of blades are influencing the wake and thus, whether a lower number of blades has a positive effect on the inflow conditions and consequently the power output of a turbine operating in the wake of the turbine with the rotor with a varying number of blades.

METHODS

Rotordesign

The rotor design is based on the rotor developed at the Department of Energy and Process Engineering at NTNU Trondheim which is described in [3] and is also the 3-bladed rotor used in the study.

For the design of the 2-bladed turbines it was important that the rotors are comparable to the existing 3-bladed rotor. Therefore the 2-bladed rotors where designed to have the same maximum CP value as the existing 3-bladed turbine.

To achieve this goal many different rotors where designed, adjusting the chord length and the twist angle. The performance characteristics of the different designs were tested with the software QBlade. The rotors showed the best agreement in the simulation were manufactured and tested.

- **Rotor 1**: 3-bladed rotor developed at NTNU
  Optimum at TSR 6
- **Rotor 2**: 2-bladed rotor same aspect ratio
  1.0 x Chord length, 0.7 x twist angle
  optimum at TSR 7
- **Rotor 3**: 2-bladed rotor same solidity
  1.5 x Chord length, 0.95 x twist angle
  Optimum at TSR 6

The three rotors are shown in Figure 1. They were manufactured using a 3D printer based on the PolyJet technology. To see if the 3D printing technology works for manufacturing the blades the performance characteristics of the 3-bladed printed rotor were compared to the 3-bladed milled aluminium rotor already existing at NTNU.

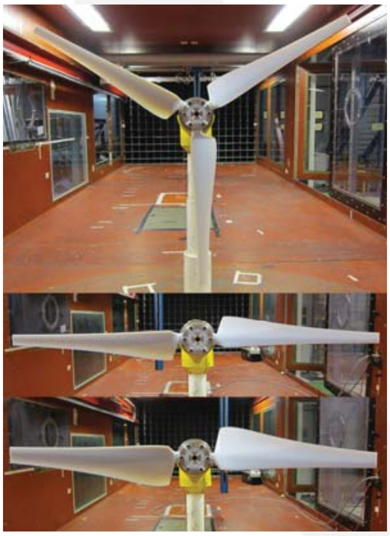

Figure 1: Three tested rotors mounted on the model turbine in the NTNU wind tunnel

Experimental Setup

The experiments were conducted in the closed-return wind tunnel of the Department of Energy and Process Engineering at NTNU. The rotors were mounted on the model turbine described in [3]. A sketch of the experimental setup is depicted in Figure 2.

- Inlet velocity $U_\infty = 10.0$ m/s
- Low turbulence $u'/U_\infty = 0.23\%$

Velocity measurement

- DANTEC 2-component LDV system

Performance measurements

- Thrust force with 6-component force balance
- Torque force with torque transducer in turbine

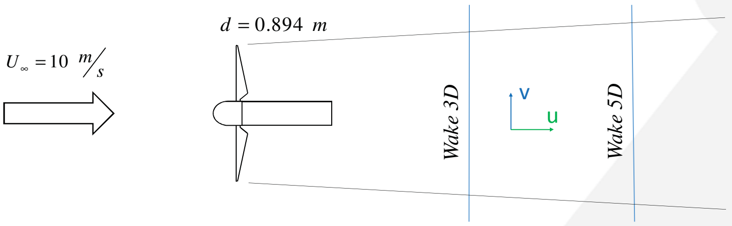

Figure 2: Sketch of experimental setup

RESULTS

Performance Characteristics

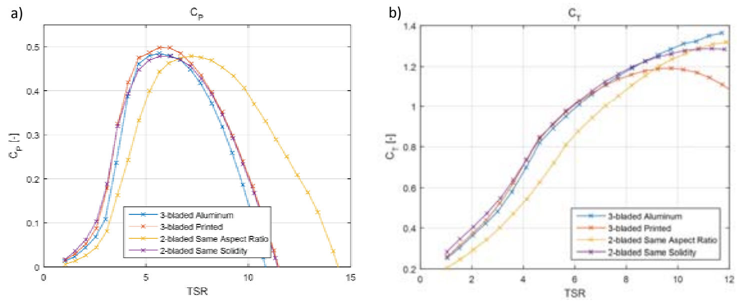

Figure 3: Performance characteristics from experiment a) power coefficient b) thrust coefficient

The maximum Power coefficients are all in the same region and the ones for the 2-bladed turbines are only 2% smaller.

The thrust coefficient shows the same behaviour at low TSR for the different rotors, only the 2-bladed rotor with the same solidity shows smaller values for the thrust coefficient in the low TSR region.

Velocity Deficit

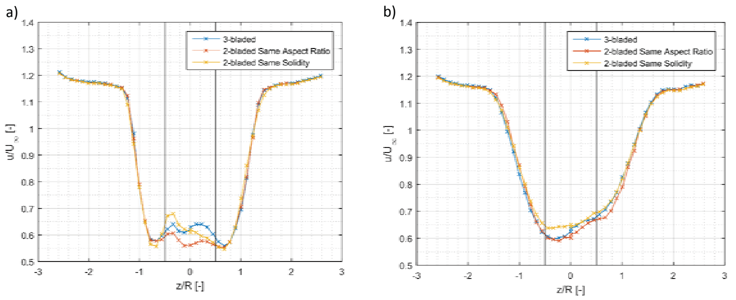

Figure 4: Normalized velocity at hub height from experiment with turbine rotor borders, a) 3D downstream of turbine, b) 5D downstream of turbine

2D Turbulence Intensity

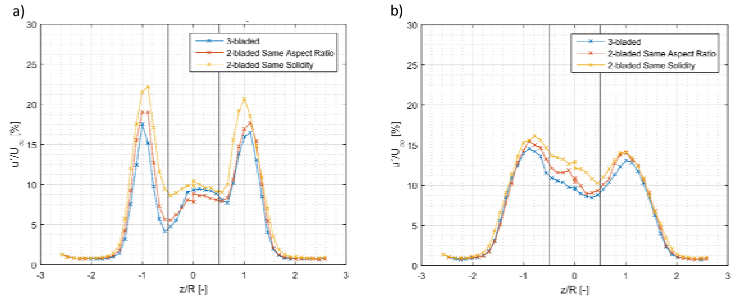

Figure 5: 2D turbulence intensity at hub height from experiment with turbine rotor borders, a) 3D downstream of turbine, b) 5D downstream of turbine

CONCLUSIONS

The performance characteristics from the experiment match the results obtained in QBlade.

The printed 3-bladed rotor has almost the same performance characteristics as the milled aluminium rotor.

The velocity deficit in the wake is very similar for all tested turbines, especially at the outer region of the wake. The major differences can be observed in the region directly behind the turbine. Consequently this regions have to be observed closer.

The turbulence intensity shows a clearer trend, whereas the 3-bladed rotor causes the smallest fluctuations followed by the rotor with the same aspect ratio and the rotor with the same solidity which generates the biggest fluctuations in the wake. Nevertheless the differences are rather small and have to be investigated closer.

REFERENCES

[1] Sanderse, B., Aerodynamics of wind turbine wakes. Energy Research Center of the Netherlands (ECN), ECN-E–09-016, Petten, The Netherlands, Tech. Rep, 2009.

[2] Hau, E. and H. von Renouard, Wind Turbines: Fundamentals, Technologies, Application, Economics. 2013: Springer Berlin Heidelberg.

[3] Krogstad, P.Å. and J. Lund, An experimental and numerical study of the performance of a model turbine. Wind Energy, 2012. 15(3): p. 443-457.

Actuator Disc Wake Modelling in RANS

N. Simisiroglou[1,2], M. Karatsioris[2], K. Nilsson[2], S.P. Breton[2], S. Ivanell[2]

[1]WindSim AS, Fjordgaten 15, N-3125 Tønsberg, Norway
[2]Department of Earth Sciences, Wind Energy section, Uppsala University Campus Gotland, Sweden

UPPSALA UNIVERSITET

Background

Accurate modelling of wind turbine wakes is essential for the design and optimization of modern wind farms. This study presents two approaches to simulate a wind turbine. This is done by employing the 1D momentum actuator disc theory (ACD) in the general purpose computational fluid dynamics software PHOENICS, developed by CHAM.

Aims

- To create an approach in RANS that will simulate a wind turbine and its wake development in an accurate and time efficient manner.
- Test the general applicability of the method for different wind turbines i.e. rated power, hub height, rotor diameter and manufacturing companies.

Methodology

Two ACD implementations

- Undistributed method: $$F_i = C_T\left(U_{1,i}\right)\frac{1}{2}\rho\left(\frac{U_{1,i}}{1-a_i}\right)^2 A_i$$
- Polynomial method: $$F_{pol,i} = 6\frac{F_{tot}}{A_{tot}}\left(\frac{r}{R}\right)^2\left(1-\left(\frac{r}{R}\right)^2\right)$$

Rotor sensitivity study

- The simulations are performed by imposing sheared inflow with hub height wind speeds ranging from 3 m/s up to 25 m/s.
- The computational parameters investigated are; the resolution of the domain, the thickness of the actuator disc and the iterative convergence criteria.
- The main output of the simulations studied are namely the wind turbine power and thrust.

Wake validation study

- It is performed by comparing comparison study between the developed methods and the state of the art Large-Eddy Simulations employing an actuator disc using airfoil data in EllipSys3D.

Results

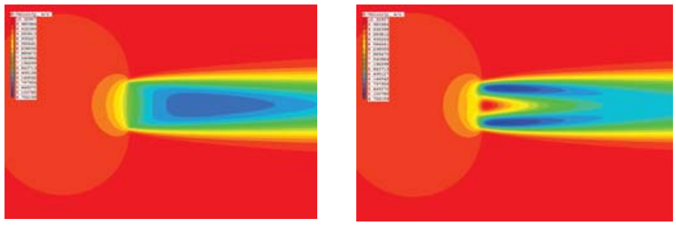

Figure 1. *Streamwise velocity contours for undistributed and polynomial method.*

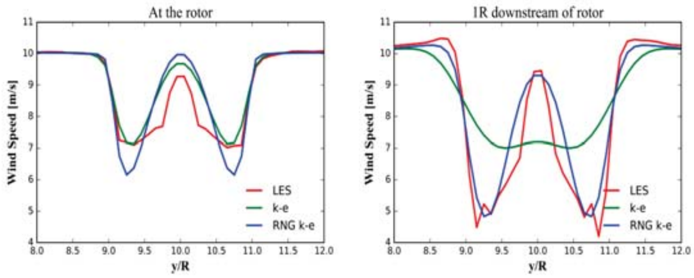

Figure 2. *Stream wise velocity at hub height along the transversal direction produced by the polynomial method using two different closure models and state of the art LES simulation, at the rotor position and 1R downstream of the rotor position.*

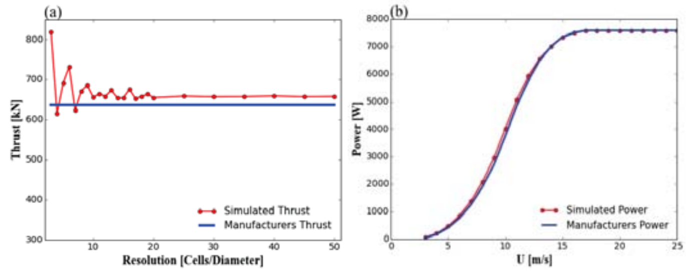

Figure 3. *Results for Enercon E-126 using the undistributed method (a) Total simulated wind turbine thrust for different grid resolutions versus the manufacturers thrust for a wind speed of 10 m/s. (b) Power production versus the manufacturers power curve for different wind speeds.*

Conclusions

The main conclusions of this study may be summarized as follows:

- The present results show that the RANS ACD methods are able to provide reasonable estimations of the conventional wind turbine power and thrust output with low computational effort.
- Changing the disc thickness had negligible effect on the estimation mentioned above.
- A grid resolution of 10 cells per rotor diameter gives sufficiently accurate results, although a grid resolution of 20 cells per rotor diameter should be preferred.
- A convergence criteria of 0.1 % is found to be sufficient.
- Lastly, the wake resulting from the RNG k-ε turbulence model with the polynomial method compares well to the LES simulations. On the other hand the standard k-ε turbulence model seems to over predict the wake recovery relatively to the other two models.

Acknowledgments

- This project was financially supported by the research council of Norway (Project no. 231831).
- A special thank you to all the members of CHAM for their technical support.

Contact

Nikolaos Simisiroglou
Uppsala University,Campus Gotland
621 67 Visby, Cramérgatan 3
Email: nikolaos.simisiroglou@windsim.com
Phone: +46 72 903 88 21

References

A. Betz, The Maximum of the theoretically possible exploitation of wind by means of a wind motor, *Wind Engineering*. 37 (2013), 441 – 446.
CHAM. Available at: http://www.cham.co.uk (accessed January 5, 2016).
S.P. Breton, K. Nilsson, H. Olivares-Espinosa, C. Masson, L. Dufresne, S. Ivanell, Study of the influence of imposed turbulence on the asymptotic wake deficit in a very long line of wind turbines, Renew. Energy. 70 (2014) 153–163. doi:10.1016/j.renene.2014.05.009

Wind farm control applications for Windscanner infrastructure

Tor Inge Reigstad

SINTEF

NOWITECH Norwegian Research Centre for Offshore Wind Technology

WindScanner.no

Windscanner

Lidar:
-> sends out a laser beam and detects the weak return, reflected or scattered from natural aerosols like dust, pollen and droplets
-> the wind speed is calculated from the Doppler shift for the backscatter in the beam direction
-> two types: pulsed or continuous wave type

Short range Windscanner:
-> three continuous wave wind lidars
-> Measuring area: a few 100 meters

Long-range Windscanner:
-> three or more pulse wave scanning lidars
-> suitable for measuring wind over a large area

Control objectives

Windscanner could:

Increase energy production: by reducing wake losses
-> reducing the power of the most upwind turbine(s)
-> controlling the yaw and redirect the wake to avoid it hitting the downwind

Increase lifetime: by reducing mechanical loads
-> improving pitch control and tip-speed ratio

Increase availability: by reducing extreme loads
-> detecting strong wind gusts and control pitch and tip-speed ratio

Improve ancillary services to the electric grid:
-> Improving production forecast

Increase lifetime performance:
-> large-area, long-time wind data are used for finding the optimal trade-off between energy production, wake losses, structural loads, downtime and revenue from sold energy.

A PI control strategy for active power control at PCC with yaw optimization and production forecast

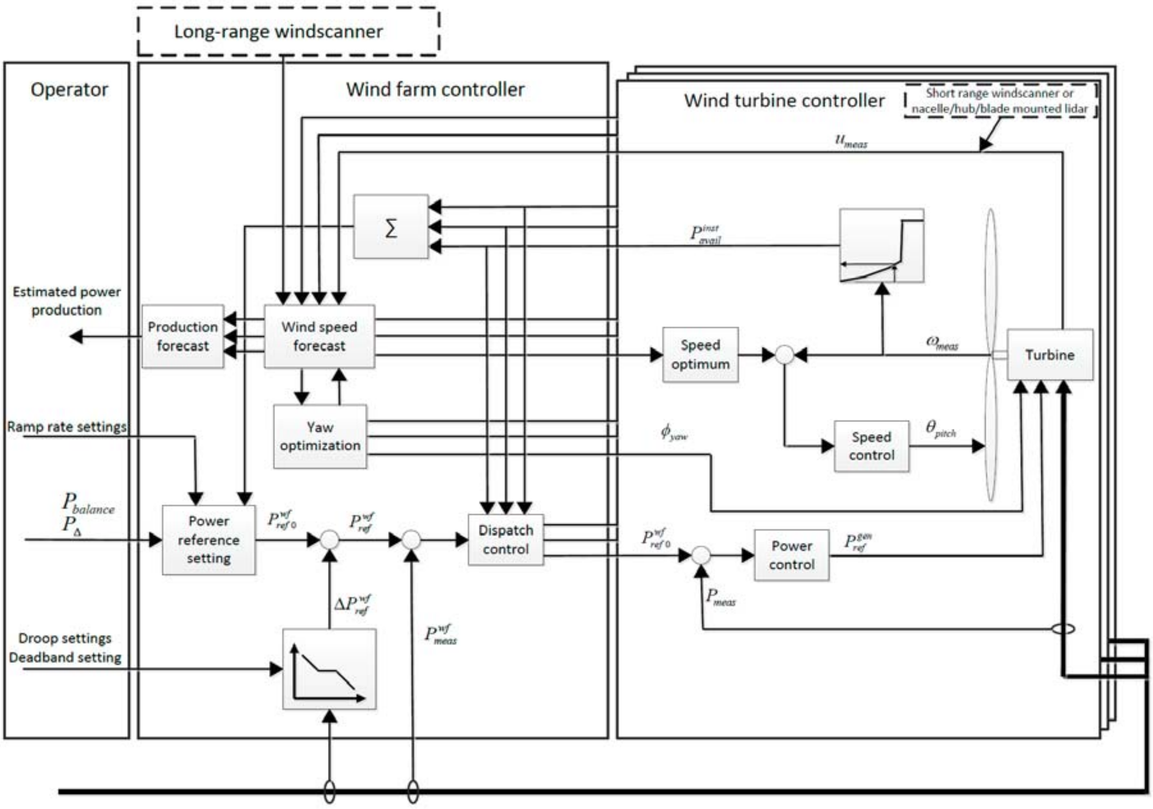

Up-front measurements

1)Mapping of wind field and wakes in different conditions with Windscanner

2)Create look-up tables or similar

3)Use these in wind farm control: "Wind speed forecast" and "Yaw optimization"

or Real-time input

Windscanner measurements -> Input to wind farm controller

1)Long-range Windscanners or

2)Short-range Windscanners (in all or some wind turbines)

High precision Windscanner measurement in real time is not presently possible

Validation of control strategies

Windscanner could:

-> Provide measurement series showing the relationships between operation condition of the turbines

-> Provide data for optimizing power production and reducing structural loads by pitching or yaw misalignment

-> Validate analysis tools

-> Provide open data

Real-Time Hybrid Model Testing of Floating Wind Turbines

Valentin Chabaud, NTNU

Maxime Thys, MARINTEK   Erin Bachynski, MARINTEK   Thomas Sauder, MARINTEK   Lars Ove Sæther, MARINTEK

Numerical Setup

- Software: SIMA (by MARINTEK)
- Hydrodynamics, kinetics and mooring dynamics modeling
- Actuators (Motor+spring+wheel+wire) modelled by a winch + winch controller + elastic cable.
- Wind turbine aerodynamics modeling for verifcation of the numerical model
- Real-time communication with the ReaTHM testing controller

The ReaTHM controller can communicate with either the physical or the numerical setup, at its option. Most of its features are compatible with both setups with only minor changes in the code.
The numerical setup provides the flexibility necessary to develop a complex ReaTHM testing project. It is also a simulation tool able to reproduce the environment of the ocean wave basin at no cost.

Real-time hybrid model (ReaTHM) testing in NOWITECH model tests

- CSC braceless semi-submersible, scale 1/30, in MARINTEK's ocean wave basin
- NREL 5MW turbine, physical tower with correct mass properties.
- Actuated wind forces. No physical wind, no rotor, but a set of 6 actuators applying in real-time the thrust force, generator torque and pitch and yaw moments calculated by NREL's AeroDyn from a turbulent wind field and online measured motions.
- No Froude-Reynolds scaling conflict, controlled wind field and aerodynamic loads, flexible inclusion of the rotor and the generator torque/blade pitch controllers

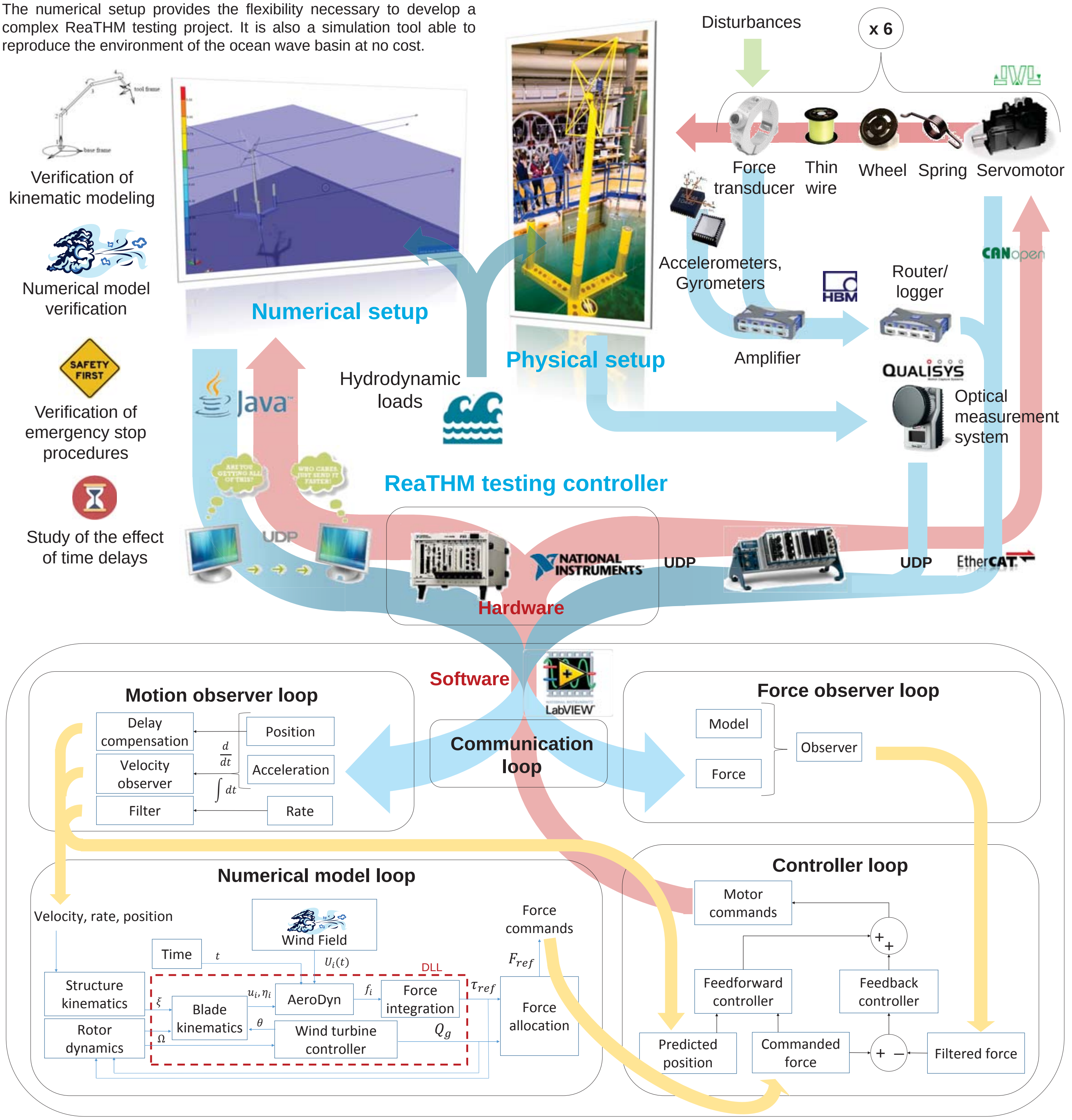

Experimental Investigations of Wind Turbine Wake Towards Offshore Wind Farm Performance Validation

Youjin Kim[1,3**] Ali Al-Abadi[1*,2] Antonio Delgado[1,3]

[1]Institute of Fluid Mechanics (LSTM), FAU-Erlangen, Germany, *ali.al-abadi@fau.de

[2]Alkawarizmi College of Engineering, University of Baghdad, Baghdad, Iraq

[3]Institute of Fluid Mechanics (LSTM), FAU Busan, South Korea , ** youjin.kim@fau.de

Motivation

- Laboratory scale representation of atmospheric turbulence and wake generated by Wind Farm
- Near wake investigation exposed to different turbulence contents
- Validation of the offshore wind-farm model performance based on experimental results
- Observation of fluid flow phenomena inside Wind farm due to wake generated turbulence

Approach

Experimental Setup

- Tests are conducted in the closed loop wind-tunnel of LSTM, FAU Erlangen
- The wind turbine is exposed to turbulent flow of different scale
- Turbulence and velocity profile of wind flow are measured by Hot-wire and Pitot-tube, respectively

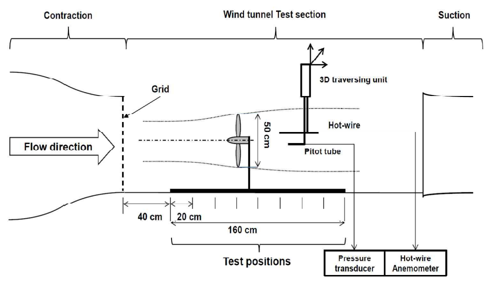

Grid Generated Turbulence

- The turbulence level increases with the installation of the fine grid at the entrance of the test section
- The same effect, but in a higher level of turbulent intensity, is depicted when using of the coarse grid
- The turbulence scale decays in the flow direction

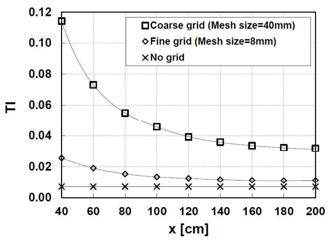

averaged oncoming wind speed of 8-16 m/s
Turbulence Intensity along the wind-tunnel test section

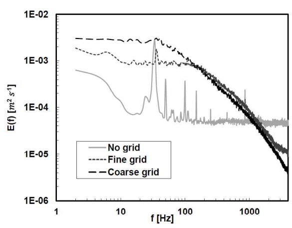

Energy Spectrum E(f) versus eddies frequencies f
at the design free-stream wind velocity 12m/s, TI=0.039
hot-wire position at x=120cm with the absence of wind turbine

Offshore Wind Farm Data and Model

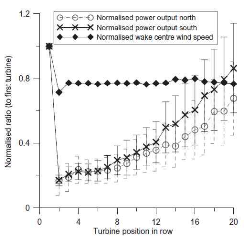

Power & Velocity output under wake
Inside Middelgrundel Offshore Wind Farm [1]

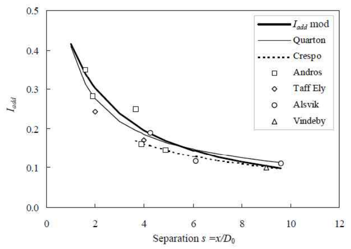

Added Turbulence Intensity versus turbine position
By different model and wind farm measurements [2]

Result & Discussion

Axial Velocity distribution of near wake

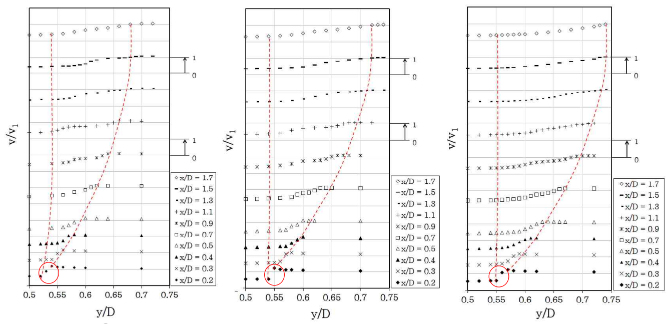

No Grid Fine Grid Coarse Grid

Downwind velocity distribution normalized by the design oncoming wind velocity of $v1=12$ m/s
x/D is the axial downwind distance normalized by the wind turbine diameter
y/D is the radial distance normalized by the wind turbine diameter

Turbulence Intensity and Energy Spectrum

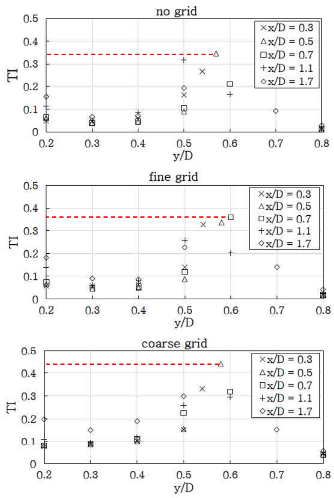

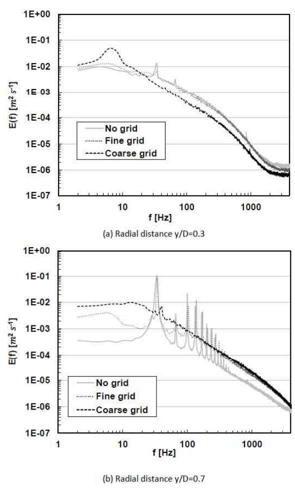

- Axial Velocity Profile shows tip-vortex, mixing and velocity restoration
- The highest turbulent intensity is observed at x/D=0.5 or 0.7 at near wake
- Wake mixing and Tip Vortex Phenomena are shown by analyzing the spectra E(f)
- E(f) distributions show suppression of tip vortex at higher turbulence
- Flow characteristics are different according to blade radial position

[1] Modelling and Measurements of Power Losses and Turbulence Intensity in Wind Turbine Wakes at Middelgrunden Offshore Wind Farm, R. J. Barthelmie, etc, Wind Energ. 2007; Wiley Inter science, DOI: 10.1002/we.238 [2] Turbulence and turbulence generated structural loading in wind turbine clusters, Sten Tronæs Frandsen, Risø National Laboratory, Roskilde, Denmark, January 2007

Conclusion

- TI from 0.07 to 0.114 and E(f) distribution of generated turbulent flow to mimic offshore wind farm atmosphere are generated in laboratory scale
- High turbulence content of oncoming wind increased wake-surrounding interaction with more energy entrainment to the wake regime as higher turbulence can penetrate through turbine rotor plane
- Higher turbulent flow brings different scales and hence more mixing in the near-wake regime with causing faster wake recovery
- Wake recovery part of axial velocity profiles were in same context of TI described by offshore wind farm models
- Experimental results describe TI distribution, tip vortex and flow mixing at near wake (up to x=1.7D)

ACKNOWLEDGMENTS - This study is supported by BB21 Project, collaboration between LSTM Erlangen, Germany and Busan Metropolitan City, South Korea

Validation of a Semi-Submersible Offshore Wind Platform through tank test

G. Aguirre (1), J. Galván (1), V. Nava (1), G. Pérez(1), M. Sanchez (1), I. Mendikoa (1), J.M. Busturia (2)

(1) Tecnalia R&I Email: goren.aguirre@tecnalia.com
(2) Nautilus floating solutions Email: jmbusturia@nautilusfs.com

ABSTRACT

The performance of a **scale model of a semisubmersible platform for offshore wind** has been identified through a varied **experimental tank test campaign**. Tests were performed by **TECNALIA** at the IHC wave tank in Santander within the framework of the **NAUTILUS** project.

The tested device consists in a **1:35 model** in a Froude scale of a four-column semi-submersible platform provided with heave plates and a ring pontoon at the bottom. The turbine held by the prototype is the NREL 5MW baseline wind turbine.

The campaign consisted in decay tests, but also tests in regular **waves** for determining the RAOs and tests in irregular waves simulating typical weather climate conditions of the Basque coasts. **Wind action** was also simulated with air fans and a rigid disk at the hub height. Different wind speed bins were tested. Finally wave, wind and **currents** conditions were replicated for extreme loads.

Outcomes in terms of hydrodynamic characteristics, RAOs, responses under irregular waves and **fairlead mooring loads** are herein reported and compared [1] with the results of numerical simulations obtained by coupling commercial and open source software (FAST and Orcaflex).

General specification	
Power rating	5 MW
Hull weight (steel mass)	1.700 tons
Total displacement	7.100 tons
WT weight	750 tons
Hub height	86 m
Hull draft	20 m
Depth	> 60 m
Catenary mooring	4 lines
Column diameter	9,5 m
Column distance	33 m
Freeboard	10 m

AERO-HYDRODYNAMIC COUPLING

The analysis of floating wind turbines (FWT) is more complicated than that of fixed-bottom wind turbines. For this particular case a **coupled aero-hydrodynamic simulator with FAST v7 and Orcaflex** has been used for simulating the response and aerodynamic performance of FWTs under wind, current and waves loads in the time domain.

For **aerodynamics**, an **unsteady BEM model and the (GDW) Generalized Dynamic Wake** has been used to calculate the aerodynamic loads and performance of the wind turbine.

For **hydrodynamics**, a **linearized BEM model** based on the frequency-dependent parameters obtained from the code AQWA has been used to calculate the hydrodynamic loads on the platform by solving the hydrostatic, **diffraction and radiation** problems.

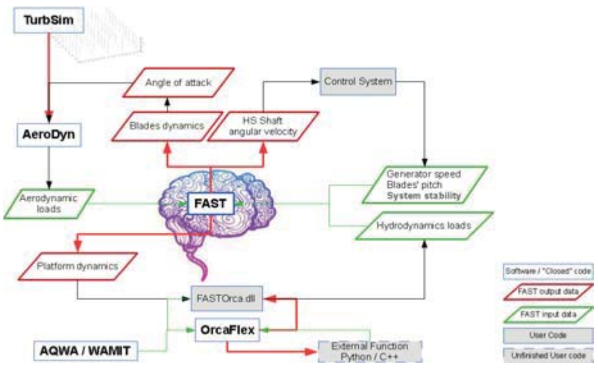

The hydrodynamic study of the floater is **combined with an aeroelasticity and a control algorithm** model to obtain a **coupled aero-servo-hydro-elastic model**. Generalized inertia forces for floating wind turbine concepts have been described for tower, nacelle, hub, platform and blades. The generalized active forces have been described for aerodynamic forces, hydrodynamic forces, gravity force, drive train force and elastic forces

TEST CAMPAIGN 1:35 SCALE MODEL

The **test campaign** carried out **included**:

1. Inclining test
2. Decay test
3. Force oscillation
4. Mooring system forces
5. Towing in regular waves
6. Regular waves
7. Wave grouping tests.

Each one had a specific **target**:

1. Stability curve
2. Eigen periods
3. Added mass and damping
4. Mooring stiffness
5. Drag coefficient
6. RAO's
7. Drift force

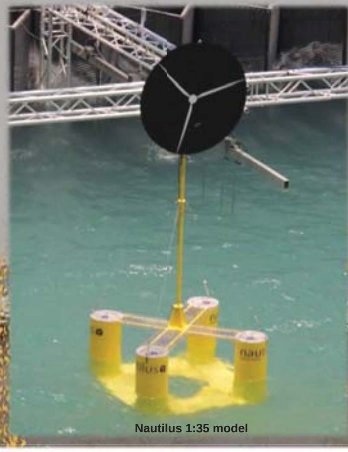

Nautilus 1:35 model

Data below shows some results from decay test (natural frequencies and calibration), validation for wave grouping and figures of operational and survival test.

Surge	Sway	Heave	Roll	Pitch	Heave
101.65 s	101.75 s	18.90 s	23.92 s	24.30 s	70.55 s

Eigen period results from decay test

Test results	Operational		Survival		
H_s	1.88		14.12		m
T_p	9.15		15		s
V_{wind}	11.5		50		m/s
$V_{current}$	0		0.9		m/s
	Offset	Peak to peak	Offset	Peak to peak	
Surge disp.	9.71	4.38	8.51	6.31	m
Heave disp.	86.5	0.47	89	5.34	m
Pitch disp.	-0.76	3.01	-0.71	3.56	deg
L1 loads	91.35	5.55	82.39	86.80	ton
L3 loads	32.21	1.46	35.73	10.45	ton
	Offset	Max	Offset	Max	
Acceleration X	0.20	0.65	0.46	1.47	m/s^2
Acceleration Z	0.09	0.29	0.47	1.41	m/s^2
Acceleration Pitch	0.12	0.47	0.27	0.90	deg/s^2

Result from operational and survival conditions

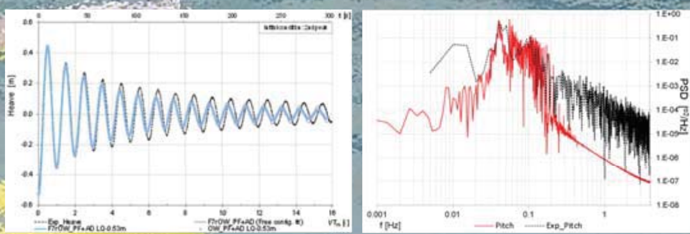

(Left) Lineal-quadratic heave calibration and (right) pitch numerical model validation for 3m significant height wave spectra.

CONCLUSIONS

- Results were **satisfactory** with expected accelerations and motions below most wind turbine manufacturer **requirements**.
- Free decay and forced oscillation test are essential for **model calibration**.
- Hydrodynamic **numerical model and test results fit** for wave excitation. Working on coupling with aerodynamic reliable model.
- Reliable numerical model **enables the simulation** of design load cases for certification.

REFERENCES

[1] Nava,V., Aguirre, G., Galvan, J., Sanchez-Lara, M., Mendikoa, I., Perez-Moran, G., Experimental studies on the hydrodynamic behavior of a semi-submersible offshore wind platform, 2015, Renewable Energies Offshore - 1st International Conference on Renewable Energies Offshore, RENEW 2014, 24-26 Nov. 2014, Lisbon, Portugal, ed. Taylor & Francis Group, pp. 709-715.
[2] Definition of the semisubmersible Floating System for Phase II of OC4; A. Roberson. NREL
[3] Integrated Dynamic Analysis of Floating Offshore Wind Turbines; Bjorn Skaare; Hydro Oil & Energy
[4] Modeling aspects of a floating wind turbine for coupled wave–wind-induced dynamic analyses; M. Karimirad; NTNU

EERA DeepWind 2016
Trondheim, 20 - 22 January 2016

Field site experimental analysis of a 1:30 scaled model of a spar floating offshore wind turbine

C.Ruzzo[1], V. Fiamma[1], V. Nava[2], M. Collu[3], G. Failla[1], F. Arena[1]

[1] Mediterranea University, Natural Ocean Engineering Laboratory, Reggio Calabria, Italy

[2] Tecnalia Research and Innovation, Energy and Environment Division, Bilbao, Spain

[3] Cranfield University, Cranfield, United Kingdom

Abstract

- System identification of offshore structures is a crucial step in the concept selection and in the design process of floating structures.
- Traditional approach consists in testing small scale models in wave basins where controlled conditions can be artificially generated. However this procedure is very expensive and often poses limitations on the testing time and the model size.
- How to characterize the dynamics of a floating structure through experiments in the open sea only?
- This work proposes a novel approach to answer the previous question, including a first-stage validation on a 1:30 model of a spar-type floating offshore wind turbine in Natural Ocean Engineering Laboratory (NOEL) of Reggio Calabria (Italy).

Traditional approach

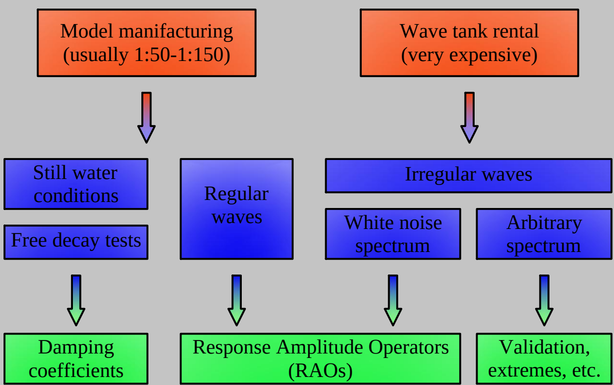

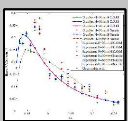

Example 1: a 1:100 scaled model of a spar support for offshore wind turbine (left) and relative experimental heave RAOs (center) (Sethuraman & Venugopal, 2012).

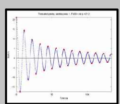

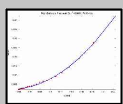

Example 2: roll FDT for a small scale model of a ship and determination of the damping coefficients with Faltinson's method (Uzunoglu & Guedes Soares, 2015; Faltinson, 1993).

Proposed approach

1. Selection of an appropriate location

NOEL laboratory of Reggio Calabria (Italy), has been chosen due to very suitable site characteristics. During certain months, typical sea states are good scale models, in Froude similarity, of severe ocean sea-storms, having H_s = 0.2-0.4 m, T_P = 1.8-2.6 s and JONSWAP-like spectra. Consequently, scale factors between 1:10 and 1:50 can be chosen.

2. Semi-permanent installation of the model

Case study is a 1:30 scaled model of the OC3-UMaine Hywind (Robertson & Jonkman,2011) where the NREL 5MW offshore wind turbine is represented as a fixed mass. It was installed in July 2015 and is still in operation. 6-DOF motions as well as wave elevation are measured.

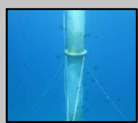

3. Identification of the model

Non-controllable metocean conditions. Local sea states must be exploited:

- calm water for free decay tests adopting an aggregate form of Faltinson's method for damping estimation.
- RAOs obtained piecewise in the wave frequency range. Wind waves are used for high frequencies (about 2.4-3.5 rad/s) while swells for lower ones (about 0.9-2.4 rad/s)

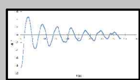

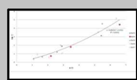

Roll free decay test executed at NOEL (left). Determination of the damping coefficient using various FDTs.

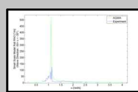

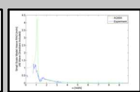

Heave and roll directional RAOs obtained from a database of 526 sea states. Horizontal motions were not investigated since their natural frequencies are too low.

Conclusions

The main differences between the traditional approach for the system identification of floating structures and the proposed one are:

- **Reduction of the costs.** Tests in natural laboratories are cheaper and may last longer than in wave tanks.
- **Larger scale factors.** Intermediate scale testing results in better scaling of hydrodynamic forces on the structures, especially with regard to viscous forces, depending on Reynolds Number.
- **Importance of the location**. The natural laboratory must present various wave conditions, including calm periods, small purely wind-generated sea states, swells with sufficiently long periods.
- **Limits of the natural laboratories**. It is not possible to investigate frequency ranges out of wave spectra domain and free decay tests are coarser than in wave tanks since water is never perfectly calm.
- **Further work** will be performed, including collection of more data, realization of new FDTs and investigation of output-only identification techniques (such as FDD) for further damping estimation.

Wind Model for Simulation of Thrust Variations on a Wind Turbine

Emil Smilden[a,b], Lene Eliassen[a]

[a]NTNU, [b]AMOS

NTNU – Trondheim
Norwegian University of Science and Technology
AMOS

Abstract

The aerodynamic thrust induced by the air passing through the wind turbine rotor is transferred on to the tower and support structure and must be considered during structural design. This paper provides a computationally simple simulation model for the aerodynamic thrust on a wind turbine. The model is based on an equivalent wind formulation accounting for the effect of wind shear, tower shadow, turbulence and rotational sampling. Wind shear is shown to have a depleting effect on the mean rotor thrust. Both wind shear and tower shadowing cause thrust variations oscillating with the blade passing frequency, the effect of wind shear is however small compared to the effect of tower shadow in this regard. Turbulent wind fluctuations will cause low-frequent thrust variations in addition to thrust oscillating with the blade passing frequency. The equivalent wind model is verified by comparison with results obtained using the software code HAWC2 by DTU Wind Energy.

Introduction

Wind turbines are dynamically sensitive structures, and especially the first tower vibration mode is prone to excitation by thrust variations induced by the wind passing through the wind turbine rotor [1]. As the blades pass through their arc of motion they will encounter a constantly changing wind field, appearing as imbalances and fluctuations in aerodynamic loading [1]. Turbulence will cause low-frequent load variations [3], and because the rotor frequency is normally higher than the turbulence frequency, turbulence will be sampled by the rotor, appearing as cyclic loads that fluctuates with the blade passing frequency (3P) [1]. In addition, 3P load variations are caused by persistent disturbances of the wind field within the rotor plane due to the presence of the tower, known as tower shadow, and air interacting with the earth surface, known as wind shear. The main contribution of this paper is the development of a wind model for fast simulation of thrust variations on a wind turbine. The model accounts for the effect of wind shear, tower shadow, turbulence and rotational sampling.

Basic Concept

The wind model is based on the concept of an equivalent wind speed, first presented in [4]. This method is based on the idea of representing the complete wind field encountered by the rotor by a single wind time-series [5]. This time-series can further be used as input to a computationally simple mathematical representation of the rotor aerodynamics for fast calculation of aerodynamic thrust using

$$T_{aero}(t) = \frac{1}{2}\rho A V(t)^2 C_T(\lambda, \beta) \qquad (1)$$

where A is the rotor area,$V(t)$ is the wind speed and $C_T(\lambda)$ is the thrust coefficient depending on the tip-speed ratio λ and blade pitch angle β.
The total wind speed is divided into two main components [3]

$$V(t) = V_0 + \tilde{v}_{eq} \qquad (2)$$

consisting of the mean wind V_0 and the equivalent fluctuating component

$$\tilde{v}_{eq} = \tilde{v}_{ws} + \tilde{v}_{ts} + \tilde{v}_0 + \tilde{v}_3 \qquad (3)$$

where $\tilde{v}_{ws}$, $\tilde{v}_{ts}$, $\tilde{v}_0$ and $\tilde{v}_3$ are the equivalent wind components accounting for wind variations caused by wind shear, tower shadow, turbulence and rotational sampling.

Acknowledgements

This work has been carried out at the Centre for Autonomous Marine Operations and Systems (AMOS). The Norwegian Research Council is acknowledged as the main sponsor of AMOS. This work was supported by the Research Council of Norway through the Centres of Excellence funding scheme, Project number 223254 - AMOS.

Mathematical model

The equivalent wind speed component accounting for turbulence $\tilde{v}_0(t)$ is calculated by its *Fourier* transform given by

$$\tilde{V}_0(f) = H_0(j2\pi f) \cdot V(f) \qquad (4)$$

where the zero harmonics filter $H_0(j2\pi f)$ is found by fitting of a rational transfer function to the admittance function for a general wind turbine rotor, and $V(f)$ is the *Fourier* transform of the fixed-point wind speed calculated by use of the Kaimal spectrum. The equivalent wind speed accounting for turbulence sampling is given by

$$\tilde{v}_3(t) = 2\mathrm{Re}\{\tilde{v}_3(t)\}\cos(3\theta) + 2\mathrm{Im}\{\tilde{v}_3(t)\}\sin(3\theta) \qquad (5)$$

where the components of $\tilde{v}_3(t)$ are calculated by their *Fourier* transforms in the same way as for $\tilde{v}_0(t)$. Further, the equivalent wind component accounting for wind shear is given by

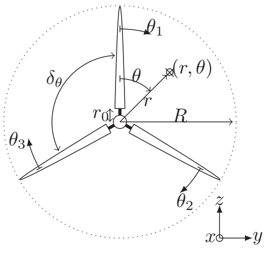

Figure 1: Rotor reference frame

$$\tilde{v}_{ws}(t,\theta) = V_0\left(\frac{\alpha(\alpha-1)}{12}\left(\frac{R-r_0}{H}\right)^2 + \frac{\alpha(\alpha-1)(\alpha-2)}{96}\left(\frac{R-r_0}{H}\right)^3\cos 3\theta\right) \qquad (6)$$

where α is the wind shear exponent, H is hub height and the other parameters are defined in Fig. 1. At last, the equivalent wind speed accounting for tower shadow is given by

$$\tilde{v}_{ts}(t,\theta) = \frac{V_0 a^2}{3R}\sum_{n=1}^{3}\left[\frac{-R}{R^2\sin^2\theta_n + b^2}\right] \qquad (7)$$

where a is the tower radius and b is the rotor overhang.

Simulations and discussion

A parameter study was performed to evaluate the importance of including the effect of wind shear and tower shadow in simulations. Further, the equivalent wind model accounting for turbulence and rotational sampling was verified by comparison with results obtained using the software tool HAWC2 by DTU Wind Energy. Simulation parameters are based on the 10MW reference wind turbine of [2]. Fig. (2) shows the effect of both wind shear and tower shadow individually and together. The primary source of thrust variations are tower shadow. Wind shear should still be included due to its depleting effect on mean thrust. Fig. (3) shows the power spectral density for thrust time-series accounting for turbulence. A high energy content is observed at low frequencies, and the peak observed in the spectrum is caused by rotational sampling with peak frequency corresponding to the 3P frequency. The equivalent wind model shows good agreement with the results obtained using HAWC2 except from a small deviation at lower frequencies which is most likely caused by small differences in aerodynamic properties for the two rotors. The second peak in the HAWC2 results is caused by 6P effects which is not modelled by the equivalent wind model.

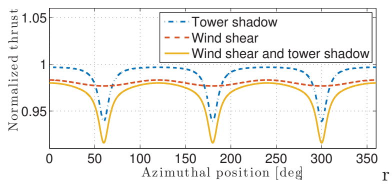

Figure 2: Normalized equivalent thrust accounting for wind shear and tower shadow

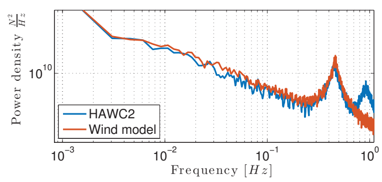

Figure 3: Power spectral density of thrust time-series using HAWC2 and equivalent wind model

References

[1] László Arany, Subhamoy Bhattacharya, John Macdonald, and S John Hogan. Simplified critical mudline bending moment spectra of offshore wind turbine support structures. *Wind Energy*, 2014.

[2] C Bak, F Zahle, R Bitsche, T Kim, A Yde, LC Henriksen, A Natarajan, and M Hansen. Description of the dtu 10 mw reference wind turbine. *DTU Wind Energy Report-I-0092*, 2013.

[3] Tony Burton, David Sharpe, Nick Jenkins, and Ervin Bossanyi. *Wind energy handbook, 2nd Edition*. John Wiley & Sons, 2011.

[4] W Langreder. Models for variable speed wind turbines. *CREST, Loughborough University of Technology*, 1996.

[5] Poul Sørensen, Anca D Hansen, and Pedro André Carvalho Rosas. Wind models for simulation of power fluctuations from wind farms. *Journal of wind engineering and industrial aerodynamics*, 90(12):1381–1402, 2002.

Numerical simulations of the NREL S826 performance characteristics

Kristian F. Sagmo, Lars Sætran, Jan Bartl
krissag@stud.ntnu.no

Introduction

The project work at hand makes use of the Computational Fluid Dynamics (CFD) software package STAR-CCM+ developed by CD-Adapco, and assesses some CFD turbulence's models ability to accurately predict performance characteristics of the NREL S826 airfoil.

Experiments on the Airfoil characteristics have already been conducted at both NTNU by Aksnes[1] and DTU by Sarlak[2], providing a large amount of data for CFD validation. Simulations were set up in a similar manner as the experiments done at NTNU's windtunnel.

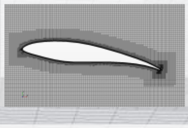

Figure 1: Exploded view of the 2D Mesh around the wing profile. cells shown are 6 mm. Chord 0.45 m.

Method

Simulations were set up in a similar manner as the experiments done at NTNU's windtunnel. After a mesh refinement study using both the Spalart-Allmaras and the Menter SST k-omega turbulence models, Reynolds dependency was investigated for low Reynolds numbers. 3D simulations were conducted using NTNU's supercomputer "Vilje" to asses effects not present in 2D simulations.

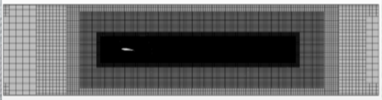

Figure 2: The 2D mesh .This mesh profile was also used for the 3D domain illustrated to the right in Figure 6.

Results and Discussion

Following the process of verification outlined in Roache[3] the grid convegence study presented in Figure 3 resulted in discretization error estimates of 6.7 % and 8.5 % for the Spalart-Allmaras and Realizable k-epsilon 2D simulations, respecively.

In Figure 4 the results for the airfoils drag coefficient is presented with experimental data, and in Figure 3 the 3D simulation results are presented.

Considering the estimated discretzation error bands and the differing results obtained by the DTU and NTNU experiments the Spalart.-Allmaras turbulence model can be said to make good predictions for lift and drag. The 2D simulations utilizing the Realizable k-épsilon model used Star-CCM+'s default k and épsilon values. This resulted in lower effective viscosity throughout the domain and lower drag prediction relative to the user specified Spalart-Allmaras turbulence parameters. The drastic difference in drag prediction highlights the importance in specifying turbulence model parameters and underlines that there really is no one RANS based turbulence model that can handle diverse flow problems without some tuning as pointed out by Versteeg et. al[3]. The 3D simulations with the Realizable k-épsilon model uses the same turbulence specifications as the Spalart-Allmaras 2D simulations.

Lift and drag coefficients were also simulated for Reynolds numbers of 50, 70 and 200 thousand, but revealed no abrubt changes in the lift and drag coefficients. This is in accordance with findings by experiments conducted at NTNU(?) but not with experiments conducted at DTU.

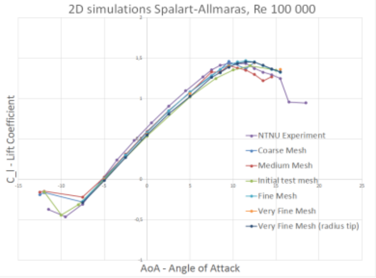

Figure 3: Lift coefficients with different mesh refinement levels. The results from the finest meshes overlap, but the solution has changed from the initial grid setup.

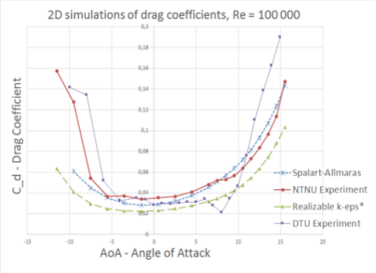

Figure 4: Drag coefficients for two different turbulence models in 2D, plotted with experimental data. under estimation of drag by the k-épsilon model is explained by the differing turbulence length scales set.

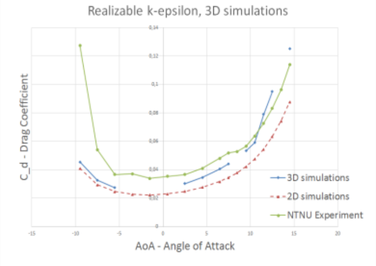

Figure 5: Drag coefficients comparing 2D and 3D simulation results. 3D effects makes for a sharper increase in drag in the stall región.

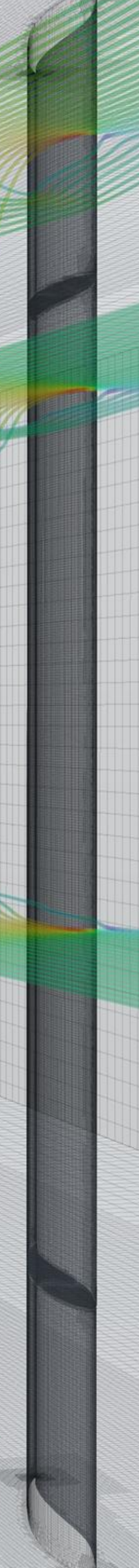

Figure 6: The 3D grid, used for simulations with the Realizable k-epsilon turbulence model. Here with an AoA of 11.5 degrees. The velocity pathlines illustrate the increase in vorticity towards the windtunnels walls, giving a sharper increase in drag prediction compared to the 2D simulations as presented in Figure 5. The outer parts of the wing separated from the center measuring section by the shaded sections are not part of lift or drag predictions.

Conclusions

It was found that 2D RANS based simulations with the Spalart-Allmaras and the Realizable k-épsilon give a reasonable estimate for lift and drag coefficients for the NREL S826 airfoil at low Reynolds numbers. The 3D simulations confirms that flow can not be considered 2D, even around the forcé measuring section of the wing, when entering the stall región. This has been previously been pointed out by Manolesos[4] among others.

Simulation results displaying Reynolds number independency and the varying results from the experiments suggest that Reynolds dependency effects might be due to unsteady flow effects. Therefore, it would be interesting to see the results from transient RANS simulations, or perhaps DES/LES simulations.

References

[1] Nikolai Yde Aksnes, *Performance characteristics of the NREL S826 airfoil - Reynolds Independency.* Master Thesis, NTNU Trondheim, 2015.

[2] H. Sarlak C., *Large Eddy Simulations of turbulent flows in Wind Energy.* Doctoral Thesis, DTU, January 2014.

[3] H.K. Versteeg & Malalasekera, *An Introduction to Computational Dynamics.*

[4] M. Manolesos, *Stall Cells, what do we know about them?* Conference Paper FORWIND Seminar, July 2015.

THE UNIVERSITY OF MAINE
Department of Mechanical Engineering

A Single-Axis Hybrid Modelling System for Floating Wind Turbine Basin Testing

Matthew Hall and Andrew Goupee

Numerical Modeling

The Problem

An important part of floating wind turbine design is simulating the coupled system response. The numerical models built for a given design require experimental validation. Experiments however have difficulty matching the full-scale coupled behavior.

Simulations

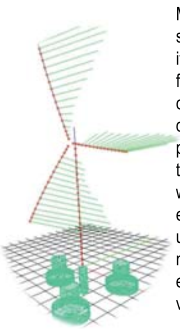

Medium fidelity coupled simulation tools are needed for iterative design processes and for loads analyses in support of certification. Engineering-level design codes like FAST[1] provide good approximations of the aero-hydro-elastic dynamics while being computationally efficient. Because of uncertainties in hydrodynamics modeling[2] and the use of empirical coefficients, model validation and tuning is crucial.

Physical Modeling

Experiments

Floating wind turbine designs are typically validated at near 1:50 scale in wind-wave laboratories. The necessity of Froude scaling results in reduced Reynolds numbers. Even with a high-quality wind tunnel and compensated rotor geometry, some aspects of the wind turbine performance have so far been unable to match the full scale values[3]. As a consequence, the aero-elastic response is altered and realistic blade-pitch controllers cannot be used.

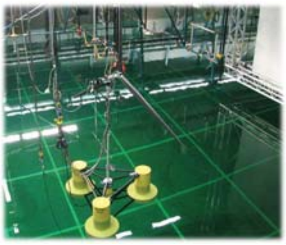

A Hybrid Solution

An alternative is to couple parts of the simulations and experiments together, an approach gaining popularity in offshore renewable energy research[4-7].

Hybrid modeling can offer wave-basin validation with more realistic wind loads by combining physical and numerical models:

- A Froude-scaled floating platform is tested in a wave basin.
- A full-scale wind turbine simulation runs beside the experiment.
- A sensor and actuation system couples the physical and numerical models together in real time. The requirements are demanding[8].

Numerical Model

A customized version of FAST models the full-scale wind turbine dynamics above the tower top at up to 15X real time. From the measured platform motions, it calculates the turbine reaction forces.

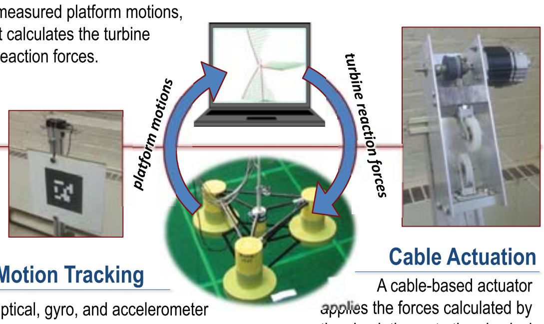

Motion Tracking

Optical, gyro, and accelerometer measurements of the floating platform motion are filtered and passed to the control system.

Cable Actuation

A cable-based actuator applies the forces calculated by the simulation onto the physical floating platform. Each winch unit incorporates force and motion feedback.

Controller

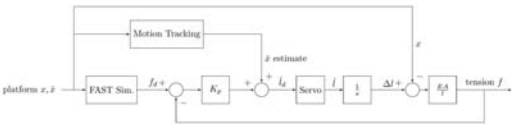

An "impedance" coupling scheme sees the actuator apply forces (calculated by the wind turbine simulation) in response to platform motions. A two-part controller deals with compensating for platform motions and ensuring the correct cable tensions.

Single-Axis Prototype

The first prototype of the hybrid coupling system uses two opposing cables to provide actuation along a single axis. It is sized to provide wind turbine thrust forces at hub height for up to 1:50-scale testing.

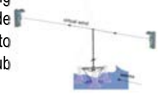

Tension Control Testing

Testing of a single winch unit in isolation allows tuning of the tension controller and quantification of system bandwidth.

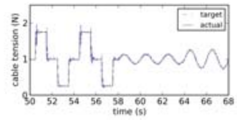

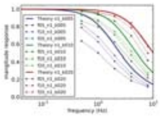

1:100-Scale Pendulum Test Rig

A 14 kg pendulum serves as a proxy floating platform and allows controlled testing of the coupling system. The pendulum approximates the DeepCwind Semisubmersible pitch response at 1:100 scale.

Free-decay tests with no numerical model (zero desired actuation force) show the actuator has a moderate effect on the pendulum, adding damping.

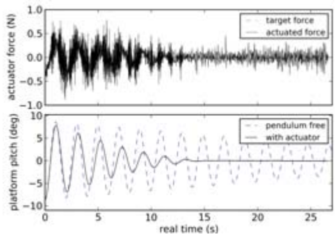

Coupled Results at 1:100 Scale

To measure and refine the coupling system's all-around performance before going to the basin, coupled tests are run in which the pendulum provides the platform dynamics and a FAST simulation provides the wind turbine dynamics. Free decay tests in steady wind give an idea of the system's performance under large platform motions and show the sensitivity of the motion to the details of the wind turbine controller. Tests in turbulent wind show the system's performance under more mild platform motion. The simulations use the NREL 5 MW reference turbine.

Numerical Results / Physical Results

Pitch free decay tests in steady 14 m/s wind

fixed pitch, fixed speed — torque and blade-pitch controllers active

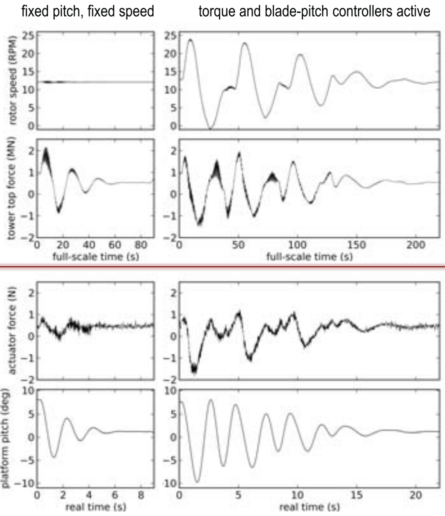

data recorded from full-scale FAST simulations running at 10X real time

data measured from 1:100-scale pendulum test apparatus

Test in 14 m/s class-A turbulent wind

torque and blade-pitch controllers active

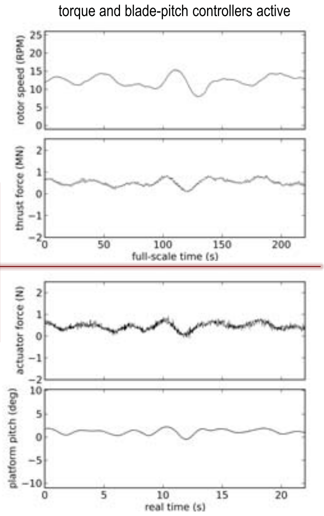

The current system has difficulty applying the dynamic wind turbine forces from high-amplitude pitch free decay tests. Nevertheless, comparing the results with and without blade pitch control active in the simulation shows a clear impact on the behavior of the physical motion, consistent with the damping issues expected from a generic blade pitch controller operating in region III.

When turbulent wind is the only excitation on the hybrid system, platform pitching is moderate and the actuator is able to match the calculated forces closely.

Conclusions

The single-axis hybrid coupling system is approaching readiness for use in basin testing of a floating wind turbine platform. Results with a proxy platform show functional coupling and noticeable effects of the turbine behavior on the platform dynamics. The force control is very effective in low-motion conditions but deteriorates during large pitch motions. More control tuning is therefore still needed. Experience has shown coupling performance increases with the cube of scale, which is promising for testing at 1:50 scale.

Future Work

Future work will include improving performance with the test rig, wave-basin testing with a floating platform, and increasing the scale. If time allows the addition of more actuation axes, tests will be done using the mooring line model MoorDyn[9] to explore the potential of avoiding physical truncated moorings.

References

1. J. M. Jonkman, "Dynamics Modeling and Loads Analysis of an Offshore Floating Wind Turbine," PhD Thesis, University of Colorado at Boulder, 2007.
2. A. Robertson, J. Jonkman, W. Musial, F. Vorpahl, and W. Popko, "Offshore Code Comparison Collaboration, Continuation: Phase II Results of a Floating Semisubmersible Wind System," in *Proceedings of EWEA Offshore 2013*, Frankfurt, Germany, 2013.
3. R. W. Kimball, A. J. Goupee, M. Fowler, E.-J. de Ridder, and J. Helder, "Wind/Wave Basin Verification of a Performance-Matched Scale-Model Wind Turbine on a Floating Offshore Wind Turbine Platform," in *Proceedings of OMAE*, San Francisco, California, 2014.
4. J. Azcona, F. Bouchotrouch, M. González, J. Garciandía, X. Munduate, F. Kelberlau, and T. A. Nygaard, "Aerodynamic Thrust Modelling in Wave Tank Tests of Offshore Floating Wind Turbines Using a Ducted Fan," *J. Phys.: Conf. Ser.*, vol. 524, no. 1, 2014.
5. V. Chabaud, S. Steen, and R. Skjetne, "Real Time Hybrid Testing of Marine Structures: Challenges and Strategies," in *Proceedings of OMAE*, Nantes, France, 2013.
6. S. J. Beatty, M. Hall, B. J. Buckham, P. Wild, and B. Bocking, "Experimental and numerical comparisons of self-reacting point absorber wave energy converters in regular waves," *Ocean Engineering*, vol. 104, Aug. 2015.
7. G. Bracco, E. Giorcelli, G. Mattiazzo, V. Orlando, and M. Raffero, "Hardware-In-the-Loop test rig for the ISWEC wave energy system," *Mechatronics*, vol. 25, pp. 11–17, Feb. 2015.
8. M. Hall, J. Moreno, and K. Thiagarajan, "Performance specifications for real-time hybrid testing of 1:50 scale floating wind turbine models," in *Proceedings of OMAE*, San Fransisco, California, 2014.
9. M. Hall. MoorDyn. Available at www.matt-hall.ca/MoorDyn.

Acknowledgements

I'm grateful to many people for their support and advice with this research, especially my advisor Andrew Goupee, and Giacomo Vissio and colleagues. Collaborations with Vissio et al. were assisted by an INORE International Collaboration Incentive Scholarship and my PhD studies are supported by the Natural Sciences and Engineering Research Council of Canada.

A design support multibody tool for assessing the dynamic capabilities of a wind tunnel 6DoF/HIL setup

Marco Belloli*, **Hermes Giberti, Enrico Fiore**

Dipartimento di Meccanica, Politecnico di Milano

Via La Masa 1, 20156, Milano, Italy. Ph:+39 0223998486, Mob:+39 3772855518

marco.belloli@polimi.it

Abstract

Within the H2020 funded project LIFES50+, the Department of Mechanical Engineering of Politecnico di Milano, is finalizing the design and building the 6-Degree-Of-Freedom (6-DoF)/ Hardware-In-The-Loop robotic setup (HIL) [1] to perform wind tunnel tests on floating offshore wind turbines (FOWT) [2], at Politecnico di Milano Wind Tunnel [3]. Due to geometric and dynamic constraints, the best suited machine for this peculiar application is represented by a parallel kinematic manipulator "Hexaslide". This work presents an integrated FEM/multibody tool for assisting the correct design of the robot. This is carried out with the multibody software ADAMS coupled with AdWiMo (which implements FAST/Aerodyn [4]) for assessing the effect of the robot's flexibility on the imposed motion of the wind turbine at the base of the tower, due to wind and wave loads. Simulations of the OC4 floating system [5] were run in ADAMS/ADWIMO (Aerodyn) and then compared to FAST output. The methodology is herein presented, along with some results about the wind rated condition.

Figure 1: Coupled flexible multibody model the robot and the FOWT.

1 The Robot

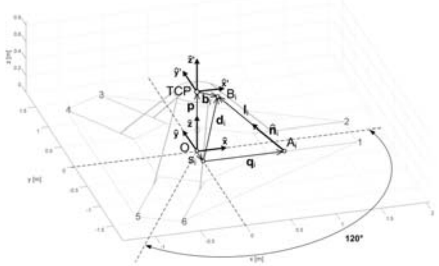

Figure 2: Hexaslide kinematics.

Hexapod, the PoliMi Hexaslide robot, is composed of a mobile platform connected to six linear guides by means of six links of fixed length, so that six independent kinematic chains belonging to the PUS family can be identified. With reference to Fig.2, the six linear guides are organized into three couples of parallel transmission units, each one out of phase by 120° with respect to the z axis. Given the TCP position $\mathbf{p}$ and the mobile platform orientation, $\Theta = \{\alpha, \beta, \gamma\}$, it is possible to find each slider position q_i by performing the inverse kinematics analysis. For the i-th kinematic chain it is possible to write:

$$\mathbf{l}_i = \mathbf{d}_i + q_i\hat{\mathbf{u}}_i \qquad \text{with} \qquad \mathbf{d}_i = \mathbf{p} + [R]\mathbf{b}'_i - \mathbf{s}_i \tag{1}$$

The [R] matrix is the rotational matrix used to switch from the mobile frame to the fixed one, and it is function of the platform orientation Θ. After some simple mathematical passages it's easy to recognize that:

$$q_i = \mathbf{d}_i^T\hat{\mathbf{u}}_i \pm \sqrt{\mathbf{d}_i^T(\hat{\mathbf{u}}_i\hat{\mathbf{u}}_i^T - [I])\mathbf{d}_i + l_i^2} \tag{2}$$

2 Multibody model

Due to the flexibility of the robot and of the wind turbine, they can't be regarded as two distinct entities. Thus it is necessary to develop a coupled FEM/flexible multibody model in order to design the system "robot + wind turbine" sufficiently rigid, not to interfere with the dynamic phenomena being investigated in the wind tunnel. Regarding the robot, the only source of flexibility is assumed to be the slender links. The mobile platform can be considered reasonably rigid.

3 Methodology

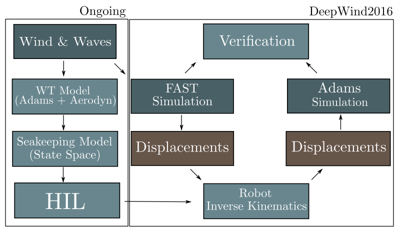

Figure 3: Numerical methodology.

In Fig. 3 the methodological approach is reported. As it can bee seen, the final target is also building a numerical tool that can be used for assessing the wind tunnel HIL implementation, that will rely on state space modelling of the seakeeping equations, due to the real-time characteristics of the application [6] (*"Ongoing"*, Fig.3) . In this work, results are reported regarding the *DeepWind 2016* section of the methodological scheme of Fig.3.

4 Numerical results and conclusion

In Fig. 4 a comparison between the ADMAS/ADWIMO output and FAST is reported, with regard to surge displacements at rated condition, where good agreement can be seen. Furthermore, Fig. 5 shows how the the natural frequencies of the system "robot+wind turbine" are well above the frequency range that will be investigated in the wind tunnel. This numerical tool is useful for a correct design of the robot, whose dynamic response is required to be at higher frequency then the range in which physical phenomena are expected to occur (e.g higher than sum-frequency second order hydrodynamics, [7], [8]).

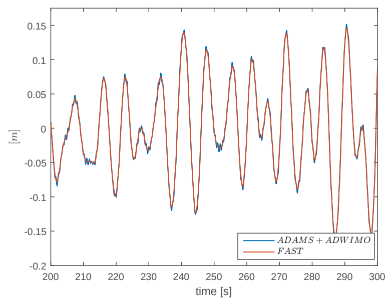

Figure 4: Comparison of the Surge response time histories (up-scaled).

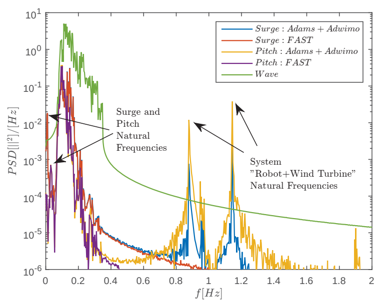

Figure 5: PSDs comparison: ADAMS+ADWIMO(Aerodyn) Vs FAST.

References

[1] Bayati I., Belloli M., Ferrari D., Fossati F., Giberti H., *"Design of a 6-DoF Robotic Platform for Wind Tunnel Tests of Floating Wind Turbines"*, Energy Procedia, pp. 313-323, 2014.

[2] Bayati I., Belloli M., Facchinetti A., Giappino S.,*"Wind Tunnel Tests on Floating Offshore Wind Turbines: A Proposal For Hardware-In-The-Loop Approach To Validate Numerical Codes"*.Wind Engineering, vol.37, N.6, 2013.

[3] Diana G., De Ponte S., Falco M., Zasso A., *"A new Large Wind Tunnel For Civil Environmental And Aeronauitcal Application"*, Journal of Wind Enegineering and Industrial Aerodynamics, 74-76, 553-565, 1998.

[4] Jonkman J.,*"Dynamics Modeling and Loads Analysis of an Offshore Floating Wind Turbine"*, PhD Thesis, 2007.

[5] Jonkman J., *"Definition of the Semisubmersible Floating System for Phase II of OC4"*, NREL/TP-5000-60601, 2014.

[6] Perez T., Fossen T., *"Practical aspects of frequency-domain identification of dynamic models of marine structures from hydrodynamic data"*. Ocean Engineering, Vol 38, pp. 426435, 2011.

[7] I.Bayati, S.Gueydon, M.Belloli, *Study of the effect of water depth on potential flow solution of the OC4 Semisubmersible Floating Offshore Wind Turbine, Energy Procedia 80 (2015) 168 176.*

[8] Bayati I., Jonkman J., Robertson A., Platt A., *"The effects of second-order hydrodynamics on a semisubmersible floating offshore wind, turbine"*, J. Phys.: Conf. Ser. 524, 2014.

Assessment of wind turbine condition using a time frequency signal processing method

Othmane El Mountassir[1], Paul McKeever*[1], Chong Ng[1], Hytham Emam[1], Wenxian Yang[2]
Offshore Renewable Energy Catapult, United Kingdom[1]
Newcastle University, School of Marine Science & Technology[2]
othmane.el.mountassir@ore.catapult.org.uk; paul.mckeever@ore.catapult.org.uk

Background

OPTIMUS is a 36-month EU funded FP7 project with 12 partners participating from six countries across Europe. The project follows on from the recently completed NIMO FP7 project. The project objectives include:

1. To improve reliability within the wind power generation industry by delivering prognostic technology.
2. Improvement in the efficiency of maintenance procedures and operational reliability of wind turbines.
3. To support implementation of the European Wind Initiative of the SET-Plan.

To efficiently capture wind energy, most large modern wind turbines operate at variable speed due to the intermittent nature of wind. As a result, the signals collected from the wind turbine condition monitoring systems are characterised by their non-linear and non-stationary features. It is believed that in order to achieve a reliable condition monitoring and diagnostic based on these signals, advanced signal processing techniques should be implemented to interpret more efficiently the condition monitoring signals collected from the turbines. This poster addresses the capability of a signal processing method, namely the spline kernelled chirplet transform (SCT), in analysing wind turbine condition monitoring data and providing a reliable diagnostic of potential anomalies.

Introduction

To investigate how the improvement of condition monitoring systems can be carried out using advanced signals processing techniques, the effectiveness of the SCT method is demonstrated. This follows up a previous work investigating the use of signal processing methods to enhance the diagnostic of wind turbines' condition monitoring systems[1]. The SCT transform is based on time frequency analyses rather than the conventional spectral analyses. It has been used and proved to be efficient in the field of machine fault detection and also in telecommunications where it is considered to be very effective for non-stationary signals [2, 3, 4]. The work proposed in this poster summarises the capability of an improved SCT to detect both the instantaneous amplitude and frequency of lengthy non-linear and non-stationary (NNS) signals.

Methodology

The SCT method is widely used and documented and its mathematical formulation can be found in [1, 2].

The proposed use of algorithm processed data collected from a WT power train test rig (Figure 1) illustrates one future wind turbine application for the SCT method. In experiments to date, various simulated wind speed inputs have been applied to a smaller test rig via its DC motor. During the study, the generator electrical imbalance was emulated on the test rig. The relevant CM signals were collected from the generator terminals and its input-side shaft.

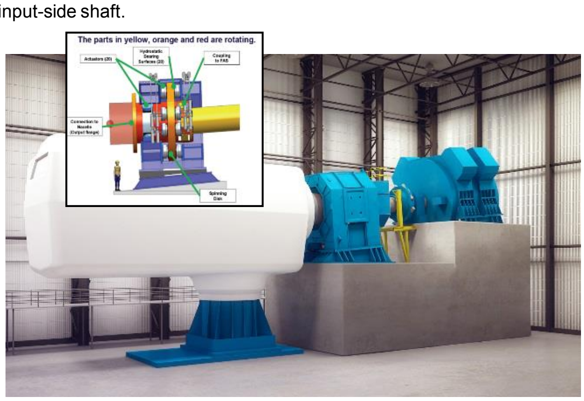

Figure 1: ORE Catapult's 15MW wind turbine drive train

Results

To extract the characteristic of the induced faults, the improved SCT was applied to the power signal. The results found are presented in Figure 2.

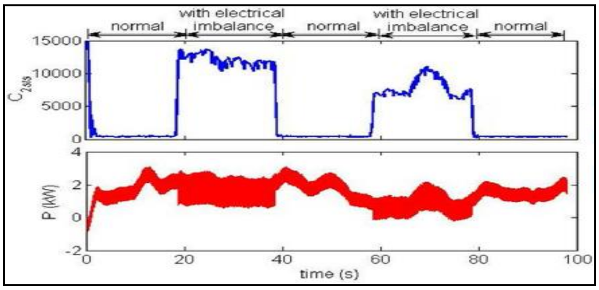

Figure 2: Diagnostic of electrical imbalance using the SCT[1]

Based on the results of Figure 2, it can be seen that the improved SCT have successfully predicted the presence of the fault.

To further verify the effectiveness of the proposed algorithm in detecting incipient fault, two different levels of rotor asymmetries were induced as faults. Figure 3 presents the results obtained by the SCT. The results also show that that both the incipient and the early developed electrical imbalance faults have been detected successfully by the improved SCT

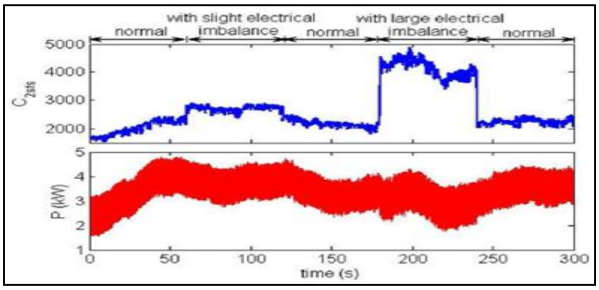

Figure 3: Diagnostic of electrical imbalance using the SCT for different severity levels of rotor imbalance [1]

Conclusion

To improve the ability of WT condition monitoring systems to analyse lengthy non-linear & non-stationary signals, an improved SCT algorithm was proposed. The improved SCT algorithm was successful in extracting potential electrical faults of non-linear and non-stationary multi-component signals at the fault frequencies of interest on a test rig.

References

[1] W. Yang, P. Tavner, W. Tian, "Wind Turbine Condition Monitoring Based on an Improved Spline-Kernelled Chirplet Transform," IEEE Transactions on Industrial Electronics, vol. 62, no. 10, pp. 6565-6574, 2015.

[2] Y. Yang, Z. Peng, G. Meng and W. Zhang, "Spline-Kernelled Chirplet Transform for the Analysis of Signals With Time-Varying Frequency and Its Application," IEEE Transactions on Industrial Electronics, vol. 59, no. 3, pp. 1612-1621, 2012.

[3] J. Zhang, A. Papandreou-Suppappola, B. Gottin and C. Ioana, "Time-Frequency Characterization and Receiver Waveform Design for Shallow Water Environments," *IEEE Transactions on Signal Processing,* vol. 57, no. 8, pp. 2973-2985, 2009.

[4] D. Marelli, M. Aramaki, R. Kronland-Martinet and C. Verron, "An Efficient Time-Frequency Method for Synthesizing Noisy Sounds With Short Transients and Narrow Spectral Components," IEEE Transactions on Audio, Speech, and Language Processing, vol. 20, no. 4, pp. 1400-1408, 2012

This project has received funding from the European Union's Seventh Framework Programme for research, technological development and demonstration under grant agreement no 322430.

http://optimusfp7.eu http://ore.catapult.org.uk

Development, Verification and Validation of 3DFloat; Aero-Servo-Hydro-Elastic Computations of Offshore Structures.

Tor Anders Nygaard, Jacobus De Vaal, Fabio Pierella, Luca Oggiano and Roy Stenbro
Institute for Energy Technology (IFE), Norway

Abstract

The aero-servo-hydro-elastic Finite-Element-Method (FEM) code 3DFloat is tailored for nonlinear, full coupling time-domain simulations of offshore structures in general, and offshore wind turbines in particular. The verification and validation histories for offshore wind turbines include the IEA OC3/OC4/OC5 projects, two wave tank tests and participation in commercial projects. Current development examples include implementation of advanced hydrodynamics in the DIMSELO project, implementation of soil/structure interaction macro-elements in the REDWIN project, and optimization of large rotors with sweep in an industry project.

Advanced hydrodynamics in DIMSELO (www.dimselo.no)

The project partners IFE, DTU, NTNU Statoil and Statkraft, develop and implement advanced hydrodynamic models. Figure 2 compares the inline force for a bottom-fixed cylinder with diameter 6m at a water depth of 35m, subject to regular waves with wave height 16.6m and period 11.4s. The 3DFloat Morison and Rainey computations use stream function of order 12 for the kinematics. The Rainey and IFE in-house CFD results agree very well. The standard Morison model underpredicts the peak force by 15% compared to the Rainey and CFD results.

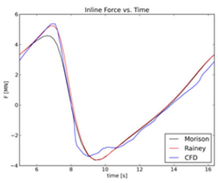

Figure 1. : Comparison of inline force for a bottom-fixed cylinder

Figure 2 shows surge and heave motions for a 80 x 30 x 8m pontoon supported by springs, used in a conceptual design study of a Submerged Floating Tunnel. The sea state corresponds to an effective wave height of 0.5m, and a peak period of 14s in the JONSWAP spectrum. As a first check of the Linear Potential Theory implementation in 3DFloat, corresponding results from SIMO are shown in the same figure.

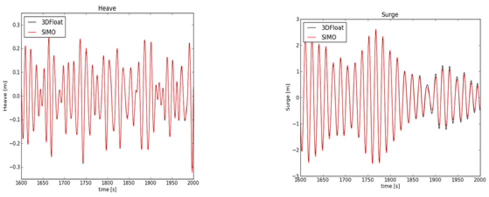

Figure 2. Pontoon heave and surge motions. Comparison between SIMO and 3DFloat results

Conclusions and further work

- 3DFloat is a platform for:
  - Innovation and technical development
  - Research on computational methods
- IFE has allocated resources for helping industrial partners getting started with computations of their in-house designs.
- The next steps for upgrades include:
  - Linear Potential Theory distributed on elements
  - Bluff body aerodynamics

Soil/structure interaction REDWIN (www.redwin.no)

REDucing cost in offshore WINd by integrated structural and geotechnical design is a R&D project supported by The Norwegian Research Council ENERGIX program. The project partners are NGI, IFE, NTNU, Dr.techn. Olav Olsen AS, Statoil and Statkraft. The primary objective of REDWIN is to contribute to reduction of costs in design of offshore wind turbines by developing and implementing soil-foundation models. As a first step, a simplified 1D-macro-element or a force resultant model has been implemented in 3DFloat. The IWAN-type model [1] consist of parallel coupled linear elastic-perfectly plastic springs, each with different stiffness and yield limits. The total load-deformation response is then represented by a nonlinear backbone curve which produce damping from its hysteresis behavior. Figure 3 shows the mudline overturning moment during an extreme operating gust starting at time 150s, combined with regular waves with wave height 3m and period 10s, for the 5MW OC3 Monopile wind Turbine. The time evolution corresponds to moving clockwise around in the hysteresis curve.

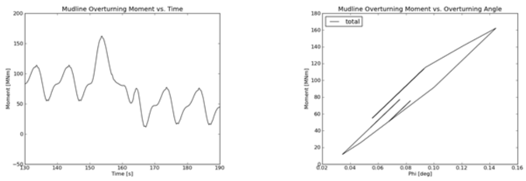

Figure 3. : Mudline overturning moment during wind gust

High-fidelity rotor aeroelastics, Statoil industry project

For long, slender and flexible rotor blades, taking into account offsets between the elastic axis and the shear- , aerodynamic- and mass centres is important. IFE is evaluating and optimizing rotors with sweep in a current industry project funded by Statoil. Figure 4 compares the aerodynamic rotor thrust during a gust for rotors with different versions of sweep. On a rotor with the blades swept backwards on the outer part of the blades, an increase in thrust on the blades produces a torsional moment, corresponding elastic twist, and thereby reduction of angle-of-attack. This reduces the peak load during the gust compared to the baseline blade. To counter the steady-state elastic twist resulting from backward sweep, a version with forward sweep on the inner part of the blade has also been designed. This reduces the peak loads further.

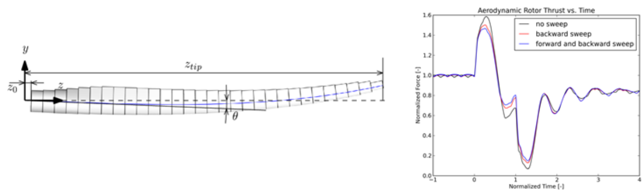

Figure 4. Load reduction during gust by rotor sweep.

Acknowledgements

We would like to acknowledge master student Steffen Aasen at NMBU and Kristoffer Skjolden Skau at NGI for the soil/structure interaction computations on the OC3 Monopile. The WADAM and SIMO computations for the pontoon of the Submerged Floating Tunnel were performed by Vegard Berge Kristensen, Dr.techn. Olav Olsen AS. Andreas Knauer at Statoil generously opened project information on advanced rotor aeroelastics for this poster. This work was in part funded by the Research Council of Norway, Statoil, Statkraft, Dr.techn. Olav Olsen AS and the Norwegian Public Roads Administration.

References

[1] Iwan, W.D. (1967). On a Class of Models for the Yielding Behavior of Continuous and Composite Systems. Journal of Applied Mechanics. [Online] 34 (3), 612–617. Available from: doi:10.1115/1.3607751.

Upstream turbine effect on the downstream turbine performance: a wind farm case optimization

Clio Ceccotti#, Andrea Spiga#, Jan Bartl#1, Lars Roar Sætran#
Department of Energy and Process Engineering, NTNU
[1]jan.bartl@ntnu.no

SINTEF

NTNU Det skapende universitet

INTRODUCTION

In a wind farm, wakes interact with each other and directly affect the downstream turbine performances. In this context, a wind tunnel turbine wake study and an analysis of the combined power output of a 2-turbine array are studied. The wake analysis is focused on the description of the wake development at different downstream stations for different turbine operating conditions and flow regimes. The performances of a turbine operating in the wake are analysed for different configurations focusing on the 2-turbine array power output; moreover a wake-rotor interaction is attempted. The array overall efficiency is found to increase by moving the second turbine further downstream, with an increased background turbulence level and by choosing a suitable operating point for each turbine.

METHODS

The experimental analysis is carried out at NTNU aerodynamic labs and the measurement set up is shown in Fig. 1. The reference wind speed is U_{ref} = 11.5 [m/s] (Eq. 1) and 2 model wind turbines of D ≈ 0.9 [m] [1] are used for the investigations. The turbines operating points are set by handling the rotor speed via a frequency converter. No variations in blade pitch angle are contemplate.

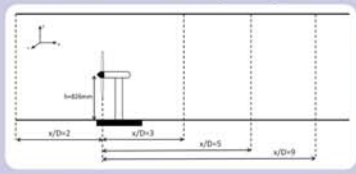

Figure 1: First turbine setup: wake measurements.

The torque (T) and the rotational speed (ω) are directly measured on the turbines shaft and the power coefficient C_P is evaluated (Eq. 2). The model turbines maximum C_P is achieved at TSR = 6 (Eq. 3). Two different turbulent flow conditions have been arranged in the tunnel:

- Wind tunnel (Low) turbulence level (TI = 0.23%).
- Similar-atmospheric (High) turbulence level (TI = 10%)

In both conditions turbine horizontal wakes behind a single turbine are measured using a hot wire anemometer. Relative velocity (U_{rel}, Eq. 1) and turbulence intensity (TI [%], Eq. 4) are analysed at 3D, 5D and 9D behind the turbine. The second turbine is located in the tunnel (Fig. 2) and for each tip speed ratio configuration (λ_1, λ_2) the array efficiency E [%] (Eq. 5) is obtained.

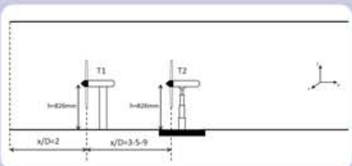

Figure 2: Two turbines setup: array efficiency optimization.

$$U_{rel}[-] = \frac{\bar{U}}{U_{ref}} \quad (1)$$

$$C_P = \frac{T\omega}{\frac{1}{2}\rho U_\infty^2} \quad (2)$$

$$TSR = \frac{\omega * R}{U_{ref}} \quad (3)$$

$$TI[\%] = \frac{u'}{\bar{U}} * 100 \quad (4)$$

$$E = \frac{C_{P,T1} + C_{P,T2}}{C_{P,T1max} + C_{P,T2max}} \quad (5)$$

RESULTS

Single turbine wake development

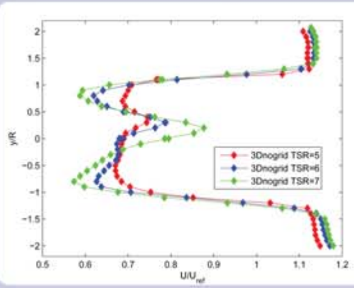

Figure 3: Relative flow velocity, 3D distance behind the turbine working at λ_1= 5,6,7.

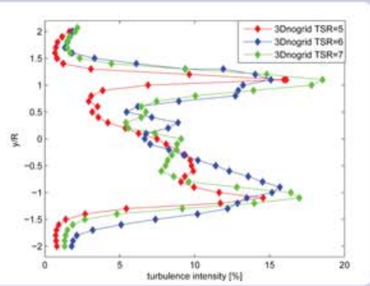

Figure 4: TI, 3D distance behind the turbine working at λ_1= 5,6,7.

- No λ dependency on radial expansion is noticed neither at 3D nor at 9D.
- At 3D (Near wake), by varying λ, the rotor inner sections feed momentum into the wake (Fig. 3) and produce big variations in TI (Fig. 4).
- At 9D (Far wake) behind the rotor, almost no difference is visible with λ variations (Fig. 5, 6).
- Generally, by increasing λ, wakes TI increases, since higher thrusts on the turbine induces strongest mean velocity gradients. Tip peaks and turbulence overall level monotonically increase.

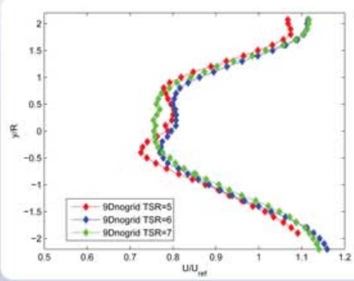

Figure 5: Relative flow velocity, 9D distance behind the turbine working at λ_1= 5,6,7.

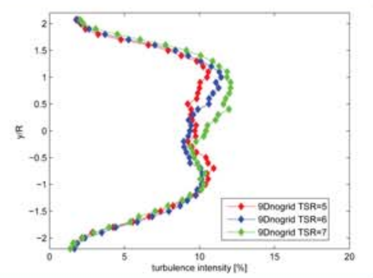

Figure 6: TI, 9D distance behind the turbine working at λ_1= 5,6,7.

Correlation between wake behind the first turbine and the power output of the second turbine

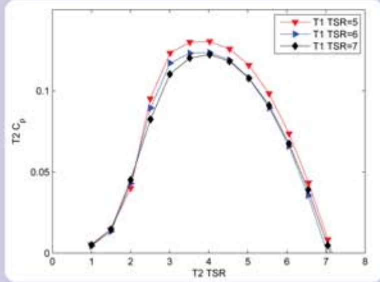

Figure 7: T2 C_P with λ_1= 5,6,7.

At 3D separations even small variations in turbine λ, strongly affect the velocity deficit in the wake (Fig. 3) resulting in a detectable C_P variation for T2 (Fig. 7). Velocity deficit peaks become deeper in the outermost region (0.5<y/R<1) leading to less T2 energy extraction.

Two turbine array case study

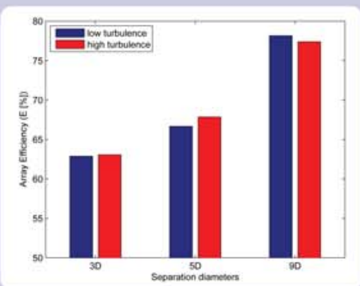

Figure 8: Max array efficiency achievable in each configuration.

Configuration	Max array efficiency [%]	Operating cond. λ_1	λ_2
0.23%, 3D	62.8	5	4
0.23%, 5D	66.5	5.5	4
0.23%, 9D	78	5	5
10%, 3D	63	5.5	4
10%, 5D	67.5	6	4.5
10%, 9D	77	6	5

Table 1: Max array efficiency for λ_1,λ_2 operating condition, each TI and separation configuration.

- Higher turbulence induced by the grid accelerates the velocity deficit recovery until the grid effect is distinct (5D); at 9D the turbulence induced is neglegible.
- A slight λ dependency on E is found. A bigger amount of energy is available for T2 if λ_1 is slightly decreased from optimum, resulting in a higher E (Tab. 1).
- A constant impact of approximately 2.5% wind farm overall efficiency recovery is found for every additional diameter separation distance between the turbines.

CONCLUSIONS

The parametric study points out a strong array efficiency dependency on:

- INFLOW TURBULENCE LEVEL: the higher the turbulence, the faster the velocity recovery, the bigger the array efficiency. High turbulence wind tunnel results are better matching the full scale reality (atmospheric inflow) [2].
- Turbines TSRs: best results of array efficiency are found with the 1st turbine running at λ slightly lower than the optimum operating point, especially for small separation distances.
- Turbines SEPARATION DISTANCE: +2.5% of array efficiency for every additional separation diameter.

Accurate management of all the parameters is advised.

References

[1] Per-Åge Krogstad and Pål Egil Eriksen. "blind test" calculations of the performance and wake development for a model wind turbine. *Renewable Energy*, 50(0):325–333, February 2013.
[2] Jan-Ake Dahlberg. Assessment of the lillgrund wind farm: power performance wake effects. *Vattenfall Vindkraft AB, 6 1 LG Pilot Report*, 2009.

SINTEF

Droplet Erosion Protection Coatings for Offshore Wind Turbine Blades

Emil André Valaker**, Astrid Bjørgum*, Shawn Wilson*, Sergio Armada*, Angelika Brink
**SINTEF Materials and Chemistry and **NTNU Department of Engineering Design and Materials

KEYWORDS: Offshore wind, Erosion, Protective coatings, Coating modification

Introduction

The work on protective coatings has been performed within the Norwegian Research Centre for Offshore Wind – NOWITECH. The objectives have been increased lifetime and reduced O & M costs for offshore wind turbines.

Water droplets impacting on high speed rotating blades are causing erosion of the leading edge. The deteriorated surface of the leading edge has a great impact on the aerodynamic efficiency of a wind turbine and therefore also on the economic efficiency.

Test-rig

In the present work, the droplet erosion as one type of leading edge erosion mechanism on wind turbine blades has been studied with polyurethane coatings, modified with nanoparticles (NP1 and NP2). As comparison a commercial tape and coating was used.

The test-rig allows speeds up to 180 m/s and different nozzle-shapes allow the control of drop-size. The droplet-size is characterised by a Phantom Multi Camera (160 000 Hz).

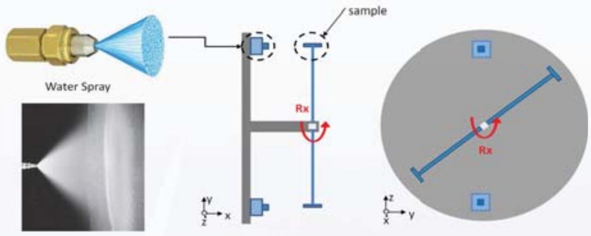

Test-rig used at SINTEF

Coatings

Dummy samples for erosion test facility

- HDPE
- PVC

Protective surface coatings

- Industrial Wind Protection Tape
- Industrial Wind Protection Coating
- Polyurethane composite coatings
  - 100% PUR
  - Modified PUR with type N1 particles (1/ 2,5 and 5 wt%)
  - Modified PUR with type N2 particles (1/ 2,5 and 5 wt%)

Results

After the test, the weigh loss of the samples were measured and the surface was investigated with a Confocal Infinite Focus Microscope (IFM), to study further the surface response of the coating to the droplets impact.

Illustration shows one of the modified coating proposed by SINTEF after a hazard test at 140 m/s for 60 min test duration.

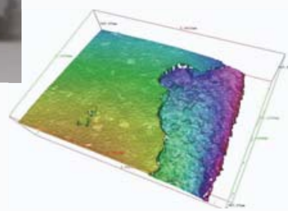

Erosion pattern observed on a PU-coating doted with 5 wt% N2 at 140 m/s for 60 min.

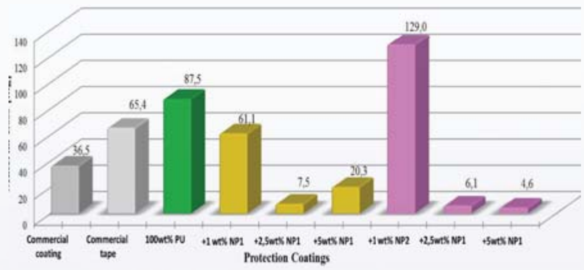

Observed material loss on the different erosion protection coatings in mg. after test program.

Summary and conclusion

Modified polyurethane composite coatings show promising mechanical and erosion resistance properties as potential protective coatings.

Commercial coatings failed at 100 m/s impact speed, while doped PU-coatings could withstand up to 140 m/s.

All coatings started to fail at the sample edge. A new sample geometry should be considered and the environmental conditions taken into account.

Further investigations should be done into the mechanisms to understand the influence of nanoparticles on the performance of the coatings.

http://www.sintef.no/Nowitech/

Design of an airfoil insensitive to leading edge roughness

Tania Bracchi, Department of Electrical Engineering and Renewable Energy NTNU

1.Introduction

During wind turbine operation dirt, salt, erosion or damage can modify the surface of the wind turbine blades, especially at the leading edge. Contamination causes earlier separation, with the consequence of reduction in wind turbine performances. The drop of lift-to-drag ratio due to contamination is inevitable, nevertheless, it can be reduced.

2.Objectives

The drop in lift-to-drag can be reduced minimizing the reduction of the maximum lift coefficient ($C_{l,max}$). The main concept behind designing an airfoil with maximum lift coefficient insensitive to leading edge roughness is to shape it such that the transition point at the suction side moves towards the leading edge just before $C_{l,max}$, hence ensuring always a turbulent boundary layer near the leading edge before stall. This should reduce the drop of Cl,max in case of leading edge roughness.

4.Assumptions

- The method of obtaining the lift coefficient from the pressure distribution results the most reliable
- The methods of obtaining the drag coefficient from the wake survey and from the pressure distribution result the most reliable respectively for low and high angles of attack.
- The results of lift and drag coefficients obtained with the balance are used to compare the different experimental set-up. That is the method which is the least time consuming, but least reliable.

3.Methodology

The airfoil was designed and its performances simulated using the program Xfoil. The airfoil was built as a two-dimensional model, with constant chord spanning the whole wind tunnel width.

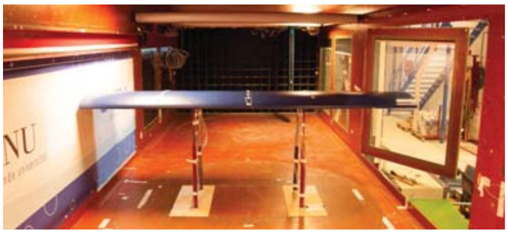

The lift and drag of the wing was measured for different angle of attack, for both clean condition (at turbulence intensities) and with applied roughness of different size and at different position at the leading edge.

- The lift was measure with both the balance on which the wing was mounted and calculated from the pressure distribution.
- The drag was measured both with the balance, by wake survey and calculated from the pressure distribution.

5.Results

Effect of turbulence. Lift and drag coefficients in function of angle of attack for turbulence intensity T.I.=0.3% (Re=$8.6\cdot10^5$) and T.I.=5% (Re=$7.4\cdot10^5$). Numerical results from Xfoil and experimental results from balance (Bal.), pressure distribution (Cp) and wake survey (Wake)

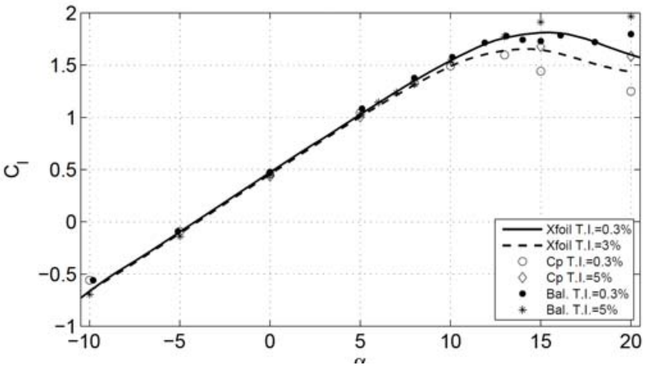

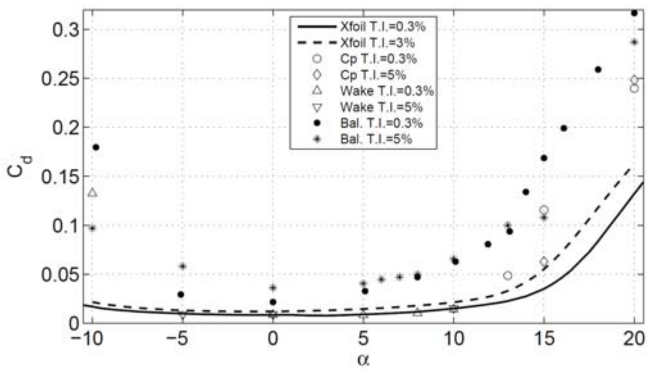

Effect of roughness. Lift and drag coefficients in function of angle of attack for Re=$8.7\cdot10^5$ obtained with the balance. Grains (size ≈0.5mm) applied on the suction side between 4% and 7% of the chord (x/c 4-7%). Tape applied around the leading edge between 0.9% on the suction side and 3.8% on the pressure side (LEtape x/c 0.9%t-3.8%b). Grains applied around the leading edge between 7.4% on the suction side and 7.9% on the pressure side (x/c 7.4%t-7.9%b).

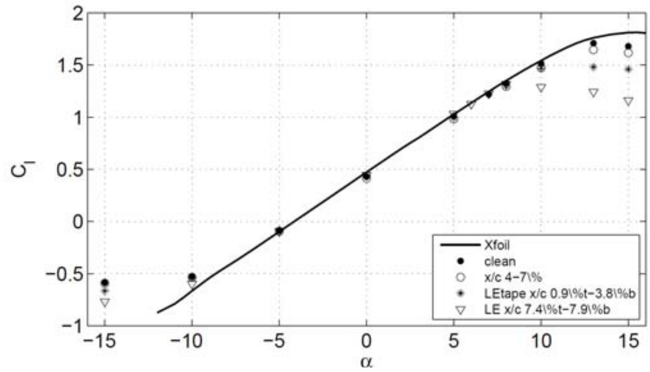

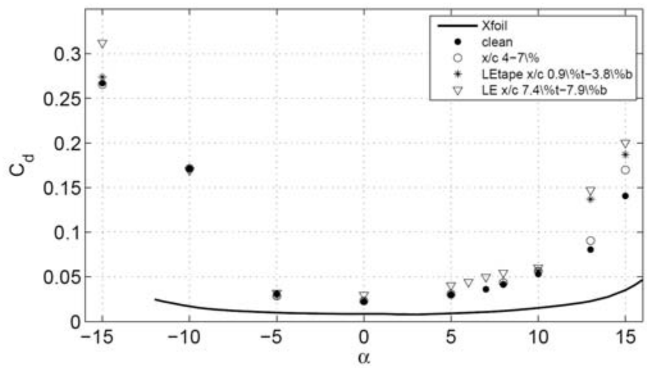

6.1. Discussion on effect of turbulence

The free stream turbulence has the positive effect of delaying stall. The drag does not increase considerably for low angle of attacks and decreases for high angles, due to the stall delay.

6.2. Discussion on effect of roughness

The aerodynamic characteristics are not affected considerably by distributed roughness of small grain size, if this is applied on the suction side downstream of 4% of the chord. In fact in this case $C_{l,max}$ drops by 4%. This means that the transition occurs naturally very close to the leading edge.

6.References

Bracchi, Tania. "Downwind Rotor: Studies on yaw Stability and Design of a Suitable Thin Airfoil." PhD thesis, 2014. .

Innovative Floating offshore wind energy

WP2: Socio-economic evaluation of floating substructures

Benveniste, G; Lerch, M; De Prada, M; Catalonia Institute for Energy Research (IREC)

WP2 Introduction

LIFES 50+ project focuses on offshore wind energy and in particular on innovative **floating substructure concepts for offshore wind turbines in water depths greater than 50 meters**. The concepts will be designed to support wind turbines in the scale of 10 MW. In order to evaluate the four designed concepts integrated in wind farm scheme from a holistic perspective, a specific work package (WP2) for **technical, economic, environmental and risk assessment has been dedicated,** led by IREC. The objective of this abstract is to present briefly the procedures and standardized tools that will be developed for the concepts evaluation and identify challenges for the project targets achievement.

Objectives

- The aim of WP2 is the **technical** and **economic evaluation** of the floating subtructure designs developed during the project.
- The **quantification** of **risk** and **uncertainties** will also be considered.

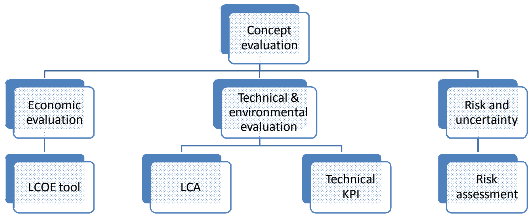

Methodology

Economic evaluation

LCOE calculation:

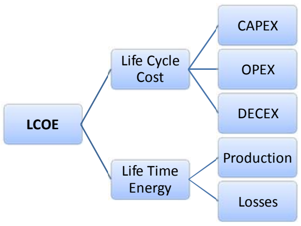

$$\text{LCOE} = \frac{\text{Sum of costs over lifetime}}{\text{Sum of electrical energy injected}} = \frac{\sum_{t=1}^{n} \frac{I_t + O\&M_t + D_n}{(1+r)^t}}{\sum_{t=1}^{n} \frac{E_t - L_t}{(1+r)^t}}$$

Life cycle cost consideration:

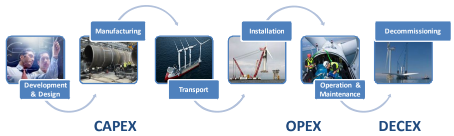

Capital expenses:
- Development and design (phase I)
- Manufacturing (phase II)
- Transportation (phase III)
- Installation (phase IV)

Operating expenses:
- Operation & Maintenance (phase V)

Decommissioning expenses:
- Dismantling of the plant (phase VI)

Cost components of an offshore wind farm

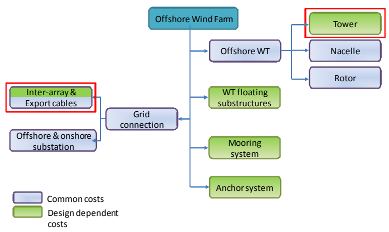

Life Time Energy

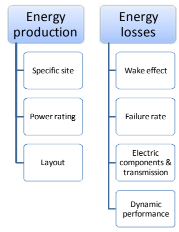

Technical and environmental evaluation

Life Cycle Assessment (LCA)

Methodology used to quantify environmental impacts of electricity generated by the floating substructures in terms of energy balance and CO_2 emissions.

Impact categories and technical KPIs:

Global Warming Potential in CO_2 equivalents
Consumption of non-renewable resources
Energy Payback time
Technical robustness and feasibility

LCA Steps

Manufacturing:
- Raw materials
- Energy consumption
- Waste generated

Installation:
- Energy consumption
- Waste generated

O&M:
- Raw materials
- Energy consumption
- Energy generated

Decommissioning
- Energy consumption
- Waste generated
- Waste Management

Life Cycle Inventory

Data collection by questionnaire

Risk and uncertainty

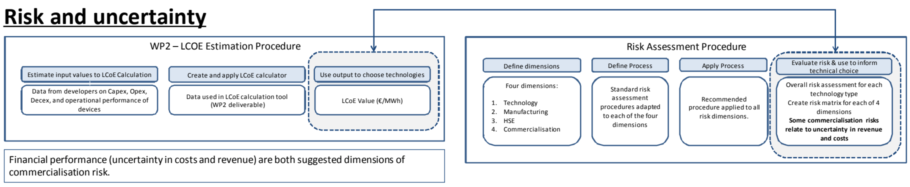

Financial performance (uncertainty in costs and revenue) are both suggested dimensions of commercialisation risk.

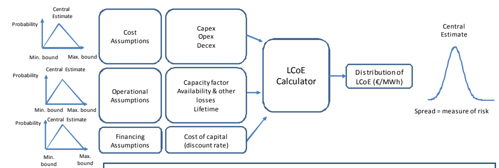

The output LCoE takes a distribution rather than a single value and the shape and spread of the distribution is driven by the input uncertainties.

Expected output

4 catergories: Each category contains parametres or KPI´s

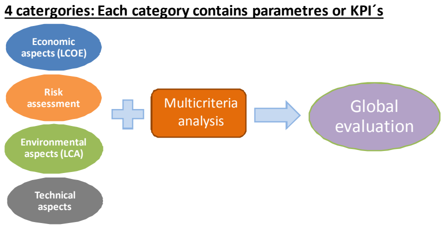

Assessment Tool

- LCOE Calculation
- Technical & Environmental KPIs
- Risk Assessment

- Tool will be developed in MATLAB
- Graphical User Interface
- Data collection in Excel
- Life-Cycle Perspective
- Graphical presentation of results

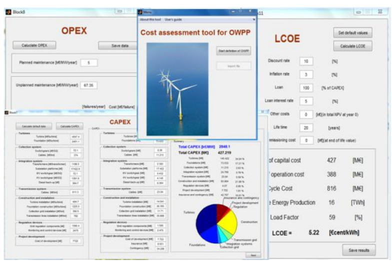

References:

-Scottish Enterprise . A Guide to Offshore Wind and Oil and Gas Capability. Glasgow, 2011.
-Multiconsult. Technological and Cost Development Trends of Renewable Offshore Energy Production. Oslo, 2012.
- C. Bjerkseter, et.al. Levelised Cost of Energy for Offshore Floating Wind Turbines Concepts., Norwegian University of Life Sciences ,2013.
- Howard. Offshore Wind Cost Reduction Pathways project . London, The Crown Estate, 2012.
- Renewables Advisory Board. Value breakdown for the offshore wind sector. London, 2010.
- National Grid. Offshore Development Information Statement. Appendix 1-4. 2011.
- Midtsund & Sixtensson. DNV KEMA, 2013.
- BVG Associates. Offshore wind cost reduction pathways – Technology work stream. 2012.
- The Crown Estate. A Guide to an Offshore Wind Farm. London, 2010.
- Douglas Westwood. Offshore Wind Assessment For Norway. Aberdeen, 2010.
- L. Fingersh, Wind Turbine Design Cost and Scaling Model, NREL 2006.
- A. Myhr, et. al. Levelised cost of energy for offshore floating wind turbines in a life cycle perspective.
- L. Castro-Santos. Methodology related to the development of the economic evaluation of floating wind farms in terms of the analysis of the cost of their life-cycle phases. 2013.
- M. Dicorato, et. al. Guidelines for assessment of investment cost for oshore wind generation.
- C. Knudsen Tveiten. HSE challenges related to offshore renewable energy. Sintef, 2011.

The research leading to these results has received funding from the European Union Horizon2020 programme under the agreement H2020-LCE-2014-1-640741.

For more information:
http://lifes50plus.eu/

Contact: gbenveniste@irec.cat

Coordinated control of DFIG-based offshore wind power plant connected to a single VSC-HVDC operated at variable frequency

Mikel de Prada[1], Jordi Pegueroles-Queralt[1], Fernando Bianchi[1] and Oriol Gomis-Bellmunt[1,2]
[1]IREC - [2]CITCEA-UPC

Objectives

This work proposes an OWPP design based on variable speed wind turbines driven by doubly fed induction generators **(DFIGs) with reduced size power electronic converters connected to a single VSC-HVDC** converter which **operates at variable frequency** within the AC collection grid. OWPP may have several VSC-HVDC converters forming clusters of wind turbines, such that each cluster operates at its own optimal frequency. The aim of this study is to evaluate the **influence of the power converter size and wind speed variability** within the OWPP **on energy yield efficiency**, as well as to **develop a coordinated control** for the **VSC-HVDC converter** and the **individual back-to-back reduced power converters of each DFIG**-based wind turbine in order to **provide control capability** for the OWPP at a **reduced cost**.

Description of the concept

This wind power plant proposal **combines DFIG** wind turbines **with reduced size power converters** (approximately 5-10% instead of 25-35% of the rated power) **and a single VSC-HVDC** converter **which dynamically changes** the collection grid **frequency** (f*) as a function of the wind speeds of each turbine.

- The common **VSC-HVDC provides variable speed control** to the whole wind power plant (or the wind turbine cluster).
- **Reduced size power converters** inside each DFIG wind turbine are in charge of **attenuating** the **mechanical loads** and of partially or totally **compensating** the **wind speed difference among turbines** due to the wake effect.
- **Improved reliability**, increased efficiency due to the **lower losses** and a **cost reduction** are expected to be achieved.
- **Wind energy captured may be reduced** owing to the narrower speed range that can be regulated by a smaller power converter.
- **HVDC transmission** link is **required** to decouple the WPP collection grid from the electrical network.
- **Especially worthwhile for offshore** wind power plants where the wind speed variability among turbines is assumed to be lower than in onshore.

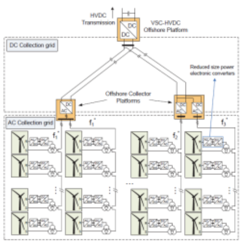

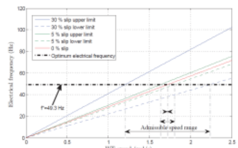

Individual power converters **optimum size** depends on various criteria such as:

- ❑ *Capital costs*
- ❑ *Increased energy capture [1]*
- ❑ *Mechanical load reduction [2-4]*
- ❑ *Fault Ride Through (FRT) capability [5-7]*

Results

Static analysis

Case of study

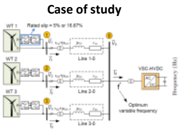

Wind speed input profile

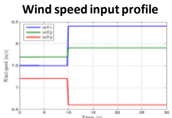

Power converter rated slip = 5% | Power converter rated slip = 16.67%

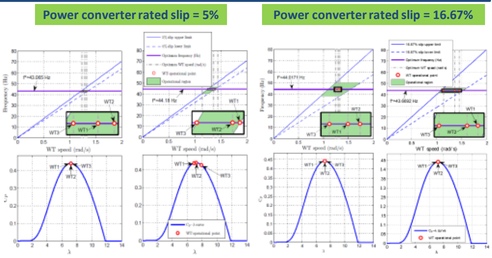

Before 10 seconds | After 10 seconds | Before 10 seconds | After 10 seconds

Dynamic analysis

Measured wind speed data [8] | **Frequency** | **Power generated**

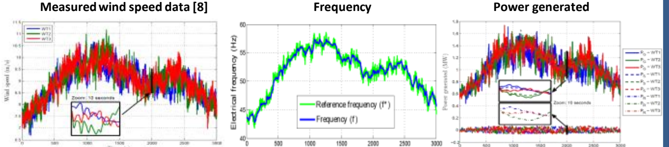

WT speed | **Rotor voltage** | **Power coeficient (Cp)**

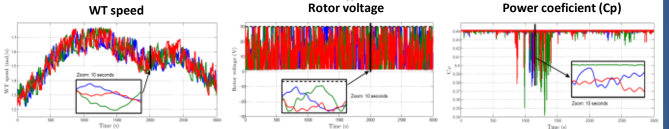

Power generated by WT3 (actual vs available)

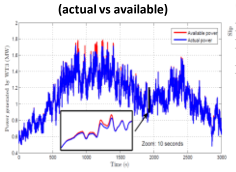

Slip | **Pitch angle**

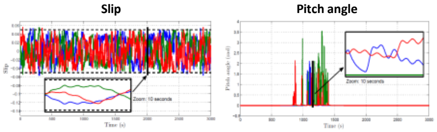

Results

Rated slip (%)	Energy (MWh) WT1	WT2	WT3	Total energy (MWh)	Energy yield efficiency (%)
5.00	0.9776	1.004	1.0172	2.9988	98.40
16.67	0.9922	1.0104	1.0280	3.0306	99.45
100.00	0.9967	1.0193	1.0315	3.0475	100.00

Influence of power converter size and wind speed variability on power generation efficiency

Steps:

1. WPP layout definition.
2. Wind conditions definition.
3. Wind speeds calculation on each WT by considering wake effects.
4. Application of the optimum electrical frequency search algorithm to maximize OWPP power generation.
5. Computation of energy generated by the OWPP during its lifetime.
6. Calculation of energy capture efficiency as a function of different wind speed variability and power converter sizes.

Case of study
- Number of WTs =12 (3 x 4)
- Power rated = 5MW
- Rotor diameter = 126 m
- WT spacing = 7 D (prevailing) x 6 D (perpendicular)
- Wind conditions:
  - ➢ Wind rose with 12 wind directions sectors.
  - ➢ One weibull distribution function (scale and shape) for each wind direction sector.

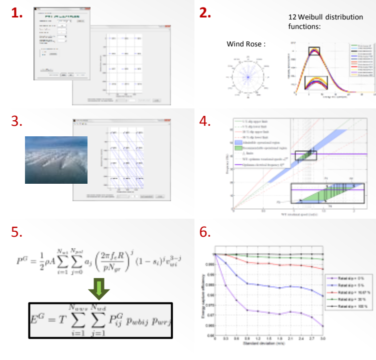

Control design

The power converter is modeled using an **average-value model (AVM)** based on switching functions, which approximates the system dynamics by **neglecting switching details**, i.e. insulated gate bipolar transistors (IGBT) are not explicitly represented. The AVM assumes that all internal variables of the MMC are perfectly controlled, all sub-modules capacitors balanced and harmonic currents circulating in each leg are suppressed.

Overall control system

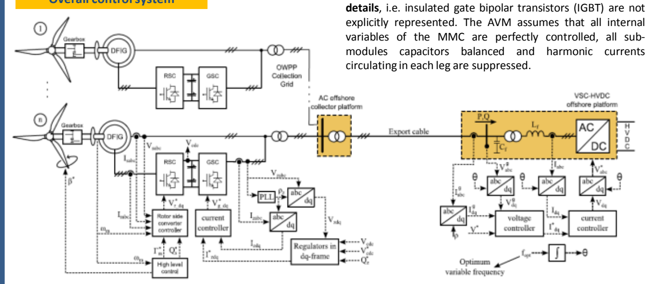

Speed control

$$K_{C_{P\_opt}} = \frac{1}{2}\left(\frac{c_1 c_2}{c_7}\right) e^{-\frac{c_6 c_7}{c_2}-1} \rho A \frac{R^3}{\left(\frac{c_2 c_7}{c_2 c_9 c_7 + c_6 c_7 + c_2}\right)^3}$$

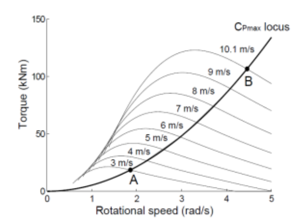

WT model block diagram

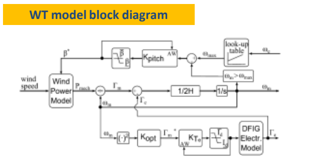

Rotor voltage saturation

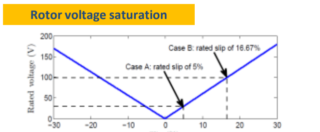

Conclusions

The **performance** of a coordinated control between a DFIG-based OWPP and a single VSC-HVDC converter is **validated** and assessed from both **static** and **dynamic** point of view.
The **results suggest a good performance** of the proposed concept **in terms of energy capture analysis**. Thus, it can be concluded that the size of the power converter installed inside the wind turbine can be potentially reduced. Consequently, **improved reliability**, **increased efficiency** due to the lower losses and a **cost reduction** are expected to be achieved. However, relevant issues such as **fault rid through capability** or **mechanical load reduction** should be also considered to fully assert the minimum admissible power converter size.

References

[1] K. E. Okedu. Impact of Power Converter Size on Variable Speed Wind Turbine. The Pacific Journal of Science and Technology, 13(1):176-181, May 2012.
[2] B. Barahona, N. A. Cutululis, A. D. Hansen, and P. Sørensen. Unbalanced voltage faults: the impact on structural loads of doubly fed asynchronous generator wind turbines. Wind Energy, June 2013.
[3] B. Barahona, R. You, A. D. Hansen, N. A. Cutululis, and P. Sørensen. Assessment of the impact of frequency support on DFIG wind turbine loads . 12th International Workshop on Large-Scale Integration of Wind Power into Power Systems as well as on Transmission Networks for Offshore Wind Power Plants, London, 2013.
[4] A. D. Hansen, N. A. Cutululis, F. Iov, P. E. Sørensen, and T. J. Larsen. Grid faults' impact on wind turbine structural loads. 4th Nordic Wind Power Conference, Roskilde, 2007. Risø National Laboratory.
[5] A. D. Hansen and G. Michalke. Fault ride-through capability of DFIG wind turbines. Renewable Energy, 32(9):1594-1610, July 2007.
[6] O. Gomis-Bellmunt, A. Junyent-Ferre, A. Sumper, and J. Bergas-Jané. Ride-through control of a doubly fed induction generator under unbalanced voltage sags. IEEE Transactions on Energy Conversion, 23:1036-1045, 2008.
[7] B. Bak-Jensen, T.A. Kawady, and M. H. Abdel-Rahman. Coordination between Fault-Ride-Through Capability and Over-current Protection of DFIG Generators for Wind Farms. Journal of Energy and Power Engineering, 4(4):20-29, April 2010.
[8] National Renewable Energy Laboratory (NREL) webpage, http://www.nrel.gov/, Access data: 24/09/2013

The research leading to these results has received funding from the European Union Horizon2020 programme under the agreement H2020-LCE-2014-1-640741.

For more information:
http://lifes50plus.eu/

Contact: mdeprada@irec.cat

Innovative floating offshore wind energy

LIFES50+

Petter Andreas Berthelsen, MARINTEK , Jan Arthur Norbeck, MARINTEK, Germán Pérez, Tecnalia, Gabriela Benveniste, IREC, Maxime Thys, MARINTEK, Henrik Bredmose, DTU, Denis Matha, Ramboll Wind, Jude Ugwu, ORE Catapult, Kolja Müller, USTUTT, Marco Belloli, POLIMI, Luca Vita, DNVGL, Juan Amate Lopez, Iberdrola, Trond Landbø, Dr. techn.Olav Olsen, Thomas Choisnet, IDEOL

Introduction

A major international collaborative project involving 12 partners from eight countries and worth €7.3 million is set to drive forward development of the next generation of floating wind substructures. The European Horizon2020-funded programme LIFES50+, led by Norway's MARINTEK, will run for 40 months starting 2015 and will focus on proving the innovative technology that is being developed for floating substructures for 10MW wind turbines at water depths greater than 50 m.

Partners:

Objectives

- Optimize and qualify to Technology Readiness Level (TRL) of 5, two innovative substructure designs for 10MW turbines.
- Develop a streamlined and KPI (Key Performance Indicator) based methodology for the evaluation and qualification process of floating substructure.

The focus of the project is on floating wind with large turbines (10 MW) installed at water depths from 50 m to 200 m. Increasing the turbine size is expected to be one of the most effective way of reducing LCOE in short term.

Approach

Four existing substructure concepts at TRL of at least 4 that can support 5MW wind turbines are used as input to the project. These floating substructures are upscaled to accomodate the 10MW DTU reference turbine[1]. This activity will be driven by concept owners, benefitting from the presence of strong research and industrial partners within the consortium, ensuring innovation both from a scientific and industrial point of view.

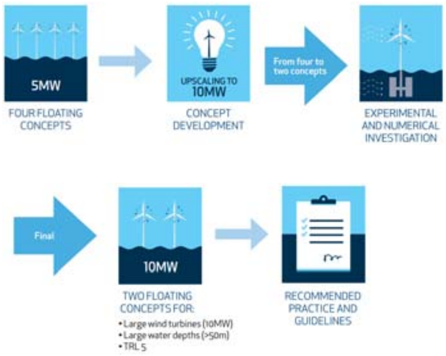

In parallel, a methodology for the evaluation of substructures, based on KPI's, will be developed. These KPI's include important parameters such as, but not limited to, CAPEX and OPEX, technology performance and integrity, deployment and installation performance, logistics and O&M costs, industrial capacity for production, Technology Readiness Level (TRL) and Manufacturing Readiness Level (MRL), time to market, adaptability to various turbines, life-cycle environmental impacts, and more. The four substructures developed in the project will undergo an evaluation based on this methodology.

Two concepts will be selected, based on the evaluation results, for further verification in order to reach the TRL level put as goal for this project. This includes numerical analysis with a range of simulation tools from simplified design simulators to high-fidelity models for specific load effects and experimental investigation based on a novel approach using Real-Time Hybrid Testing[2] in both wind tunnel and wave tank facilities. All relevant load effects and the corresponding models will be collected for a best-practice of the numerical design process for FOWTs.

The models of the two selected concepts will also be delivered as open source versions. A review of the two selected substructures will be performed after the model test campaign, with focus on the manufacturability of the concepts.

The project will also focus on uncertainties and risk assessment of the design at economic, technical and environmental levels.

The findings from the project will be included in guidelines/recommended practices written to support designers in their work and allow efficient qualification of large offshore wind substructures.

Research challenges

To realize the project goals, there is a need and clear ambition to move forward the state-of-the-art in the following:

- Multi-fidelity numerical tools in the context of qualifying and optimizing large substructures.
- Experimental techniques specific to floating offshore wind turbines.
- Concept industrialization, as an early focus in the design.
- Uncertainty and risk assessment related to unprecedented large wind turbine substructures.

Concepts

References:

1. Bak C, Zahle F, Bitsche R, Kim T, Yde A, Henriksen LC, Andersen PB, Natarajan A, Hansen MH, 2013. Description of the DTU 10 MW Reference Wind Turbine. DTU Wind Energy Report-I-0092, Roskilde, Denmark.
2. Bachynski E, Chabaud V, Suader T, 2015. Real-time hybrid model testing of floating wind turbines: sensitivity to limited actuation. 12th Deep Sea Offshore Wind R&D Conference, DeepWind'15.
3. www.nautilusfs.com
4. http://docslide.us/documents/oo-star-wind-floater-a-robust-and-flexible-concept-for-floating-wind-trond-landbo-presentation-april-2013.html
5. www.oceanlider.com, http://www.etrera2020.eu/component/phocadownload/category/2-achivied-impacts.html?download=139:tlpwind-iberdrola-project
6. http://ideol-offshore.com

The research leading to these results has received funding from the European Union Horizon2020 programme under the agreement H2020-LCE-2014-1-640741

For more information:
www.lifes50plus.eu

Aerodynamic modeling of floating vertical axis wind turbines using the actuator cylinder flow method

Zhengshun Cheng[1,2,3], Helge Aagaard Madsen[4], Zhen Gao[1,2,3], Torgeir Moan[1,2,3]
[1]Department of Marine Technology, NTNU [2]Center for Ships and Ocean Structures (CeSOS), NTNU
[3]Center for Autonomous Marine Operations and Systems (AMOS), NTNU [4]Department of Wind Energy, DTU

NTNU Norwegian University of Science and Technology

MARE-WINT new MAterials and REliability in offshore WINd Turbines technology

Abstract

Among the aerodynamic models of VAWTs, double multi-streamtube (DMST) and actuator cylinder (AC) models are two favorable methods for fully coupled modeling and dynamic analysis of floating VAWTs in view of accuracy and computational cost. This paper deals with the development of an aerodynamic code to model floating VAWTs using the AC method developed by Madsen (1982). It includes the tangential load term when calculating induced velocities, addresses two different approaches to calculate the normal and tangential loads acting on the rotor, and proposes a new modified linear solution to correct the linear solution. The effect of dynamic stall is also considered using the Beddoes-Leishman dynamic stall model. The developed code is verified to be accurate by a series of comparisons against other numerical models and experimental results. It is found that the effect of including the tangential load term when calculating induced velocities on the aerodynamic loads is very small. The proposed new modified linear solution can improve the power performance compared with the experiment data. Finally, a comparison of the developed AC method and the DMST method is performed and shows that the AC method can predict more accurate aerodynamic loads and power than the DMST method.

Actuator cylinder (AC) flow model

Considering a 2D quasi-static flow problem, the induced velocities are related to the volume force as well as the normal and tangential loads Qn and Qt, based on the continuity equation and Euler equation.
The final induced velocities can be divided into a linear part and a non-linear part.

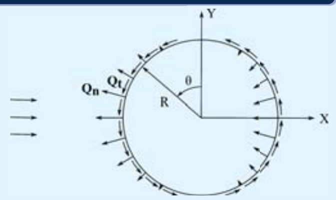

Linear solution

$$w_x = -\frac{1}{2}\int_0^{2\pi} Q_n(\theta)\frac{-(x+\sin\theta)\sin\theta+(y-\cos\theta)\cos\theta}{(x+\sin\theta)^2+(y-\cos\theta)^2}d\theta - \frac{1}{2}\int_0^{2\pi} Q_t(\theta)\frac{-(x+\sin\theta)\cos\theta-(y-\cos\theta)\sin\theta}{(x+\sin\theta)^2+(y-\cos\theta)^2}d\theta$$

$$-\left(Q_n(\arccos y)\right)^{*}+\left(Q_n(-\arccos y)\right)^{**}-\left(Q_t(\arccos y)\frac{y}{\sqrt{1-y^2}}\right)^{*}-\left(Q_t(-\arccos y)\frac{y}{\sqrt{1-y^2}}\right)^{**}$$

$$w_y = -\frac{1}{2}\int_0^{2\pi} Q_n(\theta)\frac{-(x+\sin\theta)\cos\theta-(y-\cos\theta)\sin\theta}{(x+\sin\theta)^2+(y-\cos\theta)^2}d\theta - \frac{1}{2}\int_0^{2\pi} Q_t(\theta)\frac{(x+\sin\theta)\sin\theta-(y-\cos\theta)\cos\theta}{(x+\sin\theta)^2+(y-\cos\theta)^2}d\theta$$

Modified linear solution

It's relatively time-consuming to compute the nonlinear solution directly. A correction can be applied by multiplying the velocities from the linear solution with factor

$$k_a = \frac{1}{1-a} \quad \text{(Madsen et al., 2013)}$$

$$k_a = \begin{cases} \dfrac{1}{1-a}, & (a \le 0.15) \\ \dfrac{1}{1-a}\left(0.65+0.35e^{-4.5(a-0.15)}\right), & (a > 0.15) \end{cases} \quad \text{(Present)}$$

Aerodynamic modeling of a floating VAWT

Aerodynamic loads on a 2D VAWT

Approach I

$$Q_t = \frac{BF_{tB}}{2\pi R\rho V_{wB}^2}$$

$$Q_n = \frac{BF_{nB}}{2\pi R\rho V_{wB}^2}$$

Approach II

$$Q_t = \frac{BF_{tA}}{2\pi R\rho V_{wB}^2 \sin\beta}$$

$$Q_n = \frac{BF_{nA}}{2\pi R\rho V_{wB}^2 \sin\beta}$$

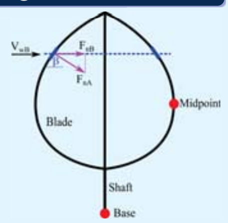

Aerodynamic modeling of a floating VAWT

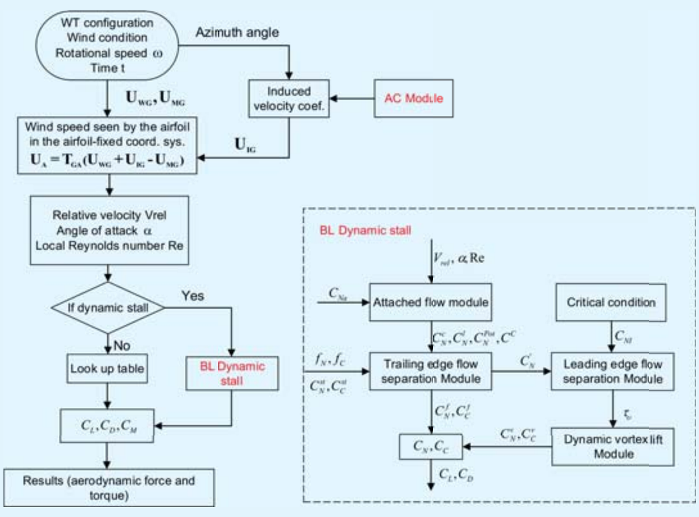

Flow chart of aerodynamic modeling of a floating VAWT using the AC method

Verifications and discussions

The developed AC code can be categorized into AC1, AC2, AC3 and AC4.

	Approach for Qn and Qt	Qt term in linear solutions	Modified linear solution
AC1	I	Neglected	Madsen et al., 2013
AC2	I	Included	Madsen et al., 2013
AC3	II	Included	Madsen et al., 2013
AC4	II	Included	Present

Verification of AC1 and AC2

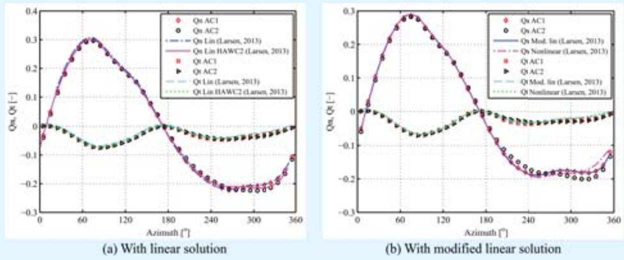

Distribution of Qn and Qt at midpoint of the blade at different azimuth angle

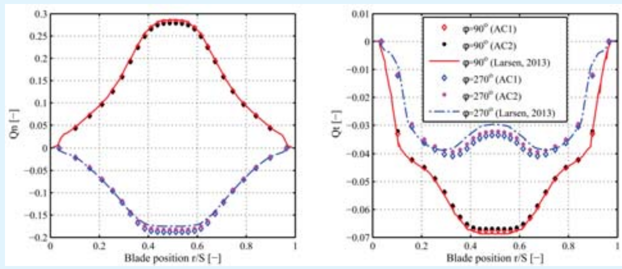

Distribution of Qn and Qt along the blade at azimuth angle of 90 and 270.

Verification of AC3 and AC4 & Comparison of AC and DMST methods

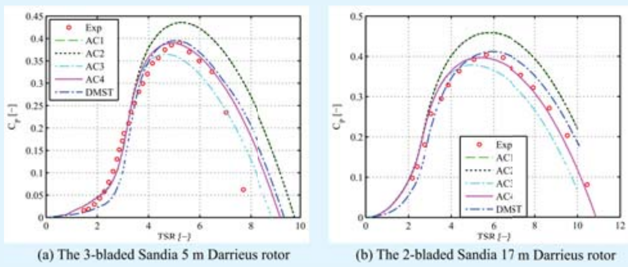

Comparison of power coefficient curve between simulation model and experimental data

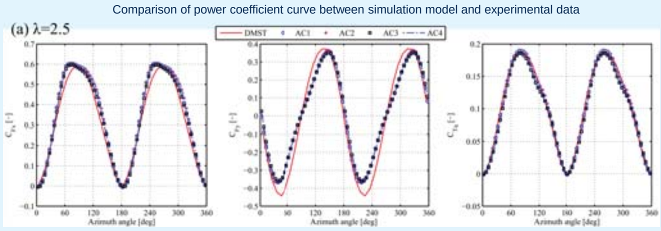

Coefficients of thrust, side force and torque for the Sandia 17 m Darrieus rotor as a function of the azimuth angle

Conclusions

- The effect of tangential load on the aerodynamic loads when calculating the induced velocities is found to be relatively very small.
- Calculating the normal and tangential loads using approach II which considers more physical phenomena predicts better aerodynamic loads than approach I.
- The modified linear solution proposed in this study gives prediction of good aerodynamic power compared with experimental data.
- The developed code AC4 can predict more accurate aerodynamic power and aerodynamic loads than the DMST method.
- This AC code can be integrated with the computer codes SIMO-RIFLEX to form a fully coupled simulation tool, i.e. SIMO-RIFLEX-AC (Cheng et al., 2016), which is capable of performing the aero-hydro-servo-elastic time-domain analysis for onshore bottom-fixed or floating VAWTs.

References

1. Ferreira, C. S., Madsen, H. A., Barone, M., Roscher, B., Deglaire, P., Arduin, I., 2014. Comparison of aerodynamic models for vertical axis wind turbines. Journal of Physics: Conference Series 524 (1), 012125.
2. Larsen, T. J., Madsen, H. A., 2013. On the way to reliable aeroelastic load simulation on VAWT's. In: Proceedings of EWEA.
3. Madsen, H. A., Larsen, T. J., Paulsen, U. S., Vita, L., 2013. Implementation of the actuator cylinder flow model in the HAWC2 code for aeroelastic simulations on vertical axis wind turbines. In: 51st AIAA Aerospace Sciences Meeting including the New Horizons Forum and Aerospace Exposition.
4. Madsen, H. A., 1982. The Actuator Cylinder: A flow model for vertical axis wind turbines. Institute of Industrial Constructions and Energy Technology, Aalborg University Centre.
5. Cheng, Z., Madsen, H. A., Gao, Z., Moan, T., 2016. A fully coupled method for numerical modeling and dynamic analysis of floating vertical axis wind turbines. Prepared for possible journal publication.

DeepWind 2016, Trondheim, 20-22 Jan. 2016

Scalability of floating Vertical Axis Wind Turbines

Elin Andersen, University of Stavanger, elin.andersen@uis.no
Arnfinn Nergaard, University of Stavanger

Universitetet i Stavanger

Background

Wind energy is moving offshore and floating wind turbines might be the next step. In floating applications, vertical axis wind turbines (VAWTs) has some advantages:

- they offer a lower center of gravity,
- they does not need a yawing mechanism,
- sensitive equipment can be located at sea level in a protected engine room
- they offer simpler operation and maintenance (O&M) activity
- they offer suppressed roll/pitch due to gyro-effects

There is a variety of rotor configurations, rotor sizes, blade profiles, blade materials etc., and it is not clear which is the most effective wind turbine rotor type. What is the optimum size and the best material choice for blade manufacturing?

Objective

To investigate the possibility of upscaling floating vertical axis wind turbines (FVAWTs) *to a size where it can produce energy at a competitive levelized cost of energy.*

Examples

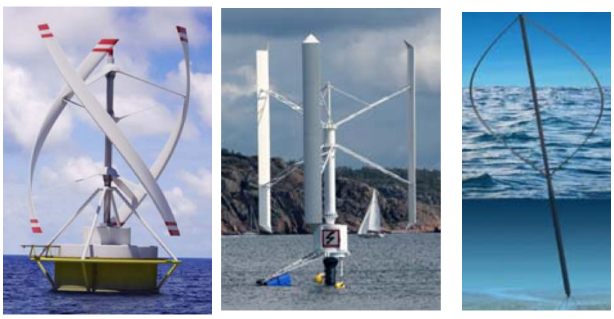

Figur 1 Examples of VAWTs: a) Gwind [1] b) Seatwirl [2] c) Deepwind [3]

Methodology

When VAWTs are scaled up to a commerzial size, i.e 5MW, there will be new challenges in the structural design. For a Darreius-type rotors, see figure 1 a-c, with two or three blades, the loads will vary with 2P or 3P, and the wake effects might be considerable.

The wind loads will be determined utilizing the aeroelastic tool HAWC2 [4], and its newer module for VAWTs. Hydrodynamic effects will be included as rotations and translations from global maotion analysis.

The newer developments on isogeometric analysis in finite element methods gives new opportunities for analyzing structures that has a smooth geometry [5]. New finite element types are developed to be capable of modeling the highly anisotropic properties of composite material layups [6].

Fluid-Structure Interaction is a useful tool to evaluate how the rapid change in angle of attack leads to high frequency and high-amplitude variations in aerodynamic torque acting on the rotor [7].

Expected results

Full-scale finite element analysis will be performed to structurally evaluate to what extent floating Vertical Axis Wind Turbines can be scaled up to MW power range.

References:
[1] http://www.gwind.no [2] http://seatwirl.com [3] http://www.deepwind.eu [4] http://www.hawc2.dk
[5] M-C. Hsu, Y. Bazilevs. Fluid–structure interaction modeling of wind turbines: simulating the full machine. (Journal of Computational Mechanics), (Vol. 50, Issue 6), 2012.
[6] J. Kiendl, Y.Bazilevs, M.-C. Hsu, R. Wüchner, K.-U. Bletzinger. The bending strip method for isogeometric analysis of Kirchhoff–Love shell structures comprised of multiple patches. (Journal of Computer Methods in Applied Mechanics and Engineering), (Vol. 199, issue 37-40), 2010.
[7] Y. Bazilevs, A. Korobenko, X. Deng, J. Yan, M.Kinzel, J. O. Dabiri. Fluid-Structure Interaction Modeling of Vertical-Axis Wind Turbines. (Journal of Applied Mechanics), (Vol. 81, issue 8), 2014.

AWESOME
PhD'S IN WIND POWER O&M

Advanced Wind Energy Systems Operation and Maintenance Expertise

AWESOME is a Marie Curie Innovative Training Network (ITN) for early stage researchers (ESR) funded by the European Commission under the H2020 Programme, the EU framework programme for research and innovation

AWESOME network aims to educate eleven young researchers in the wind power operation and maintenance (O&M) field by constructing a sustainable training network gathering the whole innovation value chain. The main EU actors in the field of wind O&M have worked together, under the umbrella of the European Wind Energy Academy (EAWE), in order to design a training program coping with the principal R&D challenges related to wind O&M while tackling the shortage of highly-skilled professionals on this area that has been foreseen by the European Commission, the wind energy industrial sector and the academia

OBJECTIVES

The main goal of AWESOME is to shape **a critical mass of new expertise** with the fundamental skills required to power the scientific and technological challenges of Wind Energy O&M in order to achieve the following specific objectives:

1. To develop better O&M planning methodologies of wind farms for maximizing its revenue
2. To optimize the maintenance of wind turbines by prognosis of component failures
3. To develop new and better cost-effective strategies for Wind Energy O&M

> These main goals have been divided into **11 specific objectives (projects)**, which have been assigned to the fellows, for them to focus their R&D project, PhD Thesis and professional career.

> Each fellow will be exposed to **three different research environments** from both, academic and industrial spheres.

> The established training plan answers the challenges identified by the SET Plan Education Roadmap.

> Personal Development Career Plans will be tuned up for every fellow, being their accomplishment controlled by a Personal Supervisory Team.

THE CHALLENGES

INDUSTRIAL SECTOR

- Wind energy sector: 10% of anual increase in the last 10 years, mainly offshore
- Aging of existing onshore parks
- O&M costs might have an average share of 20%-25% of total levelised cost per kWh produced

ACADEMIC SECTOR

- Networks of universities and other relevant higher education institutions
- Programs to be developed linked to the current EAWE status
- High education programmes, Masters and PhD levels

PARTNER ORGANIZATIONS

CETASA, Enel Green Power, ALSTOM, DONG energy, Ingeteam, DNV·GL, sgurr energy, Politecnico di Milano

BENEFICIARIES

RAMBOLL, DTU, TUM, University of Strathclyde Glasgow, Loughborough University, NTNU, ForWind, UCLM, circe

TRAINING ACTIVITIES

LOCAL TRAINING	INTRA-NETWORK TRAINING	INTER-NETWORK TRAINING
• PhD enrollment	• Academic & Industrial Secondments • Specific AWESOME Courses	• Scientific Conferences coordinated with EAWE • Summer schools • Industrial Workshops

www.awesome-h2020.eu

11 PROJECTS

ESR 1 Performance monitoring techniques for operation and maintenance of wind turbines
CIRCE - SPAIN

ESR 2 Very-short term wind field forecasts for wind farm operation and grid stability improvements
FORWIND - GERMANY

ESR 3 Stochastic Wind Park modelling and maintenance scheduling under uncertainty - a serious game
NTNU - NORWAY

ESR 4 Improved wind farm operation and control
TUM - GERMANY

ESR 5 Development of Wind Turbine Fault Detection Algorithms
LBORO - UK

ESR 6 Hardware in the Loop Testing of Wind Turbine Condition Monitoring Systems
USTRATH - UK

ESR 7 Advanced diagnosis of wind turbines
UCLM - SPAIN

ESR 8 Structural health monitoring for wind turbine extended life operation
RAMBOLL - GERMANY

ESR 9 Wind Farm O&M cost reduction through predictive maintenance
DTU - DENMARK

ESR 10 Wind Farm management cost optimization
CIRCE - SPAIN

ESR 11 Cost effective maintenance of wind turbines using components reliability
CIRCE - SPAIN

This project has received funding from the European Union's Horizon 2020 research and innovation programme under the Marie Sklodowska-Curie grant agreement n.º 642108